Pathogenesis of Myxoma Virus

Thesis submitted for the degree of Doctor of Philosophy of

The Australian National University

Sonja Marie Best

Department of Biochemistry and Molecular Biology

The Australian National University

Canberra, ACT, Australia

December, 1998

Declaration

I hereby certify that the work embodied in this thesis is my original work. Statistical advice was obtained from Mr. Bob Forrester, Biometrics Unit, CSIRO. The embedding and sectioning of fixed tissues was done by the JCSMR histology service (ANU).

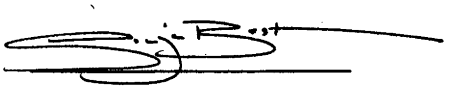

(Sonja Best)

To my family,

for your love and continued support.

Acknowledgments

To the VBCRC, and The Department of Biochemistry and Molecular Biology, ANU, thankyou for all the opportunities afforded to me; to study and to travel and discuss my work overseas.

Peter Kerr, you have my sincerest appreciation and admiration. Thankyou for all of your time, patience, support, for being constantly available and for making this study an exercise in teaching and learning. You pushed me to my limit and then guided me past it. I will always carry with me the PJK anecdotes: do you have data to support that, what are you trying to say, and discuss *your* results.

Peter Janssens, you have continually supported and believed in me, and always been able to tell it how it is. Thankyou, and thankyou for providing so many additional opportunities to extend myself beyond the laboratory door.

To Tony Robinson (VBCRC) and Alistair Ramsay (JCSMR, ANU), for your continued interest, and to Alistair for the use of your laboratory and guidance in ELISPOT and cell proliferation assays. To Michael Holland (VBCRC), for your interest and for saying the right words at the right time. To Grant McFadden (University of Western Ontareio, Canada), for the kind gifts of your myxoma virus gene-deletion mutants, and Graham Laver (JCSMR, ANU) for influenza virus. To Bob Forrester (CSIRO), for statistical advice and to Sheila Cook and Sandra Veness (JCSMR) for histology and use of the cryostat. To Frank Fenner and Ian Marshall – thankyou for your interest. I hope this thesis adds some valuable insights into the relationship between the rabbit and myxoma virus that your original work so gracefully began.

To Louise Silvers, thankyou for those many hours of rabbit work, rabbit inoculations, rabbit bleeding, rabbit autopsies (thanks for the rabbits tell your mother) and cutting up

rabbit tissues – and all before breakfast at McDonalds. To Nigel French, thanks especially for all those vero cells (and the rabbit arse cells). To Hannah Clarke, for answering all my nagging little questions, more than once. To Kathy Saint, thankyou for your superb technical help and teaching me that dilutions really aren't that hard.

To the staff and friends of the VBCRC, thankyou. Thankyou to the staff of the animal house, particularly Judi Simmons and Brenda Donges. To all my friends, in Canberra, Adelaide and further abroad, thankyou for your generosity, laughter and continued support, particularly Louise Silvers, Nigel French, James DeJersey, Brett Nixon, Karen Peisley, Tim Griffiths, Steve Parker and Brian Murphy.

To Paula Fitzgerald, for your pure generosity and making your home mine, and letting me spread my stuff through all the rooms in the house. Mostly, thankyou for your friendship and for keeping me directed through your continued belief in my ability.

To my family, my mother Valerie, father Lindsay and brother Anthony. You certainly are my cornerstone. I would not made it through all the ups and downs of this time without your continued love, phone calls, and support. Thankyou.

Table of Contents

Chapter 5. Mechanisms of host genetic resistance and myxoma virus pathogenesis

List of Tables

List of Figures

Please note: + indicates page following numbered page(s)

List of commonly used abbreviations

μCi	cicimolar
μg	microgram
μl	microlitre
μm	micrometre
^{3}H-T	tritiated thymidine
ABTS	2,2'-azino-bis(3-ethylbenzo-thiazoline-6-sulphonic acid)
AICD	activation induced cell death
APC	antigen presenting cell
ASC	antibody secreting cells
ASF	anti suppressor factor
β_2m	$\beta_2$microglobulin
BCIP	5-bromo-4-chloro-3 indolyl phosphate
BSA	bovine serum albumin
C, CC, CXC	chemokine subfamilies
cm	centimeters
CO_2	carbon dioxide
Con A	concanavalin A
CrmA	cytokine response modifying protein A
CTL	cytotoxic T cell
ddH_2O	double distilled, deionised water
DNA	deoyribose nucleic acid
dpi	days post infection
EEV	extracellular mature virion
EGF	epidermal growth factor
ELISA	enzyme linked immunosorbent assay
ELISPOT	enzyme linked immunosorbent spot assay
FBS	foetal bovine serum

FITC	fluorescein isothiocynate
g	gram
g	centifugal force
HA	influenza haemagglutinin
HAU	haemagglutinin units
HBSS	Hank's balanced salt solution
hpi	hours post infection
ICE	interferon-1β converting enzyme
ID_{50}	infectious dose of virus at which half of European rabbits are infected
IEV	intracellular enveloped virion
IFN	interferon
IgG	immunoglobulin G
IgM	immunoglobulin M
IL	interleukin
ITR	inverted terminal repitition
KM13	prototype grade III attenuated strain of mv
LPS	lippopolysaccharide
M	molar
MEM	minimal essential medium
MGF	myxoma growth factor
MHC	major histocompatability complex
min	minutes
ml	millilitre
mm	millimetre
moi	multiplicity of infection
mRNA	messenger ribose nucleic acid
NBT	nitro blue tetrazolium
NK	natural killer
°C	degrees centigrade
OD	optical density

PBS	phosphate buffered solution
pfu	plaque forming units
pfu/g	plaque forming units per gram
PHA	phytohaemagglutinin
Prp	proline rich rpotein
RL5	rabbit $CD4^+$ T cell line
Rmp1	gene encoding resistance to mousepox
RNA	ribose nucleic acid
sec	seconds
SLS	standard laboratory strain
TBS	tris buffered saline
TdT	terminal transferase
TGF-α	transforming growth factor alpha
T_H1	T helper cell type 1
T_H2	T helper cell type 2
TNF	tumor necrosis factor
TNFR	tumor necrosis factor receptor
TUNEL	terminal deoxy-nucleotide nick end labeling
UrHA	recombinant Uriarra expressing influenza haemagglutinin
v/v	volume/volume
Vero	african green monkey kidney cell line
VISF	virus induced suppressor factor
w/v	weight/volume
WBC	white blood cell

Abstract

Myxoma virus causes the lethal disease myxomatosis following infection of the European rabbit (*Oryctolagus cuniculus*), and was introduced into Australia in 1950 for the biological control of wild *O. cuniculus* populations. Shortly after its release, two, well described events occurred: attenuated strains of virus emerged and genetic resistance developed within the host rabbit populations. There have been detailed epidemiolgical and molecular studies on myxoma virus, but no coordinated study examining the mechanism of genetic resistance. This thesis provides the first detailed and coordinated study in which resistant and susceptible rabbits infected with virulent and naturally attenuated strains of myxoma virus are directly compared.

In the first part of this thesis, differences in the ability of virulent and attenuated myxoma virus to down regulate the immune response were examined. Populations of outbred laboratory rabbits were infected with the standard laboratory strain (SLS) of myxoma virus, which is 100% lethal, or with a naturally attenuated strain of myxoma virus, Uriarra, which causes myxomatosis but is lethal in less than 5% of infected rabbits. SLS but not Uriarra, suppressed the T-cell-mitogen induced proliferation of lymphocytes from lymph nodes of rabbits by 4dpi. To examine humoral immune responses, a model system of coinfections was studied, using a highly attenuated recombinant myxoma virus that expresses the influenza haemagglutinin (HA). IgG titres to HA were suppressed by coinfection of laboratory rabbits with either SLS or Uriarra. However, IgG titres to myxoma virus were strikingly higher in rabbits coinfected with SLS compared to those coinfected with Uriarra. Modulation of the immune response by SLS was associated with the depletion of lymphocytes from lymph nodes.

The next phase of this study was to determine where and when virus replication was controlled in infected rabbits. SLS replicated at the primary inoculation site in the skin,

initially in MHC II^+ dendritic cells in the dermis, followed by replication in the epidermis. Virus was probably transported to the draining lymph node in these MHC II^+ cells. In the lymph node, SLS replicated to high titres, predominantly in lymphocytes and macrophages. Virus disseminated from here to secondary sites in the skin where it grew to high titres, and to other lymph nodes, the spleen and the lung. The most severe pathology occurred in the lymph nodes which were depleted of lymphocytes. Wild rabbits were significantly resistant to SLS. A major difference between wild and laboratory rabbits infected with SLS was the local inflammatory response in the skin and lymph nodes, which was comprised predominantly of mononuclear inflammatory cells in infected wild rabbits. SLS-infected laboratory rabbits had a polymorphonuclear inflammatory response that localised deep in the dermis, away from most virus replication. Control of virus replication in wild rabbits occurred at the draining lymph node where virus titres were 10-50 fold lower than in laboratory rabbits. However, titres at the skin inoculation site were similar to laboratory rabbits. Depletion of lymphocytes occurred but in contrast with laboratory rabbits, was restricted to the draining lymph node, and this lymph node became repopulated with lymphocytes around 15dpi. Uriarra grew to similar titres as SLS at the primary inoculation site in the skin of laboratory rabbits and in the draining lymph node, but virus dissemination and growth in distal tissues was reduced, and lymphocytes were not depleted from the lymph nodes. In both Uriarra-infected laboratory rabbits and SLS-infected wild rabbits, virus was cleared from the internal tissues by between 10 and 15 days post infection and the rabbits recovered from disease.

Specific staining showed that apoptosis was a major mechanism of lymphocyte cell death in lymph nodes of all myxoma virus-infected rabbits. Apoptotic cells did not stain positive for virus. However, in SLS-infected laboratory rabbits, apoptosis was induced earlier than in the other rabbits, and was closely associated with virus replication.

This study has described where and in what cells myxoma virus replicates. By comparing resistant and susceptible rabbits it has been shown that resistance is associated with a lymphocyte-rich inflammatory response, control of virus replication in the draining lymph node and reduced replication in distal tissues. Resistance was not due to cell permissivity to virus infection. Therefore a model is proposed for resistance being due to the wild rabbit having a more effective innate and adaptive immune response to myxoma virus. This is most

likely occurring very early in infection, possibly at the level of the initially infected dendritic cells and subsequently at the draining lymph node. The mechanisms of enhanced immunity remain to be determined and particularly the role of cytokines, NK cells and CTL responses. Infection of laboratory and wild rabbits with attenuated virus supports this model, which indicates that the attenuated virus is unable to suppress or deviate the initial immune response.

Chapter 1: Introduction

1. Introduction

1.1 Introduction

The release of myxoma virus into the Australian wild European rabbit (*Oryctolagus cuniculus*) population in 1950 constituted one of the greatest natural biological experiments of host-virus coevolution ever documented. After the release of myxoma virus, which was highly lethal for *O. cuniculus*, attenuated strains of virus emerged and genetic resistance developed within the host rabbit population. The original strain of virus that was released into the Australian field and an attenuated strain isolated from the field shortly afterwards are both accessible for study, as are genetically susceptible laboratory rabbits, and wild rabbits that have been naturally selected in the field for genetic resistance to myxoma virus. This gives us a unique and exciting opportunity to study host-virus interactions.

1.2 Myxoma virus - classification, properties and replication

Myxoma virus is a member of the family Poxviridae, subfamily Chordopoxvirinae. Its genus, *Leporipoxvirus*, comprises three closely related viruses found in *Sylvilagus* species of rabbits in the Americas, two viruses of North American squirrels (*Sciurius* sp.) and the more distantly related hare fibroma virus (in *Lepus europaeus*) (Table 1.1) (Fenner, 1994b; Fenner and Kerr, 1994). There are two major geographic types of myxoma virus, the South American and Californian, which show substantial differences in their rabbit host species (Marshall and Fenner, 1960; Marshall and Regnery, 1963; Marshall *et al.*, 1963). These types also differ in the disease caused following infection of the European rabbit, *O. cuniculus,* which is not a natural host to any leporipoxvirus, and is susceptible to lethal infection with myxoma virus (Fenner and Ratcliffe, 1965).

By electron microscopy, myxoma virus virions are indistinguishable from those of the prototype poxvirus, vaccinia virus (Padgett *et al.*, 1964) appearing oval or brick shaped with a biconcave nucleoprotein core and two lateral bodies surrounded by a lipoprotein bilayer membrane (Figure 1.1). Myxoma virus shares a common antigen with species of other poxvirus genera (Woodroofe and Fenner, 1962), but there is no cross-neutralisation or cross-protection with poxviruses belonging to genera other than *Leporipoxvirus* (Woodroofe and Fenner, 1965).

Table 1.1: The natural host and types of clinical disease produced by viruses of the genus *Leporipoxvirus* (family *Poxviridae*) in the European rabbit (*Oryctolagus cuniculus*) (modified from Fenner and Ross, 1994).

Virus	Natural host	Location	Clinical signs in *Oryctolagus cuniculus*
Shope fibroma	*Sylvilagus floridanus*	eastern United States	Localised, benign fibroma
Brazilian myxoma	*Sylvilagus brasiliensis*	South America	generalised lethal disease, gross external signs
Californian myxoma	*Sylvilagus bachmani*	western United States	generalised lethal disease, few external signs
Hare fibroma	*Lepus europaeus*	Europe	localised, benign fibroma
Squirrel fibroma	*Sciurus carolinensis*	eastern United States	localised, benign fibroma
Western squirrel fibroma	*Sciurus griseus griseus*	western United States	not determined

The poxviruses have a double stranded DNA genome which varies in size, from 130 kbp (parapoxviruses) to about 375kbp (avipoxviruses) (Fenner and Nakano, 1988); the genome of myxoma virus is 163kbp in length (Russell and Robbins, 1989). The two strands of DNA form telomeric structures as they are continuous, connected by hairpin loops, but are not completely covalently bound along the entire length (DeLange and McFadden, 1990). At either end of the genome there are inverted terminal repetitions

(ITRs), which are stretches of sequence that are identical but in opposite orientation to each other. The organisation of the central region of the genome is relatively conserved between poxviruses, encoding genes essential for viral replication and production of infectious progeny (Moss, 1996). The genes adjacent to and within the ITRs are less conserved between poxviruses, and encode proteins that determine virus virulence and host specificity. These genes have been termed virulence genes (McFadden, 1995).

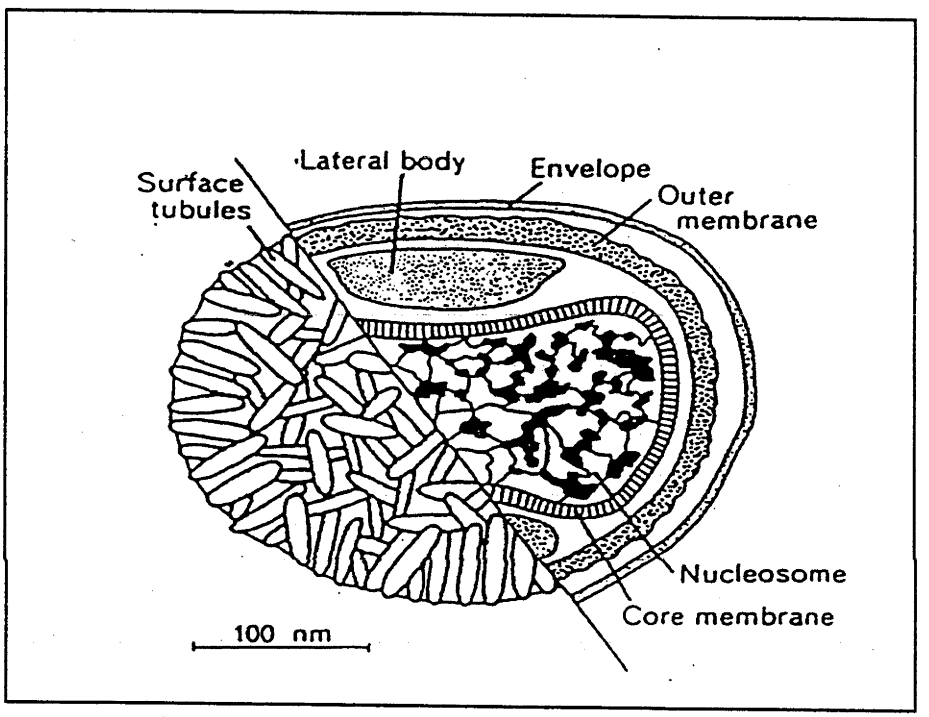

Figure 1.1: Schematic representation of the poxvirus virion. A nucleosome with a core membrane associated with lateral bodies is surrounded by an internal membrane in which are embedded surface proteins. This form of virus is infectious and found intracellularly. A second form of extracellular virus particles contain a Golgi-derived outer envelope in which virus encoded proteins are inserted. The left hand side of this diagram represents the surface structure of a non-enveloped, intracellular particle (Fenner and Nakano, 1988).

The majority of information concerning poxvirus replication is derived from studies of the prototype virus, vaccinia virus. The poxviruses, including myxoma virus, replicate in the cytoplasm of infected cells (Beaud, 1995; Moss, 1996) (Figure 1.2). Cell entry is via fusion of the virus with the plasma membrane or by endocytosis, followed by the

release of the virus core into the host cell cytoplasm (first virus uncoating). Replication appears to be independent of the cell nucleus and most of the protein components required for transcription and replication of the viral genome are encoded by the virus. (Beaud, 1995; Moss, 1996).

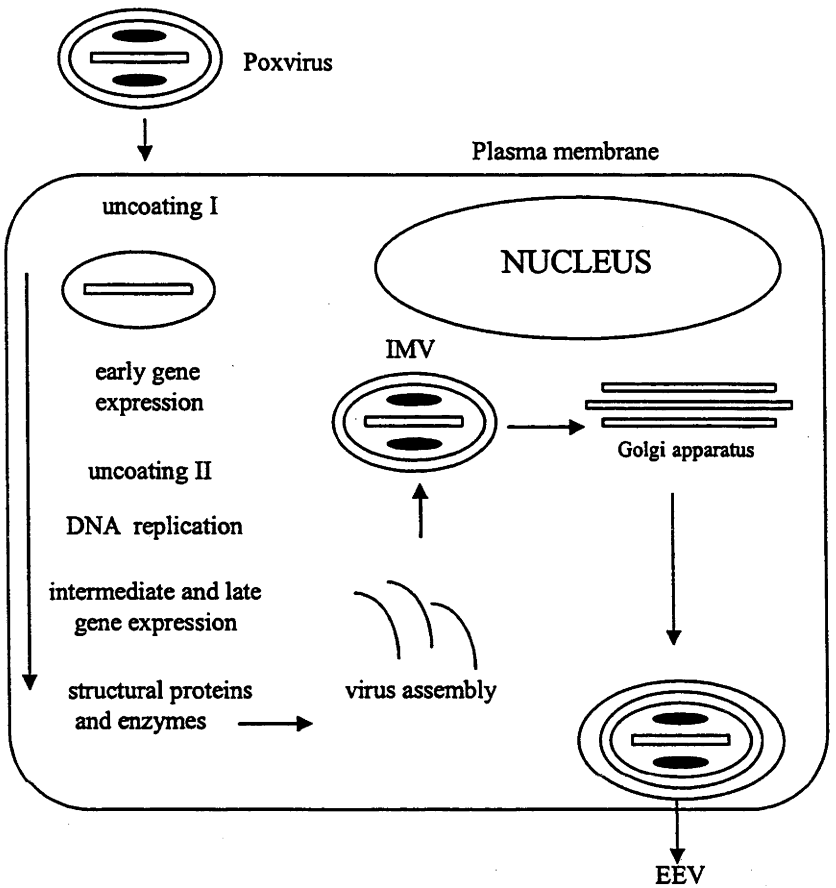

Figure 1.2: The poxvirus infection cycle in the cytoplasm of infected cells. Poxvirus replication occurs in the cytoplasm of infected cells, in virosomes (not pictured). After fusion with the plasma membrane and entry, an uncoating process releases the intact core and early gene expression occurs. This is followed by a second uncoating, DNA replication, intermediate and late gene expression and virion assembly. The intracellular mature virion (IMV) may acquire a double membrane from the Golgi apparatus. Upon release from the cell, the outer bilayer fuses with the plasma membrane, releasing an extracellular enveloped virus (EEV) with an internal membrane and an external envelope (Traktman, 1990a).

Virus replication is divided into early, intermediate and late stages. Temporal expression of genes is regulated at the transcriptional level (Moss *et al.*, 1991). Following first virus uncoating which releases the virus core, early mRNA transcription is initiated by the viral transcriptase. Transcription of intermediate and late genes is controlled by the binding of specific viral (Moss, 1996) and cellular (Rosales *et al.*,

1994; Zhu *et al.*, 1998) proteins to characteristic promoter sequences. Capped and polyadenylated mRNAs are produced, without splicing, within minutes of viral infection, due to the presence of a transcription factor, capping and methylating enzymes and a poly(A) polymerase, all included within the core of the virion. The early proteins transcribed within the proteinaceous core of the infecting virion complete the uncoating of the core (secondary uncoating) making the viral genome accessible for DNA replication. These early transcripts also encode intermediate and late gene transcription factors and the viral DNA polymerase required for DNA replication (Gershon, 1998; Moss, 1996).

DNA replication, followed by intermediate gene expression, proceeds in cytoplasmic factories called virosomes. Poxvirus DNA replication has been suggested to proceed as follows. A nick is produced in the DNA at one or both telomeres which provides a free 3'-end for priming. This is followed by an elongation of the DNA chain by the virus encoded DNA polymerase. This results in the formation of an inverted repeat which, due to complementary base pairing, folds back on itself. The leading strand synthesis of DNA from the inverted repeat is thought to result in the formation of concatemeric intermediates which are resolved into mature DNA molecules and incorporated into virus particles at the late stage of infection (Beaud, 1995; Moss, 1996).

Virus assembly requires the early recruitment of cellular membranes from the intermediate compartment, between the endoplasmic reticulum and the Golgi stack, to the virosomes, where the membranes are modified by the gradual incorporation of viral proteins (Sodeik *et al.*, 1993). These membranes are initially crescent shaped and become spherical while acquiring granular material from the virosomes. The spherical particles are known as immature virions, which mature with the condensing of the nucleoprotein core to become intracellular mature virions (IMV). These particles have the characteristic brick morphology seen by electron microscopy and constitute the majority of virus particles produced in infected cells. Virions destined for extracellular release become wrapped by cisternae from the trans-Golgi network to form a double membrane (Schmelz *et al.*, 1994), and induce actin polymerisation, forming an actin tail which propels them to the cell surface, and aids in proficient cell to cell spread through the formation of virus-tipped microvilli (Cudmore *et al.*, 1995; Mathew *et al.*, 1998; Roper *et al.*, 1998; Wolffe *et al.*, 1998). Here, the outer double membrane fuses with the plasma membrane to release virus with an internal membrane and a Golgi-derived

external envelope, termed extracellular enveloped virus (EEV). IMV are released later by cell disruption. EEV are the minority of virions produced and are thought to be important in the cell to cell spread of infection (Blasco and Moss, 1992) and thus in *in vivo* dissemination (Payne, 1980). Both intracellular and extracellular enveloped particles have been demonstrated for myxoma virus by electron microscopy (Farrent and Fenner, 1953).

1.3 The evolutionary relationships between myxoma virus and the rabbit

The natural history of myxoma virus is well documented (Fenner and Ratcliffe, 1965; Fenner and Ross, 1994). This documentation includes the natural rabbit hosts, and the changes in virus virulence and host genetic resistance following the introduction of myxoma virus into a new genus of rabbit, namely the Australian wild European rabbit. When considering the pathogenesis of myxoma virus infection of *O. cuniculus*, this natural history can be used as a tool to ask questions about the important driving forces of host-virus coevolution, and the eventual outcomes of this evolution.

1.3.1 Evolution of myxoma virus

Myxomatosis was originally described in South America as a sporadic, highly lethal disease of laboratory rabbits (*O. cuniculus*). The disease was termed 'infectious myxomatosis of rabbits' due to the production of multiple mucinous cutaneous tumors (Sanarelli, 1898). The aetiological agent of myxomatosis was at that time said to be a member of the newly defined filterable viruses, and has since been shown to be the poxvirus, myxoma virus (Fenner, 1953). The sporadic and lethal nature of the disease in *O. cuniculus* implied that the virus could not be maintained in the European rabbit population, and therefore that this animal was not the natural host of the virus. Laboratory experiments demonstrated that the disease was highly specific for rabbits. Hence, the natural reservoir of the virus was sought in wild rabbit species native to the regions where outbreaks of the disease in *O. cuniculus* occurred (Fenner and Ratcliffe, 1965).

The natural host of the South American strain of myxoma virus was found to be the tropical forest rabbit (or tapeti), *Sylvilagus brasiliensis* (Aragao, 1943), which has a wide distribution in south and central America (Figure 1.3). In this rabbit species,

myxoma virus produces a skin tumor, or lesion, that remains localised to the inoculation site and acts as a source of virus for transmission (Fenner and Ratcliffe, 1965).

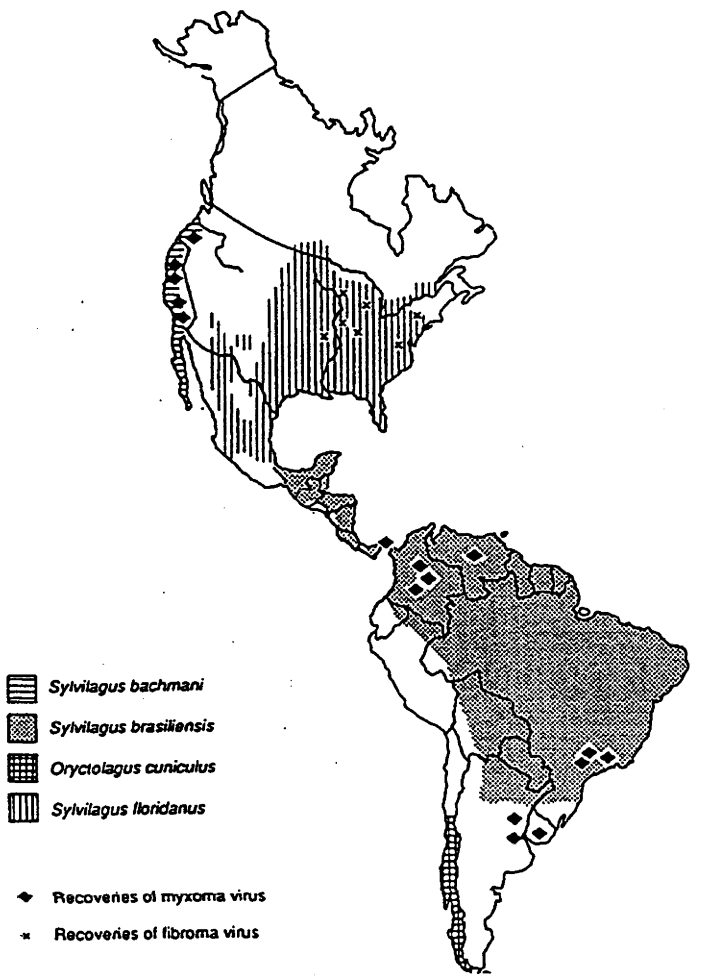

Figure 1.3: Map of the Americas showing the distribution of leporids significant in the natural history of myxomatosis (modified from Fenner, 1994c). *Sylvilagus brasiliensis* is the natural host of South American myxoma virus, *S. bachmani* the natural host of Californian myxoma virus and *S. floridanus* the natural host of Shope fibroma virus. Populations of *O.cuniculus* have been introduced into Chile.

Transmission of myxoma virus is mechanical (Aragao, 1943). It requires a biting arthropod, such as a mosquito or flea, to insert its mouthparts into the skin of a myxoma virus infected rabbit. Virus in the skin adheres to the mouthparts of the insect but does not replicate within the vector, and transmission occurs following the passive transfer of this virus to a susceptible rabbit while the arthropod vector feeds. The success rate of transmission correlates with the titre of virus in the skin of the infected rabbit (see section 1.5) (Day *et al.*, 1956; Fenner *et al.*, 1952; Fenner *et al.*, 1956).

Myxomatosis was unknown in North America until observed in the 1930s, again as sporadic outbreaks in domestic *O. cuniculus*. It was originally thought that these outbreaks were due to the importation of diseased laboratory rabbits from Mexico (Kessel *et al.*, 1931). It has since been demonstrated that myxoma virus is enzootic to the brush rabbit, *Sylvilagus bachmani,* which is distributed along the west coast of the United States (Figure 1.3) (Marshall and Regnery, 1960). The North American strains of myxoma virus are closely related, and antigenically similar, to the South American strains, and are known as the Californian strains. They too cause a benign skin fibroma which remains localised to the inoculation site following infection of *Sylvilagus bachmani* (Marshall *et al.*, 1963). However, while the Californian strains of myxoma virus are highly lethal to European rabbits, the clinical disease may differ considerably from that caused by the South American strains (Fenner and Ratcliffe, 1965).

Both the Californian and South American strains of myxoma virus are particularly adapted for transmission in their respective natural hosts. Following infection of *S. bachmani*, the Californian, but not the South American, strain of myxoma virus multiplies in the skin to a high enough titre for mosquito transmission (Marshall and Regnery, 1963). Infection of other North American *Sylvilagus* rabbit species with Californian myxoma virus results in the production of skin lesions but virus replication is insufficient for vector transmission (Regnery and Marshall, 1971). A similar specific relationship exists between South American strains of myxoma virus and *S. brasiliensis,* with the South American and not the Californian strains of myxoma virus able to replicate to high enough titres for mosquito transmission in this host. However, South American myxoma virus could be transmitted from three other North American species of rabbit, *S. auduboni*, *S. nuttallii* and *S. floridanus* (Regnery and Miller, 1972).

A third leporipoxvirus, Shope fibroma virus (or rabbit fibroma virus), is closely related to myxoma virus antigenically and genetically and is endemic to the eastern cottontail, *Sylvilagus floridanus* (Block *et al.*, 1985; Fenner, 1965; Shope, 1932; Shope, 1936). In its natural adult host, Shope fibroma virus causes a small fibroma at the inoculation site with no evidence of generalised disease (Shope, 1932). Infection of *O. cuniculus* with Shope fibroma virus also results in the production of a fibroma, but not a myxomatous lesion, at the primary inoculation site. Unlike myxoma virus, Shope fibroma virus does not disseminate from the primary lesion and is rapidly cleared by the host (Day *et al.*, 1956; Fenner and Ratcliffe, 1965).

1.3.2 The rabbit in Australia and the use of myxoma virus as a biological control agent

Domestic European rabbits *O. cuniculus*, arrived in Australia with the first fleet in 1788, but did not spread beyond the original settlements. Their successful colonisation of Australia followed the introduction of 24 wild English rabbits in 1859 at Geelong, Victoria, as well as later introductions at sites in South Australia. The clearance of property with the removal of trees, the introduction of domestic stock and the control of predators, all facilitated the establishment of rabbits (Myers *et al.*, 1994). Following these introductions, rabbits moved across Australia at an estimated rate of 100-300 km a year in one of the most dramatic mammal invasions ever recorded (Figure 1.4A). The greater proportion of the rabbits' present range was covered in just 60 years (Figure 1.4B), with the population of rabbits eventually reaching an estimated 600 million (Rolls, 1984).

Rabbits have contributed to a loss in Australian biodiversity, with the stripping and killing of seedling trees and perennial shrubs, massive soil erosion and vegetational changes, and through direct competition for food and burrow space with native mammal species (Myers *et al.*, 1994). In economic terms, rabbits are estimated to cost up to $300 million a year in lost agricultural production. Control methods have included poisoning, shooting and trapping, and the ripping and fumigation of warrens. These control methods alone are labour intensive, expensive, non-permanent, and are ineffective on a continent-wide scale.

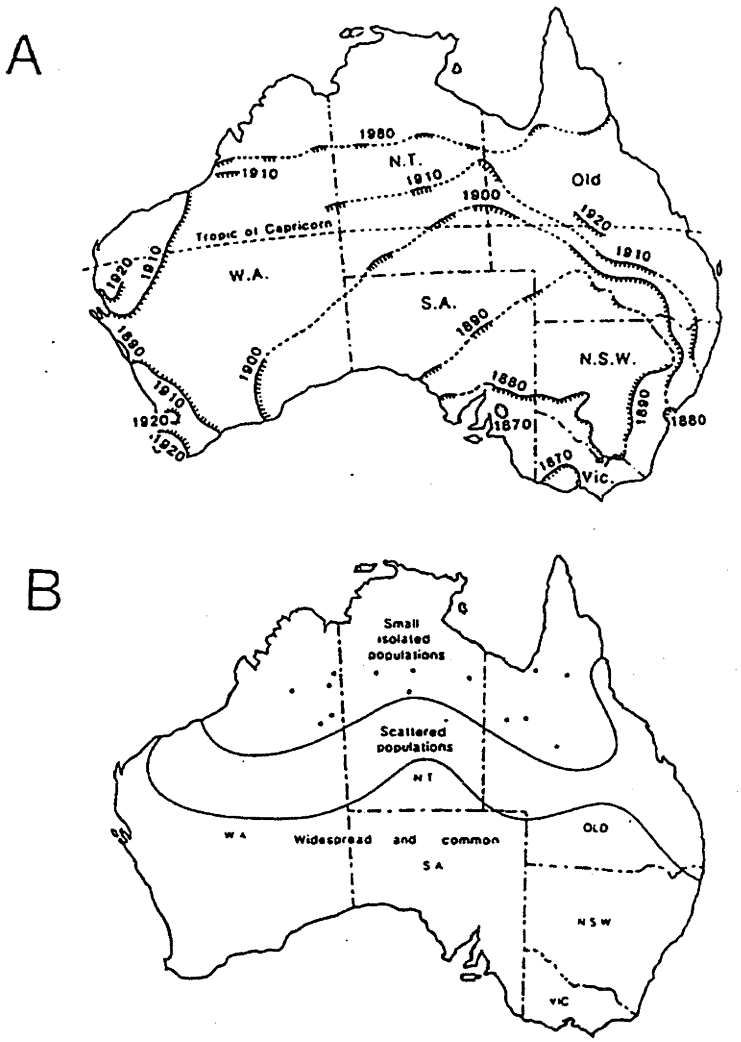

Figure 1.4: Spread of the rabbit over the mainland of Australia based on reports in newspapers and periodicals (from Stodart and Parer, 1988) (**A**) and map of the present known distribution of rabbits in mainland Australia (**B**) (Myers *et al.*, 1994).

The lethality of myxoma virus in the European rabbit suggested its use as a biological control agent for rabbits in Australia. Several trial releases of the Standard Laboratory Strain (SLS), a strain derived from a Brazilian isolate (Moses) (Moses, 1911), were conducted in the 1930s in both Australia and Europe. However, the virus appeared to remain localised to the warren at which it was released and die out after a few virus generations (Myers, 1954). In 1950, further releases of SLS in the Murray Valley of Victoria were thought to have been unsuccessful, but in the summer of 1950/51, during which time there was an explosion of the mosquito population, myxomatosis flared up near one of the abandoned trial sites and spread rapidly across south-eastern Australia (Ratcliffe *et al.*, 1952) (Figure 1.5). The natural spread of the virus was augmented by widely undertaken inoculation campaigns in the agricultural and pastoral lands of

southern Australia so that, by 1954, myxomatosis was disseminated throughout the geographic range of the rabbit in Australia (Fenner and Ratcliffe, 1965). Myxomatosis is now an enzootic disease of the Australian wild rabbit, with epizootics developing periodically in association with local and seasonal vector activity (Fenner and Ross, 1994), and the presence of susceptible rabbit kittens (Kerr and Best, 1998).

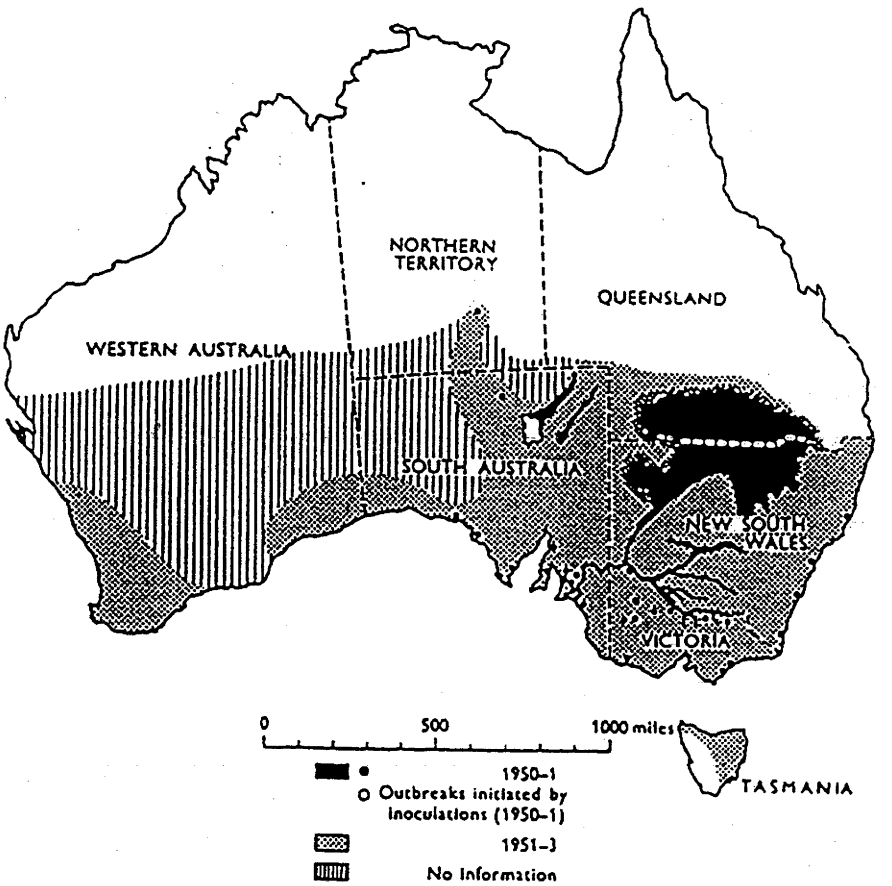

Figure 1.5: The spread of myxomatosis in Australia during the three years following its introduction in 1950 at an experimental site in northern Victoria. The major spread early in 1951 (dense black) occurred along the Murray-Darling-Murrumbidgee river system of south eastern Australia. By 1954, myxomatosis was widely disseminated throughout the distribution of the rabbit due to inoculation campaigns and the natural spread of the virus (Fenner and Ratcliffe, 1965).

1.3.3 Emergence of attenuated strains of myxoma virus in the Australian field

The case-mortality rate of rabbits during the initial Australian epidemic of myxomatosis in 1950/51 exceeded 99% and reduced many rabbit populations by greater than 90%. However, following the second summer epidemic in 1951/52, there was a greater

survival rate of infected rabbits, due to emergence of attenuated strains of the virus (Marshall and Fenner, 1958; Myers, 1954). Changes in virus virulence were monitored by the inoculation of laboratory European rabbits with field isolates collected during sequential annual epizootics. Isolates were grouped into five levels of virulence based on laboratory rabbit survival times and survival rates (Fenner and Marshall, 1957) (Table 1.2). Grade I viruses were the most virulent, killing essentially 100% of infected rabbits with an average survival time of less than 13 days. Grade V viruses were the least virulent, killing less than 50% of infected rabbits. From the testing of field isolates in this manner, it became apparent that within three years of successful myxoma virus release, the majority of myxoma virus field isolates were of grade III virulence, killing 70-95% of infected laboratory rabbits in 17-28 days (Marshall and Fenner, 1960) (Figure 1.6).

Table 1.2: Classification of strains of myxoma virus into grades of virulence based on mean survival time and case mortality rate of infected laboratory European rabbits (Fenner and Ratcliffe, 1965).

Virulence grade	Mean survival time (days)	Estimated case-mortality rate (%)
I	≤13	>99
II	13 - 16	95 - 99
III	17 - 28	70 - 95
IV	29 - 50	50 - 70
V	-	< 50

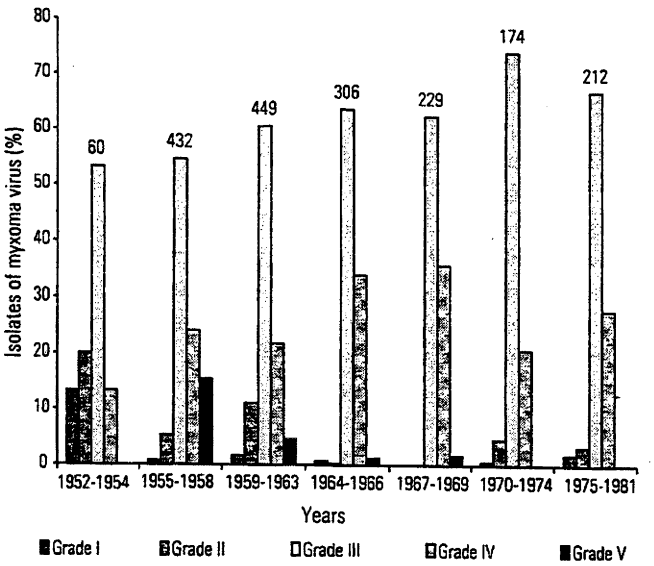

Figure 1.6: Virulence of Australian field strains recovered between 1952 and 1981. The number of isolates tested for each period is indicated, and expressed as a percentage. Virulence grades are shown in Table 1.2 (from Kerr and Best, 1998).

Transmission of myxoma virus is dependent on virus adhering to the mouthparts of arthropod vectors probing through the epidermis of infected rabbits and is most likely to occur when the virus titre in the skin exceeds 10^7 pock forming units per gram of skin (Day *et al.*, 1956; Fenner *et al.*, 1956). In an examination of the growth of viruses of varying virulence and their ability to be transmitted, grade I, III and IV viruses (grade II was not examined) replicated to sufficiently high titres in the skin to be transmissible on the mouthparts of mosquitoes (Fenner *et al.*, 1956) (Figure 1.7). In the case of grade I viruses, the infectious source was only available for a few days before the rabbit died whereas the life of the animal was prolonged during infection with grade III and IV viruses, thus providing a source of virus for a longer period. A highly attenuated grade V strain of myxoma virus, derived by serial intracerebral passage of virulent myxoma virus in rabbits (neuromyxoma) (Hurst, 1937b), did not multiply to high titre in the skin due to the ability of the host to rapidly control virus replication, and was poorly transmitted by mosquitoes. Thus, moderately attenuated viruses had the highest probability of being transmitted by arthropod vectors.

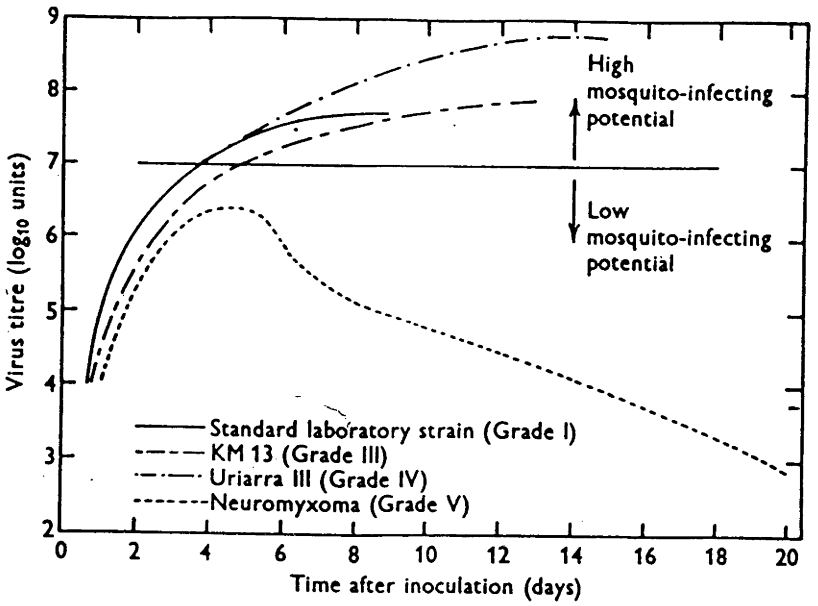

Figure 1.7: Relationship between titre of myxoma virus in primary skin lesions in *O. cuniculus* and the potential of the lesion as a source of virus for mechanical transmission by mosquitoes. Rabbits infected with virus strains of all virulence grades except grade V were highly infectious for mosquitoes. The period of availability of the infectious source was short following infection with highly virulent strains due to the rapid death of the animal. Moderately attenuated strains prolonged the life of the animal and thus produced lesions that were infectious for longer (from Fenner *et al.*, 1956).

1.3.4 Development of genetic resistance in the Australian wild rabbit population

Rapid selection for genetic resistance in the Australian wild rabbit population occurred following the emergence of attenuated strains of myxoma virus in the field. Development of genetic resistance may have been augmented by high ambient temperatures and a phenomenon known as the sire effect. This has been recently reviewed (Kerr and Best, 1998), and is discussed briefly later in this section.

The emergence of moderately attenuated strains of myxoma virus enabled approximately 10% of infected rabbits to survive in the field, and thus the rapid selection of genetic resistance. This was demonstrated by myxoma virus challenge experiments on seronegative rabbits collected from a field site at Lake Urana, New South Wales (Marshall and Douglas, 1961; Marshall and Fenner, 1958). Rabbits were captured prior to the annual/spring summer epidemic of myxomatosis from 1951, and challenged with a grade III strain of myxoma virus (KM13). This strain caused 88% and 89% mortality following infection of unselected wild and laboratory rabbits respectively. Following the first two myxomatosis epidemics, the case mortality rate of

rabbits from Lake Urana was unchanged. However, after the third epidemic, the mortality rate had dropped to 80%, and it dropped further to 50% and around 30% following the fourth and seventh epidemics respectively (Table 1.3). Interestingly, the severity of clinical symptoms in challenged rabbits was also reduced, with only 0-2% of rabbits said to have mild clinical symptoms after two epidemics, rising to 30% after seven epidemics. In the field, the animals with mild clinical symptoms are less likely to succumb to dietary and predatory pressures during the disease, and thus survive to pass on resistance genes to their offspring. Those females that recover will also provide maternal antibody to their offspring. There is some experimental evidence to suggest that this may aid survival of the young following challenge with myxoma virus (Fenner and Marshall, 1954).

Table 1.3: Case-mortality rates and severity of myxomatosis in groups of non-immune wild rabbits from Lake Urana, NSW, after successive epizootics of myxomatosis. Rabbits were challenged under standard laboratory conditions with the grade III myxoma virus, KM13 (from Fenner and Ratcliffe, 1965).

Number of epizootics to which population had been exposed	Case-mortality rate (%)	Clinical signs in challenged rabbits (%)		
		Severe (including fatal)	Moderate	Mild
0	90	93	5	2
2	88	95	5	0
3	80	93	5	2
4	50	61	26	12
5	53	75	14	11
7	30	54	16	30

In the laboratory, ambient temperature affects the severity of disease (Parker and Thompson, 1942). High ambient temperatures increased the survival rate of rabbits challenged with a moderately attenuated virus KM13a, whereas low ambient

temperatures decreased the survival rate (Marshall, 1959). Outbreaks of myxomatosis occur during the hot summer months. The high ambient temperatures at this time may increase the survival of rabbits infected with otherwise lethal strains of myxoma virus, perhaps by inhibiting virus replication (Marshall, 1959) and potentially contributing to selection of resistance (Kerr and Best, 1998). In support of this, seronegative rabbits taken from climatically hot areas of Australia were more genetically resistant to infection with highly virulent grade I strains of myxoma virus than rabbits taken from cooler regions (in Fenner and Ross, 1994).

Another factor that may be important in the enhanced survival of wild rabbits infected with myxoma virus is the sire effect. In an attempt to replicate the selection for genetic resistance in laboratory rabbits, male laboratory rabbits were challenged with strains of myxoma virus that differed in virulence. Rabbits surviving challenge were used as sires. Because the overall survival rate was very low and a small number of males could be used to impregnate a number of females, females were not challenged with virus. A response to selection for resistance was achieved, with an estimated heritability of 35-40%. The case mortality rate of the offspring was reduced from 90-95% in unselected rabbits to a minimum of around 80% after four generations (Sobey, 1969). In a reinterpretation of these data, resistance to infection was attributed to the transmission of some unknown factor from a sire that had recovered from myxoma virus infection to the dam. This factor conferred a temporary resistance to myxomatosis on the offspring that was not associated with maternal antibody (Sobey and Conolly, 1986; Williams and Moore, 1991). The risk of death of the progeny challenged with myxoma virus was reduced if kittens were born within seven months of infection of the sire and if the sire and progeny were challenged with the same strain of myxoma virus. The enhanced survival of kittens was termed the sire effect.

In areas of annual epidemics of myxomatosis, and following the emergence of attenuated strains of myxoma virus, most of the kittens born would be the progeny of males that had survived infection with myxoma virus. Thus, if the sire effect exists, it could contribute significantly to the apparent observed resistance in the field (Sobey and Conolly, 1986; Williams and Moore, 1991). However, analysis of this effect has been retrospective and the hypothesis has not been tested experimentally. If it is correct, the sire effect would have fundamental implications for the understanding of the biology of

infectious disease, especially in mammals with a short generation time (Kerr and Best, 1998).

1.4 Virus interactions with the host

The interactions of myxoma virus with the rabbit can be considered in terms of the rabbits' immune response to infection and the proteins produced by myxoma virus that modulate this response. The outcome of the interactions between the two will determine the pathogenesis of disease; whether the rabbit will control virus replication and recover from infection, or if virus replication proceeds unchecked, resulting in the animal's death. These interactions are further complicated by the level of genetic resistance of the rabbit. The pathogenesis of myxoma virus in the European rabbit, immune responses to poxviruses, immune modulation by myxoma virus and genetic resistance to virus infections are considered below.

1.4.1 Pathogenesis of myxoma virus in *O. cuniculus*

Infection of the European rabbit, *O. cuniculus*, with virulent myxoma virus results in severe, generalised disease and death. Detailed molecular and ecological studies have concentrated on either the Lausanne strain (isoalated from Brazil in 1949) or the Standard Laboratory Strain (SLS) of South American myxoma virus, or the natural variants derived after establishment of myxoma virus in wild rabbit populations of Australia and Europe. SLS (or Moses strain) is the original strain successfully released in Australia in 1950 (Fenner and Ratcliffe, 1965), and the strain utilised in the current study. It was originally recovered from a naturally infected laboratory rabbit in Rio de Janeiro in 1911 (Moses, 1911), and was subsequently maintained by passage in laboratory rabbits.

The pathogenesis of SLS following inoculation at the skin was originally studied by Fenner and Woodroofe (1953) (Figure 1.8). Virus replicates at the primary inoculation site in the skin to approximate titres of 10^8 rabbit ID_{50} units per gram of tissue, followed by replication in the regional lymph node to approximate titres of 10^7 rabbit ID_{50} units per gram. Rabbit ID_{50} is the dose of virus at which 50% of intradermally inoculated rabbits become infected. It is approximately equivalent to plaque forming units (pfu). Virus was present in the circulation after detection in the regional lymph node. This viraemia is associated with lymphoid cells as virus is not found free in the serum or

associated with red blood cells (RBC) (Fenner and Woodroofe, 1953). The virus then replicates to high titres in the testis and in distal sites in the skin and to lower titres in the lung, liver and spleen.

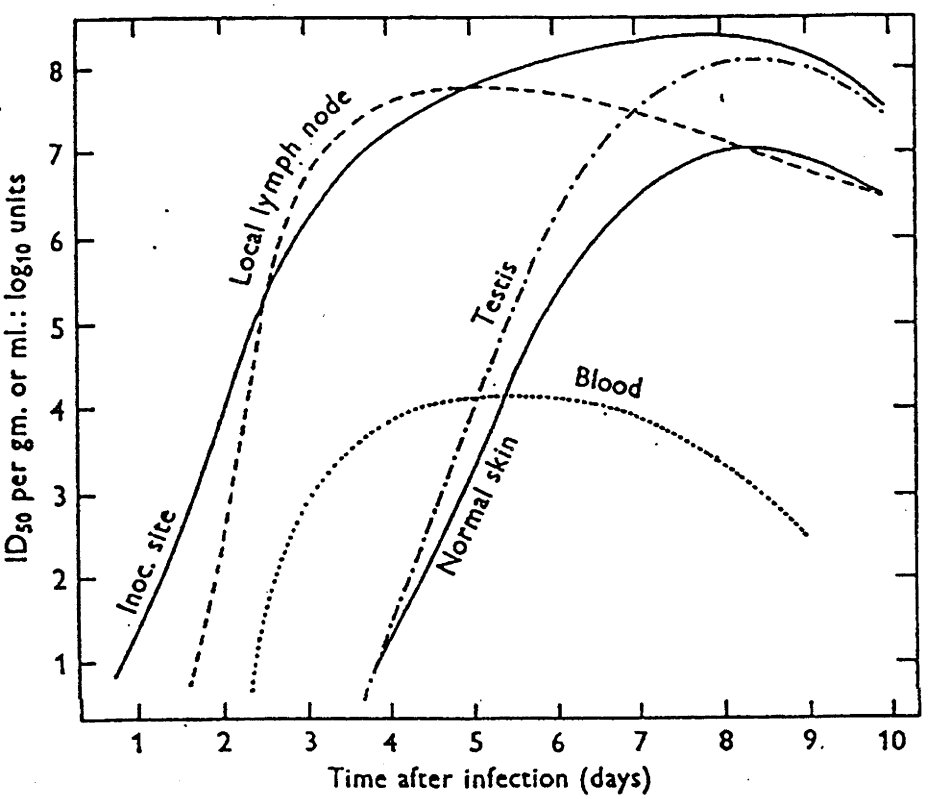

Lesions									
Inoculation site	O	+	++	+++	+++	++++	++++	+++++
Normal skin	O	O	O	O	+	++	++	++
Conjunctiva	O	O	O	±	+	++	+++	++++
Anogenital	O	O	O	O	+	++	++++	++++

Figure 1.8: The sequence of appearance and multiplication of SLS in various organs following intradermal inoculation. The times of appearance of clinical signs are indicated below the graph with an arbitrary grading of severity (± to +++++). Normal skin refers to a portion of uninoculated skin taken from the equivalent site to the inoculation site, but on the opposite side of the rabbit (Fenner and Ratcliffe, 1965).

Clinically, virus replication at the primary inoculation site results in a lump which appears on the third day after infection, and increases in size reaching a maximum of approximately 6cm in diameter on the eighth or ninth day. The lesion is at first purple

in colour and then becomes black in the centre. A secondary 'rash' which consists of lumps similar to the primary lesion but smaller, reaching approximately 2cm in diameter, appears on the sixth or seventh day. The lesions represent secondary sites of virus replication in the skin and are widely distributed over the body, being particularly obvious on the eyelids, ears and nose. The ears and eyelids become thickened, and there is an opalescent discharge from the eyelids which becomes copious and more turbid during the last two days before death. The perineum and scrotum of male rabbits becomes engorged through massive oedematous swelling, and respiration of rabbits becomes laboured (Fenner, 1994a). This is often accompanied by semipurulent nasal secretion due to secondary infection by *Pasteurella multocida* (Hobbs, 1928; Strayer *et al.*, 1983a; Strayer *et al.*, 1983b).

The cause of death of laboratory rabbits following infection with virulent myxoma virus is obscure. Death usually occurs within 10-12 days of infection. Hurst (1936a) described morbid changes in the histopathology of lymph nodes, the liver and to a lesser extent the lungs, through the proliferation, degeneration and necrosis of cells and blood vessels following infection with virulent myxoma virus. However, Mims (1964) could not attribute death to the growth of virus in a specific organ such as kidney, spleen, liver, lung or brain. Death is commonly attributed to secondary bacterial growth in the upper respiratory tract compromising the rabbits respiration (Hobbs, 1928; Strayer *et al.*, 1983a). However, rabbits infected with highly virulent Californian strains of myxoma virus often die before significant bacterial growth is evident (Marshall and Regnery, 1960)

1.4.2 The pathogenesis of ectromelia and vaccinia viruses in infected susceptible mice

Ectromelia virus is a naturally occurring poxvirus, genus *Orthopoxvirus*, of laboratory mice (Fenner, 1949). The infection of mice with ectromelia virus is a potentially important model in the consideration of the pathogenesis of, and genetic resistance to, myxoma virus infection of rabbits for a number of reasons. Firstly, the virus causes a natural infection of laboratory mice, and wild mice are a potential natural reservoir of the virus (Fenner, 1949). Secondly, the model of infection is the mouse. The availability of murine-specific monoclonal antibodies to cytokines and cell receptors, as well as inbred strains of mice that are susceptible or resistant to ectromelia virus

infection has greatly advanced the understanding of viral pathogenesis, host genetic resistance and host immune responses. Finally, the early events in ectromelia virus pathogenesis are similar to those known for myxoma virus infection of rabbits (Fenner and Woodroofe, 1953). Like myxoma virus, natural infection occurs at the skin, followed by replication at the primary inoculation site in the skin and in the regional lymph nodes in macrophages, endothelial cells and lymphoid cells. Primary viremia follows, with the infection of macrophages lining the sinusoids of the liver, replication, and the formation of infectious foci (Mims, 1959). The virus disseminates to secondary sites in the skin where it replicates and forms secondary lesions that give the name to the generalised infection of mousepox (Fenner, 1948a; Fenner, 1948b). However, the events that occur late in ectromelia virus infection of mice are different to myxoma virus-infection of rabbits. Ectromelia virus replication in the liver and spleen of infected mice is followed by extensive necrosis in these organs (Mims, 1964) that does not occur during myxoma virus infection of rabbits and which provides a potential cause of death.

Vaccinia virus is another important virus to consider in the study of myxoma virus. The animal model of vaccinia virus infection is again the mouse, and the importance of this virus both as the prototype poxvirus and as a widely used vaccine has meant that the immune responses to vaccinia virus have been extensively studied. Infection of immunocompetent mice with vaccinia virus results in an acute infection, with replication of virus to high titres in the ovary, and to a lesser extent in the skin, lung, spleen and brain (Ramshaw *et al.*, 1992). Unlike infection with ectromelia virus, immunocompetent mice recover from infection with vaccinia virus, and virus is cleared from tissues approximately 12 days after inoculation (Sharma *et al.*, 1996).

1.4.3 Host immune responses to virus infection with particular reference to poxviruses

The mammalian immune response to viral infection is comprised of two interlinked systems, namely the innate and adaptive immune systems. Innate immune responses such as natural killer (NK) cells, complement and cytokines such as interferons (IFN) and tumor necrosis factor (TNF) occur early in infection, are antigen non-specific, and act to limit the spread of virus prior to the induction of an antigen specific immune

response. The adaptive immune response involves the induction of antigen specific helper T-lymphocytes ($CD4^+$) which are important in the production of effector T lymphocytes ($CD8^+$, generated through a type 1 response) and antigen-specific antibody by B lymphocytes (generated through a type 2 response), and results in the generation of immunological memory (Janeway and Travers, 1994). The two systems are intimately linked as the innate immune response is thought crucial not only in the activation of the adaptive response, but in directing the immune response to a particular effector type (type 1 or type 2) (Medzhitov and Janeway, 1997).

The most general and simple models of type 1 or type 2 (T_H1 or T_H2) immune responses are characterised by the cytokine patterns produced by $CD4^+$ T-cells in response to activation (Abbas *et al.*, 1996); T_H1 $CD4^+$ cells secrete IFN^γ, IL-2, IL-12 and TNF^α; T_H2 cells secrete IL-4, IL-5, IL-6, IL-9, IL-10 and IL-13 (Baumgarth and Kelso, 1997). These cytokines have both direct and indirect effects on virus replication. The type 1 cytokine IFN^γ directly suppresses vaccinia virus replication. IFN^γ is also required for the direct anti-viral activity of $CD8^+$ T-cells (Ruby, 1997; Ruby and Ramshaw, 1991). IL-2 has antiviral effects, but also acts indirectly through the attraction and stimulation of NK cells to produce IFN^γ (Karupiah *et al.*, 1990a; 1990b; Karupiah *et al.*, 1993a; 1993b; Kohonen-Corish *et al.*, 1990). Like IFN^γ, TNF^α has a direct effect on vaccinia virus replication as its anti-viral effects are not dependant on the recruitment or enhancement of other cell types or responses (Sambhi *et al.*, 1991). Both the TNF type I (p55) and II (p75) receptors are involved in the antiviral effects of TNF^α (Sambhi *et al.*, 1991), although membrane-bound TNF, which has a higher affinity for TNFR2/p75, may be more important in immunity to poxviruses than soluble TNF (Ramshaw *et al.*, 1997).

In addition to the antiviral effects of the cytokines they produce, $CD4^+$ T-cells are required for the generation of optimal cytotoxic T-lymphocyte (CTL) responses to viral infection (Mizuochi *et al.*, 1989). In ectromelia virus-infected mice, $CD8^+$ CTLs are crucial for clearance of ectromelia virus from internal organs (Karupiah *et al.*, 1996). $CD4^+$ T cells are also thought to contribute directly to viral clearance since in $CD4^+$ T cell-knock out mice, although anti-viral $CD8^+$ CTL were generated, they were insufficient to clear ectromelia virus (Karupiah *et al.*, 1996) or herpes simplex virus (Nash *et al.*, 1987) from the skin. Therefore, the mechanisms of control of virus

replication and the relative roles of $CD4^+$ and $CD8^+$ T-cells appear to differ at the skin compared to the internal organs.

The role of $CD8^+$ T-cells in mice infected with vaccinia virus appears to be less crucial than during ectromelia virus infection as infection of $CD8^+$ T-cell-deficient mice with high doses of vaccinia virus resulted in 100% survival (Spriggs *et al.*, 1992a). It is thought that mice lacking $CD8^+$ T cell activity may have sufficient compensatory mechanisms for the clearance of some non-virulent (e.g. vaccinia virus) but not highly virulent (e.g. ectromelia virus) infections (Raulet, 1994), such as the increased production of IFN^{γ} (Karupiah *et al.*, 1996; Ramshaw *et al.*, 1997).

Antibody production specific to poxviruses has been demonstrated to be important in immunity to reinfection, and may be important in restricting virus dissemination within the host. However, antibody production is generally not thought to be crucial to recovery from infection (reviewed in Buller and Palumbo, 1991). Infection of rabbits with the attenuated neuromyxoma strain of myxoma virus results in the detection of anti-viral antibody in the serum later than after infection with highly virulent myxoma virus (Fenner *et al.*, 1953; Fenner and Woodroofe, 1953), suggesting that antibody is not essential for controlling myxoma virus infection. However, mice with an impaired ability to generate antiviral antibody responses develop higher virus titres following infection with vaccinia virus (Ramsay *et al.*, 1994) and can be lethally infected with ectromelia virus (in Ramshaw *et al.*, 1997). Thus the generation of virus-specific antibody may have some role in the recovery from poxvirus infections.

1.4.4 Immune modulation by myxoma virus

Immune modulation by the large DNA viruses, including poxviruses, adenoviruses and herpesviruses, has been extensively and comprehensively reviewed (Buller and Palumbo, 1991; Cuff and Ruby, 1996; Gillet and Brun, 1996; Gooding, 1992; McFadden, 1995; McFadden and Graham, 1994; McFadden *et al.*, 1995; McFadden and Kane, 1994; McNair and Kerr, 1992; Smith, 1993; Smith, 1994; Smith *et al.*, 1997b; Spriggs, 1994; Traktman, 1990a; Turner and Moyer, 1990). Each family of viruses employs different strategies of host immune modulation. Poxviruses encode numerous proteins that function to modulate immune responses including inflammation, apoptosis of infected cells, fever, and potential antigen presentation/ recognition. The proteins

known to be produced by myxoma virus are summarised in Figure 1.9 and detailed below.

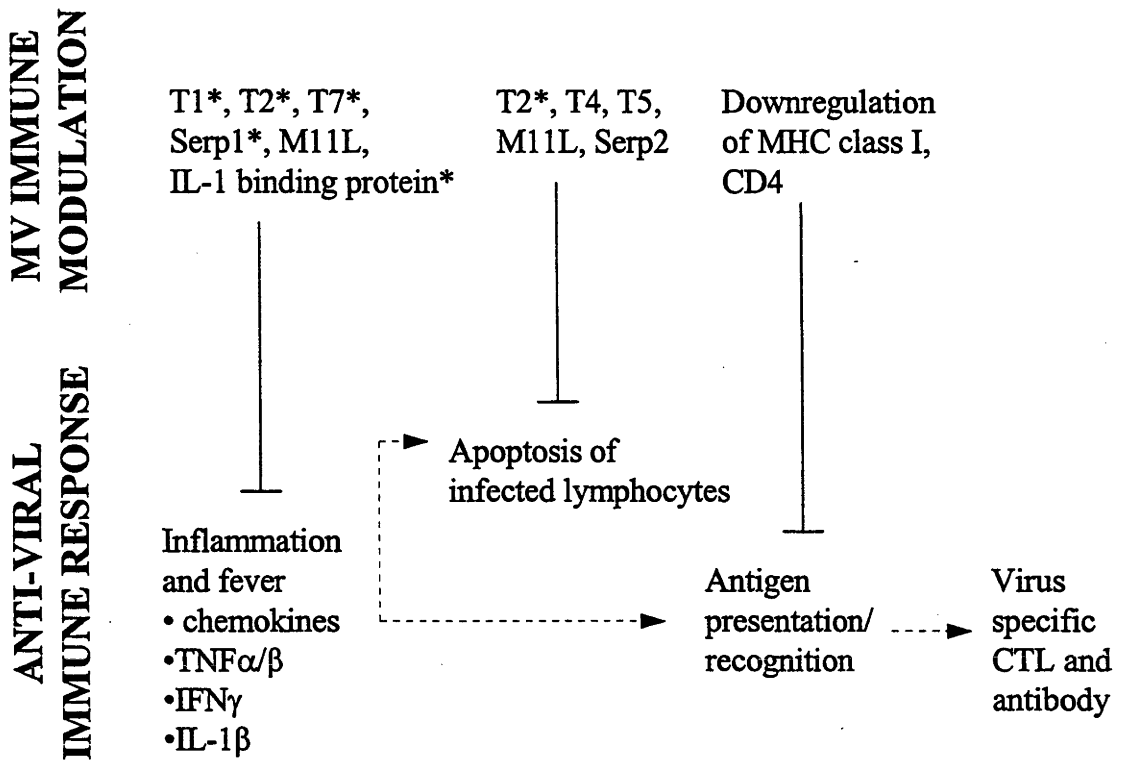

Figure 1.9: Flow diagram of the known interactions between the anti-viral immune response and myxoma virus immunomodulation. At least nine myxoma virus produced proteins are known to specifically inhibit components of the anti-viral immune response. * indicates proteins that are secreted from myxoma virus infected cells. All remaining myxoma virus immunomodulatory proteins act intracellularly except M11L which is a transmembrane protein.

The first identified immunomodulatory protein produced by myxoma virus was M-T2. M-T2 is a secreted, species-specific viral homolog of the rabbit TNF$^{\alpha}$ receptor (Schreiber and McFadden, 1994; Upton *et al.*, 1991), capable of binding and inhibiting the cytolytic activity of rabbit TNF$^{\alpha}$ and $^{\beta}$ *in vitro*. M-T2 has amino acid sequence homology with the TNFR (tumor necrosis factor receptor) superfamily, including the p55 and p75 TNF receptors, Fas, CD40, CD30 and the lymphotoxin $^{\beta}$ receptor. The N-terminal region of M-T2 contains four cysteine-rich domain motifs that are present in the ligand binding domain of TNFR superfamily members, three of which are required for the binding of M-T2 to rabbit TNF$^{\alpha}$. M-T2 binds rabbit TNF$^{\alpha}$ with an affinity similar to the mammalian TNF receptors (Schreiber and McFadden, 1994) and is

thought to prevent TNF$^{\alpha}$ produced in response to virus infection from reaching its target cells, and to prevent direct cytolysis of infected cells *in vivo*. M-T2 deletion mutants of myxoma virus are attenuated in the European rabbit (Upton *et al.*, 1991).

An intracellular form of M-T2 is also able to inhibit apoptosis of myxoma virus infected RL-5 cells, a rabbit CD4^{+} T-cell line (Macen *et al.*, 1996b). Truncated versions of M-T2, that cannot bind or inhibit TNF$^{\alpha}$, are still able to inhibit apoptosis of infected T cells (Schreiber *et al.*, 1997). These two functions of the protein are therefore distinct.

The M-T7 protein, the most abundantly secreted protein from myxoma virus infected cells, is highly homologous to the ligand binding domain of human and murine IFN$^{\gamma}$ receptors. M-T7 binds and inhibits the activity of rabbit IFN$^{\gamma}$ *in vitro* (Mossman *et al.*, 1995a; Upton *et al.*, 1992) and is thought to bind and sequester IFN$^{\gamma}$ *in vivo,* thus preventing it from reaching and signalling target cells. Inoculation of European rabbits with a recombinant myxoma virus in which the M-T7 genes have been disrupted (M-T7^{-}), results in an attenuated disease characterised by an increased inflammatory response at sites of infection and increased cellular activation in secondary lymphoid organs (Mossman *et al.*, 1996b). Thus, M-T7 is likely to be important in the blockade of early inflammatory cell migration into sites of viral replication as well as interrupting the signalling between immune cells in secondary lymphoid organs and thus the generation of adaptive immune responses.

In addition to binding IFN$^{\gamma}$, M-T7 also binds chemokines, and so like M-T2, appears to have a dual function. Chemokines are chemotactic cytokines involved in the regulation of inflammatory responses to infection (Baggiolini, 1998; Schall and Bacon, 1994) and are thought to be important in the early inflammatory responses to viruses (Cook *et al.*, 1995) . Chemokines can be divided into three subfamilies, designated CXC (or $^{\alpha}$ chemokines), CC (or $^{\beta}$ chemokines) and C, based on the position of conserved cysteine residues within the polypeptide (Schall, 1994). M-T7 binds the C-terminal heparin-binding domain of members of all three subfamilies of chemokines *in vitro* (Lalani *et al.*, 1997). It is postulated that M-T7 disrupts chemokine gradients and thus disregulates inflammatory cell migration into sites of virus infection.

M-T1 is a secreted protein, unrelated to any known receptor species, which also binds members of the CC and CXC chemokine subfamilies *in vitro* (Graham *et al.*, 1997),

although it only inhibits the *in vitro* chemotaxis of monocytes mediated by CC chemokines (Lalani *et al.*, 1998). *In vivo,* M-T1 is thought to contribute to virus virulence by inhibiting leucocyte infiltration into sites of infection, although deletion of this gene from myxoma virus does not attenuate the disease *in vivo* (Lalani *et al.*, 1998), and the deletion of the equivalent protein in rabbitpox virus (a derivative of vaccinia virus which is lethal for rabbits) did not reduce the mortality rate following infection of rabbits (Graham *et al.*, 1997).

The myxoma virus M-T5 protein is an intracellular, non-membrane-associated member of the poxviral superfamily of designated host range proteins, which determine tissue or cell type specificity rather than species specificity (Mossman *et al.*, 1996a). Infection of both primary lymphocytes and a rabbit $CD4^+$ T cell line (RL5) with a myxoma virus M-$T5^-$ mutant resulted in the complete shut down of both virus and host cell protein synthesis and the induction of apoptosis. Apoptosis did not occur following infection of adherent monocytes or primary fibroblast cell cultures. Infection of laboratory European rabbits with M-$T5^-$ resulted in an attenuated disease, with no clinical signs beyond the formation of a lesion at the inoculation site. It was concluded that M-$T5^-$ myxoma virus was incapable of disseminating past the primary inoculation site to secondary sites due to a rapid apoptotic response in infected lymphocytes and an effective inflammatory reaction at the inoculation site (Mossman *et al.*, 1996a).

The M-T4 protein contains a C-terminal endoplasmic reticulum (ER) retention sequence, -RDEL (Arg, Asp, Glut, Leu), and co-localises with calreticulin specifically to the ER of infected cells. M-T4 is synthesised early in infection and is necessary for the inhibition of apoptosis in infected lymphocytes *in vitro*; its disruption attenuates the virus *in vivo* (Barry *et al.*, 1997). Similar to M-T5, M-T4 is thought to be required for the productive infection of lymphocytes *in vivo,* with its disruption resulting in the virus being incapable of disseminating past the site of primary inoculation to secondary sites. However, unlike M-T5, M-T4 does not function by preventing the arrest of viral and host cell protein synthesis following infection of lymphocytes (Barry *et al.*, 1997).

Myxoma virus encodes at least two proteins belonging to the serine protease inhibitor (serpin) superfamily. Serine proteases regulate complex proteinase-dependent pathways, including the activation of cytokines during the inflammatory response to infection, the complement pathway (Potempa *et al.*, 1994), and apoptosis (Sarin *et al.*,

1993). Serp1 is a myxoma virus encoded, glycosylated, secreted serpin that interferes with the early inflammatory response to virus infection and its deletion results in attenuation of disease in the European rabbit. (Macen *et al.*, 1993; Upton *et al.*, 1990). Further, purified Serp1 is anti-inflammatory in rabbit atherosclerosis models (Lucas *et al.*, 1996; Maksymowych *et al.*, 1996). Serp1 is capable of functionally inhibiting the human fibrinolytic enzymes plasmin, urokinase and tissue plasminogen activator *in vitro* (Lomas *et al.*, 1993). The biological target of Serp1 in rabbits is currently unknown.

Serp2, a second serpin encoded by myxoma virus, is an intracellular protein with significant homology to cowpox CrmA protein (Petit *et al.*, 1996). CrmA inhibits human interleukin-1β converting enzyme (ICE) (Komiyama *et al.*, 1994) and is capable of inhibiting apoptosis by a variety of inducers (e.g. TNF, serum deprivation, Fas) (Gagliardini *et al.*, 1994). Similarly, Serp2 inhibits ICE, albeit not as strongly as CrmA, and inhibits granzyme B (Turner and Moyer, 1998). The vaccinia virus serpin, SPI-2, also inhibits ICE and the induction of TNF- and Fas- mediated apoptosis of infected cells (Kettle *et al.*, 1997). However, despite 93% amino acid identity between CrmA and rabbitpox SPI-2 and the ability of both to inhibit ICE *in vitro* in a similar fashion, the latter is not functionally equivalent to CrmA and is not as effective in inhibiting apoptosis of infected cells (Macen *et al.*, 1998). Thus, Serp2 of myxoma virus is a likely candidate for an inhibitor of ICE-mediated and granzyme B-mediated apoptosis of myxoma virus infected cells, but is not likely to be the only protein responsible for such inhibition in any single cell type.

The M11L protein is a type II transmembrane protein produced early in infection, which is important for the *in vivo* inhibition of inflammation by myxoma virus (Opgenorth *et al.*, 1992, Graham, 1992) and the inhibition of apoptosis of infected lymphocytes (Macen *et al.*, 1996b). M11L does not have sequence homology with any known protein, or contain motifs that might enable prediction of a biochemical function, and the mechanisms by which it functions in either process remain to be characterised. Disruption of M11L results in induction of apoptosis in infected RL-5 cells which significantly reduces the yield of progeny virus compared to infection with the wild type virus (Macen *et al.*, 1996b).

The presence of multiple inhibitors of lymphocyte apoptosis suggests that inhibition of apoptosis in these cells during viral infection is important to virus pathogenesis and may involve components of more than one cell death pathway. The inhibition of apoptosis of infected lymphocytes by myxoma virus, either through the inhibition of CTL-mediated killing (Fas and granzyme B), the direct effects of TNF, or the prevention of the arrest of protein synthesis by the host cell, prolongs the time available for the production of infectious progeny (Turner and Moyer, 1998). However, the induction of apoptosis by virus can also be advantageous, through the spread of virus and the infection of phagocytic cells (McFadden and Barry, 1998) or the suppression of immune function. At this stage, only poxvirus-encoded inhibitors of apoptosis are known, although poxviral proteins which function as inducers of apoptosis may also exist (Cuff and Ruby, 1996; McFadden and Barry, 1998)

Myxoma virus also produces a growth factor (myxoma growth factor or MGF) that displays significant homology to, and is thought to mimic the activity of, epidermal growth factor (EGF) and transforming growth factor-α (TGFα) (Upton *et al.*, 1987). Deletion of MGF results in virus attenuation *in vivo* (Opgenorth *et al.*, 1992), and virus virulence can be restored by the insertion of either VGF (vaccinia growth factor) or rat TGFα, implying that MGF is a functional growth factor (Opgenorth *et al.*, 1993). Putative biological EGF-like qualities have been demonstrated for MGF *in vitro* (Lin *et al.*, 1991), suggesting that virus-encoded growth factors are capable of competitively binding cellular growth factor receptors (Strayer and Leibowitz, 1987b) such as EGF and inappropriately stimulating cell growth.

Myxoma virus also encodes an uncharacterised IL-1β binding protein (McFadden and Graham, 1994); the role it has in virus virulence *in vivo* has not been examined. However, IL-1β, and consequently the induction of fever in response to infection, has been shown to be inhibited by the production of a secreted IL-1β binding protein by particular strains of vaccinia virus in mice (Alcami and Smith, 1992; Spriggs *et al.*, 1992b). The inclusion of an IL-1β binding protein in vaccinia virus strains attenuates these viruses, presumably due to the adverse effects the induction of endogenous pyrogens involved in fever have on the host (Alcami and Smith, 1996).

Myxoma virus also modulates the immune response by affecting immune recognition. MHC class I molecules are specifically downregulated on the surface of infected cells,

potentially inhibiting the recognition of infected cells by CTLs. This downregulation, which appears to be modulated by one or more late gene products, exceeds that achieved by complete blockage of host gene expression, and must therefore involve the masking or removal of preexisting MHC class I from the cell surface (Boshkov *et al.*, 1992). The downregulation of MHC class I on infected cells should stimulate NK cell activity, although the binding of IFN$^{\gamma}$ by secreted M-T7 may also downregulate NK cell activity. CD4 molecules are also specifically downregulated on the surface of infected T-lymphocytes and are degraded in lysosomal vesicles (Barry *et al.*, 1995). This potentially results in the inhibition of recognition of these cells by antigen presenting cells (APCs) or B-cells, thus affecting activation of T-cells and potentially the generation of cellular and humoral immune responses.

Proteins that modulate both the innate and adaptive immune responses are encoded by many other poxviruses. Cowpox, ectromelia and vaccinia viruses all produce complement control proteins which block the activity of complement through both the classical and alternate pathways (Kotwal and Moss, 1988; Miller *et al.*, 1997; Smith, 1993). Inhibitors of apoptosis in infected cells are produced by cowpox, rabbitpox, vaccinia, and variola viruses (Cuff and Ruby, 1996). Orf virus encodes an IL-10 homolog, a cytokine which has inhibitory effects both on the innate and T_H1 responses to infection (Fleming *et al.*, 1997). Both chemokine homologs and chemokine receptor-like proteins are produced by poxviruses, including molluscum contagiousum virus (Bugert *et al.*, 1998), swinepox virus (Massung *et al.*, 1993), capripox (Cao *et al.*, 1995), raccoonpox, camelpox, Shope fibroma and vaccinia viruses (Alcami *et al.*, 1998; Graham *et al.*, 1997; Smith *et al.*, 1997a) and variola and cowpox viruses (Smith *et al.*, 1997a). Encoded TNF receptor homologs have been identified from vaccinia virus, cowpox and variola viruses (Howard *et al.*, 1991; Hu *et al.*, 1994; Loparev *et al.*, 1998; Smith *et al.*, 1996). At least four proteins are produced by poxviruses that interfere with the action of IFN $^{\alpha/\beta}$ (Smith *et al.*, 1998). These include soluble IFN receptor homologs produced by vaccinia virus, swinepox, variola, cowpox and ectromelia viruses (Alcami and Smith, 1995; Mossman *et al.*, 1995b), and intracellular IFN inhibitors, of which two separate proteins are produced by vaccinia virus (reviewed in Smith *et al.*, 1998; Smith *et al.*, 1997). A soluble tanapox protein binds IFN$^{\gamma}$, IL-2 and IL-5, although the gene has not been identified (Essani *et al.*, 1994). The study of the proteins encoded by poxviruses is continually revealing new and novel strategies of

virus-induced immune modulation, and further sequencing may identify additional proteins in myxoma virus that interfere with the immune response.

1.4.5 Immunosuppression and malignant rabbit fibroma virus

Malignant rabbit fibroma virus is a recombinant between myxoma virus and the closely related Shope fibroma virus. The malignant rabbit virus genome is essentially derived from myxoma virus, with 4kb and 7kb of Shope fibroma virus sequence inserted within the left and right terminus respectively (Block *et al.*, 1985). Infection of the European rabbit with malignant rabbit virus results in a generalised disease characterised by the development of widespread lesions on the ears, face and body, and secondary bacterial infection of the respiratory tract, followed by death in 12-14 days (Strayer *et al.*, 1983a). Infection also results in severe immunosupression as measured by the inability of splenocytes from infected rabbits to proliferate in response to stimulation with mitogen (Strayer *et al.*, 1983b).

Malignant rabbit virus is closely related to myxoma virus and has been used to study the immune responses of *O. cuniculus* to poxvirus infection. In particular, the interactions between malignant rabbit virus and rabbit splenocytes have been extensively examined. Strayer *et al.* (1983b) found that lymphocytes from infected rabbits at 7dpi were suppressed in their ability to proliferate in response to stimulation with either Concanavalin A (Con A) or anti-immunoglobulin (Ig). This suppression was replicated following the *in vitro* infection of lymphocytes from uninfected rabbits with virus. The generation of antibody to sheep red blood cells by rabbits was suppressed following infection with malignant rabbit virus, although antibody responses that had been established prior to virus infection were not affected (Strayer *et al.*, 1983b). Despite the suppressed antibody responses to an unrelated antigen, rabbits developed strong neutralising antibody titres to malignant rabbit virus before death (Strayer and Leibowitz, 1987a). The ability of malignant rabbit virus-infected lymphocytes to produce and respond to IL-1 *in vitro* was unaffected, although these cells had a reduced capacity to produce IL-2 or respond to the exogenous addition of IL-2 despite the normal expression of the IL-2 receptor (Strayer *et al.*, 1986). Lymphocytes from virus-infected rabbits recovered the ability to respond to mitogen by 11dpi (Strayer *et al.*, 1983b). Despite this recovery in immune responsiveness, malignant rabbit virus infected-rabbits died by two weeks post infection.

The mechanism of malignant rabbit virus-induced immunosuppression is thought to result from two events. Firstly, the suppression of lymphoproliferation is thought to be a function of the ability of virus to replicate in lymphocytes. Shope fibroma virus is unable to replicate in lymphocytes (Strayer, Skaletsky, and Leibowitz, 1985). However, recombinant Shope fibroma virus that contained fragments of malignant rabbit virus DNA were capable of replicating in lymphocytes. These same viruses also induced a similar suppression of lymphoproliferation in response to mitogen as that induced by infection with malignant rabbit virus (Strayer *et al.*, 1990).

The second event involved in suppression of proliferative responses of lymphocytes is thought to be more indirect than virus replication in lymphocytes. Cell supernatants from splenocytes or RL-5 cells infected with ultraviolet (UV)-inactivated malignant rabbit virus suppressed lymphoproliferation and antibody responses of uninfected cells (Strayer *et al.*, 1988). It was proposed that a soluble factor generated from infected cells, termed virus induced suppressive factor or VISF, activated T-suppressor cells which then suppressed the ability of uninfected splenocytes to proliferate, presumably through cytokine production (Strayer and Dombrowski, 1988). The suppressive function of VISF could be reversed by mixing splenocytes or splenocyte supernatants taken from malignant rabbit virus-infected rabbits at 7dpi and 11dpi (Strayer and Leibowitz, 1986). This reversal was attributed to the generation of a second factor, termed anti-suppressor factor or ASF, produced by uninfected splenic T cells by 11dpi (Strayer and Dombrowski, 1988). ASF is postulated to restore proliferative responses by antagonising VISF, and provide resistance to these cells from the suppressive effects of VISF, thus explaining the recovery of immune function at 11dpi. However, neither of these factors have been purified or characterised.

Myxoma virus is commonly described as being immunosuppressive and the discovery of at least nine virus-encoded proteins that potentially modulate the immune response suggests that this is the case. However, there has been no examination of *in vivo* immune responses of laboratory rabbits following infection with myxoma virus to determine if a functional suppression of the cellular or humoral responses occurs.

1.4.6 Genetic resistance to virus infections

The mechanisms for genetic resistance of a host to a virus can be manifested either at the cellular level, through the ability of the cell to produce infectious progeny, or at the level of the host immune response. Genetic resistance to flavivirus infection, for example, is manifested at the level of the cell. Cell cultures from mice resistant to flavivirus infection, both laboratory and wild, produce lower yields of virus than cultures from susceptible mice (Webster and Johnson, 1941) through the inhibition of production of progeny virion RNA (Brinton, 1981). In contrast, resistance of mice to influenza virus is not dependant on cell permissivity, but rather correlates with genetic sensitivity of cells to IFN (Haller *et al.*, 1980).

Genetic resistance to ectromelia virus infection has been studied using inbred strains of mice and appears to be linked to the immune response to infection. Most strains of mice, such as A and A/J (both of MHC haplotype H-2^a) and BALB/c and DBA (both of MHC haplotype H-2^d), are highly susceptible to ectromelia virus infection. However, the mouse strains C57BL/6 (B6) and C57BL/10 (both of MHC haplotype H-2^b), are resistant (O'Neill, 1991; Wallace *et al.*, 1985). In susceptible mice (BALB/c), death occurs by 6-7 days post infection due to disseminated infection to the liver and spleen and consequent necrosis of these organs. In genetically resistant strains, virus spread is slower with lower titres of virus in the liver and spleen (Brownstein *et al.*, 1993), causing minimal, non-fatal lesions (Buller and Palumbo, 1991). Resistant mice infected with ectromelia virus produce high levels of the type 1 cytokines, IL-2, IL-12 and TNF$^{\alpha}$, whereas these cytokines are produced at low levels following infection of susceptible mice (in Ramshaw *et al.*, 1997). Virus specific precursor CTLs accumulate in the regional lymph node earlier in resistant than susceptible mice (O'Neill and Brenan, 1987), and strong antiviral CTL responses are generated in resistant mice which are delayed and weak in susceptible mice (in Ramshaw *et al.*, 1997). However, studies with C57BL mice indicate that resistance is operative as indicated by controlled virus replication, before the generation of virus specific CTLs (O'Neill and Blanden, 1983).

Resistance to ectromelia virus infection is controlled by multiple, unlinked, autosomal dominant genes (Brownstein *et al.*, 1989; Brownstein *et al.*, 1992) that map to chromosomes 6 (*Rmp1*) (Delano and Brownstein, 1995; Wallace *et al.*, 1985), 2 (*Rmp2*) (Brownstein *et al.*, 1992; Brownstein *et al.*, 1991) and 17 (*Rmp3*) (Brownstein *et al.*, 1991; O'Neill, 1991). *Rmp1* (resistance to mousepox) is a member of the NK gene

complex, adjacent to the *Prp* (proline-rich protein) locus. Resistance is expressed through a cell with an NK cell phenotype since infection of mice bearing the *Rmp1* resistant locus but depleted of $NK1.1^+$ cells with monoclonal antibody results in increased susceptibility (Delano and Brownstein, 1995). The NK gene complex in mice is also important in genetic resistance to cytomegalovirus (CMV) (Scalzo *et al.*, 1992) suggesting that NK cell activity is important in resistance against two unrelated DNA viruses (Delano and Brownstein, 1995).

The development of genetic resistance of European rabbits to myxoma virus in the field is well documented. However, unlike ectromelia virus infection of mice, nothing is known about the mechanisms of genetic resistance to myxoma virus in wild rabbits.

1.5 Summary and aims of this study

The study of immunological responses of rabbits to a virus infection is difficult as there are no inbred lines of rabbits available. There is substantial variation between individuals, which increases the number of animals required to achieve statistical significance. Unlike the current situation for mice, there are few immunological reagents specific for rabbits, rendering the study of specific components of immune responses difficult. However, we have in Australia the rare opportunity to study the pathogenesis of a virus evolving in a new host. The availability of the original virus strain that was released into Australia and natural attenuated variants, as well as populations of both genetically susceptible and resistant rabbits, which have been selected for by natural infection with the virus, is unique. This makes the myxoma virus/ European rabbit model an important one for the study of host-virus interactions, both in terms of biological control and in terms of emerging diseases.

Since the early studies on myxoma virus in the Australian wild rabbit population documenting changes in viral virulence and the development of genetic resistance in the host population, we have a greatly increased understanding of the viral genes required for propagation in the host, the role individual cell subsets and cytokines have in recovery from poxvirus infections, and the mechanisms involved in genetic resistance to a natural poxvirus infection. However, we have a limited understanding of myxoma virus pathogenesis and what factors are important in determining whether a susceptible rabbit will control virus replication and survive infection with virulent or attenuated

forms of myxomatosis. Further, nothing is known about the mechanism of genetic resistance to myxomatosis, and what factors are important in the control of virus replication by infected wild rabbits.

The experimental infection of genetically susceptible and resistant rabbits with virulent and attenuated strains of myxoma virus can be used to investigate important factors contributing to the pathogenesis of myxoma virus that have been previously obscured by the overwhelming lethality of the laboratory strains of myxoma virus in laboratory rabbits. The objective of this study is to use such experimental infections to develop a model of myxoma virus pathogenesis in the European rabbit and conceptualise host-virus coevolution by addressing the following questions. Firstly, does myxoma virus cause suppression of cellular and humoral immune responses in infected laboratory rabbits, similar to that caused following infection of rabbits with malignant rabbit virus, and is the ability to suppress immune responses dependent on virus virulence? This is addressed in Chapter 2. Secondly, where and when does control of virus replication occur in laboratory rabbits infected with attenuated myxoma virus, or in wild rabbits infected with virulent myxoma virus (addressed in Chapter 3)? Thirdly, what cell types within tissues become infected with myxoma virus in laboratory and wild rabbits (addressed in Chapter 4)? I also examine the pathogenic mechanisms employed myxoma virus in the lymphoid organs of rabbits that may contribute to the death of the host, and how these are dependent on virus virulence or the degree of host genetic resistance (Chapters 4 and 5). Finally, I investigate virus replication both *in vitro and in vivo* for the respective examination of the role of cell permissivity to virus replication in host resistance, and to examine the importance virus replication in dendritic cells and lymphocytes for virus virulence and dissemination (Chapter 5).

Chapter 2: Cellular and humoral responses to virulent and attenuated myxoma virus infection

2. Cellular and humoral responses to virulent and attenuated myxoma virus infection

2.1 Introduction

Myxoma virus encodes at least nine proteins that may function to suppress the host immune response. These include specific inhibitors of TNF$^{\alpha}$ and TNF$^{\beta}$ (Schreiber and McFadden, 1994; Upton *et al.*, 1991), IFN$^{\gamma}$ (Mossman *et al.*, 1995a; Upton *et al.*, 1992) and chemokines (Graham *et al.*, 1997; Lalani *et al.*, 1997), as well as inhibitors of inflammation (Graham *et al.*, 1992; Opgenorth *et al.*, 1992) including serine proteinase inhibitors (Macen *et al.*, 1993; Upton *et al.*, 1990), and inhibitors of apoptosis in infected lymphocytes (Barry *et al.*, 1997; Macen *et al.*, 1998; Macen *et al.*, 1996a; Macen *et al.*, 1996b; Mossman *et al.*, 1996a; Petit *et al.*, 1996; Schreiber *et al.*, 1997). The individual deletion of most of these genes results in the attenuation of the disease caused following infection of European rabbits. Myxoma virus also specifically downregulates the expression of MHC class I (Boshkov *et al.*, 1992) and CD4 on the surface of infected cells (Barry *et al.*, 1995). However, *in vivo* immune responses of European rabbits infected with myxoma virus have not been measured to determine if a functional suppression of the immune response occurs.

Malignant rabbit virus, a virus generated by a recombination between the closely related myxoma and Shope fibroma viruses, causes a generalised lethal disease in infected laboratory rabbits similar to that caused by infection with myxoma virus (Strayer *et al.*, 1983a). Also similarly to myxoma virus, malignant rabbit virus replicates in lymphocytes (Strayer *et al.*, 1985), encodes inhibitors of the host immune response (Upton *et al.*, 1990) and specifically downregulates MHC class I on the surface of infected cells (Boshkov *et al.*, 1992). Malignant rabbit virus-infected rabbits exhibit decreased cellular and humoral immune functions. Suppression of splenocyte proliferation in response to mitogens *in vitro* is apparent by 7dpi, with some recovery of responsiveness by 11dpi (Strayer *et al.*, 1983b). Suppression of lymphocyte responsiveness is associated with a reduced ability to produce and respond to IL-2 (Strayer *et al.*, 1986). Malignant rabbit virus-infected rabbits have a depressed ability to generate specific antibody to an unrelated antigen (sheep red blood cells) (Strayer *et al.*,

1983b) although rabbits developed substantial neutralising antibody titres to malignant rabbit virus before death (Strayer and Leibowitz, 1987a).

Malignant rabbit virus-induced suppression of lymphocyte responsiveness is thought to be a function of the ability of the virus to replicate in lymphocytes. Shope fibroma virus is unable to replicate in lymphocytes (Strayer *et al.*, 1985). Recombinants of Shope fibroma virus containing fragments of malignant rabbit virus DNA that confer the ability to replicate in lymphocytes, also induce immune suppression of infected rabbit lymphocytes (Strayer *et al.*, 1990). The importance of viral replication in lymphocytes is thought to be two fold: direct suppression of lymphocytes (Strayer and Leibowitz, 1986; Strayer *et al.*, 1985), and the induction of as yet uncharacterised soluble factors from infected cells that suppress the responses of uninfected cells (Strayer *et al.*, 1988).

Malignant rabbit virus and Shope fibroma virus provide obvious models for understanding the interactions of myxoma virus with the rabbit immune response because of their close genetic relationship with myxoma virus. In particular, whether the differences in virulence between strains of myxoma virus are due to suppression of host immune functions *in vivo*. In this Chapter, the effect that two strains of myxoma virus had on cellular and humoral responses of infected rabbits was examined. These strains were the highly virulent standard laboratory strain (SLS) which causes 100% mortality in laboratory rabbits, and the naturally attenuated Uriarra strain of myxoma virus, which causes clinical myxomatosis but results in less than 5% mortality in infected rabbits. To examine humoral immune responses, a strong antibody response to an antigen must be generated in the timespan of an SLS infection. Hence, a model system of coinfections was studied, utilising SLS or Uriarra coinfected with an extremely attenuated recombinant myxoma virus (derived from Uriarra) expressing the influenza haemagglutinin (HA). It was already known that infection of rabbits with this virus provided a strong IgG response to HA by 10dpi, although preliminary results suggested some suppression of this response in rabbits coinfected with SLS (Kerr and Jackson, 1995). Lymphocyte responsiveness *in vitro* was examined using T and B cell mitogens to stimulate cells prepared from the lymph nodes or spleen of infected rabbits.

2.2 Materials and Methods

2.2.1 Animals and viruses

2.2.1.1 Rabbit care and housing

Laboratory European rabbits (*Oryctolagus cuniculus*) were bred in the CSIRO Gungahin animal house facility. Adult rabbits over four months old were individually housed under PC2 conditions in this facility, where the temperature and lighting regimes were held constant at 20°C and 12:12 hours light:dark respectively. Rabbits were fed *ad libitum* on standard rabbit pellets supplemented with cabbage leaves.

2.2.1.2 Derivation of viruses

Standard Laboratory Strain (SLS) of myxoma virus is derived from the Moses' strain (Moses, 1911) and is the strain originally released in Australia. The SLS stock used in this study is derived from a rabbit tissue-stock freeze dried by Professor Frank Fenner in 1953 which has subsequently been passaged twice in tissue culture (RK13 cells) and then twice in rabbits. The virus has Grade I virulence for laboratory rabbits with 100% lethality and an average survival time of <13 days (Fenner and Marshall, 1957). This was confirmed for these stocks in recent retesting (Robinson *et al.*, submitted).

Uriarra strain of myxoma virus is derived from the plaque purified stock produced by Russell and Robins (1989) (Russell and Robbins, 1989) which is derived from the Uriarra/2/53-1 isolate (Myktowycz, 1953). It was passaged an unknown number of times in tissue culture (CV-1 cells) before we obtained it, and has subsequently been passaged twice in RK13 cells and then twice in rabbits. This virus is of Grade V virulence and over 95% of infected laboratory rabbits recover from infection, but all develop clinical myxomatosis (Fountain *et al.*, 1997; PJ Kerr, unpublished).

UrHA is a recombinant myxoma virus of the Uriarra strain (Uriarra/2/53-1) that encodes the influenza haemaglutinin (HA) gene under the control of the vaccinia virus P11 late promoter (Kerr and Jackson, 1995). Virus stocks were produced in RK13 cells. This virus does not cause significant clinical disease in laboratory rabbits.

2.2.1.3 Rabbit passage of virus stocks

Two adult male laboratory rabbits were infected by intradermal inoculation in the hind flank with 10^3 plaque forming units (pfu) of SLS or Uriarra strains of rabbit-passaged myxoma virus. At 8 (SLS) and 10 (Uriarra) days post infection (dpi), the rabbits were killed by barbiturate overdose and both testes removed aseptically. The two testes from each rabbit were washed in phosphate buffered saline (PBS; 0.14M NaCl, 0.003M KCl, 0.003M Na_2HPO_4, 0.003M KH_2PO_4), the tunics removed and the remainder minced with scissors and passed through a 10ml syringe. The homogenised testes were placed in a 50ml tube and approximately 10ml sterile PBS added, followed by three 5 sec bursts of sonication using a probe sonicator. The suspension was centrifuged at 230g for 10min and the supernatant removed and retained. The remaining tissue was sonicated again, followed by centrifugation. The supernatant was removed and combined with the previous supernatant. The titre of virus in the combined supernatant was determined by plaque assay (2.2.1.5) and 1ml stock aliquots stored at -70°C. These aliquots were further divided into 50µl aliquots, also stored at -70°C, that were thawed and frozen for use a maximum of two times before they were discarded.

2.2.1.4 VERO cell culture for plaque assays

Aliquots of liquid nitrogen stored VERO cells (African green monkey kidney cell line) were thawed, washed once in minimal essential medium (MEM, Gibco BRL) supplemented with 10% newborn calf serum (CSL), 200 units/ml penicillin (Sigma), 100µg/ml streptomycin (Sigma) and 2mM L-glutamine (Sigma) (complete MEM), placed with medium into a T25 flask (Nunc) and allowed to grow to confluency at 37°C in 5% CO_2 in air. When confluent, cell monlayers were washed twice in PBS, washed twice with 0.1% trypsin in diluent (0.14M NaCl, 0.005M KCl, 0.0004M Na_2HPO_4, 0.0004M KH_2PO_4, 0.006M $NaHCO_3$, 0.0003M Na_3EDTA pH 7.3) and left for 2min covered in a thin layer of 0.1% trypsin. The cells were suspended by repeated pipetting, placed in a T175 flask (Nunc) with complete MEM and allowed to grow to confluency with regular changes of complete MEM at 37°C in 5% CO_2 in air. When confluent, cells were removed from the flask as above and placed into roller bottles (Nunc) with complete MEM on a rotator at 37°C, and with regular changes of complete MEM, until they reached confluency. Cells were then removed from the roller bottle as above and counted using a haemocytometer.

2.2.1.5 Plaque assay for virus titration

VERO cells from the roller bottle cell culture were seeded into 6 well sterile plates (Nunc) at 0.8 x 10^6 cells/well in complete MEM and grown overnight at 37°C in 5% CO_2 in air to form a cell monolayer. The medium was removed leaving sufficient volume to just cover the monolayer. 100µl of serial dilutions of testis preparation (see 2.2.1.3) was added to duplicate monolayers and the plates incubated for one hour at 37°C in 5% CO_2 in air, rocking every 15min, followed by addition of 3ml of complete MEM and incubation for 7 days. After this time, the medium was poured off and 1ml of 10% formalin (v/v in PBS) added to each well. Plates were left for 1hour, followed by removal of formalin and the addition of 1ml of 0.1% aqueous crystal violet (Sigma), which was left for a further 1hour. The plates were washed in tap water, allowed to air dry and the number of plaques counted. Titres were expressed as plaque forming units (pfu)/ml of stock.

2.2.2. Infection experiments

2.2.2.1 Coinfection of laboratory rabbits with UrHA and either SLS or Uriarra

Eighteen laboratory rabbits were intradermally inoculated, in groups of three, in one flank with 10^3 pfu of the recombinant myxoma virus, UrHA. These rabbits were intradermally inoculated at the same time as the first inoculation in the opposite flank with 10^3 pfu of either the virulent SLS (n=6) or the attenuated Uriarra strain of myxoma virus (n=6) to form the UrHA/SLS and UrHA/Uriarra coinfections respectively. Control rabbits were inoculated with UrHA only (n=6). Clinical symptoms, rectal temperature and progression of the primary lesions were monitored every 24 hours. Every 48 hours, peripheral blood was taken from the marginal ear vein for peripheral white blood cell (WBC) counts (see section 2.2.2.1.1). At 10 dpi, and after a blood sample was taken, rabbits were killed by injection of barbiturate in the marginal ear vein, and the spleen and popliteal lymph node adjacent to the inoculation site of UrHA were aseptically excised and placed into cold Hanks balanced salt solution (HBSS; Flow Laboratories) supplemented with 12.5 I.U./ml heparin sodium (Fissions Pharmaceuticals) and kept on ice.

2.2.2.1.1 Peripheral WBC counts

WBC from peripheral blood samples were diluted 1:10 in WBC diluting fluid (2% glacial acetic acid, 1% of 1% aqueous gentian violet, in ddH_20), loaded into a haemocytometer and counted using a light microscope.

2.2.2.2 *Block design experiment for measuring mitogen-induced proliferation of lymphocytes* in vitro

Laboratory rabbits were intradermally inoculated with 100pfu of SLS or Uriarra on the dorsum of the hind left foot. The relatively small dose of virus was used to mimic natural infection and reduce the amount of virus reaching the node due to drainage directly from the inoculation site. Rabbits were inoculated in groups of six, with four rabbits infected with virus and two inoculated with 100µl PBS for each time point (4, 7 and 10dpi). At any one time, six rabbits were killed in a random block design (Table 2.1). This was the maximum number of rabbits that could be handled in one day. The random block design of the experiment meant that rabbits from two treatment groups were killed each time (for example, day 4 and day 10 post infection). In addition, a different combination of treatment groups was killed at each time, to randomise the effect that day of killing may have on the assay. Popliteal lymph nodes from both left and right legs (the draining and contralateral lymph nodes respectively) were removed and placed into HBSS supplemented with 12.5 I.U./ml heparin sodium (Fissions Pharmaceuticals) and kept on ice.

2.2.2.3 *Preparation of primary cells from lymph nodes and spleen*

Each spleen and lymph node was cut into small pieces with scissors and passed through a stainless steel mesh (50µm) using a glass pestle and 10ml HBSS supplemented with heparin. The cell suspension from the spleen was passed through a second mesh (40µm) to further break up cell aggregates. The resulting cell suspensions were pelleted at 230 *g* for 10min at 18°C and resuspended in 5ml of shocking solution (0.0008M KH_2PO_4, 0.15M NH_4Cl, 0.003M Na_3EDTA, pH 7.2 in ddH_2O) for 10min at room temperature to lyse red blood cells (RBC). 5ml HBSS was added to the cell suspension and it was centrifuged again as above. The cells were washed twice with HBSS before resuspending in 5ml RPMI 1640 medium (GIBCO BRL) supplemented with 10% foetal calf serum (CSL), 200 units/ml penicillin (Sigma), 100µg/ml streptomycin (Sigma) and

2mM L-glutamine (Sigma) (complete RPMI). Cells were counted in WBC diluting fluid using a haemocytometer. Cell viability was assessed by trypan blue exclusion (0.2% trypan blue in ddH_2O).

Figure 2.1: Random block design of the lymphocyte proliferation experiment. Rabbits were infected with either SLS or Uriarra at 4, 7 or 10 days before the day of killing. Rabbits were killed on six separate days (day of killing). On each of these days, three rabbits were killed from each of two treatment groups (a total of six rabbits/day). Within each treatment group, two rabbits were infected with virus and one rabbit had been inoculated with PBS. Rabbits infected with either Uriarra (blue) or SLS (red) were always killed on different days. At the end of the experiment, a total of four virus-infected rabbits and six PBS-inoculated rabbits had been killed at each time point of 4, 7 and 10 dpi (days post infection), for both Uriarra and SLS infections (a grand total of 18 rabbits per virus-infection).

Day of killing	Treatment group 1 (2 virus infected, 1 PBS)	Treatment group 2 (2 virus infected, 1 PBS)	Total number of rabbits
1	4 dpi	7 dpi	6
2	4 dpi	10 dpi	6
3	7 dpi	10 dpi	6
4	4 dpi	7 dpi	6
5	4 dpi	10 dpi	6
6	7 dpi	10 dpi	6

2.2.2.4 Mitogen stimulation of primary lymphoid cells

The ability of lymphocytes to proliferate in response to mitogen stimulation was examined using the T-cell mitogens Concanavalin A (Con A) and phytohaemagglutinin (PHA) or the B-cell mitogen, lipopolysaccharide (LPS). Primary cells from lymph nodes or spleen were seeded into 96 well flat bottomed microtitre plates (Nunc) at 1 x 10^5 cells/well in 200µl of complete RPMI. Con A, PHA or LPS (Sigma) was added to triplicate cell samples, in serial two fold dilutions from 10 to 0.625µg/ml. Cells derived from coinfected rabbits were stimulated with Con A only. Controls containing no mitogen were included. Plates were incubated for 48 hours at 37°C in an atmosphere of 5% CO_2 in air, after which 0.7µCi tritiated thymidine (^{3}H-T; ICN) in complete RPMI

was added to each well. The cells were then incubated for a further 18 hours and frozen at -20°C until harvested. Optimal incubation times for the maximal incorporation of ^{3}H-T into DNA of proliferating cells had been previously determined (K.Saint, pers. com.). The plates were thawed and harvested onto printed filtermat A glass paper (Wallac Oy, Turku, Finland) using a Wallace Betaplate cell harvester. The filtermats were dried for 10min at 60°C and placed into Wallace sampling bags and 10ml of Betaplate Scint, scintillation fluid (Wallac Oy) added. The incorporation of ^{3}H-T into the DNA of proliferating cells was counted by a 1205 Betaplate reader. The optimal mitogen concentrations assessed by maximum incorporation of ^{3}H-T into cellular DNA were 5, 5 and 10μg/ml for Con A, PHA and LPS, respectively.

2.2.3 Preparation of influenza virus

2.2.3.1 Growth and harvest of influenza virus

A/PR/8/34 influenza virus was supplied by Dr. G. Laver, John Curtin School of Medical Research, Australian National University at a concentration of 320 haemagglutinin units/ml (HAU/ml). 160 HAU influenza virus was placed into 50ml normal saline (0.15M) supplemented with 200 units/ml penicillin (Sigma) and 100μg/ml streptomycin (Sigma). 100μl was inoculated into the allantoic fluid of each of 200 ten day fertilised eggs (Parkwood Eggs, A.C.T.). The point of entry, through the shell at the air sac, was sealed with wax and the eggs incubated for three days in a humidified chamber at 37°C with regular turning of the eggs. After this, the eggs were cut open and the allantoic fluid aspirated into a flask on ice. Any eggs displaying bacterial growth were discarded. A small amount of the fluid was kept for virus titration in a haemagglutination test (section 2.2.3.3) which at this time was 2560 HAU/ml. To concentrate the virus, chicken RBC (section 2.2.3.4) were added to the remainder of the fluid to make a 2% v/v RBC suspension that was placed on ice for 60 min, shaking every 15 min to allow virus to absorb to the RBC. RBC were then pelleted at 450 *g* for 15 min at 0°C and the supernatant removed. RBC were resuspended in 50ml calcium/magnesium saline (0.01% $CaCl_2$, 0.001% $MgCl_2$ in normal saline) and incubated for 60min at 37°C with shaking every 15min, followed by centrifugation at 450 *g* for 15min at 20°C. The supernatant, which now contained the virus, was removed, the haemagglutinin titre determined, and the virus stored at 4°C.

2.2.3.2 Purification of influenza virus

The supernatant from 2.2.3.1. was centrifuged at 22 000 *g* for 3 hours at 4°C. The supernatant was removed and the pellet covered with 1ml of calcium/magnesium saline and left overnight at 4°C to resuspend. The remaining pellet was then resuspended by agitation and the suspension layered above a step gradient of 10, 40 and 55% sucrose (w/v in ddH_20). This was centrifuged at 22 000 *g* for 45min at 5°C in a SW28 rotor. The visible band of antigen (positioned a third of the way down the gradient) was collected and centrifuged for 3 hours at 35 000 *g* at 10°C and the supernatant discarded. The pellet was washed twice, without disruption, with saline and then resuspended in 1ml of saline containing 1 drop of 10% sodium azide. The final haemagglutinin titre was determined using the haemagglutination test and the virus stored at 4°C. This titre was 1.6×10^8 HAU/ml.

2.2.3.3 Preparation of chicken RBC

Chicken blood was collected from the throats of newly slaughtered adult chickens into 1% tri-sodium citrate in normal saline (0.15M). The citrated blood was passed through two layers of gauze and RBC pelleted at 450g for 15min at 0°C. RBC were washed twice (with centrifugation at 450 *g* for 15 min at 0°C) with 20ml of normal saline. The final pellet of RBC was covered with a thin layer of saline and stored at 4°C for up to seven days for use in the production of influenza virus and in the haemagglutination tests.

2.2.3.4 Haemagglutination test

The ability of antigen suspensions to agglutinate RBC was measured using the agglutination test. The test solution (allantoic fluid, unpurified and purified virus) was titrated in 2 fold serial dilutions from 1:10 in 100µl saline in duplicate in 96-well round bottomed plates (Nunc). 10µL of 10% chicken RBC (v/v in saline; section 2.2.3.4) was added to each well, mixed thoroughly and left for 30min at room temperature. The last dilution at which the RBC were not agglutinated was recorded as the titre (HAU/ml).

2.2.4 Quantification of antibody responses following coinfection of laboratory rabbits

2.2.4.1 Enzyme linked immunosorbent assay (ELISA)

The purified influenza virus (section 2.2.4.1) was used in an ELISA (see below) such that a 1:100 dilution of serum from rabbits that had been previously hyperimmunised with UrHA gave a positive reaction of 1.0 –1.2 optical density (OD) units. This concentration was a 1:5000 dilution of antigen stock.

50μL of influenza virus (section 2.2.3) or myxoma virus antigen (1:5000 or 1: 2500 respectively in PBS) was added to all wells except the first row of 96 well flat-bottomed plates (Nunc) and incubated for 3 hours at 37°C. Myxoma virus antigen was prepared from intracellular myxoma virus (Lausanne strain) grown in tissue culture (RK13 cells). Virus was released from infected tissue culture cells by sonication, pelleted by cetrifugation through two dextran/sucrose step gradients, and stored at –20°C (Kerr, 1997). Excess antigen was flicked out of the well and the plates washed three times with 5% w/v skim milk powder (Diploma) in PBS (milk/PBS). 200μL milk/PBS was added to all wells and the plates left overnight to block at 4°C. Rabbit sera were vortexed and centrifuged at 13 000 *g* for 5min to remove non-specific reactivity. Sera were diluted, in duplicate, in milk/PBS in two fold serial dilutions from 1:50 to 1:51200, and 50μl of these dilutions added to the blocked plates after the milk/PBS had been flicked out of the wells. Known positive and negative samples were included as controls. Plates were incubated for 2 hours at 37°C and then washed four times with 0.05% v/v Tween 20 (Sigma) in PBS (Tween/PBS). 50μl of goat anti-rabbit IgG (1:4000) or anti-rabbit IgM (1:1000) conjugated with horse-radish-peroxidase (Southern Biotechnology) in milk/PBS was added and the plates incubated for 60min at 37°C, followed by six washes with Tween/PBS. 100μL of a buffered ABTS (2,2'-Azino-bis(3-ethylbenzo-thiazoline-6-sulphonic acid); Sigma) solution was added to each well and left for 20min at room temperature. This consisted of 2ml stock ABTS (5mg/ml ABTS in 0.1M citrate phosphate buffer), 8ml 0.1M citrate phosphate buffer (77nM Na_2HPO_4, 61mM citrate, pH 4.0 in ddH_2O) and 0.06% H_2O_2. The OD of each well was read at 405nm with a BIORAD 3550 microplate reader using BIORAD microplate

manager 2.1 software. The antibody titre was read as the final dilution producing a positive reading at least 0.1 OD units above the OD of the 1:100 negative control.

Both the IgM and IgG ELISAs were optomised to give the highest possible signal:noise ratio. IgM was difficult to detect and so a much higher background level was accepted to enable detection of IgM compared to IgG. Hence, the ELISA titres of specific serum IgM and IgG are not comparable in a quantitative sense (Kerr, 1997).

2.2.4.2 ELISPOT

Influenza virus preparation (section 2.2.3) was diluted 1:5000 in bicarbonate buffer (0.1M $NaHCO_3$, 1mM $MgCl_2.6H_2O$, pH 9.8 in ddH_2O) and 50µl added to all wells of Millititre HA 96 well filtration plates (Millipore) with the exception of the first row, and incubated overnight at 4°C. The plates were then washed gently four times with PBS. Primary lymphoid cells from the popliteal lymph node and spleen of rabbits inoculated with UrHA were seeded into wells in serial two fold dilutions from 2×10^5 to 2.5×10^4 cells/well in triplicate. A control of no cells was included. The plates were incubated for 6 hours at 37°C to enable cells to secrete antibody, and then washed four times with Tween/PBS. 100µl of biotinylated goat anti-rabbit IgG (1:4000) or IgM (1:1000) (Southern Biotechnologies) in Tween/PBS was added and incubated at 4°C overnight. A control of no secondary antibody was included. Plates were washed four times with Tween/PBS followed by the addition of 100µl of streptavidin-conjugated alkaline phosphatase (1:2000; Amersham Life Science), followed by incubation for 60min at 37°C. Plates were again washed four times with Tween/PBS. 100µl of alkaline phosphatase substrate was added to each well and the plates left for 20min at room temperature for the colour to develop. This substrate was a filtered solution consisting of 6mg BCIP (5-bromo-4-chloro-3 indolyl phosphate; Promega), 12mg NBT (nitro blue tetrazolium; Promega), dissolved in 40ml of bicarbonate buffer plus 400µl DMF (N,N-dimethyl formamide; Sigma). Plates were washed with tap water and allowed to dry before counting spots that represented antibody secreting cells under a stereoscopic dissecting microscope. Results were expressed as antibody secreting cells (ASC) per 10^6 lymphoid cells.

2.2.5 Histology and immunohistochemistry

2.2.5.1 Fixed tissue sections and histology

Following autopsy, portions of lymph node and spleen were fixed in 4% buffered formaldehyde for 24 hours, followed by two changes in 70% ethanol, and then embedded in paraffin wax. Four 5μm sections were cut from each tissue at intervals of 500μm (and from either end of the spleen resulting in eight sections of spleen from each rabbit) and mounted on superfrost microscope slides (Menzel-Glaser). Sections were dewaxed in three changes of xylene for 2 min each and rehydrated through a graded series of ethanol (100 - 75%). Slides were then washed in tap water, stained with Gills' number 3 haematoxylin for 3 min (BDH Laboratory Supplies), washed in tap water, blued in Scotts' tap water substitute (20mM $NaHCO_3$, 80mM $MgSO_4$) for 1 min, stained with 0.025% alcoholic eosin for 2 min, differentiated in two washes of 90% ethanol and cleared in two changes of xylene. Sections were mounted under a coverslip with D.P.X. (Difco), examined by light microscopy and photographed using Fujichrome Velvia 400 film.

2.2.5.2 Frozen tissue sections

At autopsy, blocks (10mm x 2mm) of tissue from the primary site of virus inoculation in the skin, the lymph node adjacent to this inoculation site and the spleen were placed in small cups made of foil and covered in OCT fluid (Tissue Tek). These were snap frozen in liquid nitrogen and stored at -70°C. Tissue sections of 4 to 7μm thickness were cut from these blocks using a cryostat. The sections were placed onto superfrost slides (Menzel-Glaser) which had been previously coated in a 0.01% poly-L-lysine (Sigma) solution (v/v in ddH_2O) and air-dried.

2.2.5.3 Fixation of frozen sections

Within an hour of being cut, frozen sections were immersed in formol-calcium for 5 min (10% of 40% formaldehyde, 10% 1M $CaCl_2$, 80% ddH_2O), dipped in cold acetone, immersed in chloroform/acetone (1:1) for 5min at -20°C, dipped in cold acetone and washed twice in PBS. Sections were then stored at –70°C.

2.2.5.4 Preparation of rat anti-HA polyclonal antisera

To obtain primary antibody specific for the HA antigen, one adult male Wistar rat was anaesthetised with halothane and inoculated on both rear flanks with 500 HAU of

influenza virus (section 2.2.3) preparation mixed with Freunds incomplete adjuvant (Sigma). Three weeks later, the rat was given a booster inoculation with the same mixture followed by two more boosts two weeks apart. Five days following the final boost, the rat was anaesthetised with chloroform and exsanguinated. The blood obtained was centrifuged in a benchtop microfuge at 13 000 *g* for 5 min and the serum removed and stored at -20°C. The antibody titre specific for the HA antigen was measured by ELISA (section 2.2.4.1).

2.2.5.5 Immunofluorescence for influenza HA or myxoma virus localisation

Frozen tissue sections were blocked overnight at room temperature in 3% BSA (bovine serum albumin; Sigma) in PBS and washed once with 1% BSA/PBS, followed by three washes with 0.01% Tween 20 in PBS. Sections were placed in a humidified container and covered with 100µl of 1:50 rat anti-HA (section 2.2.5.4) or 1:200 mouse anti-myxoma virus monoclonal antibody (clone number 3B6E4, (Fountain *et al.*, 1997)) in 1% BSA/PBS. Controls of pre-immune rat serum, normal mouse-ascites fluid and no primary antibody were included. Sections were incubated for 2 hours at 37°C and washed again as above. 75µl of either mouse-absorbed anti-rat IgG (1:100) or goat anti-mouse IgG (1:100), both conjugated to FITC (Silenus) in 1% BSA/PBS was added to each section. The sections were incubated in the dark for 60 min at 37°C in a humidified container. Sections were then washed as above and mounted with Antifade (Molecular Probes, Oregon, USA) under a coverslip. Sections were examined with either a Leitz diaplan microscope and photographed using Fujichrome 400D colour transparency film or with a BIORAD confocal microscope with BIORAD COMOS software.

2.2.6. Statistical analysis of antibody and lymphocyte proliferation responses to infection

Significant differences in the titres of circulating serum IgM and IgG to HA and to myxoma virus at 10dpi following coinfection of rabbits were determined by one tailed Mann-Whitney U test, with a level of significance of 0.05. Differences in the numbers of ASC in the spleen and lymph nodes, secreting HA-specific IgM and IgG, at 10dpi following coinfection of rabbits were also determined by one tailed Mann-Whitney U test, with a level of significance of 0.05. The correlation coefficient, r, was determined

for comparisons of serum IgM and IgG to the number of IgM or IgG secreting cells in either the lymph node or spleen, or the two combined, for individual rabbits. Significant differences in the ability of lymphocytes from Uriarra or SLS infected rabbits to respond to stimulation with Con A, PHA or LPS were compared between days of infection and between infected and uninfected rabbits by analysis of variance (ANOVA). Multiple pairwise comparisons of means by Tukeys test were performed on groups of means that were found to be significantly different by ANOVA, to determine exactly which days post infection were significantly different from uninfected controls (Zar, 1984).

2.3 Results

2.3.1 Humoral immune responses following coinfection of rabbits with UrHA and either SLS or Uriarra

2.3.1.1 Clinical observations following coinfection of laboratory rabbits with virulent and attenuated viruses

Rabbits inoculated with UrHA alone developed a lesion at the primary inoculation site. This lesion was first evident at 3 or 4 dpi and reached a maximum diameter of approximately 4 cm at 8dpi. The lesion was flat, pink and in two of six infected rabbits, had begun to regress at 10 dpi. Mild anogenital swelling and thickening of eyelids was apparent in two of six infected rabbits. All rabbits remained alert and active throughout the period of infection.

In rabbits coinfected with UrHA and the attenuated Uriarra strain of myxoma virus, the primary Uriarra lesion on the right flank was evident at 3 dpi and reached a maximum diameter of approximately 6cm. This lesion developed a much darker colour than the lesion formed at the UrHA primary lesion, which reached a maximum diameter of 5-6 cm. Rabbits developed red eyelids, and an inflamed anogenital region by 8 to 9 dpi, followed by thickening of the eyelids and ears, some mucopurulent discharge from the nose and eyes and a depressed demeanour by 10dpi. Four animals had secondary lesions on the face or ears by 10dpi. All rabbits survived through to 10 dpi at which time they were killed by intravenous barbiturate. One rabbit did not develop a lesion at the Uriarra inoculation site and thus it is not certain that this rabbit was inoculated correctly. This rabbit has been omitted from all further results.

In rabbits coinfected with UrHA and the virulent SLS, the primary SLS lesion was evident at 3 dpi and reached a maximum diameter of approximately 7cm by 10dpi. This lesion was hard to the touch, dark purple in colour and was often surrounded by many smaller lesions. The lesion formed at the inoculation site of UrHA reached a maximum diameter of approximately 6cm. Reddened eyelids and anogenital swelling were evident by 6dpi, followed by thickened ears, a mucopurulent discharge from the eyes and nose and laboured respiration. By 10 dpi, rabbits had developed secondary lesions around the nose, eyes, ears, mouth, feet, and generally over the body and had a depressed demeanour. All rabbits survived through to 10 dpi.

On autopsy of rabbits at 10dpi, both popliteal lymph nodes, and the spleens of animals coinfected with UrHA and either Uriarra or SLS were 3-4 times the size of those from uninfected rabbits. The popliteal lymph nodes from rabbits coinfected with SLS were invariably purple in colour. However, the extent of this colouration varied, encompassing between half and the whole of the node. Lymph nodes from rabbits coinfected with UrHA and Uriarra were not discoloured. At 10dpi of rabbits with UrHA only, the popliteal lymph node regional to the UrHA inoculation site was 2-3 times normal size with no changes in colouration, and the spleen was up to 50% enlarged. The contralateral popliteal lymph node was generally not enlarged compared to lymph nodes from uninfected rabbits.

2.3.1.2 Febrile responses to coinfection

Rectal temperatures were measured daily during the course of infection and are expressed as the mean $\pm$ standard error for all rabbits on each day. The mean basal temperature of uninfected rabbits was 38.8 $\pm$ 0.3°C (n=17). The rectal temperature of rabbits coinfected with either Uriarra or SLS increased from 2dpi to 5dpi, but did not change following infection of rabbits with UrHA alone (Figure 2.1). Elevated rectal temperatures were maintained from 5 to 10dpi in rabbits coinfected with UrHA/Uriarra (n=5), attaining a maximum of 40.4 $\pm$ 0.3°C (8dpi). In rabbits coinfected with UrHA/SLS, rectal temperatures reached a maximum of 40.3 $\pm$ 0.3°C at 8dpi, but then declined rapidly to 38.5 $\pm$ 0.3°C (n=6) at 10dpi.

2.3.1.3 Changes in peripheral WBC counts

Blood samples from the marginal ear vein were taken every two days over the 10 days of infection and peripheral WBC counted. Peripheral WBC counts did not change substantially following coinfection of rabbits with UrHA and Uriarra, or infection of rabbits with UrHA alone. In contrast, coinfection of rabbits with UrHA and SLS resulted in a rapid increase in peripheral WBCs from 6dpi (Figure 2.2).

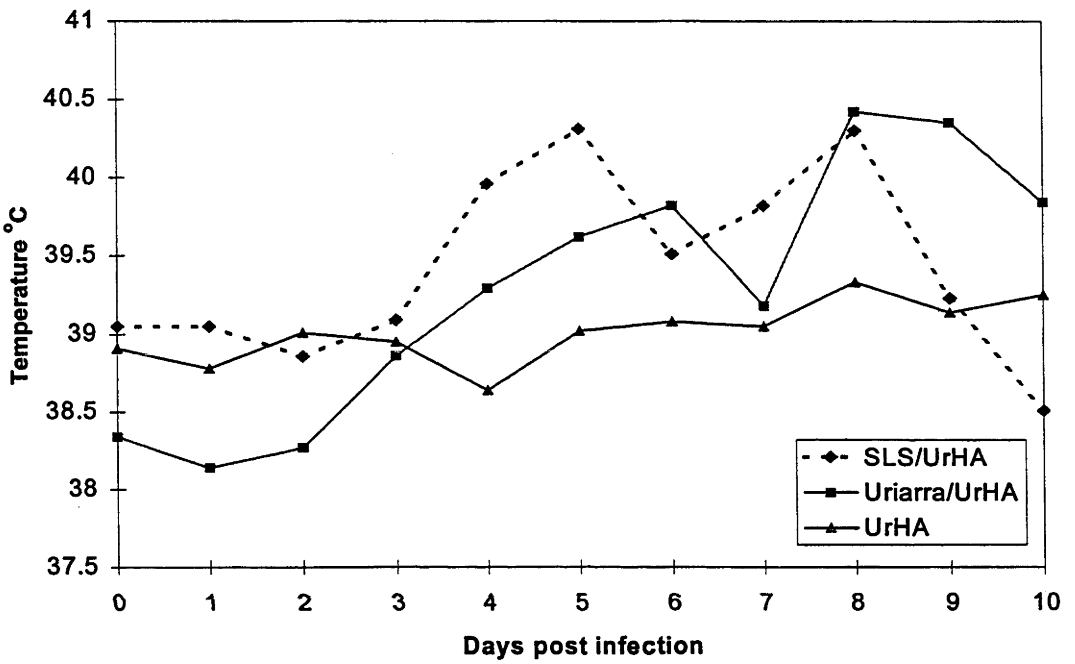

Figure 2.1: Daily mean rectal temperature (°C) of laboratory rabbits coinfected with UrHA and SLS (n=6), UrHA and Uriarra (n=5), or infected with UrHA alone (n=6). Error bars have been omitted for clarity.

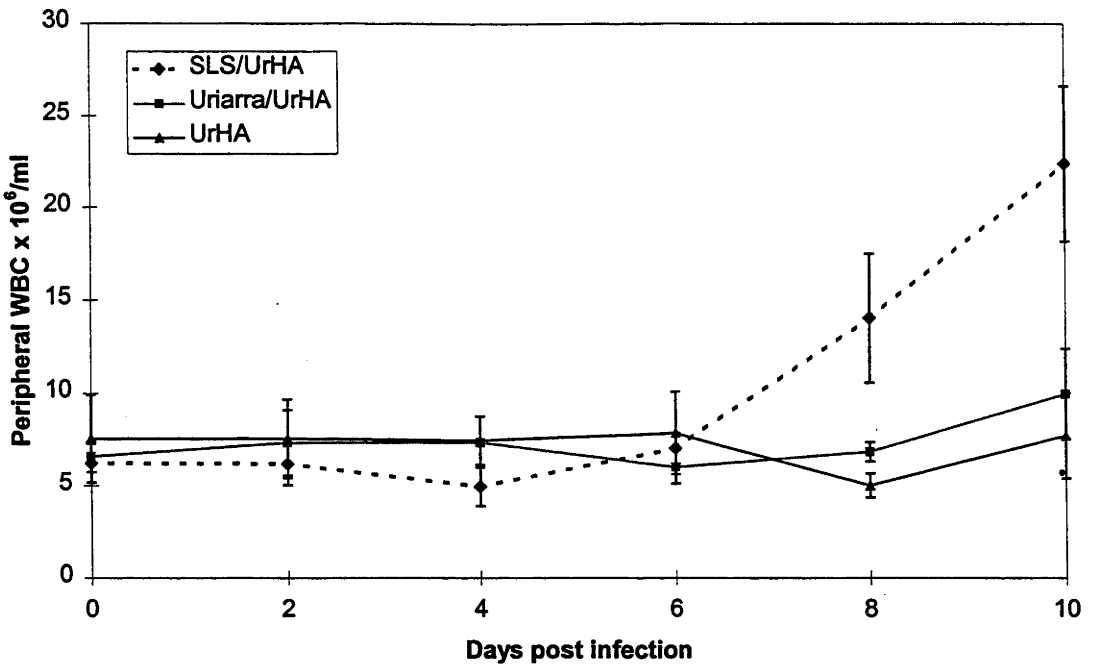

Figure 2.2: Peripheral white blood cell (WBC) counts in laboratory rabbits coinfected with UrHA and SLS (n=6), UrHA and Uriarra (n=5), or infected with UrHA alone (n=6) (mean ± SE).

2.3.1.4 Measurement of circulating serum antibody at 10dpi

2.3.1.4.1 Serum antibody specific to myxoma virus

Circulating serum IgM and IgG to myxoma virus were measured by ELISA at 10dpi in rabbits inoculated with UrHA, or coinfected with UrHA/Uriarra or UrHA/SLS (Figure 2.3). Serum was titrated in duplicate in 2 fold serial dilutions, with the endpoint titre defined as the reciprocal of the final dilution which gave a positive reading at least 0.1 OD units above the OD of the 1:100 negative control. Differences in titres between groups of rabbits were tested using a one-way Mann Whitney U test. There were no significant differences in circulating IgM to myxoma virus at 10dpi between any of the treatment groups of rabbits (Figure 2.3A). The group of rabbits coinfected with UrHA/SLS had significantly higher levels of serum IgG to myxoma virus at 10dpi than the group of rabbits inoculated with UrHA alone ($P<0.05$) (Figure 2.3B). There were no significant differences in circulating IgG to myxoma virus at 10dpi between the group of rabbits infected with UrHA and the group coinfected with UrHA/Uriarra.

2.3.1.4.2 Serum antibody specific to HA

Serum IgM and IgG to HA were measured by ELISA at 10dpi in rabbits inoculated with UrHA, or coinfected with UrHA/Uriarra, or UrHA/SLS (Figure 2.4, Table 2.2). Serum was titrated in duplicate in 2 fold serial dilutions. The endpoint titre was defined as the reciprocal of the final dilution giving a positive result at least 0.1 OD units above the OD of the 1:100 negative control. Differences in titres between groups of individual rabbits were tested using a one-way Mann Whitney U test. There were no significant differences in IgM titres between any of the groups of animals infected (Figure 2.4A). The group of rabbits coinfected with UrHA/SLS, and the group coinfected with UrHA/Uriarra, had significantly depressed levels of circulating IgG to HA at 10dpi compared to the group of rabbits inoculated with UrHA alone ($P<0.05$) (Figure 2.4B).

2.3.1.5 Proportion of B cells secreting specific IgM and IgG to HA at 10dpi in the popliteal lymph node and spleen

The proprotion of B cells secreting specific IgM or IgG to HA at 10dpi in the spleen and popliteal lymph node of infected rabbits was determined by ELISPOT. Differences in numbers of positive cells between groups were tested using a one-way Mann Whitney-U test (Table 2.2). The group of rabbits coinfected with UrHA/Uriarra had significantly lower numbers of cells secreting IgM and IgG in both the popliteal lymph node and spleen when compared to the group of rabbits inoculated with UrHA alone ($P<0.05$) (Figure 2.5; 2.6). The group of rabbits coinfected with UrHA/SLS also had significantly lower numbers of IgM and IgG secreting cells in the spleen but not the popliteal lymph node, compared to the group of rabbits inoculated with UrHA alone (Figure 2.5; 2.6). However, of the group of rabbits coinfected with SLS, one animal (identification number 197) produced considerably more IgM and IgG antibody secreting cells (ASC) in the popliteal lymph node than the other five animals in that, or any other, group. The omission of this animal from analysis resulted in a significant decrease in the number of both IgM and IgG ASC in the lymph node compared to animals infected with UrHA alone (Figure 2.5). There was no correlation between circulating serum IgM or IgG with the number of IgM or IgG ASC in the lymph node or spleen, or both combined, within individual rabbits (test of correlation coefficient, r).

A

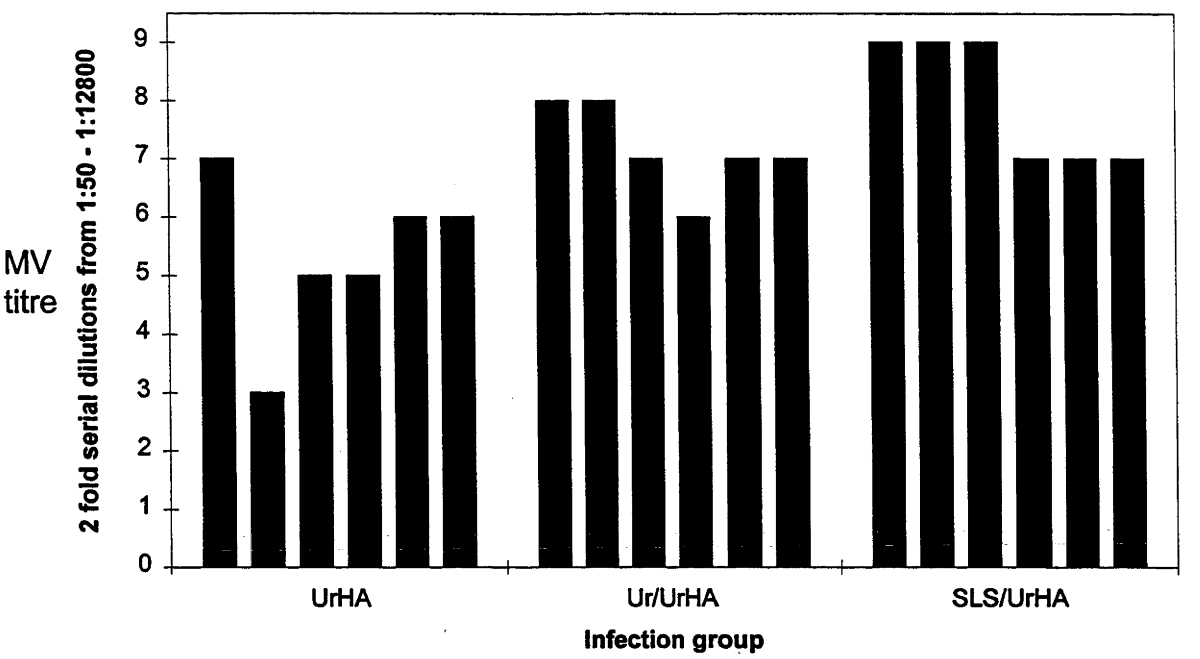

B

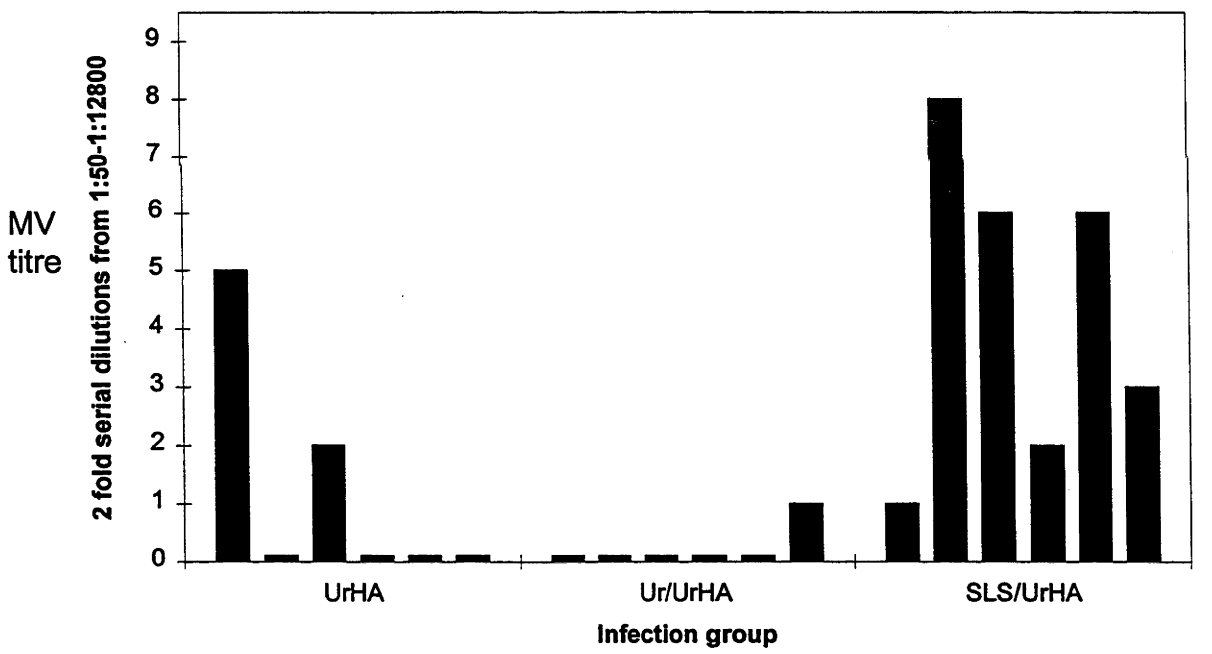

Figure 2.3: ELISA IgM (**A**) and IgG (**B**) to myxoma virus at 10dpi. Rabbits were infected with UrHA alone (n=6) and with UrHA on one flank and coinfected on the opposite flank with Uriarra (Ur/UrHA, n = 5) or SLS (SLS/UrHA, n = 6). Serum from 10dpi was diluted in duplicate in 2 fold serial dilutions, where 1 = 1:50. The endpoint titre was defined as the final dilution which was positive at least 0.1OD units above the OD of the 1:100 negative control. Each column represents the titre for an individual rabbit.

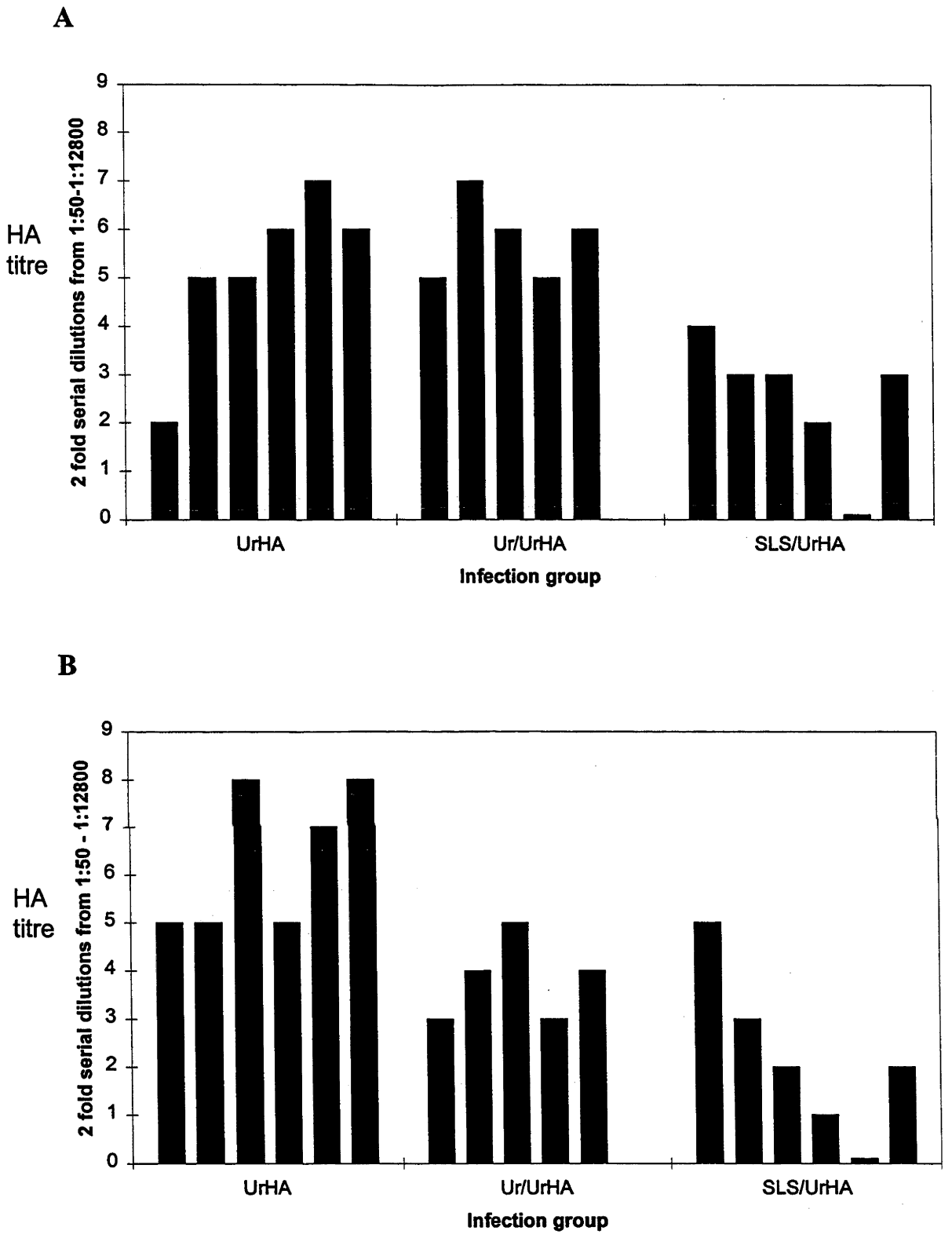

Figure 2.4: ELISA IgM (**A**) and IgG (**B**) to HA at 10dpi. Rabbits were infected with UrHA alone (n = 6) or with UrHA on one flank and coinfected on the opposite flank with Uriarra (Ur/UrHA, n = 5) or SLS (SLS/UrHA, n = 6). Serum from 10dpi was diluted in duplicate in 2 fold serial dilutions, where 1 = 1:50. The endpoint titre was defined as the final dilution which was positive at least 0.1OD units above the OD of the 1:100 negative control. Each column represents the titre for an individual rabbit.

A

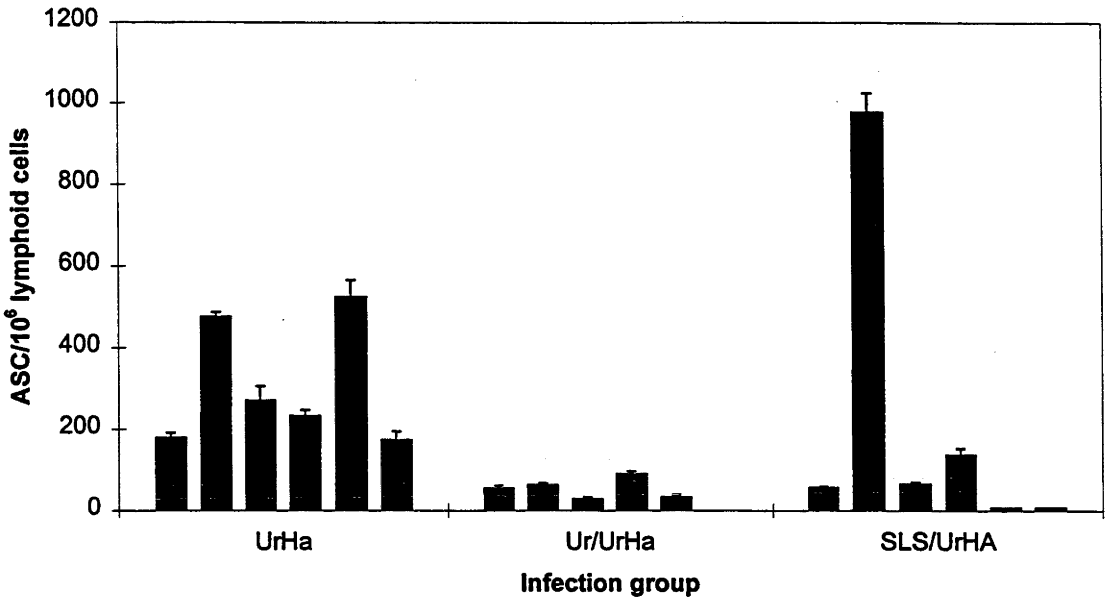

B

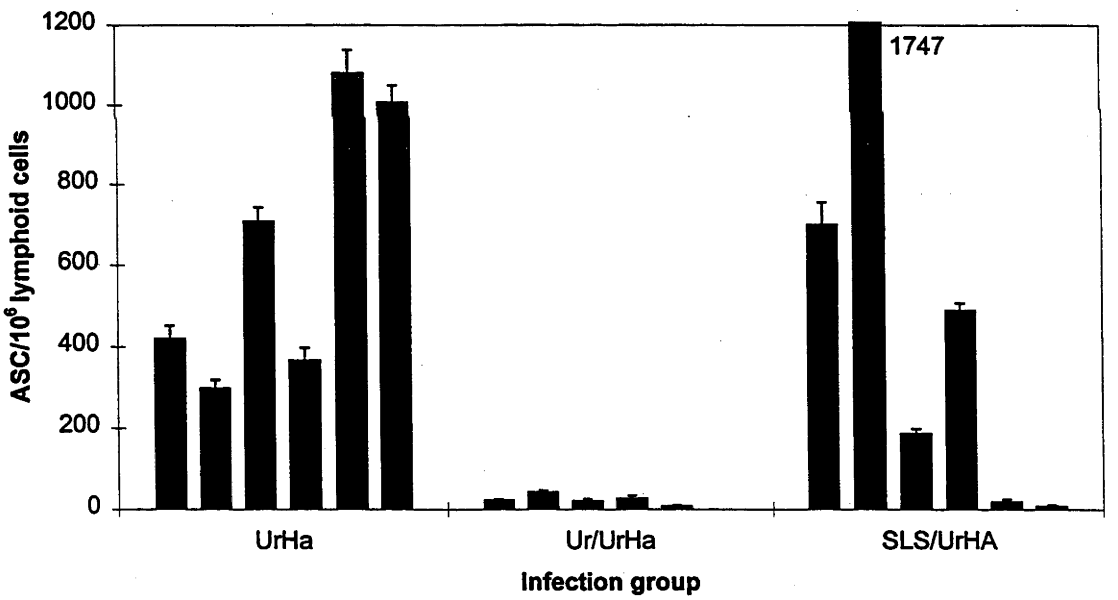

Figure 2.5: Antibody Secreting Cells (ASC) per 10^6 lymphoid cells from the popliteal lymph node of rabbits adjacent to the UrHA inoculation site, secreting specific IgM (**A**) and IgG (**B**) to HA at 10dpi, measured by ELISPOT. Rabbits were infected with UrHA on the left flank (UrHA, n = 6). Rabbits were coinfected on the right flank with either Uriarra (Ur/UrHA, n = 5) or SLS (SLS/UrHA, n = 6). Each column represents the triplicate sample from an individual rabbit ($\pm$SE). 1747 refers to the number of ASC for rabbit number 197 which was off the scale.

A

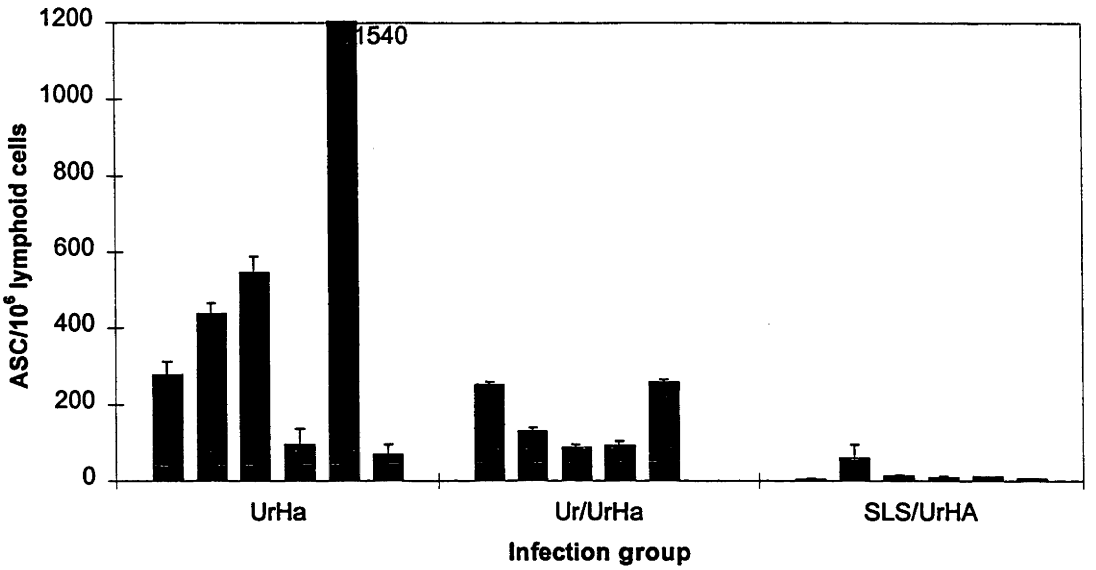

B

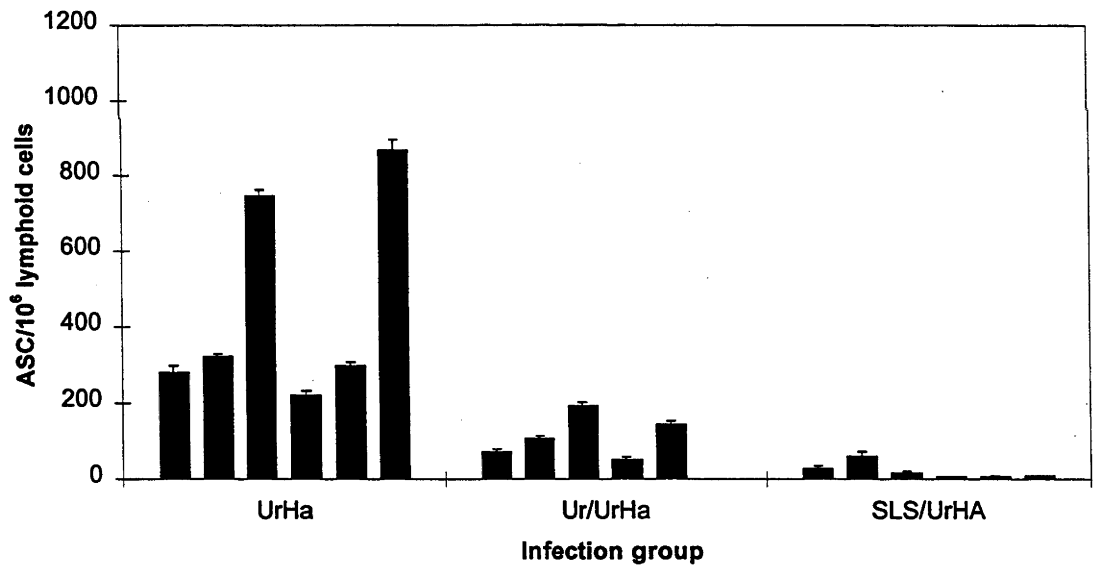

Figure 2.6: Antibody Secreting Cells (ASC) per 10^6 lymphoid cells from the spleen of rabbits, secreting specific IgM (**A**) and IgG (**B**) to HA at 10dpi, measured by ELISPOT. Rabbits were infected with UrHA on the left flank (UrHA, n = 6). Rabbits were coinfected on the right flank with Uriarra (Ur/UrHA, n = 5) or SLS (SLS/UrHA, n = 6). Each column represents the triplicate sample from an individual rabbit ($\pm$SE). 1540 refers to the number of ASC for that individual rabbit which was off the scale.

Table 2.2: Significant differences in specific IgM or IgG responses (Mann Whitney U test, $P<0.05$) to HA at 10dpi measured by ELISA or ELISPOT between groups of rabbits infected with Uriarra and UrHA (Ur/UrHA), SLS and UrHA (SLS/UrHA) or UrHA alone. (ND) no difference, (L) significantly less than. (*) indicates significance when rabbit 197 (identification number) was omitted from the analysis (see 2.3.1.4).

	ELISA	ELISPOT	
		Lymph Node	Spleen
Ur/UrHA with respect to UrHA			
IgM	ND	L	L
IgG	L	L	L
SLS/UrHA with respect to UrHA			
IgM	ND	ND/L*	L
IgG	L	ND/L*	L
SLS/UrHA with respect to Ur/UrHA			
IgM	L	ND	L
IgG	L	ND	L

2.3.1.6 Expression of HA and myxoma virus antigens at 10dpi

To determine whether UrHA replication was suppressed by coinfection, HA expression was examined in cells of the primary UrHA skin lesion, the draining lymph node and spleen of infected rabbits by indirect immunofluorescence. This provided an indirect estimate of UrHA replication. At 10dpi, HA was expressed in the lesions at the UrHA inoculation site in animals inoculated with UrHA alone and following both attenuated and virulent coinfections. The HA antigen was expressed in epidermis, apparently on the surface of cells (Figures 2.7A and C). There were no differences in the intensity of

fluorescence in any of these sections suggesting that expression of HA was not reduced by the coinfection strategy. Myxoma virus antigen was also detected by immunofluorescence in the epidermis of lesions (data not shown). In the popliteal lymph node adjacent to the UrHA inoculations site from all infections, HA antigen was detected by immunofluorescence at 10dpi, on the surface of lymphocytes in the paracortex. The number of lymphocytes expressing HA was low, at approximately one to five positive cells per $60mm^2$ of tissue (Figures 2.7B and D). HA antigen was detected on the surface of lymphocytes in the spleen of only one animal.

2.3.2 Modulation of lymphocyte proliferation in response to *in vitro* mitogen stimulation

2.3.2.1 Lymphocyte proliferation assays

At 10dpi, lymphoid cell cultures from the spleen and popliteal lymph node of rabbits from the coinfection experiments were stimulated with the mitogen Con A for 24 hours and the subsequent incorporation of ^{3}H-T into DNA measured as an index of cell proliferation. Figure 2.8 presents the Con A-induced proliferation response of lymphocytes from individual rabbits (mean of triplicate samples $\pm$ SE), and the pooled background level of cell proliferation without mitogen stimulation (no Con A) for all rabbits infected with either UrHA, UrHA/Uriarra, or UrHA/SLS, and uninfected rabbits. Cells from the lymph node and spleen of rabbits infected with UrHA alone (n=6) incorporated very high levels of ^{3}H-T, greater than 2×10^5 cpm (counts per minute). Incorporation of ^{3}H-T by lymphocytes from rabbits coinfected with UrHA/Uriarra (n=5) was not different to that from uninfected rabbits (n=4). Lymphocytes from rabbits inoculated with UrHa/SLS (n=6) did not respond to mitogenic stimulation. In each group of infected animals, the mean cpm from the lymph node was 1.5 to 6 fold greater than from the spleen.

Figure 2.7: Immunolocalisation of HA antigen expressed by UrHA-infected cells in tissue sections from rabbits infected with UrHA alone or coinfected with UrHA/SLS. Sections were labeled with rat anti-HA polyclonal antibody. HA-positive epidermal cells of the primary skin lesion **(A)** and lymphocytes from the popliteal lymph node adjacent to the UrHA primary lesion **(B)** from a UrHA infected rabbit. HA-positive epidermal cells of the primary skin lesion at the UrHA inoculation site **(C)** and lymphocytes from the popliteal lymph adjacent to the UrHA primary lesion **(D)** from a UrHA/SLS coinfected rabbit. E, epidermis; d, dermis. Bars represent (A) 100μm, (B) 25μm, (C) 120μm, (D) 10μm.

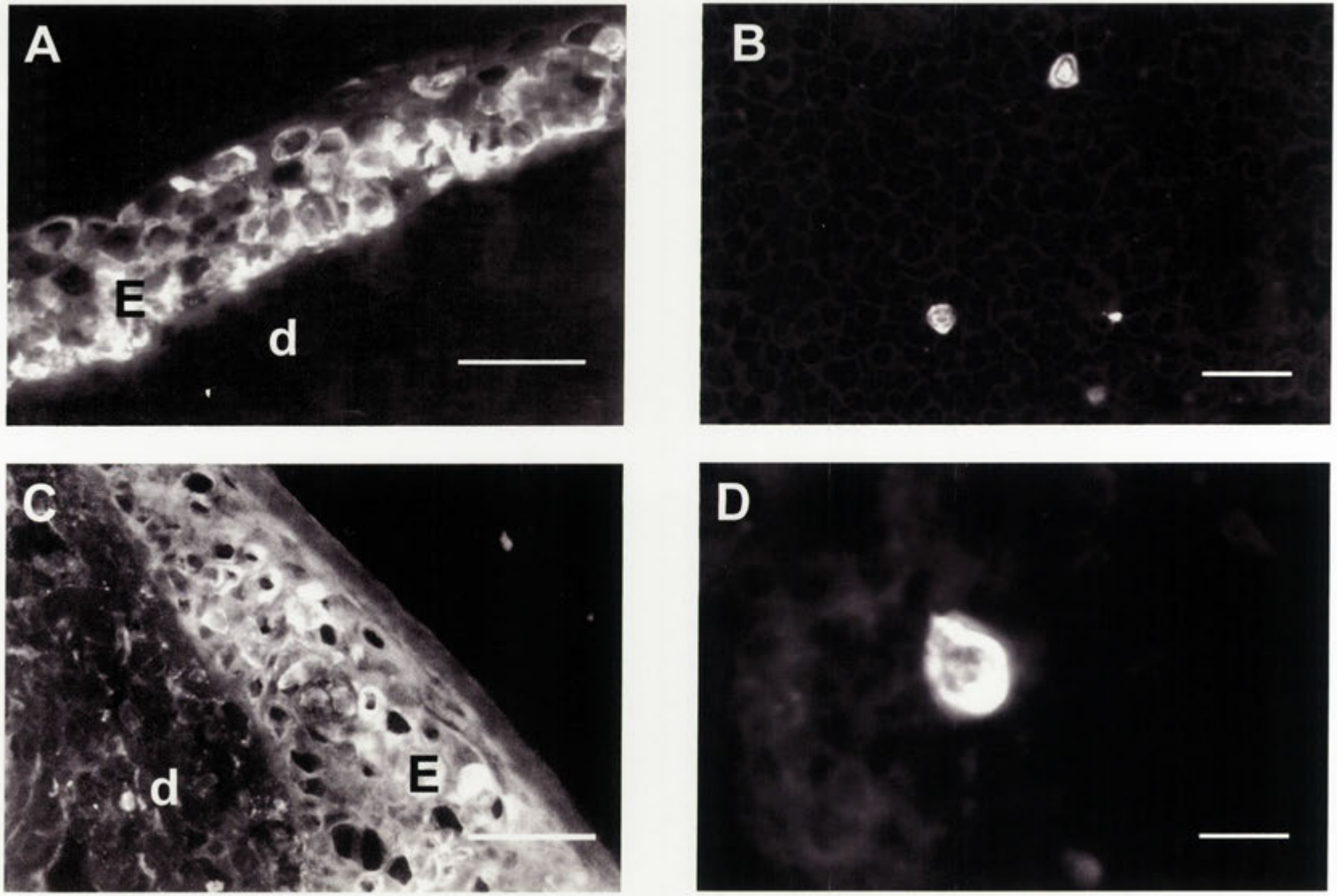
A
E
d
B
C
d
E
D

A

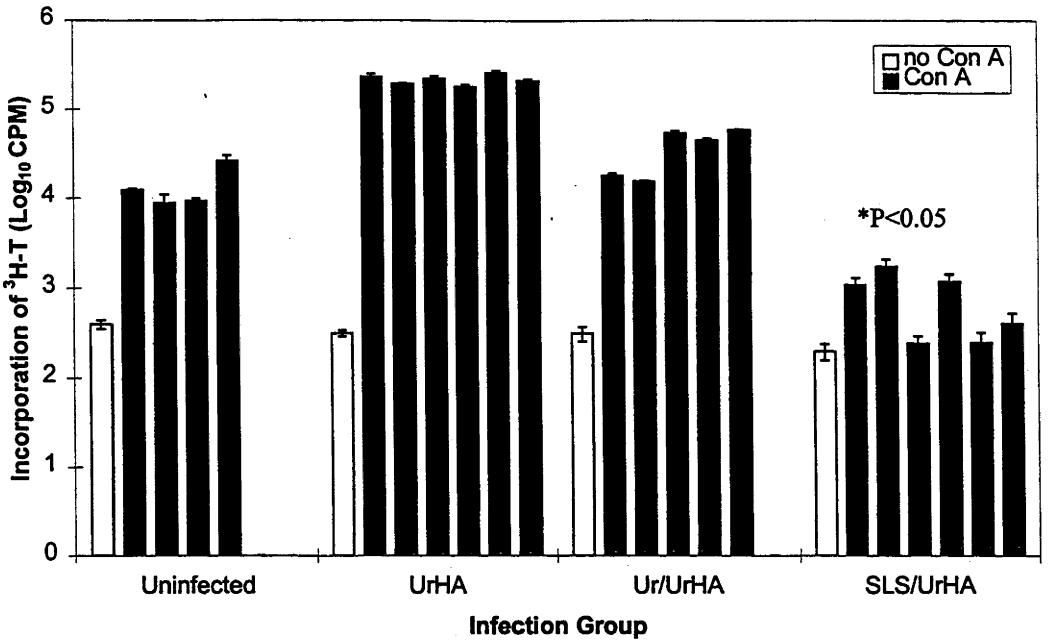

B

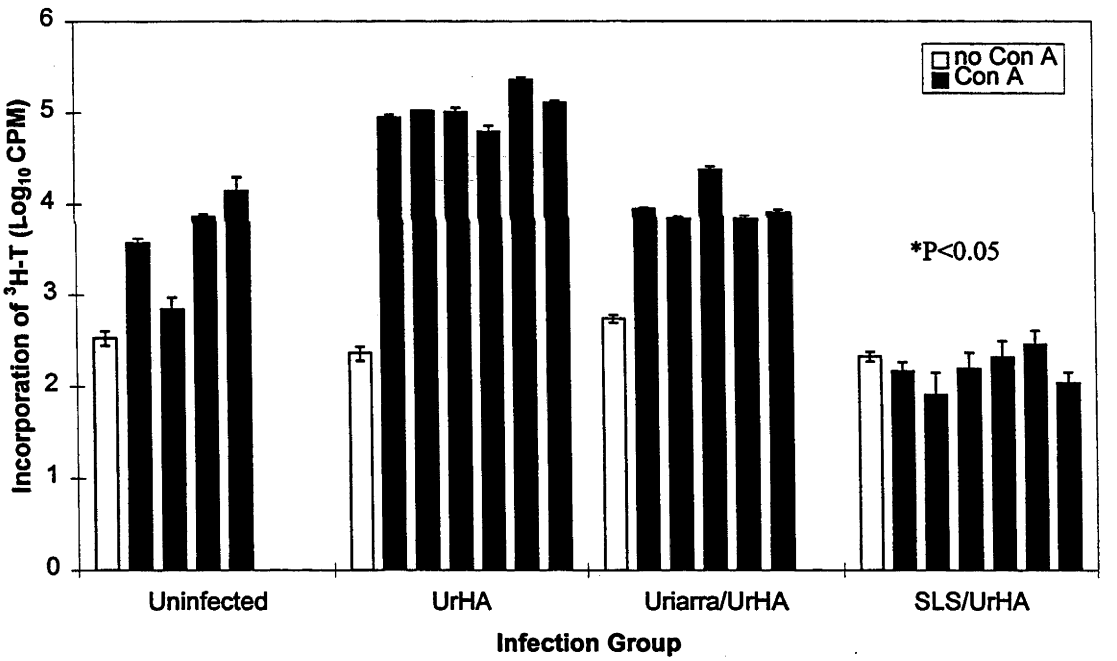

Figure 2.8: Con A stimulation of lymphocytes from the (**A**) regional lymph node and (**B**) spleen of individual rabbits infected with UrHA (n=6), UrHA and Uriarra (n=5) or UrHA and SLS (n=6) (mean ± SE of triplicate samples). Lymphocyte proliferation was measured from uninfected rabbits (n=4) as controls. Lymphocytes were stimulated with Con A, and the incorporation of [^{3}H]thymidine into proliferating cells measured in counts per minute (CPM). Controls of lymphocytes cultured without Con A were included for each rabbit, and are given as the mean of all rabbits for each group of infected rabbits (mean ± SE). A significant decrease in lymphocyte proliferation was seen in the SLS/UrHA group compared to uninfected rabbits ($P<0.05$, Mann-Whitney U test).

2.3.2.2 Lymphocyte proliferation responses to mitogen following single infection of rabbits with SLS or Uriarra

Significant suppression of the mitogen-induced proliferation of lymphocytes from rabbits coinfected with SLS was shown at 10dpi in the previous experiment. However, this suppression was potentially complicated by the infection of rabbits with two viruses. To refine these measurements, mitogen-induced proliferative responses of lymphocytes was examined in rabbits infected with either SLS or Uriarra at 4, 7 and 10dpi. These responses were measured from the lymph node draining the inoculation site of the hind foot so that the opposite popliteal lymph node could be used as a control. The design of these experiments was set up to take into account the variation in responses observed during the coinfection experiments to give statistical validity using an outbred population of rabbits. This variation included day to day variation in the proliferation assay, and the variable responses of individual rabbits as the lymphocytes from some normal control rabbits are not responsive to mitogen stimulation.

2.3.2.2.1 Statistical analysis of lymphocyte proliferation responses

To standardise variation between rabbits and between assays, rabbits were infected with virus in a random block design, which enabled the treatment of variation at two levels or strata; comparing the effect of day of killing, and the effect virus infection had at each time post infection (4, 7 or 10dpi). Non-parametric analysis is often regarded as less stringent than parametric analysis. To achieve statistical significance in a parametric test, direct comparisons between effects of infection with virulent and attenuated myxoma viruses were not incorporated into the experimental design. This was so that the sample size (n) could be as large as possible to effectively determine if the individual viruses had an effect outside the sources of variation. However, this comparison between the effect of virulent and attenuated myxoma virus was made *a posteriori* by ANOVA.

The statistical analysis used and the parameters measured are summarised in Table 2.3, and critical F values from ANOVA are provided in Table 2.4. One output of ANOVA is the least significant difference, which is the error bar displayed for Figure 2.9 to Figure 2.14 inclusively. The least significant difference is not a description of variation of the original measurements of CPM which are shown on the y-axis, but rather an

indication of variation across the entire experiment incorporating both strata of analysis (day of killing and effect of virus infection) and is based on log transformed data.

Table 2.3: Statistical tests used to determine significant effects of virulent and attenuated myxoma virus infection on the *in vitro* proliferation of rabbit lymphocytes infected *in vivo*.

Statistical test	Parameters measured
Two-way ANOVA	• effect of day of killing • effect of virus infection at each individual time post infection (4, 7 or 10dpi)
Tukey test	• multiple pairwise comparison of means to determine which time points are significantly different from uninfected controls
Multi-variate ANOVA	• comparison of significant effects between virulent and attenuated myxoma virus infection

2.3.2.2.2 Proliferative responses of lymphocytes from rabbits infected with Uriarra or SLS

Con A-induced proliferation of lymphocytes from the draining lymph node of rabbits infected with SLS was significantly suppressed at 4dpi and 10dpi, but not at 7dpi compared to that of uninfected rabbits (Figure 2.9 A). Proliferation of lymphocytes, in response to Con A, from the contralateral lymph node was suppressed at 7dpi, but not at 4dpi or 10dpi, compared to that from uninfected rabbits (Figure 2.9 B). PHA-induced proliferation of lymphocytes from the draining lymph node of rabbits infected with SLS was significantly suppressed at 4dpi and 10dpi, but not at 7dpi. At 7dpi, PHA-induced lymphocyte proliferation from these rabbits was significantly greater than at 4dpi (Figure 2.10 A). Proliferation of lymphocytes in response to PHA stimulation from the contralateral lymph node was significantly decreased at all time points of 4, 7 and 10dpi compared to that from uninfected rabbits ($P<0.05$) (Figure 2.10 B).

Lymphocytes from the draining or contralateral lymph nodes of SLS infected rabbits responded to stimulation with LPS at the same level as those from uninfected rabbits at all time points post infection (Figure 2.11).

Following infection of laboratory rabbits with Uriarra, lymphocytes harvested from the lymph nodes at 4, 7 or 10 dpi had no significant decrease in the incorporation of ^{3}H-T following Con A (Figure 2.12) or PHA stimulation (Figure 2.13) compared to lymphocytes from nodes of uninfected rabbits.

Following LPS stimulation of lymphocytes from Uriarra infected rabbits, there was no significant difference in the incorporation of ^{3}H-T into DNA of cells from the draining or contralateral lymph nodes compared to that of stimulated lymphocytes from the nodes of uninfected rabbits. At 10dpi, there was a trend towards an increased level of proliferation, although this was not significantly greater than that from uninfected rabbits at a probability level of 0.05 (Figure 2.14).

The effect of infection of rabbits with SLS on Con A- and PHA-induced proliferation of lymphocytes from both the draining and contralateral lymph node was significantly different from infection with Uriarra ($P<0.05$) (Table 2.4). There was no significant difference in LPS-induced proliferation of lymphocytes between rabbits infected with SLS or Uriarra.

Table 2.4: Obtained F values following statistical analysis by ANOVA of mitogen-stimulated proliferation of lymphocytes from the draining and contralateral lymph nodes of laboratory rabbits. An asterix indicates a significant value at a probability level of 0.05. The critical F value ($F_{0.05\,(1)\,3,14}$) was 3.34.

	Con A		PHA		LPS	
	SLS	Uriarra	SLS	Uriarra	SLS	Uriarra
Draining lymph node	8.186*	2.264	15.447*	2.99	1.447	3.105
Contralateral lymph node	5.458*	3.735*	9.845*	2.62	0.529	3.22

A

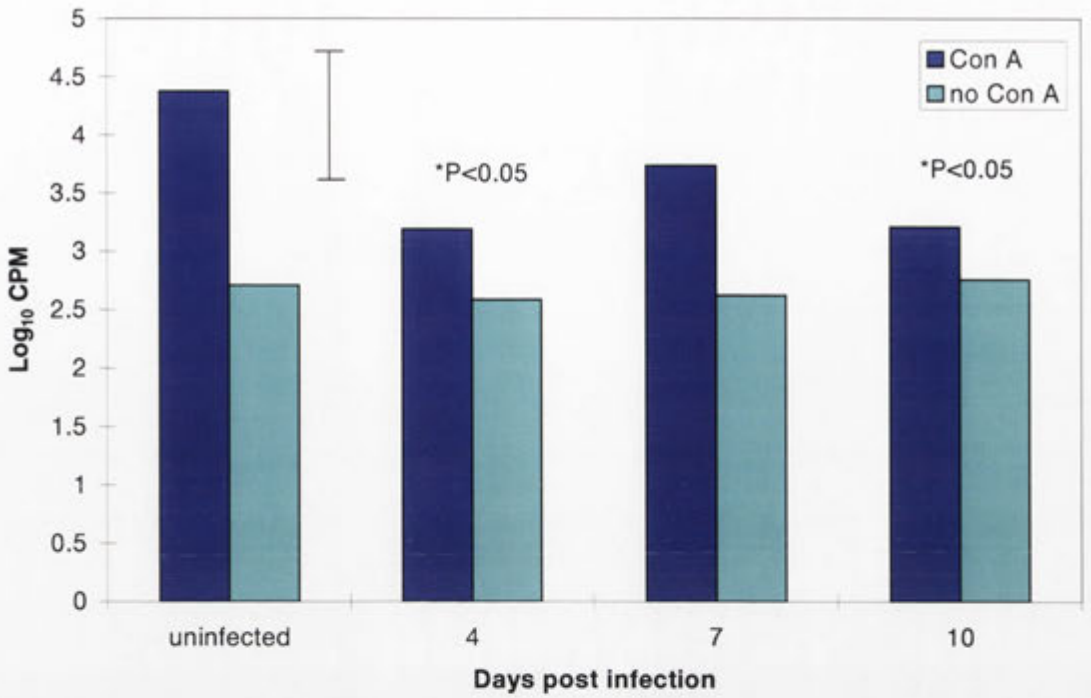

B

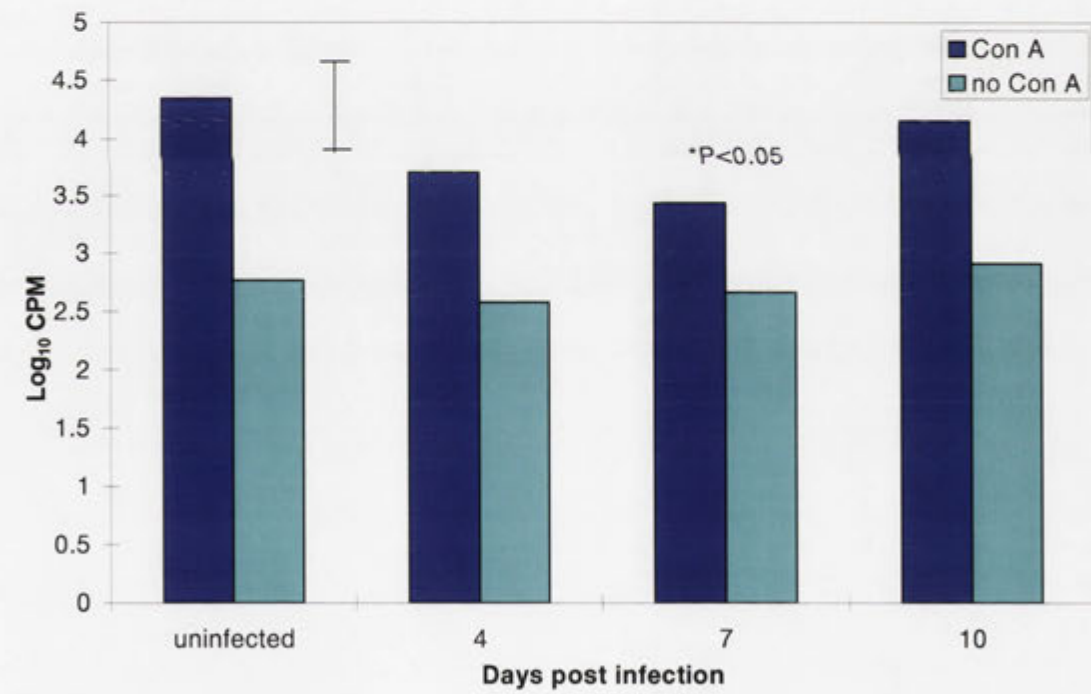

Figure 2.9: Con A stimulation of lymphocytes from the (**A**) draining and (**B**) contralateral popliteal lymph nodes of laboratory rabbits infected with SLS. Four SLS infected rabbits were killed at each of 4, 7 and 10dpi, the lymphocytes from lymph nodes stimulated with Con A, and the incorporation of [^{3}H]thymidine into proliferating cells measured in counts per minute (CPM). Control rabbits were injected with PBS, with two rabbits killed at each time point, and the data pooled. A significant decrease in lymphocyte proliferation compared to uninfected rabbits is indicated (at $P<0.05$). Error bar represents the least significant difference derived from ANOVA.

A

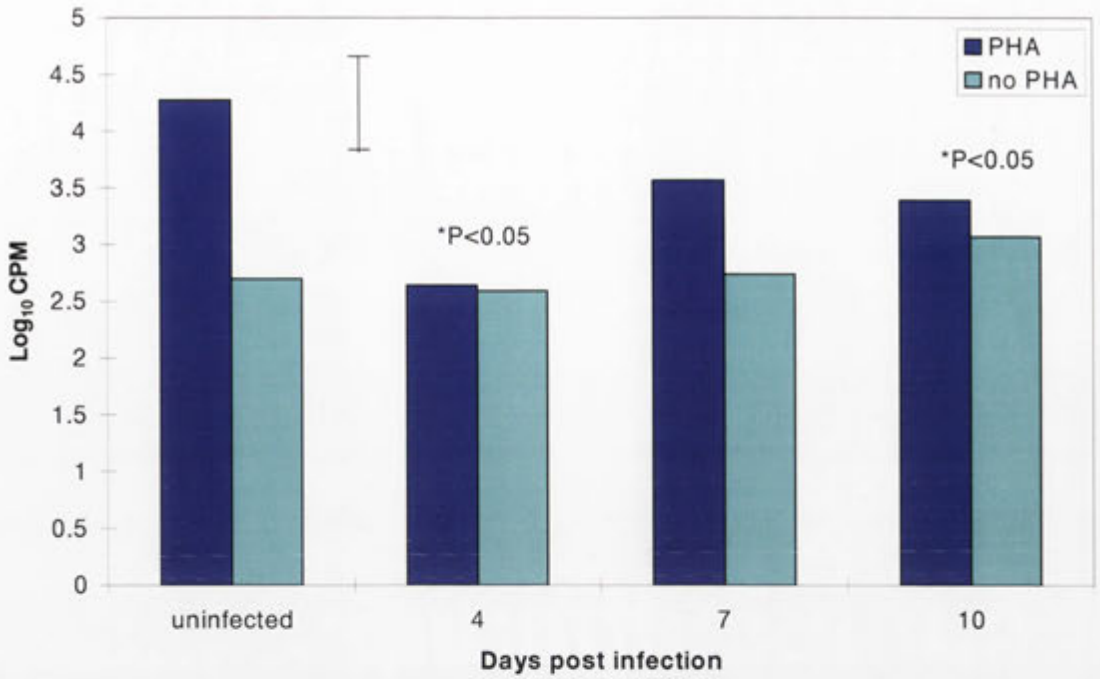

B

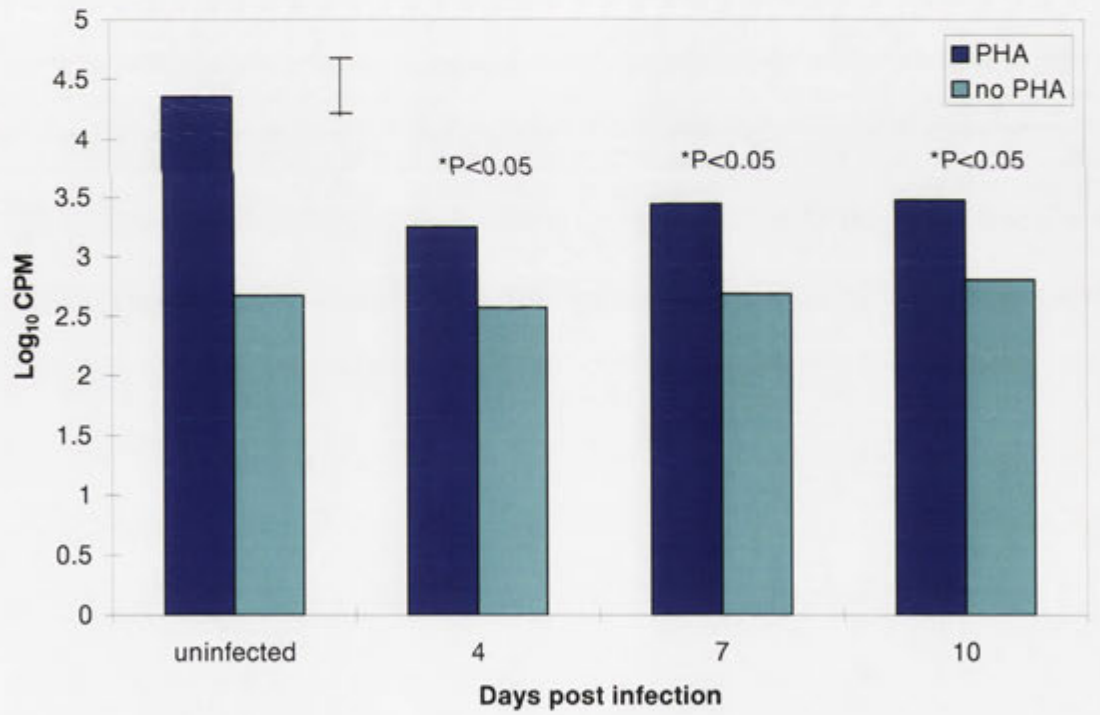

Figure 2.10: PHA stimulation of lymphocytes from the (**A**) draining and (**B**) contralateral popliteal lymph nodes of laboratory rabbits infected with SLS. Four SLS infected rabbits were killed at each of 4, 7 and 10dpi, the lymphocytes from lymph nodes stimulated with PHA, and the incorporation of [^{3}H]thymidine into proliferating cells measured in counts per minute (CPM). Control rabbits were injected with PBS, with two rabbits killed at each time point, and the data pooled. A significant decrease in lymphocyte proliferation compared to uninfected rabbits is indicated (at P<0.05). Error bar represents the least significant difference derived from ANOVA.

A

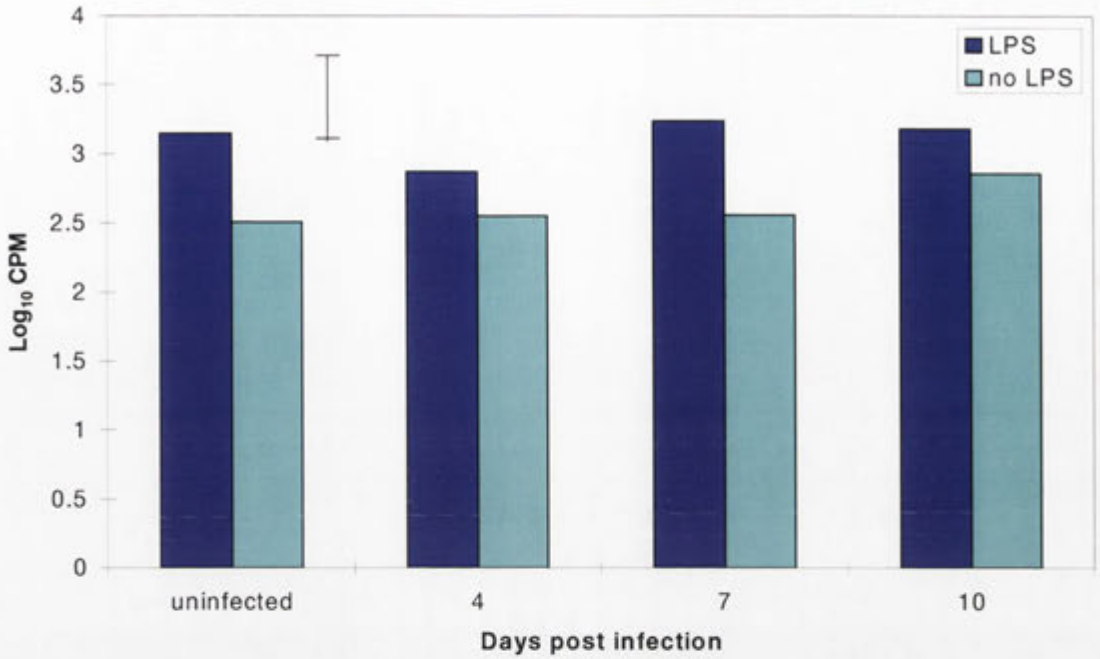

B

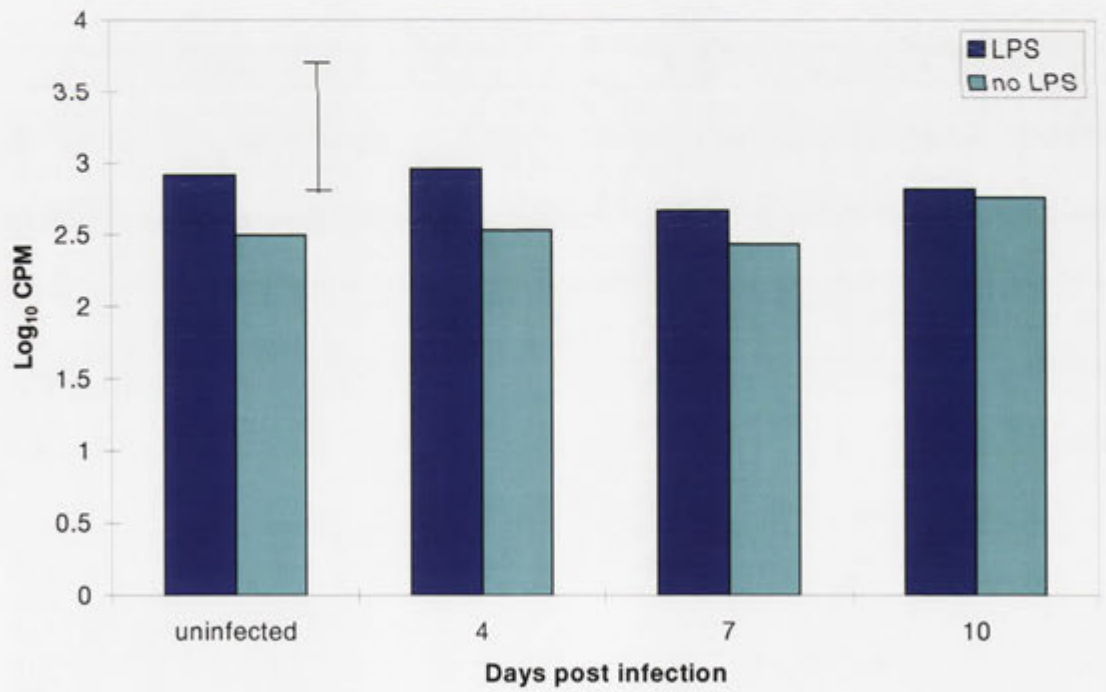

Figure 2.11: LPS stimulation of lymphocytes from the (**A**) draining and (**B**) contralateral popliteal lymph nodes of laboratory rabbits infected with SLS. Four SLS infected rabbits were killed at each of 4, 7 and 10dpi, the lymphocytes from lymph nodes stimulated with LPS, and the incorporation of [^{3}H]thymidine into proliferating cells measured in counts per minute (CPM). Control rabbits were injected with PBS, with two rabbits killed at each time point, and the data pooled. Error bar represents the least significant difference derived from ANOVA.

A

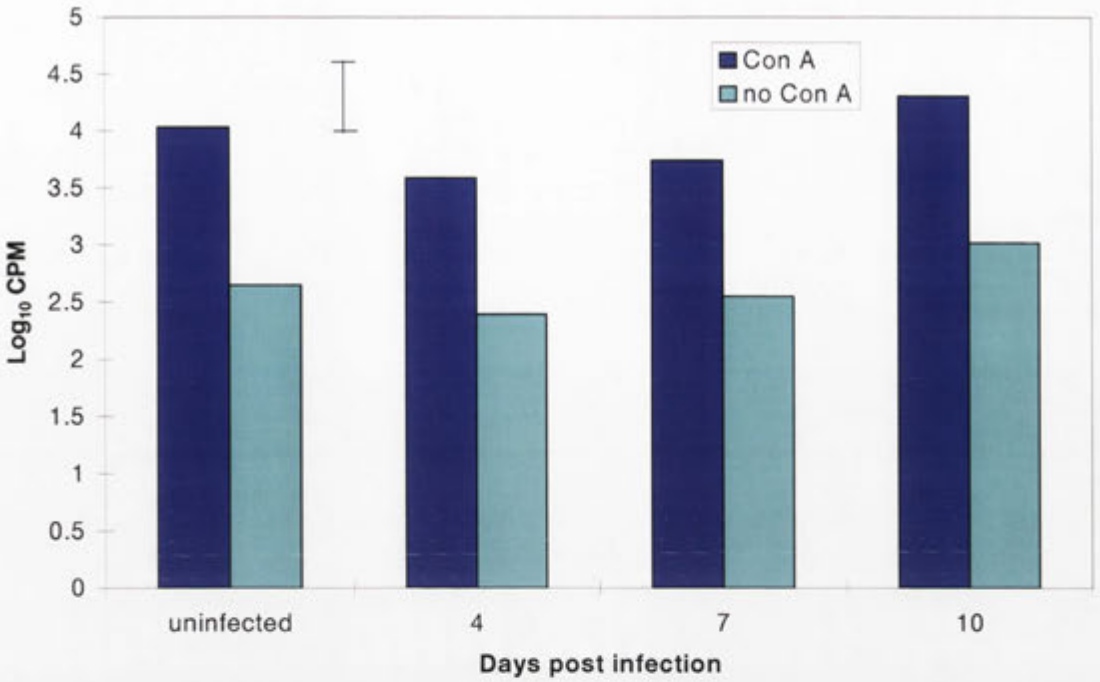

B

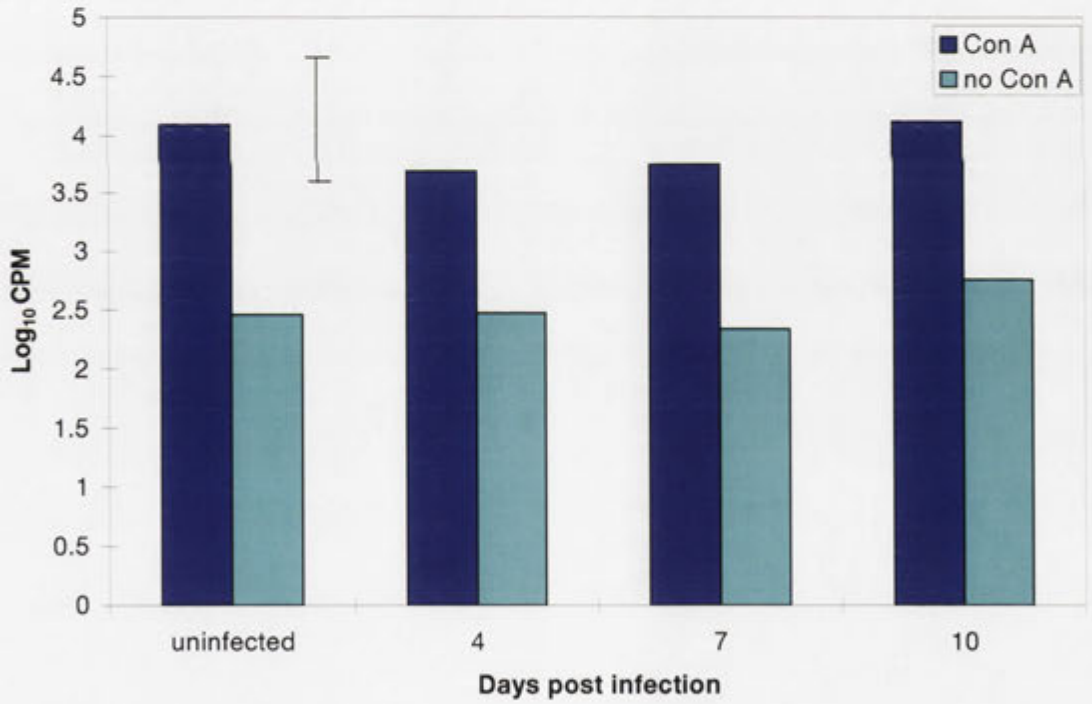

Figure 2.12: Con A stimulation of lymphocytes from the (**A**) draining and (**B**) contralateral popliteal lymph nodes of laboratory rabbits infected with Uriarra. Four Uriarra infected rabbits were killed at each of 4, 7 and 10dpi, the lymphocytes from lymph nodes stimulated with Con A, and the incorporation of [^{3}H]thymidine into proliferating cells measured in counts per minute (CPM). Control rabbits were injected with PBS, with two rabbits killed at each time point, and the data pooled. Error bar represents the least significant difference derived from ANOVA.

A

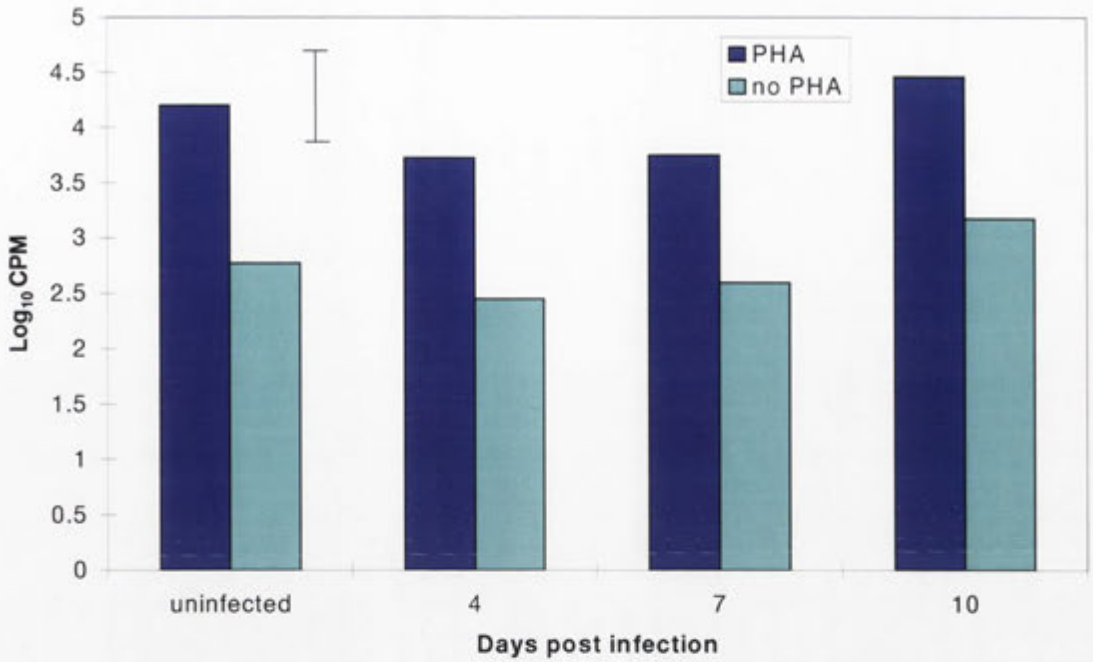

B

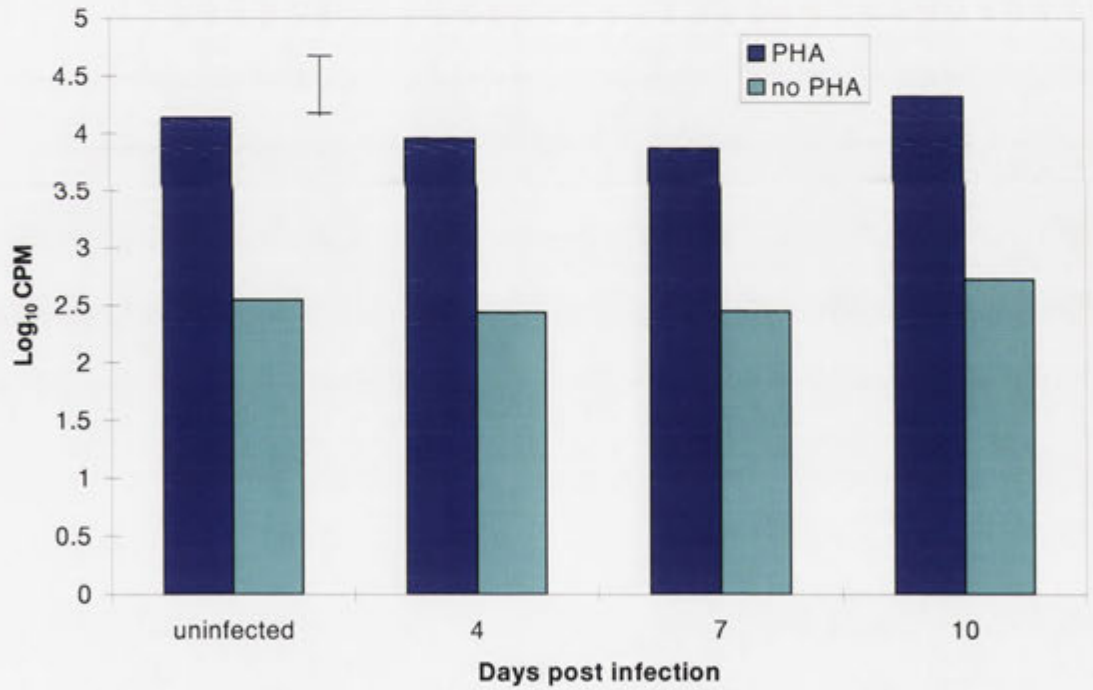

Figure 2.13: PHA stimulation of lymphocytes from the (**A**) draining and (**B**) contralateral popliteal lymph nodes of laboratory rabbits infected with Uriarra. Four Uriarra infected rabbits were killed at each of 4, 7 and 10dpi, the lymphocytes from lymph nodes stimulated with PHA, and the incorporation of [^{3}H]thymidine into proliferating cells measured in counts per minute (CPM). Control rabbits were injected with PBS, with two rabbits killed at each time point, and the data pooled. Error bar represents the least significant difference derived from ANOVA.

A

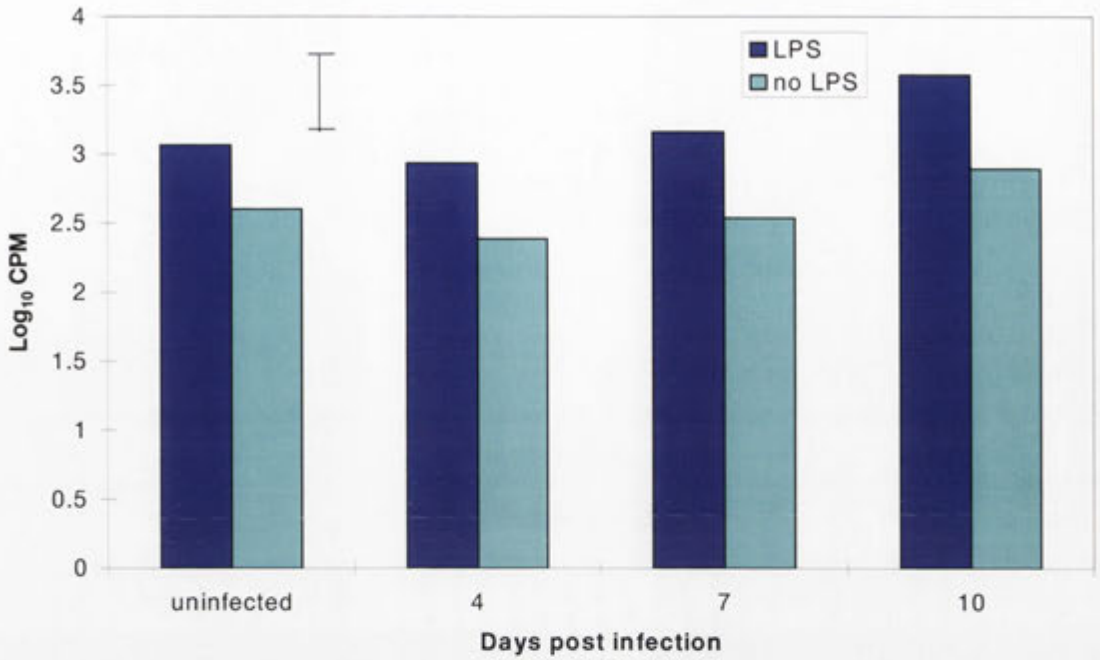

B

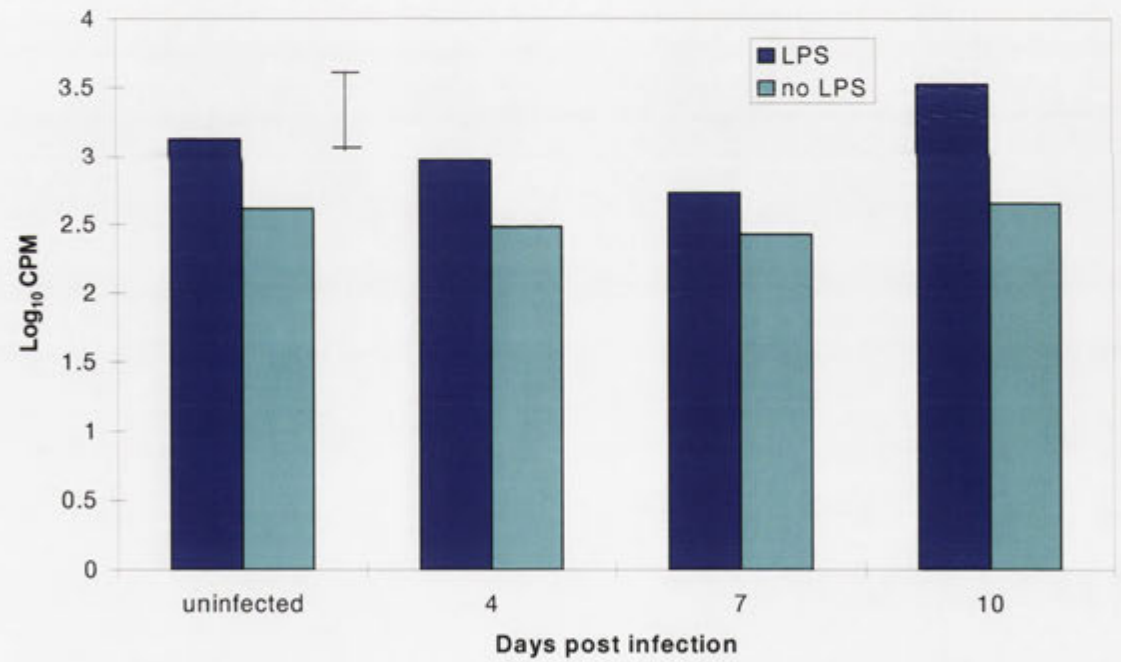

Figure 2.14: LPS stimulation of lymphocytes from the (**A**) draining and (**B**) contralateral popliteal lymph nodes of laboratory rabbits infected with Uriarra. Four Uriarra infected rabbits were killed at each of 4, 7 and 10dpi, the lymphocytes from lymph nodes stimulated with LPS, and the incorporation of [^{3}H]thymidine into proliferating cells measured in counts per minute (CPM). Control rabbits were injected with PBS, with two rabbits killed at each time point, and the data pooled. Error bar represents the least significant difference derived from ANOVA.

2.3.2.3 Histological observations of the spleen and popliteal lymph node

At 10dpi, lymph nodes from rabbits infected with UrHA alone or coinfected with UrHA/Uriarra, showed both B- and T-cell dependent areas densely populated with lymphocytes and pronounced germinal centre formation, indicative of a functioning immune response. Lymph nodes contained few neutrophils (Figure 2.15 A). In contrast, lymph nodes from laboratory rabbits coinfected with SLS were extensively depleted of lymphocytes. However, even at this advanced stage of disease, parts of the lymph node from SLS coinfected rabbits appeared relatively normal with some B- and T-dependent areas being well populated with lymphocytes. More specifically, losses of lymphocytes were consistently evident at the periphery of the nodes between the germinal centres. The germinal centres themselves also had obvious losses of lymphocytes, predominantly from the outer edges of the germinal centre and the side opposite the subcapsular sinus. Within germinal centres, high numbers of nuclear fragments were present. In addition, lymph nodes from SLS coinfected rabbits contained large numbers of neutrophils distributed throughout the nodes, particularly in areas of extensive lymphocyte depletion (Figure 2.15 B)

The histology of the spleen from rabbits spleens from UrHA infected, or UrHA/Uriarra coinfected, rabbits contained well defined germinal centres (Figure 2.15 C). The spleen from rabbits coinfected with UrHA/SLS at 10dpi did not appear markedly different to that from uninfected rabbits. There was little evidence of loss of lymphocytes from the white pulp. However, there was also little evidence of the expansion of lymphocyte populations or the extensive development of germinal centres in these spleens (Figure 2.15 D).

Figure 2.15: Histopathology of the popliteal lymph node and spleen at 10 dpi from rabbits coinfected with myxoma virus. (**A**) The paracortex of the lymph node from UrHA/Uriarra coinfected rabbits is densely populated with lymphocytes. (**B**) The lymph node paracortex from UrHA/SLS coinfected rabbits contains many neutrophils, but few lymphocytes. (**C**) The white pulp of the spleen from UrHA/Uriarra coinfected rabbits is larger and more defined compared to that of SLS infected rabbits (**D**). Tissue sections were stained with haematoxylin and eosin. GC, germinal centre; P, paracortex; M, mantle zone. Arrows indicate the edges of remnants of germinal centres in lymph nodes and the spleen. Bar represents 200μm.


A
P
GC

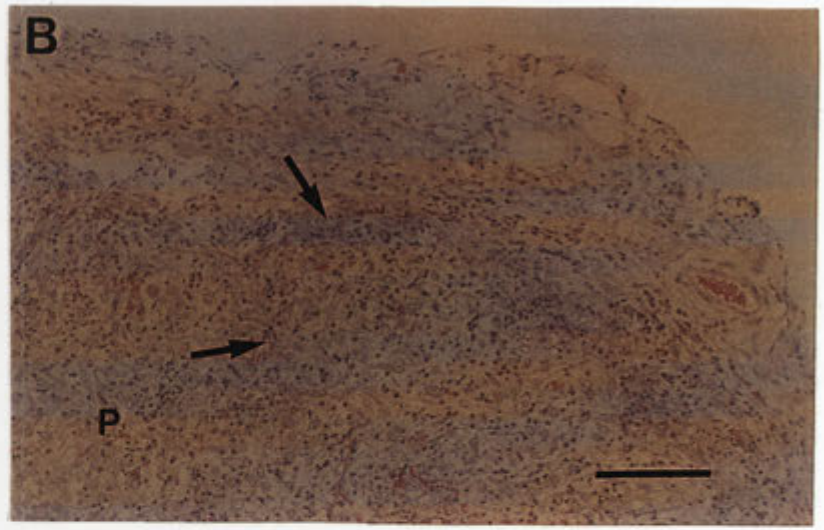
B
P

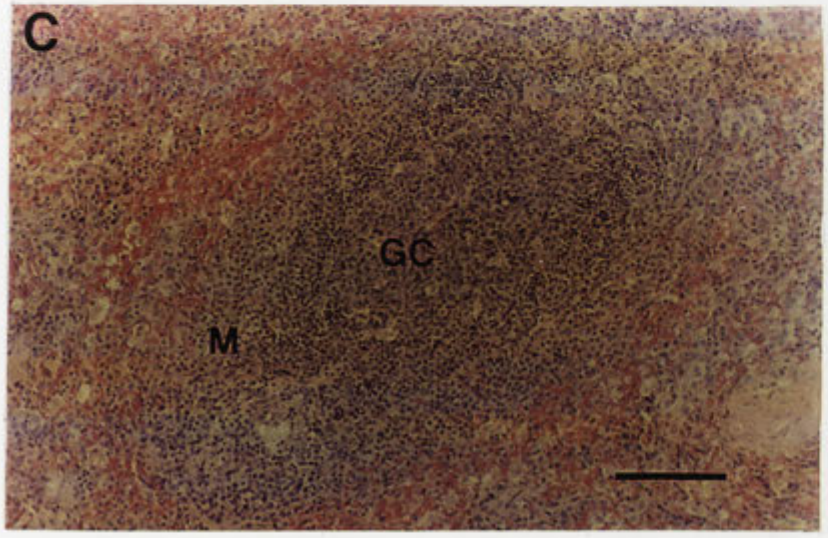
C
GC
M

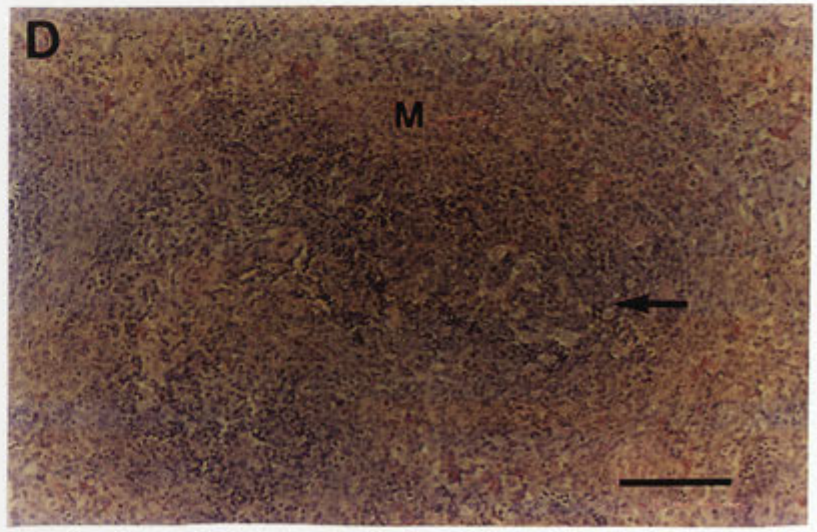
D
M

2.4 Discussion

The suppression of cellular and humoral immune responses has been examined extensively following infection of laboratory rabbits with two viruses that are closely related to myxoma virus, namely malignant rabbit virus and Shope fibroma virus (Strayer, 1992). The study described in this Chapter aimed to determine if suppression of immune functions could be demonstrated following infection of rabbits with myxoma virus, and if such suppression was a function of virulence. To achieve this, two strains of myxoma virus were used; the highly virulent SLS and the naturally attenuated Uriarra, both of which cause clinical myxomatosis in rabbits, but only SLS is uniformly lethal (Fenner and Marshall, 1957; Fountain *et al.*, 1997). The main findings were that firstly, mitogen induced proliferation of T-lymphocytes from rabbits infected with virulent virus was suppressed. Infection of rabbits with virulent myxoma virus also resulted in a rapid decline in rectal temperature from 8dpi, a rapid increase in peripheral WBC counts from 6dpi, a lack of germinal centre formation in lymph nodes and the spleen, and the extensive depletion of lymphocytes from lymph nodes by 10dpi. These responses to infection were all functions of virus virulence, as they were not observed following infection of rabbits with attenuated myxoma virus. Humoral responses were also affected by infection with myxoma virus. IgG titres to a coexpressed antigen (influenza HA) were suppressed in rabbits coinfected with either SLS or Uriarra. However, IgG titres to myxoma virus were strikingly higher in rabbits coinfected with SLS compared to Uriarra.

Virulent myxoma virus suppressed the *in vitro* proliferative responses of T-cells from lymph nodes of infected rabbits to stimulation with either Con A and PHA. In the draining lymph node, significant suppression was measured at 4dpi, well before the development of clinical illness. There was some recovery at 7dpi but suppression was significant again at 10dpi. Suppression at 10dpi was associated with pathological changes in lymph nodes, including the loss of lymphocytes and the infiltration of large numbers of inflammatory cells. Suppression of T-cell proliferation *in vitro* was also observed in cells from the contralateral lymph node of SLS-infected rabbits at 7dpi. In a separate series of experiments, suppression was observed in cells from the popliteal lymph node and spleen of rabbits coinfected with UrHA and SLS at 10dpi (the only timepoint examined). In contrast, infection of rabbits with the attenuated Uriarra strain

of myxoma virus did not cause significant suppression of mitogen-induced T-cell proliferation at any time post infection, and did not cause pathological changes in the lymph nodes at 10dpi. This suggests that these responses are functions of virus virulence.

Strayer *et al.* (1983) showed that suppression of Con A- and anti-immunoglobulin-driven proliferation of lymphocytes from the spleen of rabbits infected with malignant rabbit virus was first apparent at 7dpi, with partial recovery of proliferation at 11dpi (Strayer *et al.*, 1983b). The experiments are not directly comparable with mine as myxoma virus is likely to reach the draining lymph node earlier than the spleen. The more direct comparison between the results of Strayer *et al.* and those presented here may be the contralateral lymph node where suppression was observed at 7dpi, with some recovery at 10dpi.

Two mechanisms of suppression of lymphocyte function have been proposed for malignant rabbit virus. These are the direct replication of virus in lymphocytes (Strayer and Leibowitz, 1986; Strayer *et al.*, 1985) and the virus-induced production of soluble suppressive factor(s) by infected lymphocytes (Strayer *et al.*, 1988). The close genetic relatedness between malignant rabbit virus and myxoma virus suggests that mechanisms of suppression induced by myxoma virus may be similar. At this stage, the viral proteins responsible for this suppression have not been clearly identified for malignant rabbit virus. However, transformation of Shope fibroma virus with fragments of malignant rabbit virus DNA have led to the implication of a putative viral transcription factor in virus-induced effects on lymphocytes (Strayer and Mathew, 1993). Myxoma virus-induced suppression of lymphocyte responsiveness was clearly a function of virulence, however, there is no indication that Uriarra replicates less efficiently in lymph nodes compared to SLS (Fenner and Ratcliffe, 1965). In other experiments in our laboratory, the generation of suppressive factors by lymphocytes infected with myxoma virus *in vitro* could not be demonstrated (Cartledge, 1995).

Suppression of ConA induced T-cell proliferation may operate through the inhibition of crosslinking of cell surface antigens. Myxoma virus specifically downregulates CD4 (Barry *et al.*, 1995) and MHC class I (Boshkov *et al.*, 1992) surface antigens of infected cells, and such downregulation of these and other surface molecules could reduce the

number of surface antigens available for Con A-induced crosslinking. However, malignant rabbit virus infection of lymphocytes does not alter Con A-binding or Con A-stimulated capping (Strayer *et al.*, 1983b), although this virus also downregulates MHC class I surface antigens (Boshkov *et al.*, 1992). An alternative explanation is that viral infection of rabbits may result in lymphocyte anergy due to the partial activation of T-cells in the absence of costimulatory signals such as IL-2. Malignant rabbit virus-infected lymphocytes are defective in the production of, and the ability to respond to, IL-2 (Strayer *et al.*, 1986), the main T-cell growth factor induced in Con A-induced T-cell proliferation.

Further insights into possible mechanisms of virus-induced suppression of lymphocyte proliferation can be drawn from other systems of virus infection. Measles virus infection of peripheral blood lymphocytes *in vitro* causes suppression of lectin-induced proliferation of uninfected lymphocytes through contact between uninfected- and infected-cells. This required cell surface expression of both the F and H measles virus glycoproteins by infected cells (Schlender *et al.*, 1996). This contact appears independent of the production of soluble suppressive factors, and results in partial activation of cells followed by cell cycle arrest with a reduced capacity of uninfected lymphocytes to release or respond to IL-2 (Schnorr *et al.*, 1997). A second strategy of virus-induced immune suppression is the production of immunomodulatory proteins. African swine fever virus (ASFV) encodes a protein, A238L, that inhibits activation of both nuclear factor kappa B (NF-^{K}B) (Powell *et al.*, 1996) and nuclear factor of activated T cells (NFAT) (Miskin, 1998), and hence the gene transcription of host-cell immunoregulatory proteins. Such a protein has not been demonstrated for myxoma virus or malignant rabbit virus, although both viruses produce proteins that function to modulate the host immune response (McFadden, 1995).

As well as suppression of T-cell responsiveness, coinfection of rabbits with SLS resulted in suppression of IgG titres to an unrelated antigen (HA) expressed by the recombinant UrHA myxoma virus. Paradoxically, this was accompanied by the development of greater anti-myxoma virus IgG titres compared to coinfection with Uriarra. Although the experimental systems are quite different, similar results follow the infection of rabbits with malignant rabbit virus, which suppressed the generation of

specific antibody responses to an unrelated antigen (SRBC) inoculated at 4dpi, although rabbits developed substantial virus-neutralising antibody titres before death (Strayer and Leibowitz, 1987a). Serum antibody is normally regarded as having little role in recovery from poxvirus infections. Strayer and Leibowitz (1987a) have suggested that antibody may be involved in clearance of malignant rabbit virus from the spleen by opsonisation and phagocytosis. However, these rabbits die despite the high neutralising titres. The fact that rabbits infected with virulent myxoma virus developed high anti-viral serum IgG titres by 10dpi suggests that the production of anti-viral antibody has little positive effect on the outcome of myxoma virus infection.

The mechanism of myxoma virus-induced modulation of antibody responses is unclear. HA-specific antibody production may be suppressed if, during coinfection of rabbits, growth of virulent myxoma virus is more efficient than that of attenuated virus and suppresses the growth of UrHA and thus the expression of HA. This was not supported by immunofluorescence specific for the HA antigen, as HA was expressed on the surface of epidermal cells in the primary UrHA lesion at 10dpi with either the virulent or attenuated coinfections. HA antigen was also present on the surface of lymphocytes in the draining lymph node following coinfection with SLS, showing that UrHA did reach the draining lymph node during this coinfection; it was also associated with lymphocytes of the spleen.

If direct suppression of HA antigen production is not the cause of decreased antibody production, then it is possible that T-cell responses are critical. The specific production of serum IgG to HA is reduced by infection with virulent myxoma virus which may suggest that T-cells involved in isotype switching of antibody are not effective (Spriggs *et al.*, 1992a). In support of this, germinal centre development in the lymphoid organs of rabbits infected with virulent myxoma virus is inhibited. Germinal centres are the principal sites of isotype switching and affinity maturation of antibody and their development requires $\alpha\beta$ T-cell help (Liu and Arpin, 1997). As already discussed, T-cell proliferation *in vitro* is suppressed by myxoma virulent myxoma virus infection *in vivo*.

In the face of the suppressed IgG response to HA, the increased production of IgG specific for myxoma virus appears paradoxical. Increased anti-viral IgG may be the result of a downregulation of T_H1 T cell responses by virulent myxoma virus, and a consequent upregulation of T_H2 T cell responses. This would result in upregulation of humoral immune responses and a downregulation of CTL responses, which are known to be critical in the control of many poxvirus infections (Buller and Palumbo, 1991; Karupiah *et al.*, 1996). Indeed, myxoma virus is known to produce specific proteins that bind and inhibit T_H1 associated cytokines, particularly IFN^{γ} (Mossman *et al.*, 1995a; Upton *et al.*, 1992).

It is possible that the humoral response in coinfections represents a form of antigenic competition. However, a conventional mechanism for this during myxoma virus coinfection is unclear. Antigenic competition is described as the inhibition of the humoral immune response to one antigen by the introduction of a second antigen or determinant that is thought to compete for recognition by T-cell receptors (Guery *et al.*, 1993; Lakey *et al.*, 1986; Taussig, 1973). The conditions under which antigenic competition is most pronounced are when the antigens are structurally similar, the antigen to which the response is suppressed is introduced one to seven days after the first antigen, the dosage of the first antigen is greater than the second and the antigens are introduced into the same site (Adorini and Nagy, 1990; Babbitt *et al.*, 1986; Pross and Eidinger, 1974). A particular example is the antibody responses to bacterial pili subtypes administered as vaccines (Hunt *et al.*, 1995). The conditions described are not very similar to those in this experiment although the coinfection experiments may provide suitable conditions for antigenic competition through the inoculation of rabbits with replicating viruses that specifically disseminate to sites of antibody production (lymph nodes and spleen).

A third explanation for the alteration of humoral immune responses by virulent myxoma virus is through the generation of T-cell independent (TI) antibody responses. Viruses with highly repetitive epitopes, such as those of the glycoprotein of vesicular stomatitis virus (VSV), can extensively crosslink B-cell receptors. This results in in the $^{\alpha\beta}$ T cell-independent activation of B-cells and the production of virus-specific IgM and IgG (Bachmann and Zinkernagel, 1996; 1997) in the absence of germinal centre formation

(Maloy *et al.*, 1998). Polyomavirus infection of T-cell-deficient mice induced TI isotype switching from IgM to IgG, also without the formation of germinal centres in lymph nodes (Szomolanyi-Tsuda *et al.*, 1998). Interestingly, the co-administration of live virus and repetitive virus like-particles (VPLs) resulted in IgG production specific for the virus but not the VLPs, indicating that live virus was required to elicit the response (Szomolanyi-Tsuda *et al.*, 1998). Myxoma virus-specific IgG production may be a TI event, with a higher local concentration of antigen due to the potential greater growth of virulent myxoma virus resulting in greater IgG production (Szomolanyi-Tsuda *et al.*, 1998). In contrast, HA-specific IgG production may require the help of T-cells. It is possible that the suppressed T-cell responses in rabbits infected with virulent myxoma virus favours this outcome. TI antibody production does not occur in mice infected with vaccinia virus (Bachmann and Zinkernagel, 1996). However, myxoma virus is more lethal to rabbits than vaccinia virus is to mice and the regulation of immune responses to infection may differ substantially between both rabbits and mice, and between the different viruses.

The suppression of T-cell responsiveness, lymphocytotoxicity *in vivo* and generation of high anti-viral antibody titres by virulent myxoma virus in contrast to attenuated myxoma virus appear to be critical to the outcome of infection. Laboratory rabbits infected with SLS die within 10-14 dpi whereas laboratory rabbits infected with Uriarra develop severe clinical disease but survive infection. Previous experimental data (Fenner and Ratcliffe, 1965) suggests little difference in titres of SLS or Uriarra in draining lymph nodes. However, the results in this Chapter suggest a critical difference at this level. It is likely that interactions between rabbit lymphocytes and myxoma virus *in vitro* will strongly resemble the paradigms described for malignant rabbit virus *in vitro*. However, these events have not been examined in detail for myxoma virus *in vivo*. In particular, histological observations showed extensive lymphocytotoxicity *in vivo* for myxoma virus (although not for malignant rabbit virus) but the virus does not appear lymphocytoxic *in vitro* (Barry *et al.*, 1997; Macen *et al.*, 1998; Macen *et al.*, 1996a; Macen *et al.*, 1996b; Mossman *et al.*, 1996a; Petit *et al.*, 1996; Strayer *et al.*, 1985). In the succeeding Chapters, the replication of SLS and Uriarra *in vivo* and the cells infected will be investigated. The results obtained with virulent versus attenuated infection of laboratory rabbits with no resistance to myxoma virus suggest that infection of resistant rabbits may mimic that of laboratory rabbits infected with attenuated virus.

These relationships between laboratory and wild rabbits infected with virulent or attenuated myxoma virus will be explored.

Chapter 3: Replication and control of myxoma virus in European rabbits

3. Replication and control of myxoma virus in European rabbits

3.1 Introduction

In the years following the introduction of myxoma virus into the Australian wild rabbit population, two closely linked events were described. Firstly, the predominant strains of virus in the field were less virulent than the originally introduced SLS, with most field strains isolated being of the attenuated grade III or IV phenotype. This was due to the more efficient transmission of attenuated virus strains. The emergence of attenuated field strains of myxoma virus, which allowed the survival of over 10% of infected rabbits in the field, was probably directly responsible for the rapid selection for rabbits genetically resistant to myxomatosis (Marshall and Fenner, 1958). While a considerable amount of molecular analysis has been performed on myxoma virus, very little has been done concerning the differences between the pathogenesis of virulent and attenuated strains of virus, and there is nothing known of the mechanism of resistance of wild rabbits to myxomatosis.

In Chapter 2 it was shown that the ability of rabbits to mount a cellular response, indicated by T-cell mitogen responses *in vitro*, at least partially determined the outcome of infection. However, rabbits infected with SLS developed a strong humoral immune response to the virulent virus that was associated with lethal disease. These results indicated that early events in the immune response were important in determining the outcome of infection, but did not show how these events were related to virus growth and dissemination within the rabbit. The differences in T-cell responses from the draining lymph node and the pathology of the lymph nodes suggested that lymphoid tissue was critical in control of virus infection. In addition, the response of wild rabbits with a degree of genetic resistance to infection was not examined and in particular, whether resistant rabbits respond to infection with virulent virus in the same manner as laboratory rabbits respond to infection with attenuated virus was not explored.

The basic pathogenesis of virulent myxoma virus was described for laboratory rabbits infected with SLS by Fenner and Woodroofe (1953). Following intradermal inoculation, myxoma virus initially replicated in the skin at the primary inoculation site and in the lymph node draining the inoculation site. Virus titres reached greater than 10^7 ID_{50} per gram in both of these tissues. Virus was not found free in the blood, but was detected in blood leucocytes from 3dpi. These are presumed to be critical for systemic spread of myxoma virus. Virus was also present in the spleen and lung but did not generally reach high titres in these tissues. Virus was first detected in an uninoculated skin site situated opposite to the inoculation site at 3dpi, and reached approximately 10^7 ID_{50} per gram by 8dpi. Small, reddened swellings, or secondary lesions, in uninoculated skin were evident from 6dpi. Virus titre increased steadily in all affected organs during infection until a day or so before death when they generally declined (Fenner and Woodroofe, 1953). As laboratory rabbits do not recover from this infection, there have been no studies of viral clearance and the recovery of the rabbit. Only limited studies have been done on the pathogenesis of attenuated field strains of myxoma virus (Fenner *et al.*, 1956; Fenner and Ratcliffe, 1965). These have predominantly focussed on the relationship between virus titre in the skin and virus transmission by mosquitoes, and have not examined the details of virus replication over time in different tissues, nor have they examined control and clearance of the virus (with the exception of a detailed study of the testis (Fountain *et al.*, 1997).

The skin is a critical tissue in myxoma virus pathogenesis, both at the inoculation site and at sites where secondary lesions form. The latter are particularly important sources of virus for transmission by mosquitoes (Fenner and Woodroofe, 1953). Lymphoid tissues, particularly lymph nodes, are important sites of virus replication and the initiation of viremia and systemic dissemination. However, it is unclear how virus replication in these and other tissues such as the lung, liver and/or testis, affects the outcome of infection (Mims, 1964). More specifically, the relative importance of individual tissues over time in the control of attenuated infection is not known. Similarly, nothing is known concerning the pathogenesis of strains of myxoma virus in wild rabbits, and which tissues are involved in controlling infection of wild rabbits with a virulent virus that would be lethal in

laboratory rabbits.

Chapter 2 demonstrated that key differences between Uriarra and SLS occurred in the lymphoid tissue. These were the depletion of lymphocytes and the early suppression of lymphocyte responses. In this Chapter, I examine tissue responses in rabbits infected with attenuated or virulent virus, and compare these in laboratory rabbits which have not been selected for resistance with infection of wild Australian rabbits that have been subjected to nearly 50 years of selection. This gives the additional opportunity to re-examine WBC counts, and temperature and humoral responses reported in Chapter 2. This was done during time course experiments designed to measure virus titres in the key tissues of skin (at the inoculation site and elsewhere), lymph nodes (draining and contralateral), spleen, lung and peripheral WBC.

In developing the protocols for this study, two sets of preliminary experiments were done. Firstly, two sites in the skin were explored as primary inoculation sites; the thigh and the dorsum of the hind foot. It was necessary to identify the lymph nodes that predominantly drained these sites so that early interactions between the lymph nodes and virus could be properly examined. In particular we wanted to have a single draining lymph node so that the stages of virus dissemination could be accurately defined. Initial experiments indicated that the thigh could be used as an inoculation site. However, the virus titres at the putative draining lymph node were not commensurate with this being the sole draining node. Therefore these experiments were repeated using the foot inoculation site. The initial set of data is presented as well as the definitive set from the foot inoculation experiments. Secondly, following infection of rabbits, virus titre was to be determined in the skin. Small skin samples are difficult to homogenise and therefore the use of collagenase was investigated to assist in release of virus from the skin. A preliminary experiment was conducted to determine if this method could be used, and the optimal conditions for tissue digestion, by measuring the effect that enzyme concentration and incubation time had on tissue degradation and the viability of virus.

3.2 Materials and Methods

3.2.1 Indian ink localisation of draining lymph nodes

To determine which lymph node drained the inoculation site, 500µl of Indian ink was inoculated intradermally in both upper thighs or the dorsum of both feet of three laboratory rabbits (a total of six rabbits). At 24 hours post inoculation the rabbits were killed by an intravenous injection of barbiturate and the popliteal, inguinal and prefemoral lymph nodes excised, sliced open and examined for the presence of ink by visual observation.

3.2.2 Infection of laboratory and wild rabbits with SLS or Uriarra

Male laboratory rabbits (*O. cuniculus*) greater than four months of age, were inoculated intradermally with 100 pfu of either SLS or Uriarra (virus stocks prepared as in sections 2.2.1.2 and 2.2.1.3) in the left hind thigh or the dorsum of the left hind foot. At 2, 4, 6, 8 and 10 dpi, two rabbits inoculated with SLS and two inoculated with Uriarra in the thigh were killed by intravenous injection of barbiturate (a total of 10 rabbits infected with each virus). At 2, 4, 6 and 10 dpi, two pairs of rabbits inoculated in the dorsum of the left hind foot with SLS or Uriarra were killed. In addition, at 15 and 20 dpi, two rabbits inoculated in the hind foot with Uriarra were killed (a total of 8 rabbits infected with SLS and 12 rabbits infected with Uriarra). Rabbits had been randomly allocated to these harvest time points at the time of inoculation.

In a second experiment, male wild rabbits (*O. cuniculus*) bred in the Gungahlin animal-house and greater than four months of age were inoculated intradermally with 100 pfu of either SLS or Uriarra in the dorsum of the left hind foot. At 2 and 4 dpi, two rabbits infected with each virus were killed by intravenous injection of barbiturate. At 6, 10, 15 and 20dpi, three rabbits infected with each virus were killed (a total of 16 rabbits infected with each virus).

3.2.3 Tissue collection and monitoring of clinical signs

The tissues collected from these rabbits comprise the majority of material used in time-course experiments in this and subsequent chapters (Figure 3.1). These tissues were the skin at the primary inoculation site (primary lesion), the popliteal lymph node adjacent to

the inoculation site (the draining lymph node), the popliteal lymph node in the leg opposite the inoculation site (the contralateral lymph node), spleen, lung, and a distal skin site. The distal skin was an uninoculated piece of skin taken from the opposite hind foot to the primary lesion. Approximately 25ml of peripheral blood was taken by cardiac puncture into a heparinised syringe (50 units/ml heparin in ddH_2O; Sigma) immediately before killing each rabbit. Clinical signs of disease and rectal temperatures were recorded daily. Blood samples from the marginal ear vein were taken every 48 hours for peripheral and differential WBC counts.

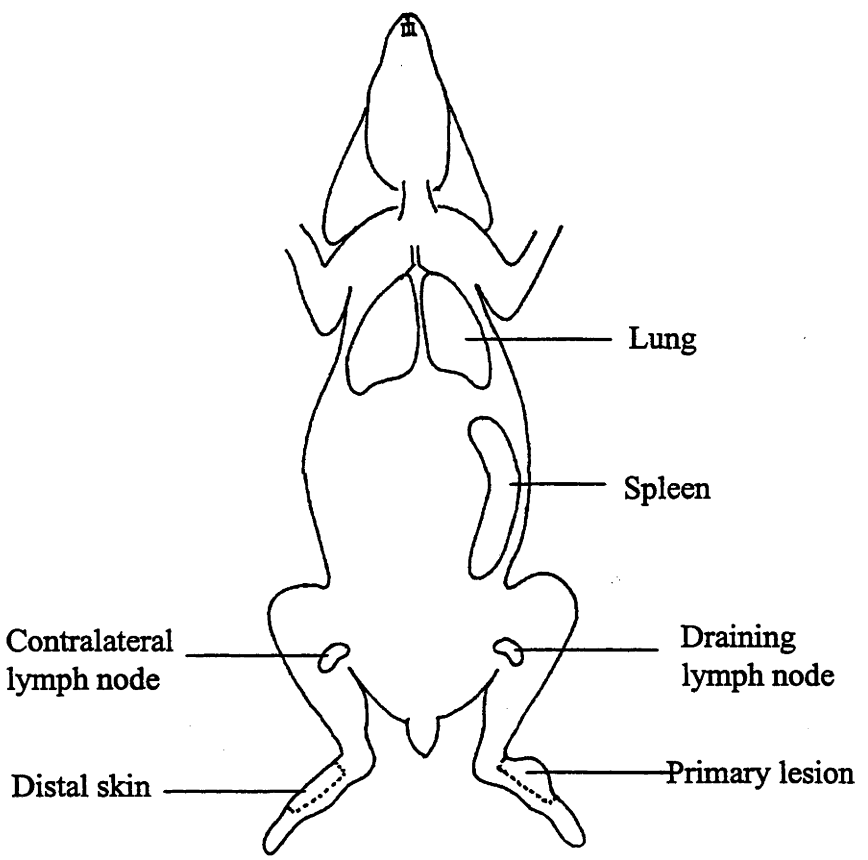

Figure 3.1: Schematic view of a rabbit at autopsy showing the tissues collected to examine virus growth. Rabbits were inoculated on the dorsum of the left hind foot with myxoma virus. Rabbits were killed at various times post infection and the following tissues collected: the inoculation site in the skin or primary lesion formed at this site, the draining and contralateral lymph nodes, spleen, lung and an uninoculated site of skin on the right hind foot (distal skin). 25ml of peripheral blood was also collected by heart puncture at the time of death. These tissues comprise the majority of material used in the time course experiments of this and subsequent chapters.

3.2.4 Ficoll-paque preparation of peripheral blood mononuclear cells

Peripheral anti-coagulated blood collected as described in section 3.2.3 was centrifuged at 500g for 20min at 18°C. The buffy coat of WBC was removed and mixed with an equal volume of PBS. Serum was also removed from the centrifuged blood sample and stored at –20°C for later assay for serum and neutralising antibody by ELISA and plaque-reduction neutralisation assay, respectively. 4ml of the diluted buffy coat in PBS was carefully layered over 3ml of Ficoll-Paque (Ficoll 400; Pharmacia) in a 10ml centrifuge tube. This was centrifuged at 400g for 20min at 18°C. The layer of mononuclear cells at the PBS/Ficoll-interface was removed using a Pasteur pipette. The remaining supernatant was discarded. The pelleted RBC/granulocytes were resuspended in shocking solution to lyse RBC as described for the preparation of lymphocyte samples from rabbit spleens (section 2.2.2.3). The mononuclear cell and granulocyte preparations were washed twice by resuspending complete MEM and centrifuging at 250 *g* for 10min at 18°C, followed by resuspension in 1ml complete RPMI. These two WBC fractions were stored at –70°C for plaque assay on Vero cell monolayers.

3.2.5 Peripheral and differential WBC counts

Peripheral blood was taken from the marginal ear vein of rabbits every 48 hours over the course of infection. Peripheral white blood cell (WBC) counts were made in as in section 2.2.2.1.1. Cell viability was separately assessed by trypan blue exclusion (0.2% trypan blue in ddH_2O). For differential WBC counts, a drop of blood taken from the marginal ear vein of rabbits was placed on a superfrost microscope slide. A second slide held at a 45° angle was used to draw the blood into a thin smear. This was allowed to air dry for 15min. Smears were covered with 1ml of Wright stain (CSL Diagnostics) for 30sec followed by the addition of 1ml of PBS. Slides were left for 1min before being washed with ddH_2O and then running tap water. Smears were allowed to air dry and mounted under a coverslip with D.P.X (Difco).

3.2.6 Preparation of tissue samples for plaque assay

Throughout these procedures, all samples were kept on ice unless otherwise stated. Lymph nodes, spleen, lung, were trimmed to remove fat, weighed, chopped with scissors or a

scalpel blade, and homogenised using a small pestle in a 1.5ml plastic tube. Tissue homogenates were suspended in complete MEM to give a 10% or 25% weight/volume (w/v) suspension. Suspensions were sonicated in three 5 sec cycles using a probe sonicator, and freeze-thawed twice. These samples were plaque assayed on Vero cell monolayers (section 3.2.7).

Counted WBC suspensions made from peripheral blood (section 3.2.4) were briefly sonicated, in two 5 sec cycles, before plaque assay on Vero cell monolayers. Preparations of mononuclear cells and granulocytes were assayed separately, although the results were pooled for each individual rabbit. Cell suspensions were assayed undiluted, at the highest possible volume of stock preparation. Hence, for a sample containing a total of 2×10^8 cells in 1ml volume, a total of 8×10^7 or 400µl was assayed on duplicate Vero cell monolayers.

Skin samples were treated with collagenase to facilitate homogenisation and release of virus. To determine optimal collagenase concentration, preliminary experiments on skin from uninfected rabbits spiked with virus of known titre were performed. Two concentrations of SLS, 1×10^3 pfu/ml and 1×10^6 pfu/ml, were mixed with either 0.1mg/ml, 1mg/ml or 0mg/ml collagenase D (Boehringer Mannheim), with or without an uninfected block of chopped and homogenised rabbit skin piece of 1cm x 0.5cm. Collagenase D (catalogue number 1088 858) was chosen as it had the lowest trypsin activity (<0.1 U/mg) of the available collagenase preparations. Replicates of each treatment were incubated for 30min, 60min, or 90min at 37°C with regular agitation. Samples were then plaque assayed to determine if collagenase treatment or incubation time at 37°C reduced virus titre. Near to maximum virus titres were recovered regardless of treatment although treatment of tissues with 0.1mg/ml collagenase resulted in slightly better recovery of virus than 1mg/ml (see section 3.3.1 for results of trials).

Hence, blocks of skin sample, 1cm x 0.5cm, carefully removed from equivalent areas of primary lesion and distal skin and shaved of hair, were washed in PBS, chopped with a scalpel blade, weighed and homogenised. Skin samples were then suspended in 1 ml of

0.1mg/ml collagenase D and placed at 37°C for 90min, with agitation every 15min, followed by three cycles of sonication. These samples were adjusted to a standard w/v of 10% or 25% in complete MEM and plaque assayed on Vero cell monolayers (section 3.2.7).

3.2.7 Plaque assay of rabbit tissues and WBC samples

Plaque assays of virus were performed on Vero cell monolayers as described in section 2.2.1.5.

3.2.8 Measurements of antibody production following infection

3.2.8.1 Detection of anti-myxoma virus IgM and IgG

Serum samples were assayed by ELISA for myxoma virus-specific IgM and IgG, as described in section 2.2.4.1.

3.2.8.2 Plaque reduction neutralisation assay

Vero cells were seeded into 6 well sterile plates (Nunc) at 0.8 x 10^6 cells/well in complete MEM and grown overnight at 37°C in 5% CO_2 in air to form a cell monolayer. The serum samples were incubated in a 56°C waterbath for 30min prior to assay to inactivate complement. Pre-immune and hyper-immune rabbit serum were included as negative and positive controls respectively. Dilutions of heat inactivated serum in complete MEM were mixed with an equal volume (150μl) of myxoma virus, strain SLS, to give a final virus titre of 1.5 x 10^3 pfu/ml and final serum dilutions of 1:5, 1:10, 1:15, 1:30, 1:50, 1:80, 1:100, 1:150, 1:200, 1:300, 1:500, 1:1000, 1:2000, 1:3000, 1:4000, 1:5000, 1:6000, 1:7000, 1:10000. Virus/serum samples were incubated for 60min in a 37°C waterbath, with a brief vortex every 20 min. Medium was removed from the cell monolayers leaving sufficient volume to cover the monolayer, and 100μl of each dilution was added in duplicate to separate monolayers. The plates were incubated for 60 min at 37°C in 5% CO_2 in air, rocking every 15 min, followed by replacement of complete MEM and incubation for 7 days. Plaques were visualised as described in section 2.2.1.5 and counted. The neutralising titre was the lowest dilution (averaged over the duplicate samples) at which myxoma virus

plaque formation was reduced by 50% or greater.

3.3 Results

Several experiments were performed to develop the protocols used in this study. These are described here prior to the detailed presentation of the time course of rabbit infections and virus replication.

3.3.1 Recovery of virus following collagenase D treatment

The effect of collagenase D (0, 0.1 or 1.0 mg/ml), incubation time at 37°C (30, 60 or 90 min) and presence or absence of skin tissue on the recovery of myxoma virus (10^3 or 10^6 pfu) from a myxoma virus suspension of known titre was determined by plaque assay (Table 3.1). None of the treatments affected virus titres greatly. However, 0.1 mg/ml collagenase resulted in slightly better recovery of virus than 1mg/ml. This may be attributable to less trypsin present in the total sample. There was a trend towards a greater reduction in virus titre following treatment with collagenase when the original virus titre was 10^3 pfu compared to 10^6 pfu. However, the standard deviation in this assay is equal to the square root of the number of plaques counted, which was approximately 100. Thus the standard variation is around 10%, indicating that there is no difference between treatment of 10^3 pfu or 10^6 pfu with collagenase. Incubation time at 0.1mg/ml of enzyme did not affect virus titre, although the longer the skin was incubated with enzyme, the better the tissue degradation. Hence, 0.1mg/ml collagenase D and 90 min incubation time was chosen to provide maximum breakdown of skin samples.

3.3.2 Localisation of lymph nodes that drain the primary inoculation site

To identify lymph nodes that drained the inoculation sites, Indian ink was inoculated into the mid-thigh of laboratory rabbits, and the presence of ink in lymph nodes examined after 8 and 24 hours. In all rabbits, the popliteal lymph node was most heavily coloured with ink such that it was obvious within the fat behind the knee without slicing the node open. In 2 of 6 inoculations, the prefemoral lymph node, also positioned in the leg, was coloured with ink but not as intensely as the popliteal lymph node. Also in 2 of 6 cases, the inguinal

lymph node was lightly discoloured with ink which was observed only after slicing the node open. It was concluded that the mid-thigh inoculation site was drained primarily by the popliteal lymph node adjacent to the inoculation site, with a small amount of drainage occurring to the prefemoral and inguinal lymph nodes.

Table 3.1: Recovery of virus following collagenase D treatment. Myxoma virus (10^3 or 10^6 pfu) was incubated in the presence or absence of a rabbit skin sample at different concentrations of collagenase D and for different incubation times. Samples were then titred by plaque assay and titres recorded as the mean of duplicate samples.

		Collagenase D concentration		
	Original virus titre, incubation time	no enzyme	0.1mg/ml	1mg/ml
Without rabbit skin sample	10^3 pfu, 30 min	1.02×10^3	0.95×10^3	0.87×10^3
	10^3 pfu, 60 min	0.96×10^3	1.12×10^3	0.99×10^3
	10^3 pfu, 90 min	1.13×10^3	1.03×10^3	0.82×10^3
	10^6 pfu, 30 min	1.28×10^6	1.33×10^6	0.77×10^6
	10^6 pfu, 60 min	1.23×10^6	1.04×10^6	0.78×10^6
	10^6 pfu, 90 min	0.97×10^6	1.07×10^6	0.7×10^6
With rabbit skin sample	10^3 pfu, 30 min	0.92×10^3	0.91×10^3	0.87×10^3
	10^3 pfu, 60 min	1.1×10^3	0.95×10^3	0.91×10^3
	10^3 pfu, 90 min	1.01×10^3	0.98×10^3	0.78×10^3
	10^6 pfu, 30 min	1.24×10^6	1.16×10^6	0.96×10^6
	10^6 pfu, 60 min	1.12×10^6	1.32×10^6	0.88×10^6
	10^6 pfu, 90 min	1.03×10^6	1.03×10^6	0.89×10^6

3.3.3 Titres of myxoma virus in laboratory rabbits following virus inoculation in the thigh

To compare the pathogenesis of SLS and Uriarra, 100pfu of each virus was inoculated intradermally into the left hind thigh of laboratory rabbits. Virus titres were determined in

the popliteal lymph node regional to the inoculation site, the contralateral popliteal lymph node, spleen and peripheral blood at 2, 4, 6, 8 and 10dpi (Table 3.2). SLS was first present in the spleen of one animal, and in the spleen, popliteal and contralateral lymph nodes of the second rabbit at 4dpi. SLS replicated to relatively low titres in the spleen, reaching a maximum of 4.5 x 10^5 pfu/g in one rabbit at 10dpi. Maximum virus titres in all tissues examined following SLS infection occurred from 6dpi. There was no difference in the titre of virus between the draining and contralateral lymph nodes. Virus was present in the blood of rabbits infected with SLS earlier, and reached a higher level, than during Uriarra infection. Uriarra was first present in the spleen of one rabbit at 4dpi. Uriarra also replicated to relatively low titres in the spleen, reaching a maximum of 7.6 x 10^3 pfu/g in one rabbit at 10dpi. Maximum titres in the draining and contralateral lymph nodes, spleen and peripheral blood following Uriarra infection occurred from 6dpi. From this time, virus titres were generally higher in SLS infected rabbits than in rabbits infected with Uriarra.

The virus titres of SLS in the draining lymph node following inoculation of rabbits in the thigh were lower and were detected later than those obtained by Fenner and Woodroofe (1953). Based on these studies, it was also unexpected to first detect virus in the lymph node and the spleen simultaneously. This suggested that virus was not draining principally to the popliteal lymph node. Therefore, the inoculation site in the thigh did not provide an optimal experimental system to examine virus dissemination. Although localisation of draining lymph nodes by Indian ink inoculations in the skin demonstrated that the popliteal lymph node predominantly drained the inoculation site, it was necessary to resolve the differences between these results and those of Fenner and Woodroofe (1953). In order to select a better inoculation site, Indian ink was inoculated intradermally into the dorsum of the hind foot of three rabbits and the lymph nodes subsequently examined for the presence of ink at 24 hours. After 5 of the 6 inoculations, the popliteal lymph node was the only regional lymph node that was coloured by ink. In the sixth case, the inguinal lymph node was lightly discoloured with ink, as observed after slicing the node open. The popliteal lymph node thus was the predominant lymph node draining the lower leg inoculation site.

Table 3.2: Virus titres following mid-thigh inoculation of 100pfu of SLS or Uriarra into laboratory rabbits. Titres for organs are expressed as Log_{10} pfu/gram of tissue. Titres for white blood cells (WBC) are expressed as pfu per 10^6 cells. (dLN) draining lymph node, (cLN) contralateral lymph node, (*) below detectable levels of 50 pfu/g or 0.1 pfu/10^6 WBC.

	URIARRA					SLS				
Day	rabbit number	dLN	cLN	spleen	WBC	rabbit number	dLN	cLN	spleen	WBC
2	769	*	*	*	*	941	*	*	*	*
	2159	*	*	*	*	958	*	*	*	*
4	555	*	*	*	*	494	*	*	2.08	*
	741	*	*	2.4	*	557	2.4	2.3	3.15	14.9
6	833	5.99	5.98	2.95	*	748	4.71	5.27	2.95	1.0
	868	4.74	4.55	3.18	1.4	198	7.46	6.81	4.59	6.7
8	789	4.74	4.78	3.41	0.7	867	5.66	5.25	2.98	79.2
	840	6.21	4.7	3.08	*	939	5.27	5.39	*	3.4
10	841	6.45	5.11	3.88	0.1	777	6.72	7.06	*	6.9
	772	3.4	5.38	*	0.3	821	7.33	6.69	5.65	0.1

To confirm this result, myxoma virus was inoculated into the dorsum of a hind foot to determine if utilising an inoculation site that was more exclusively drained by the popliteal lymph node would change the kinetics of virus replication in the lymph nodes and spleen. Two rabbits inoculated with SLS or Uriarra were killed at 2 and 4 dpi. The virus titres obtained from the popliteal lymph nodes and spleen of these rabbits were similar to those obtained by Fenner and Woodroofe (1953) with SLS at these time points. Hence, this work was repeated with rabbits infected in the hind foot with SLS or Uriarra as described in 3.2 and the results presented below.

Table 3.3: Time of onset of clinical symptoms in wild and laboratory rabbits following hind foot inoculation of 100 pfu of SLS or Uriarra.

	Laboratory rabbits		Wild rabbits	
Days post infection	SLS	Uriarra	SLS	Uriarra
2	- pink inoculation site	- no clinical signs	- pink inoculation site	- no clinical signs
3		- pink inoculation site		
4				- pink inoculation site
5			- anogenital inflammation - inflamed conjunctiva	
6	- anogenital inflammation and scrotal oedema - inflamed conjunctiva and watery discharge - secondary lesion formation	- anogenital inflammation and scrotal oedema - inflamed conjunctiva and watery discharge	- thickened eyelids	
7	- difficulty breathing		- anogenital inflammation and scrotal oedema - secondary lesions	- inflamed conjunctiva

Table 3.3 continued: Time of onset of clinical symptoms in wild and laboratory rabbits following hind foot inoculation of 100 pfu of SLS or Uriarra.

	Laboratory rabbits		Wild rabbits	
Days post infection	SLS	Uriarra	SLS	Uriarra
9		- secondary lesion formation	- difficulty breathing in 1 of 9 rabbits	
10	- mucopurulent discharge - depressed demeanour - extensive anogenital odema -RABBITS KILLED	- mucopurulent discharge - difficulty breathing and depressed demeanour - extensive anogenital odema	- mucopurulent discharge - depressed demeanour	- anogenital odema - secondary lesion formation - watery conjunctival discharge
12			-regression of lesions - difficulty breathing in most rabbits	
15		- secondaries over body	- reduction of anogenital swelling - reduced mucopurulent discharge	- regression of lesions
17		- regression of lesions		

3.3.4 Clinical symptoms and gross pathology following intradermal inoculation of myxoma virus in the dorsum of the hind foot

Clinical symptoms are described below for rabbits inoculated in the hind foot and summarised at the end of the descriptions in Table 3.3 for SLS and Uriarra infected laboratory and wild rabbits. Clinical signs did not differ in laboratory rabbits between thigh and foot inoculations, nor did they differ from those described in Chapter 2. However in Chapter 2, autopsies were only performed at 10dpi.

3.3.4.1 SLS infection of laboratory rabbits

At 2dpi, the primary inoculation site in the skin was pink. On autopsy, the draining lymph node was slightly enlarged, but all other tissues appeared normal. At 4dpi, the inoculation site was thickened and pink. The draining lymph node was approximately 75% enlarged in size (approximately 0.75cm high, 1.5cm long), and the distal skin sample was visibly thickened. At 5dpi, the primary lesion was approximately 1cm in diameter. At 6dpi, this had increased to approximately 2cm in diameter (Figure 3.2). Clinical signs other than at the primary inoculation site developed between 4 and 6dpi. At 6dpi, the anogenital area was inflamed. The conjunctivae were red and swollen and there was a clear, watery discharge from the eyes. The base of the ears were thickened and hot to the touch. Secondary lesions in the skin were evident over most of the body, including the distal skin site. These were small, round, red and raised areas of the skin that were first apparent at approximately 4mm in diameter. On autopsy at 6dpi, the draining lymph nodes were enlarged to four times normal size and were purple in colour. The contralateral lymph nodes were up to three times normal size and the spleens were swollen to approximately twice normal size. The livers appeared mottled on the uncut surface, although the lungs and kidneys were normal. By 7dpi, rabbits had impaired respiration and a clear, watery discharge from the eyes and nose. Clinical signs continued to develop in severity and by 10dpi, the primary lesion was up to 7 x 4 cm (length x breadth) and 2cm high, purple in colour, and hard to the touch (Figure 3.3). Secondary lesions, approximately 0.75cm in diameter, were evident around the nose and mouth, and over the eyelids and ears, and approximately 1cm in diameter on the feet and chest of the animals.

The anogenital region and scrotum were swollen and oedematomous and there was a thick, opaque mucopurulent discharge from the eyes (which were closed) and nose (Figure 3.3). Both the draining and contralateral lymph nodes were 3-4 times normal size; the spleens were approximately three times normal size. The livers appeared mottled and were fragile (tearing easily when handled); the lungs appeared normal. The cortex of the kidneys of one of two rabbits was pale. Rabbits had a depressed demeanour. The study of SLS-infected laboratory rabbits was not continued beyond 10dpi as the rabbits were very ill and, based on previous studies, rabbits would have invariably died in the following one to two days if not

Figure 3.2: Laboratory rabbit infected with SLS at 6 dpi. This rabbit has a protuberant primary lesion (arrow, **A**). The skin around the face and ears is red, and is thickened over the eyelids. There is a clear, watery discharge from the eyes (**B**).

A

B

Figure 3.3: Laboratory rabbit infected with SLS at 10 dpi. This rabbit has a protuberant primary lesion (**A**), swollen anogenital region (**B**) and the skin over the face and ears is thickened. There are several secondary lesions around the nose (closed arrow, **C**). In this figure, the base of the ears is thickened (open arrow), the eyes are shut due to swelling of the eyelids and an opaque mucopurulent discharge.

A

B

C

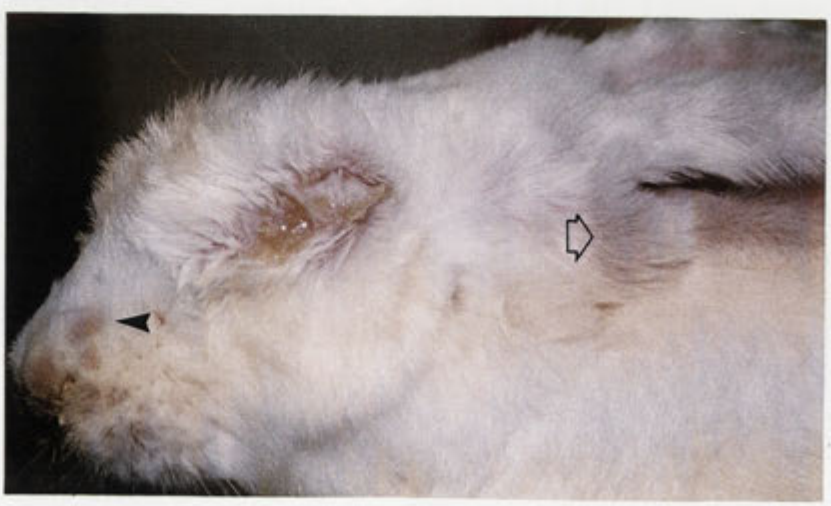

killed at this time (Fenner and Ratcliffe, 1965; Robinson *et al.*, submitted).

3.3.4.2 Uriarra infection of laboratory rabbits

Rabbits autopsied at 2dpi with Uriarra appeared normal. The first clinical signs of myxomatosis following infection of laboratory rabbits with Uriarra were observed at 3dpi when the primary inoculation site was pink and slightly raised. By 4dpi, this had swollen to approximately 1cm in diameter. On autopsy at 4dpi, the draining lymph node was approximately 1.5 times normal size, but other tissues appeared normal. At 6dpi, the primary lesion was up to 3cm in diameter. The eyelids of the rabbits were thickened and red with a limited, clear discharge from 2 of 8 infected rabbits. Half of the infected rabbits showed slight anogenital swelling and scrotal oedema. On autopsy at 6dpi, the draining lymph nodes were 3-4 times normal size and purple, and the contralateral lymph nodes were 1.5-2 times normal size. By 9dpi, secondary lesions of approximately 0.5cm in diameter were evident around the eyes, and the ears were thickened and hot to the touch. At 10dpi, all six rabbits had extensive scrotal oedema and anogenital inflammation. Secondary lesions were obvious on the eyelids and ears with some mucopurulent discharge from the eyes and nose. The primary lesion was up to 6cm in diameter, but remained light in colour (Figure 3.4). Respiration was impaired and rabbits had a depressed demeanour. On autopsy, the draining and contralateral lymph nodes and the spleens were all 3-4 times normal size. The livers, lungs and kidneys were normal. By 14dpi, the testes were palpably shrunken although scrotal oedema remained extensive. At 15dpi, secondary lesions were present over the nose, feet and body (Figure 3.5). The primary lesions were circumferenced by a dark ring, had darkened in colour and were shrunken in the centre.

Although both draining and contralateral lymph nodes were enlarged, there was no evidence of haemorrhage in the nodes. The lungs and kidney were normal, but the livers were mottled and fragile. The spleens were 3-4 times normal size. By 17dpi, a scab had begun to form over the primary lesion of both remaining rabbits. When these rabbits were autopsied at 20dpi, the spleens were approximately twice normal size and the lymph nodes approximately three times normal size. The livers were mottled but the lungs appeared normal. By this time, an extensive scab had formed over the primary lesions. No deaths

Figure 3.4: Laboratory rabbit infected with Uriarra at 10 dpi. This rabbit has a protuberant lesion at the primary inoculation site (arrow, **A**). The anogenital region is swollen (**B**). The eyelids are thickened and there is a clear, watery discharge from the eyes (**C**).

A

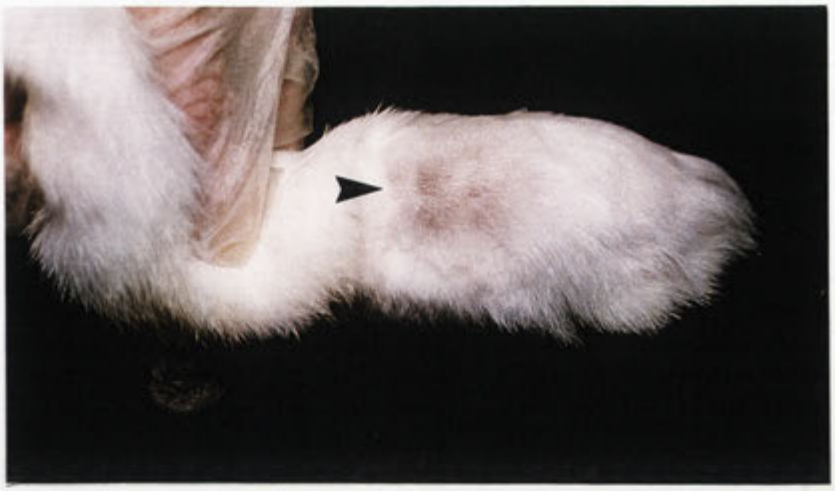

B

C

Figure 3.5: Laboratory rabbit infected with Uriarra at 15 dpi. This rabbits has a swollen anogenital region and scrotal odema (**A**) and discharge from the conjunctiva of the eyes, thickened eyelids and the formation of red swellings or small secondary lesions on the face (arrow) (**B**).

A

B

occurred apart from those planned up to 20 days of infection with Uriarra when the final rabbits were killed, and based on previous experience, most rabbits would have recovered completely if allowed (Fountain *et al.*, 1997).

3.3.4.3 SLS infection of wild rabbits

At 2dpi with SLS, the primary inoculation site in wild rabbits was pink. On autopsy, the draining lymph node of 1 of 2 rabbits was light purple in colour, although it was not enlarged. The draining lymph node of the other rabbit, and other tissues of both rabbits, were normal. By 4dpi, the primary lesions were slightly raised and 0.5cm in diameter (Figure 3.6). At autopsy, the draining lymph nodes were approximately twice normal size and purple in colour, but other tissues were normal. By 5dpi, the primary lesions were approximately 1cm in diameter and the anogenital regions and eyes of 3 of 12 infected rabbits were reddened. At 6dpi, the primary lesions were flat and approximately 3 x 1.5 cm (length x breadth) in size. All of the rabbits had red and visibly thickened eyelids. On autopsy, the draining lymph node was 2-3 times normal size and approximately half of the node was purple in colour, appearing haemorrhagic. The spleen was up to twice normal size, the liver was slightly congested and fragile while the lungs were normal. By 7dpi, the anogenital regions of most rabbits were inflamed. The primary lesions had developed a purple centre and small secondary lesions, approximately 3-4mm in diameter, were evident on the eyelids of 7 of 9 rabbits. One of these rabbits had a clear, watery discharge from both eyes. By 8dpi, secondary lesions (approximately 0.5cm in diameter) were evident over the eyes, ears feet and body of all rabbits. The primary lesions were no longer flat, being approximately 1.5cm high and purple in colour. By 9dpi, the primary lesion was 2.5-3cm high with blood breaking through the surface. One of nine rabbits had laboured breathing. By 10dpi, all rabbits had a discharge, which ranged from clear and watery to opaque and thick in consistency, from the nose and eyes, and anogenital odema was extensive (Figure 3.7). The primary lesions were dark purple in colour and rabbits had a depressed demeanour. On autopsy at this time, the draining lymph nodes were grossly enlarged, 4-5 times normal size, and purple in colour. The contralateral lymph nodes were approximately 1.5 times normal size. The spleens were swollen, up to three times normal size. Both the liver and lungs appeared mottled and congested, with livers being fragile to

Figure 3.6: Wild rabbit infected with SLS at 4 dpi. This rabbit has a small pink primary lesion (arrow, **A**). The anogenital region (**B**) and face and ears (**C**) have no clinical signs of myxomatosis.

A

B

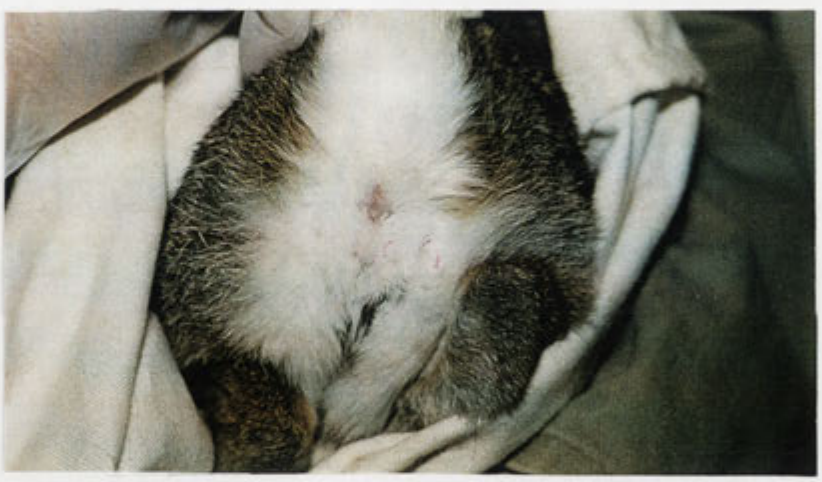

C

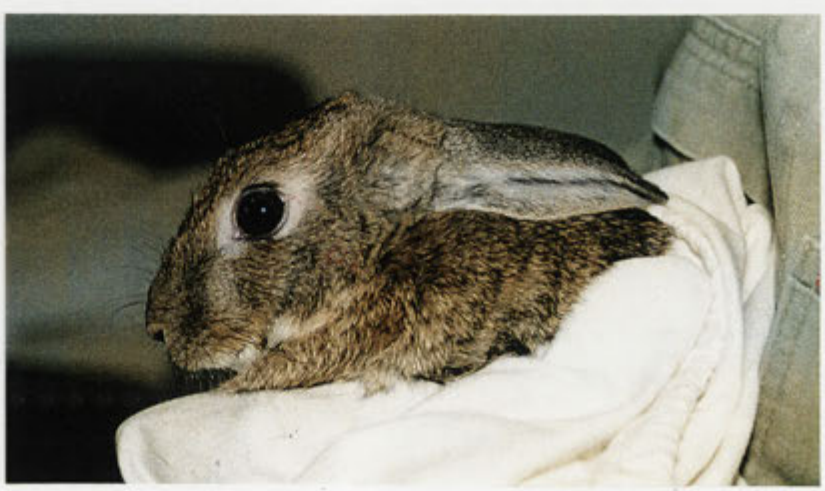

Figure 3.7: Wild rabbit infected with SLS at 10 dpi. This rabbit has a protuberant primary lesion (**A**), an inflamed anogenital region (**B**) and reddened, distorted eyelids, with some clear, watery discharge from the eyes (**C**).

A

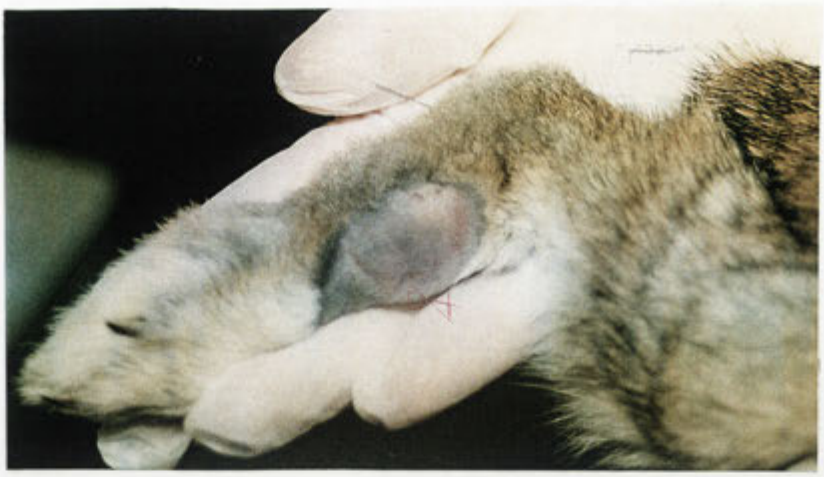

B

C

touch. The one rabbit that was experiencing difficulty breathing on day 9 and 10 died during that night. This rabbit had the most extensive primary and secondary lesions of all SLS infected animals. On autopsy, the lungs of this rabbit were congested and filled with blood, although other tissues appeared similar to those of rabbits killed at 10dpi. By 12dpi, weeping and scabbing was evident over the primary and secondary lesions. However, all 5 remaining rabbits were experiencing difficulty breathing, possibly due to obstruction of the nasal passages by the mucopurulent discharge. By 15dpi (Figure 3.8), respiration had improved in all rabbits. Scrotal oedema was limited and anogenital swelling was reduced compared to 10dpi. Rabbits had lost considerable body condition by 15dpi, although on autopsy, the stomachs of rabbits were half-full to full. Granulomas were apparent in the epididymis of 1 of 3 rabbits autopsied. The lungs of these rabbits were normal although the livers appeared engorged. The draining lymph nodes were up to 3 times normal size, the spleens were about twice normal size, while the contralateral lymph nodes remained at approximately 1.5 times normal size. At 20dpi, primary and secondary lesions were scabbed over and there was no mucopurulent discharge from the eyes or nose (Figure 3.9). On autopsy, both the draining and contralateral lymph nodes were enlarged but there was no evidence of haemorrhage within these tissues. Both the lungs and livers were normal. The testes were considerably shrunken with granulomas on the epididymides of 2 of 3 animals.

3.3.4.4 Uriarra infection of wild rabbits

The first clinical signs of myxomatosis following infection of wild rabbits with Uriarra were observed at 4dpi when the inoculation site was raised and pink. There were no signs of abnormalities in tissues from rabbits autopsied at 2dpi or at 4dpi. By 6dpi, the primary lesions were flat, pink and up to 3cm in diameter. On autopsy, the draining lymph nodes were approximately twice normal size, but all other tissues were normal. By 7dpi, one rabbit had red, visibly thickened eyelids. By 10dpi (Figure 3.10), 2 of 9 rabbits had a clear, watery discharge from the conjunctiva, although their eyelids were only slightly swollen and there was no mucopurulent discharge. One rabbit had a secondary lesion on the eyelid. Seven of 9 rabbits had mild anogenital swelling and scrotal odema. The primary lesions had reached approximately 4 x 2.5 cm (length x breadth), and were raised and red. On

Figure 3.8: Wild rabbit infected with SLS at 15 dpi. This rabbit has a protuberant primary lesion (arrow, **A**), and an inflamed anogenital region (**B**). The eyelids show limited swelling and redness although mucopurulent conjunctival discharge is evident (**C**). Extensive, rash-like secondary lesions have developed over the back (**D**)


A


B


C

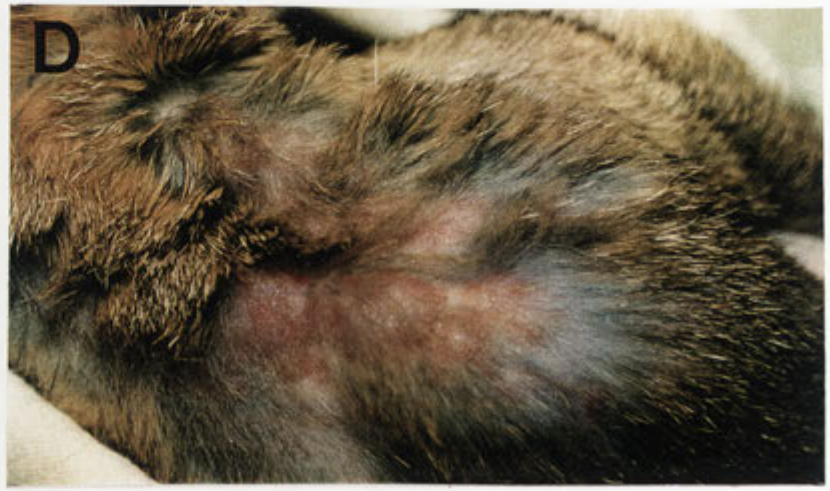
D

Figure 3.9: Wild rabbit infected with SLS at 20 dpi. The primary lesion of this rabbit is scabbing over (**A**), as are the anogenital region (**B**) and the small secondary lesions on the eyelids (**C**).

A

B

C

Figure 3.10: Wild rabbit infected with Uriarra. At 10dpi, rabbits have a small primary lesion (**A**) but no thickening or reddening of the eyelids (**B**). At 20 dpi, the primary lesion has begun to scab over (**C**). The face and ears of this rabbit remained free of secondary lesions and discharge (**D**).


A


B


C


D

autopsy, the draining lymph node was 3-4 times normal size but did not appear discoloured or haemorrhagic. The spleens were swollen to approximately twice normal size. The contralateral lymph nodes were not enlarged. By 12dpi, another one of the remaining six rabbits had developed a small secondary lesion on the eyelid. By 15dpi, the primary lesions had a dark and sunken centre, often with a dark ring at the lesion circumference. Anogenital swelling had increased from 10dpi in all infected rabbits, but was at no time considered severe. On autopsy, the draining lymph nodes were approximately twice normal size while the contralateral lymph nodes varied between normal to three times normal size. By 20dpi, the primary lesions and small secondary lesions on eyelids had formed scabs and had begun to regress (Figure 3.10). The anogenital swelling and scrotal oedema were mild and reduced compared to 15dpi. Both draining and contralateral lymph nodes were approximately twice normal size with no evidence of haemorrhage. The spleens were twice normal size. Wild rabbits infected with Uriarra remained relatively bright, did not suffer from obvious loss of body condition and apart from the small secondary lesions on the eyelids, did not develop discrete secondary lesions on the body. The lungs, livers and kidneys appeared normal at all times.

3.3.5 Titres of virulent and attenuated myxoma virus in laboratory and wild rabbits following virus inoculation in the hind foot

Virus titres in rabbit tissues following inoculation of 100pfu of either SLS or Uriarra in the hind foot were measured by plaque assay. The lowest limit of detection for this assay was 50 pfu/g tissue or 0.1 pfu/10^6 peripheral WBC. However, this represented two plaques for a sample, and such low titres should thus be interpreted as a positive indication of virus present rather than as an absolute measure of virus titre.

3.3.5.1 Titres of myxoma virus in the skin at the primary inoculation site

In laboratory rabbits inoculated with either SLS or Uriarra, virus was present at 2dpi between approximately 50 pfu/g and 1.2 x 10^5 pfu/g (Figure 3.11A). Maximum SLS titres occurred at 4, 6 and 10dpi, with 4 of 6 laboratory rabbits having SLS titres greater than 10^8 pfu/g skin. At 4dpi, the Uriarra titre was greater than 10^7 pfu/g in 1 of 2 laboratory rabbits,

and in both rabbits killed at 6dpi. Maximum titres of both SLS and Uriarra occurred at 4, 6 and 10dpi, ranging from 1.9 x 10^8 to 1.0 x 10^9 pfu/g. At 15 and 20dpi, titre of Uriarra was below 10^7 pfu/g. During the first 10 days of infection, virus titres per gram of tissue of Uriarra were not different from those of SLS at the primary inoculation site in laboratory rabbits, although the size of the lesion was generally smaller (see section 3.3.3).

In wild rabbits at 2dpi, titres of both SLS and Uriarra ranged between 9.5 x 10^3 and 1.1 x 10^6 pfu/g (Figure 3.11B). At 4dpi, the titre of both Uriarra and SLS was greater than 10^7 pfu/g in 1 of 2 wild rabbits. At 6dpi, maximum titres of SLS, greater than 10^8 pfu/g, were reached in all three infected wild rabbits. Similarly to SLS infections, maximum titre of Uriarra, greater than or equal to 10^8 pfu/g, occurred at 6dpi in all three wild rabbits. At 10 and 20dpi, the titre of both Uriarra and SLS was between 2.0 x 10^6 and 1.2 x 10^8pfu/g, but were slightly lower, between 3.8 x 10^4 and 3.7 x 10^6 pfu/g, at 15dpi. There was no difference between virus titre of SLS and Uriarra at the primary inoculation site in wild rabbits, although Uriarra infection resulted in the formation of a smaller primary lesion than SLS.

3.3.5.2 Titres of myxoma virus in the draining and contralateral lymph nodes

There was no difference between titres of Uriarra and SLS (10^2-10^4 pfu/g) at 2dpi in the draining lymph node of laboratory rabbits (Figure 3.12A). SLS reached maximum titres, greater than 10^7 pfu/g, at 4, 6 and 10dpi, in 5 of 6 laboratory rabbits. Similarly, Uriarra also had maximum titres at 4, 6 and 10dpi; these ranged from 1.1 x 10^4 to 8.7 x 10^6 pfu/g. At 15 and 20dpi, Uriarra was not present in the draining lymph node of laboratory rabbits infected with Uriarra.

SLS was present in the draining popliteal lymph node of 1 of 2 wild rabbits at 2dpi (Figure 3.12B). At 4dpi, SLS was present in the draining lymph node of both wild rabbits. The highest titres reached were 1.6 x 10^4 to 5.0 x 10^5 pfu/g at 4 and 6dpi. From 6 to 20dpi, there was a steady decline in titre of SLS with virus detectable in the draining lymph node of 2 of 3 rabbits at 15dpi and of 1 of 3 wild rabbits at 20dpi. In each case, titres were less than 10^4 pfu/g. Following inoculation of Uriarra into wild rabbits, virus was not present in the

Figure 3.11: Myxoma virus titres (plaque forming units/gram tissue) at the primary inoculation site following intradermal inoculation of SLS or Uriarra in (**A**) laboratory and (**B**) wild European rabbits. Each point represents an individual rabbit. Two laboratory rabbits infected with SLS or Uriarra were killed at 2, 4, 6 and 10dpi. Two laboratory rabbits infected with Uriarra were killed at 15 and 20dpi. Two wild rabbits infected with SLS or Uriarra were killed at 2 and 4dpi. Three wild rabbits infected with SLS or Uriarra were killed at 6, 10, 15 and 20dpi (except for 15dpi with SLS, when one rabbit had previously died). (-----) virus titre required in skin for transmission (Fenner *et al.*, 1956).

A

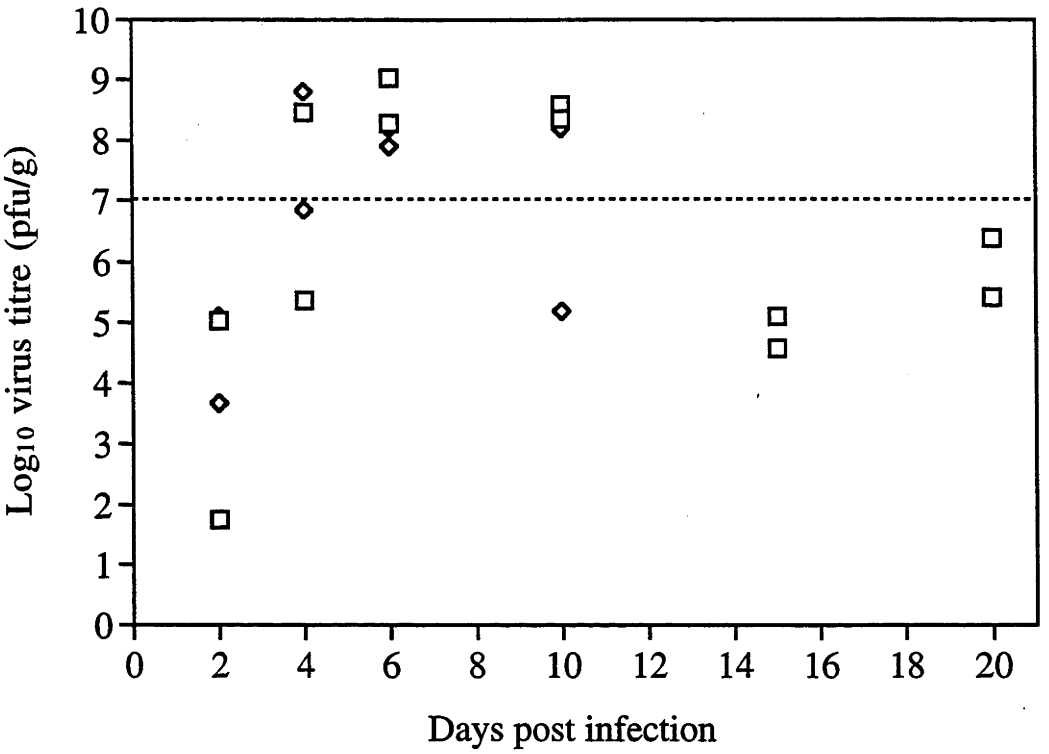
Log10 virus titre (pfu/g)
0
1
2
3
4
5
6
7
8
9
10
0
2
4
6
8
10
12
14
16
18
20
Days post infection

B

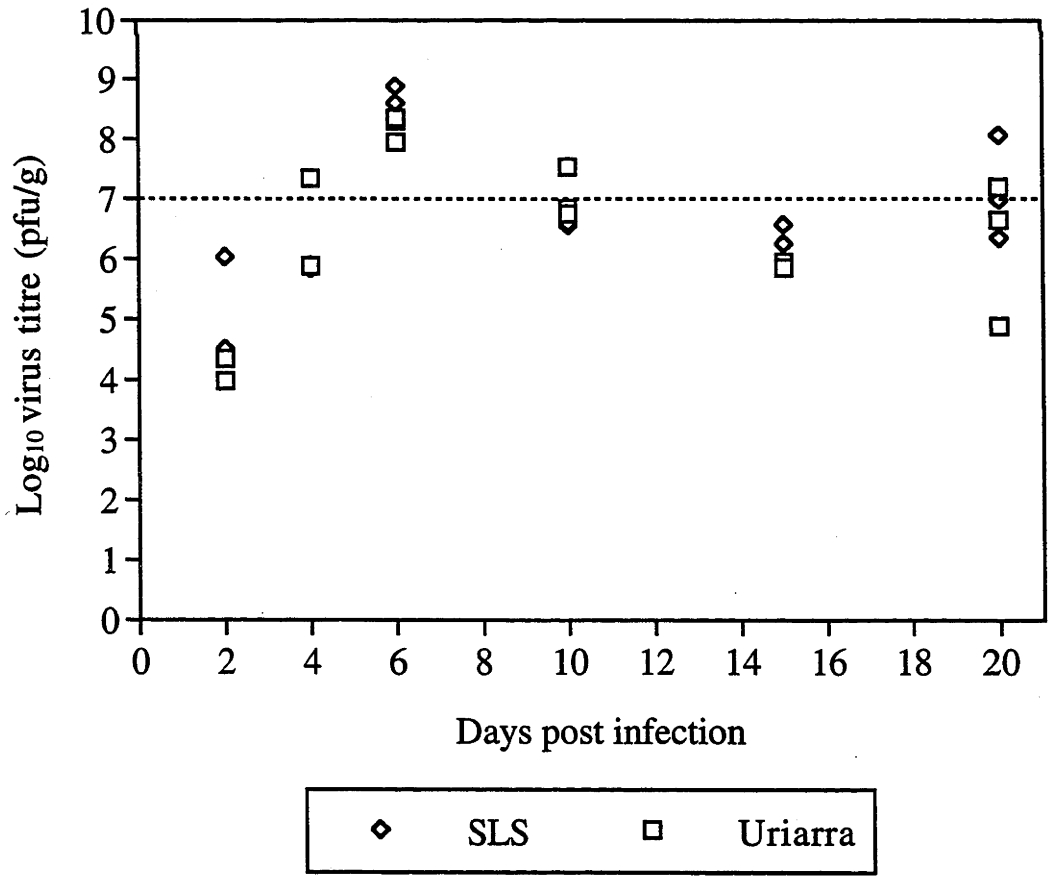
Log10 virus titre (pfu/g)
0
1
2
3
4
5
6
7
8
9
10
0
2
4
6
8
10
12
14
16
18
20
Days post infection
SLS
Uriarra

Figure 3.12: Myxoma virus titres (plaque forming units/gram tissue) in the draining lymph nodes of laboratory (**A**) and wild (**B**) rabbits infected with SLS or Uriarra. Each point represents an individual rabbit. Two laboratory rabbits infected with SLS or Uriarra were killed at 2, 4, 6 and 10dpi. Two laboratory rabbits infected with Uriarra were killed at 15 and 20dpi. Two wild rabbits infected with SLS or Uriarra were killed at 2 and 4dpi. Three wild rabbits infected with SLS or Uriarra were killed at 6, 10, 15 and 20dpi (except for 15dpi with SLS, when one rabbit had previously died).

A

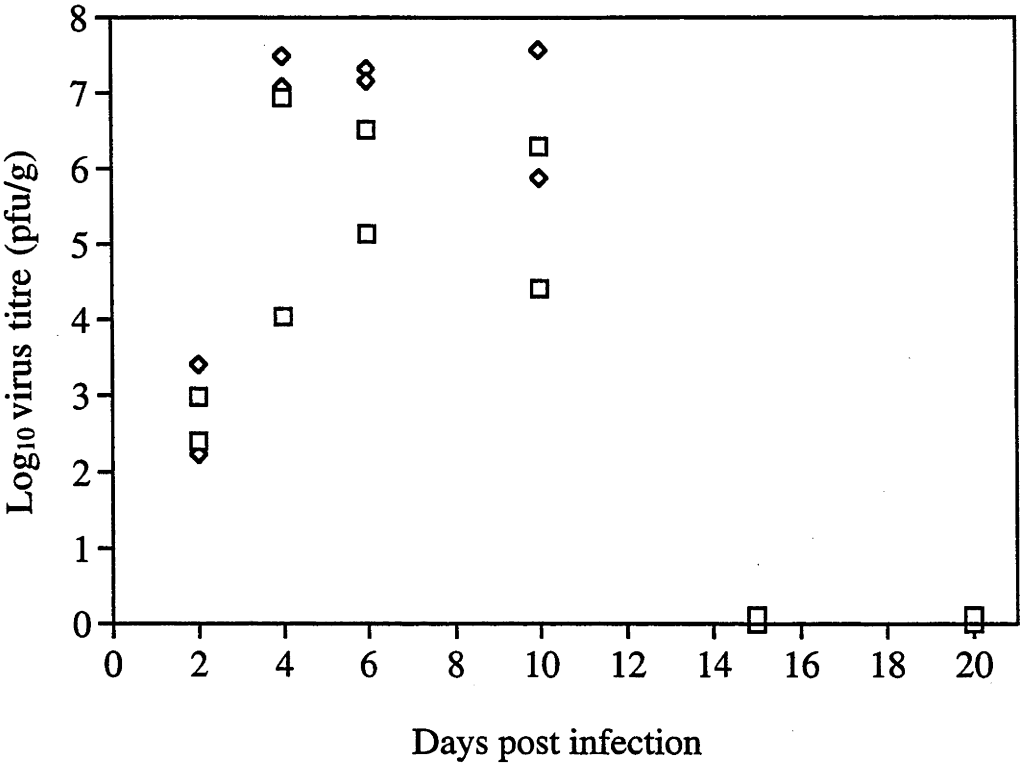
Log10 virus titre (pfu/g)
0
1
2
3
4
5
6
7
8
0
2
4
6
8
10
12
14
16
18
20
Days post infection

B

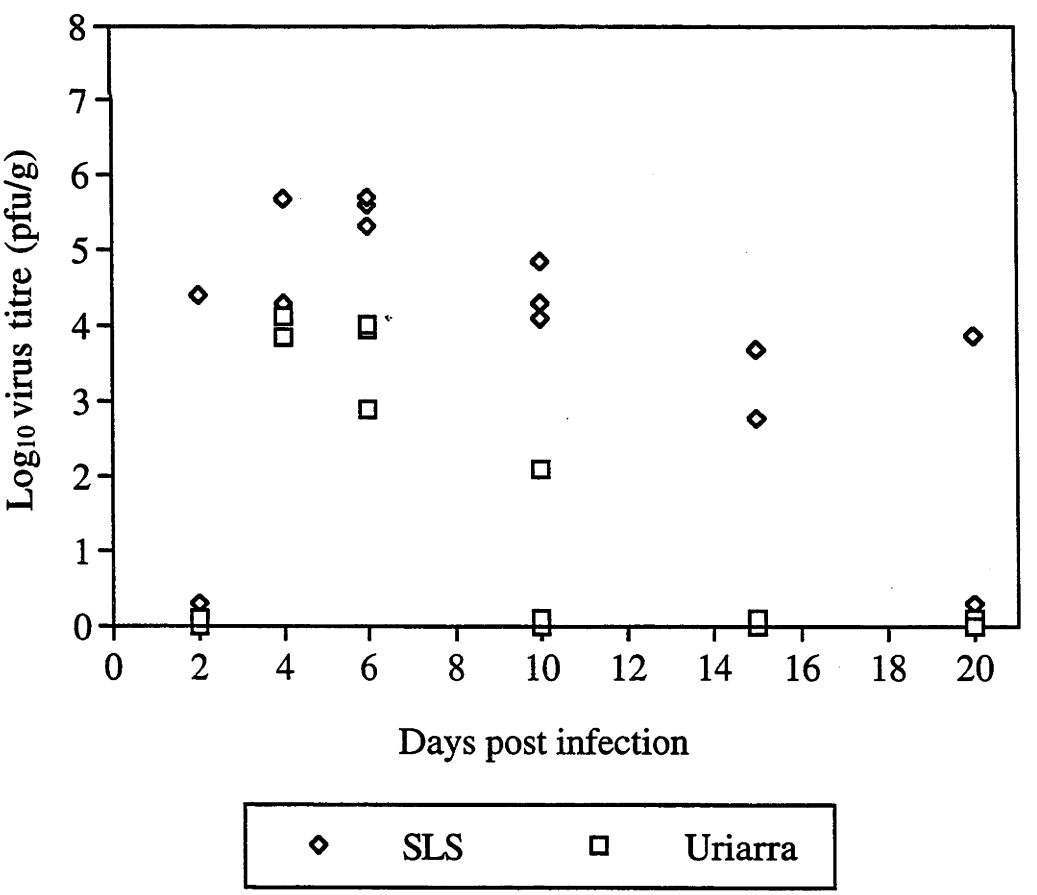
Log10 virus titre (pfu/g)
0
1
2
3
4
5
6
7
8
0
2
4
6
8
10
12
14
16
18
20
Days post infection
SLS
Uriarra

Figure 3.13: Myxoma virus titres (plaque forming units/gram tissue) in the contralateral lymph nodes of laboratory (**A**) and wild (**B**) rabbits infected with SLS or Uriarra. Each point represents an individual rabbit. Two laboratory rabbits infected with SLS or Uriarra were killed at 2, 4, 6 and 10dpi. Two laboratory rabbits infected with Uriarra were killed at 15 and 20dpi. Two wild rabbits infected with SLS or Uriarra were killed at 2 and 4dpi. Three wild rabbits infected with SLS or Uriarra were killed at 6, 10, 15 and 20dpi (except for 15dpi with SLS, when one rabbit had previously died).

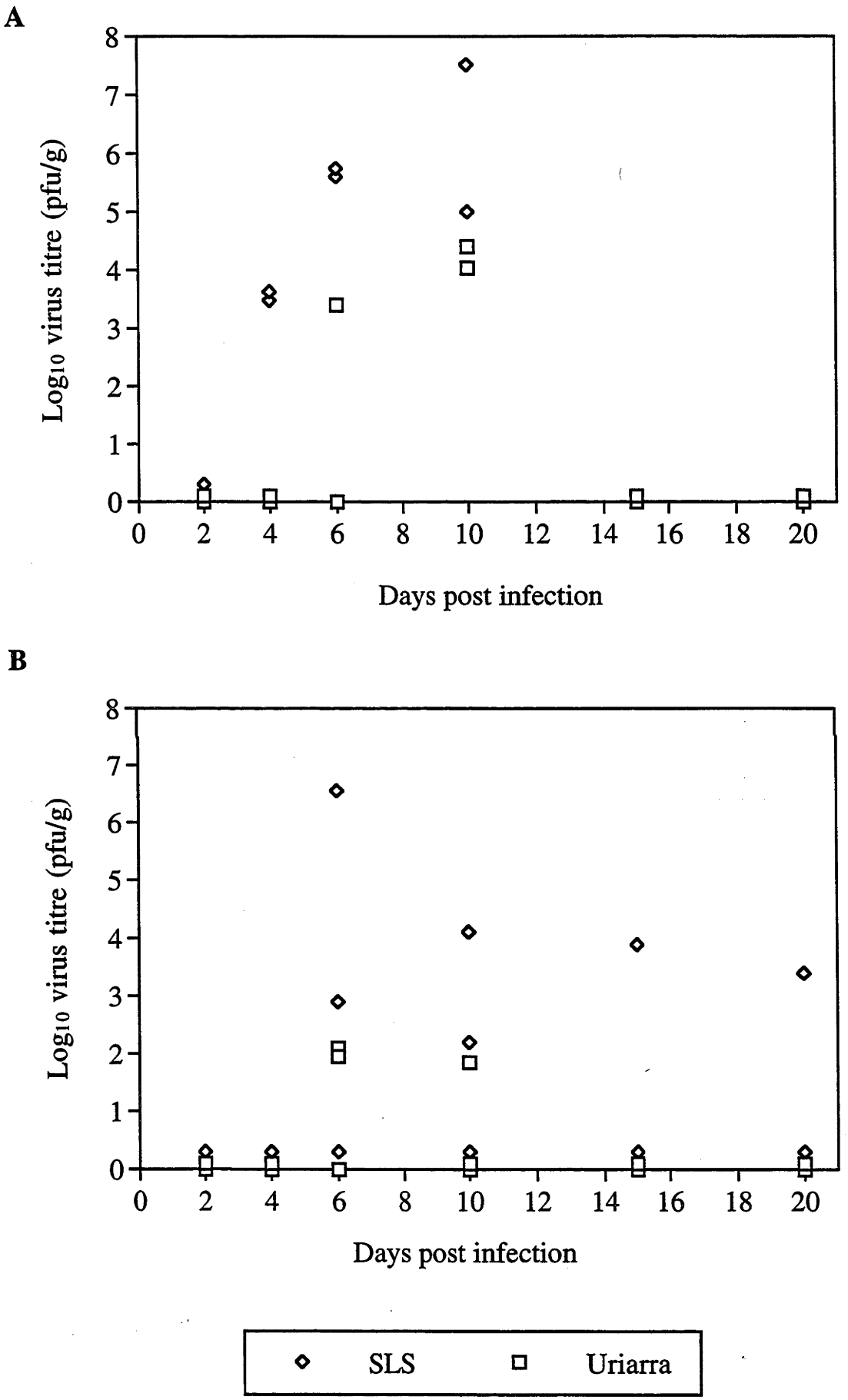
A
Log10 virus titre (pfu/g)
0
1
2
3
4
5
6
7
8
0
2
4
6
8
10
12
14
16
18
20
Days post infection
B
Log10 virus titre (pfu/g)
0
1
2
3
4
5
6
7
8
0
2
4
6
8
10
12
14
16
18
20
Days post infection
SLS
Uriarra

Figure 3.14: Myxoma virus titres (plaque forming units/gram tissue) in the spleen following intradermal inoculation of SLS or Uriarra in (**A**) laboratory and (**B**) wild European rabbits. Each point represents an individual rabbit. Two laboratory rabbits infected with SLS or Uriarra were killed at 2, 4, 6 and 10dpi. Two laboratory rabbits infected with Uriarra were killed at 15 and 20dpi. Two wild rabbits infected with SLS or Uriarra were killed at 2 and 4dpi. Three wild rabbits infected with SLS or Uriarra were killed at 6, 10, 15 and 20dpi (except for 15dpi with SLS, when one rabbit had previously died).

A

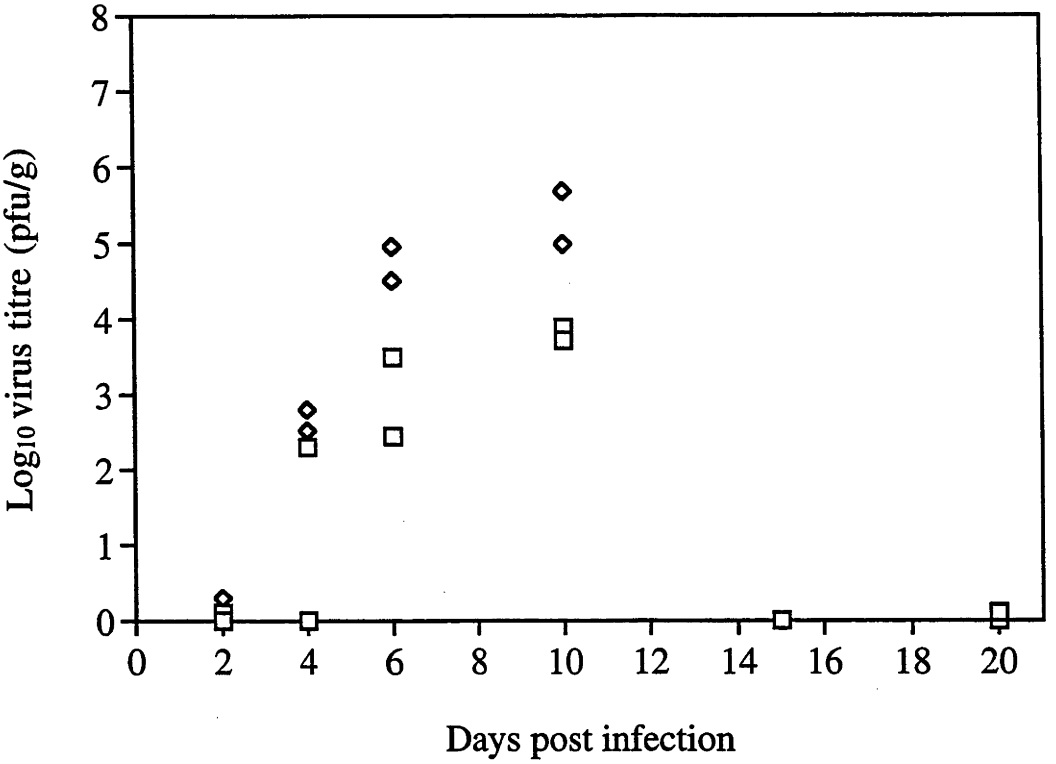
Log10 virus titre (pfu/g)
0
1
2
3
4
5
6
7
8
0
2
4
6
8
10
12
14
16
18
20
Days post infection

B

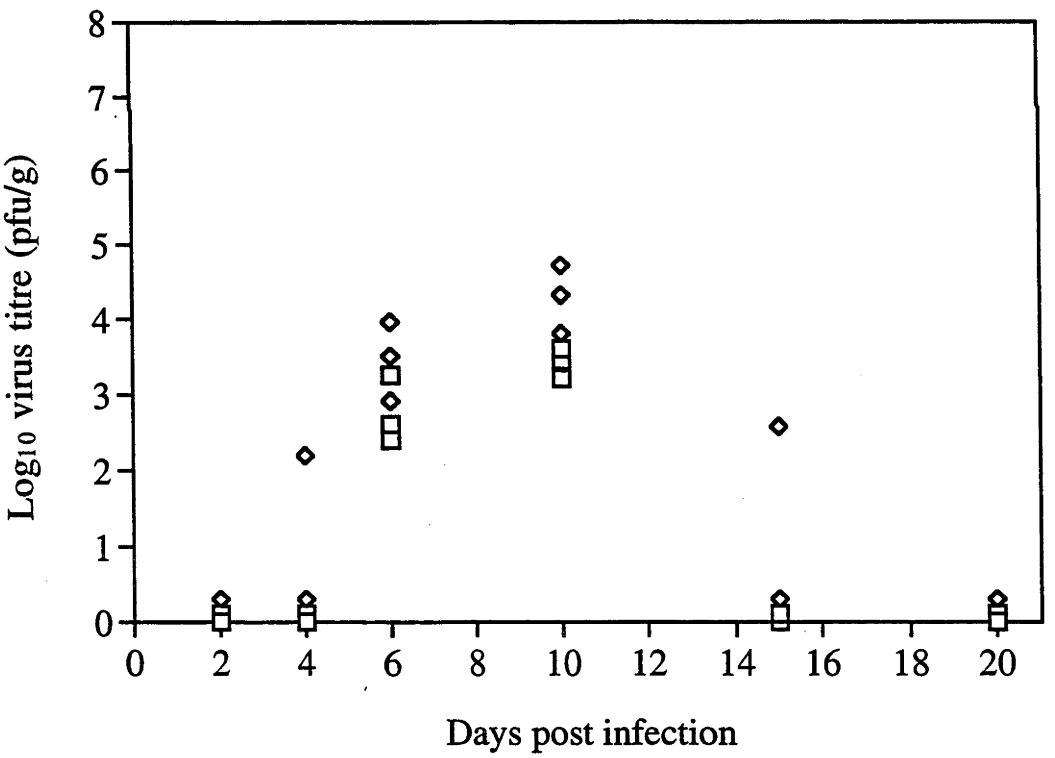
Log10 virus titre (pfu/g)
0
1
2
3
4
5
6
7
8
0
2
4
6
8
10
12
14
16
18
20
Days post infection


SLS
Uriarra

Figure 3.15: SLS and Uriarra virus titres (plaque forming units/ 10^6 white blood cells) in the peripheral blood of infected laboratory rabbits. Each point represents an individual rabbit. Two laboratory rabbits infected with SLS or Uriarra were killed at 2, 4, 6 and 10dpi. Two laboratory rabbits infected with Uriarra were killed at 15 and 20dpi.

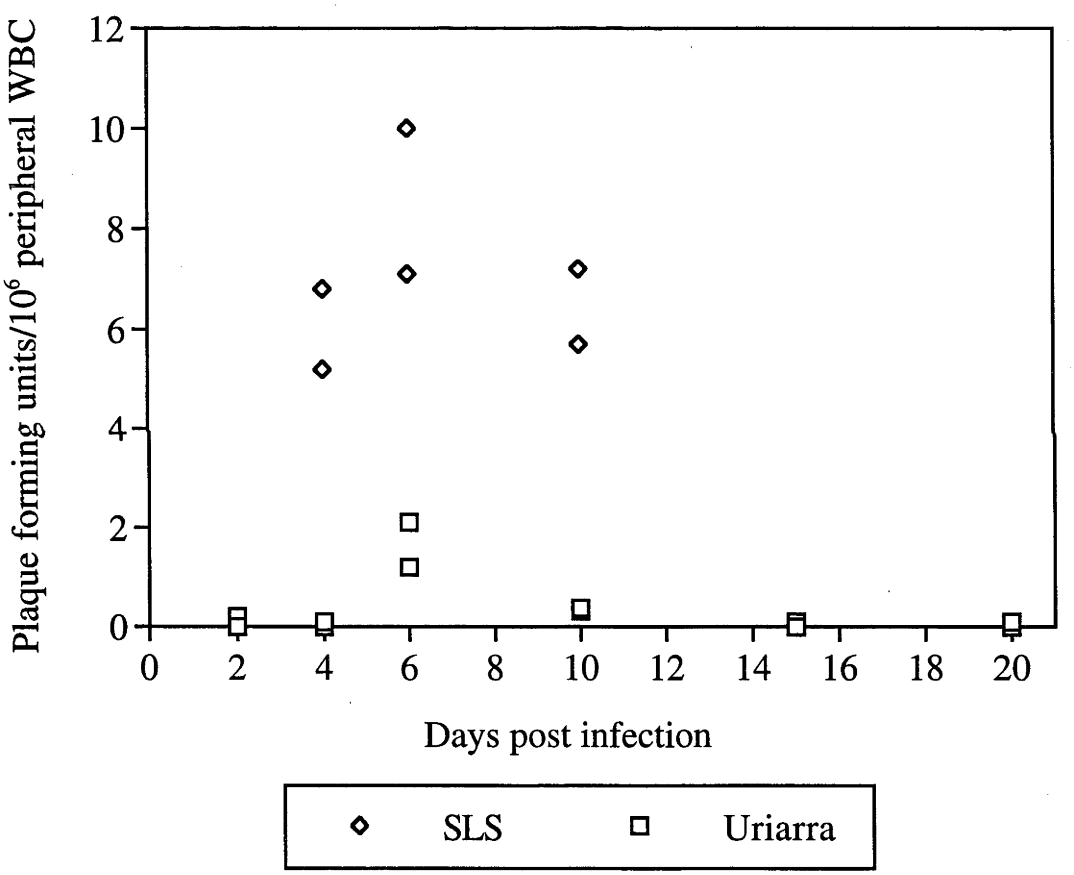
Plaque forming units/10^6 peripheral WBC
12
10
8
6
4
2
0
0
2
4
6
8
10
12
14
16
18
20
Days post infection
SLS
Uriarra

Figure 3.16: Myxoma virus titres (plaque forming units/gram tissue) in the lung following intradermal inoculation of SLS or Uriarra in **(A)** laboratory and **(B)** wild European rabbits. Each point represents an individual rabbit. Two laboratory rabbits infected with SLS or Uriarra were killed at 2, 4, 6 and 10dpi. Two laboratory rabbits infected with Uriarra were killed at 15 and 20dpi. Two wild rabbits infected with SLS or Uriarra were killed at 2 and 4dpi. Three wild rabbits infected with SLS or Uriarra were killed at 6, 10, 15 and 20dpi (except for 15dpi with SLS, when one rabbit had previously died).

A

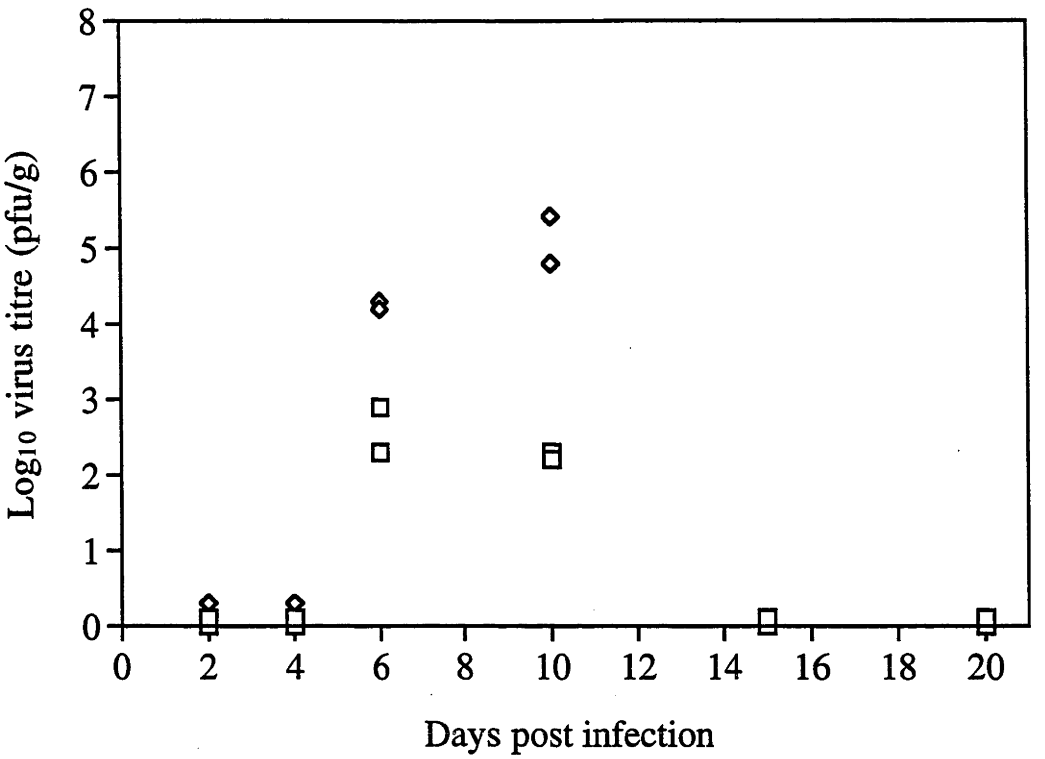
Log10 virus titre (pfu/g)
0
1
2
3
4
5
6
7
8
0
2
4
6
8
10
12
14
16
18
20
Days post infection

B

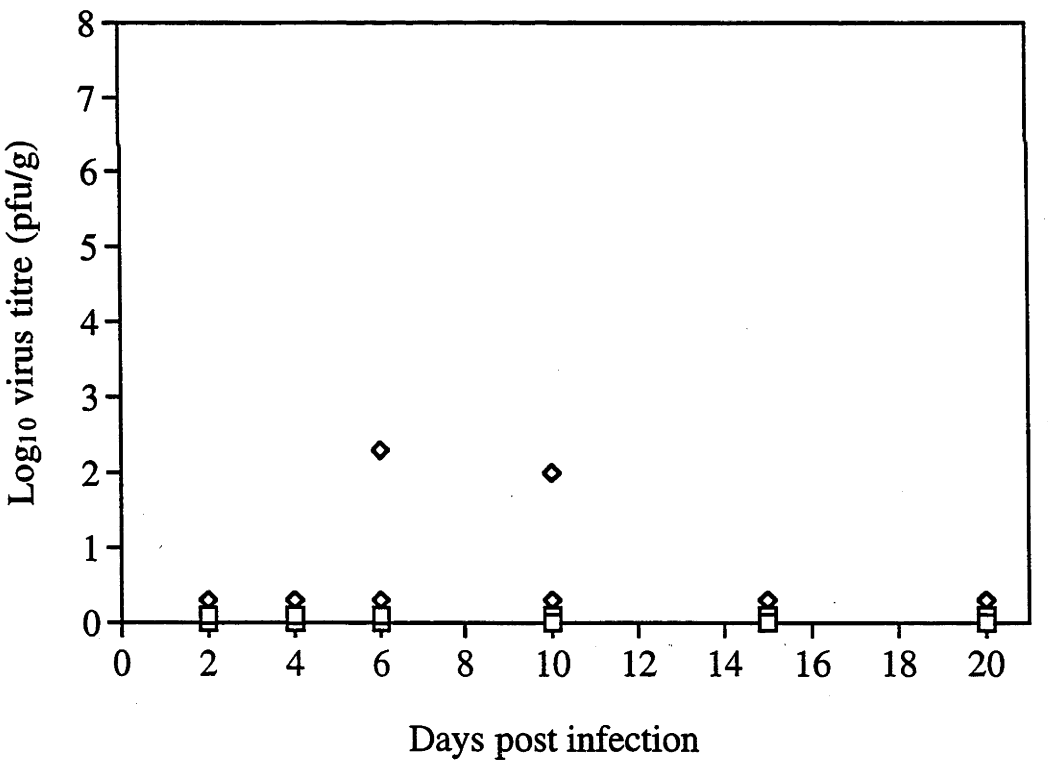
Log10 virus titre (pfu/g)
0
1
2
3
4
5
6
7
8
0
2
4
6
8
10
12
14
16
18
20
Days post infection

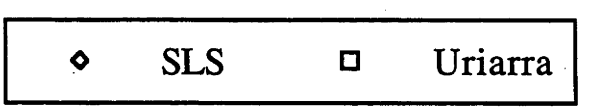
SLS
Uriarra

assay at any time.

3.3.5.5 Titres of myxoma virus in the distal skin

Virus titre was measured at an uninoculated skin site on the opposite side of the body to the inoculation site (termed distal skin) (Figure 3.17A). In laboratory rabbits inoculated with SLS, virus was first detected in distal skin at 4dpi. Maximum titres were reached at 6 and 10dpi, at which times the titre was greater than 10^7 pfu/g. In laboratory rabbits inoculated with Uriarra, virus was present at 6dpi, but not at 2 or 4dpi. Maximum titres of Uriarra were present at 6 and 10dpi, but were only 5.0 x 10^2 and 1.3 x 10^4pfu/g; at 10dpi, virus was present in the distal skin of only 1 of 2 laboratory rabbits. At 15 and 20dpi, 1.3 x 10^2 to 1.3 x 10^3pfu/g of Uriarra was present in 3 of 4 laboratory rabbits. Discrete secondary lesions were not observed at the distal skin site from laboratory rabbits infected with Uriarra, but were observed at this site in one rabbit killed at 6 dpi and both rabbits killed at 10 dpi with SLS.

At the distal skin site of wild rabbits, SLS was present at 4 dpi in both rabbits, but not at 2dpi (Figure 3.17B). SLS was present in skin from this area for the 20 days of infection at titres generally between 10^3 and 10^5pfu/g, except for two rabbits, one with a virus titre of 1.3 x 10^2 pfu/g at 4dpi, and one with a titre greater than 10^7pfu/g at 15dpi. The latter wild rabbit had a secondary lesion at the distal skin site. Uriarra was not detected in the distal skin of wild rabbits until 15 dpi, when it was present in 1 of 3 rabbits (3.3 x 10^3 pfu/g). At 20 dpi, Uriarra was present in the distal skin of 1 of 3 wild rabbits (2.0 x 10^2 pfu/g). Discrete secondary lesions were not observed at the distal skin site from wild rabbits infected with Uriarra, but were observed in 2 of 9 wild rabbits killed at or after 10 days of infection with SLS, including the rabbit with a virus titre of greater than 10^7 pfu/g at this site.

3.3.6 Humoral immunity to myxoma virus infection

The production of circulating serum antibody specific for myxoma virus was measured in serum samples taken when the infected rabbits were killed. Circulating serum IgM and IgG were measured by ELISA. Neutralising antibody was measured by plaque reduction neutralisation assay.

Figure 3.17: Myxoma virus titres (plaque forming units/gram tissue) at the distal skin following intradermal inoculation of SLS or Uriarra in **(A)** laboratory and **(B)** wild European rabbits. Each point represents an individual rabbit. Two laboratory rabbits infected with SLS or Uriarra were killed at 2, 4, 6 and 10dpi. Two laboratory rabbits infected with Uriarra were killed at 15 and 20dpi. Two wild rabbits infected with SLS or Uriarra were killed at 2 and 4dpi. Three wild rabbits infected with SLS or Uriarra were killed at 6, 10, 15 and 20dpi (except for 15dpi with SLS, when one rabbit had previously died). (-----) virus titre required in skin for transmission (Fenner *et al.*, 1956).

A

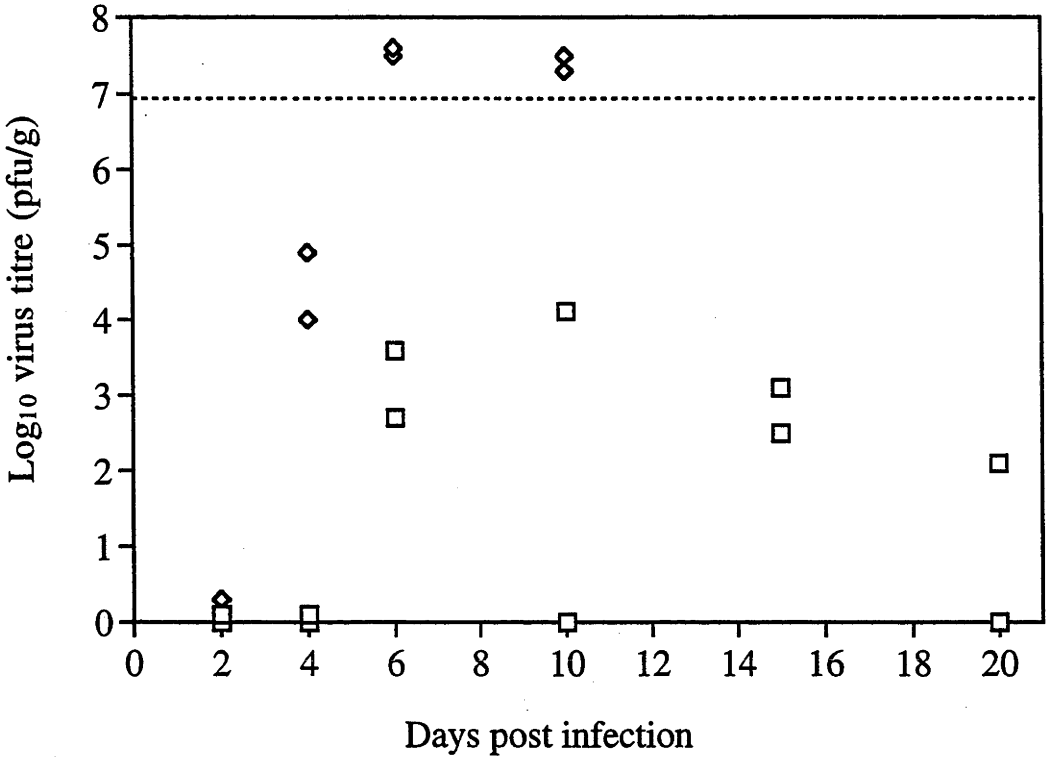
Log10 virus titre (pfu/g)
0
1
2
3
4
5
6
7
8
0
2
4
6
8
10
12
14
16
18
20
Days post infection

B

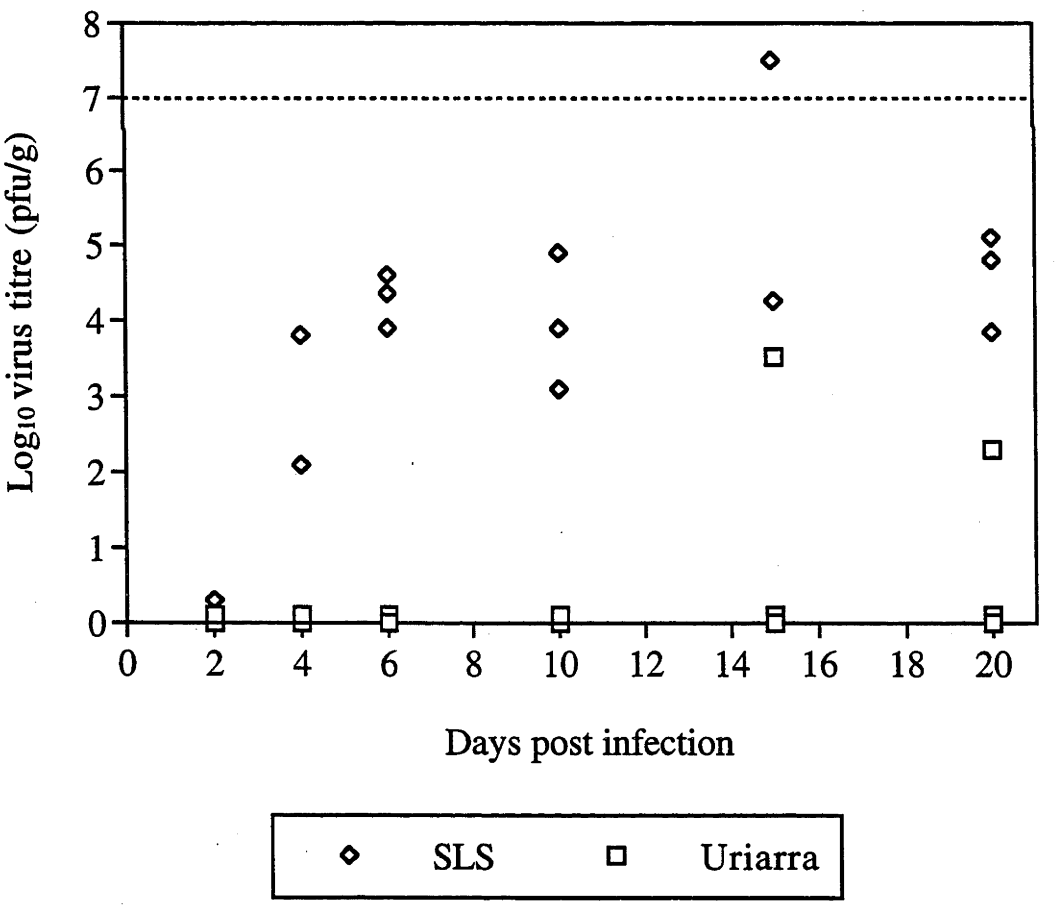
Log10 virus titre (pfu/g)
0
1
2
3
4
5
6
7
8
0
2
4
6
8
10
12
14
16
18
20
Days post infection
SLS
Uriarra

IgM was not present in sera at 2dpi. A low titre of IgM (50-100) was present in several laboratory rabbits infected with SLS or Uriarra at 4 and 6dpi (Table 3.4). IgG was not present in laboratory rabbits infected with SLS or Uriarra at 2, 4 or 6dpi, but was present at 10dpi. At 10dpi, there was no significant difference in ELISA IgM or IgG titres between viruses. However, titres were not substantially higher in the two SLS-infected laboratory rabbits compared to the Uriarra-infected laboratory rabbits. Neutralising antibody was first present in both rabbits infected with SLS or Uriarra at 10dpi, but was higher in SLS-infected rabbits. Uriarra-infected laboratory rabbits developed high neutralising antibody titres by 15 and 20dpi.

There were dramatic differences in the development of both IgG and neutralising antibody to myxoma virus in wild rabbits (Table 3.5). IgG was first present at 6dpi in 1 of 3 SLS-infected wild rabbits, but was not present in Uriarra-infected wild rabbits. By 10dpi, IgG titres in SLS-infected wild rabbits were substantially higher than in Uriarra-infected wild rabbits, and remained higher at 15 and 20dpi. Similarly, neutralising antibody was first present at 6dpi of wild rabbits with SLS, but were not present in Uriarra-infected rabbits at 6dpi. At 10 and 15 dpi, SLS-infected wild rabbits had considerably greater neutralising antibody titres than Uriarra-infected rabbits. At 20dpi, neutralising antibody titres were similar in SLS- and Uriarra-infected wild rabbits.

3.3.7 Febrile responses to infection

Rectal temperatures were measured daily during the course of infection, and are shown in Figure 3.18A expressed as the mean of all rabbits on each day. Basal temperature of both laboratory and wild rabbits ranged between 38.0 and 39.6°C, with a mean of 38.8°C $\pm$ 0.6 ($\pm$ standard error). The rectal temperature of laboratory rabbits infected with either Uriarra or SLS increased from 2dpi to 5dpi (Figure 3.18A). Elevated rectal temperatures were maintained from 5 to 20dpi with Uriarra, attaining a maximum of 40.6°C $\pm$ 0.6 (9dpi). However, after attaining a maximum of 40.3°C $\pm$ 0.4 at 8dpi, temperatures rapidly declined at 9 and 10dpi in laboratory rabbits infected with SLS to a mean of 38.9°C.

The rectal temperatures of wild rabbits infected with either Uriarra or SLS increased from 2dpi to 5dpi (Figure 3.18B). Elevated rectal temperatures were maintained from 5 to 20dpi in wild rabbits infected with SLS, with a maximum of 40.6°C $\pm$ 0.3 at 7dpi. Wild rabbits infected with Uriarra maintained elevated rectal temperatures from 5 to 14dpi (maximum of 39.9°C $\pm$ 0.3 at 4dpi), after which time there was a steady decline.

Table 3.4: Neutralising and ELISA antibody following Uriarra and SLS infection of laboratory rabbits. Neutralising antibody (N) was measured by plaque reduction neutralisation assay and indicates the reciprocal serum dilution at which 50% or greater of myxoma virus plaque formation was neutralised. To determine ELISA IgM and IgG, serum was titrated in duplicate in two fold serial dilutions. The endpoint titre was defined as the final dilution 0.1OD units above the OD of the 1:100 negative control.

	Uriarra				SLS			
Day	Rabbit	N	IgM	IgG	Rabbit	N	IgM	IgG
2	2160	-	-	-	984	-	-	-
	749	-	-	-	989	-	-	-
4	936	-	-	-	987	-	-	-
	975	-	50	-	982	-	50	-
6	167	-	50	-	269	-	-	-
	156	-	50	-	272	-	100	-
10	160	15	50	200	165	300	400	800
	158	50	400	400	179	300	200	400
15	169	4000	3200	3200				
	217	2000	3200	6400				
20	163	3000	1600	3200				
	207	3000	1600	3200				

Table 3.5: Neutralising and ELISA antibody following Uriarra and SLS infection of wild European rabbits. Neutralising antibody (N) was measured by plaque reduction assay and indicates the reciprocal serum dilution at which 50% or greater of myxoma virus plaque formation was neutralised. To determine ELISA IgM and IgG, serum was titrated in duplicate in two fold serial dilutions. The endpoint titre was defined as the final dilution 0.1OD units above the OD of the 1:100 negative control.

	Uriarra				SLS			
Day	Rabbit	N	IgM	IgG	Rabbit	N	IgM	IgG
2	298	-	-	-	193	-	-	-
	428	-	-	-	501	-	-	-
4	426	-	-	-	188	-	-	-
	427	-	50	-	194	-	-	-
6	401	-	-	-	190	300	50	200
	402	-	50	-	189	150	50	-
	429	-	50	-	505	5	50	-
10	343	80	800	50	250	3000	1600	1600
	344	50	400	-	504	2000	800	3200
	403	30	400	100	508	300	400	3200
15	768	50	400	800	498	3000	800	25600
	473	30	200	3200	506	500	800	25600
	467	50	200	6400	502	died		
20	466	2000	200	12800	500	2000	400	51200
	502	300	100	1600	499	3000	800	51200
	324	6000	100	25600	860	6000	800	51200

3.3.8 Haematology

Blood samples from the marginal ear vein were taken and peripheral WBC counted and differential blood cell counts made every two days over the period of infection.

3.3.8.1 Changes in peripheral WBC counts

Peripheral WBC counts did not change over the 20 days of infection of laboratory rabbits with Uriarra or wild rabbits with either Uriarra or SLS. SLS infection of laboratory rabbits resulted in a rapid increase in peripheral WBCs from 6dpi to approximately three-fold greater than that of other infections by 10dpi (Figure 3.19).

A

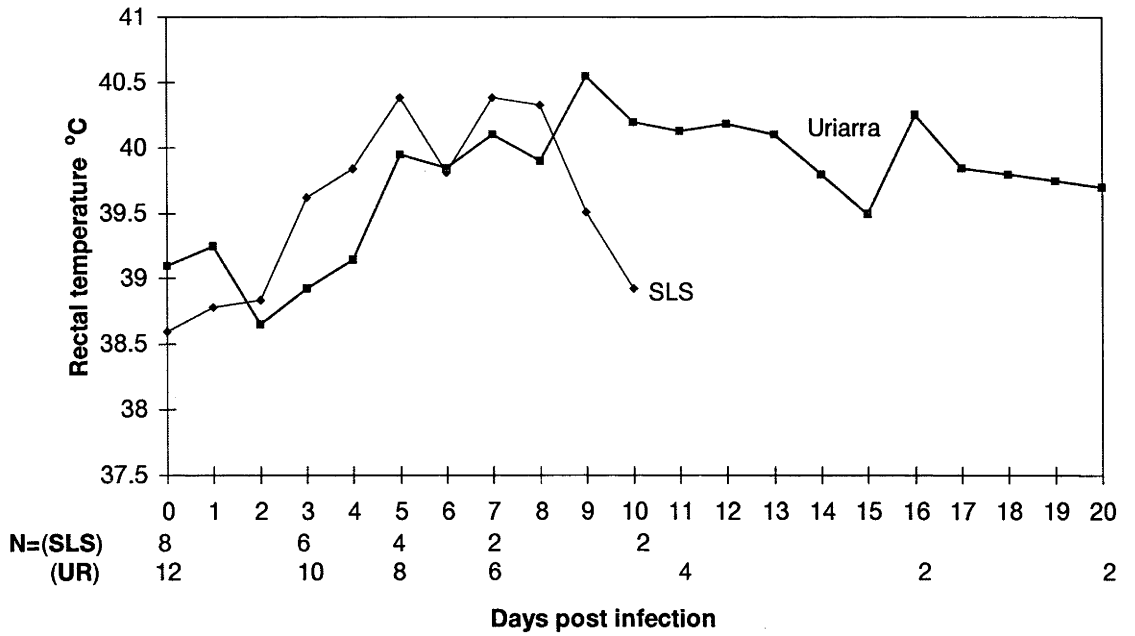

B

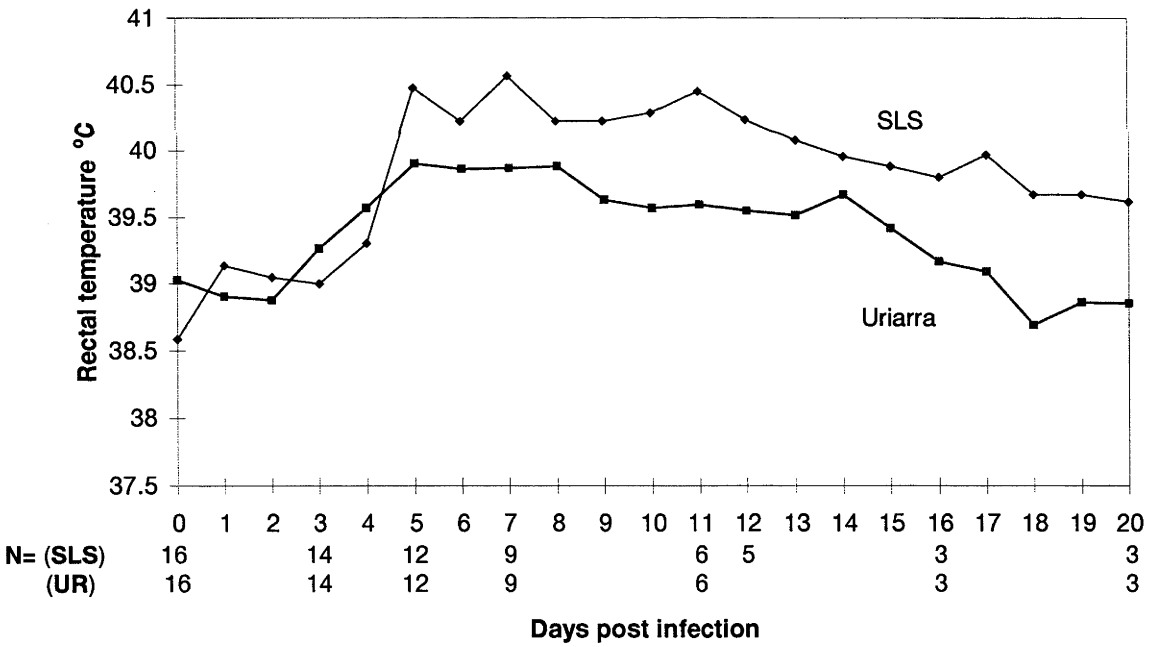

Figure 3.18: Daily mean rectal temperature (°C) of laboratory (**A**) and wild (**B**) rabbits infected with SLS or Uriarra. A change in the number of rabbits (N) infected with each virus at each time post infection is indicated below the graph.

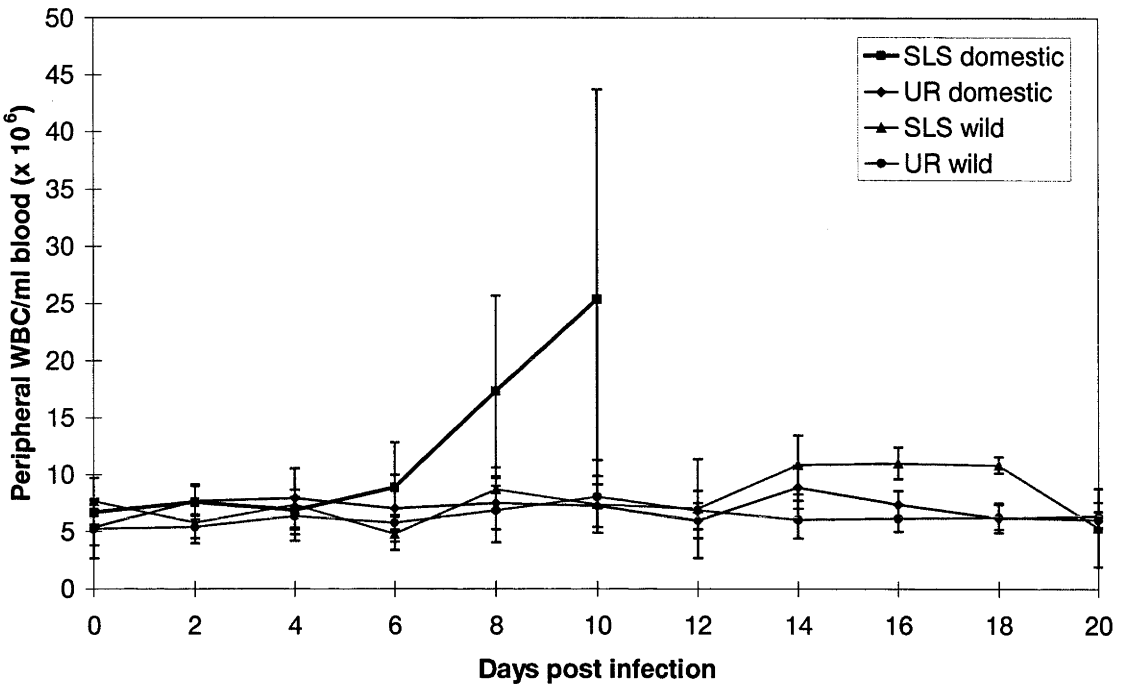

N laboratory									
(SLS)	8	6	4	2	2				
(UR)	12	10	8	6	4		2		2
N wild									
(SLS)	16	14	12	9	6	5	3		3
(UR)	16	14	12	9	6		3		3

Figure 3.19: Peripheral white blood cell (WBC) counts in laboratory and wild rabbits infected with SLS or Uriarra (mean ± SE of all rabbits for each time except where n=2 [for SLS-infected laboratory rabbits from 7dpi, and Uriarra-infected laboratory rabbits from 16dpi]. The bars then indicate a range about the mean). A change in the number of laboratory or wild rabbits (N) infected with each virus at each time post infection is indicated below the graph.

Figure 3.20: Differential WBC counts following infection of *O. cuniculus* with myxoma virus. The percent number of monocytes (**A**), eosinophils (**B**) and basophils (**C**) were determined from blood samples taken from laboratory and wild rabbits infected with SLS or Uriarra (mean $\pm$ SE of all rabbits for each time except where n=2 [for SLS-infected laboratory rabbits from 7dpi, and Uriarra-infected laboratory rabbits from 16dpi]. The bars then indicate a range about the mean). Changes in the number of rabbits (N) infected with each virus at each time point after infection are indicated below.

Days post infection

	0	2	4	6	10	12	15	20
N laboratory								
(SLS)	8	6	4	2				
(UR)	12	10	8	6	4		2	2
N wild								
(SLS)	16	14	12	9	6	5	3	3
(UR)	16	14	12	9	6		3	3

A

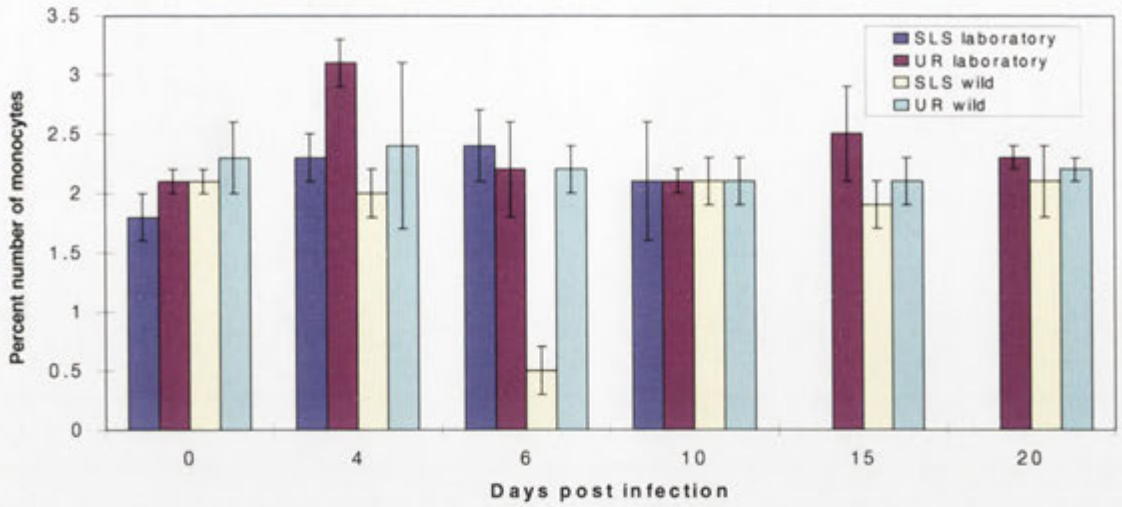
Percent number of monocytes
3.5
3
2.5
2
1.5
1
0.5
0
SLS laboratory
UR laboratory
SLS wild
UR wild
0
4
6
10
15
20
Days post infection

B

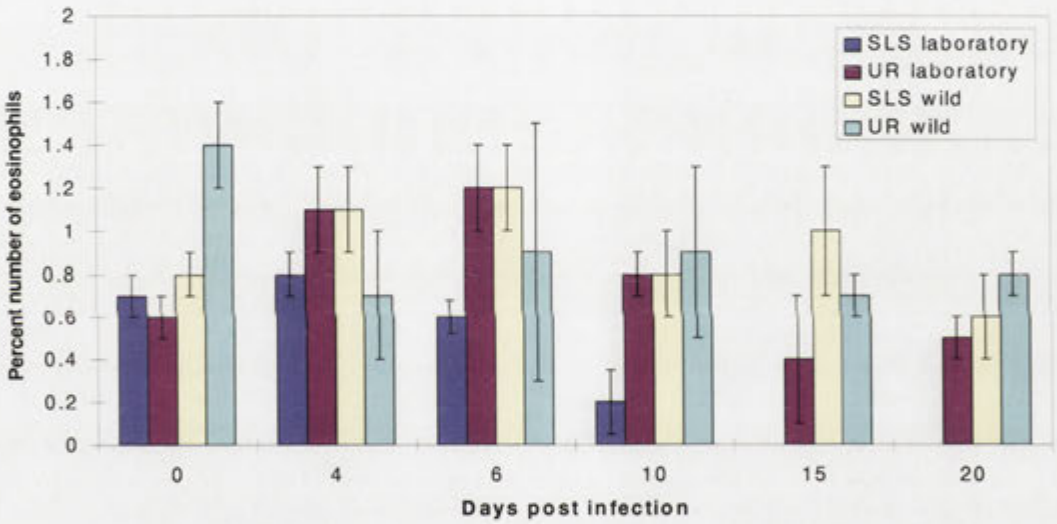
Percent number of eosinophils
2
1.8
1.6
1.4
1.2
1
0.8
0.6
0.4
0.2
0
SLS laboratory
UR laboratory
SLS wild
UR wild
0
4
6
10
15
20
Days post infection

C

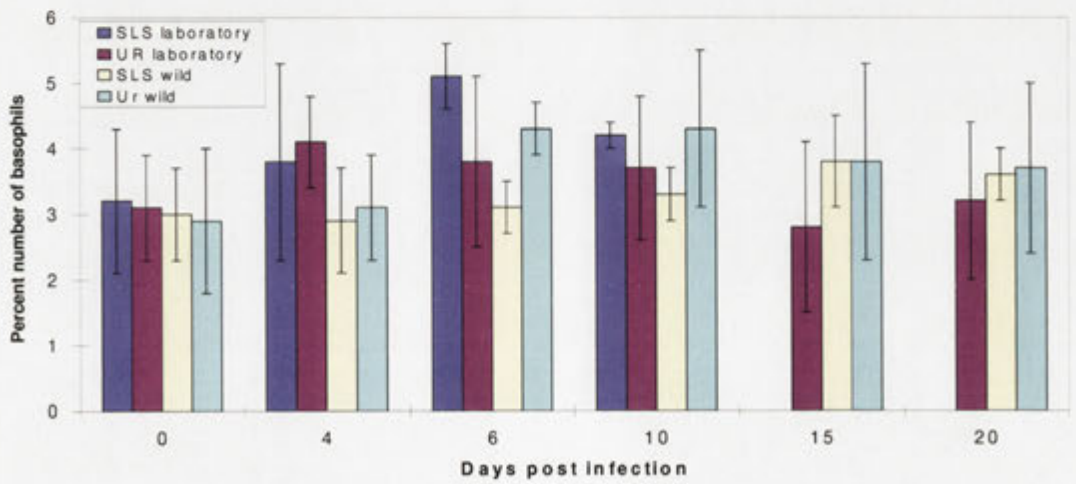
Percent number of basophils
6
5
4
3
2
1
0
SLS laboratory
UR laboratory
SLS wild
Ur wild
0
4
6
10
15
20
Days post infection

3.3.8.2 Differential WBC counts

Percent changes in numbers of basophils, eosinophils, mononuclear cells, lymphocytes and neutrophils in peripheral blood smears were monitored over the course of infection with myxoma virus. Laboratory rabbits infected with Uriarra, or laboratory and wild rabbits infected with Uriarra, did not demonstrate any changes in relative cell numbers (Figure 3.20, Figure 3.21). The percent cell numbers of basophils and monocytes in laboratory rabbits inoculated with SLS did not change over 10 days of infection, although there was a slight decrease in the percent number of eosinophils present at 10dpi (Figure 3.20). There was a large increase in the percent of neutrophils in the peripheral blood from 6 dpi which was concomitant with a decrease in the percent of lymphocytes present (Figure 3.21). The change in the proportion of lymphocytes in blood smears was not due to a change in the number of lymphocytes counted in a sample, but due to the increase in neutrophils, resulting in proportionally less lymphocytes in a sample.

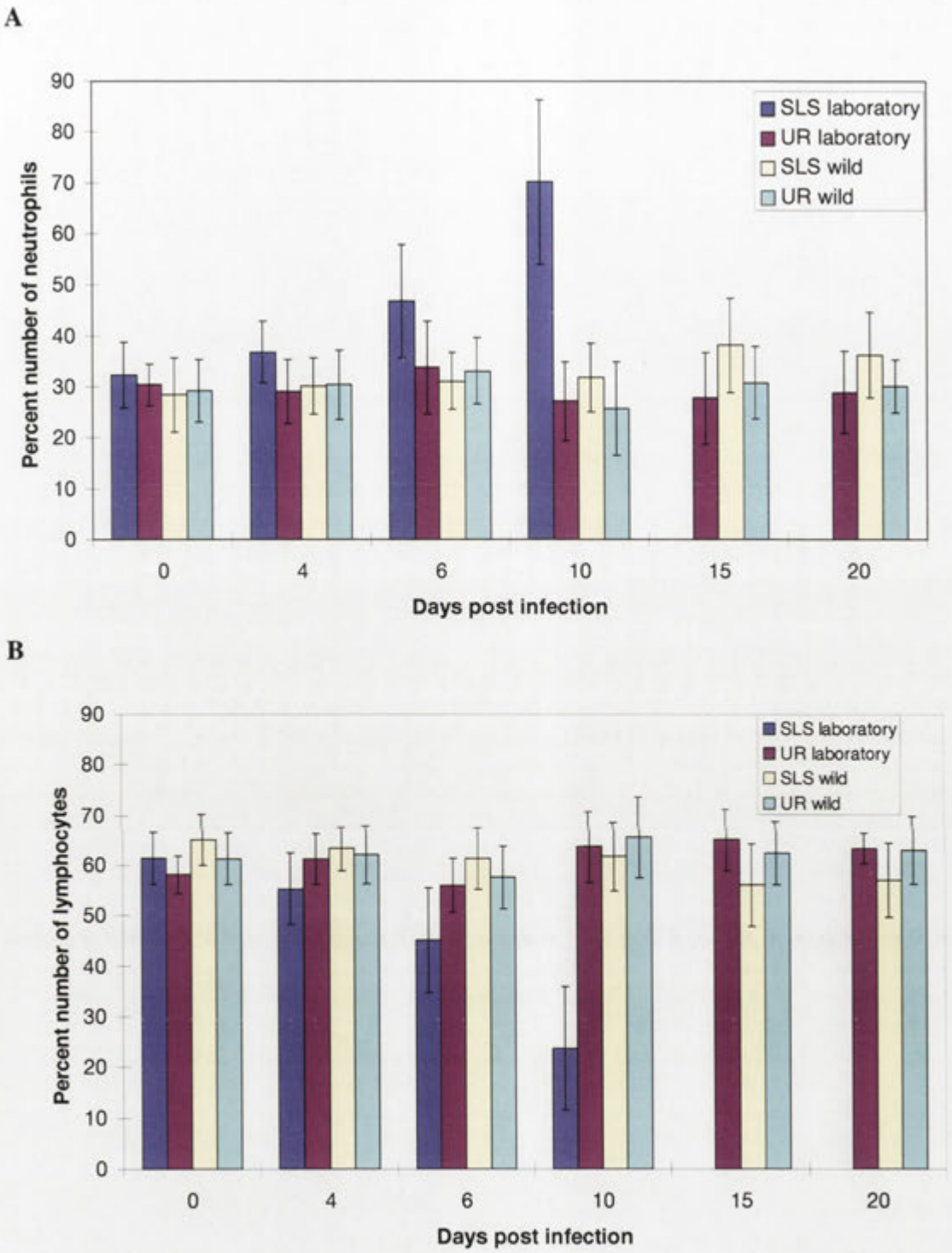

Figure 3.21: Differential WBC counts of peripheral blood samples following infection of *O. cuniculus* with myxoma virus. The percent number of neutrophils (**A**) and lymphocytes (**B**) were determined from blood samples taken from laboratory and wild rabbits infected with SLS or Uriarra (mean ± SE of all rabbits for each time except where n=2. The bars then indicate a range about the mean). Changes in number of rabbits infected with each virus at each time point are the same as indicated for Figure 3.19.

3.4 Discussion

The study described in this Chapter examined virus titres in tissues from laboratory and wild rabbits infected with SLS or Uriarra, to investigate when and in which tissues control of virus replication occurs. This study also examined the rectal temperature, peripheral WBC and antibody responses of wild and laboratory rabbits infected with SLS and Uriarra which confirmed the results obtained in Chapter 2, and extended these for wild rabbits. Differences between individual rabbits in each group were observed, especially following infection of rabbits with attenuated myxoma virus. This is unavoidable in outbred populations and especially as only two or three animals could be used at each time point. However, the investigation of virus titres at up to six time points, and in four groups of infected rabbits, made the results very clear. These are discussed below for each set of infected rabbits.

The first samples in which virus titres were measured were collected at 2dpi. At this time in laboratory rabbits, SLS was present only in the primary inoculation site and draining lymph node. However by 4dpi, rabbits had a generalised infection, with SLS present in the contralateral lymph node, spleen, WBC and distal skin. Rectal temperature increased between 2 and 5dpi, and a discrete primary lesion formed over this time at the inoculation site, but rabbits were not showing any other clinical signs of myxomatosis. These commenced at 6dpi, when rabbits had inflammation of both the anogenital region and conjunctivae. Secondary lesions are an obvious clinical feature of virus generalisation and were present over the face and body of SLS-infected laboratory rabbits from 6dpi. Clinical signs of myxomatosis progressed in severity, such that rabbits were having difficulty breathing because of mucopurulent discharge from the nose due to secondary bacterial infection of the upper respiratory tract, and hence experiments were not continued beyond 10dpi. Virus titres in the tissues had peaked at 6dpi, and were similar at 10dpi. Virus titres and clinical signs were consistent with the pathogenesis described by Fenner and Woodroofe (1953) in which virus spread from the primary inoculation site to the draining lymph node, where monocytes/lymphocytes became infected, which subsequently disseminated virus to other tissues. It is not possible to examine the clearance of virus and

recovery of rabbits, as SLS infection of laboratory rabbits is uniformly lethal (Fenner and Ratcliffe, 1965).

Infection of laboratory rabbits with the attenuated Uriarra strain of myxoma virus had a similar pattern to SLS, with virus replication in the skin and draining lymph node by 2dpi. Uriarra was disseminating by 4dpi as it was present in the spleen. However, a generalised infection of the contralateral lymph node, spleen, lung, distal skin and in WBC was not present until 6dpi. Similarly to SLS-infected laboratory rabbits, the rectal temperatures of Uriarra-infected rabbits became elevated between 2 and 5dpi, and the first clinical changes in eyelids and anogenital regions were observed at 6dpi. However, inflammation of these areas was milder and progressed more slowly than in SLS-infected laboratory rabbits. Secondary lesions were not observed over the face until 9dpi, indicating that the generalisation of Uriarra infection in laboratory rabbits was slower than in SLS-infected laboratory rabbits. There was little difference in Uriarra titres between 6 and 10dpi, with both peak titres and peak temperatures measured during this time. In general, Uriarra was present at lower titres than SLS. This was more obvious in distal tissues, particularly the lung and skin. Severity of clinical symptoms peaked between days 12 and 13. By 15dpi, the reduction in severity of clinical myxomatosis was associated with clearance of virus from many tissues; a reduction in virus titre in the primary inoculation site at 15dpi presaged the beginnings of resolution of the primary lesion observed at 17dpi.

SLS infection of wild rabbits is not an inconsequential disease. These rabbits became significantly ill, but as with Uriarra infection of laboratory rabbits, were able to control virus infection and mostly survive the disease. At 2dpi of wild rabbits with SLS, only one of two rabbits had virus in the draining lymph node, although both had titres in the skin comparable to laboratory rabbits infected with SLS. At 4 and 6dpi, virus was present in the draining lymph node of all infected wild rabbits but at titres considerably less than in laboratory rabbits, and virus persisted in this tissue throughout the 20 days of infection. Virus was present in the spleen of one wild rabbit at 4dpi and in the distal skin of both, indicating that dissemination was occurring by this time, but it was not present in the lymph node draining the distal skin at 4dpi. Moreover, SLS was only detected in peripheral WBC

from one wild rabbit. By 6dpi, SLS was present in the contralateral lymph node of two of three wild rabbits, but at all subsequent time points, there was at least one rabbit in which virus was not detectable in this tissue. In the lung, virus was present in only one of three rabbits at each of 6 and 10dpi at titres around 10^2 to 10^3 pfu/g. Similarly to laboratory rabbits infected with SLS, changes in the anogenital region and eyelids were first observed at 6dpi and rectal temperatures increased between 2 and 5dpi. Clinical signs progressed rapidly and peaked around 12dpi, but progression appeared a day or so behind in comparison with laboratory rabbits. Another difference was in the secondary lesions of SLS-infected wild rabbits which were small and retained discrete margins, unlike the indefinite and merged secondary lesions on the eyelids and ears of laboratory rabbits. Unlike laboratory rabbits infected with Uriarra, some wild rabbits cleared SLS completely in the draining lymph node and spleen by 15dpi, although there was usually one rabbit which still had virus in this tissue, and all rabbits had SLS present in the distal skin but at relatively low titres.

Wild rabbits infected with Uriarra showed only mild clinical signs of myxomatosis, which were limited to the primary inoculation site and occasional mild anogenital swelling. Secondary lesions did not form in the majority of infected wild rabbits, and while temperatures were elevated, the average temperature did not reach 40°C. Virus titres in the skin were similar to the other infections, but virus was not present in the draining lymph node until 4dpi. At 10dpi, Uriarra was present in the draining lymph node of one of three rabbits but was not detected after 10dpi. Despite the lack of secondary skin lesions, systemic dissemination of Uriarra was occurring in wild rabbits as virus was present in the spleen at 6dpi, and low virus titres were present in the contralateral lymph node from 6dpi. Uriarra was not detected in peripheral WBC. Uriarra was detected in the distal skin of only one of three wild rabbits at each of 15 and 20dpi, at 10^2 to 10^3 pfu/g, indicating that it did reach the skin but appeared unable to replicate to high titres. In contrast to SLS infection, Uriarra was cleared from both lymph nodes between 10 and 15 days of infection. This is similar to what occurred in Uriarra-infected laboratory rabbits although infected laboratory rabbits had much more severe clinical signs.

Despite the differences in clinical signs and outcomes of infection, there was little difference between virus titres in the primary inoculation site in any of the treatments. However, there were clear differences in timing of dissemination and in titres reached in both the draining lymph node and distal tissues in laboratory rabbits infected with attenuated virus and in rabbits with a degree of genetic resistance. These differences in timing of dissemination were correlated with slower development of clinical signs. Despite dissemination being apparently delayed, virus does reach distal tissues but replicates to lower titres, indicating that replication is being constrained. It is not clear whether the delay in dissemination is due to the less efficient replication in the draining lymph node. In Uriarra-infected laboratory rabbits, titres in the draining lymph node and timing of virus dissemination to distal tissues were similar to those infected with SLS. However, replication in the distal tissues was limited. In contrast, SLS infected wild rabbits had lower virus titres in the draining lymph node, dissemination was somewhat slower, and the titres in the distal tissues were reduced. Thus it appears that in wild rabbits, there is a distinct constraint of virus replication in the draining lymph node, which was not present in laboratory rabbits, as well as a constraint of virus replication in distal tissues, which was observed in Uriarra-infected laboratory rabbits. The subsequent clearance of virus from internal organs and resolution of clinical signs were closely linked. However, virus persisted at the primary inoculation site in all rabbits for the 20 days of the experiment despite the rapid recovery of wild rabbits and the beginnings of resolution of the primary lesion.

Critical events in control of virus infection appear to be mediated very early in infection. I have shown in Chapter 2 that the ability of lymphocytes from the draining lymph node of SLS-infected laboratory rabbits to respond to mitogenic stimulation is suppressed by 4dpi, and this may be critical in allowing the overwhelming infection that occurs both in this node and in distal tissues. Myxoma virus encodes proteins that are expected to suppress mediators of the anti-viral immune response, including TNF$^{\alpha/\beta}$ and IFN$^{\gamma}$ (Mossman *et al.*, 1995a; Schreiber and McFadden, 1994; Schreiber *et al.*, 1997; Upton *et al.*, 1991; Upton *et al.*, 1992), and this suggests that wild rabbits are more effective at combating these viral proteins and mounting an effective immune response. My data indicate that this occurs

within the first four days of infection, and so most likely reflects a more effective innate immune response of wild rabbits, particularly in the draining lymph node. The stimulation of a strong and appropriate innate immune response is more likely to enable an effective cell-mediated immune response, with the appropriate balance of T_H1 and T_H2 responses, to allow rabbits to control virus replication and survive infection (Fearon and Locksley, 1996; Kos and Engleman, 1996).

In another poxvirus system, resistance to ectromelia virus infection by inbred strains of mice is manifested by reduced virus replication in the spleen and liver following intravenous inoculation (Brownstein *et al.*, 1993). This constraint of virus replication is evident early in infection, before the generation of virus-specific CTL (O'Neill and Blanden, 1983). Resistance to ectromelia virus has been mapped to loci from the NK gene complex, and involves NK cells (Delano and Brownstein, 1995; Jacoby *et al.*, 1989) as well as interferons (Jacoby *et al.*, 1989), especially interferon-γ (Karupiah *et al.*, 1993a), as blocking the activity of NK cells or interferon-α/β or -γ abrogates resistance. In addition, mice that are resistant to ectromelia virus infection produce higher levels of T_H1 associated cytokines (Ramshaw *et al.*, 1997), and develop earlier and stronger virus-specific CTL responses (O'Neill and Brenan, 1987) compared to susceptible mice. Based on the similarities in the early control of replication, it is possible that similar mechanisms of control are involved in the resistance of wild rabbits to myxoma virus infection, but which are more important remains to be examined.

The greater antibody titres produced by SLS-infected compared to Uriarra-infected laboratory rabbits in Chapter 2 led to the suggestion that production of high titres of virus specific antibody in laboratory rabbits may indicate a poor prognosis. However, wild rabbits infected with SLS, and which it is presumed would have survived infection post 20 days, produced high titres of anti-viral antibody from 10dpi compared to rabbits infected with Uriarra. Whether this antibody has a role in control of virulent myxoma virus infection is unclear. The data from studies with vaccinia virus in mice suggest that antibody may have a role in controlling poxvirus infections. Infection of IL-6 knockout mice, which have a reduced capacity to produce antibody in response to infection, results in

higher titres of virus in the ovary compared to infection of wild-type mice (Ramsay *et al.*, 1994). In particular, neutralising antibody may be important in controlling spread of virus from cell-to-cell by preventing the release of extracellular enveloped virus (EEV) from the surface of infected cells (Vanderplasschen *et al.*, 1997). The early dissemination of SLS may thus be important in determining the outcome of infection, with the early and high production of neutralising antibody by wild rabbits reducing virus dissemination or replication in particular tissues.

Despite the involvement of respiratory difficulties in the clinical pathogenesis of myxoma virus infection of both laboratory and wild rabbits, gross pathology of the lung was rarely observed, and virus did not replicate to high titres in the lung. This is supported by Hurst (1937a) who found no clear correlation of clinical signs (difficulty breathing) with lung histopathology. Respiratory distress may thus be attributable to pathology of the upper respiratory tract. This was demonstrated in laboratory rabbits inoculated with malignant rabbit virus (Strayer *et al.*, 1983a) which developed secondary bacterial infection with *Pasteurella multocida* of the conjunctiva and nasal mucosa, but not of the lungs or trachea.

An interesting and unexpected finding in this Chapter concerns the comparison of virus growth in the skin with the internal tissues. Virus titres at the primary inoculation site remained high over the course of infection of laboratory rabbits with Uriarra, or of wild rabbits with SLS or Uriarra, while virus was cleared from the internal tissues of most rabbits by 15 or 20dpi. It has been suggested that different immune response mechanisms are employed in the control of replication of ectromelia and herpes simplex viruses in the skin compared to the internal organs of mice (Karupiah *et al.*, 1996; Nash *et al.*, 1987). During infection with these viruses, specific $CD8^+$ T-cells are critical in the control of virus replication in internal tissues. However in the skin, $CD8^+$ T-cells were not sufficient for control of virus replication and $CD4^+$ T-cells were required for virus clearance in a role which was independent of their provision of help to $CD8^+$ T-cells. This suggests that $CD4^+$ T-cells have an active role in the elimination of virus in the skin, perhaps through the production of cytokines. It was speculated that IFN^γ production by $CD4^+$ T-cells may be important in controlling virus replication in the skin. Indeed, IFN^γ is critical in the control

of ectromelia virus infection, but this is not the mechanism of T-cell mediated virus clearance. Inhibition of the function of IFN$^{\gamma}$, and to a lesser extent IFN$^{\beta}$, in mice exacerbated titres of ectromelia virus in internal tissues but had no effect on virus titres in the skin, again suggesting that control of virus infection in the skin and internal tissues may operate through different mechanisms (Karupiah *et al.*, 1993a). However, the relative roles of individual components of the rabbit immune response such as IFN or $CD4^+$ and $CD8^+$ T-cell subsets, to myxoma virus infection of laboratory and wild rabbits are unknown. In the case of myxoma virus, virus-encoded mediators of the immune and inflammatory responses have evolved to allow the virus to persist in the skin of the natural host where as far as it known, systemic dissemination does not occur (Marshall *et al.*, 1963). If virus replicating in the skin of these animals reaches the draining lymph node, which is perhaps likely in antigen presenting cells (dendritic cells and/or macrophages), it must not replicate efficiently at this site. This supports the possibility of different control mechanisms of myxoma virus replication in the skin and lymph node. However, the failure of myxoma virus to disseminate past the skin in its natural host may be a result of differential permissivity of cells in the skin compared to the lymph nodes to myxoma virus replication.

In studies of virus pathogenesis, it is important to know when and in which tissues virus is replicating. It is also important to know what is happening at the cellular level within individual tissues, such as which cell types are involved in virus replication. The skin and lymph nodes are important sites of myxoma virus replication in both laboratory and wild rabbits, infected with either virulent or attenuated virus. However, it is not known which cells become infected with myxoma virus following inoculation into the skin, how virus is transported from the skin to the draining lymph node, where virus replicates within lymph nodes, and how these may differ between virulent and attenuated myxoma virus, and between infected resistant and susceptible rabbits. To address these questions, the histopathogenesis and cellular localisation of virulent and attenuated myxoma virus in the skin and lymphoid tissues of infected laboratory and wild rabbits are examined in Chapter 4.

Chapter 4: Virus localisation and histopathology in the skin, lymph nodes and spleen

4. Virus localisation and histopathology in the skin, lymph nodes and spleen

4.1 Introduction

In Chapter 3, the titres of virulent and attenuated myxoma virus in individual tissues from infected laboratory and wild rabbits were determined. The determination of virus titres in these animals yields information of where the virus is replicating, but not what cells become infected, what pathology is being caused in the tissue, and how this differs between infection of laboratory and wild rabbits with virulent or attenuated myxoma virus. To examine these factors of myxoma virus pathogenesis, it is necessary to examine the histopathology and virus localisation within individual tissues from infected rabbits. The histopathology of tissues from laboratory rabbits infected with virulent myxoma virus has been described for advanced stages of myxomatosis (Rivers, 1930; Hurst, 1937a). These studies examined the skin, lymph nodes, spleen, lung, liver, kidney, testis and brain of infected rabbits, and highlighted myxomatosis as a proliferative and degenerative disease, predominantly affecting the epidermis and vascular-endothelium of the skin, and cells of the reticular and vascular systems in the lymph nodes and spleen. The pathology of myxomatosis was also characterised by the appearance of large, stellate cells called myxoma cells in the dermis of the skin, lymph nodes and spleen (Hurst, 1937a). Hurst (1937a) hypothesised that myxoma virus replicates in vascular endothelial cells causing them to proliferate, bud off and migrate into the tissue as myxoma cells. However, the cellular localisation of myxoma virus in the blood vessels of various tissues has not been examined to investigate this further. The pathological changes in tissues from laboratory rabbits infected with the attenuated neuromyxoma strain of myxoma virus have also been described (Hurst, 1937b). However, Hurst (1937b) concluded that the disease caused by this virus was possibly not true myxomatosis as myxoma cells were not observed in tissues from infected rabbits.

Previous pathological studies have been limited. Firstly, studies of the cellular localisation of virus within individual tissues has not been published in any detail (Mims, 1964; Strayer and Sell, 1983), and studies of tissue histopathology have not considered the localisation of virus in their interpretation, or the titres of virus within the same tissues. Secondly, the study of attenuated myxoma virus did not involve a

naturally attenuated strain of myxoma virus. In addition, there has been no study to investigate differences in the histopathology and/or cellular localisation of virulent myxoma virus in rabbits that have a degree of genetic resistance compared to susceptible rabbits. Finally, the study of virulent and attenuated myxoma virus has not been brought together in one group of rabbits and has not been described in a detailed time course study.

The study in this Chapter examined the pathology caused by virulent or attenuated myxoma virus, and the cellular localisation of virus, in the primary lesion, distal skin, draining and contralateral lymph nodes and the spleen of both laboratory and wild rabbits. The tissues investigated were portions of the same tissues in which virus titres were determined in Chapter 3, from wild rabbits, and from laboratory rabbits inoculated in both the thigh and the dorsum of the hind foot. Changes in the expression of selected cell markers (MHC class II, MHC class I, μ chain of immunoglobulin on B-cells, CD43, CD45) in lymph nodes, and of MHC class II in the skin, were determined by immunolocalisation. The visualisation of this specific staining, particularly for myxoma virus, and the corresponding histopathological changes within individual tissues of laboratory and wild rabbits was utilised to addresses the following questions relating to myxoma virus pathogenesis: what cell types are infected following inoculation of myxoma virus into the skin; what is the likely mode of transport of virus from the skin to the draining lymph node; what cell types are infected in the lymph nodes and spleen and what changes in cell populations occurs in the lymph nodes of laboratory rabbits; what immunopathologic mechanisms may occur in the lymphoid tissue; what is the extent of involvement of the spleen in virus replication and pathogenesis; where and when control of virus replication occurs and what key factors of myxoma virus pathogenesis differ between virulent and attenuated myxoma virus infection of either laboratory or wild rabbits?

4.2 Materials and Methods

4.2.1 Infection of rabbits and tissue collection

The tissues examined for histopathology and immunolocalisaton were the primary inoculation site in the skin, distal skin, draining lymph node, contralateral lymph node, and spleen, and were portions of the tissues taken from myxoma virus-infected rabbits in section 3.2.3. These tissues were from laboratory rabbits that had been inoculated either in the thigh or foot and killed at 2, 4, 6 and 10dpi with 100pfu SLS, or at 2, 4, 6, 10, 15 and 20dpi with 100pfu of Uriarra. Tissues from the additional time point of 8dpi were available from laboratory rabbits that had been inoculated with either SLS or Uriarra in the thigh. Tissues were collected from wild rabbits inoculated in the hind foot with 100pfu of either SLS or Uriarra and killed at 2, 4, 6, 10, 15 and 20dpi. The numbers of rabbits killed at each time point are shown in Table 4.1. Portions of all tissues were taken for both fixed and frozen sections. In addition, two laboratory and two wild rabbits were infected with 100pfu of either SLS or Uriarra in the dorsum of both hind feet and killed at 12 and 24 hours post infection (hpi). The inoculation site, which had been carefully shaven of hair and marked on the skin, and the draining lymph node were removed for frozen tissue sections only (see section 4.2.2.2).

4.2.2 Histology and immunohistochemistry

4.2.2.1 Histology

At autopsy, portions of tissue were fixed in 4% buffered formaldehyde and embedded in paraffin wax and processed as described in section 2.2.5.1.

Table 4.1: The number of laboratory and wild rabbits infected with SLS or Uriarra that were killed at each time post infection and their tissues examined by histology and immunofluorescence for myxoma virus and MHC II positive cells. An asterix (*) indicates the time points at which two laboratory rabbits were killed following inoculation in the hind foot and two rabbits were killed that had been inoculated in the thigh. (#) indicates where the two rabbits killed following inoculation in the thigh. All wild rabbits were inoculated in the hind foot. (hpi) hours post infection, (dpi) days post infection.

	Laboratory rabbits		Wild rabbits	
Time post infection	Uriarra	SLS	Uriarra	SLS
12 hpi	2	2	2	2
24 hpi	2	2	2	2
2 dpi	4 *	4 *	2	2
4 dpi	4 *	4 *	2	2
6 pdi	4 *	4 *	3	3
8 dpi	2 #	2 #	3	3
10 dpi	4 *	4 *	3	3
15 dpi	2	-	3	3
20 dpi	2	-	3	3

4.2.2.2 Sectioning of the primary inoculation site and draining lymph node from 12 and 24 hpi

Following intradermal inoculation of myxoma virus into the dorsum of the hind feet, the point of penetration through the skin and the margins of the skin that had become raised following injection of virus inoculum, were marked. At 12 or 24 hpi, rabbits were killed and this entire area of skin, and the draining popliteal lymph node removed. The skin was divided into thirds; the middle third containing the needlestick point, and the first and third portions containing the remaining skin that had been marked. The draining lymph node was trimmed of fat and cut in halves lengthwise along the dorsum. All portions of tissue were placed in individual small foil cups, covered in OTC embedding fluid (Tissue Tek), snap frozen in liquid nitrogen and stored at –70°C. The entire tissue blocks were sectioned on a cryostat; sequential tissue sections (serial sections) of 4-7μm were placed onto superfrost slides (Menzel-Glaser) which had been previously coated in a 0.01% poly-L-lysine (Sigma) solution (v/v in ddH_2O) and air-dried. Sections were labeled, and fixed as described in section 2.2.5.3 for the

identification of specific antigens by immunohistochemistry.

At all other time points, blocks (10mm x 2mm) of tissue from the primary site of virus inoculation, the skin site distal to the inoculation site, the draining and contralateral lymph nodes, and the spleen were placed in individual small cups made of foil and covered in O.C.T. embedding fluid. These were treated as described above for the early time points, although the sectioning regime was different. Ten serial sections were made and placed onto slides. The tissue was sectioned through a further 100μm and the sections discarded, ten more serial sections were made and retained, a further 100μm of tissue was sectioned through and discarded, and ten more serial sections made and retained. The serial sections were placed on slides and fixed as above.

4.2.2.3 Primary and secondary monoclonal antibodies

The mouse monoclonal antibodies used to detect specific rabbit cell antigens were supplied by Serotec (Raleigh, North Carolina, US), and used at a 1:10 dilution. These were: anti-CD43 (L11/135) which has high affinity for T-cells, and low affinity for monocytes and macrophages (Wilkinson *et al.*, 1992); anti-Ig$^{\mu}$ (NRBM) which recognises the Fc chain of IgM expressed on the surface of B-cells; anti-CD45 (L12/201) (Jackson *et al.*, 1983) which recognises the leucocyte common antigen and hence is a pan leucocyte marker; MHC class I (73-2), MHC class II RLA-DQ (2C4) (Lobel and Knight, 1984). To detect SLS or Uriarra, the mouse anti-myxoma virus monoclonal antibody (3B6E4) was used at a 1:200 dilution. By western blot, 3B6E4 recognises a late protein of the virus core. It is cross-reactive for the North and South American strains of myxoma virus as well as Shope fibroma virus, but is not cross-reactive with the *Orthopoxvirus*, vaccinia virus. In myxoma virus-infected tissue culture cells, the monoclonal antibody recognises virus in the cytoplasm, as discrete virus factories early in infection and in the entire cytoplasm late in infection (P.J. Kerr, unpublished).

Secondary antibodies used were FITC-conjugated goat anti-mouse Ig (Boehringer Mannheim; 1:50), Rhodamine-conjugated goat anti-mouse Ig (Boehringer Mannheim, 1:10), biotin-conjugated sheep anti-mouse Ig (Boehringer Mannheim; 2μg/ml or 1:500), and unconjugated sheep anti-mouse Ig (Silenus; 1:50).

4.2.2.4 Single stained immunofluorescence for myxoma virus

Frozen tissue sections were stained for myxoma virus as described in section 2.2.5.5.

4.2.2.5 Alkaline phosphatase single staining for cell markers

Frozen sections of lymph nodes and spleen from uninfected and myxoma virus-infected rabbits were blocked overnight at 4°C in 5% skim milk powder (Diploma) in 1x Tris Buffered Saline (TBS; 10mM TrisHCl, 0.15M NaCl, pH 8.0) and then washed four times in TBS. 50µl of the primary antibody L11/135, NRBM, L12/201, 73-2 or 2C4 was added, ensuring complete coverage of each section, and sections were incubated for 2 hours at 37°C. The primary and secondary antibodies and the streptavidin enzyme conjugate were all diluted in 1% milk/TBS. Sections were washed four times in TBS and 100µl of secondary antibody applied (sheep anti-mouse Ig conjugated with biotin). Sections were incubated for 2 hours at 37°C and washed four times in TBS. 100µl of streptavidin conjugated alkaline phosphatase (Amersham Life Science) at 1:150 was added and incubated for 1hour at 37°C, followed by four washes with TBS. The binding of specific antibody was visualised by development with fast red. One fast red tablet (Boehringer Mannheim) was dissolved in 2ml 0.1M Tris HCl, pH 8.2, filtered and 100µl added to each section, which were left at room temperature for 5min before rinsing with ddH_2O. The fast red substrate was used in preference to BCIP/NBT due to the resulting red product which was readily counterstained with haematoxylin. Sections were immersed in Gills Number 3 haematoxylin for 20 seconds, rinsed in water, immersed in Scotts tap water substitute for 20 seconds, rinsed in water and finally coverslipped using Girrs' aqueous mounting agent, Aquamount improved (BDH Laboratory Supplies).

4.2.2.6 Double immunofluorescence staining for myxoma virus and MHC II

Fixed frozen tissue sections of lymph node and skin were blocked in 3% BSA in PBS overnight at 4°C, followed by four washes in PBS. 50µL of 2C4, 1:10 in 1% BSA/PBS, was added to each section, followed by incubation for 2 hours at 37°C. Sections were washed as above and 100µl of goat anti-mouse conjugated to FITC (1:50 in 1%BSA/PBS) added and sections incubated for a further 1 hour at 37°C. FITC was utilised first as it is a smaller molecule than rhodamine. From this point, all steps were

completed in a box covered in foil to limit light penetration. Slides were washed and 100µl of 1:50 sheep anti-mouse Ig in 1% BSA/PBS added to each section. Slides were incubated for 1 hour at 37°C, washed and the second primary antibody added. This antibody was mouse anti-myxoma virus monoclonal (3B6E4) diluted 1:200 in 1%BSA/PBS. Slides were incubated for 1 hour at 37°C, washed and 50µl of 1:10 sheep anti-mouse Ig conjugated to rhodamine (section 4.2.2.3) added to each section, followed by a further 1hour incubation at 37°C. Sections were washed and mounted with coverslips using Antifade. Control sections for this procedure included staining of tissue sections from uninfected rabbits and the use of normal mouse ascites fluid in place of either primary antibody. For each section that was stained for both myxoma virus and MHC class II, the section that was cut from the block immediately before and after it was stained for either myxoma virus or MHC class II, but not both.

4.3 Results

The following is a description of the cellular localisation of myxoma virus within the skin at the primary inoculation site, the distal skin, the draining and contralateral lymph nodes and the spleen, from both wild and laboratory rabbits infected with either SLS or Uriarra. It also includes a description of the histopathology of myxoma virus within these tissues, and a description of changes in the presence of cells staining positive for selected cell markers. Tissue sections were examined for every rabbit from each time point, including from laboratory rabbits inoculated both in the dorsum of the hind foot and in the thigh. For each rabbit killed (Table 4.1), at least three sections were examined from every tissue for each of histology, immunofluorescent staining for myxoma virus, and for MHC class II. The immunolocalisation of all other specific cell markers was performed on tissue sections from laboratory rabbits only.

Histopathological changes in the skin, the lymph nodes and the spleen of laboratory rabbits late in infection with SLS were not markedly different from those described by Hurst (1937a). However, the descriptions by Hurst (1937a) did not examine many time points early in infection or describe the cellular localisation of virus. Hence, the following is a description of the time course of infection and highlights the differences in virus localisation and pathology following infection of laboratory and wild rabbits with either SLS or Uriarra.

4.3.1 The primary inoculation site

4.3.1.1 Uninfected skin

Skin was taken from the dorsum of the hind feet of uninfected rabbits, and from the primary lesion and uninoculated distal skin site of myxoma virus infected rabbits. Uninfected skin is shown in Figure 4.1. Rabbit skin consisted of a thin epidermis and the dermis, with a number of large hair follicles (Figure 4.1A). The epidermis (Figure 4.1B) consisted of a single layer of cuboidal cells with oval nuclei, the stratum basale, which was overlaid by layers of progressively flattened cells (the stratum spinosum). The next cell layer, the stratum granulosum, consisted of cells containing keratohyaline granules, but was not always obvious in the thin skin located over the foot. The outermost layer consisted of flattened dead cells, the stratum corneum, from which desquamating keratin was usually observed.

The dermis (Figure 4.1C) consisted of connective tissue of collagen and elastic fibres, as well as many fat cells and blood vessels (Figure 4.1D). There were a number of cell types represented in the dermis that could be identified by their nuclear morphology including lymphocytes, mast cells, macrophages, and fibroblasts. The most common of these were lymphocytes and fibroblasts (Figures 4.1 B and D). Bundles of superficial striated muscle layers were located immediately below the dermis.

When uninfected skin sections were stained for MHC class II by immunofluorescence (Figure 4.2), positive staining cells localised to areas directly under or at the epidermal/dermal junction, around the margins of hair follicles or directly outside blood vessels (Figure 4.2A). These cells were elongated, with a long cellular process (30μm long) extending from one or both ends of the nucleated body (approximately 30μm across) (Figure 4.2B). Deeper in the dermis, the majority of MHC class II positive cells present (at approximately 18 cells/mm^2) had the morphology of a nucleated body with multiple dendritic processes (Figure 4.2C). Other MHC class II positive staining cellular bodies did not have clear morphologies and were likely to be the cellular processes and portions of similar cells that had been sectioned through.

4.3.1.2 Histopathological changes, cellular localisation of myxoma virus and MHC class II positive cells in the skin at the primary lesion of rabbits

Changes in the skin at the primary inoculation site following infection of rabbits with

Figure 4.1: Skin from the dorsum of the hind foot of an uninfected laboratory rabbit showing the structure and visible cell types. **(A)** The epidermis and dermis which contains hair follicles. **(B)** The epidermis of uninfected rabbit skin. **(C)** The dermis of uninfected rabbit skin. **(D)** Blood vessels in the epidermis showing the single layer of flattened endothelial cells. E, epidermis; HF, hair follicles; SB, stratum basale; SC, stratum corneum; K, keratin; L, lymphocyte; F, fibroblast; VE, vessel endothelium. Bars represent 100μm.

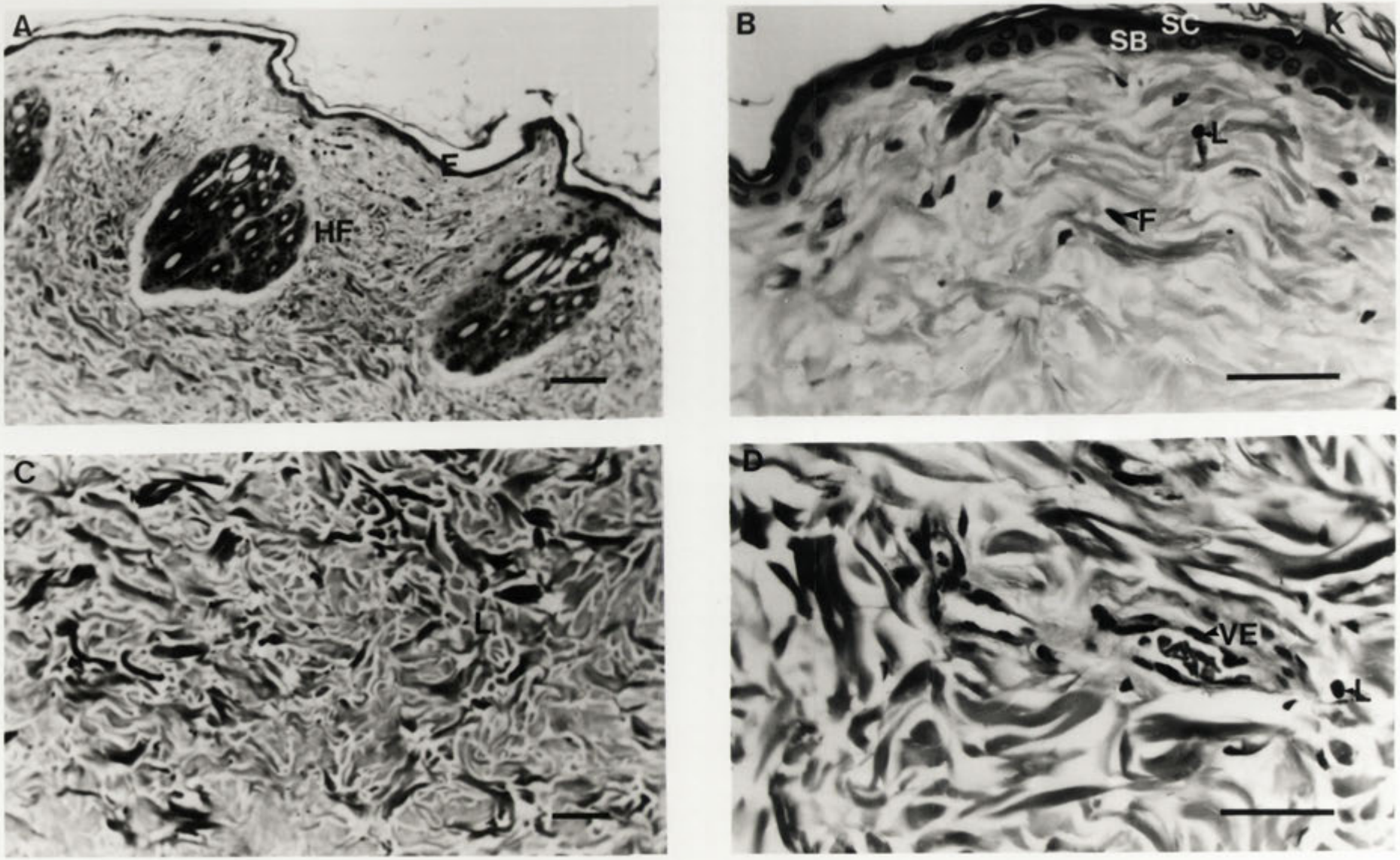
A
E
HF
B
SB
SC
K
L
F
C
L
D
VE
L

Figure 4.2: Typical MHC class II staining by immunofluorescence in the skin of an uninfected rabbit. (**A**) Distribution of MHC class II positive cells in skin. MHC class II^+ cells localised to the epidermal/dermal junction and surrounding blood vessels in the dermis. Bar represents 200μm. (**B**) Morphology of MHC class II positive cells at the epidermis/dermis junction. Bar represents 25μm. (**C**) Morphology of MHC class II positive cells in the dermis. Bar represents 10μm. E, epidermis; D, dermis, arrows indicate blood vessels.

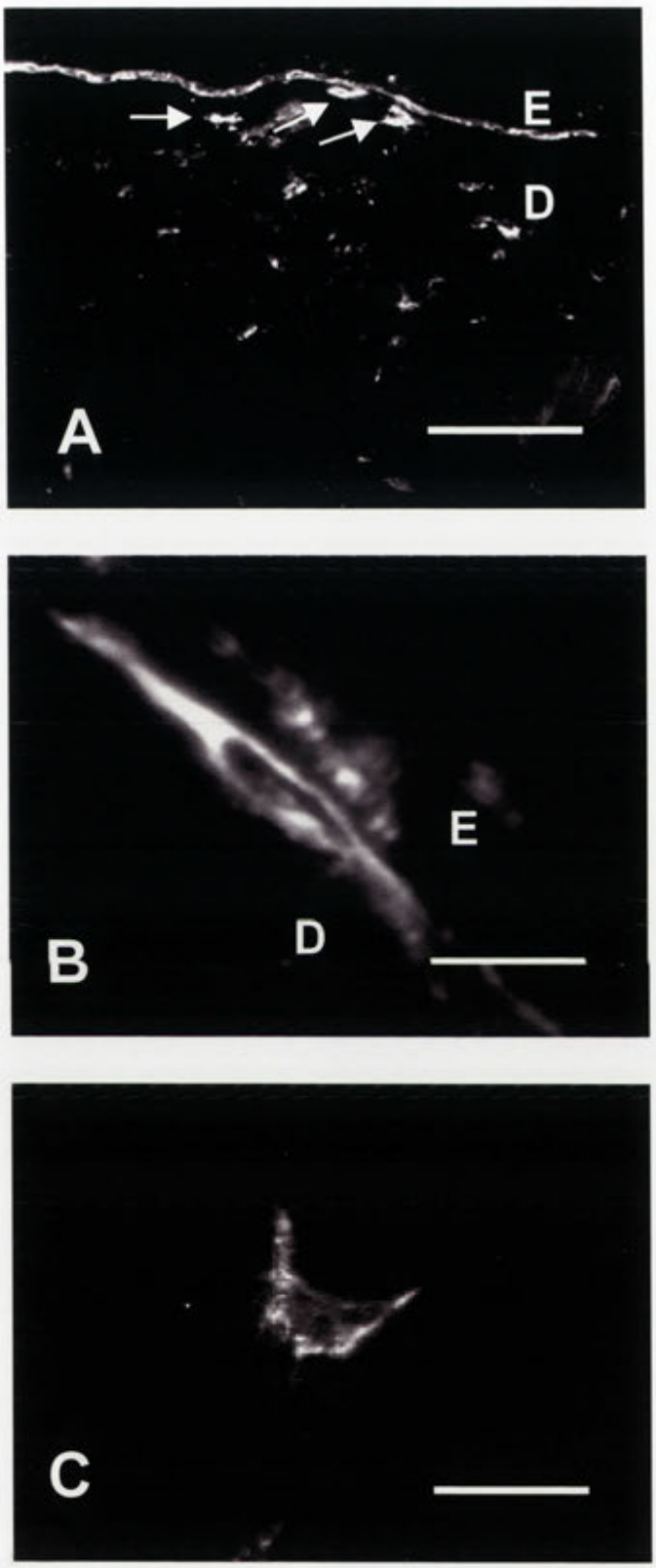
E
D
A
E
D
B
C

myxoma virus occurred particularly in the stratum basale of the epidermis, the endothelial cells of blood vessels and the connective tissue in the dermis, and in the infiltration of inflammatory cells into the dermis (Table 4.2). The changes in the epidermis and dermis are described below. The changes in the endothelial cells in the blood vessels are described separately. The changes in MHC class II positive cells, and the cells that became infected with myxoma virus in the skin, are also described below.

Table 4.2: MHC class II staining, myxoma virus localisation and histopathology in the primary inoculation site in the skin following intradermal inoculation of laboratory or wild rabbits with either SLS or Uriarra.

	SLS		Uriarra	
	Laboratory	**Wild**	**Laboratory**	**Wild**
		TWELVE HOURS POST INFECTION		
MHC class II	Fibroblast-like cells and dendritic cells of epidermis/ dermis junction and dermis	Fibroblast-like cells and dendritic cells of epidermis/ dermis junction and dermis	Fibroblast like cells and dendritic cells of epidermis/ dermis junction and dermis	Fibroblast-like cells and dendritic cells of epidermis/ dermis junction and dermis
Virus localisation	Not present	Not present	Not present	Not present
		TWENTY-FOUR HOURS POST INFECTION		
MHC class II	Fibroblast-like cells and dendritic cells of dermis	Fibroblast-like cells and dendritic cells of dermis	Fibroblast-like cells and dendritic cells of dermis	Fibroblast-like cells and dendritic cells of dermis
Virus localisation	Dendritic cells in the dermis	Dendritic cells in the dermis	Dendritic cells in the dermis	Dendritic cells in the dermis
		TWO DAYS POST INFECTION		
MHC class II	Fibroblasts and dendritic cells of dermis	Fibroblasts and dendritic cells of dermis	Fibroblasts and dendritic cells of dermis	Fibroblasts and dendritic cells of dermis
Virus localisation	Fibroblasts and dendritic cells of dermis	Fibroblasts and dendritic cells of dermis	Fibroblasts and dendritic cells of dermis	Fibroblasts and dendritic cells of dermis

Table 4.2 continued:

	SLS		Uriarra	
	Laboratory	**Wild**	**Laboratory**	**Wild**
	FOUR DAYS POST INFECTION			
MHC class II	Fibroblasts and dendritic cells of dermis	Fibroblasts and dendritic cells of dermis	Fibroblasts and dendritic cells of dermis	Fibroblasts and dendritic cells of dermis
Virus localisation	Fibroblasts and dendritic cells of dermis	Fibroblasts and dendritic cells of dermis	Fibroblasts and dendritic cells of dermis	Fibroblasts and dendritic cells of dermis
Epidermis	Intracellular edema, cell proliferation	Intracellular edema	Intracellular edema	No change
Inflammation	Mononuclear cell infiltrate into lower dermis	Mononuclear cell infiltrate throughout dermis	Mononuclear cell infiltrate throughout dermis	Mononuclear cell infiltrate throughout dermis
Blood vessels	Swollen endothelium	No change	No change	No change
	SIX DAYS POST INFECTION			
MHC class II	Round cells without dendrites in dermis, few dendritic cells	Round cells without dendrites in dermis, few dendritic cells	Round cells without dendrites in dermis, few dendritic cells	Round cells without dendrites in dermis, few dendritic cells
Virus localisation	Epidermis and external root sheath; round cells in dermis; large, rectangular cells proximal to dermal blood vessels	Epidermis and external root sheath; round cells in dermis	Epidermis and external root sheath; round cells in dermis	Epidermis and external root sheath; round cells in dermis
Epidermis	Intracellular edema, cell proliferation and degradation, virus inclusion bodies	Intracellular edema, cell proliferation	Intracellular edema, cell proliferation	Intracellular edema, cell proliferation
Inflammation	Neutrophillic infiltrate predominantly in lower dermis	Mononuclear cell infiltrate throughout dermis	Mononuclear cell infiltrate throughout dermis	Mononuclear cell infiltrate throughout dermis
Blood vessels	Swelling and proliferation of endothelial cells	Swelling of endothelial cells	Swelling of endothelial cells	No change
Stellate myxoma cells	Present	Absent	Absent	Absent

Table 4.2 continued:

	SLS		Uriarra	
	Laboratory	**Wild**	**Laboratory**	**Wild**
	TEN DAYS POST INFECTION			
Virus localisation	Epidermis and external root sheath; large, rectangular cells proximal to dermal blood vessels	Epidermis and external root sheath;	Epidermis and external root sheath;	Epidermis and external root sheath;
Epidermis	Necrotic, reticular degradation (vesicle formation), virus inclusion bodies	Intracellular edema, cell proliferation and degradation, virus inclusion bodies	Intracellular edema, cell proliferation and degradation, virus inclusion bodies	Intracellular edema, cell proliferation and degradation, virus inclusion bodies
Inflammation	Neutrophillic infiltrate predominantly in lower dermis	Mononuclear cell infiltrate throughout dermis	Massive mononuclear cell infiltrate throughout dermis	Mononuclear cell infiltrate throughout dermis
Blood vessels	Endothelial cell proliferation and necrosis	Swelling of endothelial cells	Swelling of endothelial cells	Swelling of endothelial cells
Stellate myxoma cells	Present throughout dermis	Present in deep dermis	Present in deep dermis	Absent
		FIFTEEN DAYS POST INFECTION		
Virus localisation	-	Stratum basale and external root sheath	Stratum basale and external root sheath	Stratum basale and external root sheath
Epidermis	-	Necrotic, reticular degradation, scab formation	Necrotic, reticular degradation, scab formation	Necrotic, reticular degradation, scab formation
Dermis		Fibroblasts and collagen deposition, extravasated RBC	Fibroblasts and collagen deposition, extravasated RBC	Fibroblasts and collagen deposition
Inflammation	-	Nuclear fragments of mononuclear cells, mononuclear cells throughout dermis	Nuclear fragments of mononuclear cells, mononuclear cells throughout dermis particularly at lesion margins and deep dermis	Mononuclear cells throughout dermis, particularly in deep dermis
Blood vessels	-	Swelling of endothelial cells reduced	Swelling of endothelial cells reduced	Swelling of endothelial cells reduced
Stellate myxoma cells	-	Present in deep dermis	Present in deep dermis	Absent
		TWENTY DAYS POST INFECTION		
Virus localisation	-	Stratum basale and external root sheath	Stratum basale and external root sheath	Stratum basale and external root sheath
Epidermis	-	New stratum basale, extensive scab formation	New stratum basale, extensive scab formation	New stratum basale, extensive scab formation
Inflammation	-	Mononuclear cells throughout dermis	Mononuclear cells throughout dermis particularly at lesion marginsis	Mononuclear cells throughout dermis, particularly in deep dermis

4.3.1.2.1 The dermis and epidermis of the primary lesion

Virus was detected by immunofluorescence in the dermis at the primary inoculation site of both laboratory and wild rabbits infected with either SLS or Uriarra at 24 hpi, but was not observed at 12hpi. At 24hpi, myxoma virus was present in two cell types. The first was a flattened, elongated cell located in the upper dermis, often proximal to the epidermis/dermis junction. These cells resembled fibroblasts. Figure 4.3 A and C are histological sections showing the architecture of the skin and the cell types that myxoma virus localised to (Figures 4.3 B and D). The second cell type was also located in the upper dermis, approximately 130 to 300 µm below the epidermis (Figure 4.4A), and had prominent dendritic cell processes. In Figure 4.4A, there is some autofluorescence associated with keratin in hair follicles. However, this was obviously different from the specific fluorescence obtained by the specific binding of the monoclonal antibody. To examine if cells containing virus costained for MHC class II, sections of 4 to 7 µm were cut sequentially from blocks of tissue (serial sections). One of the sections in a series was stained for myxoma virus, another for MHC class II, and another section was double stained for both antigens. The staining of serial sections in such a manner ensures that the same population of cells, and often the same cell, is being examined in each section. It is also an effective way to work up the protocols for double staining of sections to ensure that the monoclonal antibodies are binding antigens specifically, particularly when the monoclonal antibodies are raised in the same species. Both of the cell types described above that contained virus also stained positive for MHC class II in serial sections (Figure 4.4B) or in double stained sections (Figures 4.4 C and D). These cells were probably both dendritic cells.

By 2 and 4dpi with either SLS or Uriarra, the dermis of the primary lesion of all laboratory and wild rabbits examined contained many cells that stained positive for virus antigen, with little difference observed between the two time points, or between treatment groups. Figure 4.5 shows a typical example of the staining of virus in the cells of the dermis of SLS-infected laboratory and wild rabbits at 4dpi (Figures 4.5 A and C), and the histology of the skin at the primary inoculation site at the same time (Figures 4.5 B and D). There is little difference between the number or distribution of virus-positive cells. There was an increase in the number of elongated fibroblast-like cells in the upper dermis at 4dpi of both laboratory and wild rabbits infected with SLS or Uriarra. At this time, inflammatory mononuclear cells had infiltrated into the dermis of the primary inoculation site of all infected rabbits. However, in SLS-infected rabbits,

Figure 4.3: The histology of the primary inoculation site and immunofluorescent immunolocalisation of myxoma virus at 24 hpi of SLS-infected laboratory rabbits. (**A**) Histological section of the skin at 24 hpi. The cell type that myxoma virus commonly localised to at this time is indicated by an arrow. Bar represents 90μm. (**B**) Myxoma virus positive cell at the epidermal/dermal junction of the skin, similar to the cell indicated in (**A**) Bar represents 30μm. (**C**) Histological section of the skin at 24 hpi indicating fibroblast-like cells in the dermis (arrows). Bar represents 90μm. (**D**) Myxoma virus positive fibroblast-like cell in the dermis at 24hpi. Bar represents 10μm. E, epidermis; D, dermis.

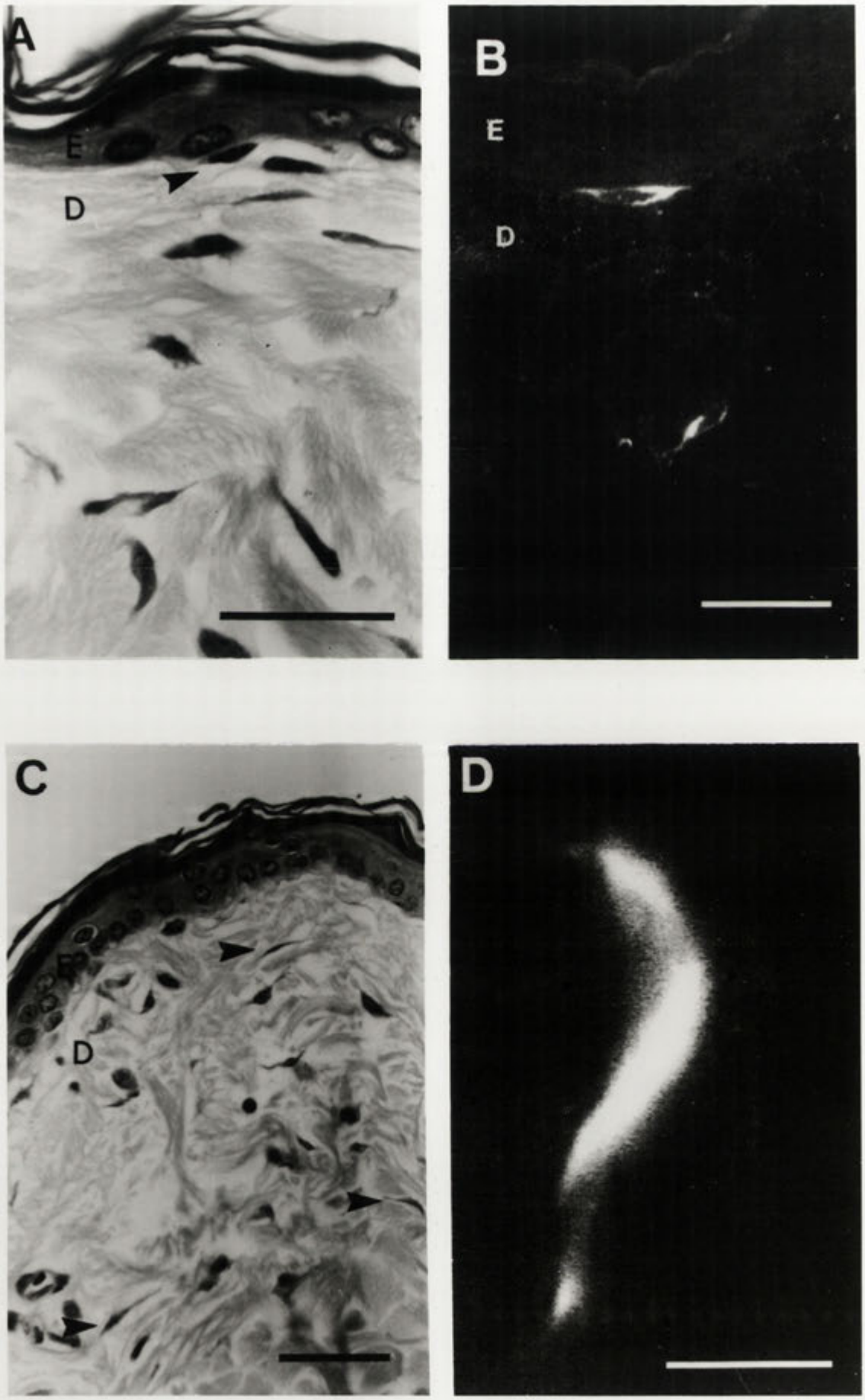
A
E
D
B
E
D
C
D
D

Figure 4.4: Immunofluorescent staining for myxoma virus and MHC class II in the primary inoculation site at 24hpi. **(A)** Skin showing myxoma virus positive cells with dendritic processes in the dermis. Bar represents 225μm. **(B)** Serial section, taken 7μm from **(A)** showing MHC class II staining of cells in the dermis that have a dendritic morphology. Bar represents 225μm. In tissue sections **A** and **B**, the keratin in hair follicles is visible due to autofluorescence. Tissue sections were also double stained for myxoma virus and MHC class II. **(C)** Myxoma virus staining. Bar represents 10μm. **(D)** MHC class II staining of the same cell as in **C**. Bar represents 10μm. E, epidermis; D, dermis; HF, hair follicle.

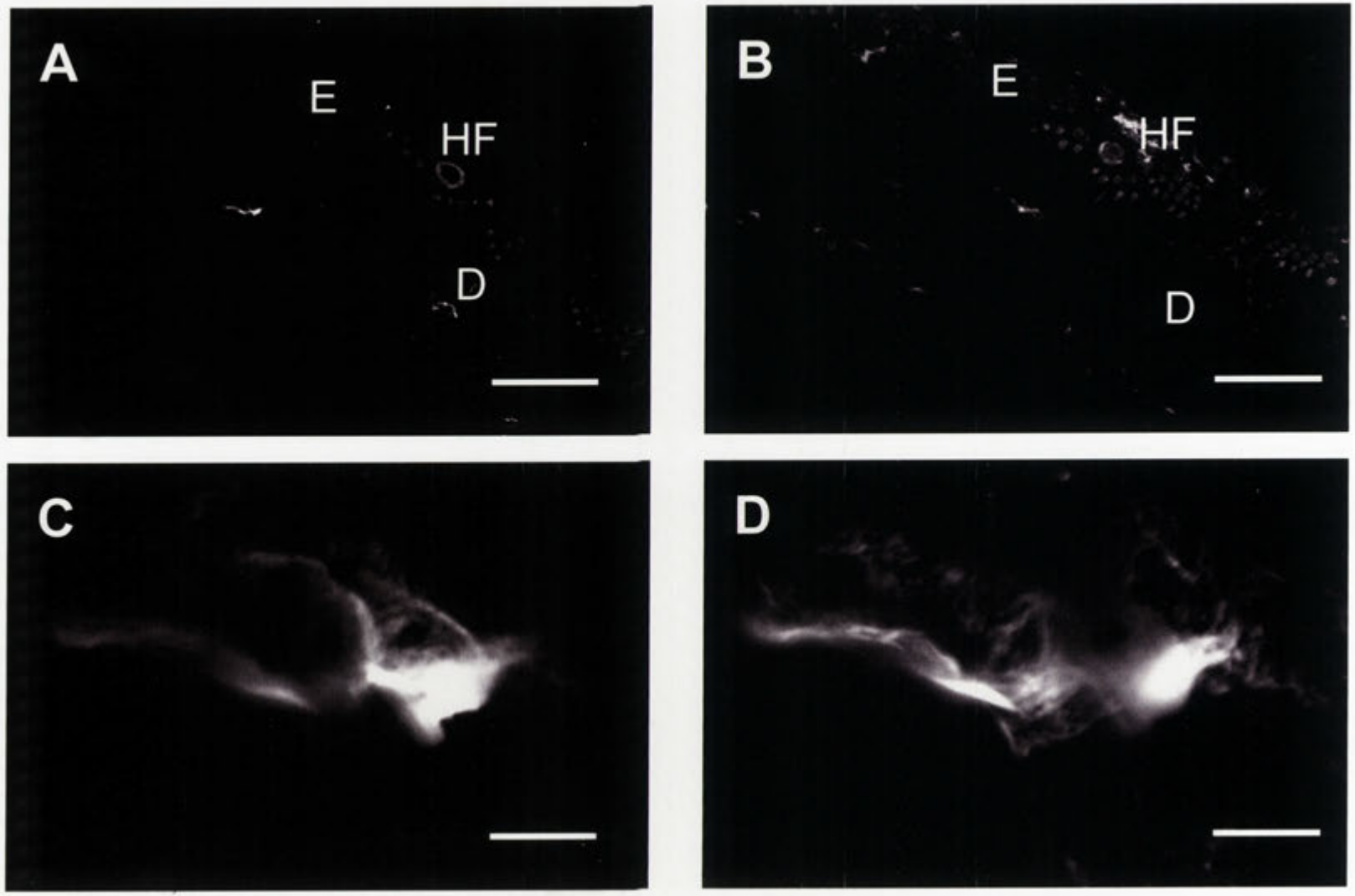
A
E
HF
D
B
E
HF
D
C
D

Figure 4.5: Virus localisation by immunofluorescence and the histology of the skin at the primary inoculation site of SLS-infected laboratory and wild rabbits at 4dpi. (**A**) Myxoma virus positive cells in the dermis of SLS-infected laboratory rabbits at 4dpi. Virus positive cells were not present in the epidermis at this time. Bar represents 150μm. (**B**) The histology of the skin of an SLS-infected laboratory rabbit at 4dpi. Bar represents 100μm. (**C**) Myxoma virus positive cells in the dermis of SLS-infected wild rabbits at 4dpi. Virus positive cells were not present in the epidermis at this time. Bar represents 150μm (**D**) The histology of the skin of an SLS-infected wild rabbit at 4dpi. Bar represents 100μm. E, epidermis; D, dermis.

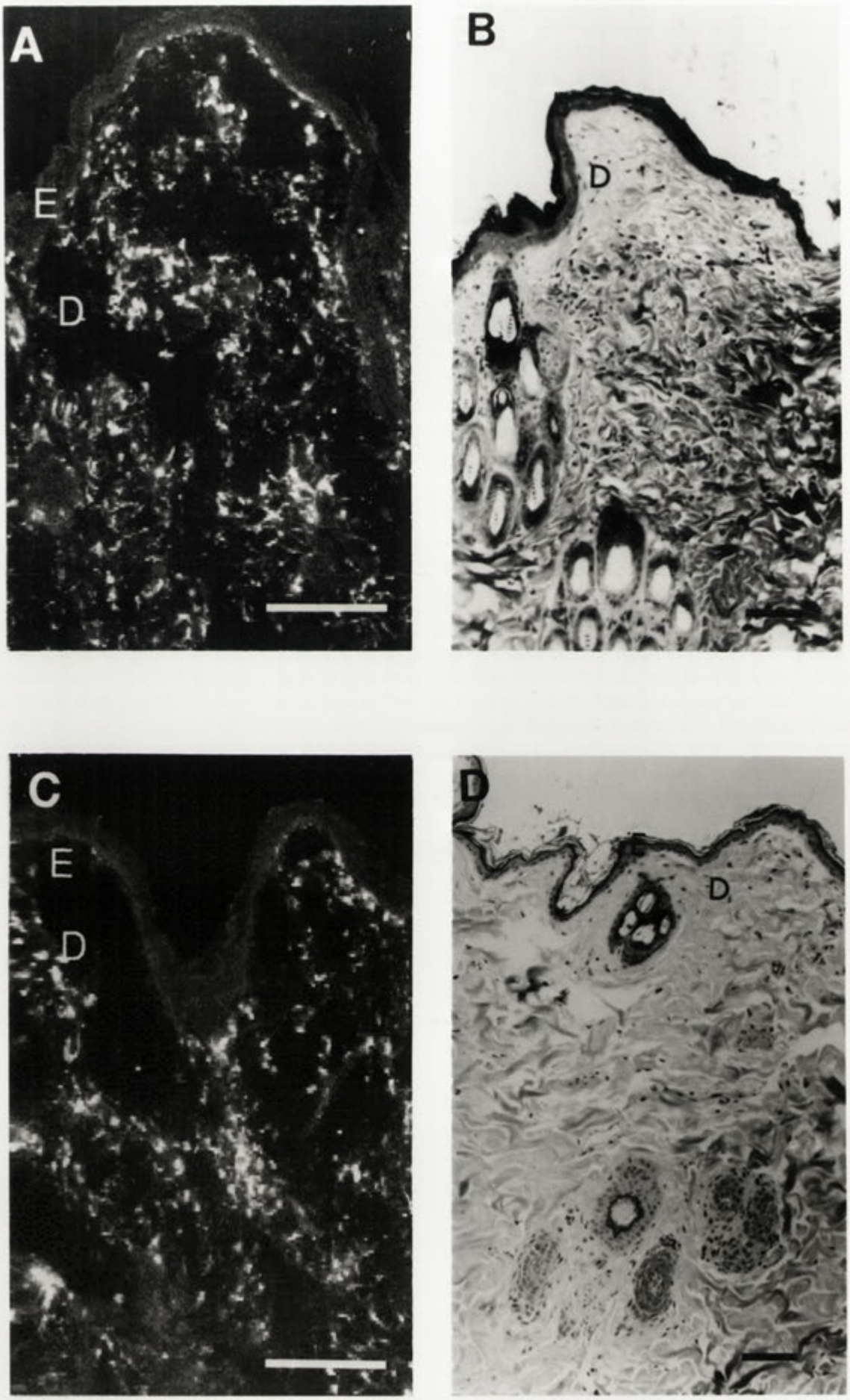
A
E
D
B
D
C
E
D
D
D

these cells were not in the very upper epidermis, close to the epidermal/dermal junction as they were in other infections. In addition, as shown in Figure 4.6, round cells of approximately 10μm in diameter, with a large round nucleus that occupied most of the cell and a thin cytoplasm, stained positive for myxoma virus in dermis from SLS-infected wild rabbits (Figure 4.6 A and B), but not in SLS-infected laboratory rabbits (Figure 4.6 C and D). These cells were probably inflammatory lymphocytes.

In sections stained for MHC class II expression, the number of MHC class II positive cells in the upper dermis at the inoculation site had increased substantially from 24hpi in both SLS- and Uriarra-infected laboratory and wild rabbits (an example is shown in Figure 4.7A; compare with Figure 4.5A), although due to the extent of processes of these cells, they were difficult to quantify. In sections double stained for virus and MHC class II (Figure 4.7B), myxoma virus localised to the cytoplasm of these cells, which had a maximum diameter across the main body containing the nucleus of 15μm, with two to three dendrites that also stained positive for virus (Figure 4.7C and D). By 4dpi of laboratory rabbits with SLS, the spaces between the connective tissue of the dermis of infected rabbits had increased, perhaps indicating some edema. Fibrin had been deposited in localised areas of the dermis.

From 6dpi of laboratory or wild rabbits with SLS or Uriarra, only a small number of cells in the dermis with a dendritic morphology stained positive for myxoma virus or MHC class II (Figure 4.8A). In SLS-infected laboratory rabbits, myxoma virus localised to the endothelium of some blood vessels and virus-positive cells were clustered around these blood vessels (Figure 4.8B). The endothelial cells of these vessels were always swollen and had increased in number (see section 4.3.1.2.2). Endothelial cells did not stain positive for MHC class II, and were not observed positive for virus in the primary lesion from Uriarra-infected laboratory rabbits, or in wild rabbits infected with either SLS or Uriarra. Other dermal cells that did costain for MHC class II and myxoma virus in both laboratory and wild rabbits infected with SLS or Uriarra, were round, approximately 10μm in diameter with no discernable nuclear morphology (Figure 4.8C). However at 6dpi, most of the virus was associated with the epidermis and the epithelial cells of the external root sheath in hair follicles.

Figure 4.9 shows a typical example of myxoma virus localisation and the architecture of the epidermis and hair follicles at 6dpi of laboratory rabbits infected with SLS. Virus

Figure 4.6: Immunofluorescent localisation of myxoma virus in the dermis of the primary inoculation site of SLS-infected laboratory and wild rabbits at 4dpi. **(A)** Myxoma virus positive cells in the dermis of SLS-infected wild rabbits. Bar represents 100μm. **(B)** Myxoma virus positive cells in the dermis of SLS-infected wild rabbits at higher magnification showing infected lymphocytes. Bar represents 15μm. **(C)** Myxoma virus positive cells in the dermis of SLS-infected laboratory rabbits. Bar represents 100μm. **(D)** Myxoma virus positive cells in the dermis of SLS-infected laboratory rabbits at higher magnification showing infected dendritic cells. Bar represents 15μm.

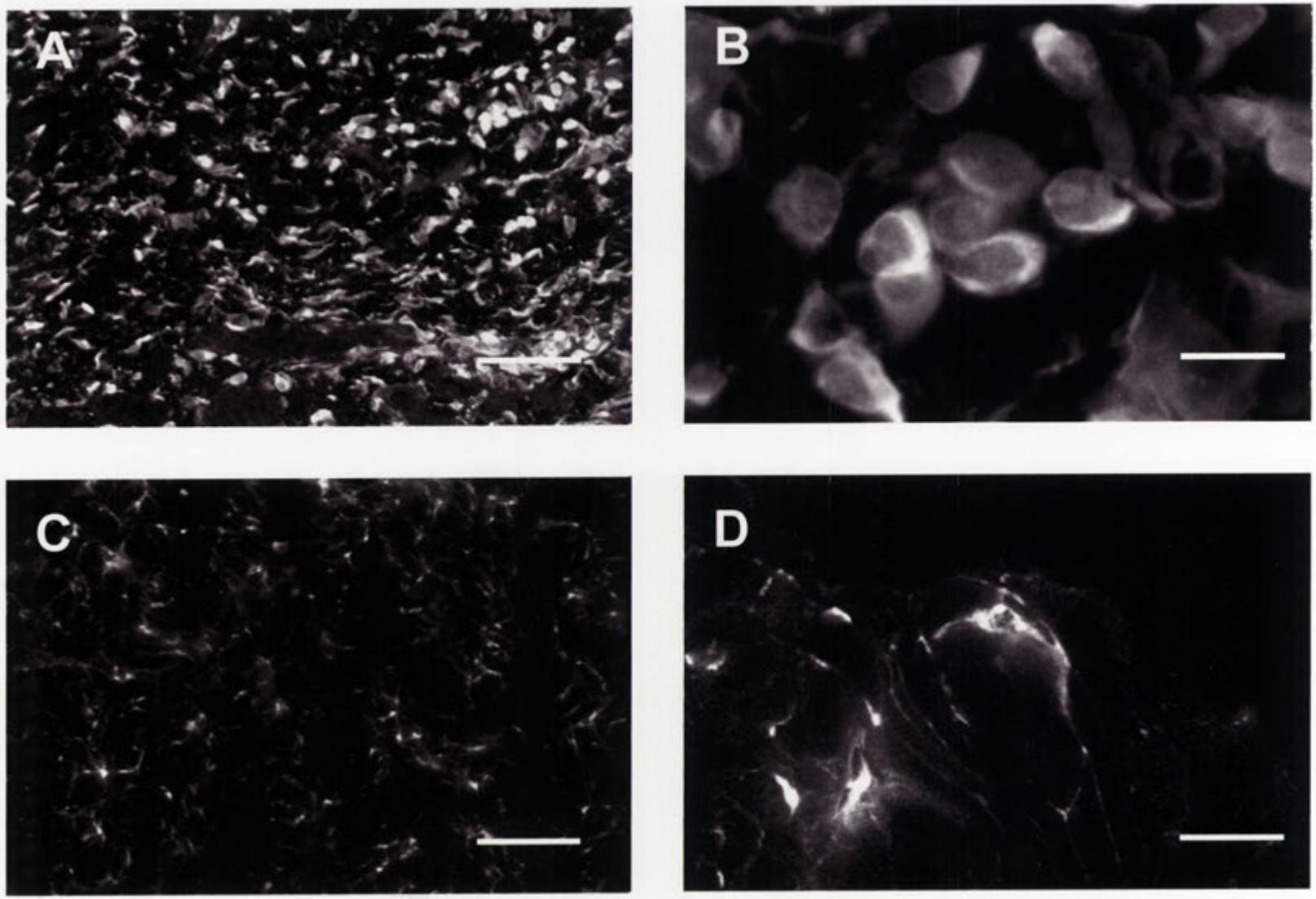
A
B
C
D

Figure 4.7: Skin sections from the primary inoculation site of SLS-infected laboratory rabbits at 4dpi and double stained by immunofluorescence for MHC class II and myxoma virus. (**A**) MHC class II positive staining of dendritic cells in the dermis. Bar represents 160μm. (**B**) Double stained section showing myxoma virus (green) and MHC class II (red) in the dermis. The colocalisation of both myxoma virus and MHC class II in the same cells gives yellow. Bar represents 80μm. (**C**) Colocalisation (shown in yellow) of myxoma virus (green) and MHC class II (red) in a dermal dendritic cell. Bar represents 10μm. (**D**) The staining of the two antigens shown in (**C**) has been digitally split using BIORAD software to show the individual staining of myxoma virus (green) in the cytoplasm of infected cells, and MHC class II (red) on the surface of infected cells. Bar represents 10μm.

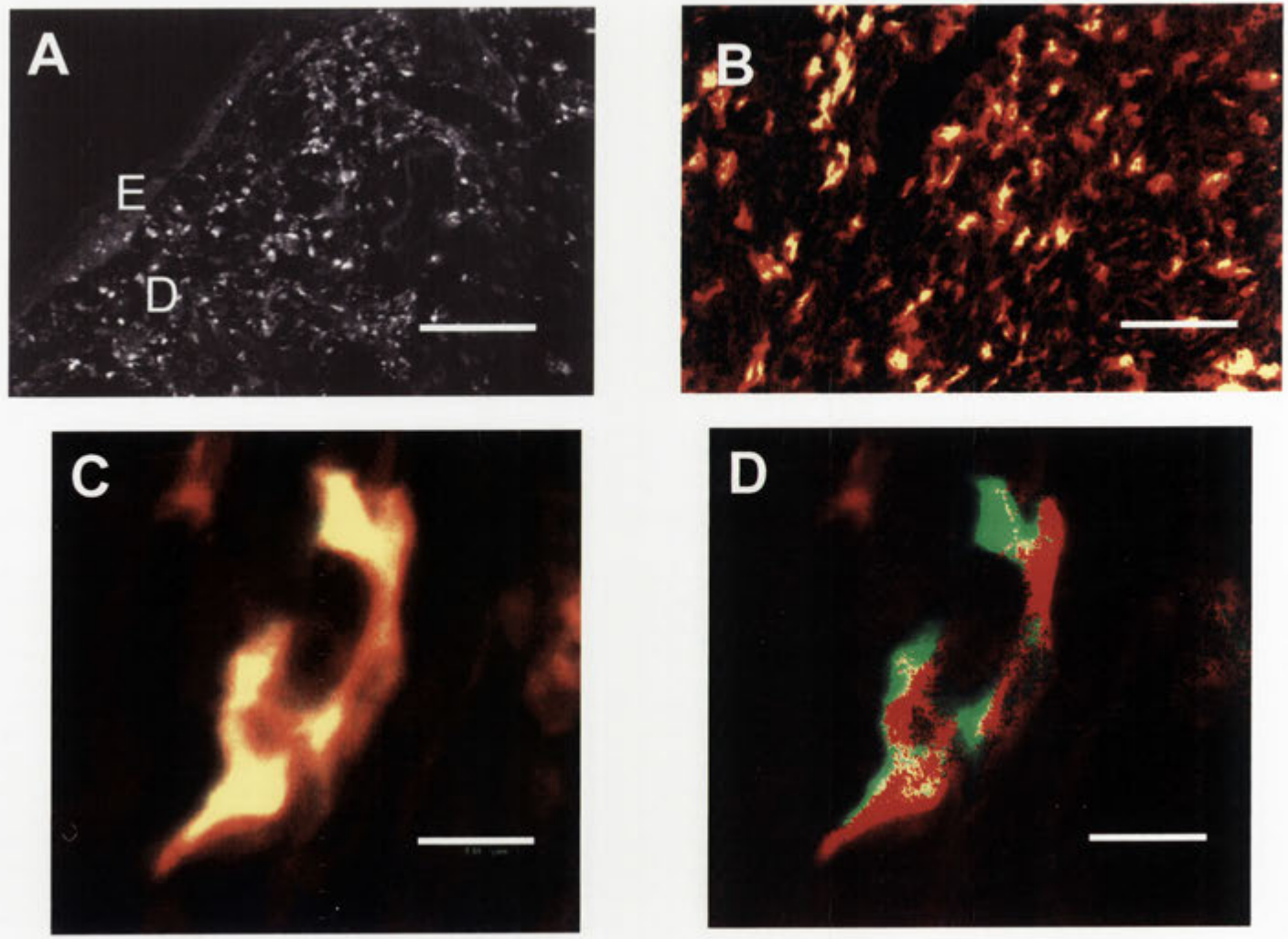
A
E
D
B
C
D

Figure 4.8: MHC class II and myxoma virus staining in the dermis at the primary inoculation site of SLS-infected laboratory rabbits at 6dpi. (**A**) MHC class II positive cells in the dermis of the inoculation site. Bar represents 200μm. (**B**) Myxoma virus positive cells in the blood vessel endothelium and in the dermis immediately surrounding these vessels. Bar represents 8μm. (**C**) Myxoma virus positive cells in the dermis at 6dpi. Bar represents 5μm. E, epidermis; D, dermis; VE, vessel endothelium.

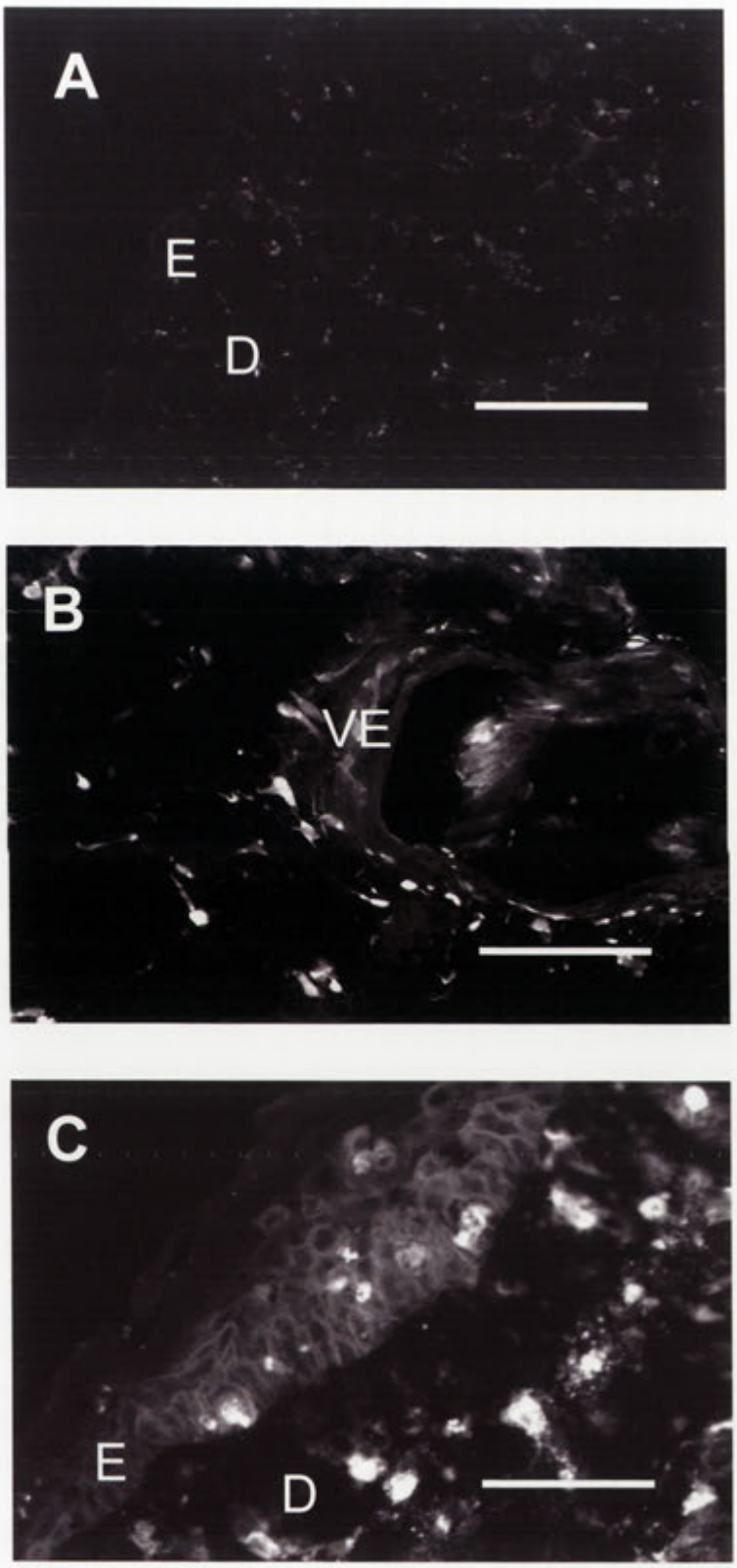
A
E
D
B
VE
C
E
D

Figure 4.9: Histopathology and virus immunolocalisation in the epidermis and hair follicles at the primary inoculation site of SLS-infected laboratory rabbits at 6dpi. **(A)** Histopathology of the epidermis. **(B)** Myxoma virus staining in the epidermis. **(C)** Histopathology of the hair follicle. **(D)** Myxoma virus staining in the hair follicle. E, epidermis; D, dermis; HF, hair follicle. Bars represent 150μm.

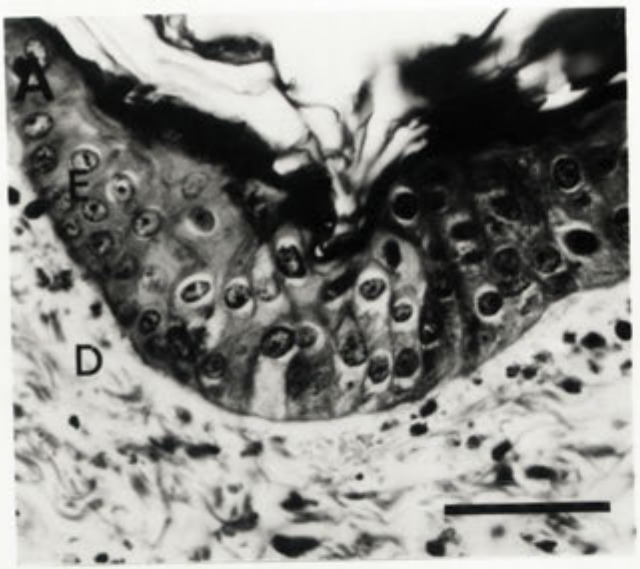
A
E
D

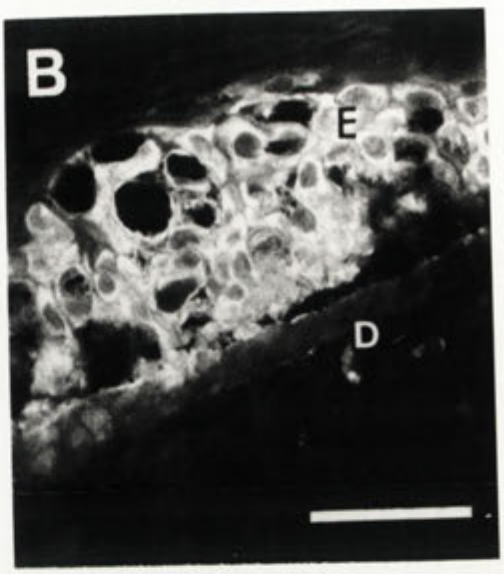
B
E
D


HF

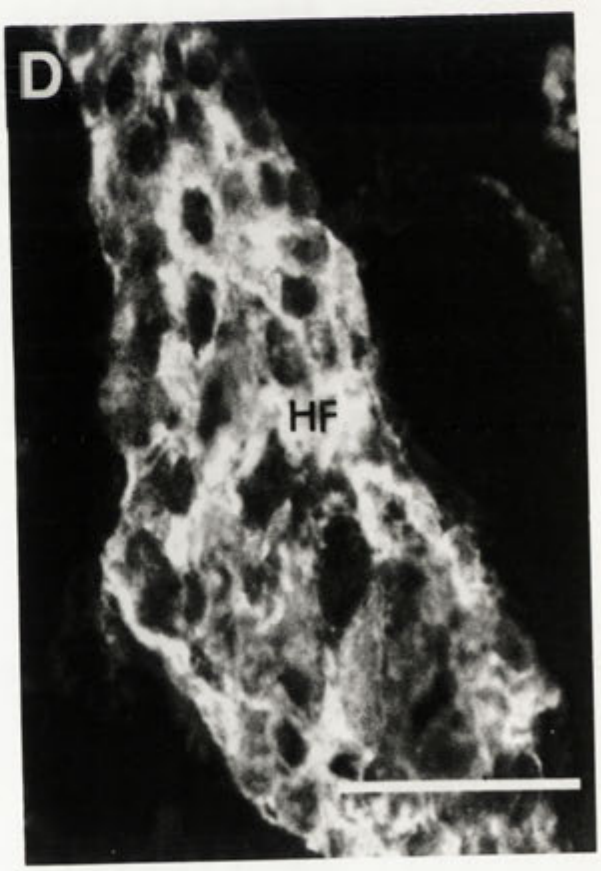
D
HF

replication in the epidermis was associated with a number of cellular changes, particularly in the cells of the stratum basale (Figure 4.10A). There was an increase in the number of cuboidal cells in the lower epidermis, although mitotic figures were not observed at any time post infection. The obvious thickening of the epidermis by 6dpi, and the loss of flattened cells of the upper epidermis could be due either to cell proliferation or differentiation. The elongation and swelling of cells and the cell nucleus indicated pathological changes in epidermal cells. The cytoplasm of these cells became foamy, indicating intracellular edema or hydropic degeneration, and appeared to be compartmentalised to one end of the cell. The nucleus was located at the opposite end of the cell to the cytoplasmic material, and stained heavily at the periphery, indicating marginalisation of nuclear chromatin. The centre of the nucleus appeared either vesicular or contained blocks of dark staining chromatin. In the most severely affected areas of the epidermis, both the nuclear and cellular membranes were poorly defined, indicating degradation and necrosis of cells. At this stage, the cytoplasm of many of the epidermal cells was no longer obvious and round or semi-lunar shaped granules were present at the opposite end of the cell to the nucleus. Others of these cells, some of which did not have a nucleus (which may be an artifact of sectioning of the tissue), contained acidophilic inclusion bodies at one end of the cell (Figure 4.10B). Virus antigen was present at all layers throughout the epidermis in which these changes were observed, with no difference between SLS- or Uriarra-infected laboratory and wild rabbits.

Although the pathology described above was similar for both SLS- and Uriarra-infected laboratory and wild rabbits, differences were observed in the timing and the extent of the changes (Figure 4.11). At 6dpi of laboratory rabbits with SLS (Figure 4.11A), the changes and necrosis of cells in the epidermis were more extensive than following infection with Uriarra at the same time (Figure 4.11B). The cells of the stratum basale had increased in number and size over more diffuse areas, and cell layers of the epidermis appeared more disrupted. It was not until 8dpi of laboratory rabbits inoculated with Uriarra in the thigh, that cells were necrotic, with the nucleus located at one end of the cell, the nuclear membrane was poorly defined and the cytoplasm was foamy. Infection of wild rabbits with SLS or Uriarra induced the same changes in the epidermis of the primary lesion as observed in laboratory rabbits, but the timing of these changes closely followed those in Uriarra-infected laboratory rabbits.

Figure 4.10: Pathological changes in the skin at the primary inoculation site of myxoma virus-infected rabbits at 6dpi. **(A)** The pathological changes in the epidermis are indicated with numbers. (1) swelling of cells of the stratum basale, (2) cellular elongation, (3) increase in the number of cuboidal cells in the stratum basale and the appearance of a foamy cytoplasm, and (4) marginalisation of nuclear chromatin, and presence of viral inclusion bodies within the cytoplasm. At 6dpi, the dermis and the cells within the dermis appeared relatively normal. Bar represents 50μm. **(B)** Cytoplasmic viral inclusion bodies in the epidermis. Bar represents 15μm. BV, blood vessel; F, fibroblast; IB, inclusion body; L, lymphocyte.

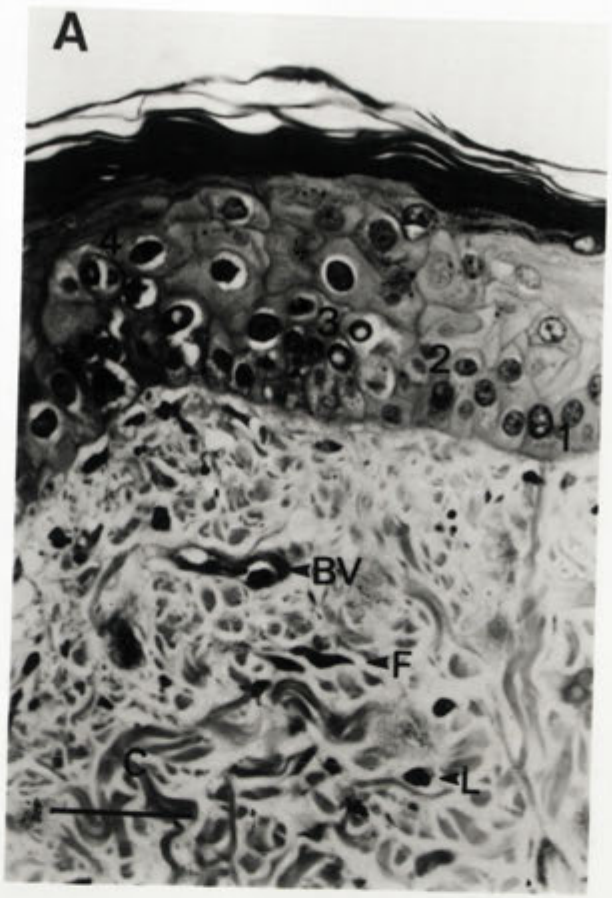
A
4
3
2
1
BV
F
L


B
IB

Figure 4.11: Histopathology of the skin at the primary inoculation site of SLS and Uriarra-infected laboratory rabbits at 10dpi. **(A)** SLS-infected laboratory rabbit. **(B)** Uriarra infected-laboratory rabbit. **(C)** SLS-infected laboratory rabbit. **(D)** Uriarra-infected laboratory rabbit. E, epidermis; HF, hair follicle; IB, inclusion body; nf, nuclear fragments; P, plasma cell; L, lymphocyte. Bars represent 150μm.

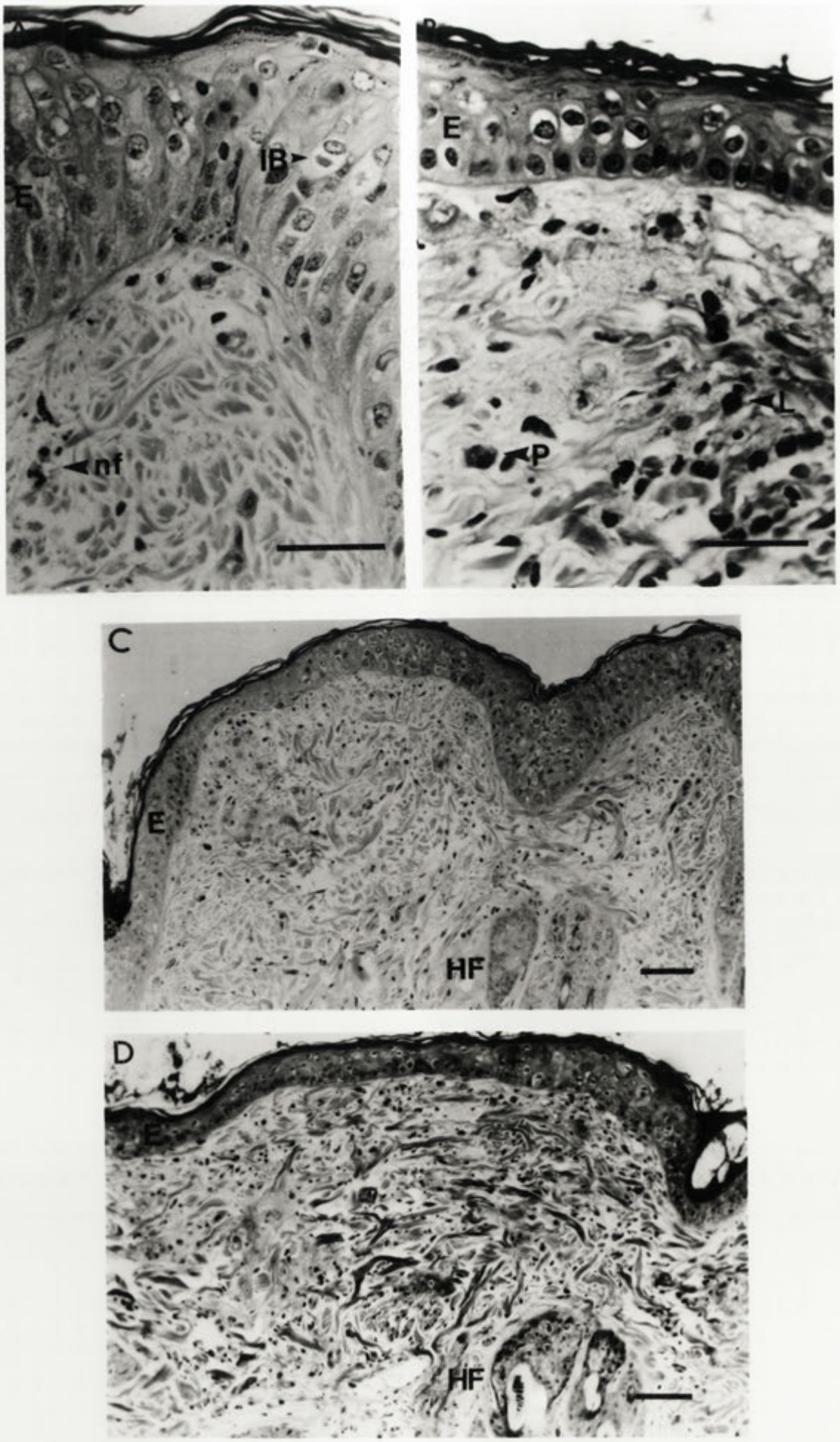
IB
E
nf
E
L
P
C
E
HF
D
E
HF

Figure 4.11 also depicts the differences in the distribution and composition of inflammatory cell infiltrate into the primary lesion of SLS (Figure 4.11 A and C) and Uriarra-infected rabbits at 6dpi (Figure 4.11 B and D). The dermis of the primary inoculation site from laboratory rabbits infected with Uriarra, or wild rabbits infected with either Uriarra or SLS, contained large numbers of mononuclear cells; macrophages, small lymphocytes and some plasma cells. These inflammatory cells were concentrated in the upper dermis, with aggregates of cells at the epidermis/dermis junction, directly below areas of epidermis with the changes associated with cell proliferation and pathology described above (Figure 4.11D). These changes were always associated with staining for myxoma virus by immunofluorescence. The influx of inflammatory cells into the dermis of infected wild rabbits was similar in composition to Uriarra-infected laboratory rabbits but always involved more cells. In contrast, inflammatory cells in the dermis of SLS-infected laboratory rabbits were predominantly neutrophils, which often appeared karyorrhectic or apoptotic, although lymphocytes and macrophages were also present. Similarly to 4dpi, inflammatory cells were less concentrated in the upper dermis of SLS-infected laboratory rabbits compared to Uriarra-infected laboratory rabbits, or to wild rabbits infected with either SLS or Uriarra, and were instead aggregated in the deep dermis, proximal to, and throughout, the superficial muscle layer (Figure 4.12). The muscle layer itself appeared shrunken and less organised in SLS-infected laboratory rabbits (Figure 4.12A) compared to rabbits infected with Uriarra (Figure 4.12B). In both SLS- and Uriarra-infected laboratory rabbits, myxoma virus was present in cells throughout the superficial muscle layer at the primary inoculation site (Figure 4.12 C). Myxoma virus was not observed at the superficial muscle layer of infected wild rabbits.

At 10dpi of laboratory or wild rabbits with either SLS or Uriarra (Figure 4.13), virtually all of the epidermis across the primary lesion stained positive for virus. Histologically, the epidermis of SLS-infected laboratory rabbits showed a marked progression of the changes described at 6dpi (Figure 4.13A). The stratum spinosum was loose and disorganised and contained large, fluid filled vesicles. These vesicles often contained polymorphonuclear leucocytes. The nucleus of many epidermal cells was semi-lunar shaped, shrunken and/or pyknotic, and appeared to be joined to the cell membrane by strands of remnant cytoplasm. Viral inclusion bodies were prominent in many epidermal cells. In Uriarra-infected laboratory rabbits (Figure 4.13B), and in wild rabbits infected with SLS at 10dpi, the epidermis of the primary inoculation site

Figure 4.12: Histopathology and virus localisation at the superficial muscle layer of the primary inoculation site of SLS and Uriarra-infected laboratory rabbits at 10dpi. **(A)** Histopathology of skin from an SLS-infected laboratory rabbit. **(B)** Histopathology of skin from a Uriarra infected-laboratory rabbit. Note the shrunken appearance of muscle in SLS-infected skin and the numerous inflammatory cells deep in the dermis compared to that in skin from Uriarra-infected laboratory rabbits. **(C)** Myxoma virus immunolocalisation in cells proximal to the superficial muscle layer of an SLS-infected laboratory rabbit. D, dermis; SM, superficial muscle. Bars represent 100μm.

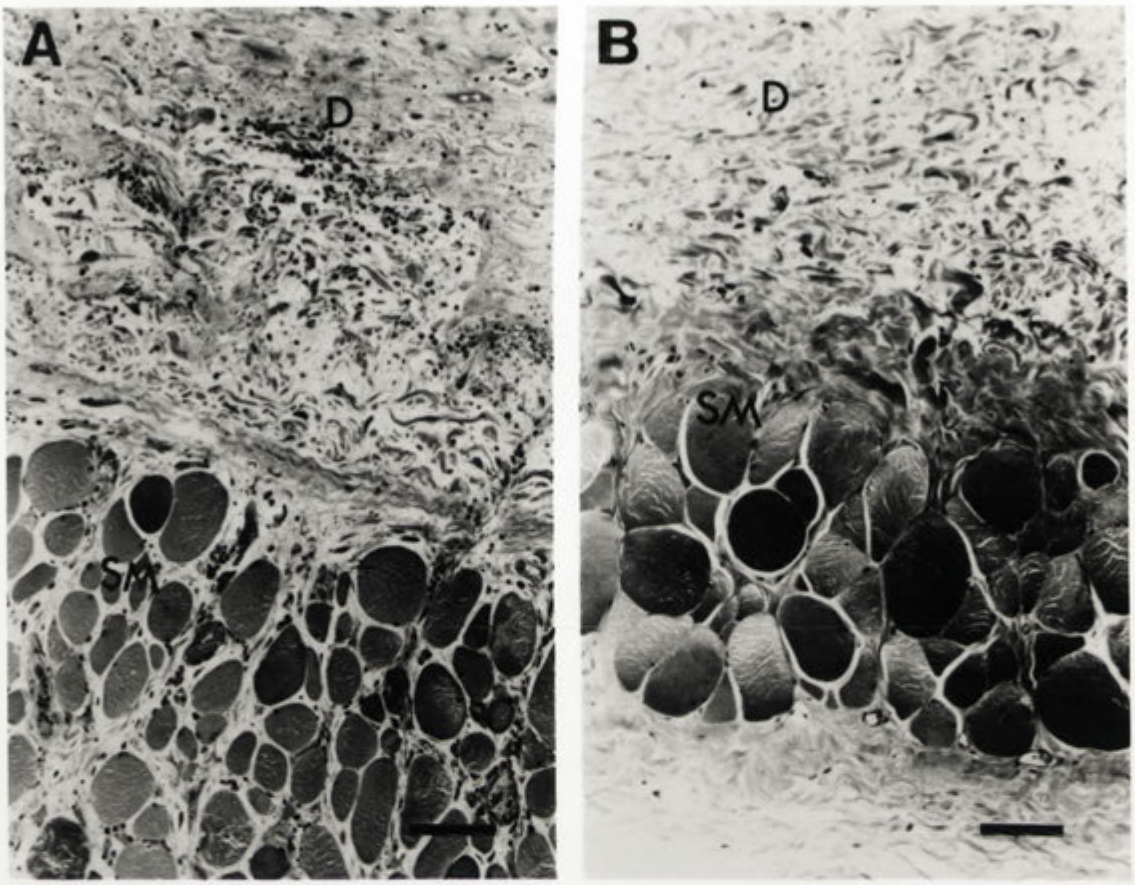
A
D
SM
B
D
SM

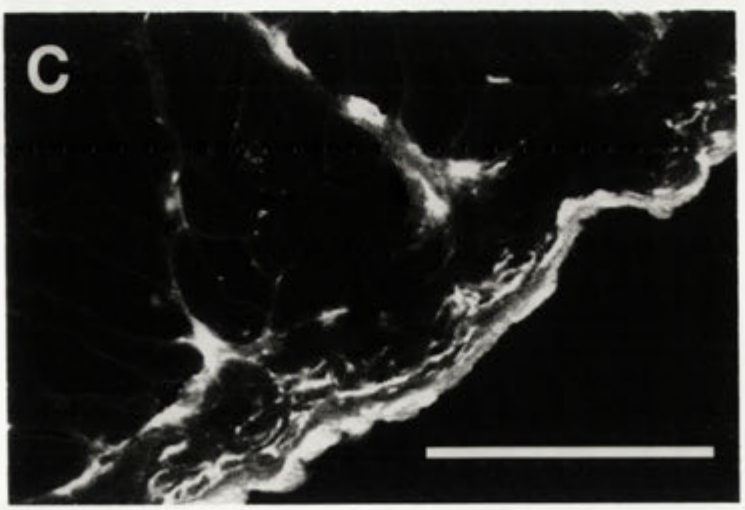
C

Figure 4.13: Histopathology and virus localisation in the epidermis of the primary inoculation site of SLS and Uriarra-infected laboratory rabbits at 10dpi. **(A)** Histopathology of skin from an SLS-infected laboratory rabbit. **(B)** Histopathology of skin from a Uriarra-infected laboratory rabbit. **(C)** Myxoma virus immunolocalisation in the epidermis of an SLS-infected laboratory rabbit. E, epidermis; D, dermis. Bars represent 100μm.

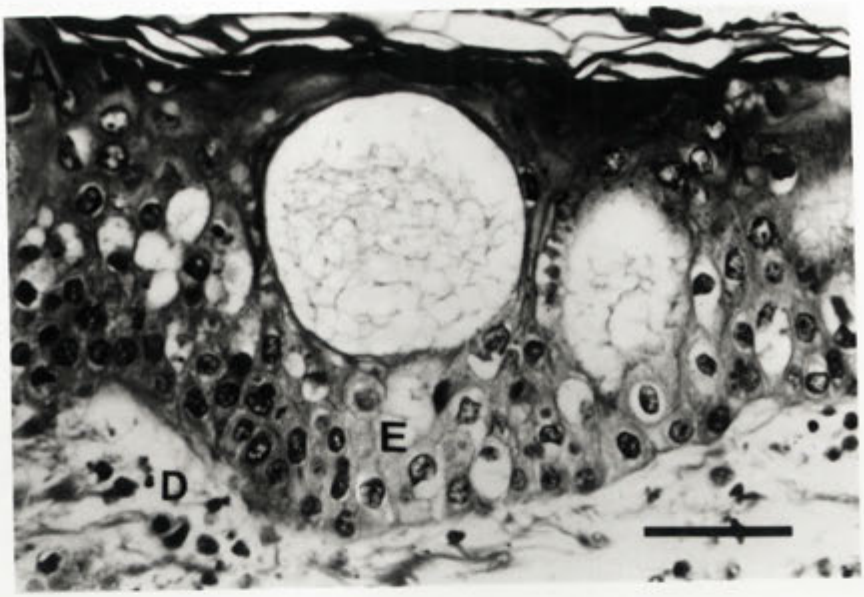
E
D

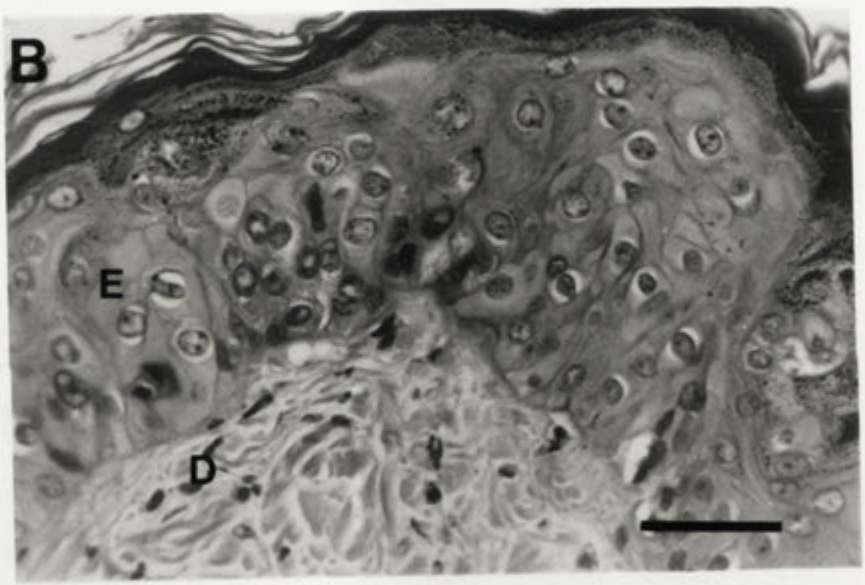
B
E
D

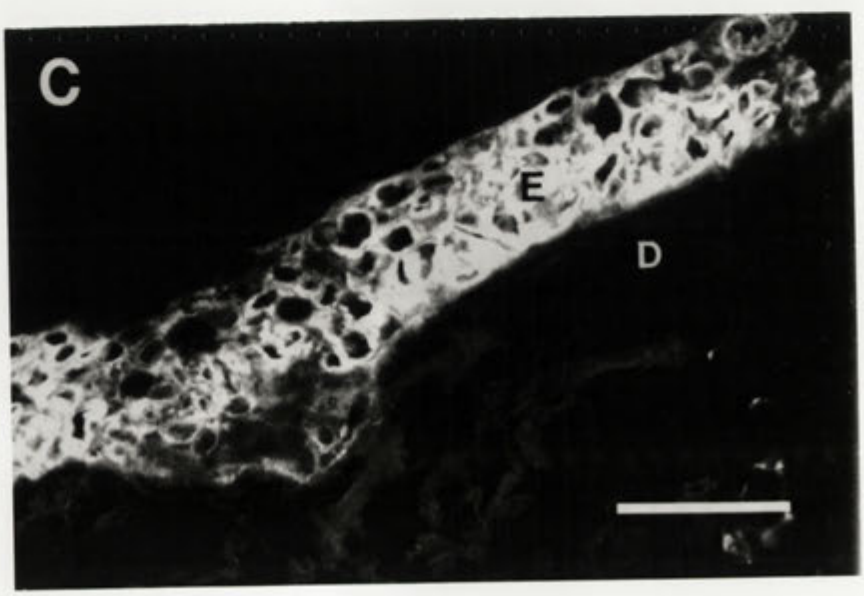
C
E
D

resembled that described at 6dpi for SLS-infected laboratory rabbits. Cells of most of the stratum basale showed changes associated with cell proliferation and pathology, and cells in the upper epidermis contained inclusion bodies.

Figure 4.14 shows differences between infections in the dermis of the primary inoculation site. These were the inflammatory responses and the organisation of the connective tissue. In SLS-infected laboratory rabbits (Figure 4.14A), the upper dermis contained nuclear fragments and cellular debris. Similarly to earlier time points in infection, inflammatory cells were concentrated deep in the dermis. The concentration of dermal collagen fibres was generally reduced compared to uninfected skin, especially directly under the epidermis and proximal to the superficial muscle layer. Collagen fibres that were present were of a disorganised appearance with either fibrin or large spaces between fibres and dermal fibroblasts were enlarged. In Uriarra-infected laboratory rabbits (Figure 4.14B), and wild rabbits infected with SLS (Figure 4.14C) or Uriarra, the upper dermis contained numerous lymphocytes and some monocytes. Spaces in the connective tissue of the dermis were larger than in the dermis from uninfected rabbits, however, pathologic changes did not progress much further, with the collagen fibres remaining well organised. The deposition of fibrin was much less extensive than following SLS infection of laboratory rabbits, and fibroblasts were of normal size.

From 15dpi of laboratory rabbits with Uriarra (Figure 4.15A) or of wild rabbits with SLS (Figure 4.15B), areas of the primary lesion had scab material consisting mainly of damaged epidermis and inflammatory cells. Many small, dark staining nuclear fragments of inflammatory cells were in the upper dermis proximal to the epidermis/dermis junction. Virus antigen was present in the epidermis of the primary skin lesion, but the numbers of infected cells were considerably less than at earlier time points. The strongest fluorescence was in the stratum basale of the epidermis, and in the epithelial cells of the external root sheath of hair follicles (Figure 4.15C). From 15dpi, mitotic figures were occasionally observed in the cells of the stratum basale. Long, thin fibroblast-like cells extended from underneath the stratum basale, and were positioned under the necrotic tissue The pathology of the epidermis at 15dpi in these rabbits was similar to those described at 10dpi in SLS-infected laboratory rabbits; the stratum basale was up to three layers thick, many cells appeared necrotic and large vesicles had formed in the epidermis of the primary lesions.

Figure 4.14: Histopathology of the dermis at the primary inoculation site of myxoma virus-infected rabbits at 10dpi. **(A)** SLS-infected laboratory rabbit. **(B)** Uriarra-infected laboratory rabbit. **(C)** SLS-infected wild rabbit. nf, nuclear fragment; F, fibroblast; BV, blood vessel. Bars represent 100μm.


nf
F

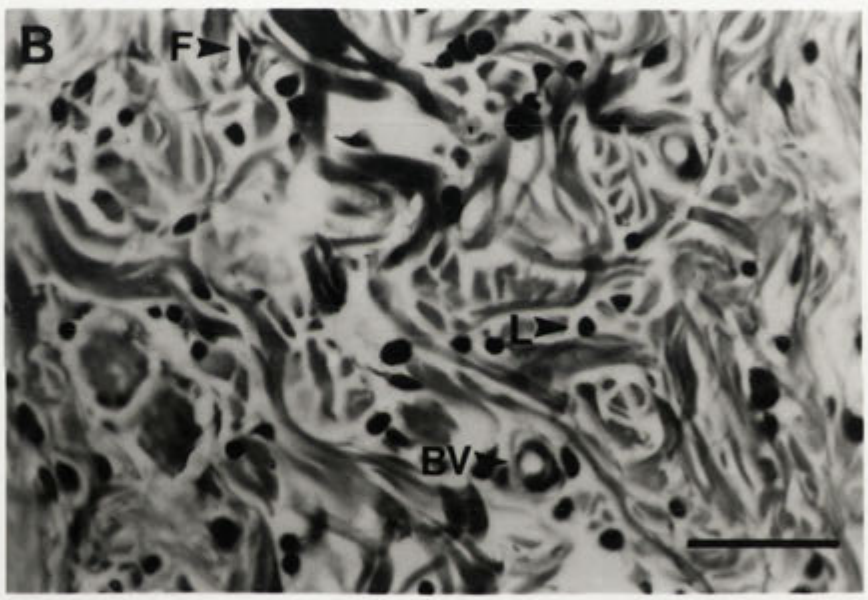
B
F
L
BV

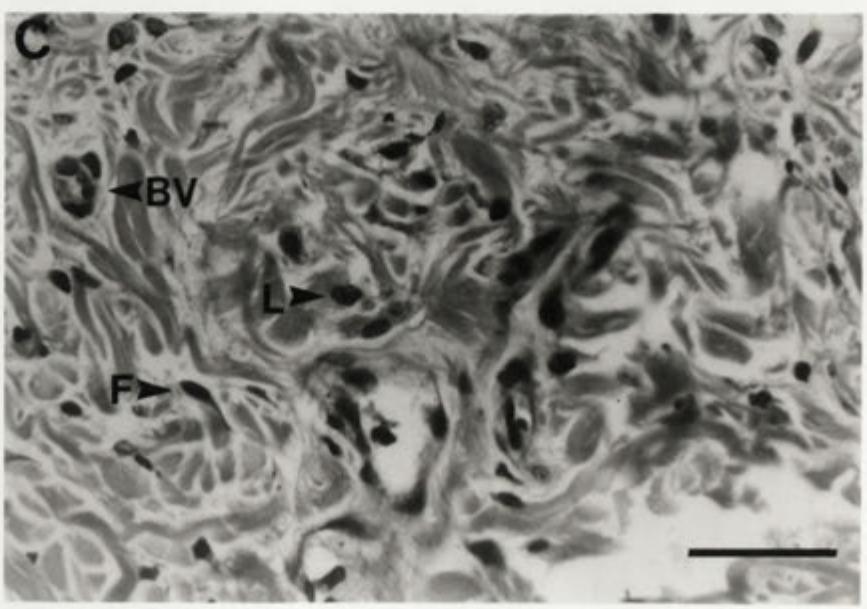
C
BV
L
F

Figure 4.15: Histopathology and virus localisation in the epidermis of the primary inoculation site of Uriarra-infected laboratory rabbits and SLS-infected wild rabbits at 15dpi. **(A)** Histopathology of skin from a Uriarra-infected laboratory rabbit. The stratum basale is indicated with an arrow. **(B)** Histopathology of skin from an SLS-infected wild rabbit. The stratum basale is indicated with an arrow. **(C)** Myxoma virus localisation in the stratum basale in the epidermis of a infected laboratory rabbit. Immunolocalisation was performed on frozen tissue sections and some of the epidermis has been torn away in the sectioning process. E, epidermis. Bars represent 100μm.

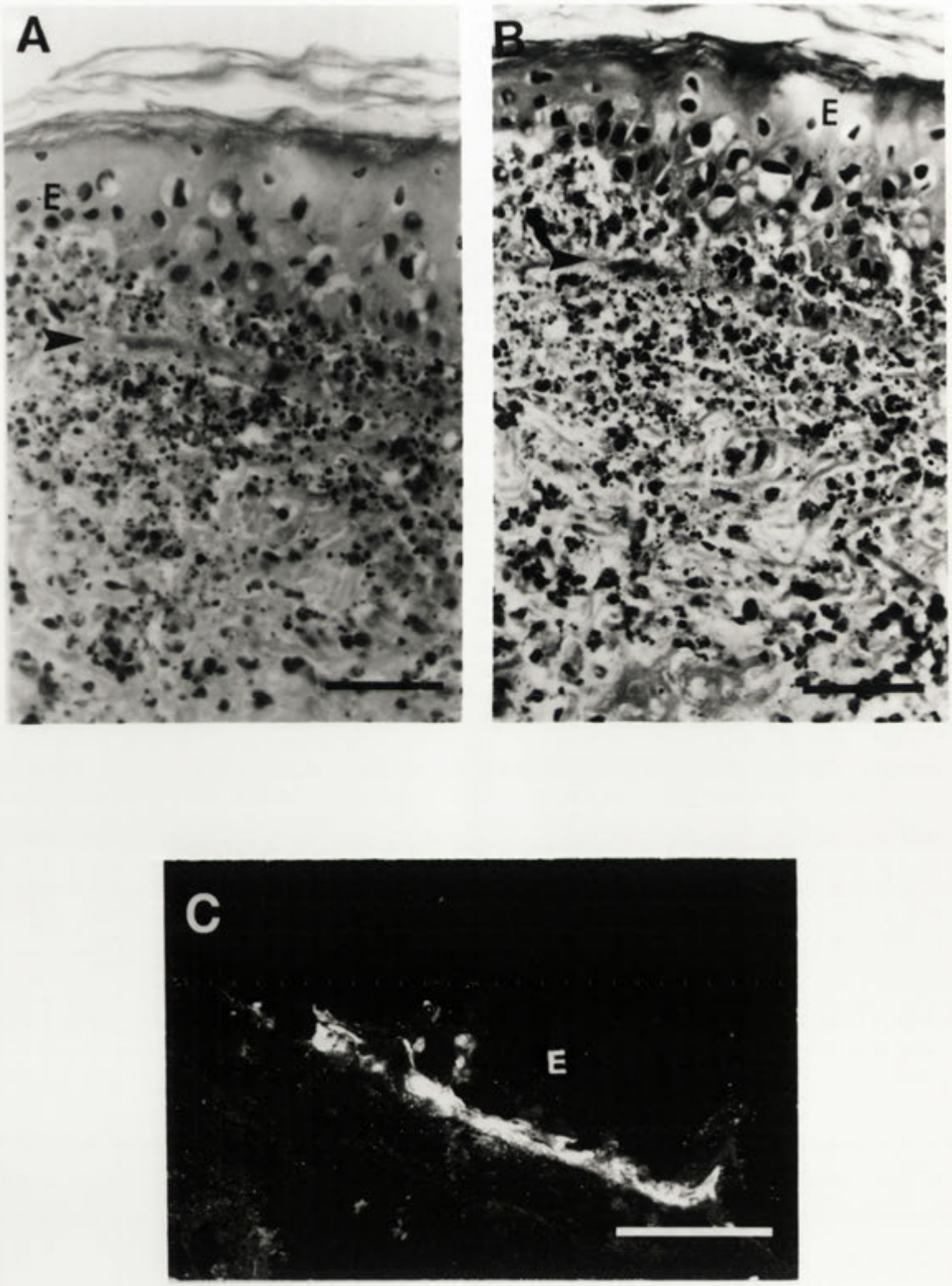
A
E
B
E
C
E

By 20dpi, thick scab material overlaid the lesion of Uriarra-infected laboratory rabbits (Figure 4.16A) or of SLS-infected wild rabbits (Figure 4.16B). Similarly to 15dpi, virus was present in cells of the stratum basale of the epidermis, and in the epithelial cells of the external root sheath of hair follicles, but was not observed in the dermis (Figure 4.16C). Massive aggregations of inflammatory cells, mainly lymphocytes, were located at the margins of the scab material and extending down into the dermis and throughout the deep dermis. This was observed particularly in infected wild rabbits. The number of nuclear fragments and inflammatory cells, and the amount of cellular debris, in the dermis proximal to the dermis/epidermis junction and in the centre of the primary lesion was decreased compared to 15dpi. The density and organisation of collagen fibres had increased throughout the dermis, especially surrounding blood vessels, and coincided with a greater number of fibroblasts in the dermis. The amorphous fibrin material was condensed. Extravasated RBCs were located throughout the dermis.

4.3.1.2.2 The endothelial cells of small blood vessels and the appearance of myxoma cells in the dermis

The endothelial wall of capillaries consists of a single layer of cells (Figure 4.17A). At 4dpi of laboratory rabbits with SLS, the endothelium of some capillaries and venules in the dermis appeared swollen, as cells were enlarged and both the nuclear and cellular membranes appeared distended (Figure 4.17B). Changes in the endothelium of these vessels, but not the larger arterioles, were extensive by 6dpi, especially of the vessels in the deep dermis proximal to the superficial muscle layer (Figure 4.17C). Endothelial cells were enlarged, and the nucleus was pale staining except at the periphery, and appeared slightly vacuolated. The number of cells in the endothelium had increased by 6 and 10dpi (Figure 4.17D). This increase in cells was particularly obvious in capillaries. The vessel type could still be determined despite the increase in cell number and swelling of cells, by the size of the vessel lumen and the extent of the elastic tissue associated with the vessel. Cells which resembled those described as myxoma cells by Hurst (1937a) were present by 6dpi proximal to blood vessels that contained abnormal endothelial cells. Myxoma cells were typically large, polygonal or stellate shaped cells with large, pale staining, hypertrophic nuclei (Figure 4.17E). Myxoma cells did not stain positive for MHC class II. Endothelial cells of capillaries did not stain positive for MHC class II and rarely stained positive for myxoma virus. By 10dpi, many of the blood vessels were surrounded by extravasated RBCs and the endothelial cells appeared necrotic. Myxoma cells were highly stellate in shape, and the nuclear membrane in

Figure 4.16: Histopathology and virus localisation in the epidermis of the primary inoculation site of Uriarra-infected laboratory rabbits and SLS-infected wild rabbits at 20dpi. (**A**) Histopathology of skin from a Uriarra-infected laboratory rabbit. (**B**) Histopathology of skin from an SLS-infected wild rabbit. (**C**) Myxoma virus localisation in the stratum basale in the epidermis and the hair follicle of a infected laboratory rabbit. E, epidermis; D dermis; HF, hair follicle. Bars represent 100μm.

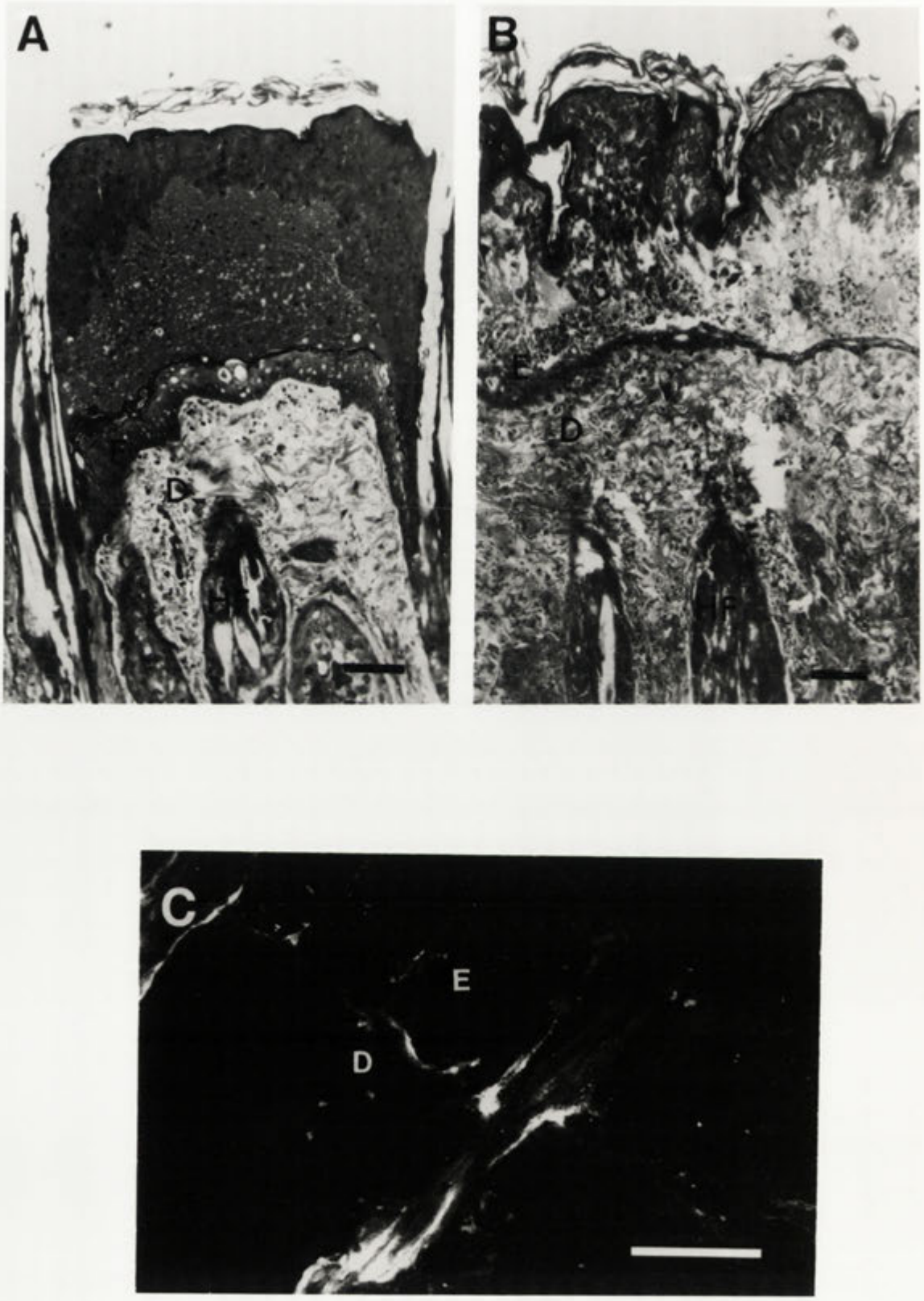
A
E
D
B
E
D
F
C
E
D

Figure 4.17: Changes in the endothelium of blood vessels and the appearance of myxoma calls in SLS and Uriarra infected laboratory rabbits. **(A)** Capillary from an uninfected rabbit. **(B)** Capillary from an SLS-infected rabbit at 4dpi. **(C)** Capillary from an SLS-infected rabbit at 6dpi. **(D)** Capillary from an SLS-infected rabbit at 10dpi. . **(E)** Stellate myxoma cell. **(F)** Capillary from a Uriarra-infected rabbit at 10dpi. Arrows indicate the blood vessel endothelium. Bars represent 30μm.

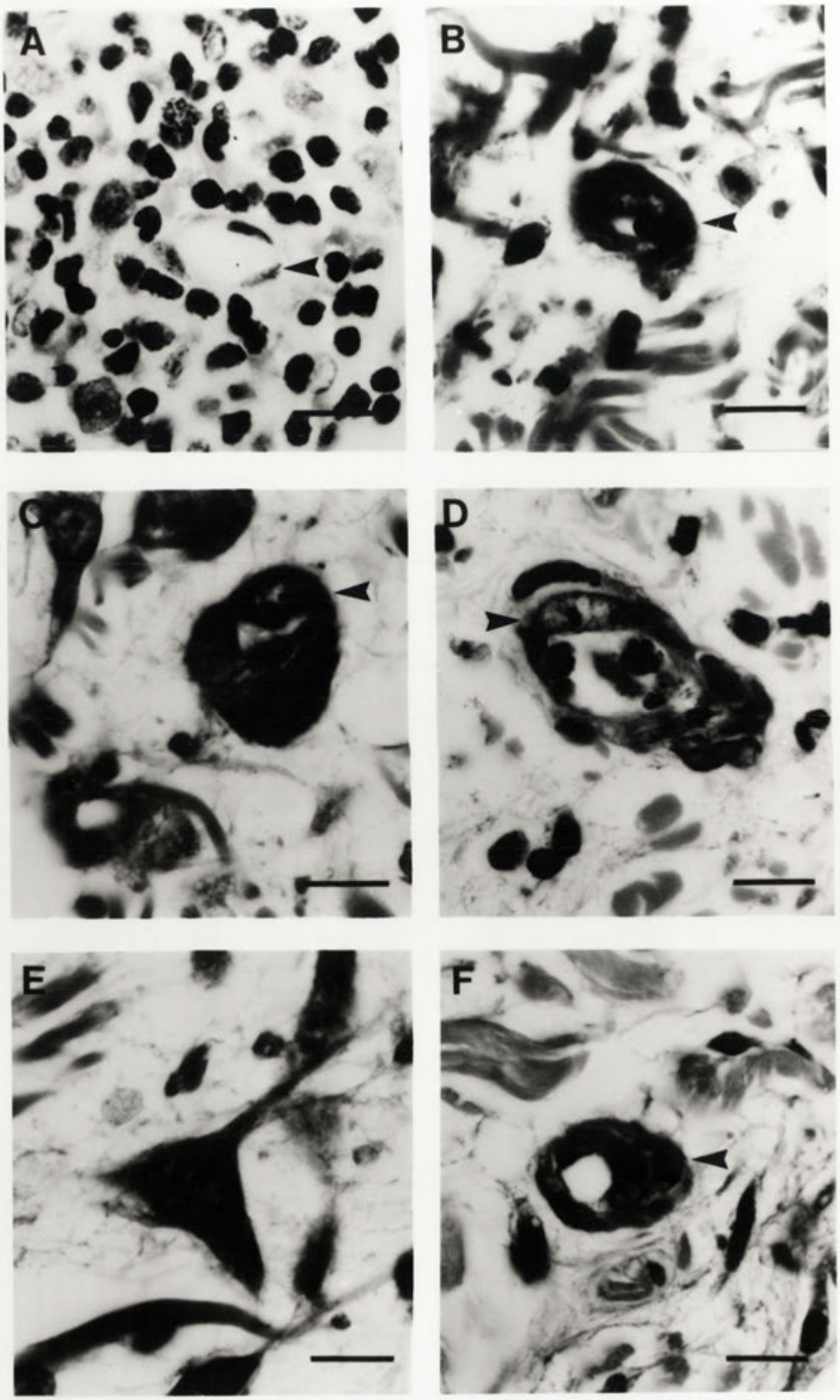
A
B
C
D
E
F

many cells was poorly defined, indicating that these cells were also necrotic. These myxoma cells were often surrounded by aggregates of neutrophils.

At 6dpi of laboratory rabbits with Uriarra, or of wild rabbits infected with SLS, endothelial cells of capillaries and venules were swollen. This swelling was also evident at 10dpi (Figure 4.17F), but in general, no further changes in the blood vessels were observed. Myxoma virus antigen was not detected in the blood vessel endothelium. Large, stellate myxoma cells were not prominent in the dermis at any time post infection of laboratory or wild rabbits infected with Uriarra. However, myxoma cells were occasionally observed from 10dpi in the deep dermis of Uriarra-infected laboratory rabbits. Stellate myxoma cells were also rare in the dermis of wild rabbits infected with SLS.

4.3.2 The distal skin

Skin was removed from the dorsum of the opposite hind foot (distal skin) to the primary inoculation site in myxoma virus-infected rabbits. The pathologic changes in the distal skin closely resembled their counterparts at the primary inoculation site and are described below.

In SLS-infected laboratory rabbits virus was first present in the dermis of the distal skin in MHC class II positive dendritic cells, in one of two rabbits at 4dpi, but was not present at 2dpi. These dendritic cells had increased in number at 4dpi compared to the numbers present in uninfected skin samples. By 6dpi, myxoma virus was present in dermal dendritic cells in both SLS-infected laboratory rabbits that had been inoculated in the hind foot. This was associated with the infiltration of mononuclear cells, predominantly lymphocytes, into the deep dermis, and the swelling of endothelial cells of some capillaries. In localised areas of the epidermis, cells of the stratum basale were swollen, with both the nuclear and cellular membranes distended, and had increased in number (Figure 4.18A).

By 10dpi of laboratory rabbits with SLS, virus was present in the epidermis of distal skin, with few virus-positive cells in the dermis. The pathological changes in the epidermis of the distal skin resembled that described for the primary inoculation site of SLS-infected laboratory rabbits at 6dpi; the cytoplasm of nucleated cells was vesicular,

and virus inclusion bodies were present in some cells. Inflammatory cells, predominantly neutrophils, remained localised to the deep dermis. Endothelial cells of dermal capillaries had increased in number and small stellate myxoma cells were present. Myxoma cells in the distal skin samples did not stain positive for myxoma virus.

Virus was first present in the distal skin of Uriarra-infected laboratory rabbits and SLS-infected wild rabbits at 6dpi and 4dpi respectively. Similarly to SLS-infected wild rabbits, myxoma virus-infected cells were dendritic cells that costained positive for MHC class II. However, cells positive for virus were distributed in the upper dermis and proximal to blood vessels and did not have the uniform distribution throughout the dermis that was observed in the primary inoculation site of the same rabbits or either skin site from SLS-infected laboratory rabbits. In addition, the number of MHC class II positive dendritic cells had increased in the dermis of Uriarra-infected laboratory rabbits and SLS-infected wild rabbits by 6dpi, but not to the extent observed in SLS-infected laboratory rabbits. However, the most striking difference between these rabbits and laboratory rabbits infected with SLS was the early infiltration of mononuclear cells throughout the dermis from 4dpi and particularly at 10dpi. At 6dpi of laboratory rabbits with SLS, inflammatory cells in the upper dermis were predominantly neutrophils and included lymphocytes (Figure 4.18A). The inflammatory response in the distal skin of wild rabbits infected with SLS was monocytic (Figure 4.18B). Lymphocytes and macrophages were particularly prominent proximal to small blood vessels and at the epidermis/dermis junction of the distal skin by 4dpi, before virus was present in the epidermis. This was in contrast to the primary inoculation site, where inflammatory cells were present at this junction at the same time as myxoma virus. This early infiltration of mononuclear cells was most prominent in SLS-infected wild rabbits (Figure 4.18B).

At 10dpi in SLS-infected wild rabbits and in Uriarra-infected laboratory rabbits, virus generally remained localised to the dermis of distal skin. Spread of virus from the dermis to the epidermis was observed in one SLS-infected wild rabbit only. The inflammatory response in the distal skin was distributed extensively throughout the dermis of SLS-infected wild rabbits and Uriarra-infected laboratory rabbits although generally involved more cells in infected wild rabbits.

Figure 4.18: Histopathology of the distal skin from SLS-infected laboratory and wild rabbits at 6dpi. (**A**) SLS-infected laboratory rabbit. (**B**) SLS-infected wild rabbit. E, epidermis; L, lymphocyte; M, monocyte, N, neutrophil. Bars represent 100μm.

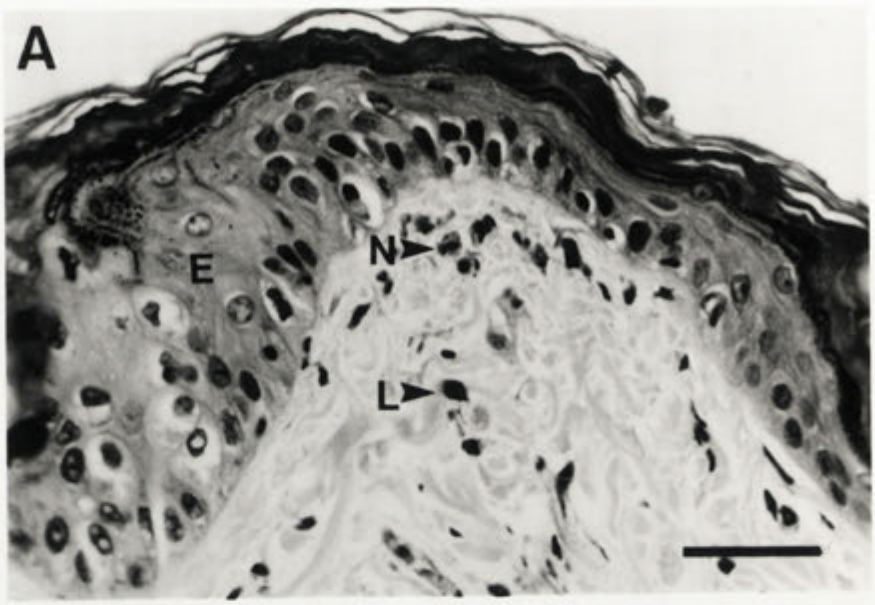
A
E
N
L

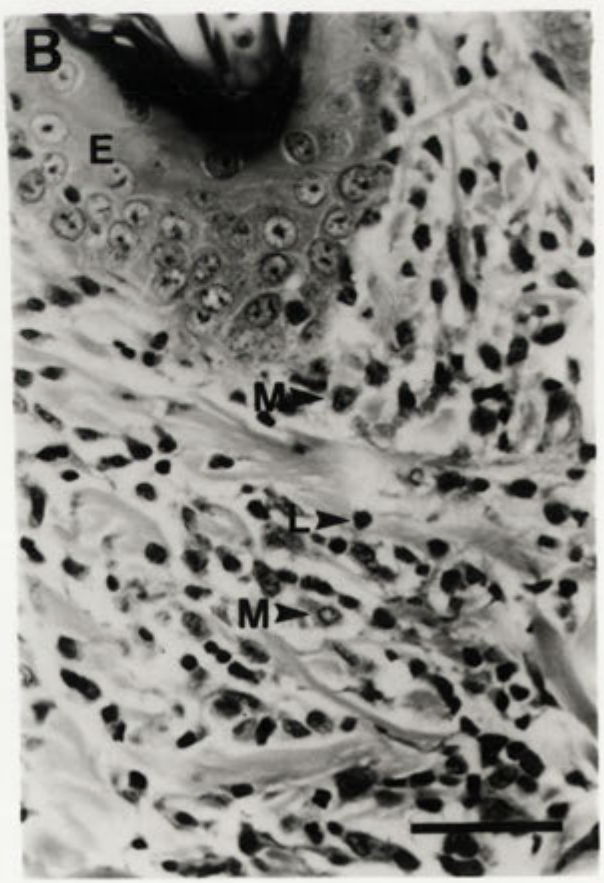
B
E
M
L
M

At 15dpi, one of two SLS-infected wild rabbits had a secondary lesion at the distal skin site and virus was present in the epidermis from both SLS-infected wild rabbits. However, virus did not infect the epidermis of the entire tissue section. Instead, virus localised to short stretches, up to 30 cells of the stratum basale in length (Figure 4.19). Cellular changes associated with virus replication in the epidermis were similar to those in the primary lesion at 6dpi for these rabbits. In the dermis, endothelial cells of blood vessels were swollen with distended cellular and nuclear membranes, but generally had not increased in number and myxoma cells were not observed. Virus was not present in the epidermis of distal skin in Uriarra-infected laboratory rabbits or Uriarra-infected wild rabbits.

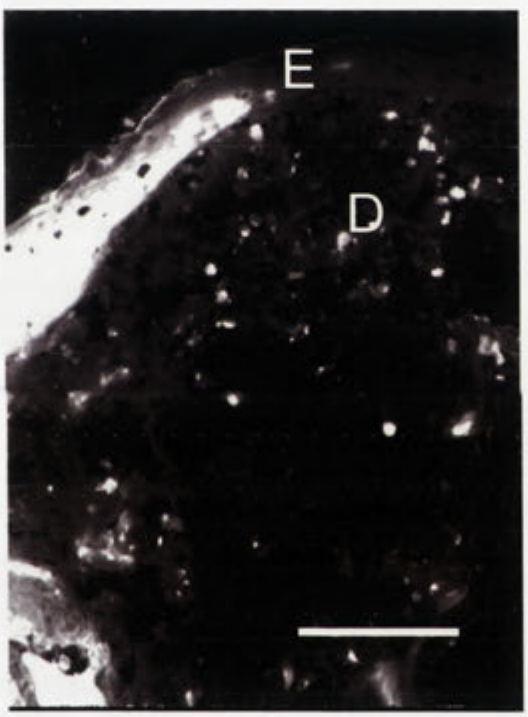

Figure 4.19: Myxoma virus localisation in the dermis and epidermis of distal skin from an SLS-infected wild rabbit at 15dpi. E, epidermis; D, dermis. Bar represents 150μm.

By 20dpi, virus was present in the distal skin in the stratum basale of the epidermis and in the external root sheath of some hair follicles in two of three SLS-infected wild rabbits. This was similar to virus localisation in the skin of the primary lesion at the same time. Virus was not present in the distal skin of the third SLS-infected wild rabbit. Similarly, virus was not present in the epidermis of laboratory or wild rabbits

infected with Uriarra. In all rabbits, the dermis contained numerous mononuclear inflammatory cells, particularly concentrated at the epidermis/dermis junction and in the deep dermis.

4.3.3 The draining and contralateral lymph nodes

4.3.3.1 Uninfected lymph nodes

The anatomy of the popliteal lymph node from an uninfected rabbit is depicted schematically in Figure 4.20. and in micrographs in Figure 4.21. The lymph node is surrounded by a capsule, into which the afferent lymphatics enter and bathe the cortex via the subcapsular sinus. Fibrous radial bands called trabeculae extend into the node from the lymph node capsule, and in many species, divide the main body of the node, the diffuse cortex, into lobules (Figure 4.20). These bands did extend through the cortex of rabbit lymph nodes, but did not divide it into obvious lobules (Figure 4.21 A and B). The structural network of the lymph node consists of reticular cells and fibres, although these are not readily observed in lymph nodes from uninfected rabbits by light microscopy and staining with haematoxylin and eosin. Lymph nodes are generally located in fatty tissue within the animal, and a network of adipose tissue surrounds the outside of the lymph node in section.

A histological section of a lymph node can be divided into two general zones; the cortex and the medulla. The cortex consists of two areas, namely the T cell-dependent paracortex in which B cell-dependent germinal centres form in response to antigenic stimulation (Figure 4.21A). The cortex contains high endothelial venules (HEV) which are bordered by cortical sinuses (Gretz *et al.*, 1997); the entire structure constitutes the paracortical cord (Kelly, 1975). The medulla is constituted with cords of reticular cells that are lined with macrophages and immediately surrounded by sinuses. The lymph drains into the medullary sinuses. Efferent lymphatics arise in the hilus from these sinuses.

The diffuse cortex of lymph nodes from uninfected rabbits contained lymphocytes, macrophages (Figure 4.21C) and plasma cells. Neutrophils were rarely present in lymph nodes from uninfected rabbits. In the cortex of uninfected lymph nodes, both germinal centres and clusters of small lymphocytes called follicles were present. Care must be taken as to the interpretation of these clusters as follicles or as a section taken

through one edge of a germinal centre. Similar to other species such as mouse or human (Liu and Arpin, 1997), germinal centres in rabbit lymph nodes had a number of zones, the dark zone containing centroblasts, the light zone containing centrocytes and follicular dendritic cells, and the mantle zone containing small, newly differentiated lymphocytes. Cells undergoing mitotic division or with fragmented nuclei were occasionally observed in the light and mantle zones (Figure 4.21D). Plasma cells were present in the paracortex below germinal centres, in the subcapsular sinus and amongst the medullary cords.

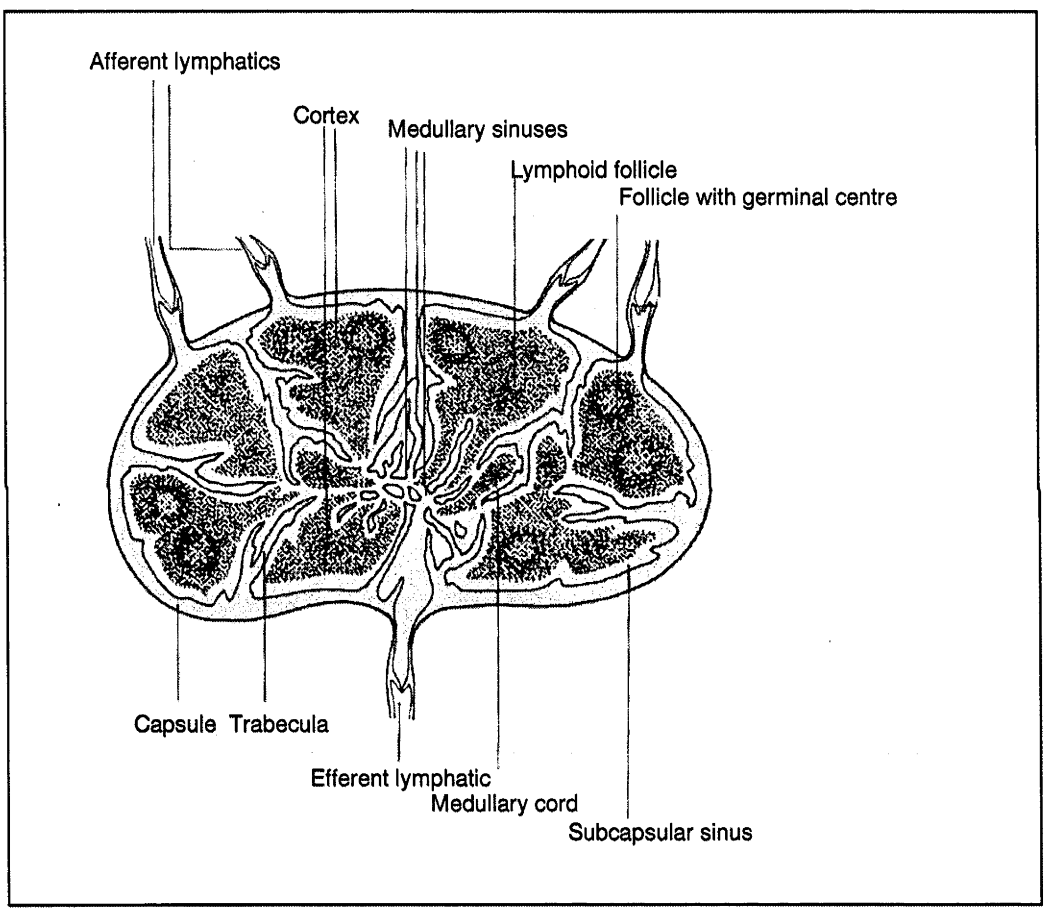

Figure 4.20: Schematic drawing of a lymph node showing its strucure. The node is encapsulated by dense connective tissue (capsule). Lymph drains into the node via the afferent lymphatics, through the subcapsular sinus and the medullary sinuses to the efferent lymphatics (modified from Wheater *et al.*, 1987).

Figure 4.21: Popliteal lymph node from an uninfected rabbit. **(A)** The cortex of a rabbit lymph node showing the T-cell-dependent paracortex and a B cell-dependent germinal centre. **(B)** The cortex of a rabbit lymph node in which the T-cell-dependent paracortex and a B cell-dependent follicle are indicated. **(C)** Paracortex of a lymph node from an uninfected rabbit, in which lymphocytes, macrophages and a blood vessel are indicated. **(D)** The light zone of a germinal centre showing lymphocytes, a cell in mitotic division (arrow) and an apoptotic cell containing nuclear fragments. A, apoptotic cell; BV, blood vessel; GC, germinal centre; F, follicle; PC, paracortex; M, macrophage. Bar represents 100μm.

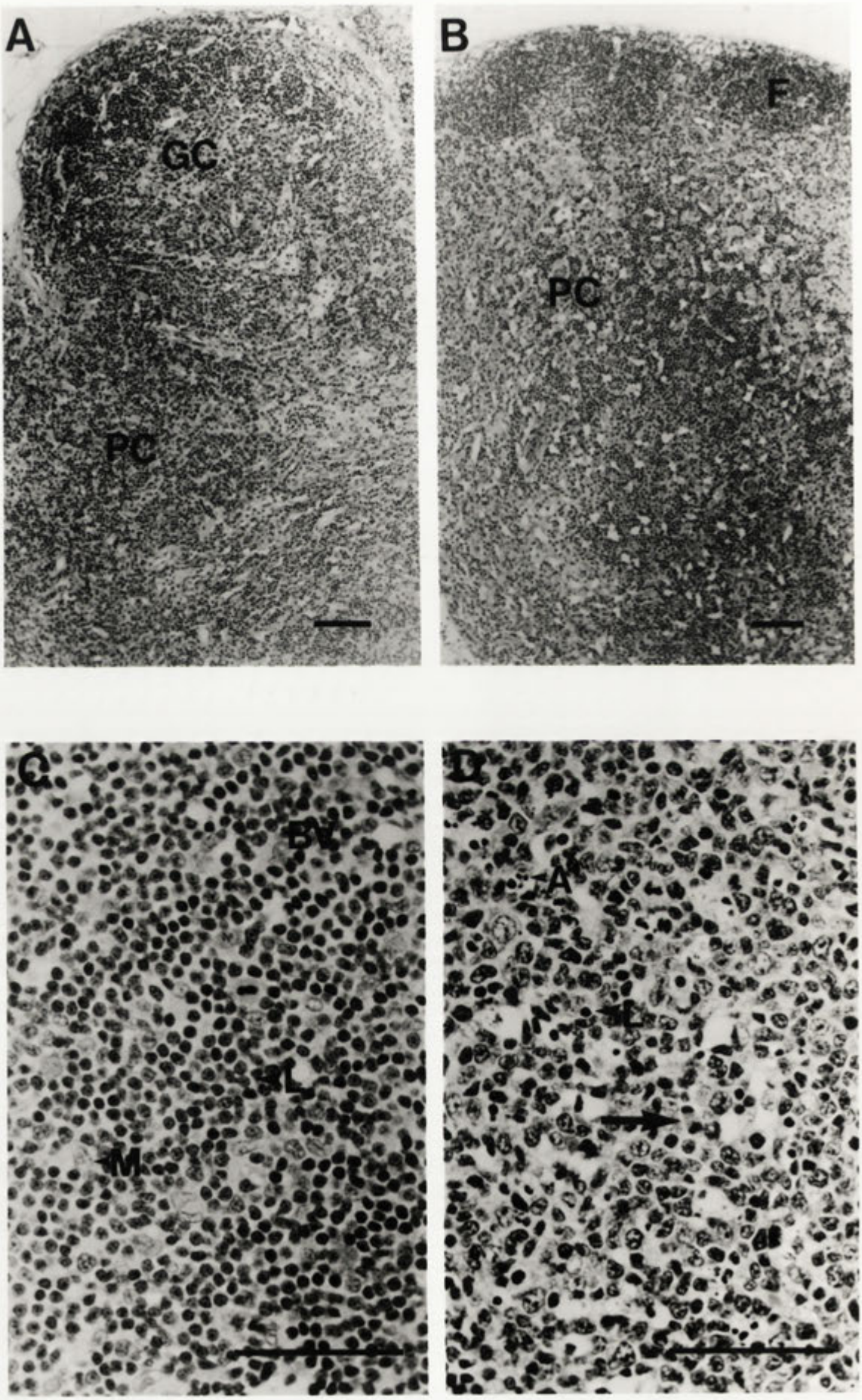
A
GC
PC
B
F
PC
C
BV
L
M
D
A

4.3.3.2 Virus antigen, histopathological changes and immunohistochemical staining in the draining and contralateral lymph nodes of rabbits infected with myxoma virus

Changes in the lymph nodes following infection of rabbits with myxoma virus occurred particularly in the paracortex and germinal centres. These included a general depletion of lymphocytes, the proliferation and degeneration of reticular and endothelial cells, and an influx of inflammatory cells into the nodes. These changes are described in detail below (and summarised in Table 4.3), as well as the cellular localisation of myxoma virus and changes in cell populations detected by immunohistochemistry.

Table 4.3: Myxoma virus localisation and histopathology of lymph nodes from laboratory or wild rabbits infected with either SLS or Uriarra. Virus was not present in the draining lymph node at 12 hours post infection.

	Laboratory		Wild	
	SLS	**Uriarra**	**SLS**	**Uriarra**
		24 HOURS POST INFECTION		
Virus antigen	Mononuclear cells in paracortex	Mononuclear cells in paracortex	Mononuclear cells in paracortex	Not present
		TWO DAYS POST INFECTION		
Virus antigen	Continuous lines spanning the paracortex; lymphocytes	Continuous lines spanning the paracortex; lymphocytes	Continuous lines spanning the paracortex; lymphocytes	Continuous lines spanning the paracortex
		FOUR DAYS POST INFECTION		
Virus antigen	Lymphocytes and macrophages in paracortex of draining and contralateral lymph nodes, lymph node capsule	Lymphocytes and macrophages in paracortex of draining lymph node	Lymphocytes and macrophages in paracortex of draining and contralateral lymph nodes, lymph node capsule	Virus not observed in draining or contralateral lymph nodes
Paracortex	Interfollicular hypoplasia of lymphocytes in draining lymph node	Hyperplasia of lymphocytes in paracortex of draining and contralateral lymph nodes	Interfollicular hypoplasia of lymphocytes in draining lymph node	Hyperplasia of lymphocytes in paracortex of draining lymph node
Germinal centres	No increase in size, definition or number	Hyperplasia of lymphocytes and increase in number of germinal centres	Limited hyperplasia	Hyperplasia of lymphocytes
Blood vessels	Swelling of endothelial cells in the draining lymph node	No change	Swelling of endothelial cells in the draining lymph node	No change

Table 4.3 continued:

	Laboratory		Wild	
	SLS	Uriarra	SLS	Uriarra
	SIX DAYS POST INFECTION			
Virus antigen	Lymphocytes and macrophages in paracortex of draining and contralateral lymph nodes, lymph node capsule	Lymphocytes and macrophages in paracortex of draining and contralateral lymph node	Lymphocytes and macrophages in paracortex of draining and contralateral lymph nodes, lymph node capsule	Not present
Paracortex	Extensive depletion of lymphocytes from both draining and contralateral lymph nodes	Hyperplasia of lymphocytes	Extensive depletion of lymphocytes from draining but not contralateral lymph nodes	Hyperplasia of lymphocytes
Germinal centres	Extensive depletion of lymphocytes from both draining and contralateral lymph nodes, neutrophil infiltration	Hyperplasia of lymphocytes	Extensive depletion of lymphocytes from draining but not contralateral lymph nodes	Hyperplasia of lymphocytes
Blood vessels	Swelling and increase in number of endothelial cells in draining and contralateral lymph nodes	Swelling of endothelial cells in the draining lymph node	Swelling of endothelial cells in the draining lymph node	Swelling of endothelial cells in the draining lymph node
Stellate myxoma cells	Present	Absent	Absent	Absent
	TEN DAYS POST INFECTION			
Virus antigen	Reticular or myxoma cells associated with degenerating germinal centres in draining and contralateral lymph nodes	Lymphocytes and macrophages in paracortex of draining and contralateral lymph node	Lymphocytes in paracortex of draining and contralateral lymph nodes, lymph node capsule	Lymphocytes in paracortex of draining and contralateral lymph nodes
Paracortex/ germinal centres	Extensive infiltration of neutrophils and reticular cell proliferation in draining and contralateral lymph nodes	Mild depletion of lymphocytes from interfollicular and mantle zones of draining and contralateral lymph nodes	Highly variable between rabbits – ranging between extensive depletion and reticular cell proliferation to relatively heathy. Some infiltration of neutrophils	No further changes
Blood vessels	Swelling and increase in number of endothelial cells in blood vessel walls of draining and contralateral lymph nodes	Swelling of endothelial cells in the draining lymph node	Swelling of endothelial cells in the draining lymph node	Swelling of endothelial cells in the draining lymph node
Stellate myxoma cells	Present in draining and contralateral lymph nodes	Absent	Present in draining lymph nodes	Absent

Table 4.3 continued:

	Laboratory		Wild	
	SLS	Uriarra	SLS	Uriarra
		FIFTEEN DAYS POST INFECTION		
Virus antigen	-	Present in a few lymphocytes in paracortex of draining lymph node	Not present	Not present
Paracortex/ germinal centres	-	No further changes	Repopulation of draining lymph node with small lymphocytes in paracortex and hyperplasia of lymphocytes in germinal centre	No further changes
Blood vessels	-	Swollen endothelium	Swollen endothelium	No change
Stellate myxoma cells	-	Absent	Absent	Absent
		TWENTY DAYS POST INFECTION		
Virus antigen	-	Not present	Continuous lines of antigen in the paracortex of draining lymph node but not associated with lymphocytes	Not present
Paracortex/ germinal centres	-	No further changes	No further changes	No further changes
Blood vessels	-	Reduced swelling of endothelium	Reduced swelling of endothelium	No change
Stellate myxoma cells	-	Absent	Absent	Absent

4.3.3.2.1 Twenty-four hpi, two and four days post infection of laboratory and wild rabbits with myxoma virus.

The earliest detection of myxoma virus was at 24 hpi in the paracortex of the draining lymph node of laboratory rabbits infected with SLS or Uriarra, or wild rabbits infected with SLS (Figure 4.22). Cells infected with myxoma virus at this time were mononuclear cells; small cells which had short processes at opposite ends to each other (Figure 4.22A) and slightly larger cells that possessed two slender dendritic processes (Figure 4.22B). Cells infected with myxoma virus were always located close to each other. Virus was not detected until 2dpi in the draining lymph node of wild rabbits infected with Uriarra.

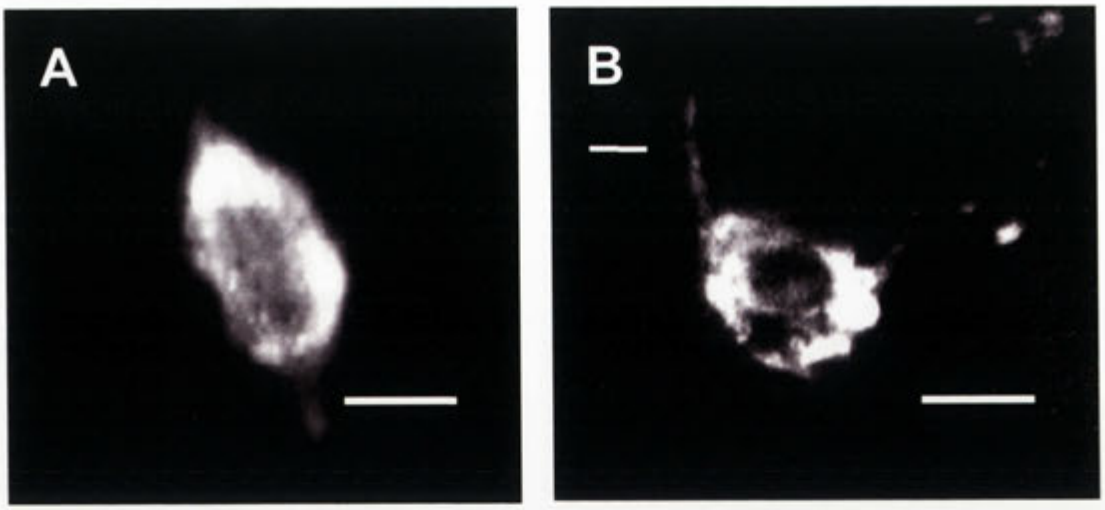

Figure 4.22: Myxoma virus infected cells in the paracortex of the draining lymph node at 24hpi. These cells were not characterised further than their morphology. (**A**) Small, mononuclear cell, approximately 6μm in diameter, with short processes at opposite ends to each other. Bar represents 3μm. (**B**) Larger mononuclear cell with long, slender dendritic processes (arrow). Bar represents 8μm.

By 2dpi, virus was localised in cells directly under the capsule of the draining lymph node (Figure 4.23A), and spanning the paracortex as continuous lines (Figure 4.23B), with no difference observed between wild or laboratory rabbits infected with Uriarra or SLS. The lines of virus antigen varied in the intensity of fluorescence. It was not clear if lines of antigen of low intensity represented virus aggregates that were not cell-associated or infected cell debris, that was draining directly into the lymph nodes from the primary inoculation site in the skin. The lines of virus antigen of high staining intensity were associated with the cytoplasm of lymphocytes in both the draining and contralateral lymph nodes of infected rabbits (Figure 4.23C) and hence are likely to depict early replication of virus within the draining lymph node. Virus was also present in separate cells that were not associated with the continuous lines of virus in the cortex of lymph nodes (Figure 4.23D), or in clusters of two to five cells adjacent to each other. These cells resembled lymphocytes as they had a single round nucleus and a narrow cytoplasm.

At 4dpi of laboratory rabbits with either SLS or Uriarra, virus was present in lymphocytes and was evenly distributed throughout the diffuse cortex of lymph nodes draining the inoculation site (Figure 4.24 A and B). This infection of T-cell-dependent areas at 4dpi was more extensive in popliteal lymph nodes from rabbits that had been

Figure 4.23: Myxoma virus localisation in the draining lymph node of an SLS-infected laboratory rabbit at 2dpi. **(A)** Myxoma virus staining cells of the outer lymph node cortex, directly under the lymph node capsule. Bar represents 25μm. **(B)** Myxoma virus infection of continuous lines of cells that spanned the paracortex. Bar represents 100μm. **(C)** High magnification of **(B)** showing myxoma virus localisation in the cytoplasm of infected cells. Bar represents 25μm. **(D)** Myxoma virus-infected lymphocyte in the cortex of the draining lymph node. Bar represents 15μm. C, capsule.

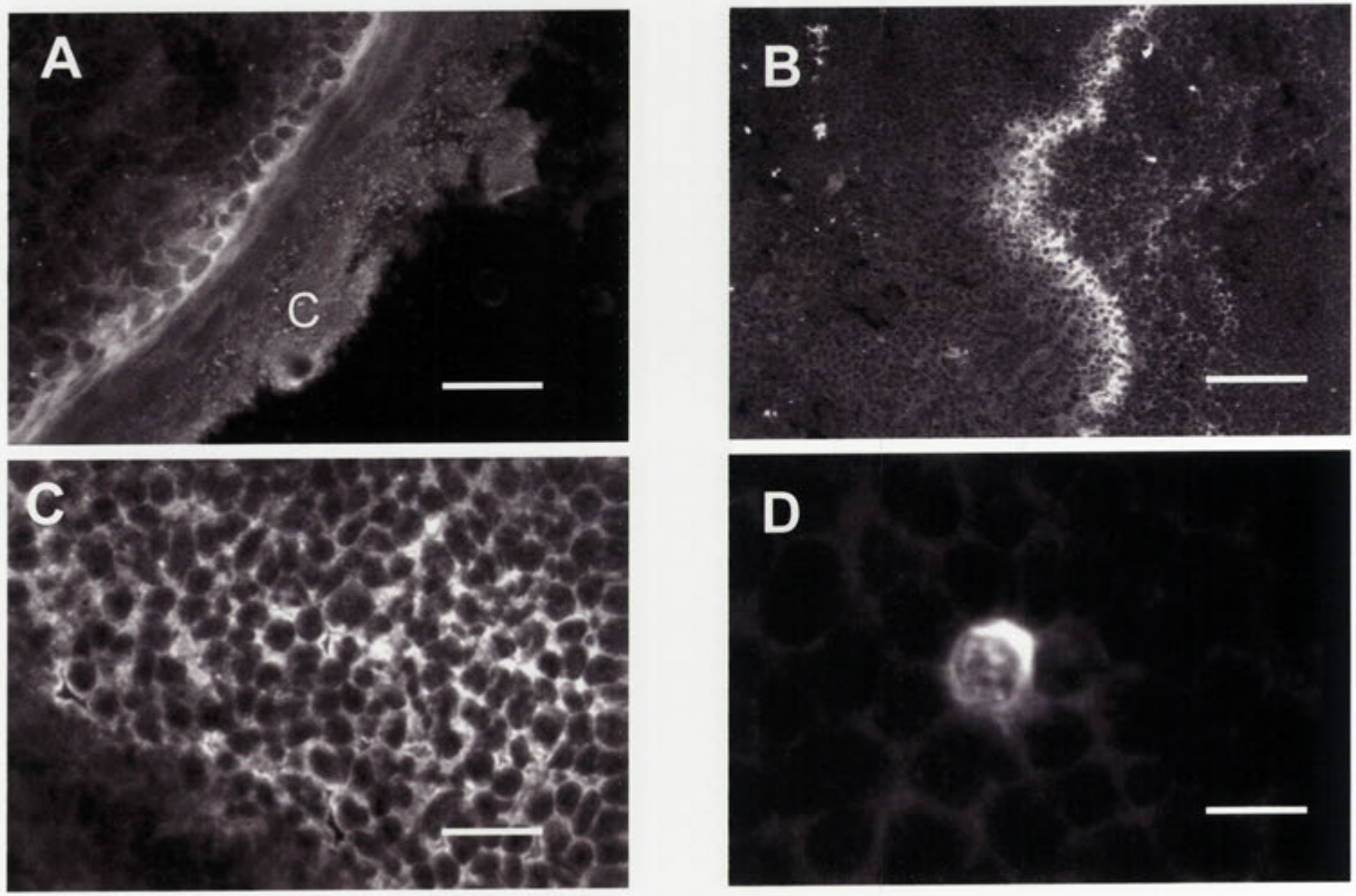
A
C
B
C
D

Figure 4.24: Myxoma virus localisation in the draining and contralateral lymph nodes of an SLS and Uriarra-infected laboratory rabbits at 4dpi. (**A**) Draining lymph node of an SLS-infected laboratory rabbit. Bar represents 300μm. (**B**) Draining lymph node of a Uriarra-infected laboratory rabbit. Bar represents 150μm. (**C**) Contralateral lymph node of an SLS-infected laboratory rabbit. Bar represents 300μm. (**D**) Contralateral lymph node of a Uriarra-infected laboratory rabbit. Bar represents 150μm. (**E**) Myxoma virus-infected lymphocyte in the paracortex. Bar represents 10μm. (**F**) Myxoma virus-infected macrophage-like cell in the paracortex. Bar represents 10μm. GC, germinal centre; P, paracortex.

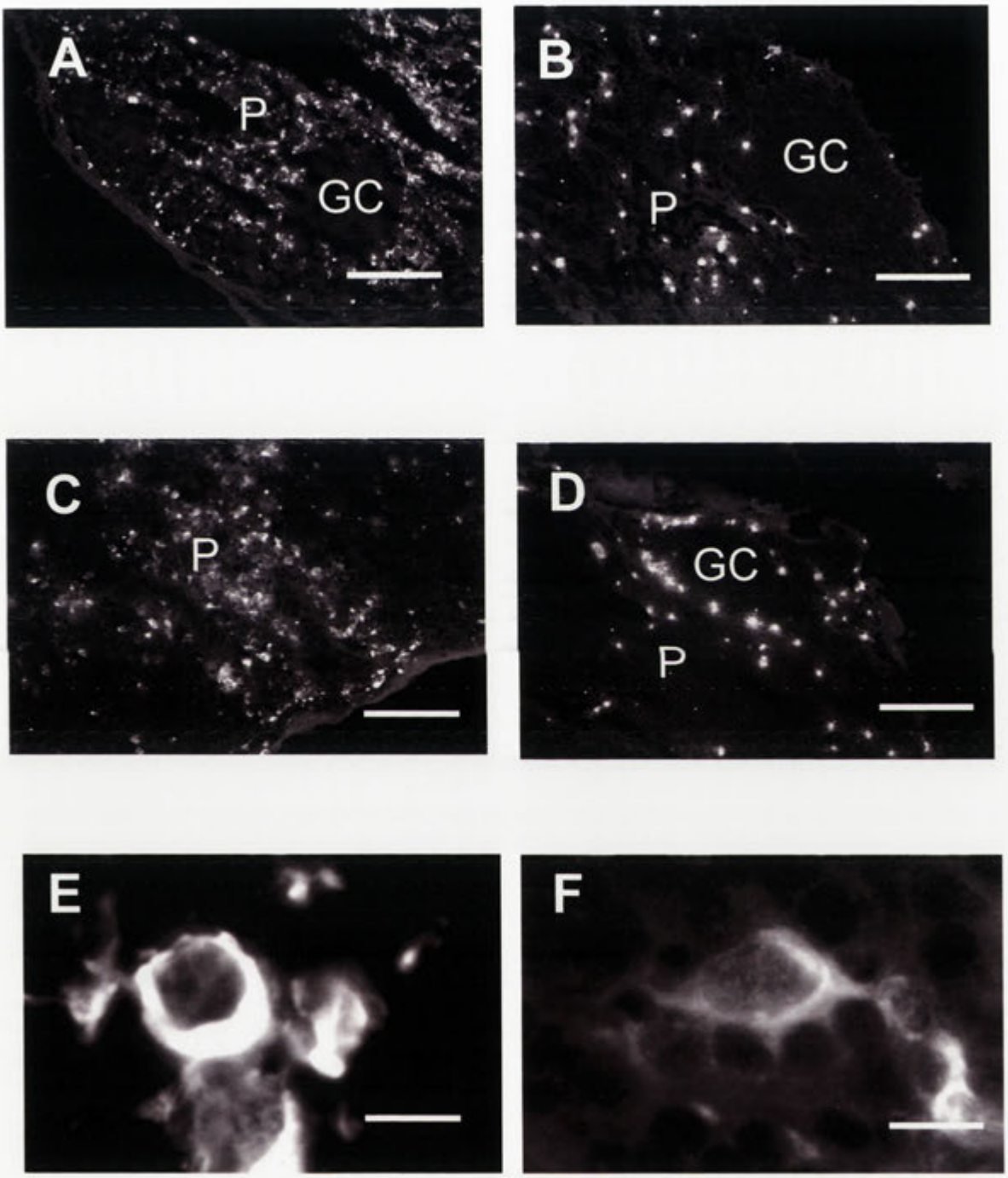
A
P
GC
B
GC
P
C
P
D
GC
P
E
F

inoculated in the foot compared to that of rabbits that had been inoculated in the thigh, and was more extensive in SLS-infected laboratory rabbits. Virus was not associated with germinal centres in the draining lymph node of laboratory rabbits infected with either SLS or Uriarra. However, in the contralateral lymph node of infected rabbits (Figures 4.24 C and D), virus had infected lymphocytes (Figure 4.24E) in both the diffuse cortex and in the newly forming mantle zones of germinal centres, particularly in the contralateral lymph nodes of infected laboratory rabbits. Virus had also infected large mononuclear cells that resembled macrophages in the paracortex in both the draining and contralateral lymph nodes (Figure 4.24F). Infection of the T-cell-dependent zones in the contralateral lymph nodes was less extensive than the draining lymph node, particularly in Uriarra-infected rabbits. From 4dpi, cells within the wall of the lymph node capsule from SLS, but not Uriarra, infected laboratory rabbits stained positive for virus antigen (Figure 4.25A). These cells were elongated, approximately 90μm across, with a large central nucleus (Figure 4.25B).

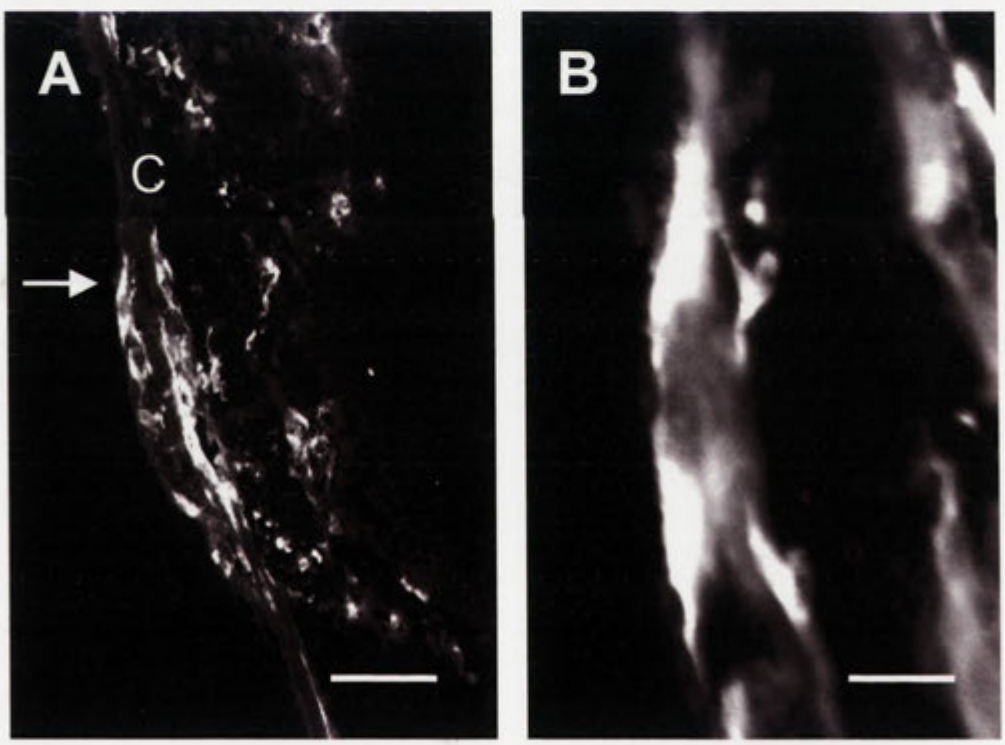

Figure 4.25: Localisation of SLS in the draining lymph node of a laboratory rabbit at 4dpi. (**A**) SLS localisation in cells of the lymph node capsule. Bar represents 100μm. (**B**) Higher magnification of (**A**) showing localisation of SLS in the cytoplasm of an infected cell. Bar represents 15μm. Arrow indicates the cell shown at higher magnification in (**B**). C, capsule.

In wild rabbits infected with SLS at 4dpi, virus was present in lymphocytes in the diffuse cortex of the draining lymph node, but less cells were infected than in the

draining lymph node of SLS-infected laboratory rabbits at the same time. In the contralateral lymph node, SLS was present in lymphocytes in the cortex of one of two infected rabbits. Uriarra was not present in the draining or contralateral lymph nodes of wild rabbits at 4dpi.

The earliest striking difference between the draining lymph nodes from myxoma virus-infected rabbits was the number of primary follicles and germinal centres at 4dpi. In SLS-infected rabbits, these numbered up to eight per tissue section (Figures 4.26 A and B show the range of follicle development), whereas there were up to 40 in Uriarra-infected rabbits (Figure 4.26C). The number of follicles and germinal centres was generally greater in SLS-infected wild rabbits compared to laboratory rabbits, but was never as great as in the lymph nodes of Uriarra-infected rabbits. In the tissue sections from two of four laboratory rabbits infected with SLS at 4dpi, there were no germinal centres present in the draining or contralateral lymph nodes, although there were numerous follicles in the very outer cortex. In SLS-infected wild rabbits, germinal centre formation was limited in the draining lymph node (Figure 4.27A), but in the contralateral lymph node, was more comparable to that of Uriarra-infected laboratory rabbits (Figure 4.27B). In some follicles from SLS-infected laboratory or wild rabbits, there was an increase in the area represented by the light zone but with no concomitant increase in the area of the mantle zone. However, in lymph nodes from Uriarra-infected rabbits, there were more cells in mitotic division in the mantle zones of germinal centres indicating that cell division was occurring following infection of rabbits. There was also an increased number of cells with apoptotic nuclei. Apoptotic cells had small, globular, dark staining fragments instead of a single nucleus. In the lymph nodes from these rabbits, there was also a general increase in the number of small lymphocytes in the paracortex compared to uninfected lymph nodes.

In addition to the development of germinal centres, differences in lymph nodes between laboratory or wild rabbits infected with either virulent or attenuated myxoma virus were observed in the paracortex. Endothelial cells of capillaries and venules within the paracortex of lymph nodes from SLS-infected laboratory rabbits were swollen by 4dpi, and in some vessels, had increased in number. Neutrophils were present within the lumen of blood vessels in both the draining and contralateral lymph nodes at 2 and 4dpi with SLS, but were not present outside the blood vessels (Figure 4.28A). The nucleus of lymphocytes proximal to blood vessels containing neutrophils contained dark-

Figure 4.26: Histopathology of the draining lymph node of SLS or Uriarra-infected laboratory rabbits at 4dpi. (**A**) Lymph node from one SLS-infected laboratory rabbit that contains follicles in the cortex, but no germinal centres. (**B**) Lymph node from the other SLS-infected laboratory rabbit which contains several germinal centres in the cortex at 4dpi. (**C**) Lymph node from a Uriarra-infected laboratory rabbit which has numerous, well defined germinal centres in the outer cortex and throughout the paracortex. Bars represent 100μm. F, follicle; GC, germinal centre; PC, paracortex.

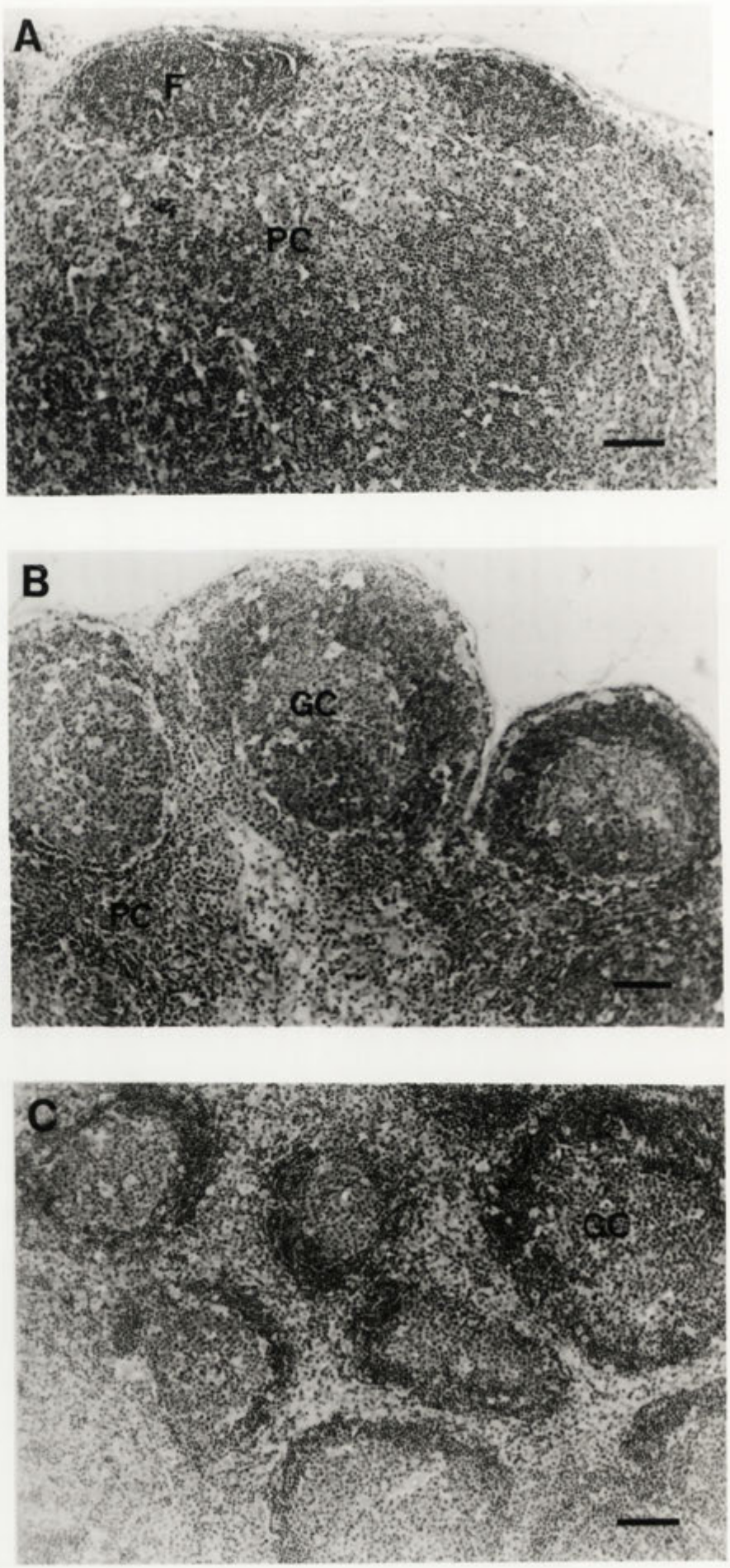
A
F
PC
B
GC
PC
C
GC

staining blocks of chromatin or were apoptotic. In SLS-infected wild rabbits or in Uriarra-infected wild or laboratory rabbits, blood vessel endothelia were similar to those in the lymph nodes of uninfected rabbits, and neutrophils were not routinely observed in the blood vessel lumen (Figure 4.28B). However, on autopsy at 2dpi, the draining lymph node from one SLS-infected wild rabbit was purple in colour and contained a large aggregation of neutrophils associated with extravasated RBC in a localised area of the subcapsular sinus and cortex. There were numerous nuclear fragments in this area. The contralateral lymph node of the same rabbit appeared normal, with no neutrophils in the lumen of blood vessels.

By 4dpi, there was depletion of lymphocytes from both the draining and contralateral lymph nodes of SLS-infected laboratory rabbits (Figure 4.29 A and B). The decrease in the number of lymphocytes was in the cortex, directly under the subcapsular sinus and in the interfollicular regions, and was associated with the deposition of fibrin. Some lymphocytes in the interfollicular zones stained darker at the periphery of the nucleus and in dark blocks in the centre of the nucleus, indicating condensation and marginalisation of chromatin. The nucleus of lymphocytes present in the blood vessel lumen also stained heavily at the periphery. In SLS-infected wild rabbits, depletion of lymphocytes had occurred by 4dpi from the interfollicular zones of draining lymph nodes, similar to that described for SLS-infected laboratory rabbits, but the contralateral lymph nodes were normal. The diffuse cortex of both draining and contralateral lymph nodes of Uriarra-infected laboratory or wild rabbits was well populated with lymphocytes and macrophages, with no evidence of cell depletion by 4dpi (Figures 4.29 C and D).

4.3.3.2.2 Six days post infection of laboratory and wild rabbits with SLS or Uriarra

At 6dpi of laboratory or wild rabbits with either SLS or Uriarra, virus had infected mononuclear cells resembling lymphocytes and macrophages in both the draining and contralateral lymph nodes. In all rabbits inoculated with myxoma virus, infected cells were evenly distributed throughout the much of the diffuse cortex of both draining and contralateral lymph nodes (Figure 4.30A) and in the mantle zones of germinal centres. However, in SLS-infected wild rabbits (Figures 4.30 B and C), or Uriarra-infected laboratory rabbits (Figures 4.30 D and E), some areas of the cortex had very few cells infected with virus. In the draining lymph node, lymphocytes within both the paracortex

Figure 4.27: Histopathology of the draining and contralateral lymph nodes from an SLS-infected wild rabbit at 4dpi. (**A**) Draining lymph node from one SLS-infected wild rabbit that contains a follicle and a small germinal centre in the cortex. (**B**) The contralateral lymph node from the same SLS-infected wild rabbit as (**A**) which has several germinal centres in the cortex at 4dpi. Bars represent 100μm. F, follicle; GC, germinal centre; PC, paracortex.

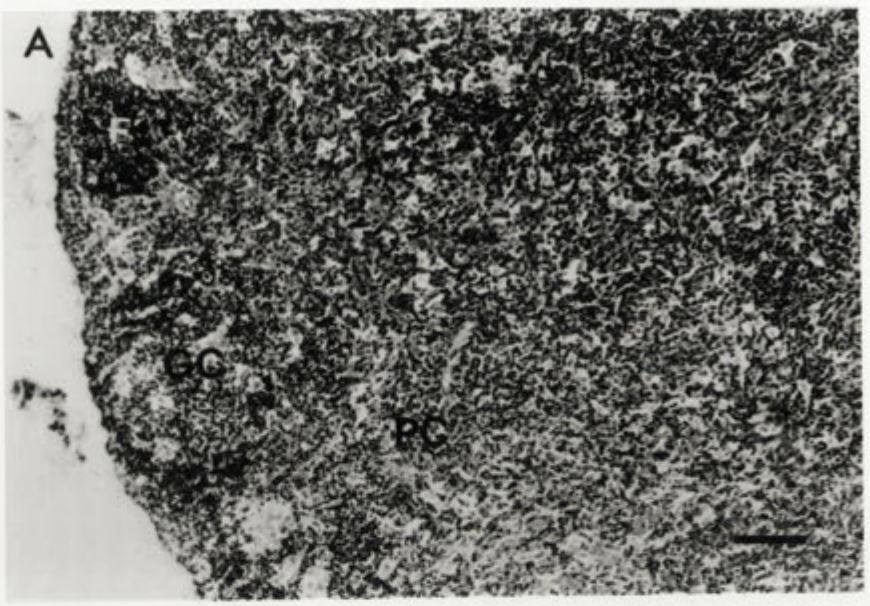
A
F
GC
PC

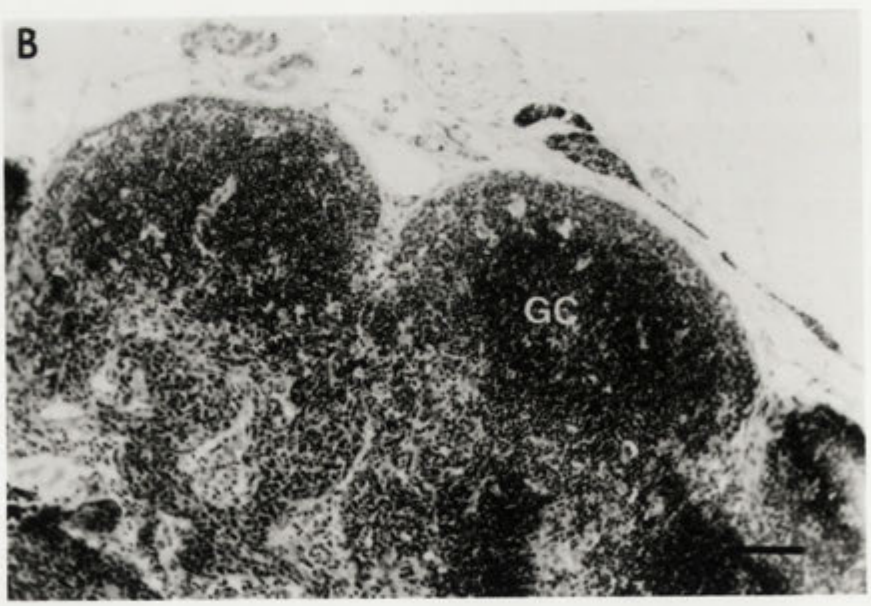
B
GC

Figure 4.28: Histopathology of in the draining lymph node of SLS or Uriarra-infected laboratory rabbits at 4dpi. (A) Blood vessel in the lymph node paracortex from an SLS-infected laboratory rabbit. Note the number of neutrophils within the vessel lumen and the cell with an apoptotic nucleus near the blood vessel. (B) Blood vessel in the lymph node paracortex from a Uriarra-infected laboratory rabbit. The lumen of this blood vessel contains lymphocytes and a single neutrophil. Bars represent 25μm. A, apoptotic cell; L, lymphocyte; N, neutrophil.

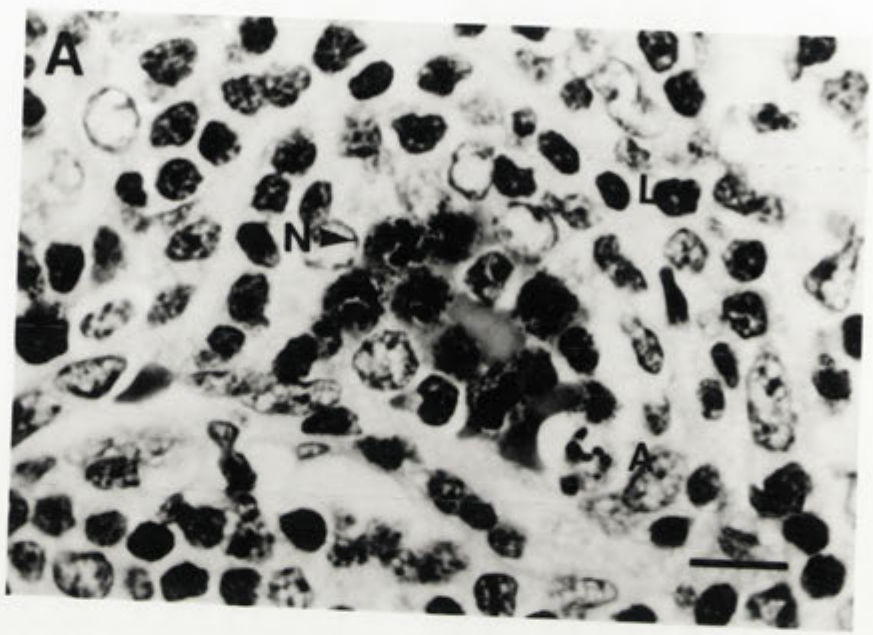
A
N
L
A

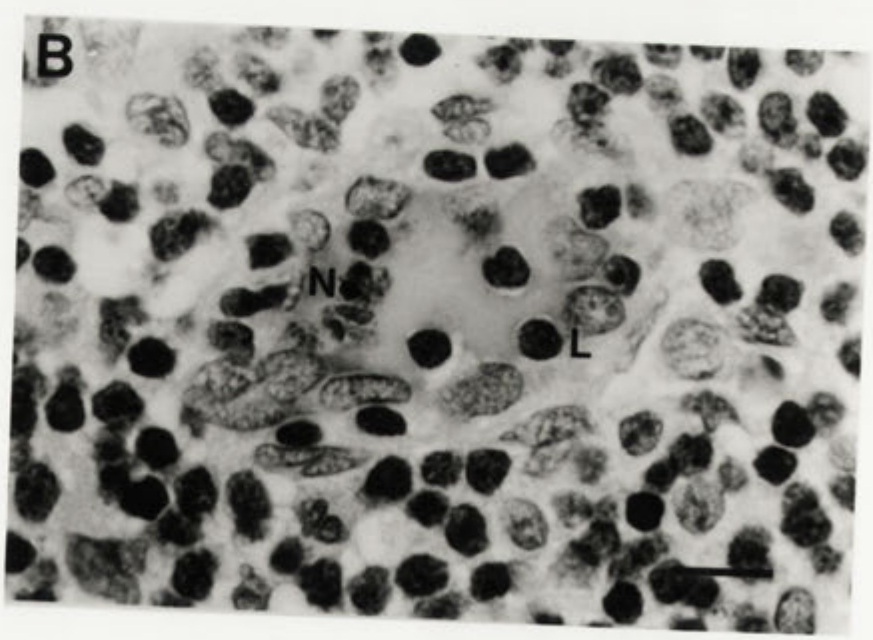
B
N
L

Figure 4.29: Histopathology of the draining lymph node of SLS or Uriarra-infected laboratory rabbits at 4dpi. **(A)** Lymph node from an SLS-infected laboratory rabbit. Lymphocytes have been depleted from the interfollicular zones. **(B)** Higher magnification of an interfollicular zone in the draining lymph node from an SLS-infected laboratory rabbit. **(C)** Lymph node from a Uriarra-infected laboratory rabbit. **(D)** Higher magnification of an interfollicular zone in the draining lymph node from a Uriarra-infected laboratory rabbit. Bars represent 100μm. C, capsule; IF, interfollicular zone; GC, germinal centre; L, lymphocyte; M, macrophage; PC, paracortex.

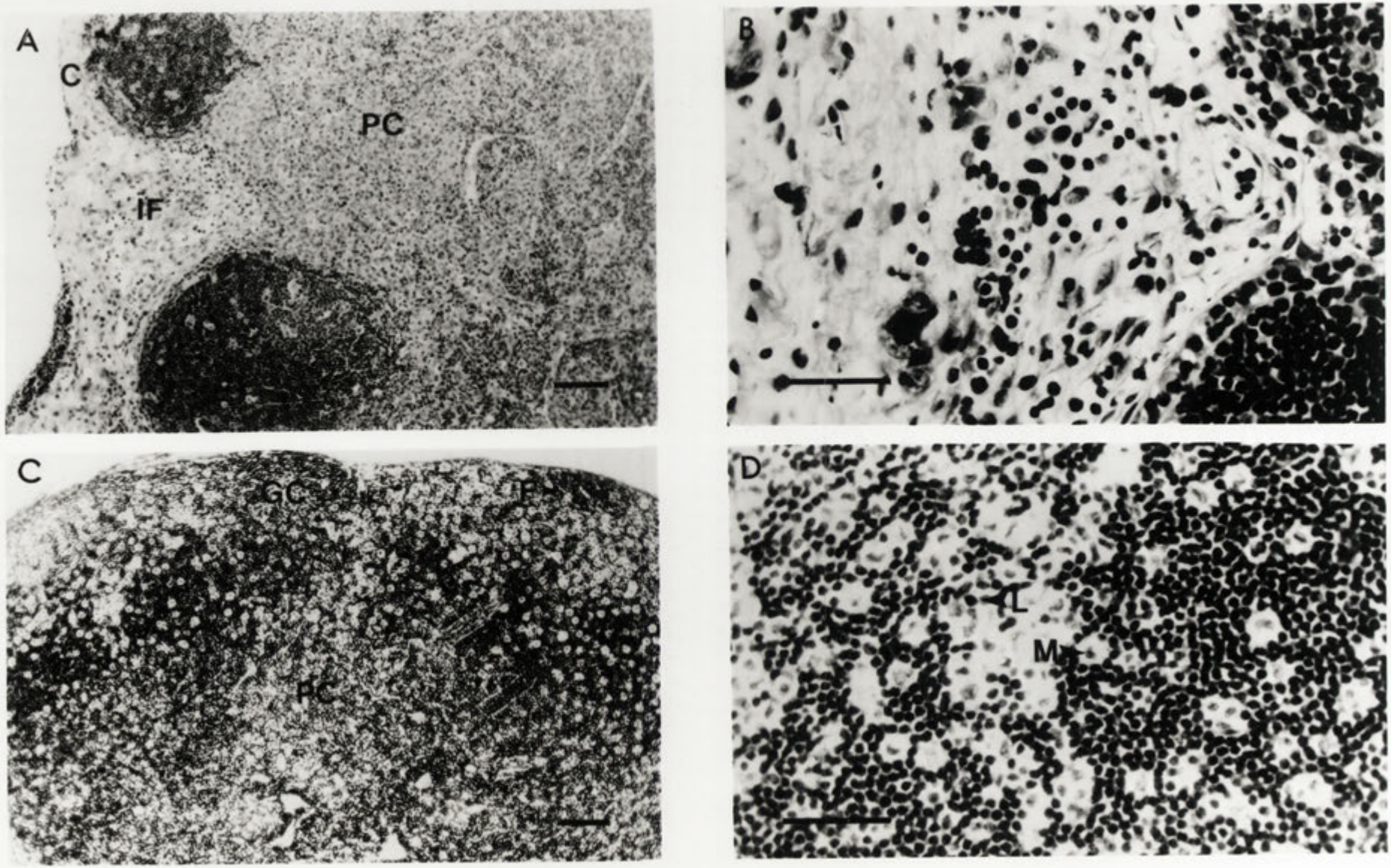
A
C
PC
IF
B
C
GC
IF
PC
D
L
M

Figure 4.30: Myxoma virus localisation in the draining lymph nodes of myxoma virus-infected laboratory and wild rabbits at 6dpi. **(A)** Draining lymph node from an SLS-infected laboratory rabbit. Bar represents 200μm. **(B)** Draining lymph node from an SLS-infected wild rabbit. Bar represents 200μm. **(C)** A different region of the draining lymph node from the same SLS-infected wild rabbit as **(B)**. Bar represents 200μm. **(D)** Draining lymph node from a Uriarra-infected laboratory rabbit. Bar represents 200μm. **(E)** A different region of the draining lymph node from the same Uriarra-infected laboratory rabbit as **(D)**. Bar represents 200μm. P, paracortex.

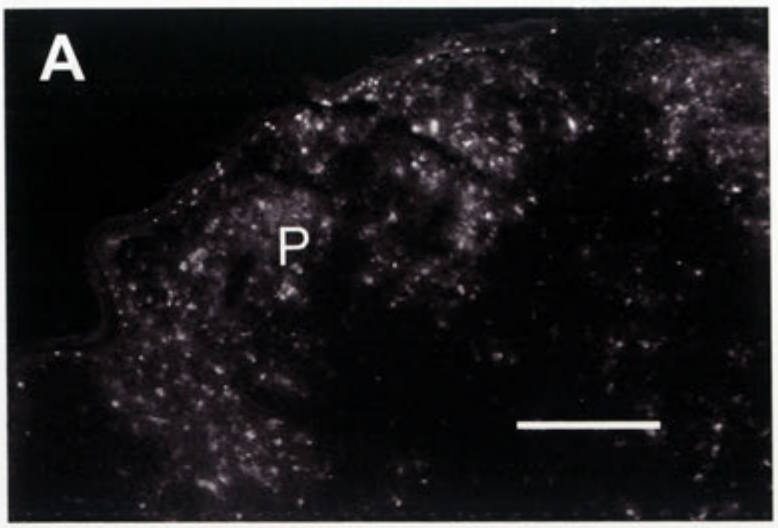
A
P

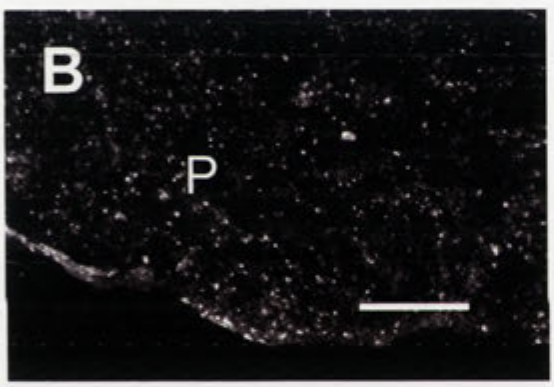
B
P


C

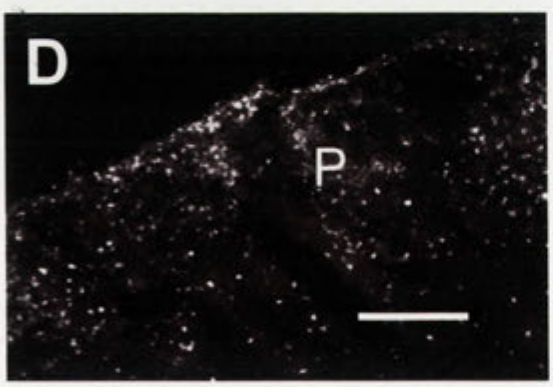
D
P


E

and mantle zones were infected (Figure 4.31A). In the contralateral lymph nodes, infection of lymphocytes of the mantle zones of germinal centres occurred without extensive infection of surrounding T-dependent areas (Figure 4.31B). Also in the contralateral lymph nodes, WBC contained in the lumen of blood vessels were positive for myxoma virus (Figure 4.31 C). These cells included lymphocytes, some of which were positioned between the endothelial cells of the vessel (Figure 4.31D) and hence were possibly migrating across the vessel wall. Mononuclear cells distinguished by a horseshoe shaped nucleus in the subcapsular sinus of contralateral lymph nodes stained positive for myxoma virus (Figure 4.31E). In both draining and contralateral lymph nodes, areas of the paracortex often remained relatively virus free with only one or two positive lymphocytes even when other areas contained high numbers of infected cells. Virus was not detected by immunofluoresence in the draining or contralateral lymph nodes of wild rabbits infected with Uriarra at 6dpi.

The differences in virus localisation between groups of myxoma virus-infected rabbits at 6dpi were mainly observed in the cell types infected. Similarly to 4dpi, SLS infected cells of the lymph node capsule in both laboratory and wild rabbits, but not in rabbits infected with Uriarra. In SLS-infected laboratory rabbits, areas of the paracortex containing high numbers of infected lymphocytes also had large cells that stained intensely for virus antigen. These large cells were located immediately surrounding blood vessels, although the endothelial cells of the vessel wall remained uninfected. These cells resembled myxoma cells, but were rectangular rather than stellate in shape, and were not infected following SLS infection of wild rabbits, or Uriarra infection of either laboratory or wild rabbits. In SLS-infected wild rabbits only, virus antigen was often present in the cytoplasm of lymphocytes in limited areas of the cytoplasm rather than as a generalised staining of the cytoplasm. These resembled virus factories in the cytoplasm and may indicate that virus replication is limited in primary cells from wild rabbits.

At 6dpi of both SLS-infected laboratory and wild rabbits, pathological changes were most extensive in the germinal centres and the paracortex of draining lymph nodes and were associated with the depletion of lymphocytes from these areas. In germinal centres, the depletion of lymphocytes resulted in poor definition of the light and dark zones. Similarly to 4dpi, depletion of lymphocytes had occurred in the interfollicular areas and extending into the paracortex, which contained increased numbers of swollen

Figure 4.31: Myxoma virus localisation in the draining and contralateral lymph nodes of SLS-infected laboratory rabbits at 6dpi. **(A)** Draining lymph node from an SLS-infected laboratory rabbit. Bar represents 200μm. **(B)** Contralateral lymph node from the same SLS-infected laboratory rabbit as **(A)**. Bar represents 200μm. **(C)** Contralateral lymph node from an SLS-infected laboratory rabbit. Myxoma virus was present in white blood cells within the lumen of a blood vessel (solid arrow indicates the blood vessel). Bar represents 100μm. **(D)** Contralateral lymph node from an SLS-infected laboratory rabbit. Myxoma virus was present in white blood cells located within the lumen and between endothelial cells of the blood vessel (open arrow indicates the connective tissue of the blood vessel). Bar represents 30μm. **(E)** Myxoma virus localisation in the cytoplasm of cells within the lymph node subcapsular sinus. These cells include a mononuclear cell with a horseshoe-shaped nucleus (slender arrow). Bar represents 20μm. C, capsule; GC, germinal centre; Lu, lumen of blood vessel; P, paracortex.

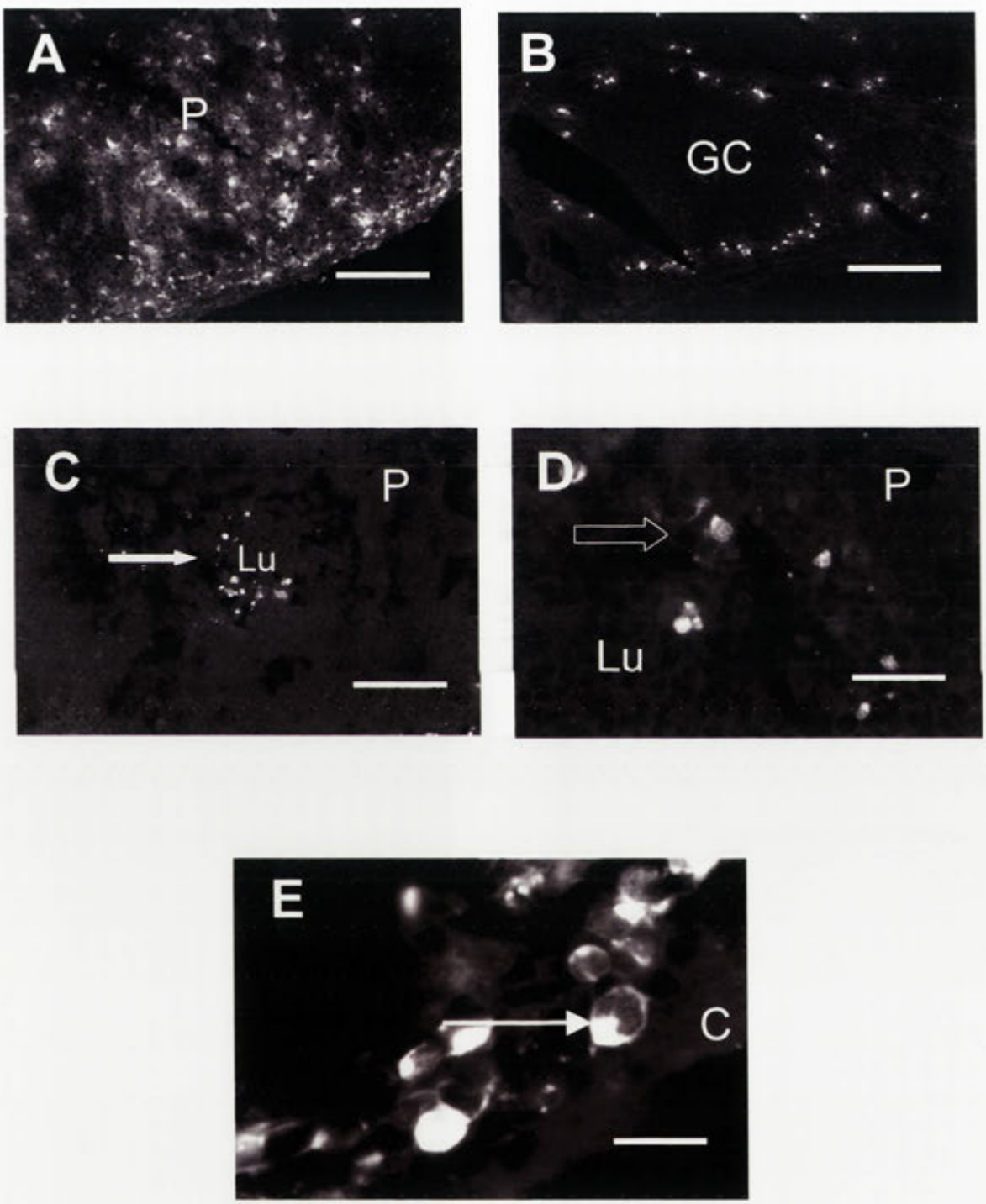
A
P
B
GC
C
P
Lu
D
P
Lu
E
C

reticular cells and neutrophils as well as fibrin deposits. However, areas of the paracortex more central in the node, towards the medulla, remained populated with lymphocytes.

Other changes in the draining lymph nodes of SLS-infected laboratory or wild rabbits included the presence of high numbers of neutrophils in the subcapsular sinus and throughout the adipose tissue, but only low numbers were present in the body of the node. Similarly to 4dpi of laboratory rabbits with SLS, the endothelial cells of SLS-infected laboratory and wild rabbits were swollen and in some vessels, had increased in number. Large, rectangular cells that resembled myxoma cells were present in areas of the lymph node depleted of lymphocytes, especially proximal to damaged blood vessels. However, stellate myxoma cells were present in the lymph nodes of SLS-infected laboratory rabbits only.

Despite the similarities in the pathology of the draining lymph node from SLS-infected laboratory and wild rabbits at 6dpi, the contralateral lymph nodes from the two groups of infected rabbits were quite different. The pathology of the contralateral lymph node from SLS-infected laboratory rabbits resembled that described above for the draining lymph node, except that the infiltration of neutrophils into the subcapsular sinus and interfollicular regions appeared greater in contralateral lymph nodes. However, the contralateral lymph nodes from wild rabbits infected with SLS were not depleted of lymphocytes, and instead resembled the contralateral lymph nodes from Uriarra-infected laboratory rabbits, described below.

At 6dpi of laboratory and wild rabbits with Uriarra, the paracortex of the draining and contralateral lymph nodes was densely populated with large and small lymphocytes and often appeared punctuated with other, larger mononuclear cells resembling macrophages. Germinal centres were generally large and well defined within the cortex of lymph nodes, and contained macrophages which had phagocytosed numerous dark staining nuclear fragments. However, in one laboratory rabbit there was a much more limited response as shown by underdeveloped germinal centres with no obvious hyperplasia of small lymphocytes within the paracortex. This lymph node contained the most amount of virus by immunofluorescence and by plaque assay, of any rabbit at 6dpi. In the paracortex of lymph nodes from Uriarra-infected rabbits, there was some swelling of the reticular and endothelial cells, however, changes in blood vessels and

reticular cells in lymph nodes were never as severe as those infected with SLS. In contrast to SLS-infection at the same time, the subcapsular sinus and adipose tissue contained more mononuclear cells than neutrophils.

Following inoculation of laboratory rabbits with Uriarra in the thigh, lymphocytes were depleted from the interfollicular areas of both the left and right popliteal lymph nodes by 8dpi. This depletion was mild, giving the impression of a general reduction in the number of lymphocytes rather than a devastation of cells, and had not progressed further in lymph nodes from rabbits inoculated in the thigh and killed at 10dpi.

4.3.3.2.3 Ten days post infection of laboratory and wild rabbits with myxoma virus

By 10dpi of laboratory rabbits with SLS, virus was present in both the draining and contralateral lymph nodes in a circular distribution in germinal centres that had been depleted of lymphocytes (Figure 4.32A). Cells containing virus antigen were not lymphocytes, but rather were large (20-25μm in diameter) with no discernible nuclear morphology (Figure 4.32B). It is probable that these cells were proliferated reticular cells or possible myxoma cells as these were the predominant cell type observed by haematoxylin and eosin staining of the same lymph nodes. Throughout the course of infection, SLS was rarely associated with cells in the medulla, except in one laboratory rabbit at 10dpi, when virus localised to lymphocytes in this area. In SLS-infected wild rabbits, virus was present in lymphocytes of the paracortex of both the draining and contralateral lymph nodes, regardless of the extent of lymphocyte depletion. However, the number of virus-positive cells was considerably less than at 6dpi.

At 10dpi, the distribution of virus in the draining and contralateral lymph nodes of one of two laboratory rabbits infected with Uriarra in the hind foot resembled that at 6dpi. Virus was present in lymphocytes in an even distribution throughout the paracortex, but was not closely associated with germinal centres. In the other rabbit, tissue sections contained only one to two positive lymphocytes in the paracortex. Following infection of wild rabbits with Uriarra, 10dpi was the only time point besides 2dpi when virus was observed in lymph nodes. At this time, virus was present in the cytoplasm of a small number of lymphocytes within the paracortex of both the draining and contralateral lymph nodes.

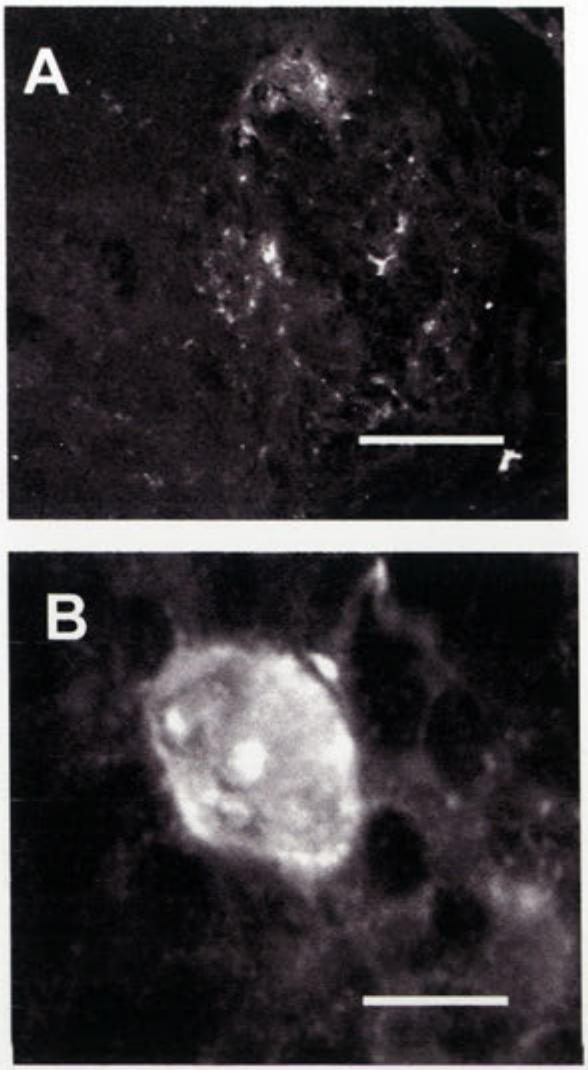

Figure 4.32: Myxoma virus localisation in the draining lymph node of an SLS-infected laboratory rabbit at 10dpi. (**A**) Myxoma virus localised to cells in a circular distribution within the remnants of germinal centres. Bar represents Draining lymph node from an SLS-infected laboratory rabbit. Bar represents 300μm. (**B**) Higher magnification of (**A**) showing the morphology of cells containing myxoma virus. The identity of these cells is unknown. Bar represents 15μm.

At 10dpi of laboratory rabbits with SLS, the pathological changes in the lymph nodes involved half to all of the node and while some areas were completely devoid of lymphocytes, others appeared well populated. Lymph nodes were always affected from the periphery inwards, with marked increases in the number of reticular cells spreading inwards along the trabeculae of the node towards the medulla (Figure 4.33A). In laboratory rabbits, these changes did not differ markedly between the draining and contralateral lymph nodes. By 10dpi, neutrophils had infiltrated extensively into areas

Figure 4.33: Histopathology of the draining lymph node of SLS-infected laboratory rabbits at 10dpi. (A) Trabeculum which is thickened and contains increased numbers of swollen reticular cells compared to that in lymph nodes from uninfected rabbits. Bar represents 100μm. **(B)** The diffuse cortex of a draining lymph node that has been depleted of lymphocytes. The continuous line of dark staining cells are predominantly neutrophils. Bar represents 100μm. (C) High magnification of the paracortex of an SLS-infected draining lymph node showing a stellate myxoma cell, some intact lymphocytes and cellular debris. Bar represents 50μm. **(D)** Germinal centres from SLS-infected lymph nodes sometimes appeared with dark central zones and a lighter outer zone. Bar represents 100μm. L, lymphocyte; MC, myxoma cell.

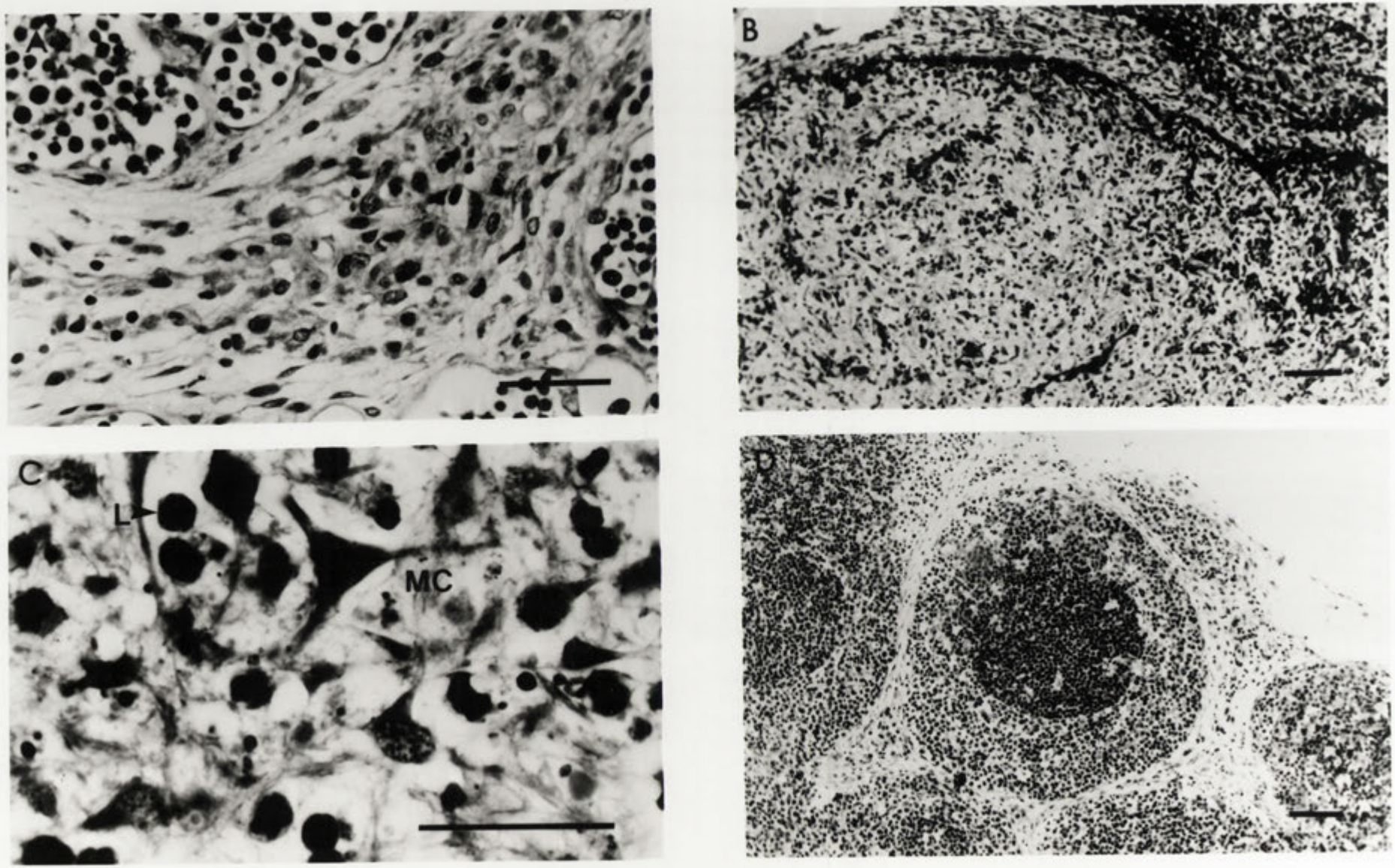
A
B
C
L
MC
D

from which lymphocytes were completely absent, and were often observed in clusters surrounding myxoma cells, or in rings one or two cells deep surrounding germinal centres that had been completely destroyed (Figure 4.33B). Extracellular fibrin was observed between myxoma cells, enlarged reticular cells and macrophages (Figure 4.33C). Some germinal centres contained macrophages and lymphocytes within the light zones although lymphocytes had disappeared from the light zones. These macrophages were full of nuclear fragments and cellular debris. The germinal centres thus appeared as though they had been inverted, with a very light staining area in the mantle zone surrounding a dark staining area in the light zone (Figure 4.33D).

At 10dpi with Uriarra, both the germinal centres and paracortex were richly populated with lymphocytes and macrophages with the occasional mitotic figure observed in these areas. Some depletion of lymphocytes had occurred in the interfollicular areas, which contained macrophages rather than myxoma cells, but there was limited neutrophil infiltration into lymph nodes. The adipose tissue surrounding the lymph node was filled with small lymphocytes. Lymphocytes with morphological characteristics of cells undergoing apoptosis were present in the paracortex of lymph nodes. These cells ranged from having marginalised chromatin within the nucleus, to being shrunken with a fragmented nucleus. At 10dpi of laboratory rabbits with Uriarra, plasma cells were present in the medullary cords and the paracortex of nodes. Some germinal centres appeared to either have shrunken in size compared to 6dpi through a depletion of lymphocytes from areas of the marginal zone closest to the lymph node capsule or, in fewer cases, to have not developed during earlier days of infection.

At 10dpi with SLS, the histopathology of lymph nodes from wild rabbits varied greatly (Figure 4.34). In one draining and two contralateral lymph nodes all from separate rabbits killed at 10dpi, the lymph nodes appeared relatively healthy. These lymph nodes contained many nuclear fragments in the paracortex although this area remained generally well populated, with limited evidence of increased numbers of swollen reticular cells or the infiltration of neutrophils, despite the presence of neutrophils in the subcapsular sinus of lymph nodes and throughout the adipose tissue surrounding the node. Large clusters of small lymphocytes were in areas where germinal centres would be expected to have formed. However, these aggregations of cells were not defined into dark, light and mantle zones. In the two other draining lymph nodes and one contralateral lymph node from SLS-infected wild rabbits, the nodes contained large

Figure 4.34: Histopathology of lymph nodes from SLS-infected wild rabbits at 10dpi. (**A**) Draining lymph node from an SLS-infected wild rabbit showing extensive depletion of lymphocytes throughout. (**B**) Higher magnification of (**A**) showing some intact lymphocytes and cellular debris in the form of nuclear fragments. (**C**) A second area of the same draining lymph node as shown in (**A**). This area contains clusters of lymphocytes in the outer cortex and is well populated with lymphocytes in the paracortex. (**D**) Higher magnification of (**C**) showing numerous intact lymphocytes. Bars represent 100μm. L, lymphocyte; nf, nuclear fragments; P, paracortex.

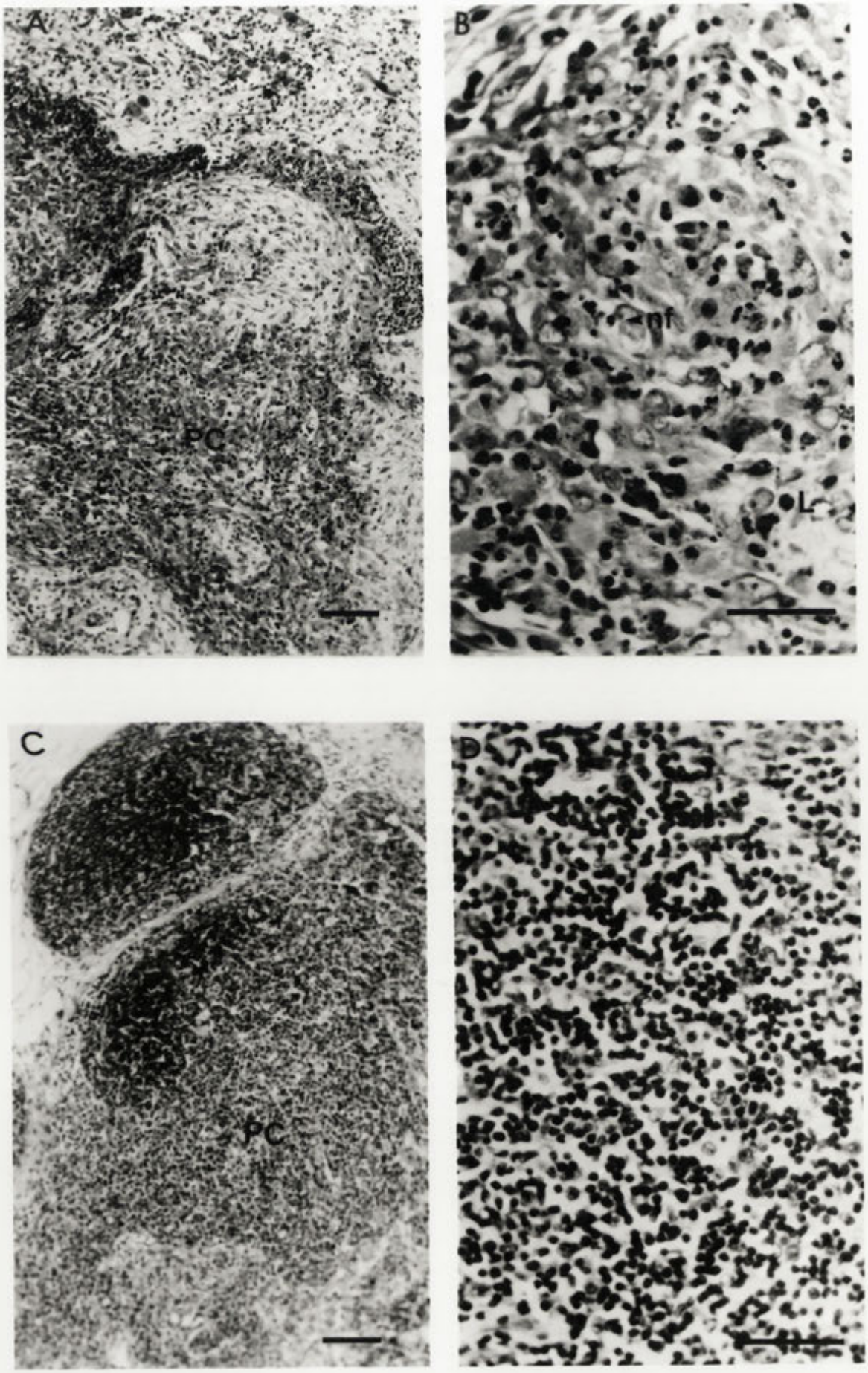
A
PC
B
nf
L
C
PC
D

areas from which lymphocytes were completely depleted (Figure 4.34A) and where there were large numbers of swollen reticular cells (Figure 4.34B). However, these areas were localised within lymph nodes, with other areas of the paracortex remaining relatively unaffected and well populated with lymphocytes (Figures 4.34 C and D). Other pathological changes, such as the presence of large myxoma cells, deposition of extracellular fibrin, neutrophil infiltration into the lymph node and adipose tissue, were more extensive than those observed following infection of laboratory rabbits with Uriarra, and resembled the changes following infection of laboratory rabbits with SLS described at 6dpi.

4.3.3.2.4 Fifteen days post infection of laboratory and wild rabbits with myxoma virus

Uriarra was not detected in lymph nodes from Uriarra-infected laboratory rabbits at 15dpi. Histologically, the paracortex was well populated with large and small lymphocytes and macrophages although areas of lymphocyte depletion were evident. However these were constrained to the interfollicular zones of the cortex of draining lymph nodes. Germinal centres were numerous and well defined. In general, the lymph nodes contained numerous nuclear fragments and some neutrophils had infiltrated into the nodes from the subcapsular sinus. The leucocytes in the lumen of blood vessels were predominantly lymphocytes. Some extravasated RBCs were present in the paracortex around these vessels.

Virus was not detected by immunofluorescence in the lymph nodes of SLS- or Uriarra-infected wild rabbits at 15dpi. The paracortex of both draining and contralateral lymph nodes SLS-infected wild rabbits resembled that described for the healthy areas of lymph nodes that remained at 10dpi; it was well populated with large and small lymphocytes and macrophages. The formation of new germinal centres, consisting of large light zones and relatively small mantle zones, was apparent in some lymph nodes of SLS-infected wild rabbits and plasma cells were observed in the paracortex. Neutrophils were observed in areas of lymph node where lymphocytes remained scarce, or at the edge of areas that were repopulated with lymphocytes. However, the number and distribution of neutrophils was never as extensive as in the lymph nodes from SLS-infected laboratory rabbits, and neutrophils were not present in areas containing numerous lymphocytes. The lumens of blood vessels and the adipose tissue were filled with small lymphocytes.

4.3.3.2.5 Twenty days post infection of laboratory and wild rabbits with myxoma virus

At 20dpi of wild rabbits with SLS, virus antigen was detected in the draining lymph nodes as faintly staining, continuous lines of antigen spanning the paracortex. Similarly to very early in infection, this antigen appeared outside cells. Virus was not detected in the contralateral lymph nodes of infected rabbits. The draining lymph nodes that had previously been depleted of lymphocytes were now populated with small lymphocytes and macrophages and newly forming, well defined germinal centres were present. Thick, eosin-staining, fibres were present in localised areas of the paracortex of the draining lymph nodes, and to a lesser extent in the contralateral lymph nodes.

Virus was not detected in the draining or contralateral lymph nodes of Uriarra-infected rabbits at 20dpi. Histologically, these lymph nodes were not distinguishable from those described at 15dpi.

4.3.3.3 Changes in lymphocyte populations in the lymph nodes of myxoma virus-infected laboratory rabbits determined by immunohistochemistry

The draining and contralateral lymph nodes of laboratory rabbits inoculated in the thigh with either SLS or Uriarra were stained for cell surface expression of MHC class I, MHC class II, CD43, CD45 or Ig-$^{\mu}$. This staining does not indicate the definitive timing of changes in these cell populations as it was performed on tissues obtained following thigh and not foot inoculations. Hence, the staining of lymph node cell populations was compared between tissues from rabbits killed at 6 and 10dpi with those from uninfected rabbits as an indication of which populations were affected.

CD43 was strongly expressed by leucocytes in the T-cell-dependent areas of uninfected lymph nodes (Figure 4.35A). The intensity of CD43 staining in the paracortex of Uriarra-infected laboratory rabbits was reduced at 10dpi compared to that from uninfected rabbits (Figure 4.35B). By 6dpi with SLS, the number of $CD43^+$ cells in the interfollicular zones was reduced and $CD43^+$ cells of the paracortex stained with a reduced intensity. By 10dpi with SLS, localised areas of the paracortex contained $CD43^+$ cells, although most of the paracortex contained greatly reduced numbers of positive cells (Figure 4.35C). This was due to a generalised depletion of cells from these areas by 10dpi.

Figure 4.35: Immunolocalisation of cells expressing CD43 in the lymph nodes of laboratory rabbits. The binding of anti-CD43 was detected using an alkaline phosphatase-conjugated secondary antibody and fast red as a substrate. The presence of CD43 is shown in red. **(A)** Lymph node from an uninfected rabbit. CD43 was strongly expressed on leucocytes in the paracortex. **(B)** Lymph node from a Uriarra-infected rabbit at 10dpi. The intensity of CD43 staining in the paracortex of Uriarra-infected laboratory rabbits is reduced compared to uninfected rabbits. **(C)** Lymph node from an SLS-infected laboratory rabbit. The loss of CD43-specific staining in lymph nodes was associated with the depletion of lymphocytes. Bars represent 100μm. F, follicle; GC, germinal centre; P, paracortex; arrow head indicates the remnants of a germinal centre.

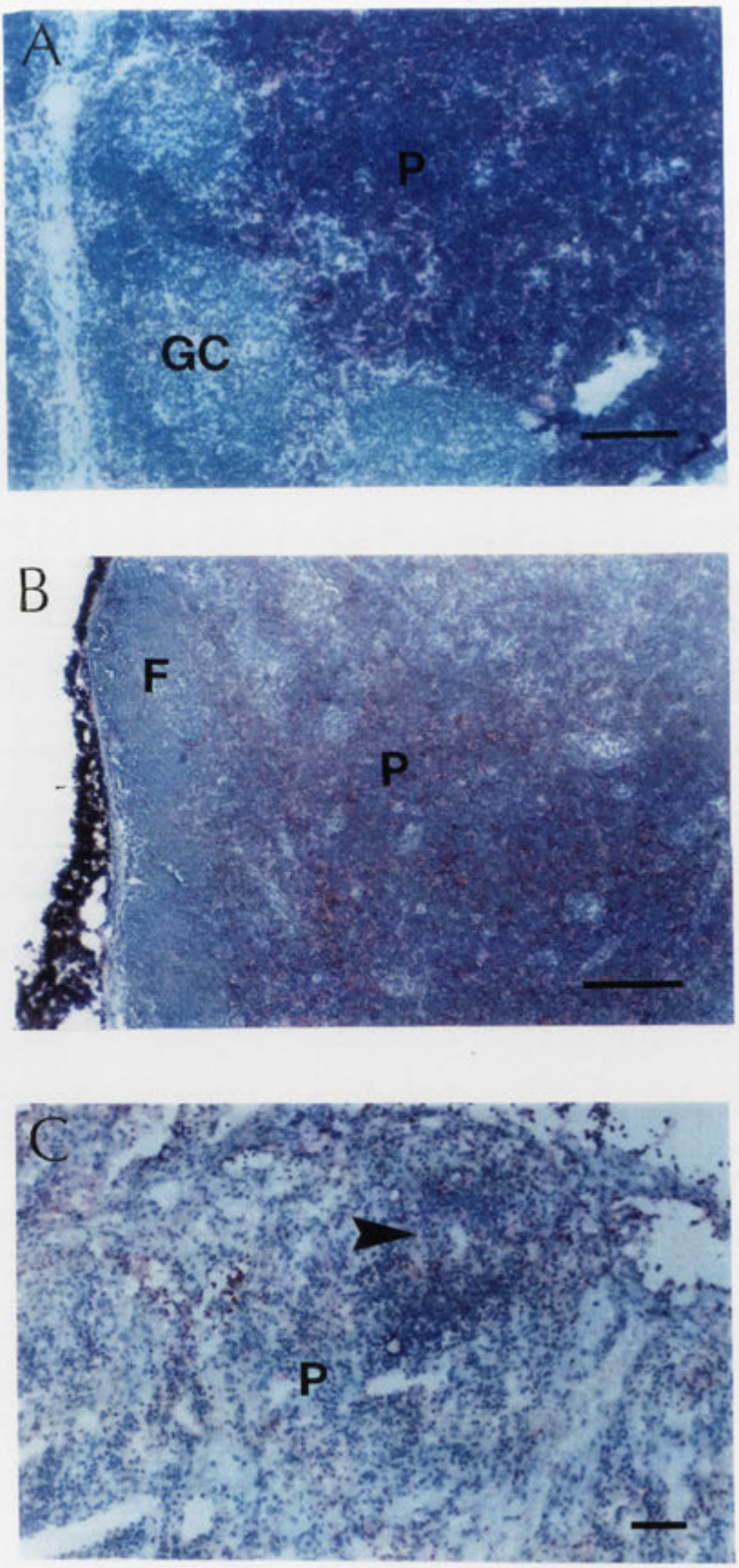
A
P
GC
B
F
P
C
P

Leucocytes in the T-cell-dependent areas of uninfected lymph nodes (Figure 4.36A) generally expressed CD45. The number and staining intensity of $CD45^+$ cells was reduced following ten days of infection with either Uriarra or SLS. However, this staining intensity did not differ substantially between infections (Figures 4.36 B and C).

MHC class I was expressed on cells throughout the T-cell and B-cell dependent areas of uninfected lymph nodes (Figure 4.37A). Staining for MHC class I in lymph nodes differed from CD43 as it stained the light zones of germinal centres, which CD43 did not. The distribution of MHC class I^+ cells in lymph nodes from Uriarra-infected laboratory rabbits at 10dpi was similar to that of uninfected lymph nodes although some areas stained with greater intensity (Figure 4.37B). It was not determined if this was due to an upregulation of MHC class I surface expression, or due to an increase in the number of MHC class I^+ cells. The distribution of cells expressing MHC class I in SLS-infected lymph nodes by 10dpi was reduced compared to nodes from uninfected rabbits or from rabbits infected with Uriarra, and were often clustered together in the localised areas of the paracortex that contained numerous lymphocytes (Figure 4.37C). Areas of the paracortex that were depleted of lymphocytes contained low numbers of cells expressing MHC class I.

MHC class II positive cells were distributed throughout entire lymph nodes from uninfected rabbits, as well as rabbits infected with either SLS or Uriarra. However, at 10dpi of Uriarra infected rabbits, the intensity of staining in the light zone of germinal centres increased compared to in that of uninfected lymph nodes. This increased staining intensity occurred in the light zones of two germinal centres from the contralateral lymph nodes of SLS-infected laboratory rabbits at 6dpi, but was not present in the lymph nodes at 10dpi (data not shown).

In lymph nodes from uninfected rabbits, Ig-μ was expressed throughout the cytoplasm of plasma cells, and on the surface of some lymphocytes (B-lymphocytes) and cells of the light zone of germinal centres, most probably indicating antibody on the surface of dendritic cells. In uninfected lymph nodes, plasma cells localised throughout the paracortex, in the mantle zone of germinal centres located most central to the node (Figure 4.38A) and in the medullary cords. Staining for this marker yielded the greatest amount of background staining in the tissue, particularly after infection of rabbits with myxoma virus, which may correspond to the detection of secreted antibody in the lymph

Figure 4.36: Immunolocalisation of cells expressing CD45 in the lymph nodes of laboratory rabbits. The binding of anti-CD45 was detected using an alkaline phosphatase-conjugated secondary antibody and fast red as a substrate. The presence of CD45 is shown in red. (**A**) Lymph node from an uninfected rabbit. CD45 was expressed on leucocytes in the paracortex. (**B**) Lymph node from a Uriarra-infected rabbit at 10dpi. (**C**) Lymph node from an SLS-infected laboratory rabbit. CD45-specific staining is reduced in lymph nodes from both Uriarra and SLS-infected laboratory rabbits. Bars represent 100μm. P, paracortex.

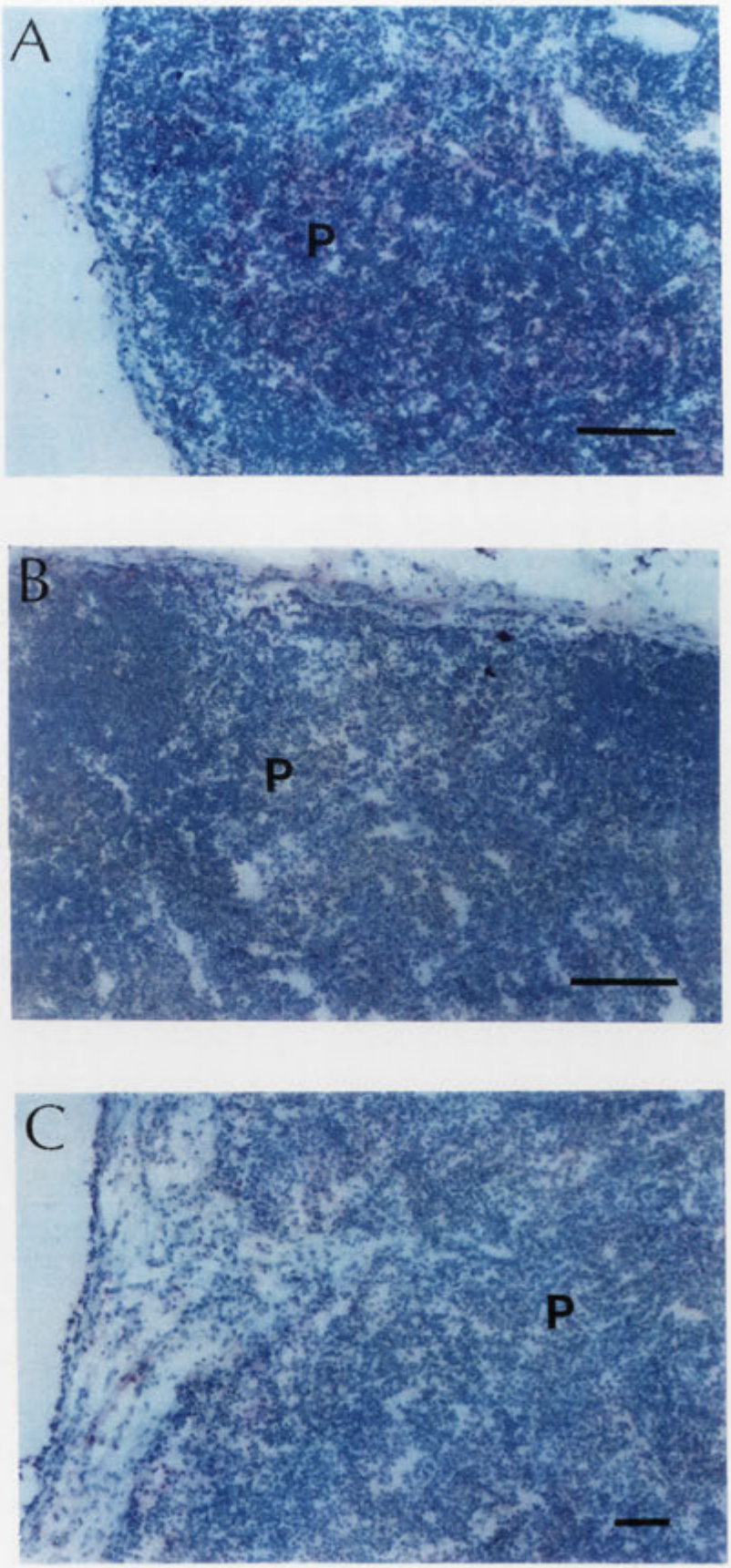
A
P
B
P
C
P

Figure 4.37: Immunolocalisation of cells expressing MHC class I in the lymph nodes of laboratory rabbits. The binding of anti-MHC class I was detected using an alkaline phosphatase-conjugated secondary antibody and fast red as a substrate. The presence of MHC class I is shown in red. **(A)** Lymph node from an uninfected rabbit. MHC class I was expressed throughout the paracortex and germinal centres. **(B)** Lymph node from a Uriarra-infected rabbit at 10dpi. The staining intensity of MHC class I increased following infection of laboratory rabbits with Uriarra. **(C)** Lymph node from an SLS-infected laboratory rabbit. The distribution of MHC class I-positive cells thoughout the paracortex was reduced compared to that in (A) or (B). Bars represent 100μm. GC, germinal centre; P, paracortex.

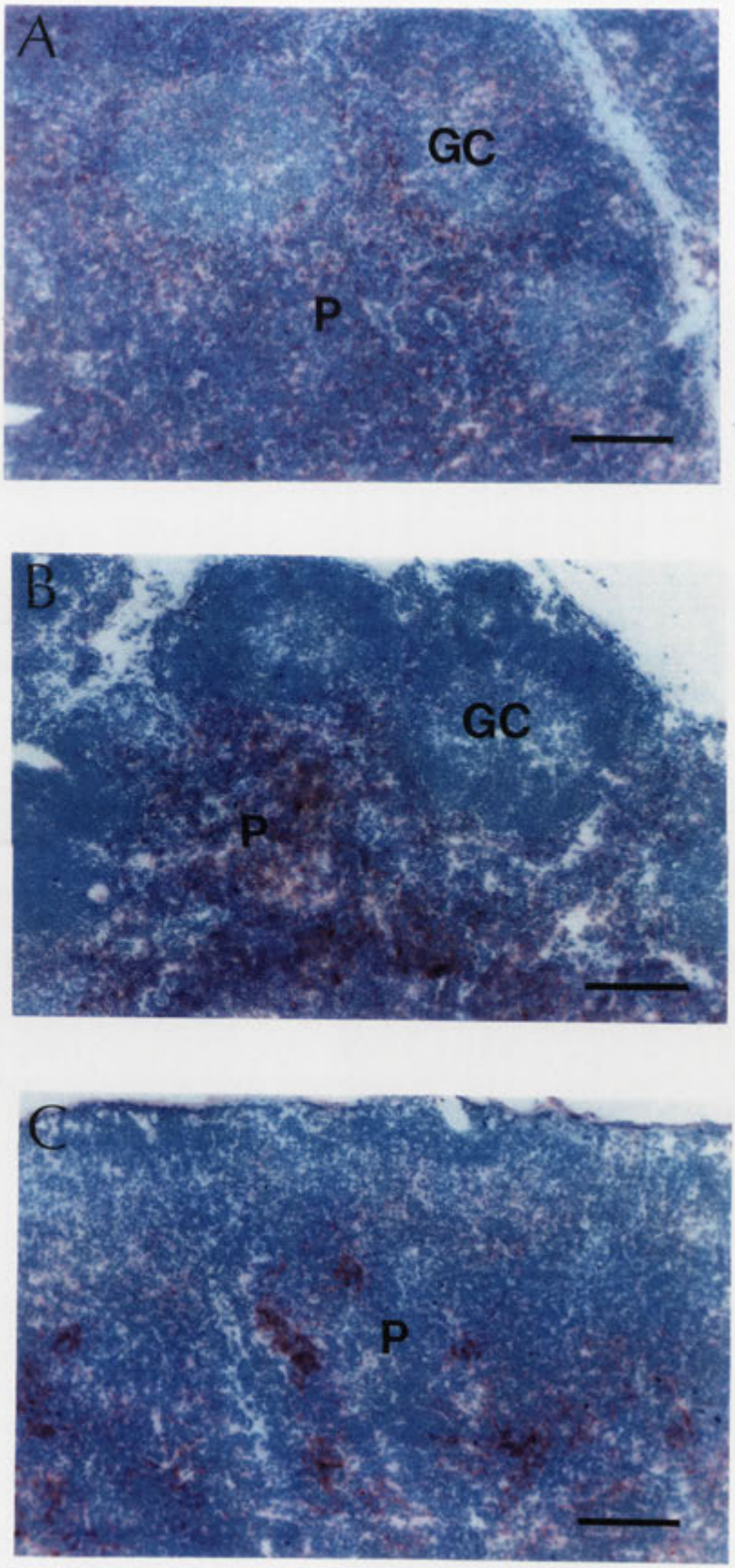
A
GC
P
B
GC
P
C
P

and serum. The distribution of Ig-μ^+ cells in the lymph nodes from Uriarra-infected laboratory rabbits was similar to that of uninfected lymph nodes. However, the number of Ig-μ^+ cells was usually less (Figure 4.38B). Similarly, in SLS-infected laboratory rabbits at 6dpi, the number of Ig-μ^+ cells in the paracortex or associated with B-cell dependent areas of lymph nodes was reduced compared to lymph nodes from uninfected rabbits. However, by 10dpi, diffuse areas of the paracortex contained numerous Ig-μ^+ cells (Figure 4.38C). These cells were distributed evenly throughout the paracortex and were not proximal to germinal centres.

4.3.4 The spleen

4.3.4.1 Uninfected spleen

The spleen from uninfected rabbits consisted of two general areas, the red and white pulp (Figure 4.39). The red pulp contained primarily RBCs, lymphocytes, granulocytes and plasma cells. The white pulp was lymphoid tissue and formed nodules surrounding branches of the splenic artery and vein (or periarteriolar lymphoid sheath; PALS). Many small follicles, and occasional germinal centres that had formed around a central arteriole, were observed within these nodules. The marginal zone surrounded the white pulp and was filled with large lymphocytes. The spleen pulp is surrounded by a capsule of dense connective tissue from which trabeculae projected into the pulp (Figure 4.39A). The capsule, trabeculae, accompanying reticular fibres and blood vessels constituted the connective architecture of the spleen.

4.3.4.2 Virus antigen and histopathological changes

The histopathology of the spleen can be considered using rabbits inoculated in either the foot or the thigh as both the timing of virus dissemination and virus growth in this tissue was similar for the two groups. Changes in the spleen following infection of rabbits with myxoma virus resembled, but were not as severe as, those described in the lymph nodes, and were the most variable of all the tissues described. These changes were apparent in the both the red and white pulp and included a general depletion of lymphocytes, the proliferation and degeneration of reticular and endothelial cells, and a

Figure 4.38: Immunolocalisation of cells expressing Ig-μ in the lymph nodes of laboratory rabbits. The binding of anti-Ig-μ was detected using an alkaline phosphatase-conjugated secondary antibody and fast red as a substrate. The presence of Ig-μ is shown in red. **(A)** Lymph node from an uninfected rabbit. Ig-μ was strongly expressed on cells associated with germinal centres. **(B)** Lymph node from a Uriarra-infected rabbit at 10dpi. The distribution of Ig-μ-positive cells throughout the paracortex and associated with germinal centres in the lymph nodes of these rabbits was similar to uninfected rabbits although the number of positive cells was generally less. **(C)** Lymph node from an SLS-infected laboratory rabbit. Ig-μ-positive cells were distributed throughout the lymph node paracortex and were not associated with well defined germinal centres. Bars represent 100μm. GC, germinal centre; P, paracortex.

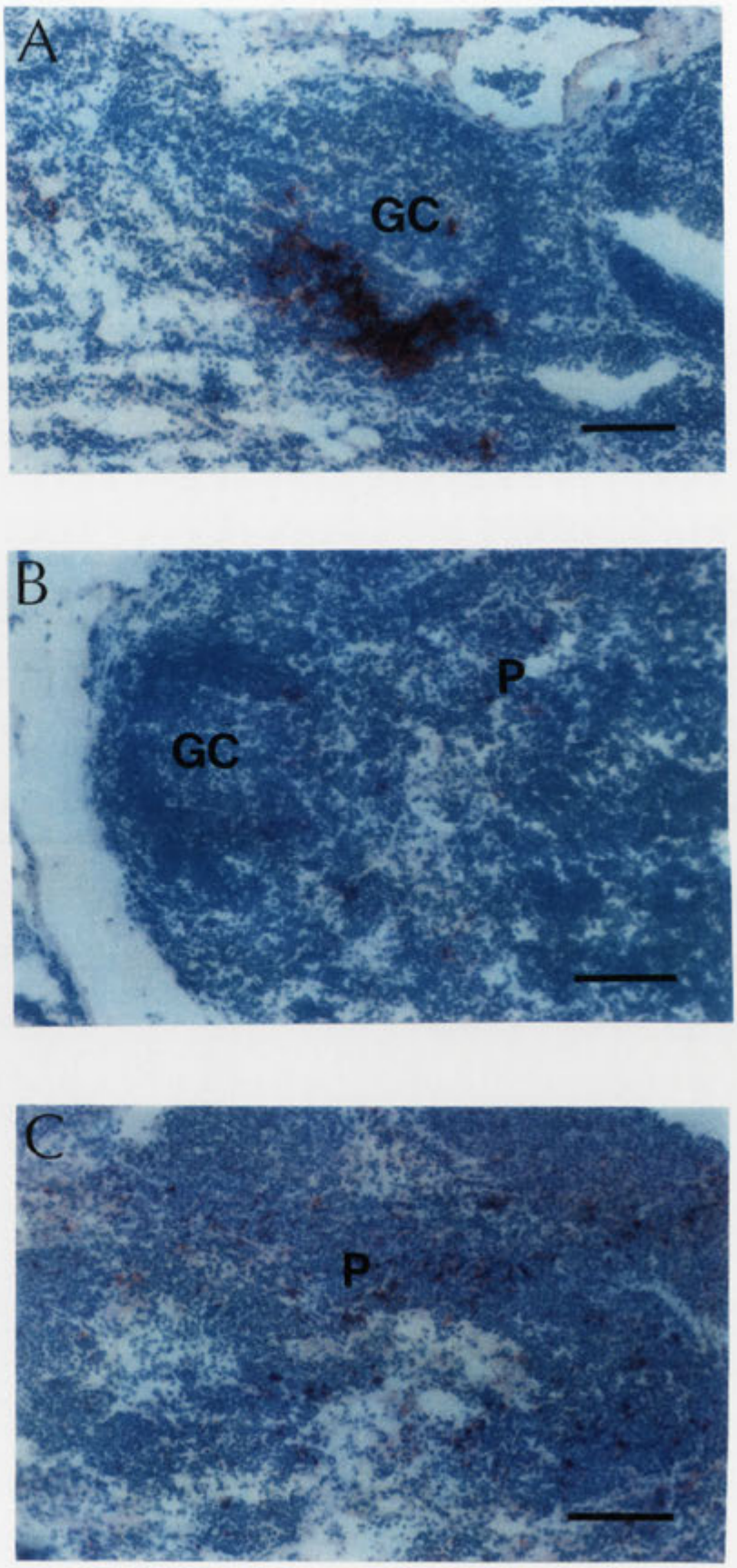
A
GC
B
P
GC
C
P

Figure 4.39: Histology of the spleen from an uninfected laboratory rabbit. **(A)** The spleen is divided into two main areas, the red pulp and the white pulp (lymphoid tissue). A nodule of white pulp is seen here in cross-section. The spleen is surrounded by the capsule (connective tissue). **(B)** The white pulp surrounds splenic arteries and in longitudinal section, appears as a sheath rather than as nodules. Bars represent 100μm. C, capsule; PALS, periarteriolar lymphoid sheath; RP, red pulp; WP, white pulp.

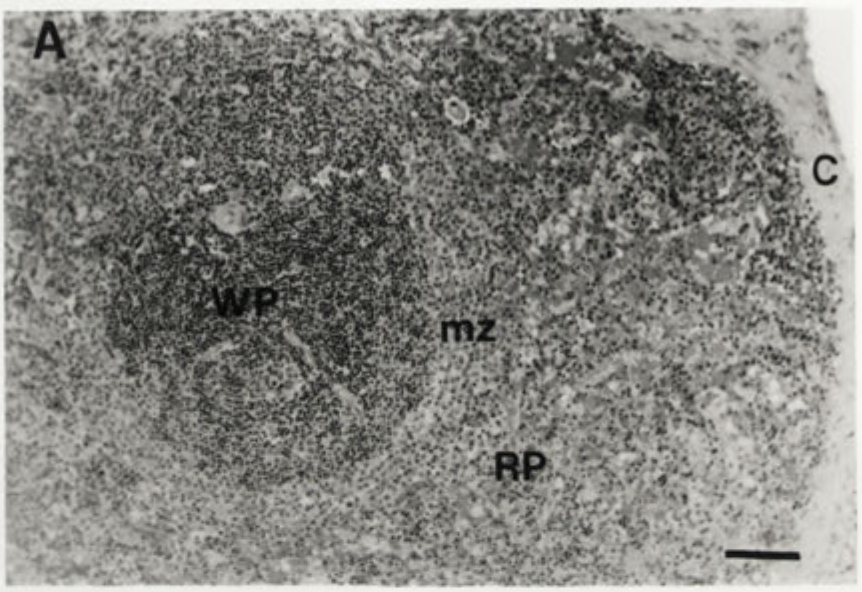
A
C
WP
mz
RP

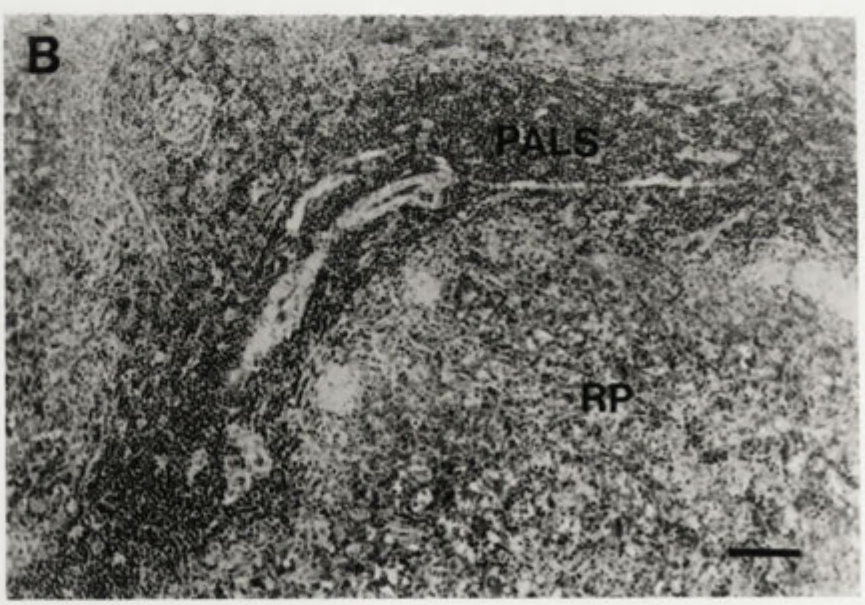
B
PALS
RP

limited influx of inflammatory cells. The enlargement of the spleen in SLS-infected laboratory rabbits described in Chapter 3 (see section 3.3.4.1) was probably due to the engorgement of the spleen with blood. Virus antigen was detected in the spleen following infection of laboratory rabbits at 6dpi with SLS (Figure 4.40A) and Uriarra (Figure 4.40B). In both cases, virus localised to the cytoplasm of lymphocytes within the white pulp. However, the number of infected cells detected was low. Virus was also present in clusters of mononuclear cells in the white pulp of SLS but not Uriarra-infected laboratory rabbits. Some of these cells were approximately 16µm in diameter and resembled macrophages (Figure 4.40C). Virus antigen was not detected in the spleen of wild rabbits infected with either Uriarra or SLS at any time. The histopathological changes in the spleen are described in sequence below.

4.3.4.2.1 Four days post infection of laboratory and wild rabbits with myxoma virus

Obvious changes in the spleens from laboratory rabbits infected with SLS were first observed at 4dpi in one of four infected rabbits (Figure 4.41A). This rabbit had the highest virus titre in the spleen of the four infected rabbits. Changes included a moderate hyperplasia of lymphocytes resulting in an increased area of the spleen occupied by the white pulp. The number of germinal centres had increased, and these contained an increased number of cells with apoptotic nuclei or with mitotic figures, particularly in the light zones. The reticular cells of the capsule appeared swollen, with foamy nuclei. There was an increase in the number of neutrophils in the red pulp directly under the capsule. Localised areas of the red pulp also contained swollen reticular cells that were proximal to areas of deposition of scanty extracellular fibrinous material. The spleens of the remaining three of the four infected rabbits examined showed few changes, and contained many small germinal centres with well defined zones in which numerous cells were undergoing mitotic division.

Changes were also observed in the spleen of Uriarra infected laboratory rabbits at 4dpi (Figure 4.41B). These included a moderate hyperplasia of lymphocytes in the white pulp, with cellular activity evident in newly forming germinal centres (nuclear fragments of apoptotic bodies and cells with mitotic figures) resulting in a general increase in the number of small lymphocytes within mantle zones. There was an increase in the numbers of neutrophils present in the red pulp, and the deposition of fibrinous material in small areas of red pulp.

Figure 4.40: Myxoma virus localisation in the spleen of laboratory rabbits at 6dpi. (**A**) Spleen from an SLS-infected laboratory rabbit. (**B**) Spleen from a Uriarra-infected laboratory rabbit. In both (**A**) and (**B**), virus was present in the cytoplasm of a small number of lymphocytes in the white pulp. Bars represent 170μm. (**C**) SLS also infected clusters of cells in the white pulp, including macrophage-like cells. Bar represents 20μm. RP, red pulp; WP, white pulp. Thin arrows indicate myxoma virus-infected lymphocytes, green arrow heads indicate cell nuclei in clusters of virus-infected cells.

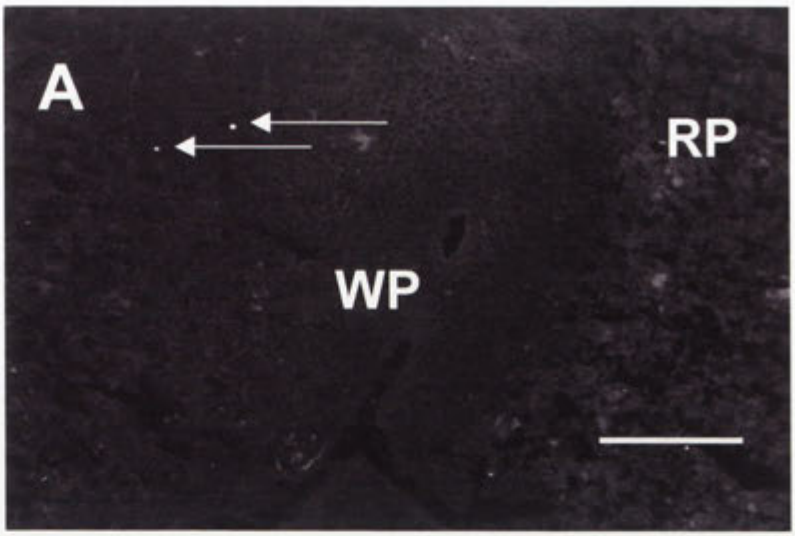
A
RP
WP

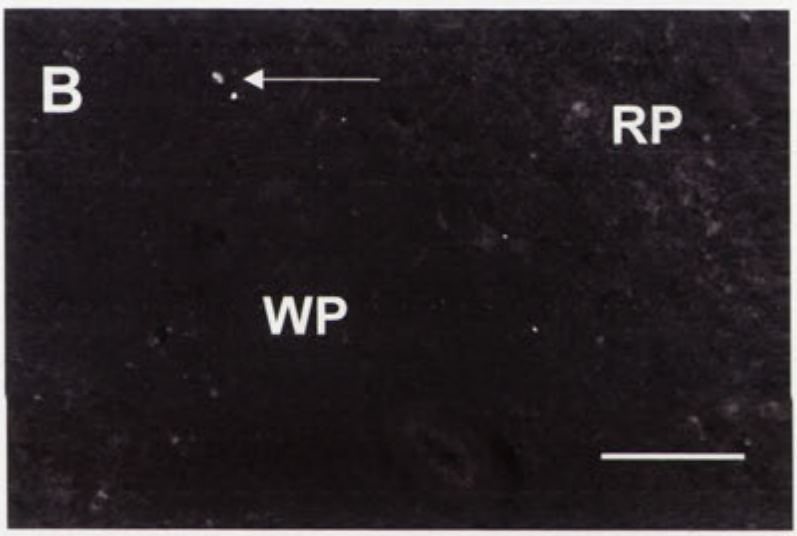
B
RP
WP

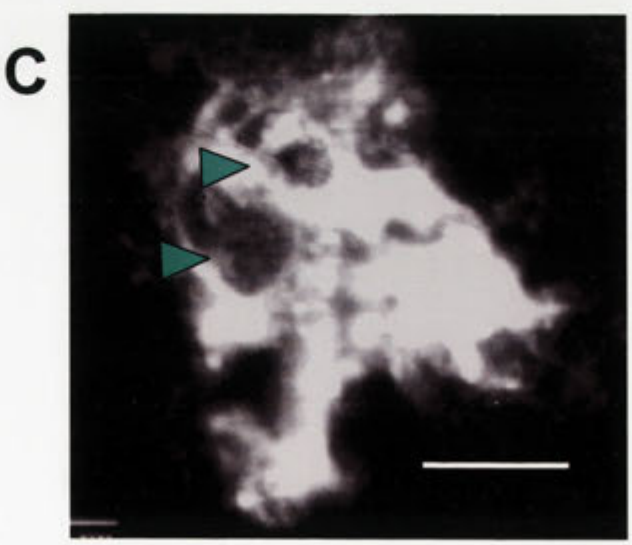
C

Figure 4.41: Histopathology of the spleen from laboratory rabbits at 4dpi (A) Spleen from an SLS-infected laboratory rabbit. There was a moderate hyperplasia of lymphocytes associated with germinal centres in the white pulp of this rabbit. (B) Spleen from a Uriarra-infected laboratory rabbit. The spleen of this rabbit had large, well defined germinal centres. Bars represent 100μm. GC, germinal centre.

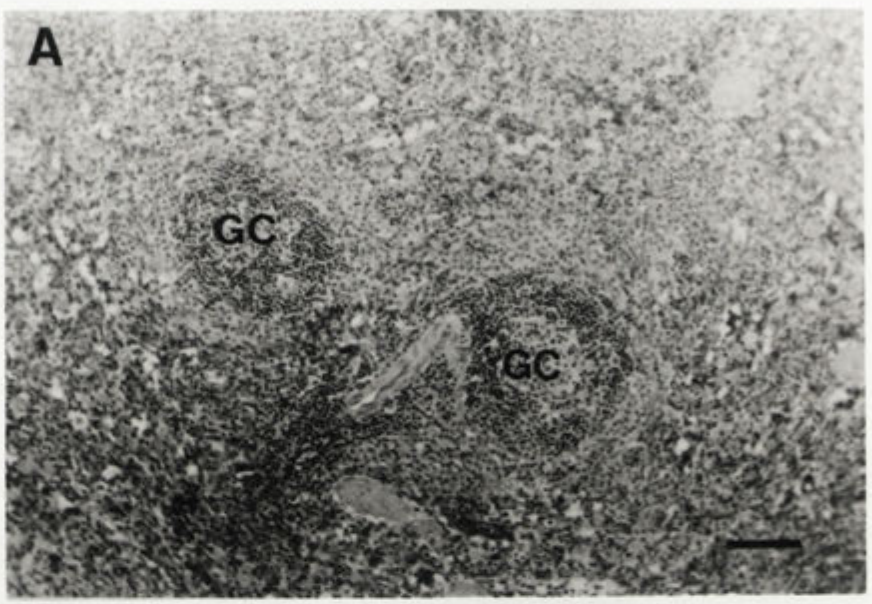
A
GC
GC

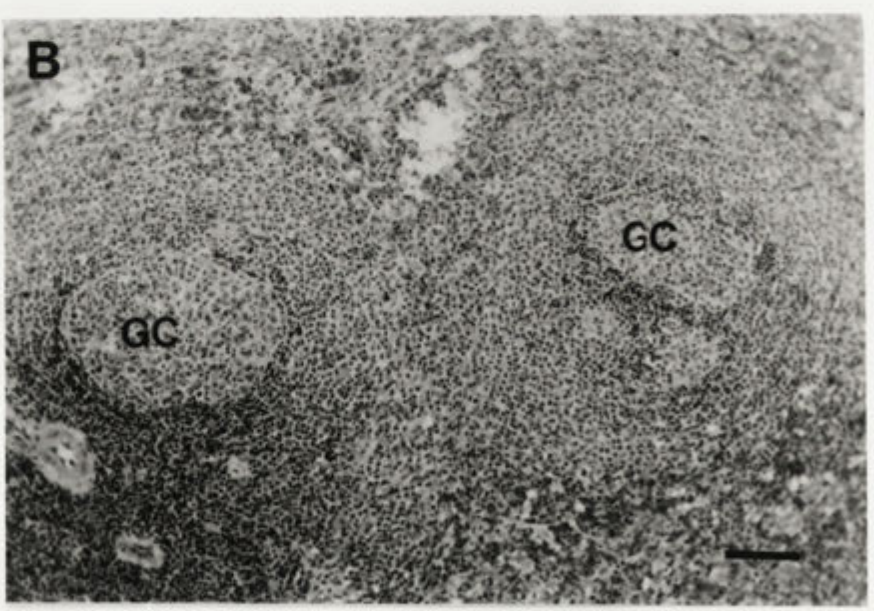
B
GC
GC

4.3.4.2.2 Six days post infection of laboratory and wild rabbits with myxoma virus

At 6dpi of both laboratory and wild rabbits with SLS, the red pulp stained very heavily red due to an engorgement of the spleen with RBCs (Figure 4.42A). There was a reduced density of lymphocytes in the red pulp, which may have been due to a depletion of these cells, or to the increased space between them resulting from the increase in RBCs. The cytoplasm of a number of macrophages in the red pulp contained RBCs, 3-5 neutrophils and/or a number of small, dark staining nuclear fragments. Neutrophils were observed directly under the capsule and infiltrating into the red pulp but not in the white pulp. There was a mild hyperplasia of small lymphocytes in the white pulp but no formation of germinal centres. Localised groups of lymphocytes within the white pulp had karryorhetic nuclei which stained darkly at the periphery.

At 6dpi of laboratory rabbits with Uriarra (Figure 4.42B), the spleen from one of four rabbits showed the severest changes observed at any time after infection with either SLS or Uriarra. These included a general reduction of small lymphocytes from the white pulp such that much of the white pulp resembled marginal zone. In the red pulp adjacent to the white pulp, there was an increase in the number of neutrophils and nuclear fragments present, an increase in the deposition of extracellular foamy material and the proliferation of reticulum cells. However, the spleens from the remaining three animals and wild rabbits infected with Uriarra at 6dpi, showed a moderate number of small lymphocytes present within the zones of germinal centres, although these zones were not sharply defined (Figure 4.42C). These spleens contained small, localised areas in which there were apoptotic bodies and neutrophils, and contained many macrophages with cytoplasms full of these cells and cell fragments.

4.3.4.2.3 Ten days post infection of laboratory and wild rabbits with myxoma virus

By 10dpi of laboratory rabbits with SLS, the spleen was engorged with RBCs. The cellular membranes of RBCs were not well defined and hence the cells appeared liquefied. Lymphocytes had been depleted from the white pulp such that the red and white pulps were not well defined (Figure 4.43A) and the majority of white pulp resembled marginal zone (Figure 4.43B). Polymorphonuclear cells were present in the red pulp at the edge of, and infiltrating into, marginal zones. The reticular cells in these areas were swollen, had a foamy cytoplasm and had increased in number, with the

Figure 4.42: Histopathology of the spleen from rabbits at 6dpi with myxoma virus. (**A**) Spleen from an SLS-infected laboratory rabbit. The dark staining of the white pulp was due to the engorgement of the spleen with red blood cells. Note that besides the dense staining of red blood cells, the white pulp is not well defined. (**B**) Spleen from a Uriarra-infected laboratory rabbit. The spleen of this rabbit had the most severe pathology of the all Uriarra-infected laboratory rabbits. The white pulp was engorged with red blood cells, and was poorly defined. (**C**) Spleen from a second Uriarra-infected laboratory rabbit. The spleen of this rabbit had large, well defined germinal centres. Bars represent 100μm. GC, germinal centre, RP, red pulp; WP, white pulp.

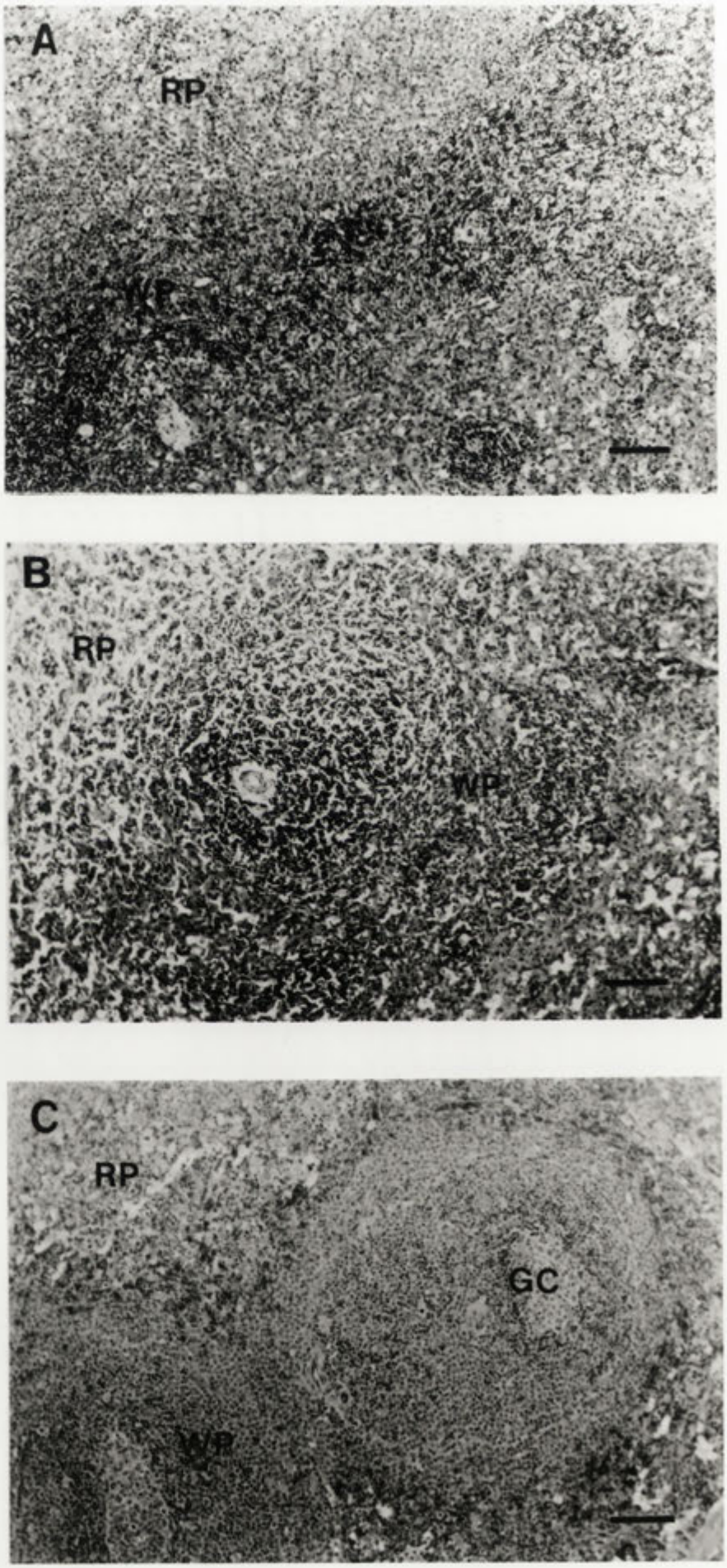
A
RP
WP
B
RP
WP
C
RP
GC
WP

Figure 4.43: Histopathology of the spleen from rabbits at 10dpi with myxoma virus. (**A**) and (**B**) Spleens from SLS-infected laboratory rabbits. The red and white pulp are poorly defined. This was due to the depletion of lymphocytes from both areas. (**C**) Spleen from an SLS-infected wild rabbit containing a large germinal centre. (**D**) The spleen of a Uriarra-infected laboratory rabbit. The red and white pulps are well defined and there was no evidence of lymphocyte depletion from these areas. Bars represent 100μm. GC, germinal centre, RP, red pulp; WP, white pulp.

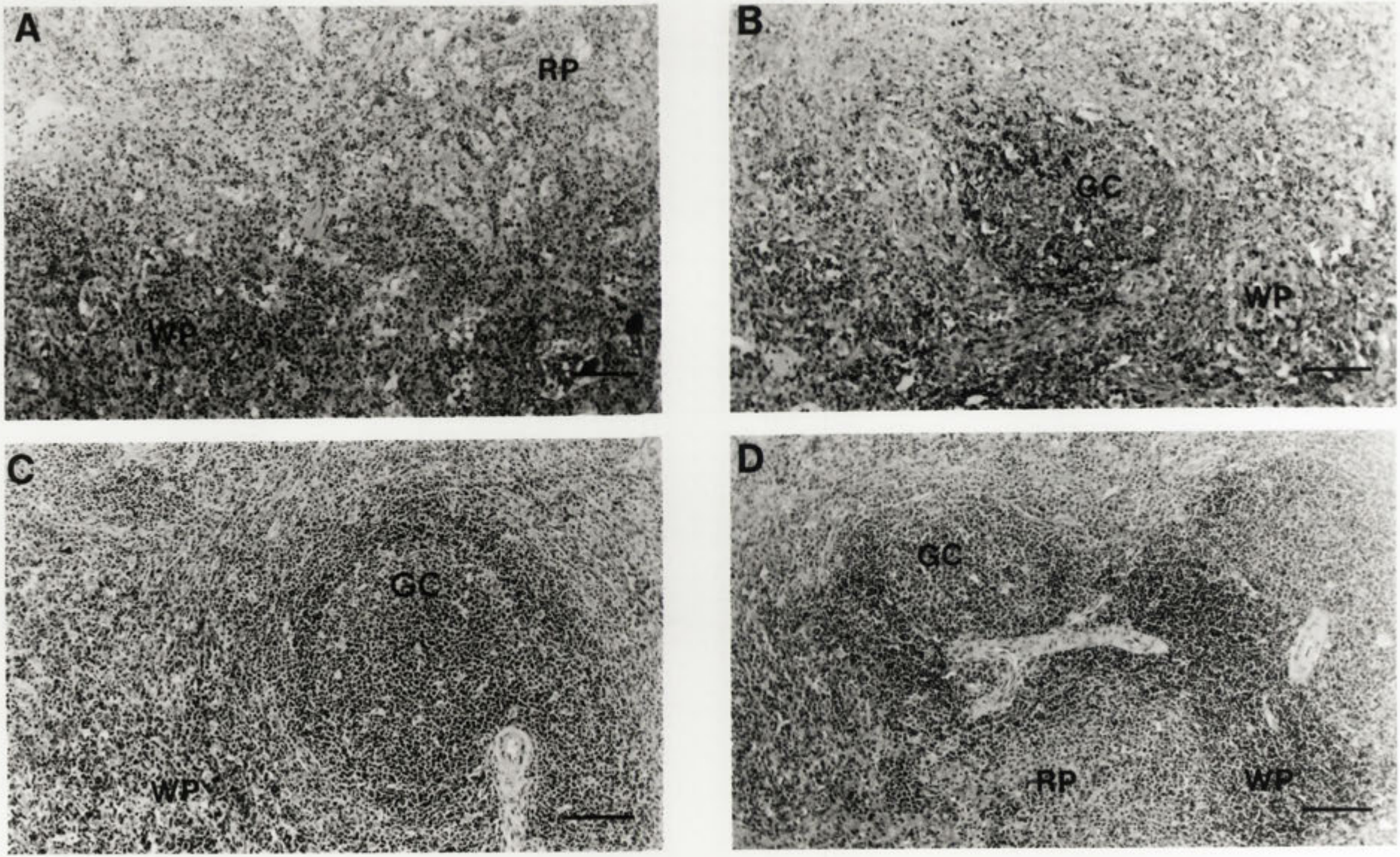
A
RP
WP
B
GC
WP
C
GC
WP
D
GC
RP
WP

spaces between cells expanded and taking on a vesicular appearance. These changes in reticular cells were also evident directly under the capsule in the red pulp. Localised areas of the capsule and trabeculae were thickened; the cells of the latter had increased in number and were swollen. The endothelial cells of small blood vessels were also swollen, with the cellular and nuclear membranes distended. Amongst the reticular fibres, there were a number of different cell types. Many large cells with a pale staining hypertrophic nucleus and a foamy cytoplasm were present in these areas. These cells resembled the myxoma cells described in the lymph nodes of SLS infected laboratory rabbits, but did not appear as stellate in shape. Other cells of the reticulum were phagocytic, containing nuclear fragments or neutrophils within their cytoplasm. A third cell type within the reticulum was giant cells that had 2-3 large nuclei.

In wild rabbits infected with SLS at 10dpi, some depletion of lymphocytes was observed from the white pulp and neutrophils had infiltrated into the red pulp of the spleen. However, the red and white pulp were well defined and germinal centres were prominent (Figure 4.43C). By 10dpi, the spleens from Uriarra-infected laboratory rabbits contained multiple large germinal centres, with no evidence of lymphocyte depletion from the white pulp (Figure 4.43D).

4.3.4.2.4 Fifteen and twenty days post infection of laboratory and wild rabbits with myxoma virus.

At 15dpi of wild rabbits with SLS, blood vessels were surrounded by cuffs of lymphocytes and at 15 and 20dpi, there was a general increase in small lymphocytes in the white pulp and the formation of well defined germinal centres compared to 10dpi (Figure 4.44A). At 20dpi, thick strands of eosin-staining connective tissue, resembling hyaline tissue, were present in between the mantle zones of germinal centres and the marginal zone (Figure 4.44B). At 15dpi and 20dpi of laboratory rabbits with Uriarra, a general expansion of the splenic area occupied by white pulp was evident containing many small lymphocytes, small follicles and well defined germinal centres (Figure 4.44C).

Figure 4.44: Histopathology of the spleen from rabbits at 15 and 20dpi with myxoma virus. (**A**) Spleen from an SLS-infected wild rabbit at 15dpi. The white pulp was densely populated with small lymphocytes. (**B**) Spleen from an SLS-infected wild rabbit at 20dpi. The white pulp contained thick strands of eosin-staining connective tissue in between the mantle zones of germinal centres and the marginal zone. (**C**) Spleen from a Uriarra-infected laboratory rabbit at 15dpi showing well defined areas of red and white pulp. Bars represent 100μm. GC, germinal centre; RP, red pup; WP, white pulp.

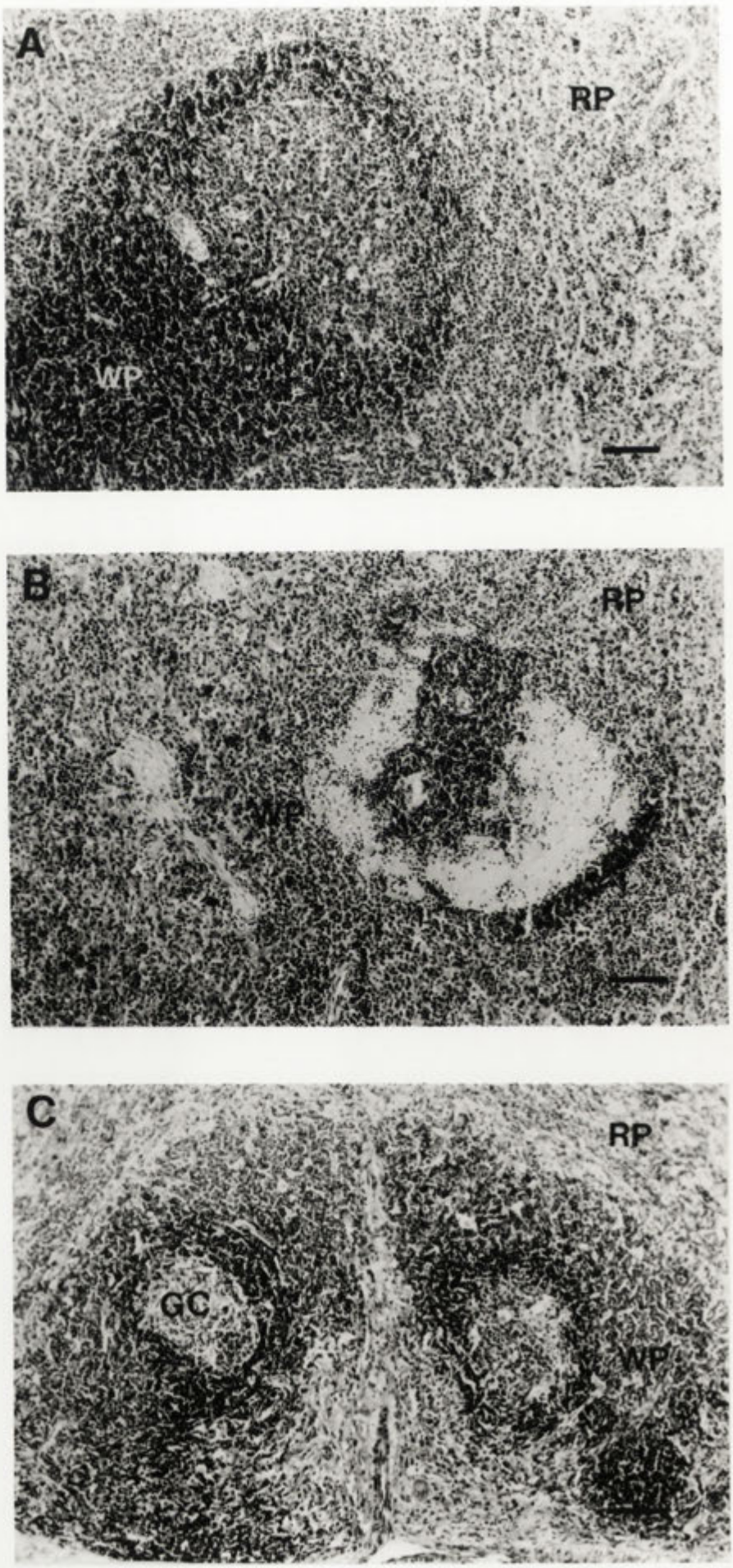
A
RP
WP
B
RP
WP
C
RP
GC
WP

4.4 Discussion

To further investigate the pathogenesis of virulent and attenuated strains of myxoma virus in infected laboratory and wild rabbits, the histopathology and cellular localisation of virus was examined in the principal target organs, the skin and lymphoid tissues. The portions of tissue used in this study were from the same tissues for which virus titres were determined in Chapter 3. Hence, for each individual rabbit killed at each time point post infection, we know which tissues the virus is replicating in, how much virus is present, what cells the virus is replicating in and what pathological changes have occurred. Furthermore, we can investigate between-virus differences by examining how each rabbit handles a virulent or an attenuated strain of virus when the differences observed depend on the virulence of the virus. In the same manner, between-rabbit differences can be examined where differences between the response of laboratory and wild rabbits to SLS or Uriarra infection depends on the evolved genetic resistance of the rabbit. The key aspects of virus pathogenesis derived from these results are discussed below for each set of infected rabbits.

Following intradermal inoculation of SLS into the hind foot of laboratory rabbits, virus was present at 24 hpi MHC II positive dendritic cells in the dermis. SLS was also present at 24hpi in the paracortex of the draining lymph node, in lymphocytes and large mononuclear, MHC II positive cells. This suggests that the early transport of virus from the primary inoculation site in the skin to the draining lymph node is likely to occur in infected MHC II positive dendritic cells. Virus that is not within cells may also drain from the skin to the draining lymph node either as free virus or associated with cell debris. This would be difficult to visualise in tissue sections by immunofluorescence, although weak staining of viral antigen that was not cell-associated was observed by 2dpi in continuous lines in the periphery of the lymph node cortex and spanning the paracortex. Whether this consists of infectious virus has not been determined. However, similar continuous lines of virus that localised to the cytoplasm of lymphocytes were observed early in infection. This could indicate that lymphocytes in the paracortex are being infected by cell-free virus draining through the subcapsular sinus.

At 2 and 4dpi, when the titre of virus in the skin was increasing, the dermis at the primary inoculation site contained numerous SLS-infected MHC II positive cells. At

4dpi in the lymph node draining the inoculation site in the foot, SLS had infected lymphocytes in the T-cell dependent paracortex, but had infected few lymphocytes associated with follicles or germinal centres. This generalised infection of lymphocytes in the paracortex of the popliteal lymph node was not observed until 6dpi following inoculation into the thigh. This indicates that the hind foot inoculation site was indeed the better site of the two for the early examination of myxoma virus interactions with the lymph nodes.

SLS was visualised in the contralateral lymph node of infected laboratory rabbits by 4dpi, and similarly to the draining lymph node, was replicating in lymphocytes of the paracortex. Infection of both the draining and contralateral lymph nodes in laboratory rabbits resulted in a lack of germinal centre development and the depletion of lymphocytes from nodes, first observed as a reduced number of lymphocytes at the periphery of the cortex by 4dpi. Depletion of lymphocytes from lymph nodes and the associated pathologic changes were consistent with the descriptions of Hurst (1937a) for infection of laboratory rabbits with SLS. This depletion progressed directionally inwards towards the centre of the node, involving both T- and B-cell populations. In areas depleted of lymphocytes, the reticular cells and the endothelial cells of small blood vessels were swollen and had increased in number, and neutrophils and large stellate myxoma cells were abundant. Despite the extensive depletion of lymphocytes, in which myxoma virus replicates, from both the draining and contralateral lymph nodes from 6dpi, the titres of SLS in these tissues were high. At this time, virus replication was predominantly in clusters of abnormally large reticular cells situated near remnants of germinal centres, and in cells of the lymph node capsule. Some depletion of lymphocytes also occurred in the spleen of SLS-infected laboratory rabbits, despite the moderate titres of virus in the spleen and the observation of virus antigen in only a small number of cells.

By 4dpi, SLS was present in the distal skin of infected laboratory rabbits. Similar to infection of skin at the primary inoculation site, SLS was first observed in MHC II positive cells in the dermis. At 6 and 10dpi, when SLS titres in the primary lesion and distal skin were the highest, the majority of virus was in the epidermis of the skin at both sites. Large numbers of inflammatory cells, predominantly neutrophils, had infiltrated the lower dermis at these sites, but did not traffic to the upper dermis proximal to the epidermis where virus replication was concentrated. Pathological

changes had occurred in the endothelial cells of dermal blood vessels and myxoma cells were abundant in the dermis, but virus antigen was visualised only very rarely in either. This observation does not support the suggestion of Hurst (1937a) that virus replication in the endothelium was responsible for pathology observed in the blood vessel walls and budding of myxoma cells from the endothelium.

Uriarra replication in the skin of laboratory rabbits was similar to that described for SLS-infected laboratory rabbits. These observations are consistent with the titres of SLS and Uriarra in the skin, which were similar to each other over the first ten days of infection. However, in contrast to SLS-infected primary lesions, inflammatory cells in the dermis of Uriarra-infected primary lesions were predominantly lymphocytes and trafficked throughout the dermis, aggregating at the dermal/epidermal junction. Changes in the cells of the epidermal stratum basale associated with virus replication were similar to SLS-infected laboratory rabbits, but their progression was generally delayed. Initial changes in the endothelium of dermal blood vessels of Uriarra-infected laboratory rabbits were also similar to SLS-infected laboratory rabbits, but did not progress as rapidly or severely, and myxoma cells were not a prominent cell type in the dermis of Uriarra-infected rabbits. In addition, Uriarra was first detected in the distal skin of laboratory rabbits at 6dpi, by immunofluorescence and plaque assay, which was delayed compared to laboratory rabbits infected with SLS. By 15 and 20dpi with Uriarra, virus replication was restricted to localised areas of the stratum basale in both the primary inoculation and distal skin sites.

The draining lymph node of laboratory rabbits infected with Uriarra was similar to that of SLS in the first six days of infection with virus, localising to the cytoplasm of infected lymphocytes and macrophages in the lymph node paracortex. However Uriarra was not present in reticular cells or cells of the lymph node capsule and by 10dpi, was present only in low numbers of lymphocytes. Uriarra was first visualised in the contralateral lymph node at 4dpi, with a similar distribution of replication to the draining lymph node, although fewer lymphocytes were infected and greater expanses of lymph node tissue remained virus-free. Mild depletion of lymphocytes in the draining lymph node occurred in the first six days of infection, particularly in the interfollicular regions. However, unlike SLS infection, numerous germinal centres had developed in lymph nodes by this time and infection was not associated with the infiltration of masses of neutrophils into the node, or with the extensive proliferation of

reticular cells. Lymphocyte depletion did not occur in the contralateral lymph node or the spleen of infected rabbits. Despite the high numbers of follicles, the number of Ig-μ+)cells in the lymph nodes was smaller in Uriarra-infected rabbits than in SLS-infected rabbits. In addition, the production of neutralising antibody and virus-specific IgG measured in Chapters 2 and 3 was slower in Uriarra-infected laboratory rabbits. Uriarra was cleared from the lymph nodes of laboratory rabbits by 15dpi as it was not detected by immunofluorescence or plaque assay at 15 or 20dpi.

The cellular localisation of SLS and Uriarra in the primary inoculation site of wild rabbits, and the pathological changes associated with virus replication, were similar to that of Uriarra-infected laboratory rabbits over the 20 days of the experiment. However, wild rabbits had a greater influx of inflammatory lymphocytes into the dermis of the primary lesion than any myxoma virus-infected laboratory rabbit. In particular, lymphocytes were densely aggregated at the margins of the lesion by 15dpi. Virus was present at 15 and 20dpi in mitotically active cells of the stratum basale directly underlying areas of damaged epidermis, and in the sheaths of hair follicles, but was not observed outside the perimeter formed by the dense aggregates of inflammatory cells. The mononuclear infiltrate into the dermis of wild rabbits infected with myxoma virus, and in particular those infected with SLS, involved more cells and was distributed throughout more of the dermis, proximal to virus replication, than in infected laboratory rabbits. This was also the case in the distal skin site of wild rabbits, in which SLS was first detected at 4dpi and Uriarra at 15dpi. The inflammatory response to myxoma virus infection in wild rabbits may thus be important in the local control of virus spread in the skin, and the restriction of the size of the primary lesion.

SLS had drained to the popliteal lymph node from the primary inoculation site of wild rabbits by 24 hours post infection. However, the appearance of Uriarra was delayed, as the first observation of virus in the draining lymph node was at 2dpi. Similarly to SLS-infection of laboratory rabbits, SLS infected the lymphocytes in the paracortex of the draining lymph node and cells of the lymph node capsule, and caused extensive depletion of lymphocytes from this node. However, the titres of virus in the draining lymph node of SLS-infected wild rabbits indicated that this tissue was involved in control of virus replication by resistant rabbits. Consistent with this, depletion of lymphocytes generally remained restricted to localised areas within lymph nodes. This lymphocyte depletion was associated with proliferation of reticular cells, but not with

severe changes in the endothelium of blood vessels, the extensive infiltration of neutrophils, or the appearance of myxoma cells in the tissue. More importantly, this depletion of lymphocytes did not occur in the contralateral lymph node of SLS-infected wild rabbits and although virus reached the contralateral lymph node, virus replication within this node was shown by plaque assay and immunofluorescence to be reduced compared to that in infected laboratory rabbits. By 15dpi, regions of the draining lymph node paracortex that contained high numbers of abnormally large reticular cells, a pathological change that was associated with the depletion of lymphocytes, appeared repopulated with small lymphocytes, and germinal centres had developed, implying immune activation within the nodes.

4.4.1 How does resistance operate?

By examining virulent and attenuated myxoma virus, where differences in pathogenesis are attributable to the virulence of the virus, and myxoma virus-infected laboratory and wild rabbits, where differences in response to infection are attributable to the evolved genetic resistance of the rabbit, we can gain clear insights into how resistance of the host operates.

4.4.1.1 The inflammatory response to infection with myxoma virus

Both virulent and attenuated myxoma virus targeted the skin and lymph nodes as major sites of replication in both laboratory and wild rabbits. However, the inflammatory response to virus replication in these tissues was markedly different between SLS-infected laboratory rabbits, and Uriarra-infected laboratory rabbits or SLS-infected wild rabbits. In the Leporid species of the Americas in which myxoma virus evolved, virus replicates in the skin at the primary inoculation site but apparently does not disseminate to secondary skin sites. Hence, virus replication and persistence in the primary inoculation site is crucial for transmission. Not surprisingly, myxoma virus has evolved proteins that bind and inhibit the action of pro-inflammatory cytokines such as TNF, interferons and chemokines, and are thought to disrupt local cytokine gradients to suppress the mobilisation of an effective inflammatory response to infection *in vivo* (Graham *et al.*, 1997; Graham *et al.*, 1992; Lalani *et al.*, 1997; Lalani *et al.*, 1998; Macen *et al.*, 1993; McFadden and Barry, 1998; McFadden *et al.*, 1997; Mossman *et*

al., 1995a; Opgenorth *et al.*, 1992; Schreiber and McFadden, 1994; Upton *et al.*, 1992).

In all rabbits infected with myxoma virus, the inflammatory response in the skin was induced by 4dpi. However, in SLS-infected laboratory rabbits, this response consisted predominantly of neutrophils deep in the skin, away from the sites of virus replication in the upper dermis and epidermis. This was in contrast to the inflammatory response of Uriarra-infected laboratory rabbits, or of wild rabbits infected with either SLS or Uriarra, in which lymphocytes predominated in the inflammatory response and were mainly in tissue proximal to virus replication. One of the most important families of cytokines involved in the orchestration of the inflammatory response are chemokines. The T1 protein encoded by myxoma virus is secreted from infected cells and binds chemokines from both the CC- and CXC-subfamilies (Graham *et al.*, 1997). T1 specifically inhibits the CC-mediated chemotaxis of monocytes *in vitro* but does not inhibit CXC-mediated chemotaxis of neutrophils (Lalani *et al.*, 1998). The inhibition of the infiltration of mononuclear cells but not neutrophils is consistent with the histopathology of the primary inoculation site of the skin of SLS-infected laboratory rabbits. CC-chemokines are involved in the attraction of T- and B- lymphocytes, NK cells and dendritic cells into the site of infection (Luster, 1998). The differences in inflammatory responses suggests that Uriarra does not modulate the inflammatory response of infected rabbits in the same way as SLS, and that the wild rabbit is able to overcome at least some SLS-induced modulation of inflammatory responses.

The inflammatory response to myxoma virus at the primary inoculation site of SLS-infected wild rabbits was not sufficient to prevent and control virus replication in the skin or prevent the dissemination of virus to the draining lymph node. However, the spread of myxoma virus to the draining lymph node and other distal tissues in wild rabbits was not associated with efficient virus replication in these tissues or the death of the infected host. The control of virus replication that was observed by both immunofluorescence and plaque assay compared to laboratory rabbits is likely to involve both the innate and adaptive immune responses, as has been shown for the poxvirus, ectromelia virus (Karupiah *et al.*, 1993a; 1993b; O'Neill and Blanden, 1983; Delano and Brownstein, 1995; Karupiah *et al.*, 1996; Ramshaw *et al.*, 1997). In Chapter 2, the responses of lymphocytes from lymph nodes of SLS-infected laboratory rabbits to stimulation with T-cell mitogens were suppressed by 4dpi, which suggests that SLS is capable of supressing T-cell function *in vivo*. These cells are critical in

developing an effective adaptive immune response. The modulation of the inflammatory response generated in the skin by myxoma virus, the early suppression of T-cell responses in the draining lymph node and the ability of wild rabbits to overcome SLS-induced immune modulation are potentially linked. The major target of early virus replication following infection of either laboratory or wild rabbits was dendritic cells in the skin. These cells are crucial in the activation of T-cells and the development of the adaptive immune response, and thus are a potential link between inflammation, immune suppression and host resistance.

4.4.1.2 Role of dendritic cells in myxoma virus pathogenesis and host resistance.

From the descriptions of myxoma virus pathogenesis above, it is likely that dendritic cells in the skin are important in the transport of virus from the primary inoculation site in the skin to the draining lymph node. Dendritic cells have been implicated in this role following flavivirus infection of mice (Johnston *et al.*, 1996), and pulmonary macrophages have been shown to transport the ectromelia virus to draining lymph node from the lung following infection of mice with aerosol (Rivers, 1930). However, this is the first demonstration of the potential importance of dendritic cells in myxoma virus infection of rabbits.

Dendritic cells in the dermis of the primary inoculation site in the skin and mononuclear cells in the paracortex of the draining lymph node were infected by myxoma virus at 24 hpi in laboratory rabbits infected with SLS or Uriarra, and in wild rabbits infected with SLS. This suggests that genetic resistance is not predominantly mediated by a block in the initial replication of virus in dendritic cells. Similarly virus attenuation did not affect replication in dendritic cells, but it did stimulate an entirely different inflammatory response. Interestingly, in wild rabbits infected with attenuated myxoma virus, the transport of virus from the skin to the draining lymph node was delayed compared to all other infections. This suggests that the role of dendritic cells in myxoma virus pathogenesis may be different depending on the virulence of the virus and the resistance of the host, but that these differences are difficult to measure using the relatively insensitive techniques of immunolocalisation or plaque assay unless host resistance and virus attenuation are combined. It is thus likely that skin dendritic cells have a role in virus replication and transport. It is also interesting to speculate that suppression of the inflammatory response may be a direct effect of SLS on dendritic cells in laboratory rabbits.

Intradermal inoculation of mice with vaccinia virus resulted in an increased number of Langerhans cells (skin dendritic cells). This increase was greater in mice infected with a virulent strain of virus than in mice infected with an avirulent strain (Sprecher and Becker, 1987). One interpretation of this is that infection with virulent virus results in an increase in these cells in the skin by the host to combat infection. The virulent virus evokes a stronger response, which may be a response by the host to perceived danger. An alternative interpretation is that the virus upregulates dendritic cells in the skin as target cells and that virulent virus is able to deviate the immune response elicited by infected dendritic cells to the hosts detriment. The local depletion of Langerhans cells by steroid treatment enhanced the lethality of virulent but not avirulent vaccinia virus (Becker and Sprecher, 1989), which supports the former interpretation. However, the actual mechanism of myxoma virus pathogenesis may lie in between these interpretations as infection of rabbits with myxoma virus is more lethal than vaccinia virus-infection of mice. The host may upregulate the number of dendritic cells in the skin in response to myxoma virus infection, and this upregulation may be greater in response to infection with virulent virus. Both virulent and attenuated viruses replicate in these cells, but the virulent virus is able to modulate their response to a greater extent than the attenuated virus. Following contact with antigen in the skin, Langerhans cells migrate to lymph nodes where they are thought to have a pivotal role in the activation of lymphocytes (Banchereau and Steinman, 1998). The infection of these cells, and the early interactions between infected cells and T-lymphocytes in the draining lymph node, is thus potentially important in the early activation of T-cell dependent responses of infected rabbits.

4.4.2 Replication of myxoma virus in lymphocytes

Replication of myxoma virus in lymph nodes occurred predominantly in lymphocytes of the T-cell dependent paracortex. *In vitro*, myxoma virus infects 100% of RL5 cells, a rabbit CD4+ T cell line (Cartledge, 1995). These results suggest that T-cells are a major target of virus replication in the lymph nodes. Early virus replication in lymph node was visualised as continuous lines of virus-infected cells spanning the paracortex and in groups of lymphocytes immediately adjacent to each other. It is possible that infection of lymphocytes in the nodes requires cell-to-cell contact, and may imply a role for extracellular enveloped virus (EEV) budding from the surface of infected cells to infect adjacent cells, which has been demonstrated as important in the dissemination of

vaccinia virus between cells (Payne, 1980; Vanderplasschen *et al.*, 1997). Lymphocyte depletion was an important aspect of pathology of the lymphoid tissue in both laboratory and wild rabbits infected with SLS. Lymphocyte depletion will almost certainly affect local immune responses to infection, and virus replication in T-cells is likely to be critical in the depletion of lymphocytes following infection with myxoma virus, and in suppressed T-cell responses observed in SLS-infected laboratory rabbits.

In vitro, replication of virulent myxoma virus in lymphocytes does not cause cell death (Macen *et al.*, 1996b; Strayer *et al.*, 1985). At least four proteins encoded by myxoma virus are known to inhibit apoptosis of infected lymphocytes (Barry *et al.*, 1997; Macen *et al.*, 1996b; Mossman *et al.*, 1996a; Schreiber *et al.*, 1997). Deletion of any one of these proteins induces apoptosis in infected lymphocytes. As Uriarra replicates to similar titres to SLS in RL-5 cells and does not induce apoptosis, all of these proteins are obviously functioning (P.J. Kerr, unpublished). However, it is not known if lymphocyte depletion and/or immune suppression are direct consequences of virus replication in lymphocytes *in vivo*, or if indirect mechanisms of cell death are operating. Although both SLS and Uriarra induced depletion of lymphocytes from the lymph nodes, laboratory rabbits infected with Uriarra and wild rabbits infected with SLS were able to restrict the loss of lymphocytes in the draining lymph node and control the depletion in the contralateral lymph node. In both cases this was associated with control of virus replication.

Following replication of myxoma virus in the draining lymph node, systemic dissemination of myxoma virus occurs in infected peripheral WBC (Fenner and Woodroofe, 1953). This implies that initiation of virus replication in distal tissues occurs following the migration of infected WBC into tissues. Alternatively, it has been suggested that virus growth across the endothelium may be important for virus invasion of immune privileged sites, such as the central nervous system (CNS) and the testis into which diapedisis, and thus invasion by infected leucocytes, may be limited (Mims, 1964). Hurst (1937a) speculated that virulent myxoma virus replicated in the endothelial cells of blood vessels. However, virus antigen was rarely observed in endothelial cells of blood vessels in the skin and lymph nodes, although massive proliferation of endothelial and reticular cells occurred following infection of laboratory rabbits with SLS. This was consistent with the descriptions of Hurst (1937). Hence, the

main mode of myxoma virus dissemination throughout the rabbit is likely to be in infected leucocytes.

Myxoma virus infected small numbers of lymphocytes in the spleen of rabbits which correlates with the lower virus titres recorded in this organ compared to the skin and lymph nodes. However, infection of laboratory rabbits with SLS resulted in a lack of germinal centre formation in the spleen as well as some depletion of lymphocytes and the swelling and increase in number of reticular cells. The pathology in the spleen of laboratory rabbits when SLS titres were relatively low may indicate a generalised systemic suppression of the host immune response. However, the spleen does not appear to be a major site of SLS replication or virus-induced pathology. This is similar to the descriptions of myxoma virus-induced pathology in the spleen by Hurst (1937a) and to malignant rabbit virus-infection of rabbits (Strayer and Sell, 1983), but is in contrast to ectromelia virus infection of mice. Ectromelia virus growth and the resulting necrosis of the spleen is an important aspect of disease and death (Mims, 1964).

4.4.3 Myxoma virus replication and transmission

At 15 and 20dpi of laboratory rabbits with Uriarra or wild rabbits with SLS, virus was present in the basal cells of the epidermis in the primary lesion. The histology of the skin at this time suggests continued proliferation and renewal of the basal cells of the epidermis. Hence, this is a likely site of continued virus replication in the skin and of continued virus drainage into the lymph nodes. The amount of virus antigen in the epidermis in the skin at 15dpi was considerably less than at 10dpi, although the virus titres were similar at these two time points, at approximately 10^6 - 10^7 pfu/g. This may be attributable to the presence of infective cell-free virus in the tissue that does not stain well by immunofluorescence. However, when considering transmission of virus from the primary lesion, the scab material formed over the lesion at this stage will prevent the probing of mosquito vectors at the primary lesion, with transmission of virus relying on the presence of less advanced secondary lesions on eyelids (Day *et al.*, 1956). In Uriarra-infected laboratory rabbits, secondary lesions had not scabbed over at this time and may be a continued source of infective virus for mosquitoes. In SLS-infected wild rabbits, scabbing of secondary lesions was rapid, suggesting that these rabbits would be poor transmitters of SLS in the field.

The early pathological changes and localisation of myxoma virus in the skin and draining lymph nodes are similar in both laboratory and wild rabbits infected with either SLS or Uriarra. However, as shown by both virus localisation and virus titres, laboratory rabbits infected with Uriarra and wild rabbits infected with SLS were able to control replication of virus in the draining lymph node and limit subsequent virus dissemination, replication and pathology in distal tissues. It was suggested that the early inflammatory response together with NK cells and the subsequent adaptive immune response to infection is important in determining the outcome of infection in rabbits with a degree of genetic resistance. However, the permissivity of primary cells from laboratory and wild rabbits to virus replication may also be involved. The ability of myxoma virus to replicate in lymphocytes, and deplete them from the draining lymph node may contribute to the overwhelming of the immune response. As discussed previously, the *in vitro* replication of myxoma virus in lymphocytes does not cause cell death, and a number of proteins produced by myxoma virus function to inhibit apoptosis of infected cells *in vitro*. The histopathology of the lymph node suggests that both apoptosis and necrosis are major mechanisms of cell destruction. It is thus not clear to what extent the depletion of lymphocytes can be attributed to apoptosis, how this may differ between virulent and attenuated myxoma virus, or how the depletion of lymphocytes may relate to suppression of the immune response in laboratory rabbits. In addition, there is limited information on the role of viral anti-apoptosis proteins in virus virulence, replication and dissemination. These questions concerning cell permissivity and cell death following infection of rabbits with myxoma virus are addressed in Chapter 5.

Chapter 5: Mechanisms of host genetic resistance and myxoma virus pathogenesis

5. Mechanisms of host genetic resistance and myxoma virus pathogenesis

5.1 Introduction

The growth of myxoma virus in rabbits is characterised by replication at the primary inoculation site in the skin, followed by transport to and replication in the draining lymph node. Virus disseminates from here to distal tissues, including other lymph nodes and the spleen, and to secondary sites in the skin where it grows to high titres. Laboratory rabbits infected with virulent SLS die at 10 to 12 days post infection. The most severe pathology is in the lymph nodes which are depleted of lymphocytes. Infection of laboratory rabbits with the attenuated Uriarra strain of myxoma virus results in the growth of virus to similar titres as SLS in the primary inoculation site and the draining lymph node, but virus dissemination to and growth in distal tissues is reduced, and lymphocytes are not depleted from the lymph nodes. SLS-infection of wild rabbits results in similar virus titres in the primary inoculation site, but SLS titres in the draining lymph node of wild rabbits are less than in laboratory rabbits. Depletion of lymphocytes occurs but is restricted to the draining lymph node, and lymph nodes become repopulated with lymphocytes around 15dpi. In both Uriarra-infected laboratory rabbits and SLS-infected wild rabbits, virus is cleared from the internal tissues by between 10 and 15 days post infection and the rabbits recover from disease. From these depictions of myxoma virus pathogenesis, obvious important factors of virulence and host resistance are the ability of virus to replicate in the draining lymph node, cause lymphocyte depletion and disseminate to distal tissues, and in the ability of the host to control virus replication, dissemination and tissue pathology.

The results presented in this thesis suggest that wild rabbits have an enhanced immune response to SLS and that this controls viral replication. However, resistance to viral infection could also be mediated at the level of the cell. The innate and heritable resistance of inbred strains of mice to flavivirus infection is mediated by cell permissivity, which restricts virus replication and the production of infectious progeny (reviewed in Shellam *et al.*, 1998). Such restricted permissivity of cells from wild rabbits to myxoma virus infection could result in reduced virus titres, reduced virus-induced pathology and more efficient virus clearance. A comparison of the growth of virulent myxoma virus in primary cells from laboratory and wild rabbits has not

previously been performed to address this possibility.

Histopathology of lymph nodes from myxoma virus-infected rabbits in Chapter 4 indicated that both necrosis and apoptosis of cells were occurring and associated with lymphocyte depletion. Other viruses induce cell death by apoptosis both in cultured cells, for example influenza virus (Price *et al.*, 1997), and *in vivo*, for example African swine fever virus causes apoptosis of lymphocytes in the lymphoid tissue of infected pigs (Summerfield *et al.*, 1998). In the case of some infections, such as HIV infection of humans, depletion of lymphocytes by apoptosis is associated with immune suppression (Finkel *et al.*, 1995). Myxoma virus encodes at least four genes which have been shown to inhibit the apoptosis of infected lymphocytes *in vitro*, and these cells are not killed by infection (Barry *et al.*, 1997; Macen *et al.*, 1996b; Mossman *et al.*, 1996a; Schreiber *et al.*, 1997). However, the consequences of replication *in vivo* may be quite different as indicated by the histological results presented in Chapter 4. In addition, a fifth myxoma virus anti-apoptotic gene Serp2, does not function as an inhibitor of apoptosis *in vitro*, but is reported to inhibit apoptosis of lymphocytes *in vivo* (Messud-Petit *et al.*, 1998). Therefore the induction of apoptosis was examined in lymph nodes and spleen from infected rabbits to determine if this was a major cause of cell death and whether apoptosis was occurring in virus-infected cells.

Lymphocytes have been postulated as a major cell type in which myxoma virus disseminates within the infected rabbit (Fenner and Woodroofe, 1953). As already discussed, myxoma virus replicates well in lymphocytes *in vitro* and there are at least four genes which are critical for this replication. These are M11L, M-T2, M-T4 and M-T5 (Barry *et al.*, 1997; Macen *et al.*, 1996b; Mossman *et al.*, 1996a; Schreiber *et al.*, 1997). Single gene knockout mutants for these genes are at least partially defective in replication in lymphocytes, induce apoptosis in infected lymphocytes *in vitro* and are highly attenuated *in vivo* (Table 5.1). However, the M-T5 knockout virus replicates in primary macrophage/monocytes, but is reported not to disseminate beyond the site of inoculation (Mossman *et al.*, 1996a). My observations indicate that MHC II positive dendritic cells are sites of primary replication and are probably involved in dissemination to the draining lymph node. If virus could not replicate in these cells, it might be expected to be less able to suppress an inflammatory response in the skin as has been reported for the single-gene knockout viruses for M11L, MT-5 and MT-4 (Barry *et al.*, 1997; Graham *et al.*, 1992; Mossman *et al.*, 1996a; Opgenorth *et al.*,

1992). It may also be important that virus-infected dendritic cells are the first cells to reach the draining lymph node as these may influence subsequent events in the draining lymph node. In addition, since the knockout viruses for M11L, MT-2, MT-4 and MT-5 cannot replicate productively in lymphocytes *in vitro,* there should be limited replication of these viruses in the draining lymph node and very limited systemic dissemination unless other mechanisms of virus spread are operating. Therefore these viruses have been used not to examine apoptosis or virulence, but to begin to explore the roles of these genes in replication in dendritic cells and lymphocytes *in vivo* and in dissemination *in vivo*.

Table 5.1: Replication of myxoma virus gene-deletion mutants, vMyxlacT2$^-$, vMyxlacT4$^-$, vMyxlacT5$^-$ or vMyxlacM11L$^-$, in primary lymphocytes and RL-5 cells

Myxoma virus gene deletion mutant	Apoptosis of infected lymphocytes *in vitro*?	Productive *in vitro* replication in RL-5 cells ?	Productive *in vitro* replication in primary lymphocytes ?	Attenuated *in vivo*?	References
vMyxlacT2$^-$	Yes	No	Unknown	Yes	Macen et al., 1996b; Schreiber et al., 1997
vMyxlacT4$^-$	Yes	Reduced	Unknown but induces apoptosis	Yes	Barry et al., 1997
vMyxlacT5$^-$	Yes	Reduced	Unknown but induces apoptosis	Yes	Mossman et al., 1996a
vMyxlacM11L$^-$	Yes	No	Productive infection in mitogen-stimulated cultures only	Yes	Opgenorth et al., 1992; Macen et al., 1996a

5.2 Materials and Methods

5.2.1 *In vitro* infection of primary cell culture from laboratory and wild rabbits

To examine the permissivity of primary cells to SLS infection, primary lymphoid cells from the lymph nodes and spleen and fibroblasts from the tunics of the testes were made from each of three uninfected laboratory and three uninfected wild, male rabbits. These cells were infected with SLS and the virus titre as well as the proportion of infected cells determined at 24, 48 and 72 hours post infection.

5.2.1.1 Preparation of primary lymphoid cells from lymph nodes and spleen

The popliteal lymph nodes and the spleen were excised aseptically from each rabbit and placed into HBSS on ice. Primary lymphoid cells were obtained as described in section 2.2.2.3.

5.2.1.2 Preparation of primary fibroblast cell cultures

The scrotum of each rabbit was incised and the testes removed aseptically into a petri dish on ice. The testes were washed in sterile PBS and the tunics removed using sterile forceps and scissors. The tunics were cut with a scalpel blade into 1mm^2 pieces, placed into T25 flasks (six pieces per flask, six flasks per rabbit), and each piece covered with a drop of complete MEM supplemented with 20% fetal bovine serum (FBS). The tissue explants were incubated for 24 hours at 37°C in 5% CO_2 in air, followed by the addition of fresh medium. When fibroblasts surrounding the tissue explant were confluent, the explants were gently dislodged and discarded. Fibroblast monolayers were washed twice with PBS, twice with 0.1% trypsin in diluent (section 2.2.1.4) and left for 2 min covered in a thin layer of 0.1% trypsin. Fibroblasts were gently removed from the flask and re-seeded into T25 flasks. Complete MEM containing 10% FBS was added and cells were grown to confluency. When confluent, fibroblast monolayers were washed twice with PBS and removed from the flask using 0.1% trypsin as above. Fibroblasts from each individual rabbit were pooled and pelleted by centrifugation (230g for 5min at 18°C). The supernatant was removed and cells were resuspended in 6ml of 10% DMSO in FBS (filtered). 1ml aliquots in cryotubes (Nunc) of the cell suspension were placed in the centre of a large, cottonwool-filled container and frozen overnight at

-70°C, before being stored in liquid nitrogen.

5.2.1.3 Infection of primary cells

Primary cells from the lymph nodes or spleen were counted and 1 x 10^7 cells in 3ml of compete medium placed in 10ml tubes. Myxoma virus (SLS) was added at a MOI of 3, to ensure at least 95% of primary cells were infected. Virus and cells were mixed, followed by an hour incubation at 37°C in a waterbath, shaking every 10 min. The cells were centrifuged at 230g for 10min, the supernatant removed and the cells were resuspended in 12ml fresh medium. The cells were centrifuged as above, the supernantant removed and the cells resuspended at 1 x 10^6 cells/ml. 1ml aliquots of cells were seeded into wells of a sterile, 24 well plates (Nunc) and cultured for 24, 48 and 72 hours at 37°C in 5% CO_2 in air. At each harvest point, the cells were gently resuspended using a pasteur piptette and wells were checked by microscopy to ensure that all cells were removed. Cells were placed in a 1.5ml tube and stored at –70°C until virus titre could be determined by plaque assay.

Aliquots of primary fibroblasts were thawed, washed once in complete MEM, placed with complete MEM into a T25 flask, and allowed to grow to confluency at 37°C in 5% CO_2 in air. When confluent, cells were washed twice with PBS, washed twice with 0.1% trypsin in diluent and left for 2min covered in a thin layer of 0.1% trypsin. The cells were resuspended using a pasteur pipette, and the cells were counted using a haemocytometer. 2 x 10^5 cells in 1ml of complete medium were seeded into each well of sterile 24 well plates, and allowed to grow to confluency overnight. The estimated number of cells per confluent monolayer was 2 x 10^8 cells. SLS was added at a MOI of 3 in 75µl complete medium, and allowed to absorb for an hour with rocking every 10min. The medium was aspirated from the cells, which were then washed by two changes of fresh complete MEM. 1ml of complete MEM was added and the SLS-infected cells cultured for 24, 48 or 72 hours at 37°C in 5% CO_2 in air. At each time point, medium was removed from the fibroblasts, and 75µl SSC (0.15M NaCl, 0.015M $C_6H_5Na_3O_7$, pH 7.0) added. Cells were left for 2min and removed from the wells using a pasteur piptette. Wells were checked by microscopy to ensure that all cells had been removed. Cells were placed in a 1.5ml tube and stored at –70°C until virus titre could be determined by plaque assay.

5.2.1.4 Immunofluorescence assay for myxoma virus in SLS-infected primary cell cultures

At 24, 48 and 72 hours post infection, SLS-infected lymphoid cells were harvested by repeated pipetting and placed into a 1.5ml tube. These cells were fixed briefly in acetone:methanol (1:1), washed twice in PBS and centrifuged onto poly-L-lysine coated slides using a cytospin (Shandon Cytospin 2). Cells were then blocked in 3% BSA/PBS at room temperature for 60 min, followed by a further two washes in PBS. Slides were placed in a humidified container and 100µl of primary mouse anti-myxoma virus monoclonal antibody (clone number 3B6E4), 1:200 in 1% BSA/PBS was added. Slides were incubated for 2 hours at 37°C, followed by two washes in PBS. Sections were then incubated in the dark for 60min at 37°C with 75µl of 1:100 goat anti-mouse IgG conjugated to FITC (Boehringer Mannheim) in 1% BSA/PBS in a humidified container. Sections were washed as above and mounted with Antifade under a coverslip, and viewed using confocal microscopy.

Primary fibroblasts were grown on glass coverslips placed in the bottom of 24 well plates and cells were infected with SLS as described in section 5.2.1.3. At 24, 48 and 72 hours post infection, infected-fibroblasts were fixed for 5min at 4°C with acetone:methanol (1:1), washed twice with PBS and blocked in 3% BSA/PBS at room temperature for 60 min, followed by a further two washes in PBS. Cells were stained for myxoma virus using the 3B6E4 monoclonal antibody as described above. After the final wash with PBS, the coverslips were removed from the 24 well plates and inverted onto glass slides using Antifade as a mounting medium, and viewed using confocal microscopy.

5.2.1.5 Vero cell culture and plaque assay for virus titration

Primary cells infected with SLS were harvested and virus titre determined by plaque assay on monolayers of Vero cells. Vero cell culture conditions and plaque assay are described in sections 2.2.1.4 and 2.2.1.5, respectively.

5.2.2 Detection of apoptotic cells *in vivo*

The number and distribution of apoptotic cells were examined in paraffin embedded tissue sections of the popliteal lymph nodes and spleens taken from laboratory and wild

rabbits infected with either SLS or Uriarra in Chapter 3. These tissues are the same tissues for which virus localisation and histopathology were described in Chapter 4 and the numbers of rabbits infected with each virus and killed at each time point are shown in Table 4.1.

5.2.2.1 Terminal deoxy-UTP nick end labelling of tissue sections

Tissues were fixed in 10% formaldehyde, paraffin embedded within 24 hours of fixation, and sectioned onto 0.1% poly-L-lysine coated slides. Sections were dewaxed by passing them through the following alcohol series to water: three changes of xylene (1 x 10min, 2 x 1 min), three changes of 100% ethanol (3 x 2min), 95% ethanol (1 x 2min), 75% ethanol (1 x 2min), 50% ethanol (1 x 2min), ddH_2O. Sections were soaked in 2x SSC for 20min at 80°C, soaked in ddH_2O for 10min at room temperature and immersed in prewarmed 0.1M Tris/EDTA at 42°C for 2min. Sections were placed into a humidified container and covered with 100µl of 0.1mg/ml proteinase K in Tris/EDTA for 10min at 37°C, followed by a rinse in ddH_2O. Sections were blocked in 1% BSA in PBS for 5min at room temperature, and then permeablised for 2min at 4°C in 0.1% sodium citrate with 1:1000 Triton X-100 (Sigma) followed by two immediate washes with PBS. Sections were returned to the humidified container, covered with 50µl of the reaction mix and incubated for 1hour at 37°C. Per tissue section, the reaction mix consisted of 31µl ddH_2O, 10µl 5x TdT (terminal transferase) buffer (1M potassium cacodylate, 125mM Tris-HCl, 1.25 mg/ml BSA, pH 6.6; Boehringer Mannheim), 2µl 25mM $CoCl_2$ (Boehringer Mannheim), 3µl 1mM dATP (Boehringer Mannheim), 3µl 1:100 FITC conjugated dUTP (1mM; Boehringer Mannheim) and 1µl TdT enzyme (25 x 10^3 units/ml; Boehringer Mannheim). The reaction mix without enzyme was added to lymph node sections as a negative control. Tissue sections of ovary and liver were included as positive and negative controls respectively. The reaction was terminated by the addition of 50µl 0.05M EDTA. Coverslips were mounted with Antifade and sections viewed by confocal fluorescent microscopy.

To quantitate the number of apoptotic cells in each tissue section, a grid (1000µm^2) was superimposed over the field of view and the number of TUNEL$^+$ cells counted. Counting of cells was segregated into the different zones of lymphoid tissue (paracortex and germinal centres for the lymph nodes and red and white pulp for the spleen). Up to 20 individual units of the grid were counted for each microspcope field of view at low magnification (10x). If a unit of the grid in which cells were counted overlaid more

than one zone of lymphoid tissue, the proportion of the field occupied by that zone was estimated and the number of cells adjusted accordingly. Four microscope fields of view were used for each section of lymph node tissue, and five fields were used for each section of spleen tissue. Three different sections were used from each tissue from each rabbit (see Table 4.1 for the number of rabbits at each time point). The number of $TUNEL^+$ cells were expressed as the mean $\pm$ standard error, and included all counts for a group of infected rabbits killed at the same time point.

5.2.2.2 Staining of sections for myxoma virus and $TUNEL^+$ cells using double labeling and serial sections.

To examine if apoptosis occurred in virus-infected cells, double staining for myxoma virus and apoptotic cells was performed on frozen tissue sections of lymph nodes that had been made and fixed as described in sections 2.2.5.2 and 2.2.5.3. These tissues were stained for myxoma virus by immunofluorescence as described in section 2.2.5.5 with the exception that sections were labeled using a sheep anti-mouse secondary antibody conjugated to rhodamine (Boehringer Mannheim; at a dilution of 1:10 in 1% BSA/PBS) rather than conjugated to FITC. Frozen tissue sections were then stained using the TUNEL reaction described in section 5.2.2.1 with the following exceptions. Sections were not treated with 2xSSC at 80°C, digested with proteinase K or permeablised with sodium citrate/Triton-X as sections were permeablised during the fixative process by acetone.

To confirm that neither positive signal for virus or $TUNEL^+$ cells was being lost during double labeling, serial frozen sections were made of lymph nodes and spleen. Sequential sections were either stained for myxoma virus or using the TUNEL reaction. This indicated that the number of virus-infected cells was reduced in double stained tissue sections and sometimes the number or staining intensity of $TUNEL^+$ cells was also reduced. Hence, serial sections were routinely used in the examination of virus localisation and apoptotic cells in tissue sections and it is the results generated from these tissue sections presented in 5.3.2.

5.2.3 Infection of laboratory rabbits with $vMyxlac^+$, $vMyxlacM11L^-$, $vMyxlacT2^-$, $vMyxlacT4^-$ or $vMyxlacT5^-$

The myxoma virus gene-deletion mutants, $vMyxlacM11L^-$ (Graham *et al.*, 1992), $vMyxlacT2^-$ (Macen *et al.*, 1996b; Schreiber *et al.*, 1997), $vMyxlacT4^-$ (Barry *et al.*,

1997) or vMyxlacT5$^-$ (Mossman *et al.*, 1996a) and a control virus with vMyxlac$^+$ (Macen *et al.*, 1993) were kindly supplied by Professor Grant McFadden, John P. Robarts Research Institute and Department of Microbiology and Immunology, University of Western Ontario, Canada. In each case, the gene of interest has been insertionally inactivated by the *E. coli lacZ* gene. vMyxlac$^+$ has *lacZ* inserted intergenically. All viruses are derived from the highly virulent Lausanne strain (Brazil campinas 1949). The titre of virus stocks was determined by plaque assay on Vero cells (section 2.2.1.5). Nine laboratory rabbits were inoculated intradermally with 1000pfu of each virus in the dorsum of the left hind foot. Three rabbits were killed by intravenous injection of barbituate at each of 24 and 48hpi and 6dpi. The skin at the primary inoculation site, and the draining and contralateral popliteal lymph nodes were removed. Tissues taken at 24 and 48hpi were processed for frozen tissue sections (section 4.2.2.2) and stained for virus by immunofluorescence (section 2.2.5.5). Tissues taken at 6dpi were processed for the titration of virus by plaque assay (section 2.2.1.5).

5.3 Results

5.3.1 Growth of myxoma virus in primary cells from laboratory and wild rabbits.

To determine whether host resistance to myxoma virus infection was associated with resistance to virus replication within cells, primary cultures of lymphoid cells from the lymph nodes and spleen, and of fibroblasts from the tunics of the testes, were made from each of three wild and three laboratory rabbits. Lymphoid cell suspensions and fibroblast cell monolayers were infected with SLS at a MOI of 3 which should ensure infection of 95% of cells, and cultured for 24, 48 and 72 hours. By 24hpi, SLS had replicated to similar titres in cells from the lymph node of either laboratory or wild rabbits, at mean titres of 3.9×10^5 and 3.3×10^5 respectively (Figure 5.1). These titres did not change substantially at 48 and 72 hpi. SLS grew to similar titres in primary mononuclear cells from the spleen of both laboratory and wild rabbits at 24, 48 and 72 hpi (Figure 5.2). By 24hpi, SLS had replicated to titres of 1.6×10^5 and 3.1×10^5 in fibroblasts from the testes of either laboratory or wild rabbits, respectively (Figure 5.3). At 48 and 72 hpi, titres of SLS in primary fibroblasts were also similar between cultures from laboratory and wild rabbits.

SLS-infected primary cells were stained by immunofluorescence for myxoma virus. By 24 hpi, approximately 50% of primary cells from either the lymph nodes (Figure 5.4 A)

or spleen (Figure 5.4 B) of laboratory rabbits were infected with myxoma virus. By 48 and 72 hpi, there was no increase in the proportion of infected cells, with approximately 50% of cultured cells containing virus. Similarly, myxoma virus infected approximately 50% of primary cells cultured from the lymph nodes and spleens of wild rabbits at 24 (Figure 5.4 C and D), 48 or 72 hpi. Cell suspensions made from the spleen were often clumped together. The counts of myxoma virus-positive cells indicated that approximately 50% of cells in a sample were infected, although this is not clear from the subsample depicted in Figure 5.4D. By 24hpi, SLS had infected 95 to 100% of primary fibroblasts cultured from the testis of either laboratory or wild rabbits (data not shown).

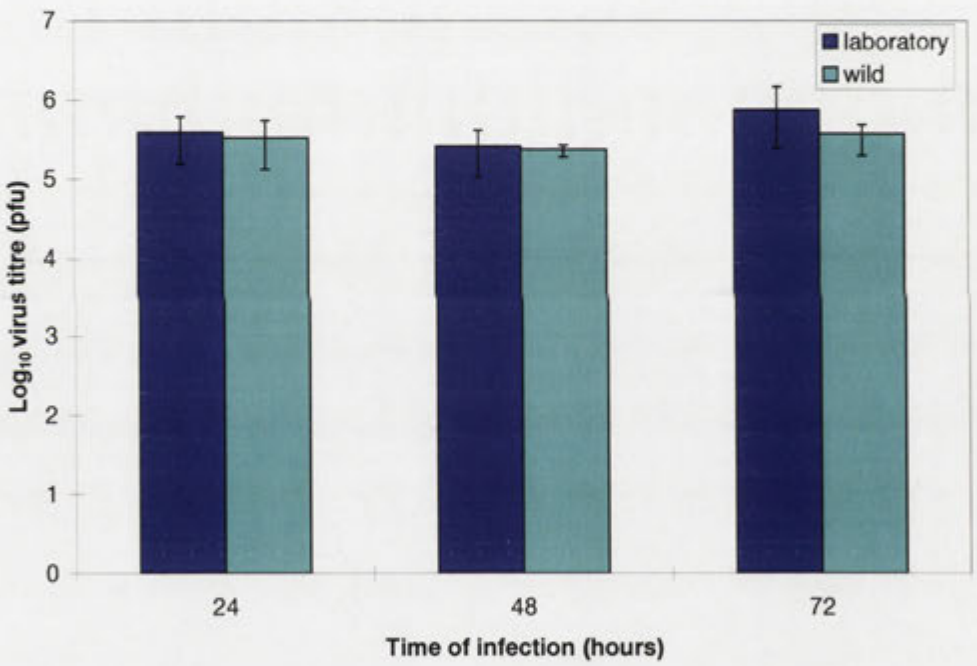

Figure 5.1: SLS titre following infection of primary lymphocytes from lymph nodes of laboratory and wild rabbits. Primary cells were cultured from each of three laboratory and three wild rabbits and infected with SLS at a moi of 3. Triplicate samples of infected cells were cultured for 24, 48 or 72 hours, and the virus titre determined by plaque assay (±SE between rabbits).

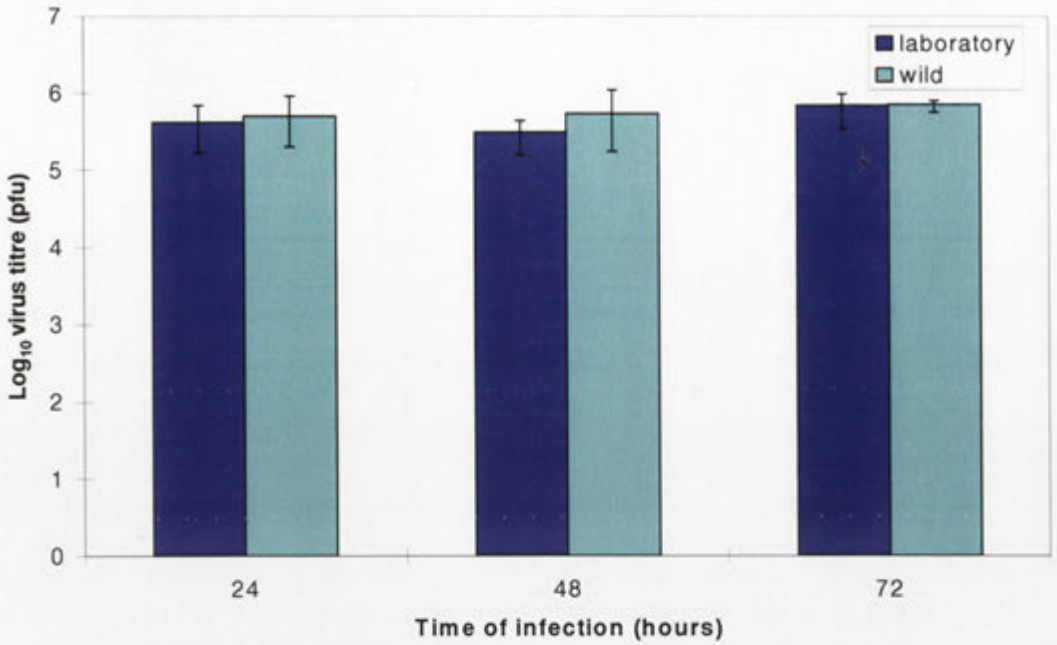

Figure 5.2: SLS titre following infection of primary lymphocytes from spleens of laboratory and wild rabbits. Primary cells were cultured from each of three laboratory and three wild rabbits and infected with SLS at a moi of 3. Triplicate samples of infected cells were cultured for 24, 48 or 72 hours, and the virus titre determined by plaque assay (±SE between rabbits).

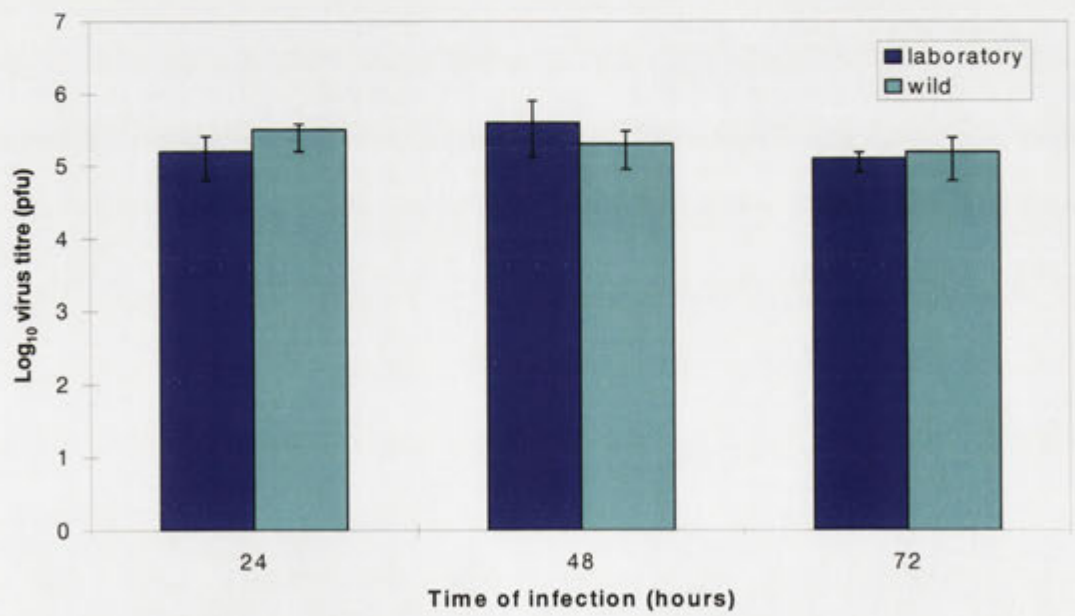

Figure 5.3: SLS titre following infection of primary fibroblasts from testes of laboratory and wild rabbits. Primary cells were cultured from each of three laboratory and three wild rabbits and infected with SLS at a moi of 3. Infected cells were cultured for 24, 48 or 72 hours, and the virus titre determined by plaque assay (±SE between rabbits).

Figure 5.4: Primary lymphocytes from the lymph nodes and spleen of rabbits infected with SLS *in vitro*. Lymphocytes were infected with SLS at a moi of 3, cultured for 24 hours and stained for myxoma virus. (**A**) lymph node lymphocytes from a laboratory rabbit, (**B**) splenic lymphocytes from a laboratory rabbit, (**C**) lymph node lymphocytes from a wild rabbit, (**D**) splenic lymphocytes from a wild rabbit. In each case, approximately 50% of cells were positive for myxoma virus, except in (**D**), which is an artifact of cell distribution on the slide rather than the number of virus-positive splenocytes.

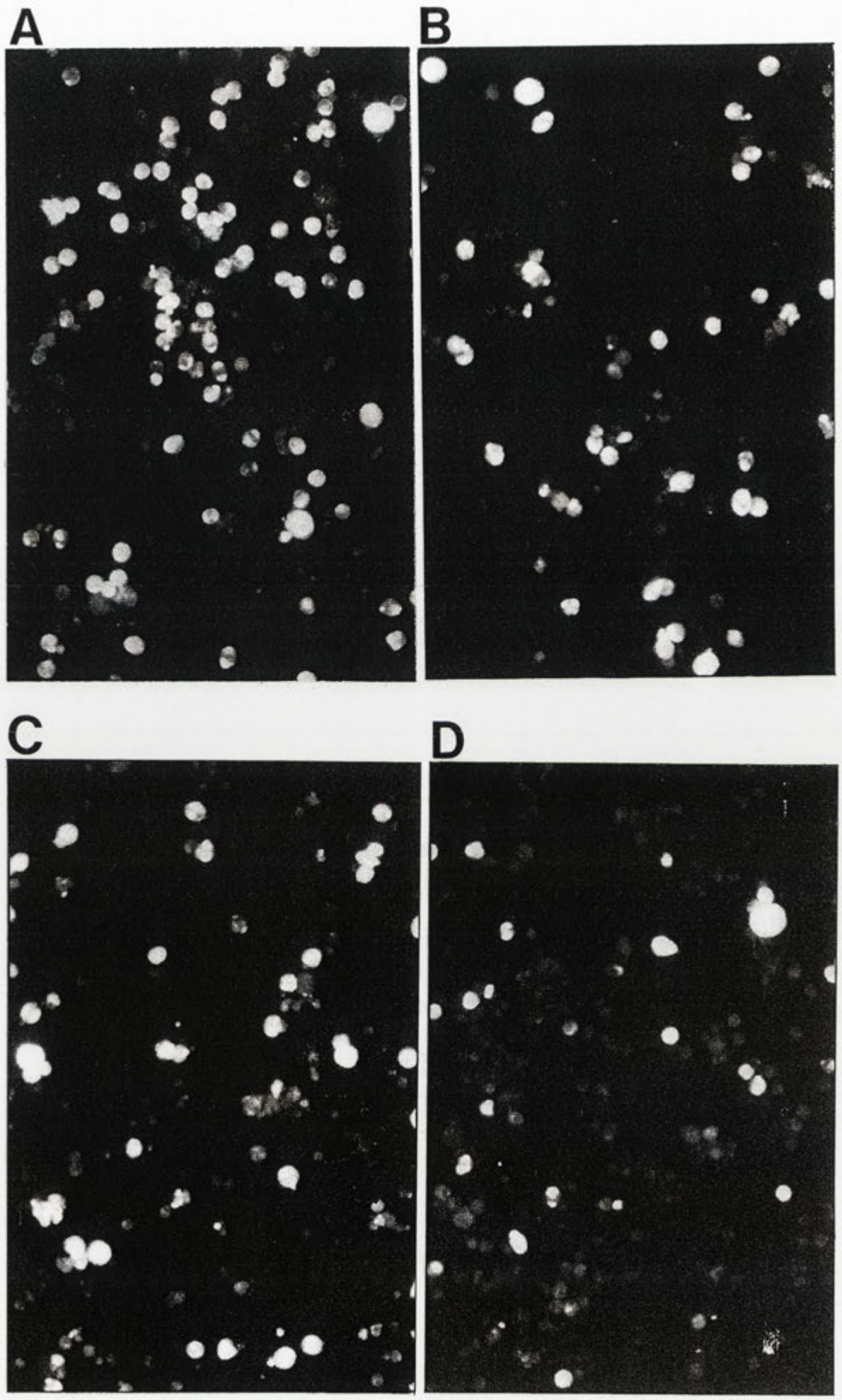
A
B
C
D

5.3.2 Cell death in lymph nodes due to apoptosis

Changes in the number and distribution of cells with apoptotic nuclei in the lymph nodes and spleens following infection of laboratory or wild rabbits with SLS or Uriarra were examined by TUNEL reaction in fixed tissue sections. Tissue sections from ovary and liver were included as positive and negative controls respectively (Figure 5.5). The distribution of cells with apoptotic nuclei in the lymph nodes of uninfected rabbits and the changes following infection are described below.

5.3.2.1 Lymph nodes from uninfected rabbits

The lymph nodes from 11 uninfected laboratory rabbits were labelled by the TUNEL reaction to determine the distribution of apoptotic cells in uninfected lymph nodes (Figure 5.6A). Apoptotic cells were often clustered in a group of 3-15 cells in the centre of dark zones or at the edge of light zones in germinal centres (Figure 5.6B). Some germinal centres were surrounded by a ring of apoptotic cells, or had 3-10 apoptotic cells at the border of germinal centres and the paracortex. Apoptotic cells in the paracortex of uninfected lymph nodes were evenly distributed at a density of 2.3 ± 1.1 cells/100μm^2 (Figure 5.6C). Fluorescence was usually only observed in intact cells, with apoptotic bodies rarely observed.

5.3.2.2 Changes in the number and distribution of apoptotic cells in draining and contralateral lymph nodes following the infection of laboratory or wild rabbits with either SLS or Uriarra

The density of apoptotic cells in the paracortex of draining lymph nodes is shown in Figure 5.7. This indicates that SLS-infection of laboratory rabbits resulted in an increase in the number of cells with apoptotic nuclei in the draining lymph node by 4dpi. Apoptotic cells were a prominent feature in the lymph nodes from 6dpi in all other rabbits. By 10dpi when most other infections had high numbers of apoptotic cells in the paracortex, the draining lymph nodes from SLS-infected laboratory rabbits had low numbers. This was associated with depletion of lymphocytes from the lymph nodes. Changes in the density of apoptotic cells in the contralateral lymph node were similar to the draining lymph node and are shown in Figure 5.7B.

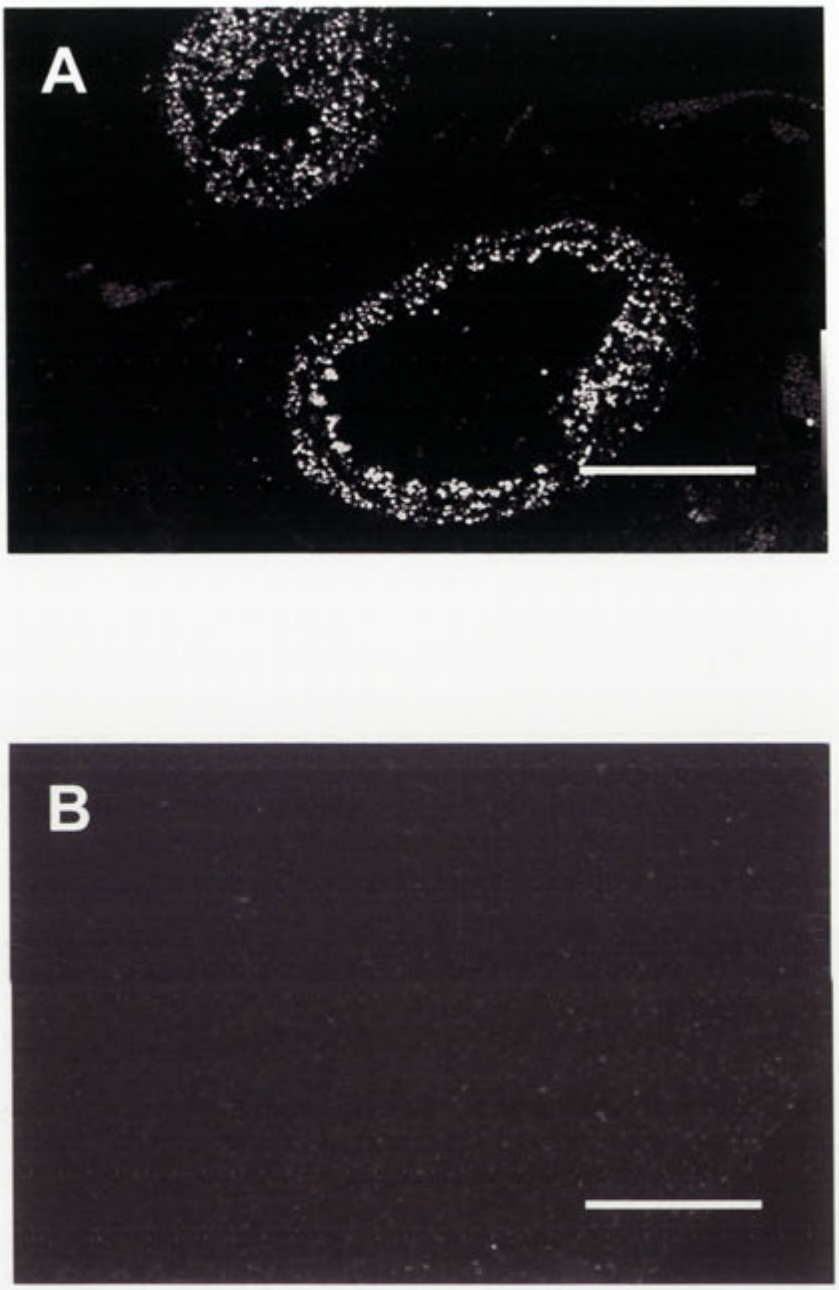

Figure 5.5: Tissue sections of rabbit ovary (**A**) and liver (**B**) stained with the TUNEL reaction. Cells of the ovary granulosum have a high rate of apoptosis, and thus this tissue was used as a positive control for the TUNEL reaction. Apoptosis is not a major mechanism of cell turn over in the liver, and thus this tissue was used routinely as a negative control for this assay. Bar represents 400μm.

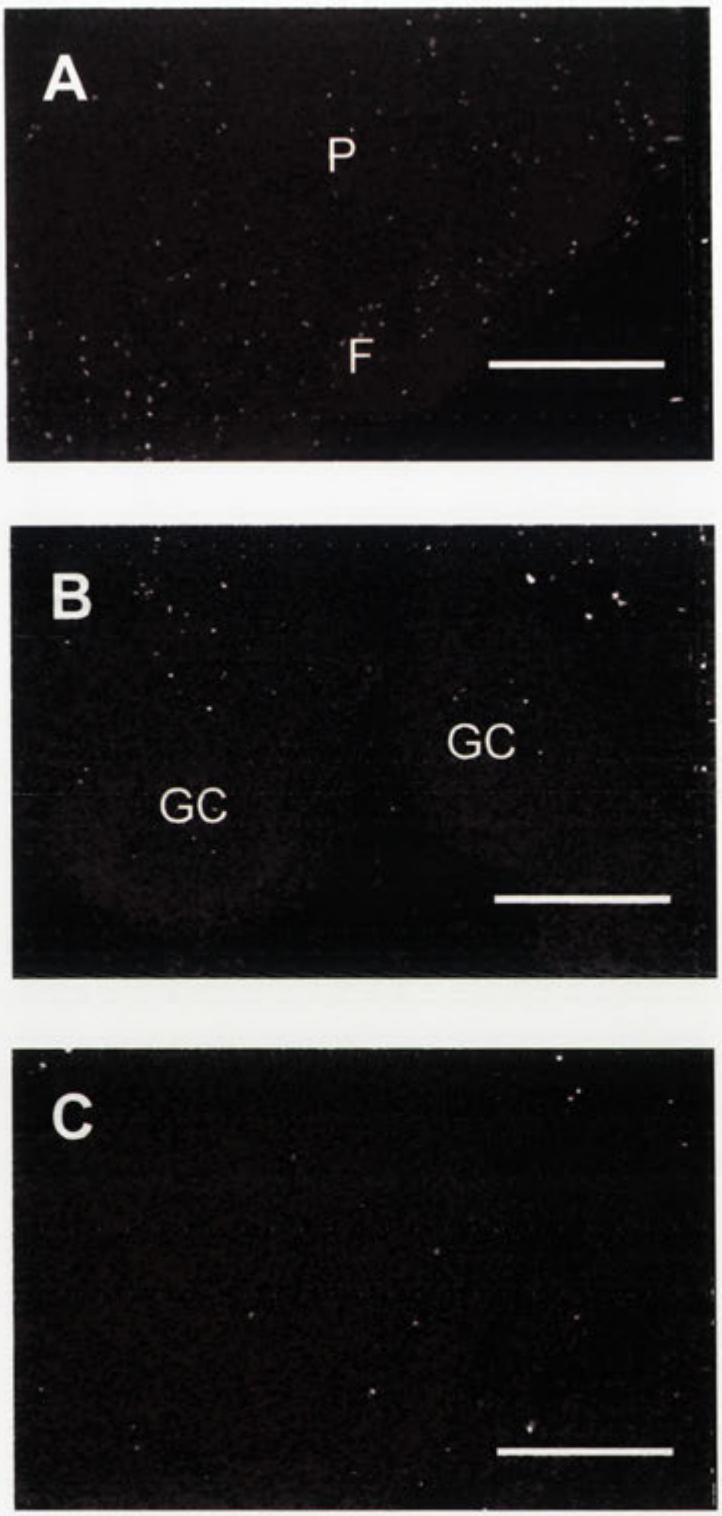

Figure 5.6: TUNEL$^+$ cells in the popliteal lymph nodes from uninfected rabbits. (**A**) TUNEL$^+$ cells in the paracortex and follicles. Note the even distribution of TUNEL$^+$ cells in the paracortex and in small clusters associated with follicles of uninfected lymph nodes. Bar represents 300μm. (**B**) TUNEL$^+$ cells in germinal centres. Bar represents 150μm. (**C**) TUNEL$^+$cells in the paracortex. Bar represents 150μm. P, paracortex; F, follicles; GC, germinal centres.

A

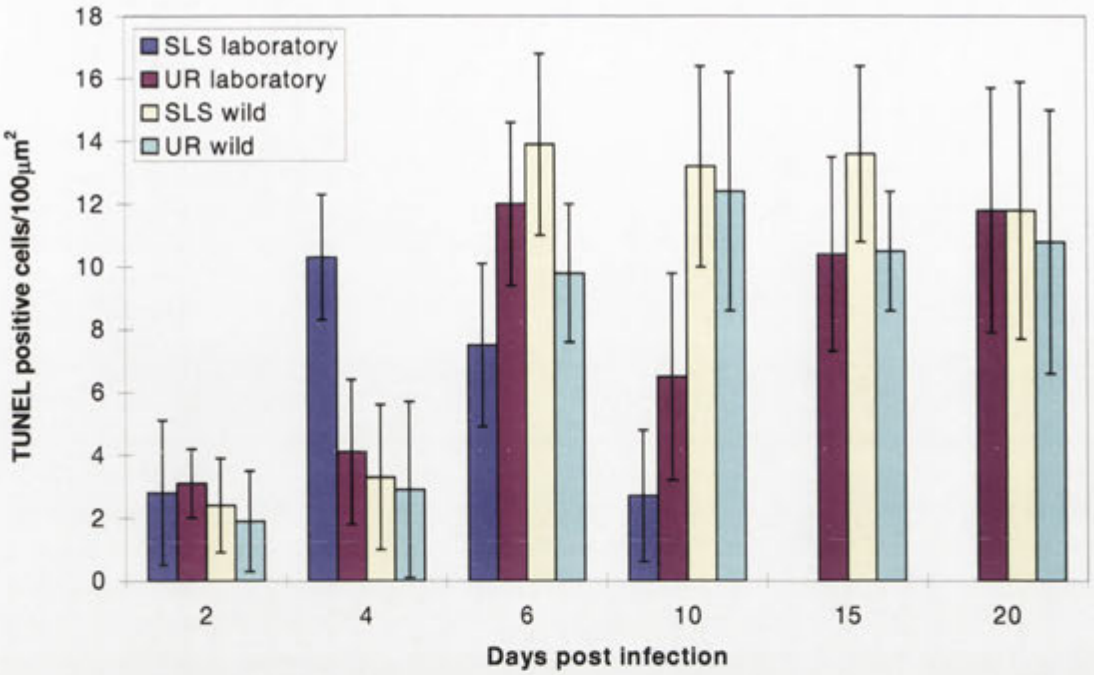

B

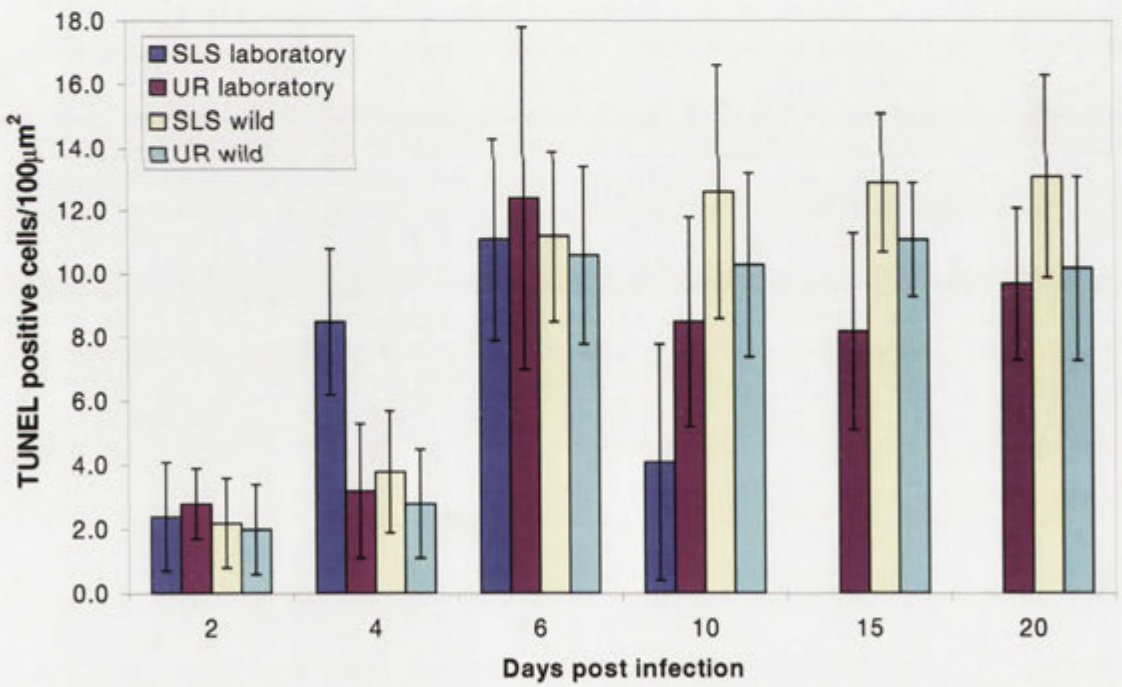

Figure 5.7: Numbers of TUNEL$^+$ cells in the paracortex of (**A**) draining and (**B**) contralateral lymph nodes from SLS and Uriarra infected laboratory and wild rabbits (cells/100µm^2 ± SE). Using fixed tissue sections, the nucleus of cells containing fragmented DNA was labeled using the TUNEL reaction. A grid was superimposed over the field of view (4 fields were used per section, three tissue sections per tissue, see Table 4.1 for the number of rabbits at each time point) and up to 20 individual units of the grid counted. The SE is calculated for all tissue sections from all rabbits.

In addition to changes in the density of apoptotic cells, the distribution of TUNEL$^+$ cells in the lymph nodes of myxoma virus-infected rabbits also differed between infections. These differences in distribution were particularly associated with the paracortex and germinal centres of lymph nodes, and are described below. Using serial sections, lymph node tissues from infected rabbits were stained for cells with apoptotic nuclei By TUNEL reaction. Sequential tissue sections of 4μm thickness were stained for myxoma virus. The results are described below.

5.3.2.3 Changes in the distribution of apoptotic cells and localisation of myxoma virus

5.3.2.3.1 The paracortex

In SLS-infected laboratory rabbits, apoptotic cells were first seen in the paracortex immediately under the subcapsular sinus, over the cortex and extending down between follicles and germinal centres (Figure 5.8A). This was observed in both the draining and contralateral lymph nodes at 4dpi, although many areas of the paracortex were normal (Figure 5.8B). In other cases, a continuous line of positive cells, seen as a band of positive cells approximately 400μm across, or as a line one to two cells deep, spanned the paracortex directly under the follicles (Figure 5.8C and D). These lines of TUNEL$^+$ cells were usually associated with continuous lines of myxoma virus-infected lymphocytes, but cells staining positive for myxoma virus generally did not have apoptotic nuclei. This is shown in Figure 5.9 in serial sections with the TUNEL$^+$ cells shown in Figure 5.9A and virus localisation in a second but sequential tissue section shown in Figure 5.9B. At 4dpi of laboratory rabbits with SLS, high numbers of apoptotic cells in the cortex of the lymph nodes was associated with the presence of virus-infected lymphocytes. However, apoptotic cells were not infected with SLS (Figure 5.10). Although myxoma virus was present in the lymph nodes of Uriarra-infected laboratory rabbits, and SLS- or Uriarra-infected wild rabbits at the same time, the distribution of apoptotic cells in the paracortex of Uriarra-infected laboratory rabbits was similar to that in lymph nodes from uninfected rabbits.

Apoptotic cells became evenly distributed throughout large areas of the cortex and paracortex of the draining and contralateral lymph nodes of all infected rabbits by 6dpi (Figure 5.11A and B). There was an even distribution of myxoma virus-infected lymphocytes in the paracortex from all infected rabbits (an example is shown in Figure 5.11C) except Uriarra-infected wild rabbits. WBC contained within the lumen of blood

vessels also stained positive by the TUNEL reaction in all infected rabbits (Figure 5.12A). Endothelial cells did not have apoptotic nuclei. In draining lymph nodes from SLS-infected laboratory rabbits but not from other rabbits, there was an increase in the number of cells containing nuclei that stained intensely positive immediately surrounding the blood vessels (Figure 5.12B) and trabeculae (Figure 5.12C) of the diffuse cortex.

Figure 5.8: TUNEL$^+$ cells in the paracortex of the draining lymph node of SLS-infected laboratory rabbits at 4dpi. **(A)** TUNEL$^+$ apoptotic cells in the paracortex immediately under the subcapsular sinus, over the cortex and extending down between follicles and germinal centres. Bar represents 150μm. **(B)** Diffuse cortex in another area of the same lymph node as **(A)**. Bar represents 150μm. **(C)**. Continuous band of TUNEL$^+$ cells spanning the paracortex. Bar represents 100μm. **(D)** Continuous band of TUNEL$^+$ cells spanning the paracortex. Bar represents 100μm. (GC) germinal centre.

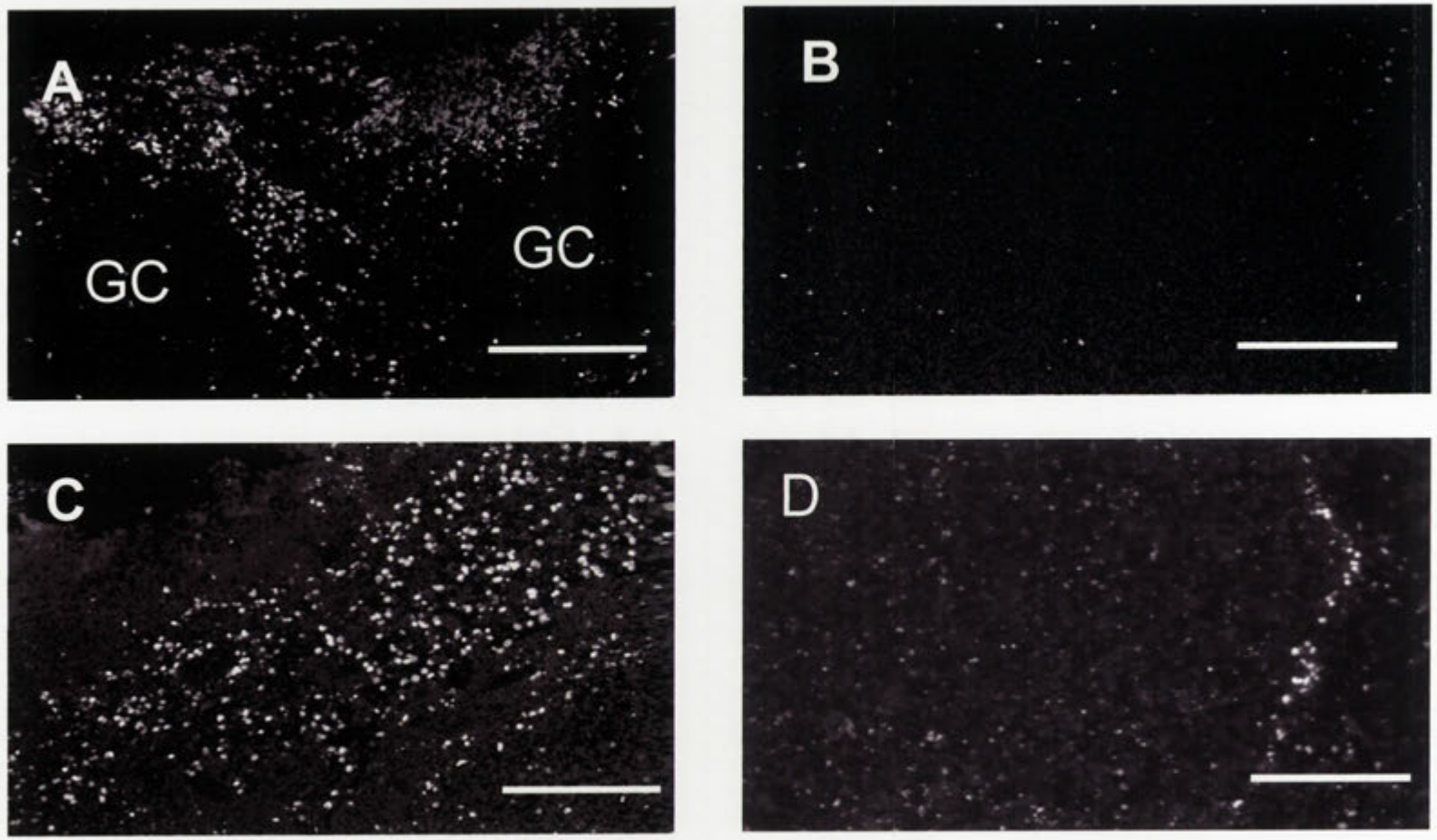
A
GC
GC
B
C
D

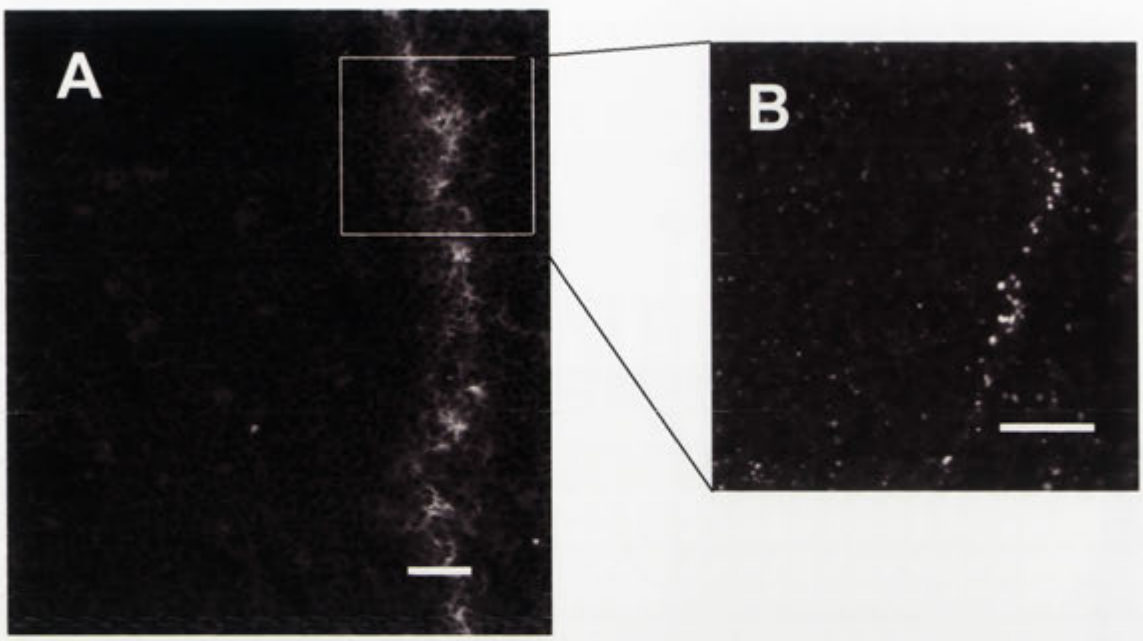

Figure 5.9: Serial sections of lymph nodes from an SLS-infected laboratory rabbit at 4dpi stained by TUNEL reaction or by immunofluorescence for myxoma virus. (**A**) Myxoma virus positive lymphocytes in the paracortex. (**B**) Serial section taken 4μm from (**A**) showing the $TUNEL^+$ cells spanning the paracortex. $TUNEL^+$ cells were adjacent to myxoma virus infected lymphocytes. Bars represent 100μm.

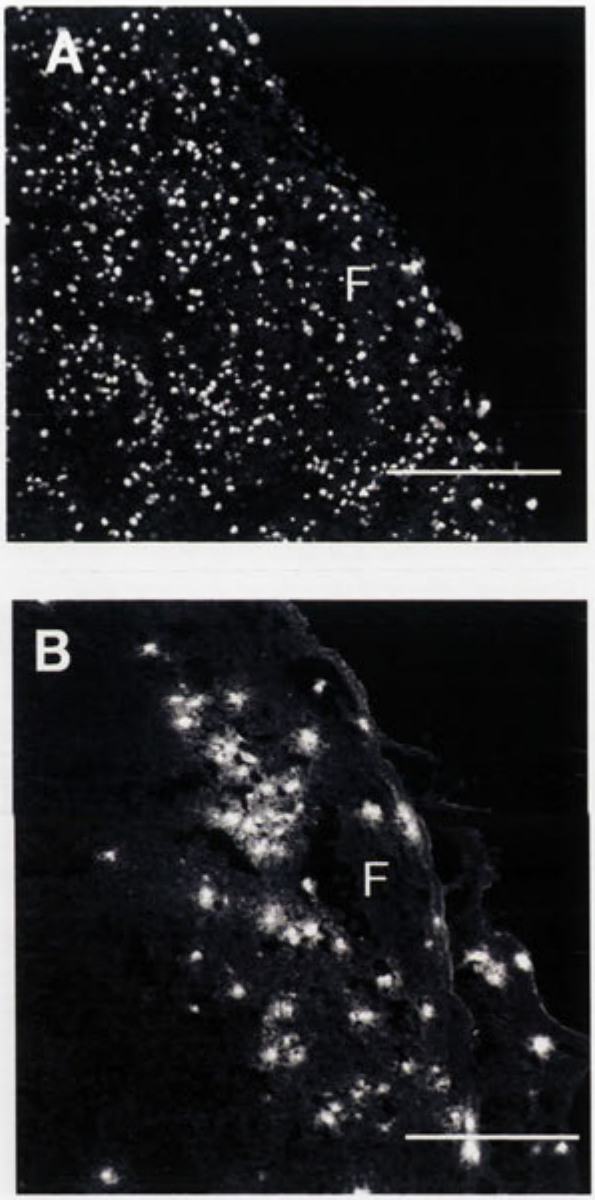

Figure 5.10: Serial sections of a lymph node from an SLS-infected laboratory rabbit at 4dpi. (**A**) TUNEL$^+$ cells in the cortex and throughout a follicle. (**B**) Localisation of SLS . F, follicle. Bars represent 100μm.

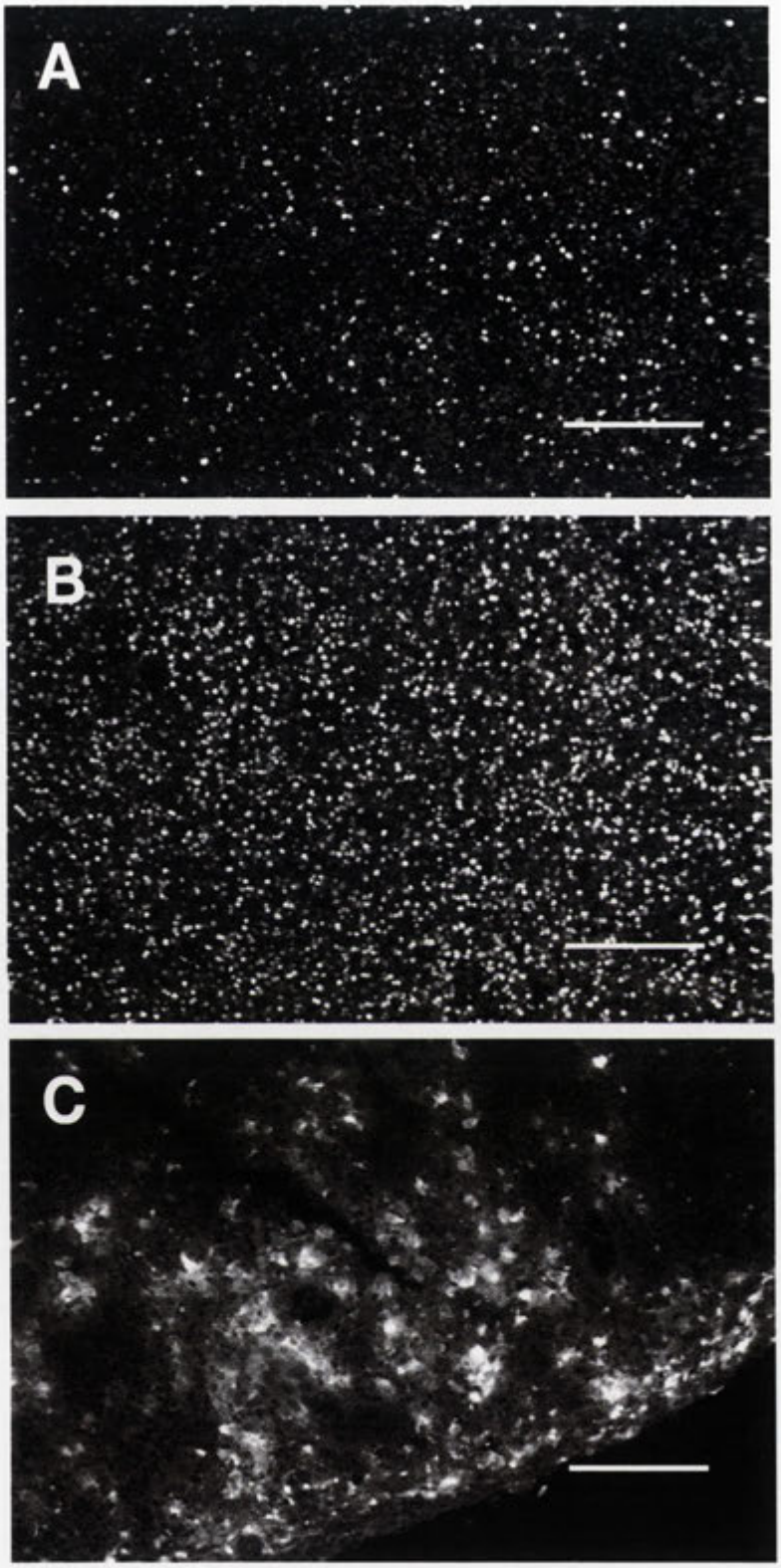

Figure 5.11: TUNEL$^+$ cells and myxoma virus positive cells in the paracortex of draining lymph nodes at 6dpi. (**A**) TUNEL$^+$ cells in the lymph node paracortex from an SLS-infected laboratory rabbit. (**B**) TUNEL$^+$ cells in the lymph node paracortex from an SLS-infected wild rabbit. (**C**) Myxoma virus staining in the lymph node paracortex from an SLS-infected laboratory rabbit. Bars represent 150μm.

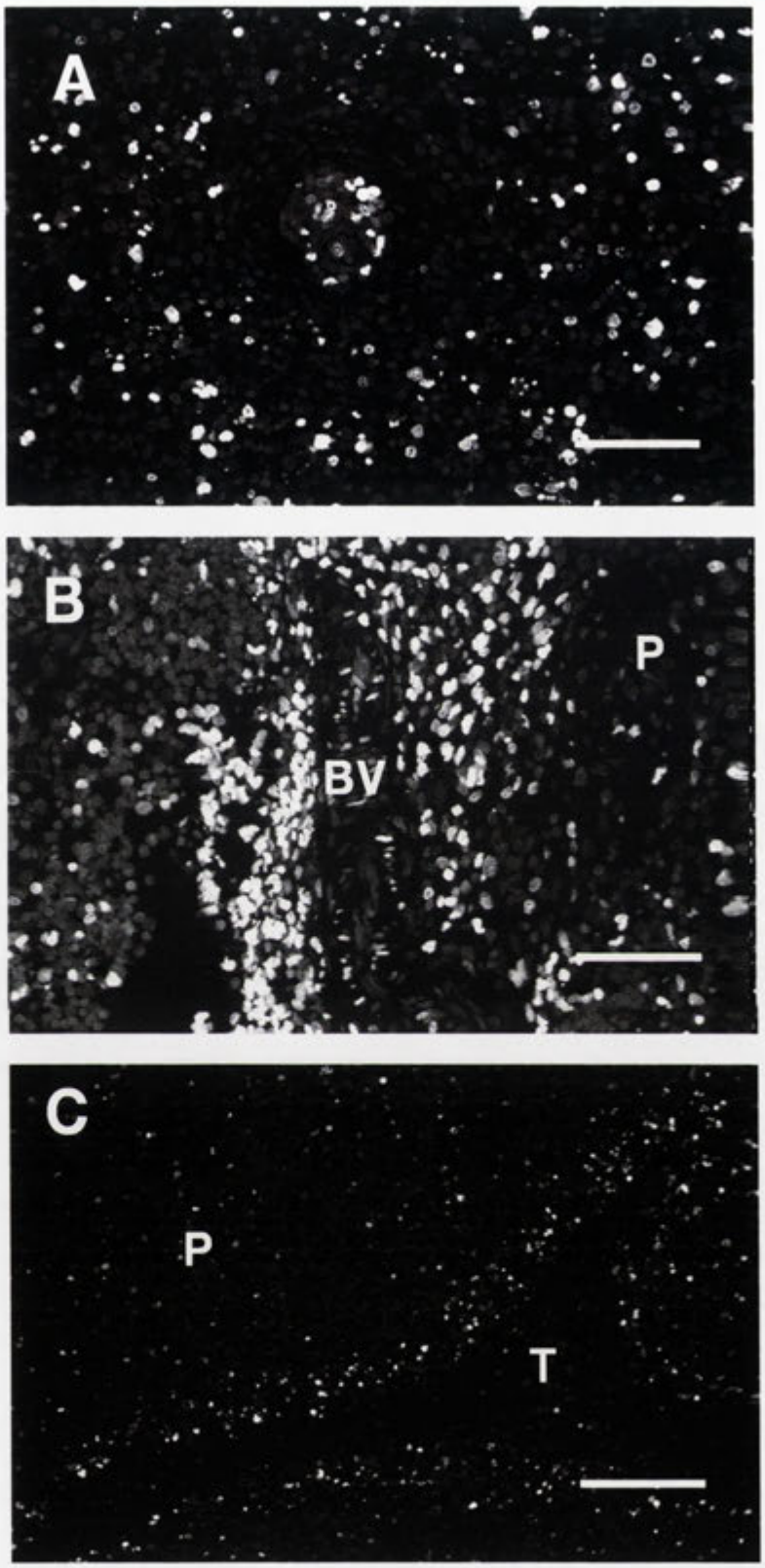

Figure 5.12: TUNEL$^+$ cells associated with blood vessels and connective structures in the paracortex of lymph nodes at 6dpi. (**A**) TUNEL$^+$ WBC in the lumen (arrow) of a blood vessel from an SLS-infected laboratory rabbit. Bar represents 100μm. (**B**) TUNEL$^+$ cells surrounding blood vessels in the lymph node paracortex from an SLS-infected laboratory rabbit. Bar represents 100μm. (**C**) TUNEL$^+$ cells surrounding the trabeculus in the lymph node paracortex from an SLS-infected laboratory rabbit. Bar represents 200μm. BV, blood vessel; P, paracortex; T, trabeculus.

The number and staining intensity of apoptotic cells in the cortex and paracortex of most draining and contralateral lymph node sections taken from SLS-infected rabbits at 10dpi were generally reduced compared to 6dpi. This reduction was associated with the depletion of lymphocytes from the lymph nodes. In contrast, the paracortex of lymph nodes from Uriarra-infected laboratory rabbits, or from wild rabbits infected with either SLS or Uriarra, contained evenly distributed $TUNEL^+$ cells at medium to high densities (Figure 5.13 A), similar to that at 6dpi, even when virus was not present in serial sections (Figure 5.13B). This general distribution of cells with apoptotic nuclei was maintained in the diffuse cortex of lymph nodes from Uriarra-infected laboratory rabbits, or from wild rabbits infected with either SLS or Uriarra, over the 20 days of infection, although virus was not detected by immunofluorescence in lymph nodes from 15 and 20dpi.

5.3.2.3.2 Germinal Centres

Changes in the distribution of $TUNEL^+$ cells and myxoma virus-infected lymphocytes associated with germinal centres in lymph nodes were substantially different between infections. In Uriarra-infected laboratory rabbits (Figure 5.14A) and in wild rabbits infected with either SLS (Figure 5.14B) or Uriarra, the number of apoptotic cells in the newly forming germinal centres of the draining lymph node increased slightly at 4dpi, and was substantial by 6dpi. This increase was most obvious in the dark zones of germinal centres and throughout the side of the mantle zone closest to the lymph node paracortex. Myxoma virus was present in lymphocytes in the paracortex of these rabbits, but was not associated with germinal centres. By 10dpi of these rabbits, large macrophage-like (approximately 35µm across) were present in the light zone of many germinal centres in both the draining and contralateral lymph nodes. These cells contained 10-20 apoptotic bodies within their cytoplasm (Figure 5.14C). In SLS-infected wild rabbits, myxoma virus localised to the mantle zones of some germinal centres by 6dpi. $TUNEL^+$ cells were distributed evenly over the entire area of these germinal making distinct zones difficult to define. The generalised distribution of $TUNEL^+$ cells over germinal centres was not observed in the lymph nodes from Uriarra-infected laboratory rabbits.

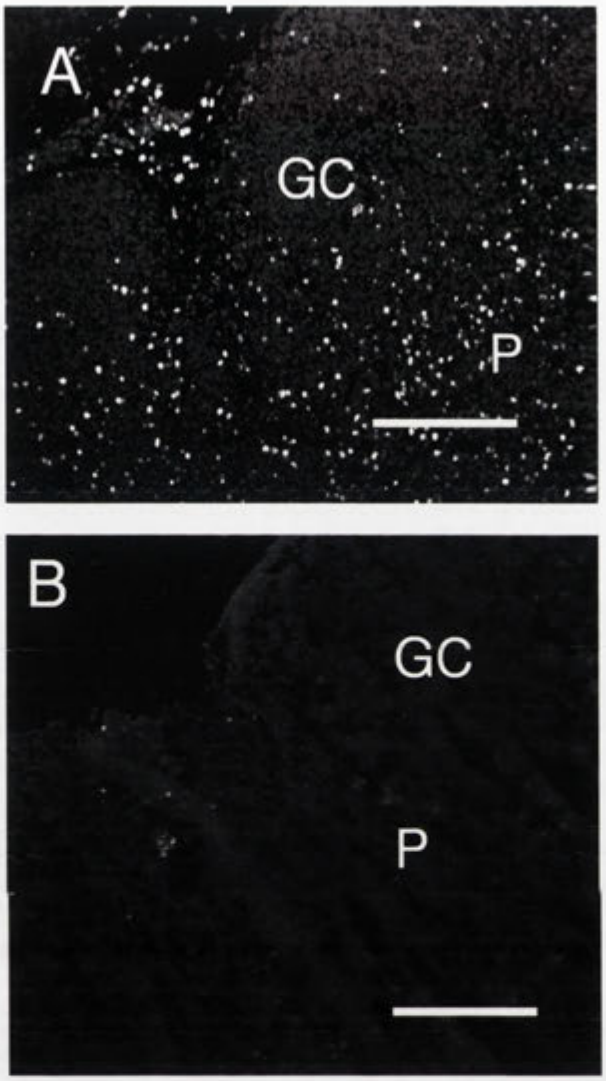

Figure 5.13: TUNEL staining and virus localisation in serial sections of lymph node from a Uriarra-infected laboratory rabbit at 6dpi. (**A**) TUNEL$^+$ cells were distributed throughout the paracortex and inner mantle zone of germinal centres. (**B**) Myxoma virus localisation in a serial section taken 4μm from (**A**). The germinal centre indicated (GC) is the same one in each case. Bars represent 200μm. P, paracortex.

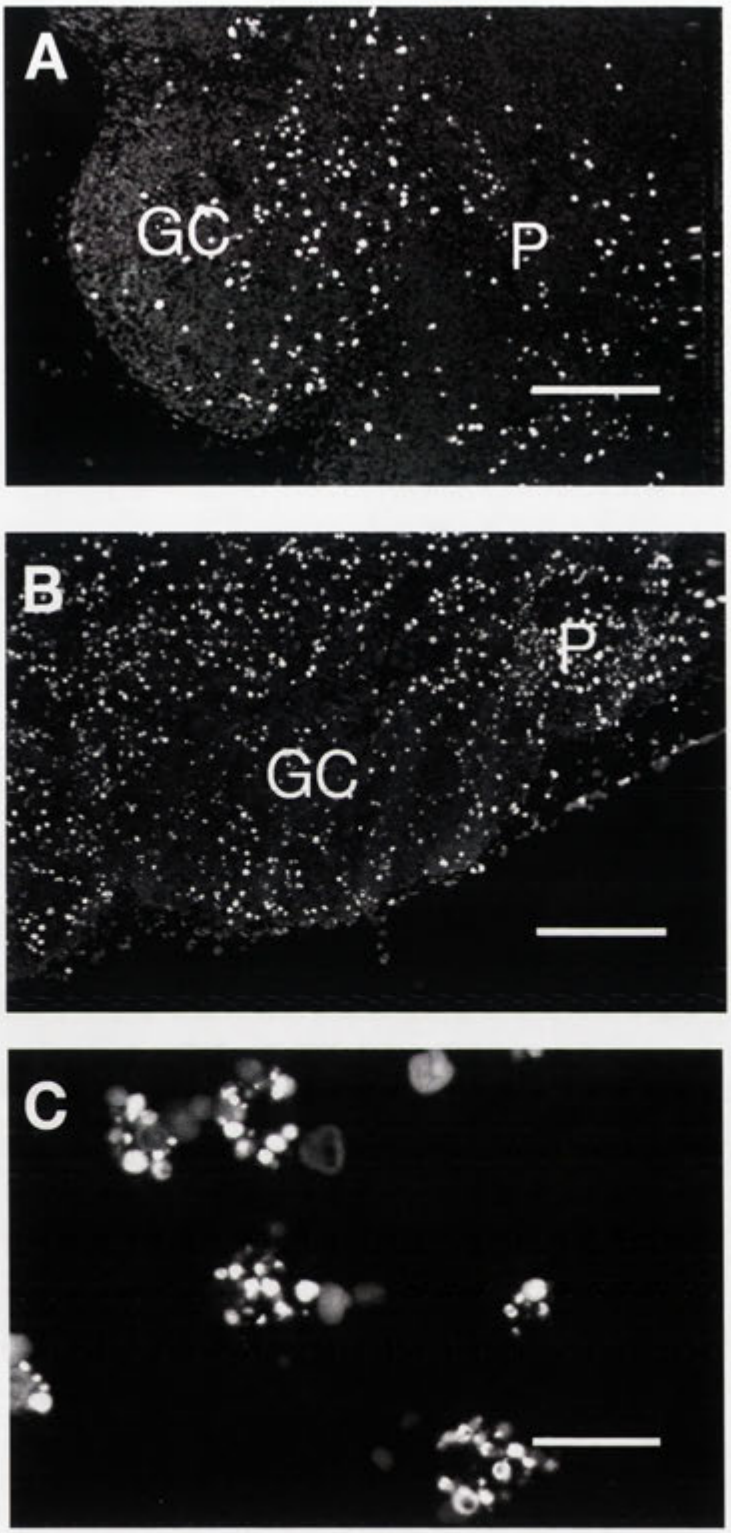

Figure 5.14: TUNEL^{+} staining of germinal centres in draining lymph nodes from myxoma virus-infected rabbits. (**A**) Uriarra-infected laboratory rabbit at 6dpi. Bar represents 100μm. (**B**) SLS-infected wild rabbit at 6dpi. Bar represents 100μm. (**C**) Macrophage-like cells containing TUNEL+ apoptotic bodies within the cytoplasm. These were present in the light zones of germinal centres from 10dpi of Uriarra-infected laboratory rabbits or SLS-infected wild rabbits. Bar represents 35μm. P, paracortex; GC, germial centre.

In SLS-infected laboratory rabbits, myxoma virus localised in lymphocytes of the mantle zones of some germinal centres by 4dpi, and there was an increase in $TUNEL^+$ cells in germinal centres by 6dpi. Both the virus localisation and the distribution of apoptotic cells were highly variable. In some germinal centres, the distribution of $TUNEL^+$ cells was clustered in the dark or inner mantle zones (Figure 5.15A). SLS was not present in the mantle zones of these germinal centres. In other germinal centres that did contain SLS, $TUNEL^+$ cells were distributed throughout most of the germinal centre (Figure 5.15B) or contained large numbers of rounded fluorescent particles of two general sizes. The first and smallest were distributed throughout the dark and light zones of the germinal centres and were likely to be nuclear fragments corresponding to apoptotic bodies. The second, larger particles were distributed throughout the mantle zone of germinal centres and were the size of intact cells with apoptotic nuclei (Figure 5.15C). Germinal centres containing numerous nuclear fragments were never present in Uriarra-infected laboratory rabbits and was observed only at 20dpi in one SLS-infected wild rabbit.

The number of TUNEL+ cells in the germinal centres of lymph nodes from SLS-infected laboratory rabbits declined at 10dpi (Figure 5.15D), but was generally maintained over the course of infection in Uriarra-infected laboratory rabbits or in wild rabbits infected with either SLS or Uriarra.

As has been discussed, SLS localised to the mantle zones of germinal centres in both the draining and contralateral lymph nodes of laboratory rabbits by 4dpi (Chapter 4). This was associated with an increase in the number of $TUNEL^+$ cells. However, in serial sections taken at 4μm intervals, cells within germinal centres that had apoptotic nuclei did not stain positive for myxoma virus. Two examples of TUNEL staining and myxoma virus localisation in germinal centres from the lymph nodes of SLS-infected rabbits are shown in Figure 5.16.

Figure 5.15: TUNEL staining in germinal centres from the draining lymph nodes of SLS-infected laboratory rabbits. (**A**) Germinal centre at 6dpi. $TUNEL^+$ cells are present in the dark zone or in the area of the mantle zone closest to germinal centres from the paracortex. (**B**) Germinal centres from the same draining lymph node shown in (**A**). $TUNEL^+$ cells are evenly distributed over the germinal centres. (**C**) Germinal centre at 6dpi containing $TUNEL^+$ fragments of two sizes; small apoptotic bodies (open long arrow) and larger, intact lymphocytes (open short arrows). (**D**) Remnants of a draining lymph node germinal centre at 10dpi containing few $TUNEL^+$ cells. The closed arrow indicates the edge of the remnant centre. GC, germinal centre; P, paracortex. Bars represent 150μm.

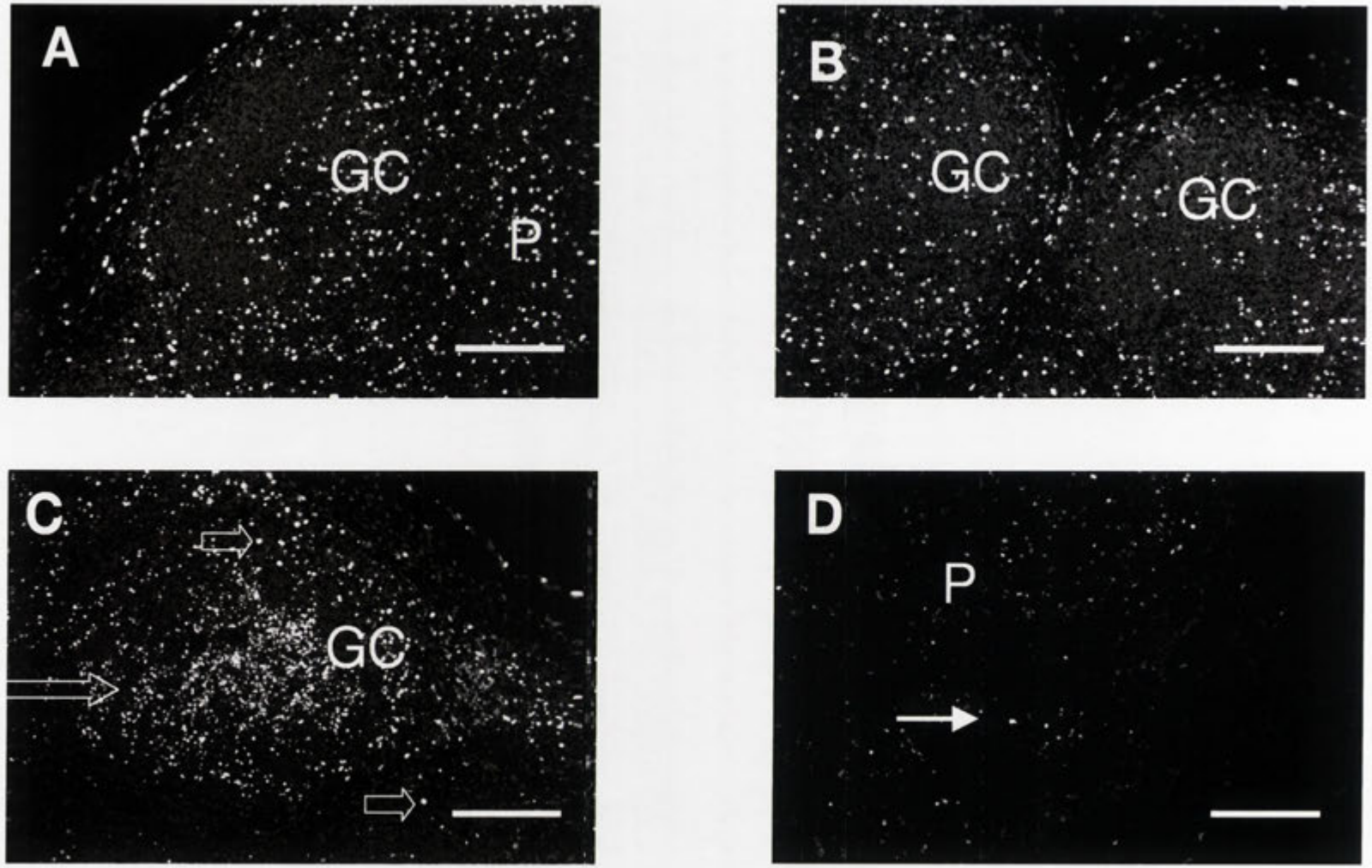
A
GC
P
B
GC
GC
C
GC
D
P

Figure 5.16: TUNEL staining (left hand side) and myxoma virus localisation (right hand side) in two germinal centres from SLS-infected laboratory rabbits. $TUNEL^{+}$ cells were clustered in the middle of the germinal centres whereas myxoma virus-infected cells were present in the mantle zones. In addition, more cells were apoptotic than were infected with virus.

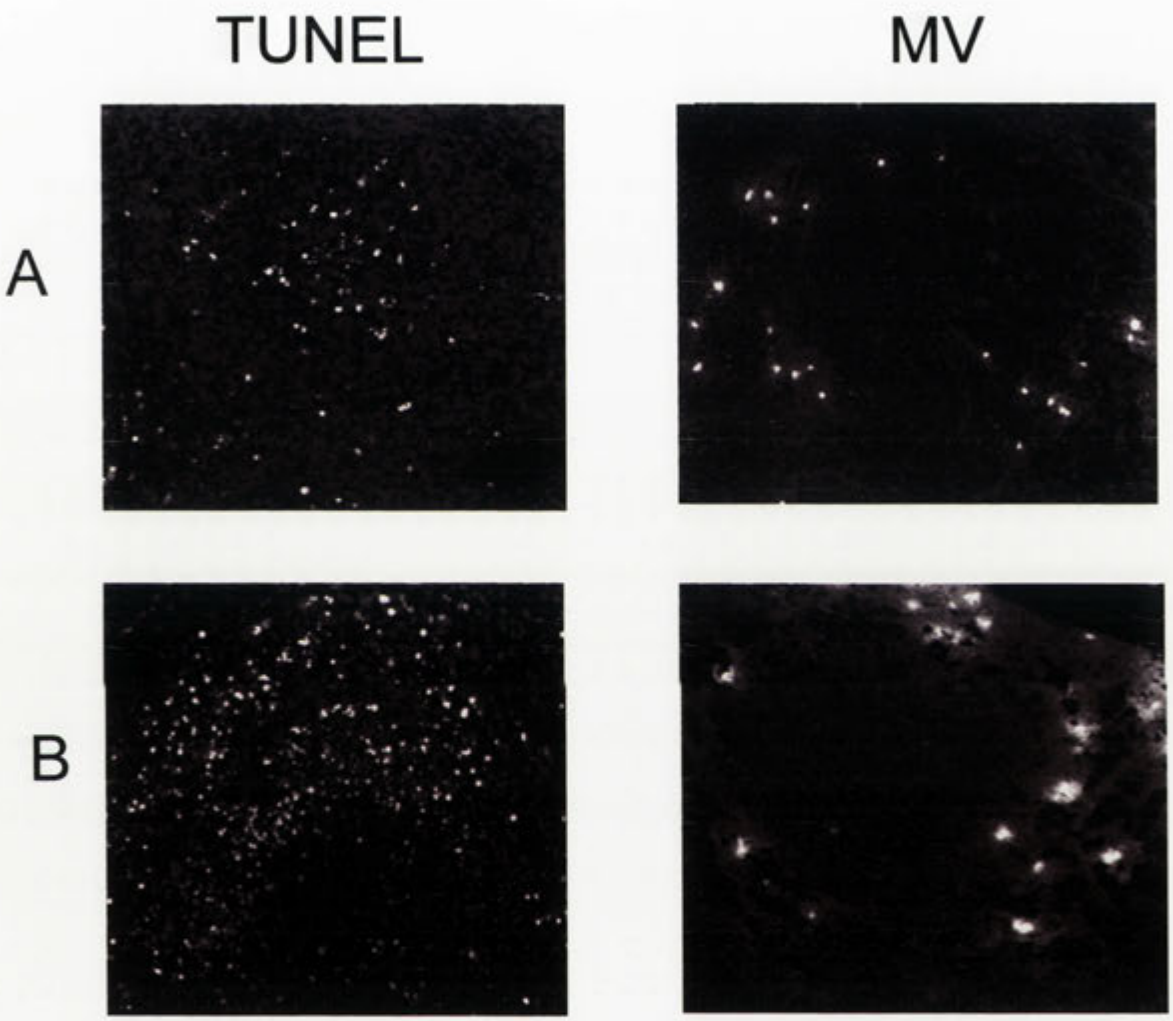
TUNEL
MV
A
B

5.3.3 Cell death in the spleen due to apoptosis

5.3.3.1 Spleens from uninfected rabbits

Uninfected spleens contained low densities of TUNEL$^+$ lymphocytes throughout the white pulp at 1.7 $\pm$ 1.0 cells/100μm^2 and many clusters of positive staining mononuclear cells in the red pulp (Figure 5.17A). These cells in the red pulp were of two types. The first were macrophages as they were large, and contained numerous TUNEL$^+$ nuclear fragments within their cytoplasm, although the cell nucleus was not positive (Figure 5.17B). The nucleus of the other mononuclear cell type stained positive by TUNEL. These were probably lymphocytes and were present in the red pulp at 2.6 $\pm$ 1.2 cells/100μm^2.

5.3.3.2 Changes in the number and distribution of apoptotic cells in the spleen following the infection of laboratory or wild rabbits with either SLS or Uriarra

In general, the changes in the number of TUNEL$^+$ cells in the red and white pulp of the spleen (Figure 5.18 A and B) were small compared to the lymph nodes. However, SLS infection of laboratory rabbits was clearly different from Uriarra-infected laboratory rabbits or SLS-infected wild rabbits. The two prominent differences shown by TUNEL staining were seen at 10dpi. The first of these was a decrease in the number and staining intensity of lymphocytes in the white pulp of SLS-infected laboratory rabbits (Figure 5.19A) compared to other infections (Figure 5.19B). Secondly, by 10dpi there was a decrease in the number of macophages containing apoptotic bodies in the splenic red pulp of SLS-infected laboratory rabbits (Figure 5.19C) compared to other groups of infected rabbits (Figure 5.19D).

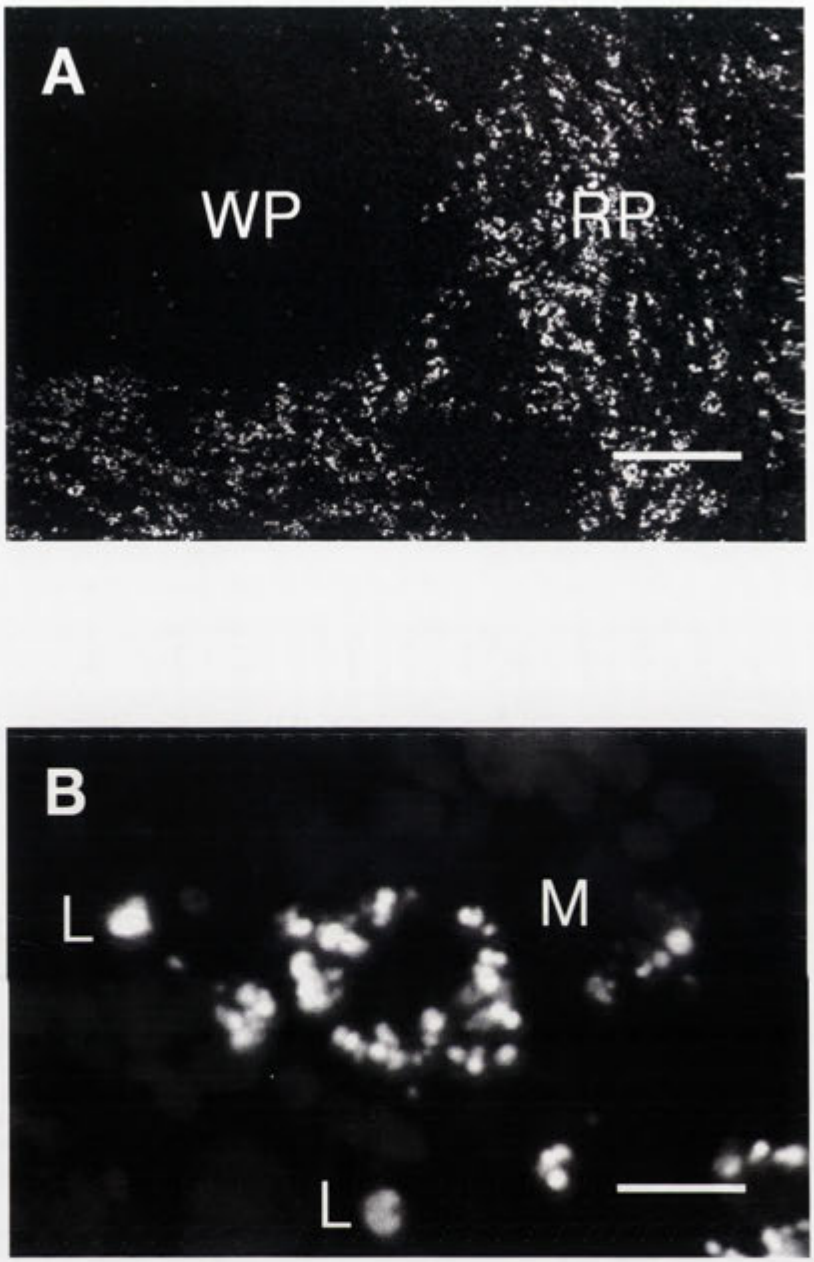

Figure 5.17: TUNEL staining of the spleen from an uninfected rabbit. (**A**) TUNEL$^+$ cells in the red and white pulp of the spleen. The majority of TUNEL signal in the red pulp localised to macrophages. Bar represents 150μm. (**B**) TUNEL$^+$ lymphocytes and macrophages in the red pulp of the spleen. The macrophage cytoplasm contains TUNEL$^+$ apoptotic bodies. Bar represents 15μm. RP, red pulp; WP, white pulp; L, lymphocyte; M, macrophage.

A

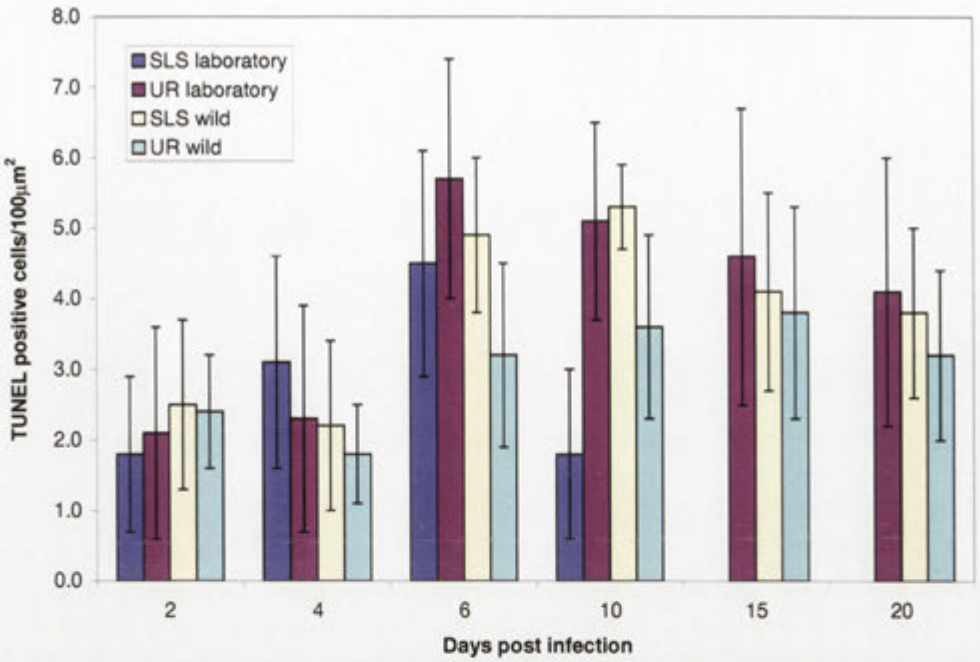

B

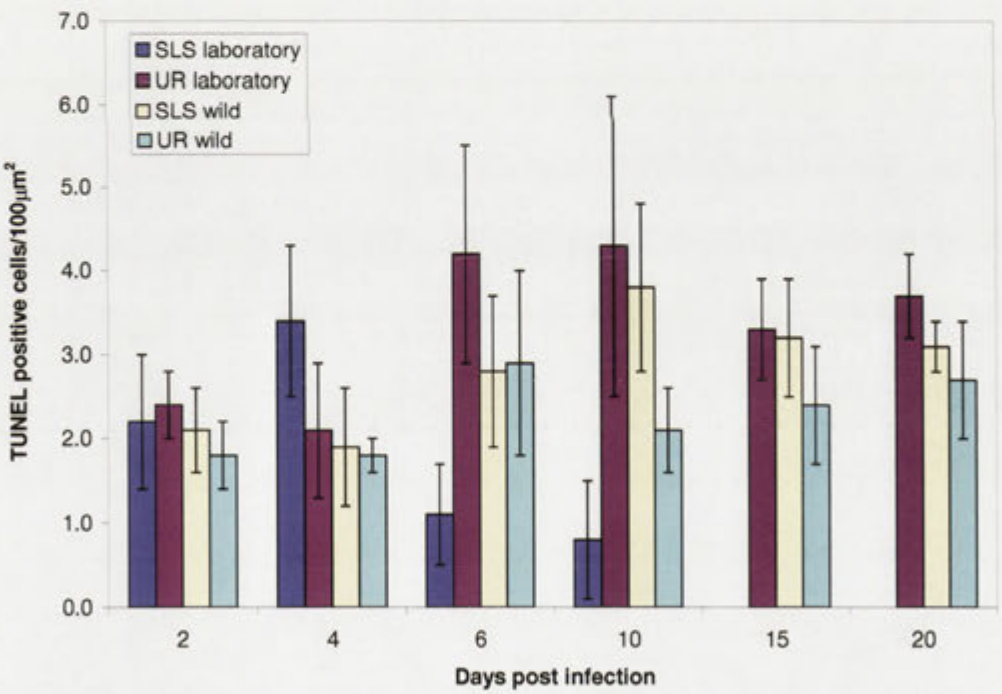

Figure 5.18: Numbers of TUNEL$^+$ cells in the (**A**) red pulp and (**B**) white pulp of spleens from SLS and Uriarra infected laboratory and wild rabbits (cells/100µm^2 ± SE). Using fixed tissue sections, the nucleus of cells containing fragmented DNA was labeled using the TUNEL reaction. A grid was superimposed over the field of view (5 fields were used per section, three tissue sections per tissue, see Table 4.1 for the number of rabbits at each time point) and up to 20 individual units of the grid counted. Day 0 has not been shown as this was not different to 2dpi.

Figure 5.19: TUNEL$^+$ cells in the spleen of SLS and Uriarra-infected laboratory rabbits at 10dpi. Bar represents 400μm. (**A**) TUNEL$^+$ cells in the white pulp of SLS-infected laboratory rabbits. (**B**) TUNEL$^+$ cells in the white pulp of Uriarra-infected laboratory rabbits. Bar represents 400μm. (**C**) TUNEL$^+$ cells in the red and white pulp of SLS-infected laboratory rabbits. Bar represents 400μm. (**D**) TUNEL$^+$ cells in the red and white pulp of Uriarra-infected laboratory rabbits. Bar represents 200μm RP, red pulp; WP, white pulp.

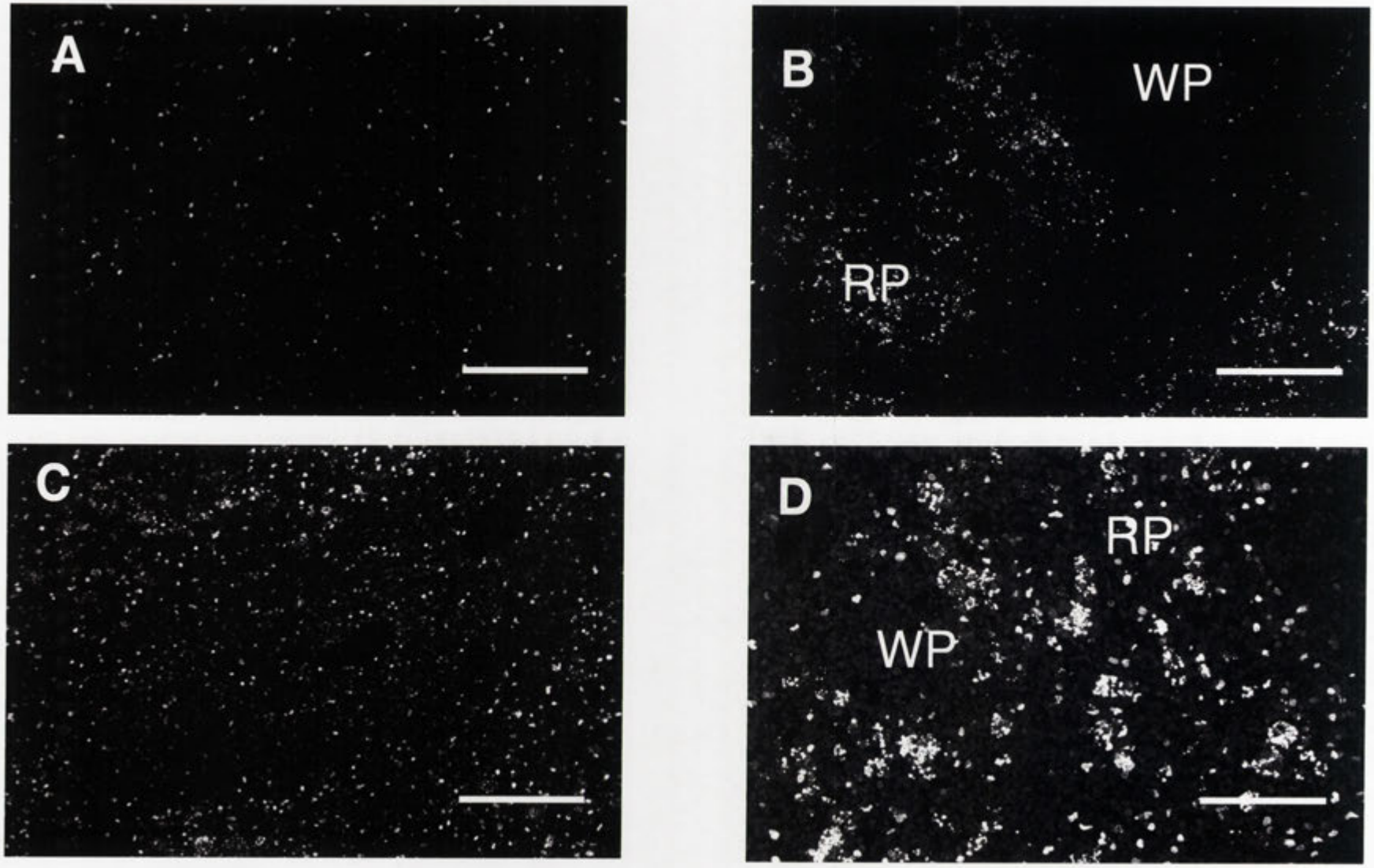
A
B
WP
RP
C
D
RP
WP

5.3.4 Infection of rabbits with myxoma virus deletion mutants, vMyxlacM11L$^-$, vMyxlacT5$^-$, vMyxlacT4$^-$ or vMyxlacT2$^-$

To examine if the myxoma virus genes known to function as inhibitors of apoptosis in infected cells are important in virus replication and transport from the primary inoculation site in the skin to the draining lymph node, laboratory rabbits were inoculated with vMyx-lac$^+$, or the vMyxlacM11L$^-$, vMyxlacT5$^-$, vMyxlacT4$^-$ or vMyxlacT2$^-$ myxoma virus gene-deletion mutants. These viruses were visualised in tissue sections of the primary inoculation site and the draining lymph node by immunofluorescence at 24 and 48 hpi. To examine the ability of these viruses to replicate at the primary inoculation site and the draining lymph node, and to disseminate to and replicate in the contralateral lymph node, virus titres were determined in these tissues at 6dpi.

5.3.4.1 Autopsy findings following infection of laboratory rabbits with myxoma virus-apoptosis gene deletion mutants or vMyx-lac$^+$

There were no gross changes at the inoculation site or in the draining or contralateral lymph nodes of rabbits at 24 or 48 hpi. The gross pathological changes following six days of infection of laboratory rabbits with myxoma virus-apoptosis gene deletion mutants or vMyx-lac$^+$ are summarised in Table 5.1 and described below.

At 6dpi with the control myxoma virus, vMyx-lac$^+$, the inoculation site was approximately 1.5cm in diameter, raised and red. The draining lymph node was enlarged to approximately three times normal size, and had localised patches of dark purple discolouration. The contralateral lymph node generally did not appear enlarged, but was slightly purple in colour.

At 6dpi with the vMyxlacM11L$^-$, the skin at the primary inoculation site was thickened, slightly raised and pink. Both the draining and contralateral lymph nodes were enlarged to approximately twice normal size, and the draining lymph node had small areas of purple discolouration. The primary inoculation sites of vMyxlacT2$^-$, vMyxlacT4$^-$ and vMyxlacT5$^-$ were raised and red, with the vMyxlacT2$^-$ primary lesion being the greatest in diameter and the vMyxlacT5$^-$ lesion the smallest. The draining lymph node following infection with all three viruses was grossly enlarged, at four to five times

normal size and very haemorrhagic in appearance. However, the contralateral lymph node following infection of rabbits with these viruses was generally not enlarged and remained ivory in colour.

Table 5.2: Autopsy findings at 6dpi of laboratory rabbits with myxoma virus deletion mutants and vMyxlac$^+$.

Myxoma virus deletion mutant	Primary inoculation site	Draining lymph node	Contralateral lymph node
vMyx-lac$^+$	1.5cm x 1.5cm, raised, red	3 x normal size, discoloured	not enlarged, slighty discoloured
vMyxlacM11L$^-$	thickened, pink *	2 x normal size, discoloured	2 x normal size, discoloured
vMyxlacT2$^-$	3cm x 1.5cm, raised, red	4 x normal size, purple	1.5 x normal size, not discoloured
vMyxlacT4$^-$	2cm x 1.5cm, raised, red	5 x normal size, purple	no change
vMyxlacT5$^-$	1cm x 1cm, slightly raised, red	4 x normal size, purple	no change

* lesion could not be accurately defined

5.3.4.2 Localisation of myxoma virus deletion mutants at 24 and 48hpi by immunofluorescence

At 24hpi, all five viruses were present in dendritic cells in the dermis, and in mononuclear cells in the paracortex of the draining lymph node. vMyx-lac$^+$, vMyxlacT5$^-$, vMyxlacT4$^-$ and vMyxlacT2$^-$ were present in the skin from all three rabbits inoculated with each virus, whereas vMyxlacM11L$^-$ was only present in the skin of two of three infected rabbits. At 48hpi, vMyx-lac$^+$, vMyxlacT5$^-$, vMyxlacT4$^-$, vMyxlacT2$^-$ and vMyxlacM11L$^-$ were present in dendritic cells of the dermis in all three rabbits inoculated with each virus. However, visually, the overall number of infected cells in the dermis from two rabbits inoculated with vMyx-M11L$^-$ was slightly less than those inoculated with vMyx-lac$^+$, vMyxlacT5$^-$, vMyxlacT4$^-$ or vMyxlacT2$^-$ (Figure 5.20).

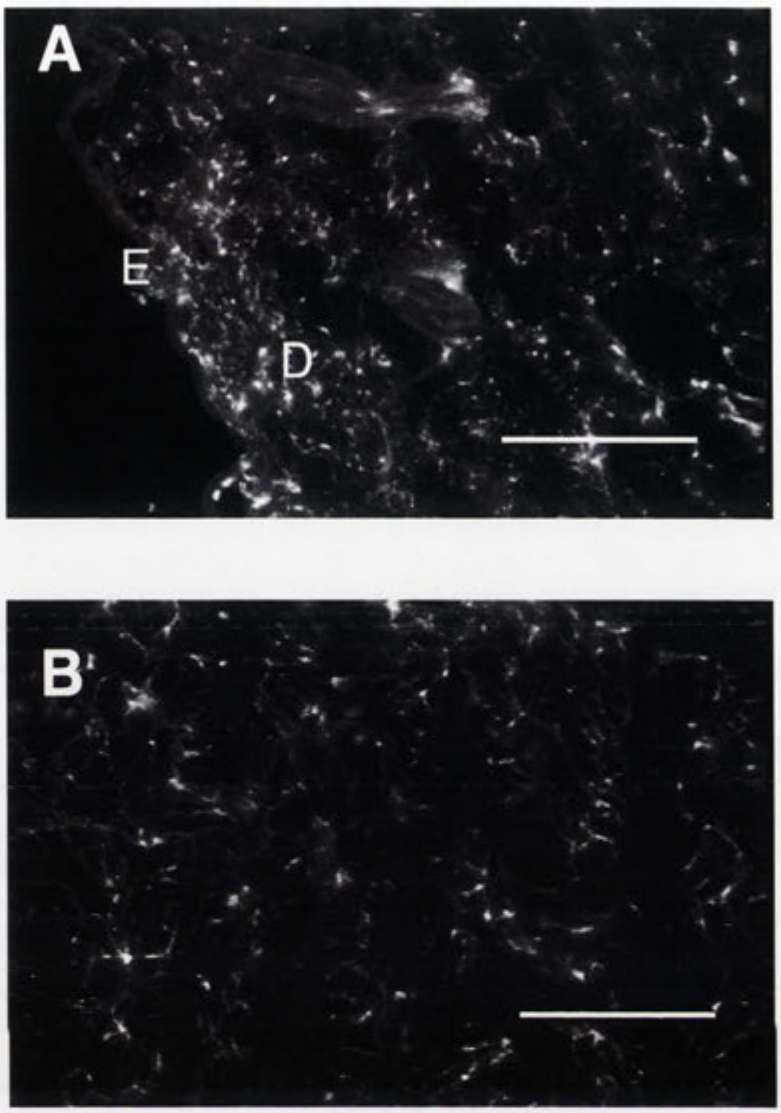

Figure 5.20: Localisation of vMyx-lac^{+} (**A**) and vMyxlacM11L^{-} (**B**) in the dermis of the primary inoculation site at 48hpi. E, epidermis; D, dermis. Bar represents 300μm.

vMyx-lac^{+}, vMyxlacT5^{-}, vMyxlacT4^{-} and vMyxlacT2^{-} were present in the paracortex of the draining lymph node at 24hpi in mononuclear cells resembling lymphocytes and macrophages. At 48hpi, all five viruses, including vMyxlacM11L^{-}, were present in lymphocytes positioned in continuous lines, one to three cells deep, spanning the cortex and paracortex of draining lymph nodes. Lymphocytes not contiguous with other lymphocytes or in clusters of 3 to 5 lymphocytes were also positive for myxoma virus in the draining lymph nodes of all infected rabbits at 48hpi.

5.3.4.3 Titres of virus in the primary lesion, draining and contralateral lymph nodes at 6dpi

Following intradermal inoculation, the titre of the control virus, vMyx-lac$^+$, was greater than 10^8 pfu/g at 6dpi in the primary lesions. At 6dpi, the titres of vMyxlacM11L$^-$ and vMyxlacT5$^-$ were 100-1000 fold less than the control virus in the primary inoculation site of two of three infected rabbits in each group. vMyxlacT2$^-$ and vMyxlacT4$^-$ were present in the primary lesion of all three infected rabbits in each group at titres approximately 10 fold less than the control virus (Figure 5.21A). In the draining lymph node at 6dpi, vMyx-lac$^+$ titres were greater than 10^6 pfu/g in all rabbits and reached a maximum titre of 1.3 x 10^8 in one infected rabbit. By 6dpi, vMyxlacM11L$^-$ and vMyxlacT5$^-$ were present at 10-100 fold lower titres, and vMyxlacT2$^-$ and vMyxlacT4$^-$ were present at approximately 10 fold lower titres, than the control virus, vMyx-lac$^+$ (Figure 5.21B). The control virus and all four gene-deletion mutant viruses disseminated to the contralateral lymph node. In this lymph node, vMyx-lac$^+$ titres ranged between 10^3 and 10^4 pfu/g. vMyxlacM11L$^-$ and vMyxlacT4$^-$ viruses were present in the contralateral lymph node of all three rabbits inoculated with either virus, although in two vMyxlacM11L$^-$-infected rabbits and in all vMyxlacT4$^-$ -infected rabbits, the titres were approximately 10 fold lower than following infection with the control virus. Virus was not present by 6dpi in the contralateral lymph nodes of one laboratory rabbit inoculated with vMyxlacT2$^-$ and in two rabbits infected with vMyxlacT5$^-$. Titres of virus present in the contralateral lymph nodes of vMyxlacT2$^-$ or vMyxlacT5$^-$ infected rabbits were 10^3 to 2.5 x 10^3 pfu/g (Figure 5.21C).

Figure 5.21: Virus titre at 6dpi in the primary lesion (**A**), draining lymph node (**B**) and contralateral lymph node (**C**) of laboratory rabbits infected with myxoma virus gene deletion mutants, vMyxlacM11L$^-$, vMyxlacT5$^-$, vMyxlacT4$^-$, vMyxlacT2$^-$ or the control virus, vMyxlac$^+$. Three rabbits were intradermally inoculated in the dorsum of the hind foot with 1000pfu of virus. Each column represents the titre of virus (pfu/g) for an individual rabbit. An asterix indicates virus was not detected by plaque assay. The limit of detection was 10^2 pfu/g tissue.

A

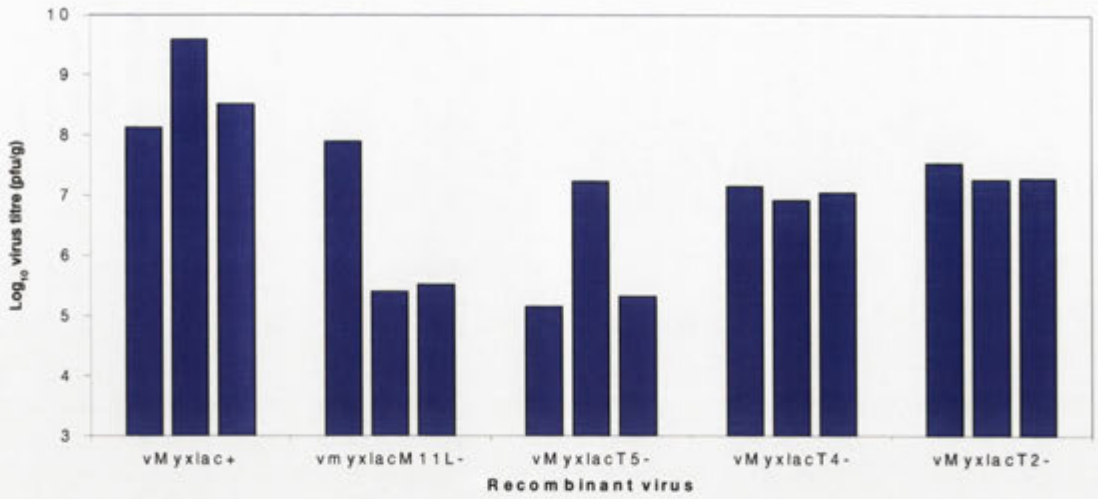
10
9
8
7
6
5
4
3
Log10 virus titre (pfu/g)
vMyxlac+
vmyxlacM11L-
vMyxlacT5-
vMyxlacT4-
vMyxlacT2-
Recombinant virus

B

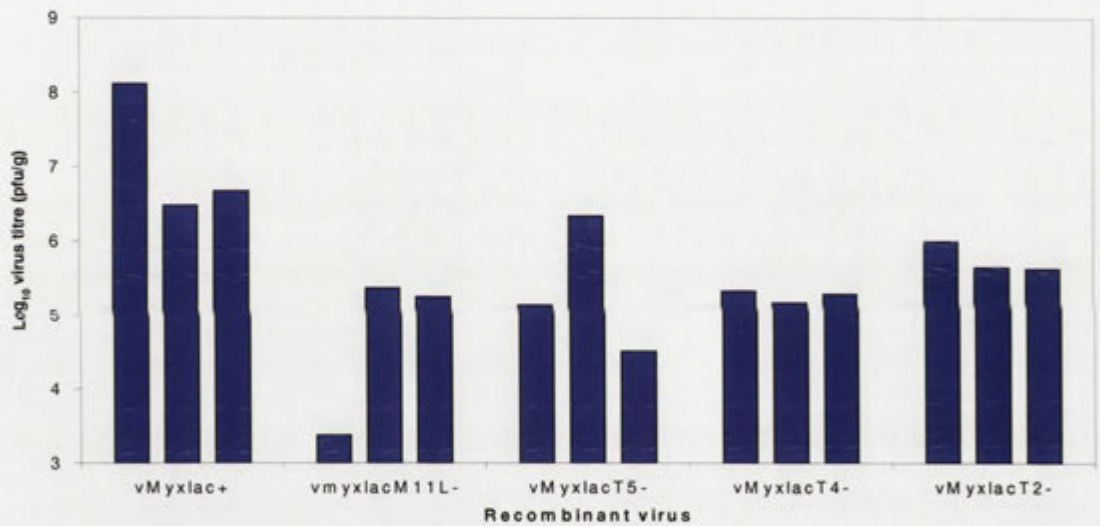
9
8
7
6
5
4
3
Log10 virus titre (pfu/g)
vMyxlac+
vmyxlacM11L-
vMyxlacT5-
vMyxlacT4-
vMyxlacT2-
Recombinant virus

C

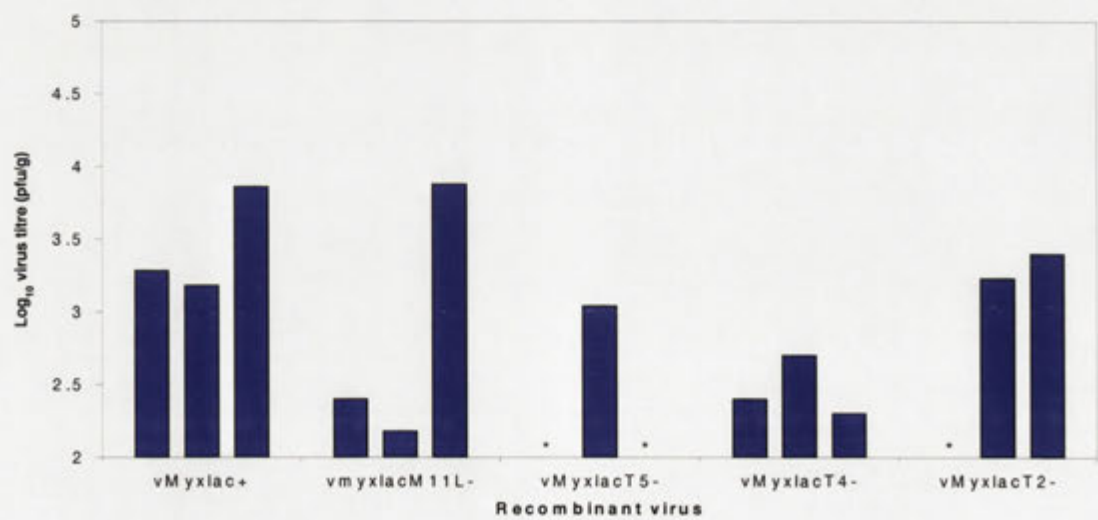
5
4.5
4
3.5
3
2.5
2
Log10 virus titre (pfu/g)
vMyxlac+
vmyxlacM11L-
vMyxlacT5-
vMyxlacT4-
vMyxlacT2-
Recombinant virus

5.3.4.4 Myxoma virus gene-deletion mutant plaque phenotypes on Vero cells

The titre of virus stocks was determined by plaque assay on Vero cells. The morphology of the plaques formed following infection of Vero cell monolayers with all five viruses as originally obtained following culture in BGMK cells was large and round, with vMyxlacM11L$^-$ yielding the plaques with the largest diameter after 6 days of culture, followed by vMyx-lac$^+$ and vMyx-T4$^-$. vMyxlacT2$^-$ and vMyxlacT5$^-$ yielded the plaques with the smallest diameter. Following six days of *in vivo* passage, the plaque morphology of vMyx-lac$^+$, vMyxlacT2$^-$, vMyxlacT4$^-$ and vMyxlacT5$^-$ did not change. However, infection of Vero cells with vMYX-M11L$^-$ after rabbit passage yielded large round plaques that had much smaller plaques in a tail formation to one side of the main plaque. These plaques are termed rocket plaques (data not shown).

5.4 Discussion

5.4.1 Cell permissivity to infection from wild rabbits

The experimental evidence presented in this thesis suggests that the control of SLS replication by wild rabbits demonstrated in Chapter 3 is mediated through the early activation of a more efficient immune response to infection compared to that of laboratory rabbits. However, the early restriction of virus replication in the draining lymph nodes of wild rabbits compared to laboratory rabbits could also have resulted from resistance at the level of cell permissivity to virus infection or replication, such as occurs in flavivirus resistant mice (reviewed in Shellam *et al.*, 1998). SLS replicated efficiently in primary cells from the spleen and lymph nodes of both resistant and susceptible rabbits and similar results were obtained in primary fibroblasts. In both cases, similar proportions of cells were infected. This suggests that the permissivity of rabbit cells to virus infection is not a crucial factor in genetic resistance to myxoma virus, and supports the hypothesis that control of myxoma virus replication in wild rabbits is mediated by the immune response.

5.4.2 The induction of apoptosis in the lymph nodes and spleen of myxoma virus-infected rabbits

The depletion of lymphocytes from the lymph nodes and spleen of laboratory rabbits

infected with virulent myxoma virus has been a constant histological finding in both this and previous studies (Hurst, 1937a). However, lymphocyte depletion was much more extensive in SLS-infected laboratory rabbits compared to Uriarra infection. Apoptosis was a major mechanism of cell death of lymphocytes in lymph nodes in both laboratory and wild rabbits infected with either SLS or Uriarra. In all rabbits, apoptosis occurred only in lymphocytes that did not contain virus antigen. However, the timing and distribution of apoptosis throughout the lymph nodes of SLS-infected laboratory rabbits was substantially different to all other infections.

Lymphocyte depletion was most obvious in SLS infections. That is, it was a function of virus virulence. Histologically, lymphocytes in infected lymph nodes were apoptotic. It was hypothesised that the cell depletion was due to apoptosis. However, staining of lymph nodes from all the infections showed that extensive apoptosis was a feature in lymph nodes whether or not cell depletion was occurring. Thus, apoptosis of lymphocytes, while a major feature of myxoma virus infection, was not sufficient to explain the extensive loss of lymphocytes from SLS-infected lymph nodes. Despite this, there was a correlation between lethal infection and earlier induction of apoptosis in lymph nodes. Thus, SLS-infected laboratory rabbits had extensive apoptosis at 4dpi whereas all other infections only showed background apoptosis at this time point. This is despite relatively similar titres of virus in Uriarra and SLS-infected laboratory rabbits (Chapter 3). It is possible that the early induction of apoptosis removes a critical population(s) of lymphocytes for the subsequent control of virus replication and that the later apoptosis is associated with an ongoing activation of lymphocytes during an immune response.

The mechanisms of induction of apoptosis following infection with myxoma virus have not been determined. Apoptosis did not occur in lymphocytes in which viral antigen could be detected. In SLS-infected laboratory rabbits it was occurring in lymphocytes adjacent to these cells. However, in all other infections, lymphocytes undergoing apoptosis were not closely associated with lymphocytes infected with virus. This supports the idea that in SLS-infection of laboratory rabbits, the mechanism of induction of apoptosis may be different than during other infections and may be a direct viral effect, perhaps by triggering apoptosis on virus-binding to adjacent cells, or an indirect effect due to activation of adjacent cells. The role, if any, of infected interdigitating dendritic cells in this remains to be determined.

Binding of vaccinia virus to non-permissive cells has been shown to induce apoptosis (Ramsey-Ewing and Moss, 1998). Following myxoma virus infection *in vitro,* around 50% of lymph node primary cells did not become infected. Apoptosis of these cells has not been reported (Barry *et al.*, 1997; Macen *et al.*, 1996b; Mossman *et al.*, 1996a; Schreiber *et al.*, 1997) and was not examined in my study. It is possible that in the environment of the lymph node, these cells do undergo apoptosis on non-permissive infection with SLS. This explanation is not completely satisfactory unless there is a significant difference between SLS infection in wild rabbit lymphocytes and laboratory rabbits, which was not apparent *in vitro.* One possible explanation is a difference in the proportion of extracellular enveloped versus intracellular mature virus (EEV and IEV, repectively) particles produced in each case, and possibly in Uriarra versus SLS infection, and the relative importance of the different surface proteins of these virus phenotypes in the interactions between virus and cell-surface proteins. Apoptosis of non-permissive cells would prevent virus infection and therefore be a defence mechanism. Without ruling this out, the lack of proximity to infected cells in SLS-infected wild rabbits or Uriarra-infected laboratory rabbits, and the fact that apoptosis continues in lymph nodes after virus is no longer detectable further suggests that apoptosis is not a defence mechanism against virus infection of lymphocytes in these animals, but is a part of the activation of the immune response.

Apoptosis is an important regulatory mechanism in immune activation, involved in the selection of lymphocytes capable of specifically interacting with antigen, the regulated cell death of lymphocytes that are partially activated by signaling with cytokines or ligands but are not capable of specifically recognising viral antigen, and the eventual reduction of clonally expanded, antigen-reactive, lymphocyte populations (Rudin and Thompson, 1997). Apoptosis is also an important killing mechanism of virus-infected cells by CTLs (through Fas and serine proteinase mediated mechanisms) or via signaling through the TNF receptors (Atkinson and Bleackley, 1995; Henkart, 1994). Myxoma virus produces multiple inhibitors of apoptosis in infected lymphocytes, including the intracellular form of the T2 protein which inhibits TNF/Fas-mediated apoptosis (Schreiber *et al.*, 1997; Sedger and McFadden, 1996), and the Serp2 protein, which inhibits interleukin-1β-converting enzyme (ICE) (Messud-Petit *et al.*, 1998; Petit *et al.*, 1996), a serine protease involved in Fas, TNF and granzyme B mediated pathways of apoptosis (reviewed in McFadden and Barry, 1998; Turner and Moyer, 1998). In myxoma virus-infected rabbits, apoptosis of cells positive for virus was not

observed suggesting that anti-viral CTL-mediated cell death was not the major contributor to apoptosis of lymphocytes in infected lymph nodes.

A possible model for the lymphocyte pathology in myxomatosis is provided by African swine fever virus (ASFV) in pigs. Significant apoptosis occurs in lymphocytes in infected lymph nodes but these lymphocytes are not infected with virus (Oura *et al.*, 1998a). The lymphocyte cell death has been attributed to virus infection of monocytes which then stimulate inappropriate cell death in lymphocytes. Interestingly, wild bush pigs which are resistant to ASFV control virus replication in lymph nodes and this is associated with reduced numbers of apoptotic lymphocytes (Oura *et al.*, 1998b).

5.4.3 The role of M11L, MT-2, MT-4 and MT-5 in virus replication and dissemination *in vivo*.

A model was proposed in Chapter 4 in which myxoma virus replicates initially in dermal dendritic cells and disseminates in these cells to the draining lymph node. Replication in the lymph node then occurs in T-lymphocytes and these cells are critical for further dissemination. The importance of virus replication in dendritic cells and lymphocytes for dissemination was investigated by examining the *in vivo* replication of gene-deletion mutants which are partially defective for replication in lymphocytes *in vitro,* and are attenuated in rabbits (Barry *et al.*, 1997; Graham *et al.*, 1992; Macen *et al.*, 1996b; Mossman *et al.*, 1996a; Opgenorth *et al.*, 1992; Schreiber *et al.*, 1997). These genes are M11L, T2, T4 and T5, which are each involved in the inhibition of apoptosis in infected lymphocytes via different pathways.

Deletion of M11L was associated with fewer infected dendritic cells in the skin of the primary inoculation site than with the other viruses, which were not different from the control virus. The control virus vMyxlac$^+$ grew to 1000 fold greater titres in the skin of rabbits than in two of three rabbits infected with either vMyxlacM11L$^-$ or vMyxlacT5$^-$, and to 10 fold greater titres than vMyxlacT2$^-$ and vMyxlacT4$^-$. All viruses reached the draining lymph node in all infected rabbits by 48hpi. The transport of vMyxlacM11L$^-$ to the draining lymph node was possibly delayed as all other viruses were detected at 24hpi. Titres of gene-deletion mutants in the draining lymph node were not particularly different from each other at 6dpi, although they were considerably lower than the control virus, vMyx-lac$^+$. Antigen was detected in lymphocytes in the draining lymph

node in all virus infections. Thus, in infected rabbits, virus was able to replicate in lymphocytes. However, far more lymphocytes were infected in the lymph nodes of rabbits infected with vMyx-lac$^+$, which was also present in cells of the lymph node capsule.

The main differences between replication of the control virus and the gene-deletion mutants was in the contralateral lymph node. At 6dpi, titres were lower for all viruses compared to the draining lymph node. Two animals infected with vMyxlacT5$^-$ and one animal infected with vMyxlacT2$^-$ had no detectable virus in the contralateral lymph node and the titres of vMyxlacM11L$^-$ and vMyxlacT4$^-$ were generally lower than vMyx-lac$^+$. At 48hpi, virus was present in the contralateral lymph node of two of three rabbits infected with vMyx-lac$^+$, but was not present in the contralateral lymph nodes of any other virus-infected rabbits.

Virus replication was limited in the gene-deletion mutants compared to the control virus, with reduced titres in the skin and lymph nodes. However, all viruses replicated in dendritic cells and reached the draining lymph node, and in some animals, virus reached the contralateral lymph node. It is interesting that replication in dendritic cells and lymphocytes occurred *in vivo* and that virus was able to reach distal lymph nodes. Obviously the presence of virus in a lymph node was not enough to ensure efficient replication of that virus. This is similar to results obtained with SLS and Uriarra in resistant rabbits and suggests that the host response to the virus will determine if the virus replicates to high titres. In this study it was not possible to dissect out whether low virus titres of the gene-deletion mutants were due to enhanced inflammatory and immune responses of the rabbits or poor replication of virus in critical cells. Thus, infection of rabbits with the gene-deletion mutants did not provide a good model for examining the importance of viral replication in particular cell types in virus dissemination.

The growth and dissemination of myxoma virus and the control of virus replication by the host will undoubtedly involve very complex signaling between the virus and the host cell, as well as signaling between host cells in the context of an immune response. The deletion of individual viral genes is essential to investigate gene and protein function, as well as providing indications as to what type of selection pressures have been important in the evolution of the virus. However, infection of rabbits with these

viruses shows that the individual functions of viral genes are not well defined *in vivo*, and that the attenuation of these viruses is more complex than can be explained by impaired replication in lymphocytes. The study of *in vivo* models of virus pathogenesis is thus highly important in the understanding of virulence and genetic resistance.

Chapter 6: Final Discussion

6. Final Discussion

The coevolution of myxoma virus and the European rabbit is one of the best described examples of host-pathogen coadaptation (Fenner and Ratcliffe, 1965). However, while the development of genetic resistance in the rabbit and the consequences for biological control have been well described, there was remarkably little information on the pathogenesis of myxoma virus, particularly in resistant rabbits. This thesis has presented a detailed study of the pathogenesis of two strains of myxoma virus, the highly virulent SLS and the naturally attenuated Uriarra. By using wild rabbits naturally selected for genetic resistance, I have focussed on the interactions of myxoma virus with the rabbit immune system and the role of particular cell types in virus replication and dissemination.

6.1 Myxoma virus pathogenesis

In Chapter 2, I examined the differences in the immune responses of rabbits to virulent and attenuated strains of myxoma virus and showed that the virulent virus suppressed T-cell responses to mitogens. In addition, virulent virus caused the almost total loss of lymphocytes from the lymph nodes and suppressed the rabbits' ability to mount an antibody response to a coexpressed antigen.

The lymphoid tissues and skin are critical for myxoma virus pathogenesis. In Chapter 3 I compared the titres of virulent and attenuated strains of myxoma virus in these tissues and for the first time, examined the titres in resistant wild rabbits. This demonstrated that wild rabbits were able to control virus replication very early in infection at the lymph node draining the skin inoculation site and also controlled replication in distal sites to which the virus disseminated. In contrast, laboratory rabbits infected with attenuated virus mostly controlled replication at distal sites following dissemination.

Using immunofluorescence to localise viral antigen, in Chapter 4, the initial cells in which myxoma virus replication occurred were MHC II positive cells in the dermis. Virus replication subsequently occurred in cells of the epidermis and the draining lymph node. The predominantly lymphocytic inflammatory response to virus infection by SLS-infected wild rabbits and Uriarra-infected rabbits indicated a difference between

the ability of SLS and Uriarra to modulate the inflammatory response and that wild rabbits could overcome the modulation caused by SLS. Massive depletion of lymphocytes occurred in SLS-infected lymph nodes in laboratory rabbits. This was a direct effect of virus infections because although apoptosis was a major feature of all infected nodes, this occurred in both SLS and Uriarra infected rabbits and continued after virus was largely cleared from the nodes (Chapter 5). Apoptosis did not occur in lymphocytes productively infected with virus. Importantly, SLS infected laboratory rabbits had earlier apoptosis and the cell death was adjacent to virus infected cells. *In vitro,* fibroblasts and lymphoid cells from wild rabbits supported myxoma virus replication equivalently to the same cells from laboratory rabbits. This showed that cell permissivity was not the cause of resistance and confirmed the immunofluorescence results from Chapter 4 where virus was present in the same cell types in wild and laboratory rabbits.

The molecular basis of attenuation of Uriarra compared to SLS is not understood. The viruses have similar replication rates in tissue culture and a similar cell host range *in vitro* [P.Kerr, unpublished]. As far as is known, both SLS and Uriarra produce the same functional proteins involved in modulation of the immune response. These include the proteins known to inhibit apoptosis of infected lymphocytes *in vitro*, as well as the IFNγ receptor homolog [P.Kerr, unpublished results]. In addition, both SLS and Uriarra downregulate MHC I on the surface of infected cells [P.Kerr, unpublished], suggesting that CTL responses are potentially limited during infection with either virus. Hence, at present, there is no molecular basis for the difference between the ability of the two viruses to modulate the immune response. Using Uriarra as the attenuated model virus does not provide the detail concerning individual genes and their functions that single gene knock-out viruses do. However, Uriarra provides a model of a naturally attenuated virus and allows the examination of the phenotypic events occurring in infection of laboratory and wild rabbits, and the events associated with replication, dissemination and control of an attenuated virus. Similar survival rates of Uriarra-infected laboratory rabbits and SLS-infected wild rabbits also suggested that this was a very useful model to compare pathogenesis and resistance. Obviously it is not possible to make the sort of molecular conclusions in outbred animals that can be made in models using inbred, knock-out or transgenic mice. However, while these systems are very powerful for examining immunological mechanism, they may not provide a good model for what happens in an outbred population of animals naturally infected in the field.

6.2 Models of myxoma virus pathogenesis in laboratory and wild rabbits

The models of myxoma virus pathogenesis for laboratory and wild rabbits infected with either SLS or Uriarra are presented in Figure 6.1, and highlight a series of important points concerning virus replication and the control of this replication. Firstly, both SLS and Uriarra replicated in dendritic cells in the dermis at the primary inoculation site, followed by replication in the epidermis. At this site, both viruses reached titres greater than 10^7 pfu/g suggesting that both viruses could be transmitted by mosquitoes from the primary lesion of either laboratory or wild rabbits (Day *et al.*, 1956; Fenner, Day, and Woodroofe, 1956). Resistance to infection and control of virus replication was not mediated by a block in the transport of virus to the draining lymph node, although in Uriarra-infected wild rabbits, the spread of virus to this node was delayed compared to the other infections.

Events in the draining lymph node were critical in determining whether virus replication was uncontrolled and virus rapidly disseminated to tissues including other lymph nodes, the spleen, lung and secondary sites in the skin, as occurred during SLS-infection of laboratory rabbits (Figure 6.1A), or if virus replication and dissemination were constrained. Titres of Uriarra in the draining lymph node of laboratory rabbits were similar to those in SLS-infected laboratory rabbits until 6dpi, after which time virus replication was controlled, leading to the eventual clearance of virus from this tissue (Figure 6.1B). Uriarra reached distal tissues later than SLS and replicated to lower titres in these tissues. Thus both dissemination to distal tissues and replication were controlled, except for the spleen where similar titres were reached. Uriarra titres in the distal skin did not reach 10^7 pfu/g, suggesting that this virus could not be transmitted from this sample of skin. However, transmission of Uriarra may occur from secondary lesions that formed over the nose and eyelids of infected laboratory rabbits (Day *et al.*, 1956; Fenner, Day, andWoodroofe, 1956; Fenner and Woodroofe, 1953). Anti-viral antibody was produced by these rabbits. However, laboratory-rabbits infected with SLS produced earlier and higher titres of virus-specific antibody than Uriarra-infected rabbits, suggesting that antibody was not critical in the control of virus replication. Rather, the observation that Uriarra replication was restricted from 6dpi suggests a role for CTL responses in virus clearance from laboratory rabbits.

Figure 6.1: Models of the replication and control of virulent and attenuated myxoma virus in infected laboratory and wild rabbits. Following intradermal inoculation at the skin, both Uriarra and SLS replicated in dermal dendritic cells and the epidermis, and all viruses were transported to the draining lymph node. In SLS-infected laboratory rabbits, virus replicated to high titres in the draining lymph node, rapidly disseminated to distal tissues and secondary sites in the skin, where it grew to high titres. The dissemination of Uriarra to distal tissues was reduced compared to SLS in infected laboratory rabbits. The draining lymph node may be important in the control of this dissemination and subsequent replication of Uriarra in distal tissues. Control of both SLS or Uriarra by wild rabbits occurred at the draining lymph node. All rabbits produced anti-viral antibody. Based on the timing, control of virus replication by laboratory rabbits is hypothesised to involve CTL responses; in wild rabbits, both NK cells and CTLs may be involved. Arrows represent virus dissemination. Uncontrolled virus replication in tissues or uncontrolled dissemination are both indicated in red. Control of virus replication or dissemination is indicated in green. Hypothesised (indicated by **?**) and known immune responses are indicated in blue. Transmission indicates measurement of 10^7 pfu/g of skin at the primary inoculation site and distal skin.

A SLS infected laboratory rabbits

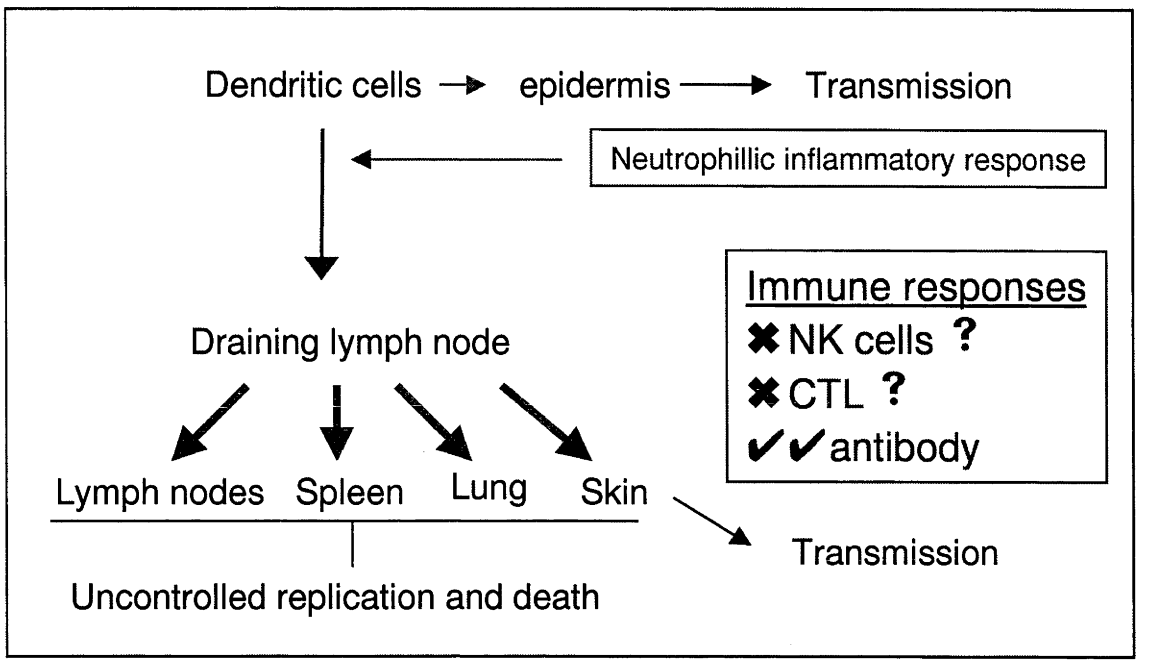

B Uriarra infected laboratory rabbits

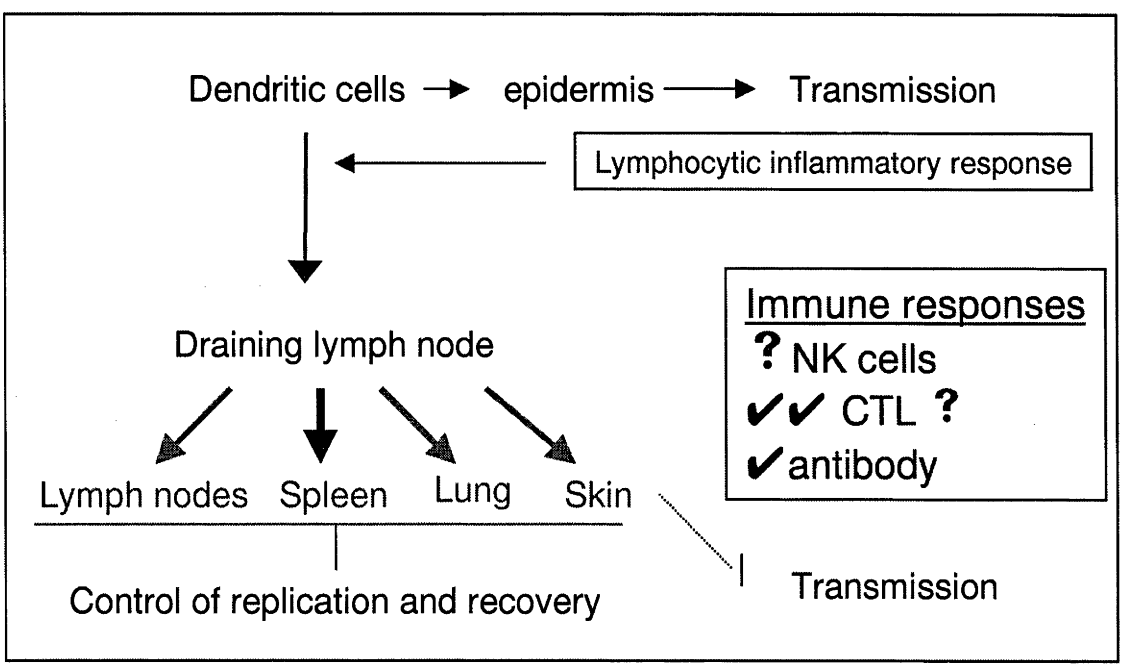

C SLS infected wild rabbits

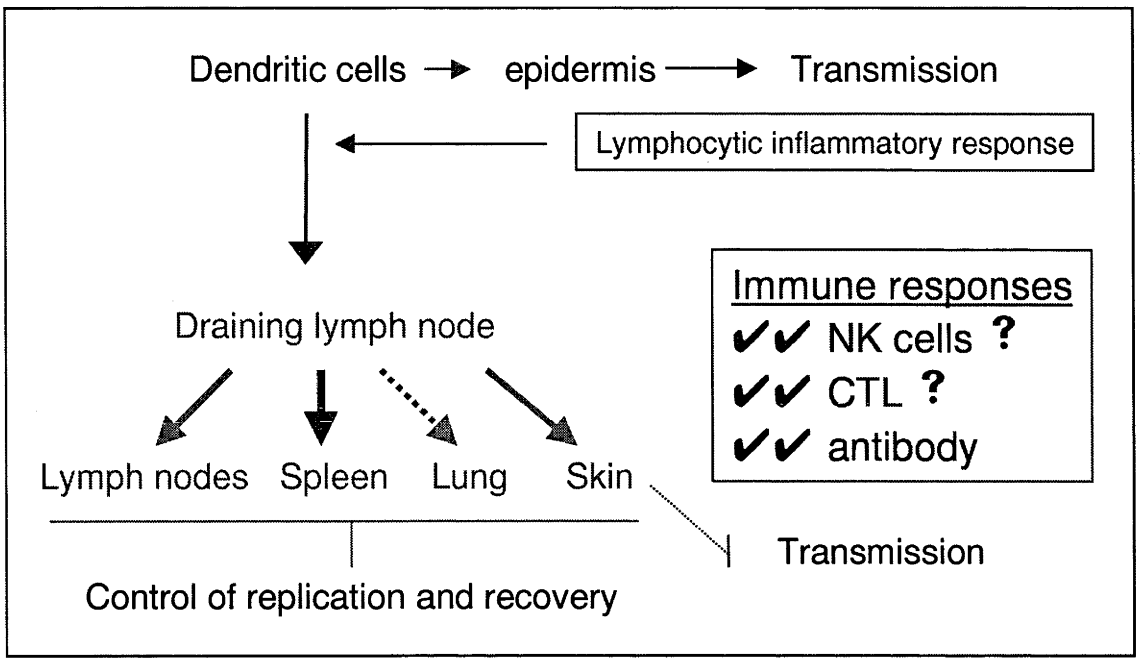

D Uriarra infected wild rabbits

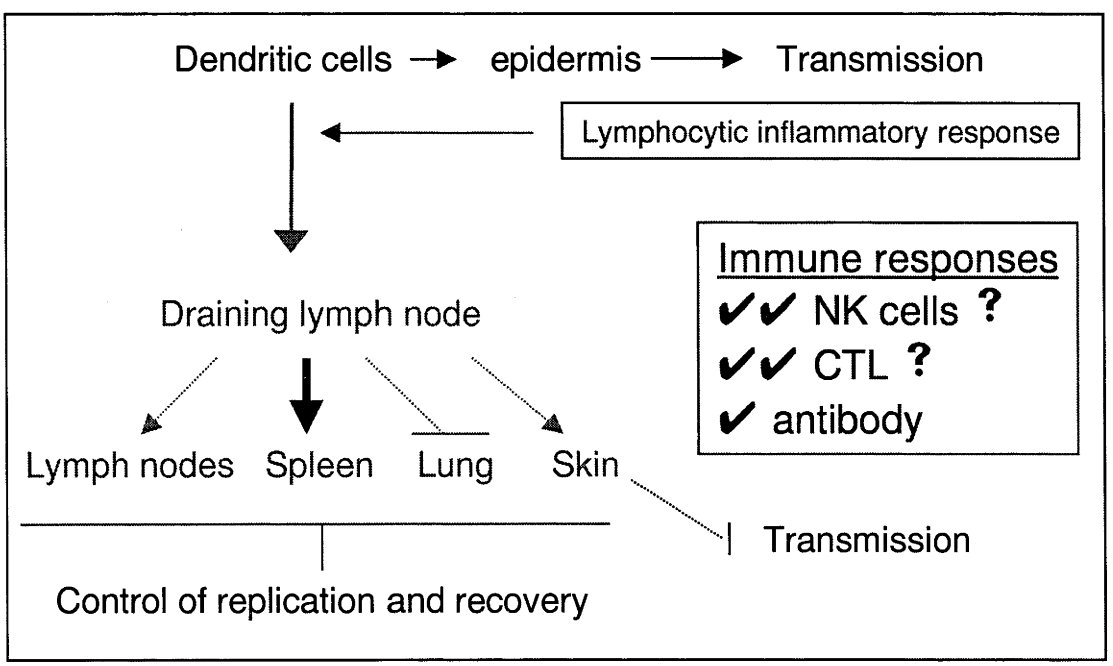

The draining lymph node was important for the control of myxoma virus replication in wild rabbits (Figure 6.1C). This control occurred earlier in SLS-infected wild rabbits than in Uriarra-infected laboratory rabbits based on the lower titres of virus. Similarly to Uriarra-infected laboratory rabbits, SLS dissemination from the draining lymph node to other tissues was constrained as it reached distal tissues later than SLS in infected laboratory rabbits, except for the spleen. SLS reached the distal skin site of wild rabbits, but did not replicate in the epidermis as efficiently as SLS in laboratory rabbits, and reached titres no greater than approximately 10^5 pfu/g. Hence, virus still reached distal tissues but was locally controlled. This control was associated with a rapid and concentrated lymphocytic inflammatory response at the distal skin. I hypothesise that early control at the draining lymph node may be due to enhanced NK cell activity and probably more effective INF α/β activity. This is then followed or accompanied by an early CTL response. High titres of virus-specific antibody were produced by wild rabbits in response to infection with SLS, and this may also be important in the restriction of virus spread (Vanderplasschen *et al.*, 1997), such as that in the distal skin. Despite this control, SLS may have been transmitted from the distal skin of the one wild rabbit in which secondary lesions containing greater than 10^7 pfu/g of virus formed, and from the secondary lesions on the face. However, these lesions rapidly scabbed over, which would limit the time virus was accessible to mosquitoes, and thus reduce the probability of transmission (Day *et al.*, 1956).

Wild rabbits infected with Uriarra limited virus dissemination and replication to the draining lymph node and to other lymph nodes, the lung and distal skin (Figure 6.1D). Transmission of Uriarra from the skin of infected wild rabbits is unlikely to occur as virus did not grow to high titres and did not cause secondary lesion formation on the face. It is interesting that despite the generalised limitation of dissemination and replication, Uriarra was able to initially replicate just as efficiently in the primary inoculation site and the spleen of wild rabbits as SLS or as Uriarra in infected laboratory rabbits. However, the actual primary lesion was smaller in Uriarra-infected wild rabbits, suggesting control of virus replication does occur in the skin, but may be dependent on effector cells generated elsewhere.

The orchestration of immune responses to viral pathogens depends on the efficient delivery of stimulatory signals, such as cytokines and antigen, to appropriate effector cells such as NK cells, $CD4^+$ and $CD8^+$ T-cells, and B-cells. Cytokines, such as IFNs

and TNF, can also have direct antiviral affects (Ramshaw *et al.*, 1997). The most potent cells involved in the delivery and organisation of this response are dendritic cells (Banchereau and Steinman, 1998). Following viral infection, the activation of dendritic cells by viral antigen and the appropriate growth factors such as IL-1, TNF and/or GM-CSF (granular macrophage-colony stimulating factor), begins a cascade of stimulatory signals which activate effector cells involved in the clearance of virus infection (Caux *et al.*, 1992). A very early response of dendritic cells is to produce IL-12. IL-12 activates NK cells which recognise and kill virus-infected cells. NK cell recognition of target cells is enhanced by low levels of MHC I expression (Trinchieri, 1995). NK cells are also an early source of high levels of IFNγ that, along with IL-12 produced by dendritic cells, stimulates $CD4^+$ T-cell precursors to secrete TNF and IFNγ, and hence become T_H1 T-cell clones. The co-stimulation of $CD4^+$ T-cells with antigen in association with MHC II by dendritic cells results in further communication between these two cell types through CD40/CD40 ligand (Schoenberger *et al.*, 1998). This enables or 'conditions' dendritic cells to stimulate $CD8^+$ T-cells to become antigen-specific killer cells (or cytotoxic T-lymphocytes; CTL) through the continued production of IL-12, and through direct signaling with antigen associated with MHC I (Banchereau and Steinman, 1998). IFNγ produced by both NK cells and $CD4^+$ T-cells also stimulates $CD8^+$ T-cells.

Dendritic cells are the first cells to become infected with myxoma virus in the skin, and probably transport virus to initiate virus infection in the draining lymph node. Infection of dendritic cells could interfere with cellular gene transcription and protein synthesis, thus disrupting cell function. In addition, myxoma virus is known to downregulate the cell surface proteins, MHC I and $CD4^+$ (Barry *et al.*, 1995; Boshkov *et al.*, 1992). This has the potential to prevent the recognition and stimulation of effector cells. Myxoma virus also encodes proteins that may interfere directly with the responses of dendritic cells and associated effector cells. In particular, myxoma virus-produced proteins interfere with the action of TNF α/β, INFγ, IL-1 and chemokines (Graham *et al.*, 1997; Lalani *et al.*, 1998; McFadden and Graham, 1994; Mossman *et al.*,, 1995a; Schreiber and McFadden, 1994; Schreiber *et al.*, 1997; Upton *et al.*, 1992). Myxoma virus also modulates immune responses through proteins with as yet undefined functions, such as M11L and the serpins, serp1 and serp2 (Macen *et al.*, 1993; Opgenorth *et al.*, 1992, Graham, 1992; Petit *et al.*, 1996; Upton *et al.*, 1990). In addition, the entire sequence of myxoma virus has not been determined and it is likely that additional immune-regulatory proteins remain to be discovered. Based on strategies of immune modulation

by other poxviruses, myxoma virus has the potential to affect IFN α/β and complement mediated responses. Infection of dendritic cells with myxoma virus thus has the potential to affect immune responses on many different levels and create a milieu in which immune function is severely compromised, both in the skin and the draining lymph node.

A specific potential example of this following myxoma virus infection of dendritic cells is the modulation of immune responses through chemokines. Following stimulation, dendritic cells produce chemokines to attract effector cells and increase the probability of contact with, and stimulation of, lymphocytes capable of reacting specifically to antigen (Banchereau and Steinman, 1998). Myxoma virus produced chemokine binding proteins inhibit the CC chemokine-mediated chemotaxis of mononuclear lymphoid cells *in vitro* (Lalani *et al.*, 1998). These myxoma virus-produced binding proteins do not inhibit CXC-mediated neutrophil chemotaxis *in vitro*. If this translates directly to the infection of dendritic cells *in vivo,* the local environment at sites of infection will be dominated by stimulatory signals associated with neutrophil granule release. This is consistent with the inflammatory response of laboratory rabbits to SLS infection in the skin. Although neutrophils have been shown to have an anti-viral function (Lidbury *et al.*, 1995; Tumpey *et al.*, 1996; West *et al.*, 1987), the generation of signals in this response will not be balanced through cytokine production by mononuclear cells involved in the promotion of specific anti-viral immune responses, and will result in continued inappropriate signaling of cell responses. Thus, infection of dendritic cells by myxoma virus need only initiate an inappropriate response; the cascade of signals between cells will serve to amplify it.

In a model of myxoma virus pathogenesis, I propose that infected dendritic cells are crucial in determining the interactions of the immune response both in the skin and in the draining lymph node. Further, that infection of dendritic cells with SLS results in inappropriate signaling between cells and the severe modulation of anti-viral immune responses. In the lymph nodes, SLS-infected of dendritic cells (interdigitating dendritic cells) may partially activate $CD4^+$ T-cells via the presentation of antigen but fail in the delivery of appropriate soluble signals to T-cells through their inhibition by viral proteins. Partially activated T-cells may be in a state of anergy and thus unable to respond to the *in vitro* stimulation with mitogens. This would render them highly susceptible to activation-induced cell death (AICD). The early death of these cells

would greatly restrict the T-cell help available for the generation of anti-viral $CD8^+$ CTL, and contribute to the failure of the rabbit to control virus replication. Indeed, murine T_H1 clones have been shown to preferentially undergo AICD via the Fas pathway of activation (Varadhachary *et al.*, 1997).

T-cell responses to mitogen were not significantly altered in Uriarra-infected rabbits (see Chapter 2), and thus T-cells are potentially available to supply help for the stimulation of anti-viral CTL in these rabbits. Uriarra infected similar numbers of dermal dendritic cells as SLS. Nevertheless, Uriarra reached distal tissues of laboratory rabbits later than SLS, and it may be that this control of virus dissemination occurred at the level of the draining lymph node. Within this model of myxoma virus pathogenesis, it is possible that Uriarra-infected dendritic cells present antigen in association with the crucial co-stimulatory signals, resulting in the efficient generation of anti-viral $CD8^+$ CTL. This is consistent with the timing of the control of virus replication, and the lymphocytic inflammatory response to Uriarra-infection in the skin.

6.3 A model of genetic resistance to myxoma virus infection

The mechanisms of immune modulation employed by SLS and Uriarra strains of myxoma virus in infected laboratory rabbits will still be operational in infected wild rabbits. However, the wild rabbits are able to overcome this modulation, control virus replication and recover from infection. Similarly to Uriarra-infection of laboratory rabbits, the control of SLS-infection of wild rabbits is mediated at the draining lymph node, and is associated with a lymphocytic inflammatory response in the skin. However, titres of SLS in the draining lymph node of wild rabbits were somewhat lower than Uriarra in laborator rabbits. This suggests that the control of SLS replication in wild rabbits occurs earlier than control of Uriarra in laboratory rabbits. The earliest anti-viral effector cells are likely to be NK cells as these do not require the adaptive arm of the immune response. In the figures of virus pathogenesis (Figure 6.1), I have suggested that two levels of resistance are operating. Firstly, unselected rabbits infected with attenuated virus are able to mount an effective CTL response and limit virus replication in distal tissues, possibly by INF α/β action making cells resistant to infection as well as by direct killing of virus infected cells. Secondly, in resistant rabbits, control of SLS replication occurs earlier in the draining lymph node and here I postulate an effective NK cell response together with by INF α/β and an earlier CTL

response. However, this does not completely clear the virus from this tissue in one rabbit at each late time point. This is probably a reflection of two things; drainage of virus from the skin and the outbred nature of the rabbits leading to variation in resistance.

This model is supported by the model of resistance to ectromelia virus infection of mice. Ectromelia virus resistance is dependent on INFγ as well as INF α/β (Karupiah *et al.*, 1990a; Karupiah *et al.*, 1993a), NK cells (Delano and Brownstein, 1995), the early generation of anti-viral CTL (O'Neill and Brenan, 1987; Ramshaw *et al.*, 1997), and the presence of high levels of T_H1-associated cytokines, IL-2, IL-12 and TNFα (in Ramshaw *et al.*, 1997). Genetic resistance to ectromelia virus infection is predominantly controlled by one locus, a member of the NK gene complex (*Rmp1* or resistance to mousepox) (Delano and Brownstein, 1995; Wallace *et al.*, 1985), but several other unlinked, autosomal dominant genes also contribute to resistance (Brownstein *et al.*, 1989; Brownstein *et al.*, 1992).

In myxoma virus-infected wild rabbits, NK cells have two potential roles in controlling virus infection. Firstly, a strong and early NK cell response to infection in wild rabbits may act as an early and concentrated source of IFNγ, capable of saturating the IFNγ binding protein of myxoma virus. Influenza virus-infected murine dendritic cells are capable of stimulating $CD8^+$ T-cells in the absence of $CD4^+$ T-cells (Ridge, Di Rosa, and Matzinger, 1998). The early production of IFNγ by NK cells, in concert with myxoma virus-infected dendritic cells, may be sufficient for the stimulation of $CD8^+$ CTL responses to infection, and the control of virus replication. However, SLS does deplete lymphocytes from the draining lymph node, implying that some disruption of the wild rabbits immune responses is occurring. The second role for NK cells in wild rabbits is potentially the recognition and killing of virus-infected dendritic cells.

The role of $CD4^+$ T-cells in these models of virus-induced immune modulation and genetic resistance is potentially in the development of a strong cellular immune response through the production of T_H1-associated cytokines. Suppression of the mitogen-induced proliferative response and/or the early apoptosis of these cells in SLS-infected laboratory rabbits may be sufficient to suppress the ensuing CTL response hypothesised to be important in the control of Uriarra by laboratory rabbits. Alternatively, the modulation of early stimulation of $CD4^+$ T-cells by SLS-infected

dendritic cells may activate a presominantly T_H2 response, resulting in anti-viral antibody production, but downregulating the activation of CTL responses. However, virus was generally cleared from internal tissues of Uriarra-infected laboratory rabbits and SLS-infected wild rabbits, but was not cleared from the skin. Clearance of ectromelia or herpes simplex viruses from the skin of mice has been shown to require $CD4^+$ T-cells (Karupiah *et al.*, 1996; Nash *et al.*, 1987). Hence, it may be that strong $CD4^+$ T-cell-mediated responses are not generated in response to myxoma virus infection.

The models of myxoma virus-induced immune suppression and genetic resistance make two predictions. These are firstly that laboratory rabbits infected with Uriarra mount a stronger CTL response to infection than SLS-infected laboratory rabbits. Secondly, SLS-infected wild rabbits mount both a stronger NK cell response than SLS-infected laboratory rabbits and an earlier CTL response. These predictions are testable in outbred rabbits, through an examination of effector cell function in laboratory and wild rabbits. It might be expected that genetically resistant rabbits may produce higher levels of proinflammatory cytokines involved in the mobilisation of NK cell responses. Potential candidate cytokines include INFγ, TNFα or IL-12. Reverse transcriptase-polymerase chain reaction (RT-PCR) assays for cytokine production by cells from laboratory and wild rabbits are currently being developed in our laboratory. Reliable commercial reagents to investigate subpopulations of rabbit T-cells involved in the immune response to myxoma virus infection are limited. However, the development of NK cell and virus-specific CTL responses can be examined by investigating the killing of non-autologous and autologous (MHC non-restricted and restricted) target cells by lymph node cells from resistant and susceptible rabbits infected with virulent and attenuated strains of myxoma virus at various times after infection.

6.4 Virus transmission and the selection for virus virulence and host resistance

The development of genetic resistance in the wild rabbit population was probably dependent on existing polymorphisms at one or more critical loci, as the occurrence of a mutational event over such a short time as observed at the Lake Urana field site (Marshall and Douglas, 1961; Marshall and Fenner, 1958) is unlikely (Kerr and Best, 1998). Resistance can be explained by selection for rabbit survival by several genetic models. The first is selection on a single locus with a single allele that mediates

resistance. A second possibility is selection on a single locus with multiple resistance alleles that encode for different levels of resistance. In this case, combinations of alleles may mediate different levels of resistance. Alternatively, resistance may be selected on multiple loci, which individually confer weak resistance, but when inherited together, confer strong resistance. A final possibility is the inheritance of combinations of resistance loci, with a single locus conferring major resistance and other loci contributing (Kerr and Best, 1998) as occurs in genetic resistance in mice to both ectromelia virus and cytomegalovirus (Brownstein, Bhatt, andJacoby, 1989; Brownstein *et al.*, 1992; Scalzo *et al.*, 1992). Obviously dominance and heterozygosity would also be involved at any resistance locus.

Myxoma virus is endemic in Australia causing frequent epidemics in wild rabbit populations. Rabbits from these populations usually show a range of resistance phenotypes following infection with a standard virus. A small proportion of infected rabbits may show no clinical signs, another larger proportion may die and the main group will develop clinical myxomatosis and recover [Kerr, Merchant and Robinson, unpublished]. It is interesting to speculate that rabbits having high genetic resistance to myxomatosis may be selected against in terms of survival from other disease or for other causes, and that this leads to populations with only a small proportion of highly resistant rabbits.

Selection of successful myxoma virus strains in the field depends on the transmission of virus from infected to uninfected animals. On average, if each infected animal fails to transmit to at least one susceptible animal, the virus will become extinct. Transmission of myxoma virus in natural hosts, the *Sylvilagus* species of rabbit, depends exclusively on high virus titres in the primary skin site as the virus does not disseminate to secondary sites of replication in the skin (Marshall and Regnery, 1960; Marshall, Regnery, and Grodhaus, 1963). In European rabbits in the absence of a reseviour *Sylvilagus* host, myxoma virus could evolve or be selected in two ways as genetic resistance develops. The first is selection of strains that are predominantly transmitted from the primary inoculation site, but do not disseminate substantially to other tissues. This strategy essentially breaks the strong relationship between success of transmission and virus dissemination and requires persistence of virus at high titres at the primary inoculation site (Anderson and May, 1982; Fenner and Ross, 1994).

The second strategy is selection towards highly virulent strains of virus that have a greater chance to produce a disseminated disease and replicate to high titres in secondary sites in the skin, causing the development of secondary lesions from where transmission would occur. These viruses would thus be likely to have a high mortality rate, at least in a proportion of infected rabbits. Strains of myxoma virus recently isolated in Australia cause a range of clinical signs. Some viruses do not cause primary lesions at the inoculation site, but virus can be transmitted from secondary lesions on the face (Kerr, Merchant and Robinson, unpublished). These viruses are thus capable of systemic dissemination and substantial replication at secondary sites in the skin of genetically resistant wild rabbits. Hence, the evidence from the field suggests that host-virus coevolution has selected for a virulent, disseminated disease rather than for persistence of virus in the skin.

6.5 Final summary

This study has provided the baseline description of pathogenesis of virulent and attenuated strains of myxoma virus in both laboratory (unselected for resistance) and wild rabbits which have undergone intense selection for resistance to myxoma virus. The genetic and molecular basis for this resistance remain to be investigated, but clearly involves an effective immune response. However, using the models presented in this thesis, we can now focus on likely mechanisms of resistance such as effector cells and the generation of effector cells in the innate and adaptive immune response.

References

References

Abbas, A. K., Murphy, K. M., and Sher, A. (1996). Functional diversity of helper T lymphocytes. *Nature* **383,** 787-793.

Adorini, L., and Nagy, Z. A. (1990). Peptide competition for antigen presentation. *Immunology Today* **11,** 21-24.

Alcami, A., and Smith, G. L. (1992). A soluble receptor for interleukin-1β encoded by vaccinia virus: a novel mechanism of virus modulation of the host response to infection. *Cell* **71,** 153-167.

Alcami, A., and Smith, G. L. (1995). Cytokine receptors encoded by poxviruses: a lesson in cytokine biology. *Immunology Today* **16,** 474-478.

Alcami, A., and Smith, G. L. (1996). A mechanism for the inhibition of fever by a virus. *Proceedings of the National Academy of Sciences* **93,** 11029-11034.

Alcami, A., Symons, J. A., Khanna, A., and Smith, G. L. (1998). Poxviruses: capturing cytokines and chemokines. *Seminars in Virology* **5,** 419-427.

Anderson, R. M., and May, R. M. (1982). Co-evolution of hosts and parasites. *Parasitology* **85,** 411-426.

Aragao, H. d. B. (1943). O virus do myxoma do coelho do mato (Sylvilagus minensis) sua transmissao pelos Aedes scapularis e aegypti. *Memorias do Instituto Oswalso Cruz (Rio de Janeiro).* **38,** 93-99.

Atkinson, E. A., and Bleackley, R. C. (1995). Mechanisms of lysis by cytotoxic T cells. *Critical Reviews in Immunology* **15,** 359-384.

Babbitt, B. P., Matsueda, G., Haber, E., Unanue, E. R., and Allen, P. M. (1986). Antigenic competition at the level of peptide-Ia binding. *Proceedings of the National Academy of Sciences* **83,** 4509-4513.

Bachmann, M. F., and Zinkernagel, R. M. (1996). The influence of virus structure on antibody responses and virus serotype formation. *Immunology Today* **17,** 553-558.

Bachmann, M. F., and Zinkernagel, R. M. (1997). Neutralising antiviral B cell responses. *Annual Review of Immunology.* **15,** 235-270.

Baeuerle, P. A., and Baltimore, D. (1996). NF-κB: ten years after. *Cell* **87,** 13-20.

Baggiolini, M. (1998). Chemokines and leukocyte traffic. *Nature* **392,** 565-568.

Banchereau, J., and Steinman, R. M. (1998). Dendritic cells and the control of immunity. *Nature* **392,** 245-252.

Barry, M., Hnatiuk, S., Mossman, K., Lee, S. F., Boshkov, L., and McFadden, G. (1997). The myxoma virus M-T4 gene encodes a novel RDEL-containing protein that is retaiined within the endoplasmic reticulum and is important for the productive infection of lymphocytes. *Virology* **239,** 360-377.

Barry, M., Lee, S. F., Boshkov, L., and McFadden, G. (1995). Myxoma virus induces extensive downregulation and dissociation of $p56^{lck}$ in infected rabbit $CD4^{+}$ T lymphocytes. *Journal of Virology* **69,** 5245-5251.

Baumgarth, N., and Kelso, A. (1997). Gamma interferon and the Th1/Th2 paradigm. *In* "Gamma Interferon in Antiviral Defense." (G. Karupiah, Ed.). R.G. Landes Company.

Beaud, G. (1995). Vaccinia virus DNA replication: a short review. *Biochimie* **77,** 774-779.

Becker, Y., and Sprecher, E. (1989). Langerhans cells in vaccinia virus infection in mouse skin. *Archives of Virology* **107,** 307-313.

Bender, B. S., Croghan, T., Zhang, L., and Small, P. A. J. (1992). Transgenic mice lacking class I major histocompatability complex-restricted T cells have delayed viral clearance and increased mortality after virus challenge. *Journal of Experimental Medicine* **175,** 1143-1145.

Benner, R., Hijmans, W., and Haaijman, J. J. (1981). The bone marrow: the major source of serum immunoglobulins, but still a neglected site of antibody formation. *Clinical and Experimental Immunology* **46,** 1-8.

Bennett, S. R. M., Carbone, F. R., Karamalis, F., Flavell, R. A., Miller, J. F. A. P., and Heath, W. R. (1998). Help for cytotoxic-T-cell responses is mediated by CD40 signalling. *Nature* **393,** 478-480.

Blanden, R. V. (1970). Mechanisms of recovery from a generalised viral infection: mousepox. I. The effects of anti-thymocyte serum. *Journal of Experimental Medicine* **132,** 1035-1053.

Blanden, R. V. (1971). Mechanisms of recovery from a generalised viral infection: mousepox. II. Passive transfer of recovery mechanisms with immune lymphoid cells. *Journal of Experimental Medicine* **133,** 1074-1089.

Blasco, R., and Moss, B. (1992). Role of cell-associated enveloped vaccinia virus in cell-to-cell spread. *Journal of Virology* **65,** 4598-4608.

Block, W., Upton, C., and McFadden, G. (1985). Tumorigenic poxvirus: genomic organisation of malignant rabbit virus, a recombinant between Shope fibroma virus and myxoma virus. *Virology* **140,** 113-124.

Boshkov, L. K., Macen, J. L., and McFadden, G. (1992). Virus-induced loss of class I MHC antigens from the surface of cells infected with myoma virus and malignant rabbit fibroma virus. *Journal of Immunology* **148,** 881-887.

Brinton, M. A. (1981). Isolation of a replication efficient mutant of West Nile virus from a persistently infected genetically resistant mouse cell culture. *Journal of Virology* **39,** 413-421.

Brownstein, D., Bhatt, P. N., and Jacoby, R. O. (1989). Mousepox in inbred mice innately resistant or susceptible to lethal infection with ectromelia virus. V. Genetics of resistance to the Moscow strain. *Archives of Virology* **107,** 35-41.

Brownstein, D. G., Bhatt, P. N., and Gras, L. (1993). Ectromelia virus replication in major target organs of innately resistant and susceptible mice after intravenous infection. *Archives of Virology* **129,** 65-75.

Brownstein, D. G., Bhatt, P. N., Gras, L., and Budris, T. (1992). Serial backcross analysis of genetic resistance to mousepox, using marker loci for *Rmp-2* and *Rmp-3*. *Journal of Virology* **66,** 7073-7079.

Brownstein, D. G., Bhatt, P. N., Gras, L., and Budtis, T. (1991). Chromosomal locations and gonadal dependence of genes that mediate resistance to ectromelia (nousepox) virus-induced mortality. *Journal of Virology* **65,** 1946-1951.

Bugert, J. J., Lohmuller, C., Damon, I., Moss, B., and Darai, G. (1998). Chemokine homolog of molluscum contagiosum virus: sequence conservation and expression. *Virology* **242,** 51-59.

Bull, L. B., and Mules, M. W. (1944). An investigation of *Myxomatosis cuniculi* with special reference to the possible use of the disease to control rabbit populations in Australia. *Journal for the Council for Scientific and Industrial Reasearch of Australia.* **17,** 79-93.

Buller, R. L. M., and Palumbo, G. J. (1991). Poxvirus pathogenesis. *Microbiological Reviews* **55,** 80-122.

Buller, R. M. L., Holmes, K. L., Huggin, A., Frederickson, T. N., and Moorse, H. C. I. (1987). Induction of cytotoxic T-cell responses *in vivo* in the absence of CD4 helper cells. *Nature* **327,** 77-79.

Cabriac, G. F., Strayer, D. S., Sell, S., and Leibowitz, J. L. (1985). Characterization, molecular cloning and physical mapping of the Shope fibroma virus genome. *Virology* **143,** 163-170.

Cao, J. X., Gershon, P. D., and Black, D. N. (1995). Sequence analysis of HindIII Q2 fragment of capripox reveals a putative gene encoding a G-protein-coupled chemokine receptor homologue. *Virology* **209,** 207-212.

Cartledge, K. (1995). Honours thesis. The Australian National University, Canberra.

Caux, C., Dezutter-Dambuyant, C., Schmitt, D., and Banchereau, J. (1992). GM-CSF and TNFα cooperate in the generation of dendritic Langerhans cells. *Nature* **360,** 258-261.

Childerstone, A., Takamatsu, H., Yang, H., Denyer, M., and Parkhouse, R. M. E. (1998). Modulation of T cell and monocyte function in the spleen following infection of pigs with African swine fever virus. *Veterinary Immunolofy and Immunopathology* **62,** 281-296.

Cook, D. N., Beck, M. A., Coffman, T. M., Kirby, S. L., Sheridan, J. F., Pragnell, I. B., and Smithies, O. (1995). Requirement of MIP-1α for an inflammatory response to viral infection. *Science* **269,** 1583-1585.

Croft, M., Carter, L., Swain, S., and others, a. (1994). Generation of polarized antigen-specific CD8 effector populations: reciprocal action of interleukin (IL)-4 and IL-12 in promoting type 2 versus type 1 cytokine profiles. *Journal of Experimental Medicine.* **180,** 1715-1728.

Cudmore, S., Cossart, P., Griffiths, G., and Way, M. (1995). Actin-based motility of vaccinia virus. *Nature* **378,** 636-638.

Cudmore, S., Reckmann, I., Griffiths, G., and Way, M. (1996). Vaccinia virus: a model system for actin-membrane interactions. *Journal of Cell Science* **109,** 1739-1747.

Cuff, S., and Ruby, J. (1996). Evasion of apoptosis by DNA viruses. *Immunology and Cell Biology* **74,** 527-537.

Day, M. F., Fenner, F., Woodroofe, G. M., and McIntyre, G. A. (1956). Further studies on the mechanism of mosquito transmission of myxomatosis in the European rabbit. *Journal of Hygiene* **54,** 258-283.

DeLange, A. M., and McFadden, G. (1990). The role of telomeres in poxvirus DNA replication. *In* "Current Topics in Microbiology and Immunology" (R. W. Moyer, and P. C. Turner, Eds.), Vol. 163, pp. 71-92.

Delano, M. L., and Brownstein, D. G. (1995). Innate resistance to lethal mousepox is genetically linked to the NK gene complex on chromosome 6 and correlates with early restriction of virus replication by cells with an NK phenotype. *Journal of Virology* **69,** 5875-5877.

Eichelberger, M., Allan, W., Zijlstra, M., Jaenisch, R., and Doherty, P. C. (1991). Clearance of influenza virus respiratory infection in mice lacking class I major histocompatability complex-restricted $CD8^+$ T cells. *Journal of Experimental Medicine* **174,** 875-880.

Essani, K., Chalasani, S., Eversole, R., Beuving, L., and Birmingham, L. (1994). Multiple anti-cytokine activities secreted from tanapox virus-infected cells. *Microbial Pathogenesis* **17,** 347-353.

Farrent, J. L., and Fenner, F. (1953). A comparison of the morphology of vaccinia and myxoma virus. *Australian Journal of Experimanetal Biology and Medical Science.* **31,** 121-126.

Fearon, D. T., and Locksley, R. M. (1996). The instructive role of innate immunity in the aquired immune response. *Science* **272,** 50-53.

Fenner, F. (1948a). The clinical features of mouse-pox (infectious ectromelia of mice) and the pathogenesis of the disease. *Journal of Pathology and Bacteriology* **60,** 529-552.

Fenner, F. (1948b). The epizootic behaviour of mouse-pox (infectious ectromelia of mice). *British Journal of Experimental Pathology.* **29,** 29-91.

Fenner, F. (1949). Mousepox (infectious ectromelia of mice): a review. *Journal of Immunology* **63,** 341-373.

Fenner, F. (1953). Classification of myxoma and fibroma viruses. *Nature* **171,** 562-564.

Fenner, F. (1994a). Myxoma Virus. *In* "Virus infections of rodents and lagomorphs." (A. D. M. E. Osterhaus, Ed.), pp. 59-70. Elsevier Science, Oxford.

Fenner, F. (1994c). Poxviruses of largomorphs. *In* "Virus Infections of Rodents and Largomorphs." (A. D. M. E. Osterhaus, Ed.), Vol. 5. Elsevier Science B.V., New York.

Fenner, F., Day, M. F., and Woodroofe, G. M. (1952). The mechanism of the transmission by myxomatosis in the European rabbit (*Oryctolagus cuniculus*) by the mosquito *Aedes aegypti. Australian Journal of Experimental Biology and Medical Science.* **30,** 139-152.

Fenner, F., Day, M. F., and Woodroofe, G. M. (1956). Epidemiological consequences of the mechanical transmission of myxomatosis by mosquitoes. *Journal of Hygiene* **54,** 284-303.

Fenner, F., and Kerr, P. J. (1994). Evolution of the poxviruses, including the coevolution of virus and host in myxomatosis. *In* "The Evolutionary Biology of Viruses." (S. S. Morse, Ed.), pp. 273-292. Raven Press, New York.

Fenner, F., and Marshall, I. D. (1954). Passive immunity in myxomatosis of the European rabbit (*Oryctolagus cuniculus*): the protection conferred on kittens born by immune does. *Journal of Hygiene* **52,** 321-336.

Fenner, F., and Marshall, I. D. (1957). A comparison of the virulence for European rabbits (*Oryctolagus cuniculus*) of strains of myxoma virus recovered in the field in Australia, Europe and America. *Journal of Hygiene* **55,** 149-191.

Fenner, F., Marshall, I. D., and Woodroofe, G. M. (1953). Studies in the epidemiology of infectious myxomatosis of rabbits. I. Recovery of Australian wild rabbits *(Oryctolagus cuniculus)* from myxomatosis under field conditions. *Journal of Hygiene* **51,** 225-244.

Fenner, F., and Nakano, J. H. (1988). *Poxviridae*: the poxviruses. *In* "The laboratory diagnosis of infectious diseases: principles and practice, vol II. Viral, rickettsial and chlamydial diseases." (E. H. Lennette, P. Halonen, and F. A. Murphy, Eds.). Springer-Verlag, New York.

Fenner, F., and Ratcliffe, F. N. (1965). "Myxomatosis." Canbridge University Press, Canbridge.

Fenner, F., and Ross, J. (1994). Myxomatosis. *In* "The European rabbit: the history and biology of a successful coloniser." (H. V. Thompson, and C. M. King, Eds.), pp. 205-239. Oxford University Press, Oxford.

Fenner, F., Wittek, R., and Dumbell, K. R. (1989). "The Orthopoxviruses." Academic Press, San Diego.

Fenner, F., and Woodroofe, G. M. (1953). The pathogenesis of infectious myxomatosis: the mechanism of infection and the immunological response in the European rabbit(*Oryctolagus cuniculus*). *British Journal of Experimental Pathology* **34,** 400-411.

Finkel, T. H., Tudor-Williams, G., Banda, N. K., Cotton, M. F., Curiel, T., Monks, C., Baba, T. W., Ruprecht, R. M., and Kupfer, A. (1995). Apoptosis occurs predominantly in bystander cells and not in productively infected cells of HIV- and SIV-infected lymph nodes. *Nature Medicine* **1,** 129-134.

Fleming, S. B., McCaughan, C. A., Andrews, A. E., Nash, A. D., and Mercher, A. A. (1997). A homolog of interlekin-10 is encoded by the poxvirus orf virus. *Journal of Virology* **71,** 4857-4861.

Fountain, S., Holland, M. K., Hinds, L. A., Janssens, P. A., and Kerr, P. J. (1997). Interstitial orchitis with impaired steroidgenesis and spermatogenesis in the testis of rabbits infected with an attenuated strain of myxoma virus. *Journal of Reproduction and Fertility* **110,** 161-169.

Gagliardini, V., Fernandez, P.-A., Lee, R. K. K., Drexler, H. C. A., Rotello, R. J., Fishman, M. C., and Yuan, J. (1994). Prevention of vertebrate neuronal death by the *crm*A gene. *Science* **263,** 826-828.

Garcia-Sastre, A., Durbin, R. K., Zheng, H., Palese, P., Gertner, R., Levy, D. S., and Durbin, J. E. (1998). The role of interferon in influenza virus tissue tropism. *Journal of Virology* **72,** 8550-8558.

Gershon, P. D. (1998). mRNA 3' end formation by vaccinia virus: mechanism of action of a heterodimeric poly(A) polymerase. *Seminars in Virology* **8,** 343-350.

Gillet, G., and Brun, G. (1996). Viral inhibition of apoptosis. *Trends in Microbiology* **312,** 312-317.

Gooding, L. R. (1992). Virus proteins that counteract the immune system. *Cell* **71,** 5-7.

Graham, K. A., Lalani, A. S., Macen, J. L., Ness, T. L., Barry, M., Liu, L. Y., Lucas, A., Clarke-Lewis, I., Moyer, R. W., and McFadden, G. (1997). The T1/35kDa family of poxvirus secreted proteins bind chemokines and modulate leukocyte influx into virus-infected tissues. *Virology* **229,** 12-24.

Graham, K. A., Opgenorth, A., Upton, C., and McFadden, G. (1992). Myxoma virus M11L ORF encodes a protein for which cell surface localization is critical in manifestation of viral virulence. *Virology* **191,** 112-124.

Gretz, J. E., Anderson, A. O., and Shaw, S. (1997). Cords, channels, corridors and conduits: critical architectural elements facilitating cell interactions in the lymph node cortex. *Immunological Reviews* **156,** 11-24.

Guery, J.-C., Neagu, M., Rodriguez-Tarduchy, G., and Adorini, L. (1993). Selective immunosuppression by administration of major histocompatibility complex class II-binding peptides. II. Preventative inhibition of primary and secondary *in vivo* antibody responses. *Journal of Experimental Medicine* **177,** 1461-1468.

Haller, O., Arnheiter, H., Lindenmann, J., and others, a. (1980). Host gene influences sensitivity to interferon action selectively for influenza virus. *Nature* **283,** 660-662.

Henkart, P. A. (1994). Lymphocyte-mediated cytotoxicity: two pathways amd multiple effector molecules. *Immunity* **1,** 343-346.

Hobbs, J. R. (1928). Studies on the nature of the infectious myxoma virus of rabbits. *American Journal of Hygeine* **8,** 800-839.

Howard, S. T., Chan, Y. S., and Smith, G. L. (1991). Vaccinia virus homologues of the Shope fibroma virus inverted terminal repeat proteins and a discontinuous ORF related to tumor necrosis factor receptor family. *Virology* **180,** 633-647.

Hu, F., Smith, C. A., and Pickup, D. J. (1994). Cowpox virus contains two copies of an early gene encoding a soluble secreted form of the type II TNF receptor. *Virology* **204,** 343-356.

Hunt, J. D., Jackson, D. C., Wood, P. R., Stewart, D. J., and Brown, L. E. (1995). Immunological parameters associated with antigenic competition in a mutivalent footrot vaccine. *Vaccine* **13,** 1649-1657.

Hurst, E. W. (1937a). Myxoma and the Shope fibroma. I. The histology of myxoma. *British Journal of Experimental Pathology* **18,** 1-15.

Hurst, E. W. (1937b). Myxoma and the Shope fibroma. II. The effect of intracerebral passage on the myxoma virus. *British Journal of Experimental Pathology* **18,** 15-23.

Ichihashi, Y. (1996). Extracellular enveloped vaccinia virus escapes neutralisation. *Virology* **217,** 478-485.

Jackson, R. J., and Bults, H. G. (1990). A myxoma virus nucleotide sequence with homology to the vaccinia virus RNA polymerase 22-kDa subunit gene. *Nucleic Acid Research* **18,** 5290.

Jackson, S., Chuses, T. M., Wilkinson, J. M., Leiserson, W. M., and Kindt, T. J. (1983). Differentiation antigens identify subpopulations of rabbit T and B lymphocytes. *Journal of Experimental Medicine* **157,** 34-46.

Jacoby, R. O., Bhatt, P. N., and Brownstein, D. G. (1989). Evidence that NK cells and interferon are required for genetic resistance to lethal infection with ectromelia virus. *Archives of Virology* **108,** 49-58.

Janeway, C. A. J., and Travers, P. (1994). "Immunobiology." Current Biology Ltd., London.

Jenkinson, D. M., Hutchison, G., Onwuka, S. K., and Reid, H. W. (1991). Changes in the MHC Class II^+ dendritic cell population of ovine skin in response to orf virus infection. *Vetinary Dermatology* **2,** 1-9.

Johnston, L. J., Halliday, G. M., and King, N. J. (1996). Phenotypic changes in Langerhans'cells after infection with arboviruses: a role in the immune response to epidermally acquired viral infection. *Journal of Virology* **70,** 4761-4766.

Karupiah, G., Blanden, R. V., and Ramshaw, I. A. (1990a). Interferon γ is involved in the recovery of athymic nude mice from recombinant vaccinia virus/interleukin 2 infection. *Journal of Experimental Medicine* **172,** 1495-1503.

Karupiah, G., Buller, R. M. L., Van Rooijen, N., Duarte, C. J., and Chen, J. (1996). Different roles for $CD4^+$ and $CD8^+$ T lymphocytes and macrophage subsets in the control of a generalised virus infection. *Journal of Virology* **70,** 8301-8309.

Karupiah, G., Coupar, B. E., Andrew, M. E., Boyle, D. B., Phillips, S. M., Mullbacher, A., Blanden, R. V., and Ramshaw, I. A. (1990b). Elevated natural killer cell responses in mice infected with recombinant vaccinia virus encoding muring IL-2. *Journal of Immunology* **144,** 290-298.

Karupiah, G., Fredrickson, T. N., Holmes, K. L., Khairallah, L. H., and Buller, R. M. L. (1993a). Importance of interferons in recovery from mousepox. *Journal of Virology* **67,** 4214-4226.

Karupiah, G., and Harris, N. (1995). Inhibition of viral replication by nitric oxide and its reversal by ferrous sulphate and tricarboxylic acid cycle metabolites. *Journal of Experimental Medicine* **181,** 2171-2179.

Karupiah, G., Xie, Q. W., Buller, R. M. L., Nathan, C., Duarte, C., and MacMicking, J. D. (1993b). Inhibition of viral replication by interferon-gamma induced nitric oxide synthase. *Science* **261,** 1445-1448.

Kelly, R. H. (1975). Functional anatomy of lymph nodes. I. The paracortical cords. *International Archives of Allergy and Applied Immunology.* **48,** 836-849.

Kerr, P. J. (1997). An ELISA for epidemiological studies of myxomatosis: persistence of antibodies to myxoma virus in Europena rabbits (*Oructolagus cuniculus*). *Wildlife Research* **24,** 53-65.

Kerr, P. J., and Best, S. M. (1998). Myxoma virus in rabbits. *Revue Scientifique et Technique* **17,** 256-268.

Kerr, P. J., and Best, S. M. (1998). Myxoma virus in rabbits. *Revue Scientifique et Technique* **17,** 256-268.

Kerr, P. J., and Jackson, R. J. (1995). Myxoma virus as a vaccine vector for rabbits; antibody levels to influenza virus haemagglutinin presented by a recombinant myxoma virus. *Vaccine* **13,** 1722-1726.

Kessel, J. F., Prouty, C. C., and Meyer, J. W. (1931). Occurrence of infectious myxomatosis in southern California. *In* "Proceedings of the Society for Experimental Biology and Medicine", Vol. 28, pp. 413-414. University of Toronto Press, Totonto.

Kettle, S., Alcami, A., Khanna, A., Ehert, R., Jassoy, C., and Smith, G. L. (1997). Vaccinia virus serpin B1 3R (SPI-2) inhibits interleukin-1b-converting enzyme and protects virus-infected cells from TNF- and Fas-mediated apoptosis, but does not prevent IL-1b-induced fever. *Journal of General Virology* **78,** 677-685.

Kohonen-Corish, M. R. J., King, N. J. C., Woodhams, C. E., and Ramshaw, I. A. (1990). Immunodeficient mice recover from infection with vaccinia virus expressing interferon-γ. *European Journal of Immunology* **20,** 157-161.

Komiyama, T., Ray, C. A., Pickup, D. J., Howard, A. D., Thornberry, N. A., Peterson, E. P., and Salvesen, G. (1994). Inhibition of interleulin-1 beta converting enzyme by the cowpox virus serpin CrmA. An example of cross-class inhibition. *Journal of Biological Chemistry* **269,** 19331-19337.

Kopf, M., LeGros, G., Bachman, M., Lamers, M. C., Bluethmann, H., and Kohler, G. (1993). Disruption of the murine IL-4 gene blocks Th2 cytokine responses. *Nature* **362,** 245-248.

Kos, F. J., and Engleman, E. G. (1996). Immune regulation: a critical link between NK cells and CTLs. *Immunology Today* **173,** 1-6.

Kotwal, G. J., and Moss, B. (1988). Vaccinia virus encodes a secretory polypeptide structurally related to complement control proteins. *Nature* **335,** 176-178.

Lakey, E. K., Margoliash, E., Flouret, G., and Pierce, S. K. (1986). Peptides related to the antigenic determinant block T cell recognition of the native protein as processed by antigen-presenting cells. *European Journal of Immunology* **16,** 721-727.

Lalani, A. S., Graham, K., Mossman, K., Rajarathnam, K., Clark-Lewis, I., Kelivin, D., and McFadden, G. (1997). The purified myxoma virus IFN-γ receptor homolog, M-T7, interacts with the heparin binding domains of chemokines. *Journal of Virology* **71,** 4356-4363.

Lalani, A. S., Ness, T. L., Singh, R., Harrison, J. K., Seet, B. T., Kelvin, D. J., McFadden, G., and Moyer, R. W. (1998). Functional comparisons among members of the poxvirus T1/35kDa family of soluble CC-chemokine inhibitor glycoproteins. *Virology* **250,** 173-184.

Lathbury, L. J., Allan, J. E., Shellam, G. R., and Scalzo, A. A. (1996). Effect of host geneotype in determining the relative roles of natural killer cells and T cells in mediating protection against murine cytomegalovirus infection. *Journal of General Virology* **77,** 2605-2613.

Lidbury, B. A., Ramshaw, I. A., and Sambhi, S. K. (1995). The role for host-immune factors in the *in vivo* antiviral effects of tumor necrosis factor. *Cytokine* **7,** 157-164.

Lin, Y.-Z., Ke, X.-H., and Tam, J. P. (1991). Synthesis and structure-activity study of myxoma virus growth factor. *Biochemistry* **30,** 3310-3314.

Liu, Y.-J., and Arpin, C. (1997). Germinal centre development. *Immunological Reviews* **156,** 111-126.

Lobel, S. A., and Knight, K. L. (1984). The role of rabbit Ia molecules in immune functions as determined with the use of an anti-Ia monoclonal antibody. *Immunology* **51,** 35-43.

Lomas, D. A., Evans, D. F., Upton, C., MgFadden, G., and Carrell, R. (1993). Inhibition of plasmin, urokinase, tissue plasminogen activator, and C_{1s} by a myxoma virus serine proteinase inhibitor. *Journal of Biological Chemistry* **268,** 516-521.

Loparev, V. N., Parsons, J. M., Knight, J. C., Panus, J. F., Ray, C. A., Buller, R. M., Pickup, D. J., and Esposito, J. J. (1998). A third distinct tumor necrosis factor receptor of orthopoxviruses. *Proceedings of the National Academy of Sciences* **95,** 3786-3791.

Lucas, A., Liu, L., Macen, J. L., Nash, P. D., Dai, E., Stewart, M., Yan, W., Graham, K., Etches, W., Boshkov, L., Nation, P. N., Humen, D., Hobman, M., and McFadden, G. (1996). A virus-encoded serine proteinase inhibitor, SERP-1, inhibits atherosclerotic plaque development following balloon angioplasty. *Circulation* **94,** 2890-2900.

Luster, A. D. (1998). Chemokines: chemotactic cytokines that mediate inflammation. *New England Journal of Medicine* **338,** 436-445.

Macen, J., Takakashi, A., Moon, K. B., Nathaniel, R., Turner, P. C., and Moyer, R. W. (1998). Activation of caspases in pig kidney cells infected with wild-type and CrmA/SPI-2 mutants of cowpox and rabbitpox viruses. *Journal of Virology* **72,** 3524-3533.

Macen, J. L., Garner, R. S., Musy, P. Y., Brooks, M. A., Turner, P. C., Moyer, R. W., McFadden, G., and Bleackley, R. C. (1996a). Differential inhibition of the Fas- and granule-mediated cytolysis pathways by the orthopoxvirus cytokine response modifier A/SPI-2 and SPI-1 protein. *Procedings of the National Academy of Science.* **93,** 9108-9113.

Macen, J. L., Graham, K. A., Lee, S. F., Schreiber, M., Boshkov, L. K., and McFadden, G. (1996b). Expression of the myxoma virus tumor necrosis factor receptor

homologue and M11L genes is required to prevent virus-induced apoptosis in infected rabbit T-lymphocytes. *Virology* **218,** 232-237.

Macen, J. L., Upton, C., Nation, N., and McFadden, G. (1993). SERP1, a serine protease inhibitor encoded by myxoma virus, is a secreted glycoprotein that interferes with inflammation. *Virology* **195,** 348-363.

Maksymowych, W. P., Nation, N., Nash, P. D., Macen, J., Lucas, A., McFadden, G., and Russell, A. S. (1996). Amelioration of antigen-induced arthritis in rabbits treated with a secreted viral serine proteinase inhibitor. *Journal of Rheumatology* **23,** 878-882.

Maloy, K. J., Odermatt, B., Hengartner, H., and Zinkernagel, R. M. (1998). Interferon γ-producing γδ T cell-dependent antibody isotype switching in the absence of germinal centre formation during virus infection. *Proceedings of the National Academy of Sciences.* **95,** 1160-1165.

Marshall, I. D. (1959). The influence of ambient temperature on the course of myxomatosis in rabbits. *Journal of Hygiene* **57,** 484-497.

Marshall, I. D. (1961). Myxomatosis investigations carried out in Central and South America. *Report to the Australian Wool Research Fund Committee.*

Marshall, I. D., and Douglas, G. W. (1961). Studies in the epidemiology of infectious myxomatosis of rabbits. VIII. Further observations on changes in the innate resistance of Australian wild rabbits exposed to myxomatosis. *Journal of Hygiene* **59,** 117-122.

Marshall, I. D., and Fenner, F. (1958). Studies in the epidemiology of infectious myxomatosis of rabbits. V. Changes in innate resistance of wild rabbits between 1951 and 1959. *Journal of Hygiene* **56,** 288-302.

Marshall, I. D., and Fenner, F. (1960). Studies in the epidemiology of infectious myxomatosis of rabbits. VII. The virulence of strains of myxoma virus recovered from Australian wild rabbits between 1951 and 1959. *Journal of Hygiene* **58,** 485-487.

Marshall, I. D., and Regnery, D. C. (1960). Myxomatosis in a Californian brush rabbit (*Sylvilagus bachmani). Nature* **188,** 73-74.

Marshall, I. D., and Regnery, D. C. (1963). Studies in the epidemiology of myxomatosis in California. III. Reponse of brush rabbits (*Sylvilagus bachmani*) to infection with exotic and enzootic strains of myxoma virus, and the relative infectivity of the tumors for mosquitoes. *American Journal of Hygeine* **77,** 213-219.

Marshall, I. D., Regnery, D. C., and Grodhaus, G. (1963). Studies in the epidemiology of myxomatosis in California. I. Observations on two outbreaks of myxomatosis in coastal California and the recovery of myxoma virus from a brush rabbit *(Sylvilagus bachmani). American Journal of Hygeine* **77,** 195-204.

Massung, R. F., Jayarama, V., and Moyer, R. W. (1993). DNA sequence analysis of conserved and unique regions of swinepox virus: identification of genetic elements supporting phenotypic observations including a novel G protein-coupled receptor homologue. *Virology* **197,** 511-528.

Mathew, E., Sanderson, C. M., Hollinshead, M., and Smith, G. L. (1998). The extracellular domain of vaccinia virus protein B5R affects plaque phenotype, extracellular enveloped virus release, and intracellular actin tail formation. *Journal of Virology* **72,** 2429-2438.

Maudsley, D. J., and Pound, J. D. (1991). Modulation of MHC antigen expression by viruses and oncogenes. *Immunology Today* **12,** 429-431.

McFadden, G., Ed. (1995). Viroceptors, virokines and related immune modulators encoded by DNA viruses. Austin, Texas: R.G. Landes Company.

McFadden, G., and Barry, M. (1998). How poxviruses oppose apoptosis. *Seminars in Virology* **8,** 429-442.

McFadden, G., and Graham, K. (1994). Modulation of cytokine networks by poxviruses: the myxoma virus model. *Seminars in Virology* **5,** 421-429.

McFadden, G., Graham, K., Ellison, K., Barry, M., Macen, J., Schreiber, M., Mossman, K., Nash, P., Lalani, A., and Everett, H. (1995). Interruption of cytokine networks by poxviruses: lessons from myxoma virus. *Journal of Leukocyte Biology* **57,** 731-738.

McFadden, G., and Kane, K. (1994). How DNA viruses perturb functional MHC expression to alter immune recognition. *Advances in Cancer Research* **63,** 117-209.

McFadden, G., Schreiber, M., and Sedger, L. (1997). Myxoma T2 protein as a model for poxvirus TNF receptor homologs. *Journal of Neuroimmunology* **72,** 119-126.

McNair, A. N. B., and Kerr, I. M. (1992). Viral inhibition of the interferon system. *Pharmacology Theory* **56,** 79-95.

Medzhitov, R., and Janeway, C. A. (1997). Innate immunity: the virtues of a nonclonal system of recognition. *Cell* **91,** 295-298.

Messud-Petit, F., Gelfi, J., Delverdier, M., Amardeilh, M. F., Py, R., Sutter, G., and Bertagnoli, S. (1998). Serp2, an inhibitor of the interleukin-1β-converting enzyme, is critical in the pathobiology of myxoma virus. *Journal of Virology* **72,** 7830-7839.

Miller, C. G., Shchelkunov, S. N., and Kotwal, G. J. (1997). The cowpox virus-encoded homolog of the vaccinia virus complement control protein is an inflammation modulatory protein. *Virology* **229,** 126-133.

Mims, C. A. (1959). The response of mice to large intravenous injections of ectromelia virus. II. The growth of virus in the liver. *British Journal of Experimental Pathology* **40,** 543-550.

Mims, C. A. (1964). Aspects of the pathogenesis of virus disease. *Bacteriological Reviews* **28,** 30-71.

Miskin, J. E. (1998). A viral mechanism for inhibition of the cellular phosphatase calcineurin. *Science* **281,** 562-565.

Mizuochi, T., Hugin, A. W., Morse, H. C. I., Singer, A., and Buller, R. M. L. (1989). Role of lymphokine-secreting CD8+ T cells in cytotoxic T lymphocyte responses against vaccinia virus. *Journal of Immunology* **142,** 270-273.

Moses, A. (1911). O Virus do mixoma does coelhos. *Memorias do Istituto Oswaldo Crus (Rio de Janeiro)* **3,** 46-53.

Moss, B. (1990). Poxviridae and their replication. 2 ed. *In* "Virology" (B. N. Fields, and D. M. Knipe, Eds.), pp. 2079-2111. Raven Press, New York.

Moss, B. (1996). Poxviridae: the viruses and their replication. *In* "Fields Virology" (B. N. Fields, D. M. Knipe, and P. M. Howley, Eds.), Vol. 2, pp. 2637-2671. Lippincott Raven Press, New York.

Moss, B., Ahn, B.-Y., Amegadzie, B., Gershon, P. D., and Keck, J. G. (1991). Cytoplasmic transcription system encoded by vaccinia virus. *Journal of Biological Chemistry* **266,** 1355-1358.

Mossman, K., Barry, M., and McFadden, G. (1995a). The myxoma virus-soluble interferon-γ receptor homolog, M-T7, inhibits interferon-γ in a species specific manner. *Journal of Biological Chemistry* **270,** 3031-3038.

Mossman, K., Lee, S. F., Barry, M., Boshkov, L., and McFadden, G. (1996a). Disruption of M-T5, a novel myxoma virus gene member of the poxvirus host range superfamily, results in dramatic attenuation of myxomatosis in infected European rabbits. *Journal of Virology* **70,** 4394-4410.

Mossman, K., Nation, N., Macen, J., Garbutt, M., Lucas, A., and McFadden, G. (1996b). Myxoma virus M-T7, a secreted homolog of the interferon-γ receptor, is a critical virulence factor for the development of myxomatosis in European rabbits. *Virology* **215,** 17-30.

Mossman, K., Upton, C., Buller, R. M. L., and McFadden, G. (1995b). Speicies specificity of ectromelia virus and vaccinia virus interferon-γ binding proteins. *Virology* **208,** 762-769.

Myers, K. (1954). Studies in the epidemiology of infectious myxomatosis in rabbits. II. Field experiments, August-November 1950, and the first epizootic of myxomatosis in the riverine plain of south-eastern Australia. *Journal of Hygiene* **52,** 337-360.

Myers, K., Parer, I., Wood, D., and Cooke, B. D. (1994). The rabbit in Australia. *In* "The European rabbit: the history and biology of a successful coloniser." (H. V. Thompson, and C. M. King, Eds.), pp. 108-157. Oxford University Press, Oxford.

Myktowycz, R. (1953). An attenuated strain of the myxomatosis virus recovered from the field. *Nature* **172,** 448-449.

Nagao, S., and Inaba, S. (1976). Langerhans cells at the site of vaccinia virus inoculation. *Archives of Dermatological Research* **256,** 23-31.

Nash, A. A., Jayasuriya, A., Phelan, J., Cobbold, S. P., Waldmann, H., and Prospero, T. (1987). Different roles for $L3T4^+$ and $Lyt\ 2^+$ T cell subsets in the control of an acute herpes simplex virus infection of the skin and nervous system. *Journal of General Virology* **68,** 825-833.

O'Neill, H. C. (1991). Resistance to ectromelia virus infection in mice. Analysis of H-2-linked gene effects. *Archives of Virology* **118,** 253-259.

O'Neill, H. C., and Blanden, R. V. (1983). Mechanisms determining innate resistance to ectromelia virus infection in C57BL mice. *Infection and Immunity* **41,** 1391-1394.

O'Neill, H. C., and Brenan, M. (1987). A role for early cytotoxic T cells in resistance to ectromelia virus infection of mice. *Journal of General Virology* **68,** 2669-2673.

Opgenorth, A., Graham, K., Nation, N., Strayer, D., and McFadden, G. (1992). Deletion analysis of two tandemly arranged virulence genes in myxoma virus, M11L and myxoma growth factor. *Journal of Virology* **66,** 4720-4731.

Opgenorth, A., Nation, N., Graham, K., and McFadden, G. (1993). Transforming growth factor alpha, Shope fibroma growth factor, and vaccinia growth factor can replace myxoma growth factor in the induction of myxomatosis in rabbits. *Virology* **192,** 701-709.

Oura, C. A. L., Powell, P. P., Anderson, E., and Parkhouse, R. M. E. (1998b). The pathogenesis of African swine fever virus in the resistant bushpig. *Journal of General Virology* **79,** 1439-1443.

Oura, C. A. L., Powell, P. P., and Parkhouse, R. M. E. (1998a). African swine fever: a disease characterized by apoptosis. *Journal of General Virology* **79,** 1427-1438.

Parer, I., Sobey, W. R., Conolly, D., and Morton, R. (1995). Sire transmission of acquired resistance to myxomatosis. *Australian Journal of Zoology* **43,** 459-465.

Parker, R. F., and Thompson, R. L. (1942). The effect of external temperature on the course of infectious myxomatosis of rabbits. *Journal of Experimental Medicine.* **75,** 567-573.

Pathak, P. N., and Tompkins, W. A. F. (1974). Interferon production by macrophages from adult and newborn rabbits bearing fibroma virus-induced tumors. *Infection and Immunity* **9,** 669-673.

Payne, L. G. (1980). Significance of extracellular enveloped virus in the *in vitro* and *in vivo* dissemination of vaccinia. *Journal of General Virology* **50,** 89-100.

Petit, F., Bertagnoli, S., Gelfi, J., Fassy, F., Boucraut-Baralon, C., and Milon, A. (1996). Characterization of a myxoma virus-encoded serpin-like protein with activity against interleukin-1β-converting enzyme. *Journal of Virology* **70,** 5860-5866.

Potempa, J., Korzus, E., and Travis, J. (1994). The serpin superfamily of proteinase inhibitors: structure, function and regulation. *Journal of Biological Chemistry* **269,** 15957-15960.

Powell, P. P., Dixon, L. K., and Parkhouse, R. M. E. (1996). IkappaB homolog encoded by African swine fever virus provides a novel mechanism for downregulation of proinflammatory cytokine response in host macrophages. *Journal of Virology* **70,** 8527-.

Price, G. E., Smith, H., and Sweet, C. (1997). Differential induction of cytotoxicity and apoptosis by influennza virus strains of differing virulence. *Journla of General Virology* **78,** 2821-2829.

Pross, H. F., and Eidinger, D. (1974). Antigenic competition: a review of non-specific antigen-induced suppression. *Advances in Immunology* **18,** 133-168.

Ramsay, A. J., Husband, A. J., Ramshaw, I. A., Bao, S., Matthaei, K. I., Koehler, G., and Kopf, M. (1994). The role of interleukin-6 in mucosal IgA antibody responses *in vivo. Science* **264,** 561-563.

Ramsey-Ewing, A., and Moss, B. (1998). Apoptosis induced by a postbinding step of vaccinia virus entry into Chinese hamster ovary cells. *Virology* **242,** 138-149.

Ramshaw, I., Ruby, J., Ramsay, A., Ada, G., and Karupiah, G. (1992). Expression of cytokines by recombinant vaccinia viruses: a model for studying cytokines in virus infections *in vivo. Immunological Reviews* **127,** 157-182.

Ramshaw, I. A., Ramsay, A. J., Karupiah, G., Rolph, M. S., Mahalingam, S., and Ruby, J. C. (1997). Cytokines and immunity to viral infections. *Immunological Reviews* **159,** 119-135.

Ratcliffe, F. N., Myers, K., Fennessy, B. V., and Calaby, J. H. (1952). Myxomatosis in Australia. A step towards the biological control of the rabbit. *Nature* **170,** 7-11.

Regnery, D. C., and Marshall, I. D. (1971). Studies in the epidemiology of myxomatosis in California. IV. The susceptibility of six leporid species to Californian myxoma virus and the relative infectivity of their tumors for mosquitoes. *American Journal of Epidemiology* **94,** 508-513.

Regnery, D. C., and Miller, J. H. (1972). A myxoma virus enzootic in a brush rabbit population. *Journal of Wildlife Research* **8,** 327-331.

Ridge, J. P., Di Rosa, F., and Matzinger, P. (1998). A conditioned dendritic cell can be a temporal bridge betwen a $CD4^+$ T-helper and a T-killer cell. *Nature* **393,** 474-478.

Rivers, T. M. (1930). Infectious myxomatosis of rabbits. *Journal of Experimental Medicine* **51,** 965-975.

Robinson, A. J., Muller, W. J., Braid, A. L., and Kerr, P. J. (submitted). The effect of buprenorphine on the course of disease in laboratory rabbits infected with myxoma virus. *Laboratory Animals.*

Rodriguez, J. R., Risco, C., Carrascosa, J. L., Esteban, M., and Rodriguez, D. (1998). Vaccinia virus 15-kilodalton (A14L) protein is essential for assembly and attachment of viral crescents to virosomes. *Journal of Virology* **72,** 1287-1296.

Rolls, E. C. (1984). "They All Ran Wild." 3rd ed. Angus and Robertson Publishers, Sydney.

Roper, R. L., Wolffe, E. J., Weisberg, A., and Moss, B. (1998). The envelope protein encoded by the A33R gene is required for formation of actin-containing microvilli and efficient cell-to-cell spread of vaccinia virus. *Journal of Virology* **72,** 4192-4204.

Ruby, J. (1997). Anitviral activity of gamma interferon. *In* "Gamma Interferon in Antiviral Defense" (G. Karupiah, Ed.). R.G. Landes Company.

Ruby, J., and Ramshaw, I. (1991). The antiviral activity of immune $CD8^+$ T cells is dependent on interferon-γ. *Lymphokine and Cytokine Research* **10,** 353-358.

Rudin, C. M., and Thompson, C. B. (1997). Apoptosis and disease: regulation and slinical relevance of programmed cell death. *Annual Reviews in Medicine* **48,** 267-281.

Russell, R. J., and Robbins, S. J. (1989). Cloning and molecular characterisation of the myxoma virus genome. *Virology* **170,** 147-159.

Sambhi, S. K., Kohonen-Corish, M. R., and Ramshaw, I. A. (1991). Local production of tumor necrosis factor encoded by recombinant vaccinia virus is effective in controlling virus replication *in vivo*. *Procedings of the National Academy of Science* **88,** 4025-4029.

Sanarelli, G. (1898). Das myxomatogene Virus. Beitag zum Stadium der Krankheitserreger ausserhalb des Sichtbaren. *Zentralblatt fur Bakteriologie, Parasitenkunde, Infectionskrankheiten und Hygiene (Abt.1).* **23,** 865-873.

Sarin, A., Adams, D. H., and Henkart, P. A. (1993). Protease inhibitors selectively block T cell receptor-triggered programmed cell death in a murine T cell hybridoma and activated peripheral T cells. *Journal of Experimental Medicine* **178,** 1693-1700.

Scalzo, A. A., Fitzgerald, N. A., Simmons, A., La Vista, A. B., and Shellam, G. R. (1990). Cmv-1, a genetic locus that controls murine cytomegalovirus replication in the spleen. *Journal of Experimental Medicine* **171,** 1469-1483.

Schall, T. J. (1994). The chemokines. 2 ed. *In* "The Cytokine Handbook" (A. Thompson, Ed.), pp. 419-460. Academic Press, San Diego.

Schall, T. J., and Bacon, K. B. (1994). Chemokines, leukocyte trafficking, and inflammation. *Current Opinion in Immunology* **6,** 865-873.

Schlender, J., Schnorr, J. J., Speilhofer, P., Cathomen, T., Cattaneo, R., Billeter, M. A., ter Meulen, V., and Schneider-Schaulies, S. (1996). Interaction if measles glycoproteins with the surface of uninfected peripheral blood lymphocytes induces immunosuppression *in vitro. Proceedings of the National Academy of Sciences* **93,** 13194-13199.

Schmelz, M., Sodeik, B., Ericsson, M., Wolffe, E. J., Shida, H., Hiller, G., and Griffiths, G. (1994). Assembly of vaccinia virus: the second wrapping cisterna is derived from the trans Golgi network. *Journal of Virology* **68,** 130-147.

Schnorr, J.-J., Seufert, M., Schlender, J., Borst, J., Johnston, I. C. D., ter Meulen, V., and Schneider-Schaulies, S. (1997). Cell cycle arrest rather than apoptosis is associated with measles virus contact-mediated immunosuppression *in vitro. Journal of General Virology* **78,** 3217-3226.

Schoenberger, S. P., Toes, R. E. M., van der Voort, E. I. H., Offringa, R., and Melief, C. J. M. (1998). T-cell help for cytotoxic T lymphocytes is mediated by CD40-CD40L interactions. *Nature* **393,** 480-483.

Schreiber, M., and McFadden, G. (1994). The myxoma virus TNF-receptor homologue (T2) inhibits tumor necrosis factor-α in a species-specific fashion. *Virology* **204,** 692-705.

Schreiber, M., Sedger, L., and McFadden, G. (1997). Distinct domains of M-T2, the myxoma virus tumor necrosis factor (TNF) receptor homolog, mediate extracellular TNF binding and intracellular apoptosis inhibition. *Journal of Virology* **71,** 2171-2181.

Scott, C. B., Holdbrook, R., and Sell, S. (1981). Cell-mediated immune response to Shope fibroma virus-induced tumors in adult rabbits. *Journal of the National Cancer Institute* **66,** 681-689.

Sedger, L., and McFadden, G. (1996). M-T2: a poxvirus TNF receptor homologue with dual activities. *Immunology and Cell Biology* **74,** 538-545.

Sharma, D. P., Ramsay, A. J., Maguire, D. J., Rolph, M. S., and Ramshaw, I. A. (1996). Interleukin-4 mediates downregulation of antiviral cytokine expression and cytotoxic T-lymphocyte responses and exacerbates vaccinia virus infection *in vivo*. *Journal of Virology* **70,** 7103-7107.

Shellam, G. R., Sangster, M. Y., and Urosevic, N. (1998). Genetic control of host resistance to flavivirus inefection in animals. *Revue Scientifique et Technique* **17,** 231-248.

Shope, R. E. (1932). A filterable virus causing a tumor-like condition in rabbits and its relationship to virus myxomatosum. *Journal of Experimental Medicine* **56,** 803.

Shope, R. E. (1936). Infectious fibroma of rabbits. III. The serial transmission of virus myxomatosum in cottontail rabbits, and cross-immunity tests with the fibroma virus. *Journal of Experimental Medicine.* **63,** 43.

Smith, C. A., Davis, T., Anderson, D., Solam, L., Beckman, M. P., Jerzy, R., Dower, S. K., Cosman, D., and Goodwin, R. G. (1990). A receptor for tumor necrosis factor defines an unusual family of cellular and viral proteins. *Science* **248,** 1019-1023.

Smith, C. A., Farrah, T., and Goodwin, R. (1994). The TNF receptor superfamily of cellular and viral proteins: Activation, co-stimulation and death. *Cell* **76,** 959-962.

Smith, C. A., Hu, F. Q., Smith, T. D., Richards, C. L., Smolak, P., Goodwin, R. G., and Pickup, D. J. (1996). Cowpox virus genome encodes a second soluble homologue of cellular TNF receptors, distinct from CrmB, that binds TNF but not LT alpha. *Viology* **223,** 132-147.

Smith, C. A., Smith, T. D., Smolak, P. J., Friend, D., Hagen, H., Gerhart, M., Park, L., Pickup, D. J., Torrance, D., Mohler, K., Schooley, K., and Goodwin, R. G. (1997a). Poxvirus genomes encode a secreted, soluble protein that preferentially inhibits β chemokine activity yet lacks sequence homology to known chemokine receptors. *Virology* **236,** 316-327.

Smith, G. L. (1993). Vaccinia virus glycoproteins and immune evasion. *Journal of General Virology* **74,** 1725-1740.

Smith, G. L. (1994). Virus strategies for evasion of the host response to infection. *Trends in Microbiology* **2,** 81-88.

Smith, G. L., Symons, J. A., and Alcami, A. (1998). Poxviruses: interfering with interferon. *Seminars in Virology* **8,** 409-418.

Smith, G. L., Symons, J. A., Khanna, A., Vanderplasschen, A., and Alcami, A. (1997). Vaccinia virus immune evasion. *Immunological Reviews* **159,** 137-154.

Sobey, W. R. (1969). Selection for resistance to myxomatosis in domestic rabbits (*Oryctolagus cuniculus). Journal of Hygiene* **67,** 743-754.

Sobey, W. R., and Conolly, D. (1986). Myxomatosis: non-genetic aspects of resistance to myxomatosis in rabbits (*Oryctolagus cuniculus*). *Australian Wildlife Research* **13,** 177-188.

Sodeik, B., Doms, R. W., Ericsson, M., Hiller, G., Machamer, C. E., van't Hof, W., van Meer, G., Moss, B., and Griffiths, G. (1993). Assembly of vaccinia virus: role of intermediate compartment between the endoplasmic reticulum and the Golgi stacks. *Journal of Cell Biology* **121,** 521-541.

Sprecher, E., and Becker, Y. (1986). Skin Langerhans cells play an important role in the defense against HSV-1 infection. *Archives of Virology* **91,** 341-349.

Sprecher, E., and Becker, Y. (1987). Herpes simplex type 1 pathogenicity in footpad and ear skin of mice depends on Langerhans cell density, mouse genetics and virus strain. *Journal of Virology* **61,** 2515-2522.

Spriggs, M. K. (1994). Poxvirus-encoded soluble cytokine receptors. *Virus Research* **33,** 1-10.

Spriggs, M. K., Hruby, D. E., Maliszewski, C. R., Pickup, D. J., J.E., S., Buller, R. M. L., and Vanslyke, J. (1992b). Vaccinia and cowpox viruses encode a novel secreted interleukin-1 binding protein. *Cell* **71,** 145-152.

Spriggs, M. K., Koller, B. H., Sato, T., Morrissey, P. J., Fanslow, W. C., Smithies, O., Voice, R. F., Widmer, M. B., and Maliszewski, C. R. (1992a). β_2-microglobulin$^-$, $CD8^+$ T-cell-deficient mice survive inoculation with high doses of vaccinia virus and exhibit altered IgG responses. *Proceedings of the National Academy of Science* **89,** 6070-6074.

Stodart, E., and Parer, I. (1988). Colonisation of Australia by the rabbit *Oryctolagus cuniculus* (L.). *Project Report No. 6, CSIRO Division of Wildlife and Ecology, Canberra.*

Strayer, D. S., Cabirac, G., Sell, S., and Leibowitz, J. L. (1983a). Malignant rabbit fibroma virus: observations on the culture and histopathologic of a new virus-induced rabbit tumour. *Journal of the National Cancer Institute* **71,** 91-96.

Strayer, D. S., and Dombrowski, J. (1988). Immunosuppression during viral oncogenesis. V. Resistance to virus-induced immunosuppressive factor. *Journal of Immunology* **141,** 347-351.

Strayer, D. S., Horowitz, M., and Leibowitz, J. L. (1986). Immunosuppression in viral ocogenesis. III. Effects of virus infection of interleukin 1 and interleukin 2 generation and responsiveness. *Journal of Immunology* **137,** 3632-3638.

Strayer, D. S., Korber, K., and Dombrowski, J. (1988). Immunosuppression during viral oncogenesis. IV. Generation of soluble virus-induced immunologic suppressor molecules. *Journal of Immunology* **140,** 2051-2059.

Strayer, D. S., Laybourn, K. A., and Heard, H. K. (1990). Determinants of the ability of malignant fibroma virus to induce immune dysfunction and tumor dissemination *in vivo. Microbial Pathogenesis* **9,** 173-189.

Strayer, D. S., and Leibowitz, J. L. (1986). Reversal of virus-induced immune suppression. *Journal of Immunology* **136,** 2649-2653.

Strayer, D. S., and Leibowitz, J. L. (1987a). Virus-lymphocyte interactions during the course of immunosuppressive virus infection. *Journal of General Virology* **68,** 463-472.

Strayer, D. S., and Leibowitz, J. L. (1987b). Inhibition of epidermal growth factor-induced cellular proliferation. *American Journal of Pathology* **128,** 203-209.

Strayer, D. S., and Mathew, J. (1993). A 34kd protein with strong homology to ras-like proteins inhibits epidermal growth factor activity. *American Journal of Pathology* **142,** 1141-1153.

Strayer, D. S., and Sell. (1983). Immunohistology of malignant rabbit fibroma virus - a comparative study with rabbit myxoma virus. *Journal of the National Cancer Institute* **71,** 105-116.

Strayer, D. S., Sell, S., Skaletsky, E., and Leibowitz, J. L. (1983b). Immunologic dysfunction during viral oncogenesis. I. Nonspecific immunosuppression caused by malignant rabbit fibroma virus. *Journal of Immunology* **131,** 2595-2600.

Strayer, D. S., Skaletsky, E., and Leibowitz, J. L. (1985). *In vitro* growth of two related Lepripoxviruses in lymphoid cells. *Virology* **145,** 330-334.

Summerfield, A., Knotig, S. M., and McCullough, K. C. (1998). Lymphocute apoptosis during classical swine fever: implication of activation-induced cell death. *Journal of Virology* **72,** 1853-1861.

Szomolanyi-Tsuda, E., Le, Q. P., Garcea, R. L., and Welsh, R. (1998). T-cell-independent immunoglobulin G responses *in vivo* are elicited by live-virus infection but not by immunization with viral proteins or virus-like particles. *Journal of Virology* **72,** 6665-6670.

Taussig, M. J. (1973). Antigenic competition. *Current Topics in Microbiology and Immunology* **60,** 125-174.

Traktman, P. (1990a). Poxviruses: an emerging portrait of biological strategy. *Cell* **62,** 621-626.

Traktman, P. (1990b). The enzymology of poxvirus DNA replication. *In* "Current Topics in Microbiology and Immunology" (R. W. Moyer, and P. C. Turner, Eds.), Vol. 163, pp. 93-123.

Tumpey, T. M., Chen, S.-H., Oakes, J. E., and Lausch, R. N. (1996). Neutrophil mediated suppression of virus replication after herpes simplex virus type 1 infection of the murine cornea. *Journal of Virology* **70,** 898-904.

Turner, P. C., and Moyer, R. W. (1990). The molecular pathogenesis of poxviruses. *In* "Poxviruses" (R. W. Moyer, and P. C. Turner, Eds.), pp. 125-151. Springer-Verlag, Berlin.

Turner, P. C., and Moyer, R. W. (1998). Control of apoptosis by poxviruses. *Seminars in Virology* **8,** 453-469.

Upton, C., Macen, J. L., and McFadden, G. (1987). Mapping and sequencing of a gene from myxoma virus that is related to those encoding epidermal growth factor and transforming growth factor alpha. *Journal of Virology* **61,** 1271-1275.

Upton, C., Macen, J. L., Schreiber, M., and McFadden, G. (1991). Myxoma virus expresses a secreted protein with homology to the tumor necrosis factor gene family that contributes to viral virulence. *Virology* **184,** 370-382.

Upton, C., Macen, J. L., Wishart, D. S., and McFadden, G. (1990). Myxoma virus and malignant rabbit fibroma virus encode a serpin-like protein important for virus virulence. *Virology* **179,** 618-631.

Upton, C., and McFadden, G. (1986). Tumongenic poxviruses: analysis of viral DNA sequences implicated in the tumongenicity of Shope fibroma virus and malignant rabbit virus. *Virology* **152,** 308-321.

Upton, C., Mossman, K., and McFadden, G. (1992). Encoding of a homolog of the IFN-γ receptor by myxoma virus. *Science* **258,** 1369-1372.

Vanderplasschen, A., Hollinshead, M., and Smith, G. L. (1997). Antibodies against vaccinia virus do not neutralise extracellular enveloped virus but prevent virus release from infected cells and comet formation. *Journal of General Virology* **78,** 2041-2048.

Varadhachary, A. S., Perdow, S. N., Hu, C., Ramanarayanan, M., and Salgame, P. (1997). Differential ability of T cell subsets to undergo activation-indeced cell death. *Proceedings for the National Academy of Sciences* **94,** 5778-5783.

Wallace, G. D., Buller, R. M., and Morse, H. C. (1985). Genetic determinants of resistance to ectromelia (mousepox) virus-induced mortality. *Journal of Virology* **55,** 890-891.

Webster, L. T., and Johnson, M. S. (1941). Comparative virulence of St. Louis encephalitis virus cultured with brain tissue from innately susceptible and innately resistant mice. *Journal of Experimental Medicine* **74,** 489-494.

Werdelin, O. (1982). Chemically related antigens compete for presentation by accessory cells to T cells. *Journal of Immunology* **129,** 1883-1891.

West, B. C., Eschete, M. L., Cox, M. E., and King, J. W. (1987). Neutrophil uptake of vaccinia virus *in vitro*. *Journal of Infectious Diseases* **156,** 597-606.

Wheater, P. R., Burkitt, H. G., and Daniels, V. G. (1987). "Functional histology: a text and colour atlas." 2nd ed. Churchill Livingstone, London.

Wilkinson, J. M., Galea-Lauri, J., Sellars, R. A., and Boniface, C. (1992). Identification and tissue distribution of rabit leucocyte antigens recognized by monoclonal antibodies. *Immunology* **76,** 625-630.

Williams, C. K., and Moore, R. J. (1991). Inheritance of acquired immunity to myxomatosis. *Australian Journal of Zoology* **39,** 307-312.

Wolffe, E. J., Weisberg, A. S., and Moss, B. (1998). Role for the vaccinia virus A36R outer envelope protein in the formation of virus-tipped actin-containing microvilli and cell-to-cell virus spread. *Virology* **244,** 20-26.

Woodroofe, G. M., and Fenner, F. (1962). Serological relationships within the poxvirus group: an antigen common to all members of the group. *Virology* **16,** 334-341.

Woodroofe, G. M., and Fenner, F. (1965). Viruses of the myxoma-fibroma subgroup of the poxviruses. I. Plaque reduction in cultured cells, plaque reduction tests, and cross-protection tests in rabbits. *Australian Journal of Experimental Medical Science* **43,** 123-142.

Zar, J. H. (1984). "Biostatistical Analysis." 2nd ed. Prentice-Hall Interantional, Inc., New Jersey, USA.

Zhu, M., Moore, T., and Broyles, S. S. (1998). A cellular protein that binds vaccinia virus late promoters and activates transcription *in vitro*. *Journal of Virology* **72,** 3893-3899.